Serbian Association for Geometry and Graphics

# The 8th International Scientific Conference on Geometry and Graphics

# moNGeometrija 2021

September 10th - 12th, Belgrade, Serbia

## Proceedings

Srebian Association for Geometry and Graphics

# PROCEEDINGS

September 10th – 12th 2021, Belgrade, Serbia

ISBN 978-86-6060-086-0

SUGIG
Beograd, 2021.

The 8th International Scientific Conference on Geometry and Graphics

# moNGeomatrija2021

**Publishers**

Serbian Society for Geometry and Graphics (SUGIG)
Faculty of Mechanical Engineering, University of Belgrade

**Title of Publication**

PROCEEDINGS

**Editor-in-Chief**

Zorana Jeli

**Co-Editors**

Branislav Popkonstantinović
Slobodan Mišić
Ratko Obradović

**Graphic design**

Zorana Jeli
Boris Kosić

**Formatters**

Zorana Jeli
Boris Kosić
Filip Mirčeski

**Print**

Planeta Print, Belgrade

Number of copies: 50

ISBN 978-86-6060-086-0

The 8th International Scientific Conference on Geometry and Graphics

# moNGeomatrija2021

## Conference Organizers

Serbian Society of Geometry and Graphics (SUGIG)

Faculty of Mechanical Engineering, University of Belgrade

## Co-organizers

Faculty of Technical Sciences, University of Novi Sad, Department of Fundamental Sciences

## Under the auspicies of

Ministry of Education, Science and Technological Development of Republic of Serbia

## Scientific Committee:

Hellmuth Stachel – Austria
Emil Molnar – Hungary
Gunter Weiss – Germany
Naomi Ando – Japan
Radovan Štulić – Serbia
Branislav Popkonstantinović – Serbia
Ratko Obradović – Serbia
Branko Malešević – Serbia
Lidija Matija – Serbia
Albert Wiltsche – Austria
Milena Stavric – Austria
Ajla Aksamija– USA
Olga Timcenko – Denmark
Ema Jurkin – Croatia
Alina Duta – Romania
Dragos-Laurentiu Popa – Romania
Carmen Marza – Romania
Laszlo Voros – Hungary
Zsuzsanna Balajti – Hungary
Michal Zamboj – Czech Republic
Monika-Sroka Bizon – Poland
Pengfei Zheng, China
Tashko Rizov – North Macedonia
Maja Čavić – Serbia
Aleksandar Čučaković – Serbia
Marija Obradović – Serbia
Sonja Krasić – Serbia
Slobodan Mišić – Serbia
GianLucca Stasi – Spain
Maja Ilić – Republic of Srpska, Bosnia and Herzegovina
Djordje Djordjević – Serbia
Marijana Paunović – Serbia
Magdalena Dragović – Serbia
Gordana Djukanović – Serbia
Maja Petrović – Serbia
Emil Veg – Serbia
Miša Stojićević – Serbia
Bojan Banjac – Serbia

## Organizing Committee:

Zorana Jeli
Miša Stojićević
Ana Petrović
Boris Kosić
Ivana Vasiljević
Aleksandra Dragičević
Aleksandra Joksimović
Isidora Zorić
Filip Mirčeski
Rodoljub Milićević

## Reviewers:

Prof. Branislav Popkonstantinović – Serbia
Prof. Ratko Obradović – Serbia
Prof. Branko Malešević – Serbia
Associate Prof. Alina Duta – Romania
Associate Prof. Dragos-Laurentiu Popa – Romania
Associate Prof. Zsuzsanna Balajti – Hungary
Associate Prof. Monika-Sroka Bizon – Poland
Associate Prof. Tashko Rizov – Macedonia
Associate Prof. Pengfei Zheng, China
Associate Prof. Aleksandar Čučaković – Serbia
Associate Prof. Marija Obradović – Serbia
Associate Prof. Sonja Krasić – Serbia
Associate Prof. Slobodan Mišić – Serbia
Associate Prof. Zorana Jeli – Serbia
Associate Prof. Emil Veg – Serbia
Ass. Prof. Magdalena Dragović – Serbia
Ass. Prof. Miša Stojićević – Serbia
Ass. Prof. Djordje Djordjević – Serbia
Ass. Prof. Gordana Djukanović – Serbia
Ass. Prof. Bojan Banjac – Serbia
Ass. Prof. Maja Petrović – Serbia

# PROCEEDINGS

## CONTENT

# TOPIC 1: ENGINEERING COMPUTER GRAPHICS AND GEOMETRY

# CONSTRUCTIVE GEOMETRIC METHOD FOR THE ANALYSIS OF THE MANUFACTURING ACCURACY OF HELICOID DRIVES

Zsuzsa Balajti

University of Miskolc, Faculty of Mechanical Engineering and Informatics, Department of Descriptive Geometry, H-3515 Miskolc, Hungary

balajtizs@ubi-miskolc.hu

***ABSTRACT***

*One of the most important condition of intelligent manufacturing is the continuous development of tool geometry. One relevant component of tool geometry is the analysis of the relationship between tool edge geometry and manufactured surface quality. During the production of worm gear, in order to achieve the required quality, after the worm gear hob testing, the cutting edge must be re-sharpened, which results in a decrease in the diameter of the hob. Changes in geometric conditions are the result of the decrease in distance between the re-sharped hob axis and the gear axis. The aim of this paper is to present the analysis method of the relation between the re-sharpening of the hob and the gear tooth surface quality.*

**Keywords:** production geometry; worm gear drive; hob; cutting edge; gear tooth surface

## 1. INTRODUCTION

One of the most important research topics of the Worm Scientific School, operating in the Difi-CAD Engineering Office having cooperation agreement with the University of Miskolc, is the continuous further development of the production geometry of the elements of worm gear drives. The unique tool that can be used for finishing machining to the gear tooth surface is one that envelopes the same surface as the worm connected to the gear (direct movement mapping). This tool is the hob in the case of serial production of gears. As the hob is an expensive tool with extremely complicated geometry, it is advisable to make their re-sharpening as many times as possible.

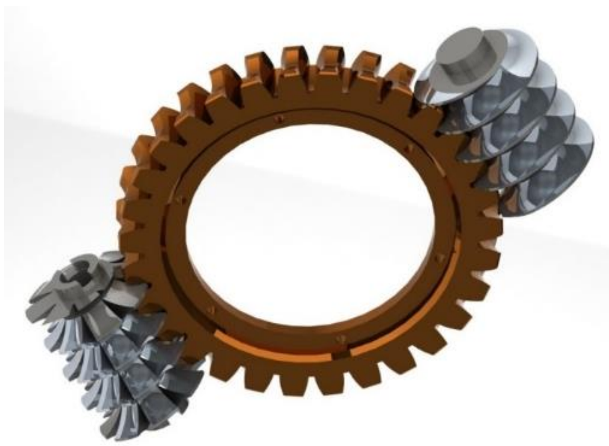

**Figure 1**: Virtual model of the worm gear drive and the hob

The wear test of the tool is necessary to achieve the required accuracy of the machined elements of drives (Bercsey et al., 2002). Several modern, highly regarded graphics systems are used to develop technical systems (Jeli et al., 2012). During research the cutting edge wear of the hob was examined with two CCD cameras to obtain the spatial position of the cutting edge curve. Visualizing the geometry of two images provides a number of tasks (Stachel, 2006), including the question of solving reproducibility. Because of all before this, the CCD cameras must be positioned mathematically correctly to ensuring the reproducibility of the V cutting edge curve, which is marked with blue colour in Figure 2 (a). To the testing the hob has to be adjusted to the predetermined position by one unchanging element of it, which can be the L intersection curve of the H face surface of the hob examined tooth and the root cylinder, which is marked with green colour in Figure 2 (a). Considering to the placement of the CCD cameras in the directions of the projection lines, the images show the Monge projections of the cutting edge of the hob (Balajti et al., 2017). The images are clearly defined by the projection directions, and since the reproducibility from the images is indifferent to the parallel shift, it was only worth examining the projection directions that fit the starting point of a fixed coordinate system. In the fixed Descartes coordinate system, the relationship between the projection lines defining the Monge projections and their defining direction angles of the projection lines as triplets of real numbers resulted the Monge-cuboid (Balajti et al., 2020). The correct positions of CCD camera pair to ensuring the reproducibility of the V cutting edge curve give us the bijective parts of Monge-cuboid that provide the bijective mapping. The border surface point between the bijective and non-bijective parts inside the Monge- cuboid respected to the V curve is signed with blue colour in Figure 2(b). The condition of the reproducibility of the V cutting edge curve has been constrained even by additional boundary condition. The border surface point between the bijective and non-bijective parts inside the Monge-cuboid respected to the L curve is signed with green colour in Figure 2(b). These border surfaces inside of the Monge-cuboid have indicated the applicable positions of CCD camera pairs in Figure 2. Solutions that satisfy two boundary conditions can also be calculated with a special mathematical background (Rontó, A. et. al, 2000), marked in red.

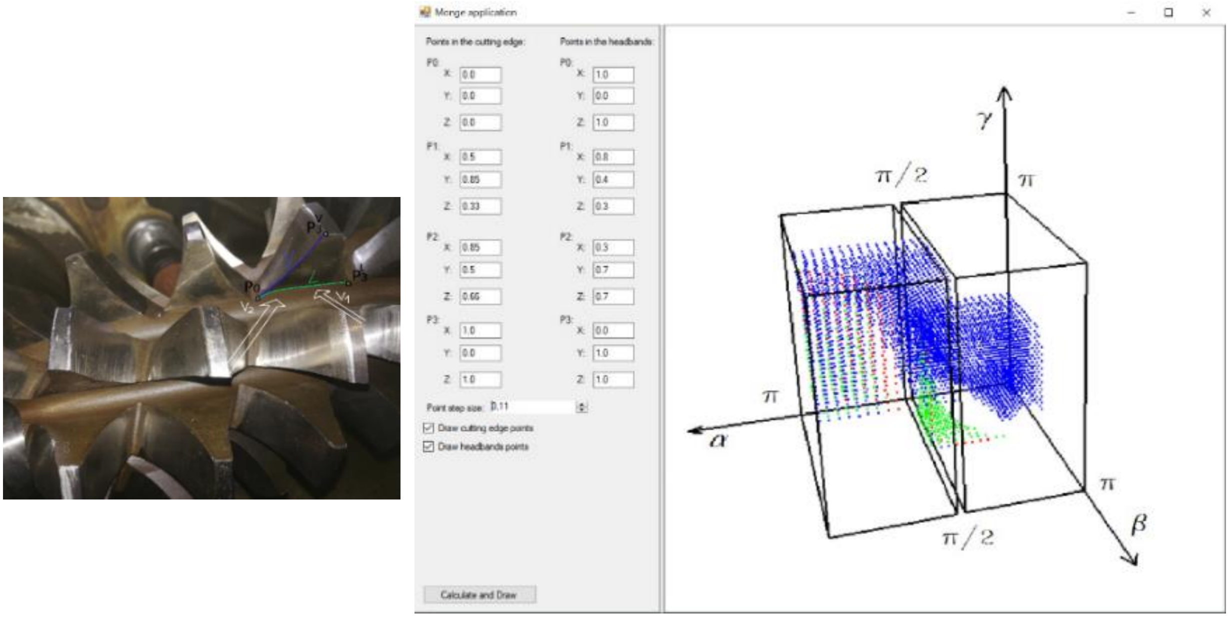


(a) (b)

**Figure 2**: (a) The V cutting edge curve and the predetermined L curve on the hob, and (b) border surfaces points between the bijective and non-bijective parts with respect to curves V and L (Source: Johansen et al. (2012)

The border surfaces inside Monge-cuboid separate points, that ensure bijectivity and give the correct positions of CCD camera pair to adjust the hob and to test the edge wear at the same time. The reconstruction of the cutting edge curve of the hob can be determined by method of descriptive geometry (Cvetković, 2019), which was developed using an interpolation Bezier curve (Ábel et al., 2018). The right projection direction was investigated using the polynomial-shaped Hermite arc, the relation of which to the interpolation Bezier curve fitted to the cutting edge is obtained by solving a linear inhomogeneous system (Raisz et. al., 2000). During the production of worm gear, in order to achieve the required quality, the hob must be tested for wear and the cutting edge must be re-sharpened, which results geometric deformation on the gear tooth surface. Because of the enveloping theorem and the direct motion mapping (Popkonstantinovic et al., 2019), the effect of worm profile on contact lines indicate the distortion of the tooth surface machined by the re-sharpened and adjusted hob (Dudás L., 2010). The contact patch on the gear tooth surface must be examined by method of the main low of contact (Máté et al., 2013). This paper proposes an analysis method of the gear tooth deformation due to the hob re-sharpening.

## 2. APPLIED PRODUCTION GEOMETRY THEORY OF CYLINDRICAL WORM GEAR DRIVES

During the of manufacturing process, from the kinematic substitution aspect, all continuous machining can be seen as mapping of relative movements informations, so the theorem of motion mapping, which is the production method of the related surfaces of special kinematic pairs, can be considered an organic part of manufacturing geometry. The analysis of the geometrically correct production of worm gear tooth surfaces was executed by applying the mathematical model based on results of kinematical geometry, tooth theory, the production geometry analysis of tools, and the mathematical description of the geometric and connection relation. The two elements of the drive pairs envelop each other in relative motion, their connection taking place along the contact line (Litvin et al., 1994). The worm gear hob created from the worm is a suitable tool machining the gear tooth surface mated to the worm. Hob design requires an extremely strong background in manufacturing technology (Felhő et. al., 2004), production geometry (Kral et al., 2013) and all areas mathematics (Vadászné Bognár, 2003). The cutting edges of the hob should be located on the tooth surfaces of the substituting worm. The substituting worm with the same tooth surface as the real worm has a larger addendum diameter and tooth thickness than the real worm, and they have common geometric axes, their diameter of reference cylinders $d_{m1}$ are identical, and their tooth surfaces on the same sided are coincident with the corresponding axial displacement. The teeth of the worm gear connected to the worm are determined by the teeth of the worm, since the contact tooth surfaces are mutually enveloping surfaces (Dudás I., 1991), and because of the hob motion produces the same result enveloped surface, as the worm, examination of the connection between the worm and the gear leads to the connection between the hob and the gear.

### 2.1 Mathematical kinematical model

The investigations have been procreated with the support of the Dudás's kinematic mathematical model, where the cylindrical and conical worms or hobs with its axis coinciding $z_{1F}$, furthermore worm-gears and tools of worms with its axis coinciding $z_{2F}$, and in which the coordinate systems and applied geometrical parameters are suitable for the production geometrical analysis (Dudás I., 2004). The examinations have been made in an improved model with changing axis distance, which is presented with special parameters in Figure 3.

Coordinate systems are interpreted as follows:

$K_0$ ($x_0$, $y_0$, $z_0$)....................stationary coordinate system,
$K_{1F}$ ($x_{1F}$, $y_{1F}$, $z_{1F}$)..............rotating coordinate system fixed to the helicoid surface,
$K_1$ ($x_1$, $y_1$, $z_1$)....…………coordinate system connected to linear moving table,
$K_{2F}$ ($x_{2F}$, $y_{2F}$, $z_{2F}$)……..…rotating coordinate system fixed to the gear or tool,
$K_2$ ($x_2$, $y_2$, $z_2$)………...….stationary coordinate system fixed to tool,
$K_{20}$ ($x_{20}$, $y_{20}$, $z_{20}$)……...…coordinate system of the generating curve on the tool of surface,
$K_k$ ($x_k$, $y_k$, $z_k$)……………auxiliary coordinate system,
$O_0$, $O_1$, $O_2$, $O_{1F}$, $O_{2F}$, $O_k$…origins of coordinate systems related to their subscripts.

Applied parameters:

$a$, $c$……………………..…distances of axes [mm],
$\alpha$………………………...tilting angle of the tool to the helical surface in a characteristic section [°],
$\gamma$…....................................lead angle on the worm's reference surface [°],
p…………………………screw parameter of the helix on the worm,
$p_a$………………………...axial screw parameter,
$p_r$………………………...radial screw parameter,
$\varphi_1$………………………..rotation angle of the helical surface [°],
$\varphi_2$……………….………rotation angle of the gear or the tool surface [°],
$\boldsymbol{\omega}_1$………………………angular velocity of the worm [$s^{-1}$],
$\boldsymbol{\omega}_2$……………………....angular velocity of the gear or the tool [$s^{-1}$],
($\eta$,$\vartheta$) ……………………parameters of worm surface [mm, °].

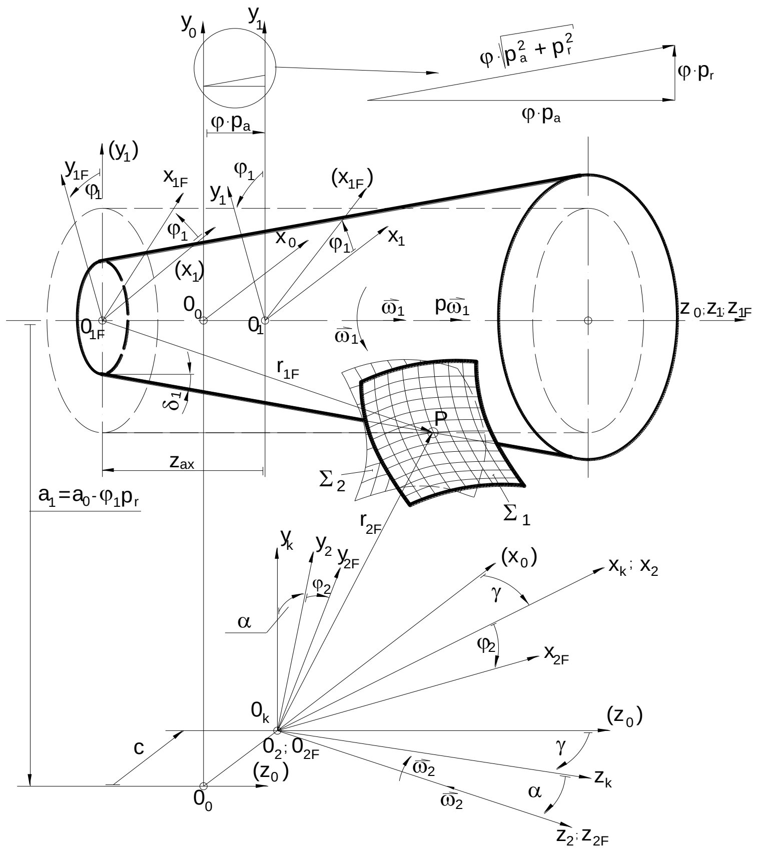

**Figure 3**: The applied coordinate systems for production geometry analyzing of conical and cylindrical worm gear drives (Balajti, 2007).

An example, the special improved model with the appropriate parameter selection refers to cylindrical worm gear drive pairs with parameters $\alpha_o$=0, $c$=0, $p_r$=0, $\gamma \equiv \Sigma$= -90°, and in this case the geometrical relations can be examined by the main rule of connection, as in case in any drive pairs.

## 2.2 Connection conditions

The tooth surface $\Sigma_1$ of the worm can be written in the following form in the $K_{1F}(x_{1F}, y_{1F}, z_{1F})$ rotating coordinate system of the worm with surface parameters $(\eta, \vartheta)$

$$\mathbf{r}_{F1} = \mathbf{r}_{F1}(\eta, \vartheta) \qquad \text{( Eq.1)}$$

The normal vector $\mathbf{n}_{1F}$ of the surface (Eq.1) can be calculated in the coordinate system $K_{F1}(x_{F1}, y_{F1}, z_{F1})$ according to the partial derivate

$$\mathbf{n}_{1F} = \frac{\partial \mathbf{r}_{1F}}{\partial \eta} \times \frac{\partial \mathbf{r}_{1F}}{\partial \vartheta} \qquad \text{( Eq.2)}$$

The $\mathbf{v}_{1F}$ relative velocity vector between the worm and the mating gear can be written

$$\mathbf{v}_{1F}^{(12)} = \mathbf{M}_{1F,2F} \frac{d}{dt}\left(\mathbf{M}_{2F,1F} \cdot \mathbf{r}_{1F}\right) = \mathbf{M}_{1F,2F} \cdot \frac{d\mathbf{M}_{2F,1F}}{dt} \cdot \mathbf{r}_{1F} \qquad \text{(Eq.3)}$$

where the $\mathbf{M}_{1F,2F}$ and the $\mathbf{M}_{2F,1F}$ are transformation matrices between the $K_{1F}(x_{1F}, y_{1F}, z_{1F})$ and $K_{2F}$ $(x_{2F}, y_{2F}, z_{2F})$ coordinate systems, and the $t$ time is included in the $\varphi_1$ motion parameter

$$\mathbf{P}_{1a} = \mathbf{M}_{1F,2F} \cdot \frac{d\mathbf{M}_{2F,1F}}{dt} \qquad \text{(Eq.4)}$$

the "kinematic transfer" matrix.

$$\mathbf{P}_{1a}=\begin{bmatrix} 0 & -1-i\cdot\cos\alpha\cdot\cos\gamma & \begin{array}{l}+i\cdot\cos\alpha\cdot\sin\gamma\cdot\sin\varphi_1\\ -i\cdot\sin\alpha\cdot\cos\varphi_1\end{array} & \begin{array}{l}-\left(a_0+i\cdot c\cdot\cos\alpha\cdot\cos\gamma+p_r+i\cdot z_{ax}\cdot\cos\alpha\cdot\sin\gamma\right)\cdot\sin\varphi_1\\ +\left(i\cdot p_a\cdot\cos\alpha\cdot\sin\gamma+p_r\right)\cdot\varphi_1\cdot\sin\varphi_1\\ -\left(i\cdot a_0\cdot\cos\alpha\cdot\cos\gamma-c-i\cdot z_{ax}\cdot\sin\alpha\right)\cdot\cos\varphi_1\\ -i\cdot\left(p_a\cdot\sin\alpha-p_r\cdot\cos\alpha\cdot\cos\gamma\right)\cdot\varphi_1\cdot\cos\varphi_1\end{array} \\ 1+i\cdot\cos\alpha\cdot\cos\gamma & 0 & \begin{array}{l}+i\cdot\sin\alpha\cdot\sin\varphi_1\\ +i\cdot\cos\alpha\cdot\sin\gamma\cdot\cos\varphi_1\end{array} & \begin{array}{l}+\left(i\cdot a_0\cdot\cos\alpha\cdot\cos\gamma-c-i\cdot z_{ax}\cdot\sin\alpha\right)\cdot\sin\varphi_1\\ +i\cdot\left(p_a\cdot\sin\alpha-p_r\cdot\cos\alpha\cdot\cos\gamma\right)\cdot\varphi_1\cdot\sin\varphi_1\\ -\left(a_0+i\cdot c\cdot\cos\alpha\cdot\cos\gamma+p_r+i\cdot z_{ax}\cdot\cos\alpha\cdot\sin\gamma\right)\cdot\cos\varphi_1\\ +\left(i\cdot p_a\cdot\cos\alpha\cdot\sin\gamma+p_r\right)\cdot\varphi_1\cdot\cos\varphi_1\end{array} \\ \begin{array}{l}-i\cdot\cos\alpha\cdot\sin\gamma\cdot\sin\varphi_1\\ +i\cdot\sin\alpha\cdot\cos\varphi_1\end{array} & \begin{array}{l}-i\cdot\sin\alpha\cdot\sin\varphi_1\\ -i\cdot\cos\alpha\cdot\sin\gamma\cdot\cos\varphi_1\end{array} & 0 & \begin{array}{l}-\left(p_a+i\cdot p_r\cdot\cos\alpha\cdot\sin\gamma\right)\cdot\varphi_1\\ -i\cdot a_0\cdot\cos\alpha\cdot\sin\gamma-i\cdot c\cdot\sin\alpha+p_a+z_{ax}\end{array} \\ 0 & 0 & 0 & 0 \end{bmatrix} \quad \text{(Eq.5)}$$

The worm surface parameters $(\eta,\vartheta)$ should be a function of parameter $u$ to describing the equation of the contact lines according to the first law of connection (Balajti, 2007) in every fixed motion parameter $\varphi_1$ in the following function relation

$$f(\eta(u),\vartheta(u),\varphi_1)=f(u,\varphi_1)=\mathbf{n}_{1F}\cdot\mathbf{v}_{1F}=0 \quad \text{(Eq.6)}$$

The tooth surface $\Sigma_2$ of the worm gear can be produced as the covering surface of the instantaneous contact lines written in the coordinate system $K_{2F}$ fixed to the worm gear

$$\left.\begin{array}{l} f(\eta,\vartheta,\varphi_1)=0\\ \mathbf{r}_{1F}=\mathbf{r}_{1F}(\eta,\vartheta)\\ \mathbf{r}_{2F\_gear}=\mathbf{M}_{2F,1F}\cdot\mathbf{r}_{1F}\end{array}\right\} \quad \text{(Eq.7)}$$

Using the procedure outlined above, the points of the $\Sigma_2$ tooth surface of the gear can be determined for any type of drive.

## 3. DISCUSSION

The cylindrical worm with circle arched profile in axial section has been patented by Dudás founding professor of the Worm Scientific School. This arched profiled cylindrical worm gear driving and worm gear hob was developed with ensuring the possibility of a hob's re-sharpening. The geometry parameters of the circle arched profile in axial section, such as $\rho_{ax}$ arc profile radius in axial section on the worm and $K$ distance between the centre of the circle arc profile and axis of the worm, as it can be seen in Figure 4. The gear tooth surface connected to the worm, can be manufactured by the hob created from the worm.

The $\mathbf{r}_{1F}$ helical surface with circle arc profile in axial section in the $K_{F1}(x_{F1}, y_{F1}, z_{F1})$ rotating coordinate system with parameters from Figure 4 can be written in the following form

$$\left.\begin{array}{l} x_{1F}=-\eta\cdot\sin\vartheta;\\ y_{1F}=\eta\cdot\cos\vartheta;\\ z_{1F}=p\cdot\vartheta-\sqrt{\rho_{ax}^2-(K-\eta)^2}\end{array}\right\} \quad \text{( Eq.8)}$$

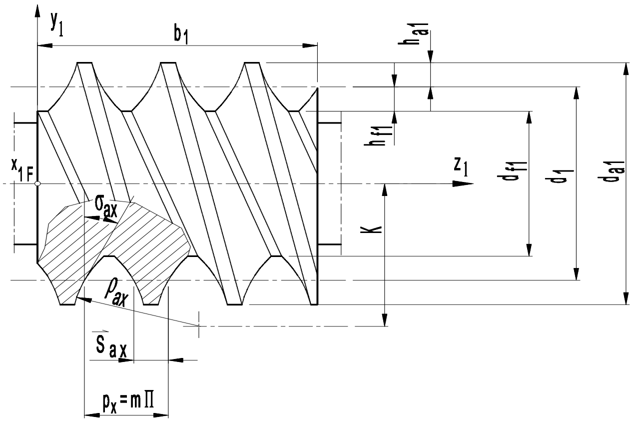


**Figure 4**: Geometrical parameters of the cylindrical worm with the circular arc profile in axial section (Source: Dudás I., 2004)

The coordinates of the normal vector $\mathbf{n}_{1F}$ of the surface (Eq.2) can be calculated in the coordinate system $K_{F1}(x_{F1}, y_{F1}, z_{F1})$ according to the partial derivate

$$\left.\begin{aligned} n_{1Fx} &= -\eta \cdot \sin\vartheta \cdot \frac{K-\eta}{\sqrt{\rho_{ax}^2-(K-\eta)^2}} + p \cdot \cos\vartheta \\ n_{1Fy} &= \eta \cdot \cos\vartheta \cdot \frac{K-\eta}{\sqrt{\rho_{ax}^2-(K-\eta)^2}} + p \cdot \sin\vartheta \\ n_{1Fz} &= \eta \end{aligned}\right\}$$

( Eq.9)

### 3.1 Geometry of the hob

The cutting edges $V_B$ and $V_J$ of the hob can be obtained as an intersection of the backward grinded side surfaces $R_B$ and $R_J$, and the face surface H. The back-machining and the technology of the processing should be carried out in such a way that the received edges $V_B$ and $V_J$ are on the tooth surface of the substituting worm, which is geometrically the same as the tooth surface of the real worm. The face surface of the hob is preferably a closed Archimedean worm surface, along which the tool is re-sharpened. Since the cutting edge V remains on the tooth surface of the same worm even after re-sharpening, it only shifts axially; the tool forms a tooth surface without profile distortion even after re-sharpening.

The face surface H of the hob is derived by the complex movement of a half-line perpendicular to the axis, which is a motion in axial direction with a screw parameter $p_h$ of the face-surface, and simultaneously a rotation about the axis.

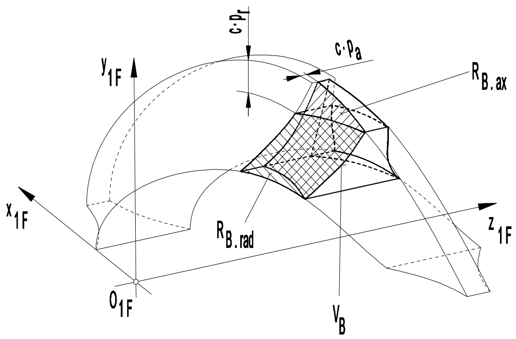


**Figure 5**: Surfaces and cutting edge of the tooth of the hob in the $K_{1F}$ motion coordinate system (Dudás, 2004)

In case of the right-handed hob the face surface H is left-handed, and its lead angle

$$\gamma_{oh} = 90^o - \gamma_o \,.$$

(Eq.8)

The equation of the face surface H can be written into the next form

$$\left.\begin{aligned} x_h &= -\eta \cdot sin(\vartheta + \varphi_{oh}); \\ y_h &= +\eta \cdot cos(\vartheta + \varphi_{oh}); \\ z_h &= -p_h \cdot sin(\vartheta + \varphi_{oh}); \end{aligned}\right\} \qquad \text{(Eq.9)}$$

where the lead parameter of the face surface H of the hob

$$p_h = \frac{d_{01} \cdot \pi \cdot \mathrm{tg}\gamma_{0h}}{2 \cdot \pi} \qquad \text{(Eq.10)}$$

then, making the appropriate substitutions,

$$-p_h \cdot (\vartheta + \varphi_{oh}) = p \cdot (\vartheta + \varphi_0) - \sqrt{\rho_{ax}^2 - (K - \eta)^2} + z_{ax} \qquad \text{(Eq.11)}$$

from which

$$\varphi_{oh} = \frac{1}{p_h} \cdot \sqrt{\rho_{ax}^2 - (K - \eta)^2} - \frac{p}{p_h} \cdot (\vartheta + \varphi_0) - \vartheta - \frac{z_{ax}}{p_h} \qquad \text{(Eq.12)}$$

Since the cutting edge V should remain on the substituting worm surface after re-sharpening, it forms a tooth on the wheel without profile distortion. Its equation in the examined case can be written in the following form

$$\left.\begin{aligned} x_v &= -\eta \cdot \sin \frac{\sqrt{\rho_{ax}^2 - (K - \eta)^2} - z_{ax}}{p + p_h} \\ y_v &= \eta \cdot \cos \frac{\sqrt{\rho_{ax}^2 - (K - \eta)^2} - z_{ax}}{p + p_h} \\ z_v &= -p_h \cdot \frac{\sqrt{\rho_{ax}^2 - (K - \eta)^2} - z_{ax}}{p + p_h} \end{aligned}\right\} \qquad \text{(Eq.13)}$$

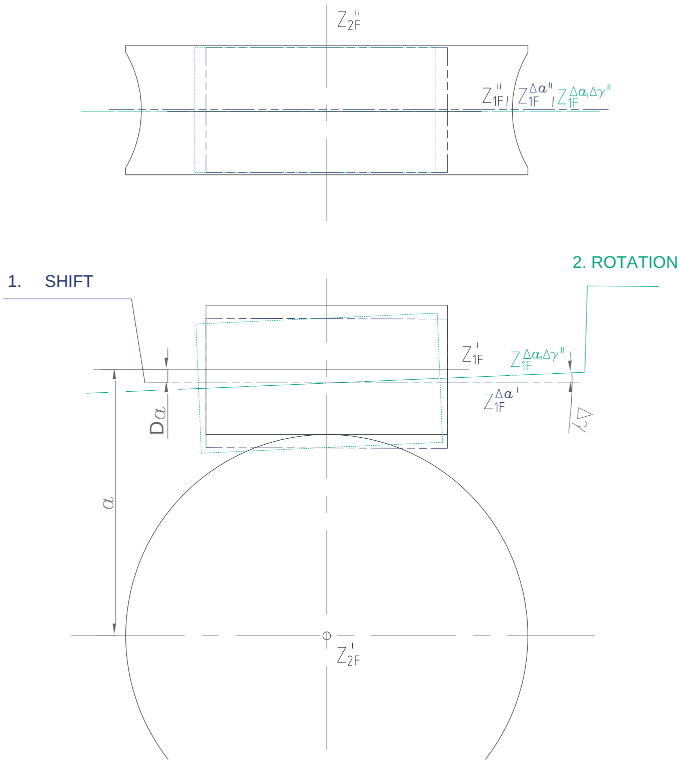


**Figure 6**: Schematic arrangement of the post-sharpening adjustment of the hob

However, in the case of radial rework, a radial dimensional change occurs after the tool has been re-sharpened. This result in a decrease in the distance between axes *a* and a change in the pitch angle γ (Balajti et al., 2020).

The worm gear hob created from the worm is a suitable tool machining the worm gear tooth surface, therefore the examination of the contact area of the worm and mated gear leads to analysis of the manufacturing accuracy of the gear machined by the post-sharped and adjusted hob.

### 3.2 Geometry of the gear resulted by the post-sharped and adjusted hob

The tool forms a tooth surface with profile distortion after re-sharpening, because of the motion relations have been changed. The re-sharpening of the hob requires shaft adjustment, which is related to the decrease in axes distance. The kinematic transfer matrix indicates the gear tooth surface distortion as a function of parameter *a*.

In the $K_{2F}$ coordinate system the coordinates of position vector $\mathbf{r}_{2F}$ pointing to the tooth surface $\Sigma_2$ of the gear depending on the adjusted hob are

$$\left.\begin{aligned} x_{2F\_gear} &= \sin\varphi_1 \cdot \sin\varphi_2 \cdot \eta \cdot \sin\vartheta - \cos\varphi_1 \cdot \sin\varphi_2 \cdot \eta \cdot \cos\vartheta \\ &\quad - \cos\varphi_2 \cdot \left(p_a \cdot \vartheta - \sqrt{\rho_{ax}^2 - (K-\eta)^2}\right) - (a + \Delta a) \cdot \sin\varphi_2 \\ y_{2F\_gear} &= \sin\varphi_1 \cdot \cos\varphi_2 \cdot \eta \cdot \sin\vartheta + \cos\varphi_1 \cdot \cos\varphi_2 \cdot \eta \cdot \cos\vartheta \\ &\quad - \sin\varphi_2 \cdot \left(p_a \cdot \vartheta - \sqrt{\rho_{ax}^2 - (K-\eta)^2}\right) - (a + \Delta a) \cdot \cos\varphi_2 \\ z_{2F\_gear} &= -\cos\varphi_1 \cdot \eta \cdot \sin\vartheta - \sin\varphi_1 \cdot \eta \cdot \cos\vartheta \end{aligned}\right\} \qquad \text{(Eq. 15)}$$

The result shows the changing in $x_{2F\_gear}$ and $y_{2F\_gear}$ coordinates, so the analysis have to been done in its plane. In a concrete case of the cylindrical worm with arched profile in axial section and connected gear was examined.

In the case of a designed and manufactured worm with data $z_1$=3, $m$=12.5, $\gamma_0$=21°2′15″, $\rho_{ax}$=50mm, $\overline{S}_{a1}$=10 to set addendum on tooth chord, $\overline{S}_{n1} = 13^{+0.0}_{-0.125}$ size of worm tooth chord, $a$=280mm, $d_{01}$=97,5mm, $H$=117,809722mm, $z_2$=35, $F_{r1}$=±0,017, $f_{p1}$=±0,016, $f_\gamma$=±0,018, $f_f$=0,08 (Dudás I., 1991).

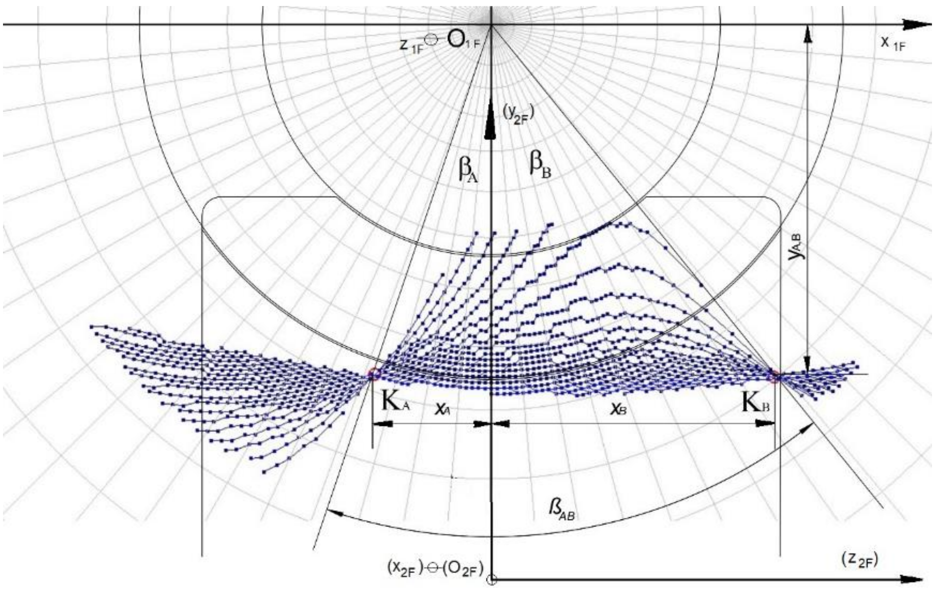


| Input: | | | Output: |
|---|---|---|---|
| $i_{21}$ =0.0857142<br>$x_2$ =1.0<br>K =69.5 mm<br>a =280.0 mm<br>$p_o$ =18.75<br>$\rho_{ax}$ =50.0 mm<br>$z_{ax}$= 0.0 mm | $d_f$ = 38.75 mm<br>$d_a$ =58.75 mm<br>$\varphi_{1Start}$= -100.0<br>$\varphi_{1Stop}$= 250.0<br>$\varphi_{1Step}$= 10.0 | $\eta_{Start}$ =35.75<br>$\eta_{Stop}$ =88.75<br>$\eta_{Step}$ =1.0<br>$\vartheta_{Start}$= -100.0<br>$\vartheta_{Stop}$ =+100.0<br>$\vartheta_{Step}$ =1.0<br>n·v<= 0.001 | $X_A$ =-20.3389<br>$X_B$ =49.3389<br>$Y_A$ =60.7890<br>$Y_B$ =60.7890<br>$\beta_A$ =18.4993<br>$\beta_B$ =38.8347<br>$\beta_{AB}$=57,3340 |

**Figure 7.** Contact lines in the plane [($x_2$), ($y_2$)] with $K_A$ and $K_B$ knots, based on a computer program developed by us

The position of the contact points on the surface of the gear is illustrated in Figure 7. The operating principle of our computer program for demonstrating the production of contact lines is that the program calculates the system of implicit equations required to start the procedure from the input data with exact mathematical background (Rontó, M. et. al., 2008). Based on the input data, the scope of the study is limited to the realistically interpretable area, so according to the boundary conditions, the search procedure calculates the contact points of the given case and then transforms the obtained point set into an ordered point group of a contact curve.

The projection in Figure 7 shows the $K_A$ and $K_B$ knots are shown, which indicate a good bearing pattern, the suitable efficiency and required considerable lifespan. In operation the worm is turning, and the knots are moving on the lines of knots. The line of knots are perpendicular position to the plane [($x_2$), ($y_2$)]. Each contact curve intersects the lines of the knots.

The spatial displacement of the contact points forming the contact lines due to the reduction of the distance between the axes can be examined in Figure 8, with respect to the limit of the required accuracy.

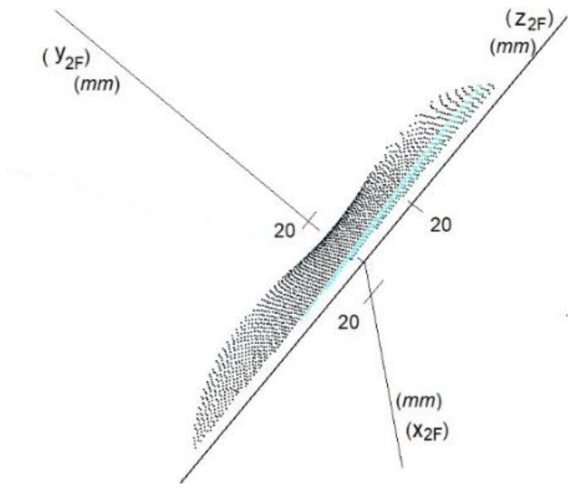


**Figure 8.** The spatial location of the gear tooth surface points in the ($K_{2F}$) coordinate system, which is parallel to the $K_{2F}$ coordinate system

In this way, the degree of re-sharpening of the hob and the distortion of the tooth surface of the wheel can be coordinated and kept within the margin of error specified by the designer.

## 4. CONCLUSIONS

The required quality of the worm gear drive pairs leads to develop the tools geometry. The unique tool that can be used for finishing machining to the gear tooth surface is the hob in the case of serial production of gears. As the hob is an expensive tool with extremely complicated geometry, it is advisable to make their re-sharpening as many times as possible. The worm gear hob created from the cylindrical worm with circle arc profile in axial section is a suitable tool machining the worm gear tooth surface. The examination of the contact area of the worm and mated gear leads to analysis of the manufacturing accuracy of the gear machined by the post-sharped and adjusted hob. Changes in geometric conditions and gear tooth surface are the result of the decrease in distance between the re-sharped hob axis and the gear axis. The spatial displacement of the contact points forming the contact lines due to the reduction of the distance between the axes can be examined for the limit of the required accuracy according to the outlined procedure. In this way, the degree of re-sharpening of the hob and the distortion of the tooth surface of the wheel can be coordinated and kept within the margin of error specified by the designer.

## REFERENCES

1. Ábel, J. and Balajti, Zs., 2018. *Examination of Tool Wear of Teeth with the Method of Descriptive Geometry*. XXVI. International Conference on Mechanical Engineering, Targu Mures, Romania. ISSN 2068-1267, pp. 12-15.

2. Balajti, Zs., 2007. *Development of production geometry of kinematical drive pairs*. PhD dissertation (in Hungarian), Miskolc, Hungary. p. 126.

3. Balajti, Zs. and Dudás, I., 2017. *The Monge Theorem and Its Application in Engineering Practice*. International Journal of Advanced Manufacturing Technology, 91. pp 739–749. DOI: 10.1007/s00170-016-9763-1.

4. Balajti, Zs. and Ábel, J., 2020. *Edge geometry test method with correctly positioned CCD cameras for production geometrical development of a worm gear hob with arched profile.* Procedia Manufacturing, 10,052,Vol 51: p. 365-372.

5. Bercsey, T. and Horák, P., 2002. *Modelling of the contact and tribological relations of spatial gear pairs.* International Conference on Gears, Munchen, Germany. ISBN 3-18-091665-6, pp. 91-105.

6. Cvetković, I. D. and Stojićević, M. D. and Stachel, H. and Milićević, R. G. and Popkonstantinović, B. D., 2019. *The Man who Invented Descriptive Geometry*. FME Transactions, 47(2). pp 331-336. DOI:10.5937/fmet1902331C.

7. Dudás I., 2004. *The Theory & Practice of Worm Gear Drives*. Kogan Page US. Sterling. USA. ISBN 1 9039 96619 9. p. 320.

8. Dudás, I., 1991. *Theory of screw surface production*. Academic doctoral dissertation, Miskolc.

9. Dudás, L., 2010. *The effect of worm profile on contact lines.* microCAD, XXIV. International Scientific Conference. Miskolc, Hungary. ISBN 978 963 661 919 0, pp. 39-44.

10. Felhő, Cs.and Szentesi, A. and Tóth, G., 2004. *Geometrical Dimensioning of Worm Drives.* Proceeding of the 11th International Conference on Tools. Miskolc, Hungary, University of Miskolc. pp. 177-182.

11. Jeli, Z. and Komatin, M. and Popkonstantinovic, B. and Regodic, M., 2012. *Usage of modern graphical presentations in development of technical systems*. 3th International Conference moNGeometrija, Novi Sad, Serbia. ISBN 978-86-7892-405-7, pp. 553-564.

12. Jr. Kral, J. and Kral, J., 2013. *Calculation of the shape of tool cutting edge for production of involute worm.* Advances in Science and Technology Research Journal. 7(17). pp. 1–5.

13. Litvin, F. L. and Fuentes, A., 1994. *Gear Geometry and Applied Theory*. Englewood Cliffs. Prentice Hall. NJ.

14. Máté, M. and Hollanda, D. and Tolvaly-Rosca, F. and Popa-Müller, I., 2013. *The localization of the contact patch by cylindrical gear having an Archimedean toothline using the method of setting the tangential displacement.* XXI. International Conference on Mechanical Engineering, Arad, Romania. ISSN 2068-1267, pp. 265-268.

15. Popkonstantinovic, B. and Stojicevic, M. and Jeli, Z. and Obradovic, M. and Dragos-Laurentiu, P., 2019. *Simulation and Motion Study of Mechanical Integrator 3D Model*. FME Transactions. 47(2). pp. 299-303. doi:10.5937/fmet1902299P.

16. Raisz, P. and Rontó, M., 2000. *Differential equations for technicians.* University of Miskolc Publishing.

17. Rontó, A. and Rontó, M., 2000. On the investigation of some boundary value problems with non-linear conditions. Miskolc Mathematical Notes, 1(1) pp. 43-55. Doi. 10.18514/MMN.2000.17.

18. Rontó, M. and Lengyelné Szilágyi, Sz., 2008. *Analysis for Program Design Informatics Students and Business Informatics Students.* Electronic note. https://www.uni-miskolc.hu/evml/database/downloads/matalap/segedletek/pr_jegyz_2008.pdf

19. Stachel, H., 2006. *Descriptive Geometry Meets Computer Vision – The Geometry of Two Images.* Journal for Geometry and Graphics. 10(2). pp. 137–153.

20. Vadászné Bognár, G., 2003. *Mathematic for IT specialists and Engineerings 2.* University Press of Miskolc, Hungary. ISBN 9636615764. p. 347.

# PARAMETRIC DESIGN AS AN APPROACH FOR DESIGNING PERSONALIZED PRODUCTS

Jelena Djokikj[1], Elena Angeleska, Tashko Rizov, Tatjana Kandikjan

Ss. Cyril and Methodius University in Skopje, Faculty of Mechanical Engineering, 1000 Skopje, Republic of North Macedonia

[1]jelena.djokikj@mf.ukim.edu.mk

***ABSTRACT***

*Parametric design (PD) and additive manufacturing (AM) form an extremely useful tool for designers liberating them from the constrains of conventional production processes. These technologies enable them to expand their creativity and generate designs with a great level of detail and differentiation. In addition, as the development of new products shifted from designing for mass production to designing for personalization, there is a constant race on the market for offering products that can be customized by the users in unique ways. The aim of this method is not only to strengthen the emotional bond with the item which results with extending the period of its use, but also to trigger grater brand attachment. Therefore, one of the most common uses of the 'PD-AM' tool is in personalization.*

*This study aims to make use of design exploration with the goal to examine principles of parametric design and apply them as a method for offering personalized products intended to be produced by AM technologies. Experimenting with shapes and techniques resulted in gaining practice with the parametric modelling process and researching options for personalization. The study suggests a simple and intuitive interface that allows users to 'play' with the parametric options changing a set of aesthetic features of the product. With this approach, users can create a wide range of solutions and all the generated designs can be different from one another.*

**Keywords:** Parametric Design; Personalization; Paneling Morph Geometry; Industrial Design; Additive Manufacturing

## 1. INTRODUCTION

Personalized design products along with the mass customized products are a must for the contemporary companies in today's consumerist society. The consumers want to distinguish themselves from others [1] and require unique and personalized products. They want a product that completely matches their personality. There is also that special feeling that the product is made just for you. In craft production, it is possible for the customer to create their own, unique product that expresses their personal tastes and preferences since all the products are custom made by someone who possess the appropriate materials, tools, and skills [2].

Product personalization refers to a process that defines or changes the appearance or functionality of a product to increase its personal relevance to an individual [3, 4]. Users need to invest mental effort to configure the product with selection of shape and color. As a result, the effect of the effort invested during the personalization process generates an emotional bond with the product. It has been shown that users will extend the period spent with this kind of product [5].

The personalization, especially in the mass production, is achievable only through parametric design. Parametric and generative design tools give the freedom in creation. Besides the freedom in creation, these software offer the users to create scripts. All possible operations and commands in CAD become part of a code that could be applied to different parts [6]. What is currently known as algorithmic, parametric or generative design software (plug-in/Add-in/…) is the platform to do such design processes in computers via CAD software [6]. Creating the 3D model parametrically allows the user to change the parameters as many times as he/she wants. Gardiner [7] describes a parametric design/model as “set up on the basis of rules and references that govern geometry and thereby provide the designer with syntax for creating an unlimited number of morphologically different versions of the same design-template”. Abdullah and Kamara [8] propose the procedures for parametric design in order to increase the idea generation in the conceptual phase. Dean [9] uses parametric and generative modelling to fully exploit the AM’s possibilities and to offer personalized products to users. The design studio Nervous Systems offers an interesting approach, by applying parametric and generative design to their products inspired by nature [10].

One element that made product personalization possible for companies and mass producers is the parametric design, but the other one is the fabrication by the additive manufacturing (AM) technologies. These technologies build the model in layers by adding material [3]. This working manner, which is completely opposite to the traditional subtractive manufacturing, offer many benefits for the designers and engineers. Some of them are freedom in creation of complex shapes, combination of different material in one go, whole assemblies build at the time and different models build on the go. All these possibilities are noteworthy for exploiting these technologies in the product personalization process.

With this paper, we are applying methodology for parametric design in order to create product personalization platform. This platform is based on parametric design, offering multiple possibilities for the users. The users can design their own products and afterwards build them using AM, making design affordable to anyone.

## 2. DESIGN EXPLORATION

### 2.1 Goal and Method

The goal of this research is to offer platform for design of personalized products. Products which allow the users to be involved in the design and fabrication phase of the whole process, rather than just being able to select from several pre-defined options, or send their preferences to the manufacturer. This kind of user involvement is one step further from the conventional personalization options, because the end-user is engaged in the creation of the product.

To achieve this goal, Rhinoceros and its visual editor Grasshopper were used, as one of the most widely used parametric design tools. The possibilities offered by this combination (Rhino and Grasshopper) provide an adequate response to AM requirements [11]. Rhino is used for modelling complex freeform shapes, while Grasshopper is utilised for additional mathematical modelling, or even programming [12]. Still, Grasshopper on its own can be used for the modelling of the whole part. Rhino offers more subtle and straightforward options for freeform creation.

The methodology that we used, underlies the methodologies for design for AM (DfAM) with addition of the parametric design [13, 14]. The parametric design is perfect for DfAM as it is working with the same logic, setting the parameters or the constrains before designing.

### 2.2 Design Application

The CAD model developed for the purpose of the research is a freeform surface with various textures applied as decoration. The combination of freeform surfaces and textures was chosen since it allows multiple possibilities for customization: defining the size, shape and flow of the surface area, as well as defining the texture type and its density.

The surface can be modified in several manners. First, the number of attractor points that define the surface orientation flow can be adjusted according to preferences (Fig.1), as well as their positions on the surface (Fig.2). This is done by a simple point movement on the MD Slider in GH. It becomes very easy to examine the effect of changing the attractor location and have the whole model update [15]. Second, the intensity of the surface curvatures can be adjusted by selecting a type of wave distribution (graph type) and adjusting the points of the graph type on the Graph Mapper in GH (Fig.3). By doing so, the surface can have literally any kind of desired shape. The surface size can also be easily adjusted by controlling x and y size sliders (Fig.4). The user can choose the desired dimensions, or this can be done in order to satisfy the technical requirements of the 3D printer used for production.

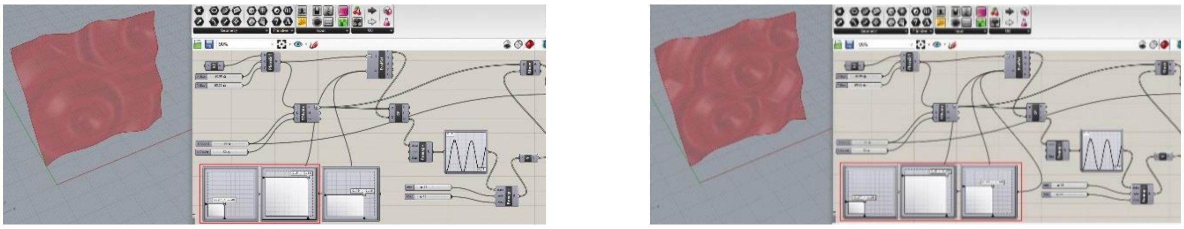

**Figure 1:** The difference between using 2 and 3 attractor points

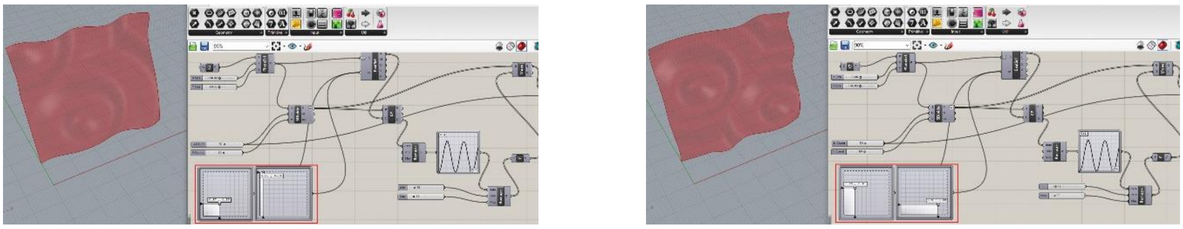

**Figure 2:** Changing the positions of attractor points

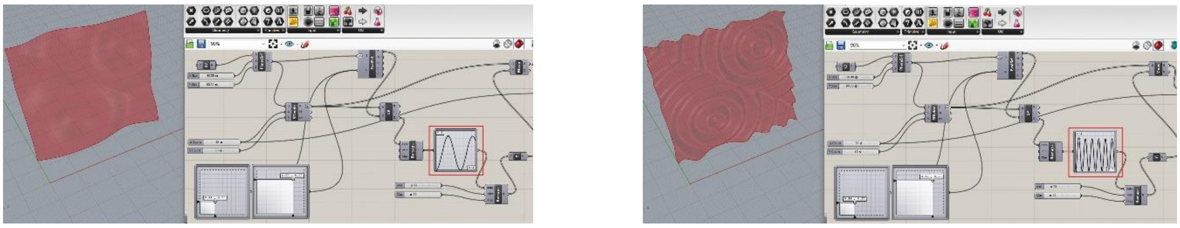

**Figure 3:** Changing the wave distribution

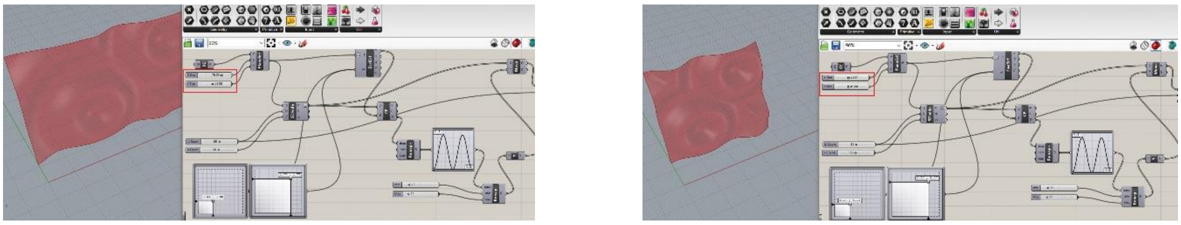

**Figure 4:** Changing the surface size

The following step was the application of textures and creating a 3D model from the surface. This was done by using the paneling tools in GH. The surface is divided in a grid (panels) out of which surface boxes are extruded (Fig.5). These boxes or cells are populated by previously modeled solid bodies – design components [15]. The final result of morphing the objects in the twisted boxes is a complex, textured, 3D, organic body (Fig.6). The thickness of the surface boxes can be adjusted using a number slider (Fig.7), and the number of cell divisions is integer defined by the designer (Fig.8).

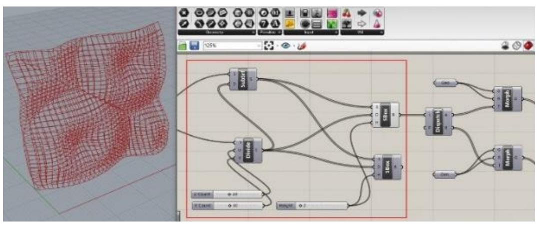

**Figure 5:** Creating surface boxes (cells)

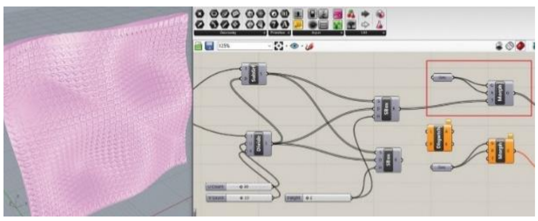

**Figure 6:** Preview of the generated design by geometry-populated cells

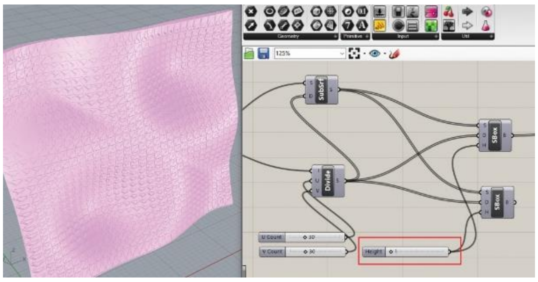

**Figure 7:** Changing the thickness of the surface boxes (cells)

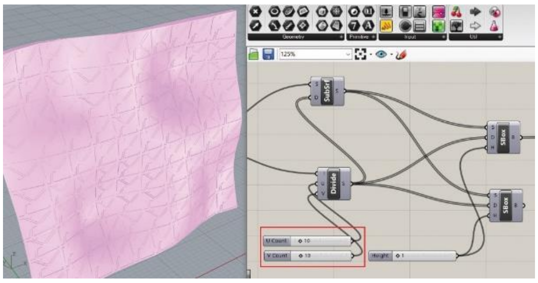

**Figure 8:** Changing the number of panels (surface box cells)

The design components that populate the cells can be chosen by the user from a provided number of models created by the designer. The designed components for this paper were modeled in SolidWorks software, exported as STL files, and then imported in Rhinoceros to be used as reference geometry for paneling. The personalization can continue by using variations of the design components (Fig.9), or using two (or more) components for the surface boxes in one model (Fig.10). This way, the final design can be more dynamic and playful.

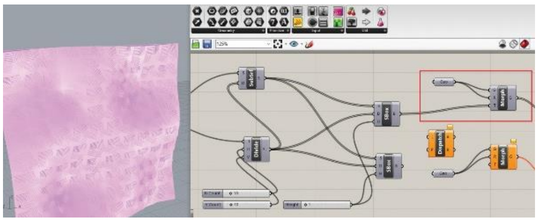

**Figure 9:** Choosing another option from the offered design components for creating the morphed geometry

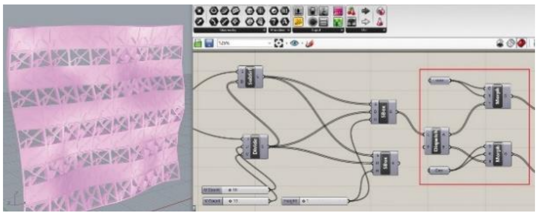

**Figure 10:** Using two types of design components for creating the morphed geometry

## 3. RESULTS & DISCUSSION

The goal of this design exploration study was to develop platform for design of personalized products. The use of parametric design software in order to design the base of the model and to offer the possibility for personalization by the user.

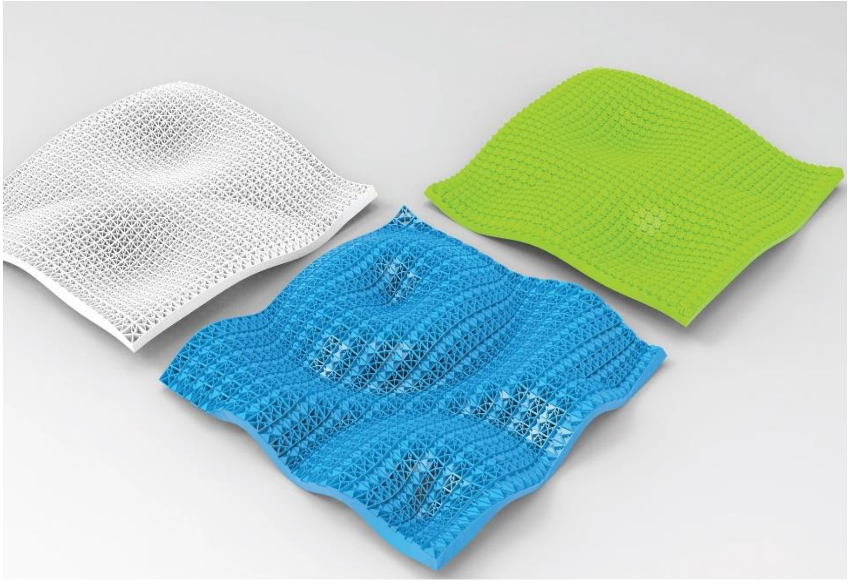

**Figure 11:** Design results due to different interface interactions

The simple manipulation of slider buttons with pre-defined maximum and minimum values is used as an interactive interface and it allows users that are not experts in 3D modeling or AM to develop their own creations. Several GH tools were used to simulate the interactive interface. The two number sliders for adjusting the surface size are an input in the surface division component and define the number of surface segments in the u and v directions. The multidimensional sliders are used as an input to evaluate the local surface properties at the UV coordinates (attractor points) defined by the MD slider positions. The graph mapper slider is used to define the surface flow. Two more number sliders that are an input in the number of u and v segments of the divide domain component are used to define the number of panels the surface will have. The number slider that is an input in the surface box can be changed in order to adjust the height of the surface boxes (panels) that will be filled with design elements. The geometry components are elements that will fill those surface boxes and they can be easily defined by selecting from an offer of CAD models. Right clicking on the geometry component on the GH interface and selecting one given CAD model will distribute that model in the defined number of surface boxes. If desired, several different geometry items can be used in order for the panel rows to vary. The strong aspect of this type of interface is not only the easy manipulation of slider components, but also in the option to limit the set of values the sliders offer and define them according to the technical requirements of the AM technology that will be used. This way, the designer can limit the interface options and make sure that it will be possible to produce the item regardless of the type of adjustments made by the user in the personalization process.

The final generated appearances are shown on the image below (Fig.11). However, by defining a different surface shape, this approach can be used for various types of products that can be personalized.

This personalization is feasible with the AM processes. We fabricated scaled samples of the personalized design (Fig.12). For the fabrication Creality Ender 3 machine was used with PLA (Polylactic acid) as build material.

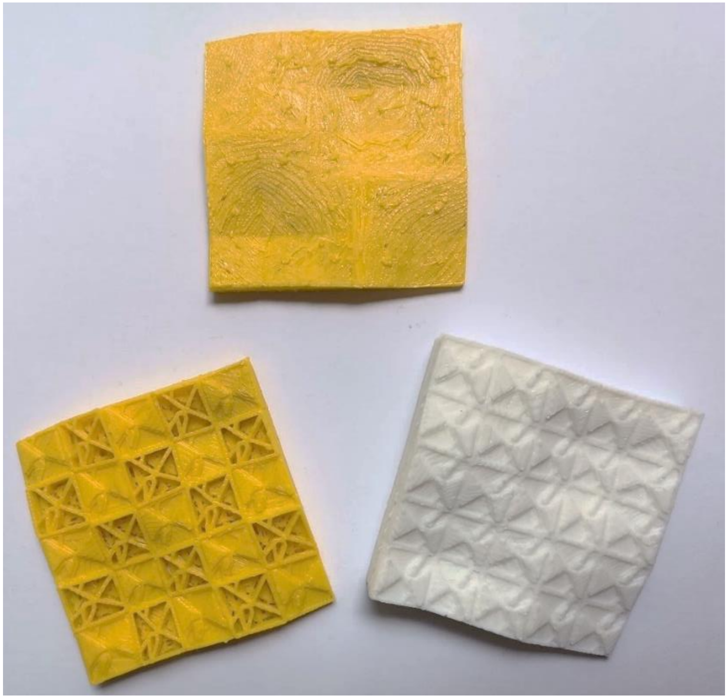

**Figure 12** Fabricated samples

Consequently, it is evident that there is a significant freedom in the customization of the end design. In this design exploration case, the surface can be produced as a decorative bowl, jewelry, or decorations for textile.

## 4. CONCLUSION

The use of parametric 3D modelling is ideal for satisfying the customer demand for unique products due to the fact that it enables the user to change the inputs as many times as he/she wants. Parametric design combined with AM can provide the possibility for users to embody their personality traits in the attributes of the products they use and thus strengthen the emotional bond with those products (and the brand).

The use of Rhinoceros and Grasshopper proved to be very beneficial for exploring the possibilities of engaging users in the creation of design solutions. The developed design variations showed several methods by which the products aesthetics can be changed parametrically.

In addition, the process should continue by using the GH data for developing a user-interface (UI) in the form of a control window that provides a simplified overview of the adjustment options and a graphical representation of the product that demonstrates the changes made in the control options in real time. This UI should then be evaluated by users in order to improve it.

**REFERENCES**


1. Jensen, R.: The Dream Society: Hot the coming shift from information to imagination will transform your business. New York, McGraw-Hill (1999).
2. Vink, N.Y.: Customization Choices: Consumer Product Decisions in Mass Customization Environments. Doctoral dissertation, TU Delft, Delft University of Technology (2003).
3. Gebhardt, A.: Understanding Additive Manufacturing – Rapid prototyping – Rapid Tooling – Rapid Manufacturing. Carl Hanser, München (2012).
4. Blom, J.: Personalization: A Taxonomy. CHI’00 Extended Abstracts on Human factors in Computing Systems. ACM, New York (2000).
5. Mugge, R., Schoormans, J.P. and Schifferstein, H.N.: Emotional bonding with personalised products. Journal of Engineering Design, 20(5), pp.467-476 (2009).
6. Kabazi, Z.: Generative Algorithms. In: Micevska, J. and Kandikjan, T.: Personalization in Design through New Technological Achievements. South East European Journal of Architecture and Design, 2016, pp.1-5 (2016).
7. Gardiner, J.:Exploring the emerging design territory of construction 3D printing-project led architectural research. Doctoral dissertation, Architecture and Design, RMIT University (2011).
8. Abdullah, H.K., Kamara, J.M.: Parametric design procedures: A new approach to generative-form in the conceptual design phase. In AEI 2013: Building Solutions for Architectural Engineering, pp. 334-343 (2013).
9. Dean, L.T.: Future factories: The application of random mutation to three-dimensional design. Doctoral dissertation. The University of Huddersfield. (2009).
10. Nervous System, I.: Nervous System. https://n-e-r-v-o-u-s.com [Accessed: 10th December 2019].
11. Akos, G., Parsons, R.: Foundations: The Grasshopper primer third edition. Modelab (2014).
12. Khabazi, M.:Algorithmic modelling with Grasshopper (Vol.1). Bukupedia (2009).
13. Djokikj, J. and Kandikjan, T.: Parametric Design as an approach for Design for Additive Manufacturing. Book of Abstracts of 7th International Symposium on Geometry and Graphics - moNGeometrija 2020 (2020).
14. Djokikj, J. and Kandikjan, T.: Methodology for integrating Parametric Design in the Design for Additive Manufacturing. IETI Transactions on Engineering Research and Practice 4(2), pp.10-16. DOI: 10.6723/TERP.202012_4(2).0002 (2020).
15. Issa, R.: Essential Mathematics for computational design. Lulu. com. http://blog.rhino3d.com/2013/11/the-essential-mathematics-third-edition.html [Accessed: 10th February 2021] (2010)

# ROBOT WELDING PATH PLANNING BASED ON GRAPHICAL COMPUTING

Pengfei Zheng[1,2], Xujiang Yu[1], Yongfei Chen[3], Zhubing Sun[3]

[1]Yiwu Industrial & Commercial College, School of Mechanical Information, 322000 Yiwu, China

[2]East China University of Science and Technology, School of Mechanical and Power Engineering, 200237 Shanghai, China

[3]Zhejiang Linix Motor Co., Ltd, 322118 Dongyang, China

pfzheng@126.com

***ABSTRACT***

*As a classic problem in artificial intelligence research, robot welding path planning has been extensively studied. Related scholars have also proposed many solutions, such as heuristic algorithm, neural network, genetic simulated annealing algorithm, improved genetic algorithm, etc. But there are still deficiencies in welding torch posture, welding position, and robot motion stability. Because of the characteristics of the welding seam have a vital influence on the path planning of the welding robot, it is also the basis for ensuring the welding accuracy. From the perspective of graphic calculation, the graphical computing method of precise welds is analyzed, the point cloud graphics of the welded parts are used to calculate the overlap of primitives, and the accurate and rapid extraction of weld features are realized by changing the graphic representation of the welded parts model. According to the connection characteristics of the weldment, the characteristics of the weldment are collected, and a simple, fast, and more versatile method for extracting and calculating weld features is designed, and the weld features are discretized. Discrete weld feature points are used as the basis for path planning of the welding robot to carry out reasonable welding path planning, which reduces the manual teaching process and workload. Finally, a robot welding path planning method based on graphical computing is proposed, and corresponding simulation experiments are carried out.*

**Keywords:** Graphical computing; Point cloud; Welding robot; Path planning

## 1. INTRODUCTION

Welding is an indispensable surface forming technique in modern industrial high quality and efficient manufacturing technology. It is a method of bonding workpieces by heat or pressure or both, and with or without filler material. In essence, it is a processing method in which metal atoms on two separated solid surfaces are brought close to the lattice distance (0.3-0.5 mm) by a suitable physicochemical process to form a metal bond, thus achieving a permanent connection. Its advantages include easy forming, low production cost, adaptability, material saving, high structural strength, good sealing, and easy automation, especially in auto body processing, the use of industrial robots for automatic welding of body is the most typical application.

In welding production, there are many types of components, variable types of welds and complex spatial distribution, and these characteristics make it much more difficult to automate welding using robots. In robotic welding technology, the proper planning of the welding path is crucial. Welding path planning, as a classical problem in artificial intelligence research, has been extensively studied by many scholars and corresponding planning algorithms have been proposed, such as artificial potential field method, genetic algorithm, simulated annealing algorithm, etc. [1]-[8]. In addition, the use of manual instruction for welding path planning is also more common, but the manual instruction method is time-consuming and the accuracy is difficult to guarantee. Therefore, a graphical computing-based robot welding path planning method is proposed in this paper from a graphical perspective and simulated in the RobotStudio environment. Finally, based on the simulation, the OTC FD-B6 welding robot is used for the corresponding example welding test, and the test verifies the effectiveness of the method for robot welding path planning.

## 2. GRAPHICAL REPRESENTATION OF WELDING PROBLEMS

In general, the welding process of any component can be abstracted as a number of three-dimensional graphics connection problem, the weld is the spatial intersection of these three-dimensional graphics. As shown in Figure 1, where (a) is the welding model of a tee pipe; (b) is the welding assembly diagram of a complex box. It is obvious that the welds are all intersecting curves of each component in the assembly attitude. Therefore, the problem of calculating the weld curve is essentially a graphical problem, and the graphical calculation can be used to find the exact weld curve. In welding robot path planning, the teaching method is based on curve fitting of several manually collected feature points to obtain the welding trajectory curve. Obviously, the more feature points collected, the more accurate and time-consuming the welding trajectory curve is. Based on this need, a discrete representation of the weld profile is used to plan the weld path.

(a) Welding diagram of tee pipe

(b) Welding assembly diagram of complex box

**Figure 1:** Weld seam characteristics in welded assemblies

## 3. GRAPHICAL CALCULATION METHOD OF THE WELD PATH

### 3.1 Parametric calculation method of the weld curve

#### 3.1.1 Establishment of the geometric model of the weld curve

The process of building the geometric model is illustrated by taking the example of a cylindrical tube docked with a flat plate. As shown in Figure 2, the projection of the cylindrical tube and the flat panel buttress is shown, and the full section of the cylindrical tube is performed. As can be seen from the figure, the left half of the cylindrical tube has the inner skin in contact with the surface of the flat plate, and the right half has the outer skin in contact with the surface of the flat plate. At the plain lines $aa_1$ and $bb_1$ of the interface surface, the inner and outer skins of the cylindrical tube are in contact with the flat surface at the same time.

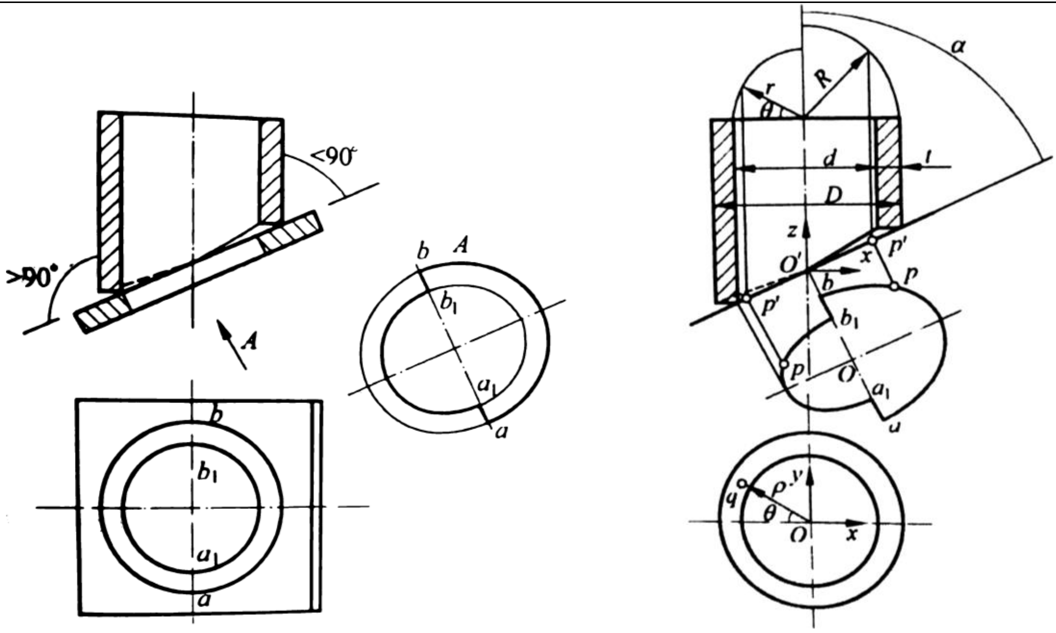


(a) Cylindrical tube butted against a flat plate (b) Geometric intersection diagram

**Figure. 2:** Mathematical model of the docking of cylindrical tube and flat plate

### 3.1.2 Establishment of mathematical model of weld curve

The mathematical model for solving the docking of a cylindrical tube to a flat plate is shown in Figure 2. The dimensions of the structure are known to be $D$, $t$ and $a$, $d = D - 2t$, $r = \frac{d}{2}$, $R = \frac{D}{2} = r + t$。Taking any point $p$, on the interface curve, it can be seen from figure 2 that, $x_p = -r\cos\theta$, $y_p = r\sin\theta$.Because, $\frac{r\cos\theta}{-z_p} = \tan\alpha$, therefore, $z_p = -\frac{r\cos\theta}{\tan\alpha}$.

Thus, the coordinates of the point on the interface curve are:

$$\begin{cases} x_p = -r\cos\theta \\ y_p = r\sin\theta \\ z_p = -\dfrac{r\cos\theta}{\tan\alpha} \end{cases} \qquad \text{(Eq.1)}$$

Where, the values of $\theta$ are: $0 \le \theta \le \frac{\pi}{2}$ and $\frac{3\pi}{2} \le \theta \le 2\pi$ .

According to equation (Eq. 1), the coordinates of the point $p$ on the epithelial interface curve can be obtained as:

$$\begin{cases} x_p = -R\cos\theta \\ y_p = R\sin\theta \\ z_p = -\dfrac{R\cos\theta}{\tan\alpha} \end{cases} \quad \text{(Eq.2)}$$

Where, the values of $\theta$ is: $\frac{\pi}{2} \le \theta \le \frac{3\pi}{2}$.

If $Q$ is any point on the interface surface and $\rho$ is the distance from that point to the axis, for the left half of the interface surface, it have:

$$\begin{cases} x_q = -\rho\cos\theta \\ y_q = \rho\sin\theta \\ z_q = -\dfrac{\rho\cos\theta}{\tan\alpha} \end{cases} \quad \text{(Eq.3)}$$

Where, the values of $\rho$ is: $r \le \rho \le R$, the values of $\theta$ is: $0 \le \theta \le \frac{\pi}{2}$ and $\frac{3\pi}{2} \le \theta \le 2\pi$.

Similarly, for the right half of the interface surface, it have:

$$\begin{cases} x_q = -\rho\cos\theta \\ y_q = \rho\sin\theta \\ z_q = -\dfrac{R\cos\theta}{\tan\alpha} \end{cases} \quad \text{(Eq.4)}$$

Where, the values of $\rho$ is: $r \le \rho \le R$, the values of $\theta$ is: $\frac{\pi}{2} \le \theta \le \frac{3\pi}{2}$.

### 3.2 General calculation method of weld curve

In order to further reduce the computational complexity of the weld curve, a reduced dimensional intersection calculation method of the geometry is proposed. As shown in Figure 3, the point cloud model of the welded part is collected using 3D digital scanning technology, and the point cloud data of the intersection area is approximated to find the mean value.

If point $P_i$ of weld 1 and point $P_j$ of weld 2 satisfy $\mathrm{dis}(P_i, P_j) \le \delta$, where $\delta$ is the preset accuracy value, then the point $P_{c(x,y)} = (P_{i(x,y)} + P_{j(x,y)})/2$ on their intersection curve. These discrete points are the feature points on the weld curve, similar to the manually taught path points. Since these weld curve characteristic points are obtained by graphical calculation method, the number of points is high and the calculation process is simple. In contrast, the graphical calculation method for path planning of the welding robot saves a lot of manual demonstration time and also improves the accuracy of the welding path. A detailed description of this generic calculation method for weld profiles can be found in the literature [9].

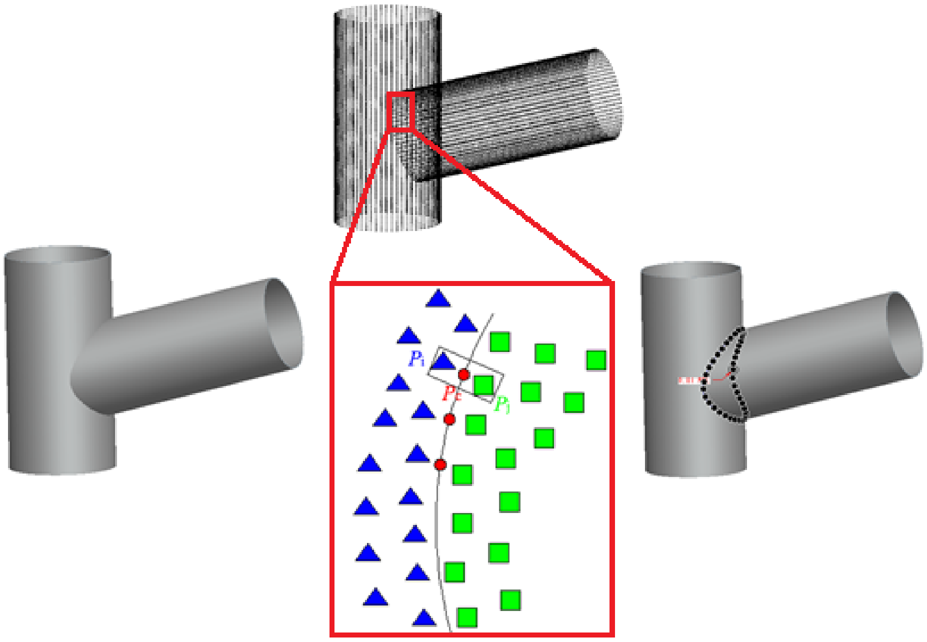


**Figure 3:** General calculation model of weld curve

## 4 EXAMPLE VERIFICATION

### 4.1 Calculation of the welding path for unequal diameter pipes

The following is an example of the unfolding correction calculation for two circular pipes with a spatially curved weld. As shown in Figure 4, a welding case of two round tubes of unequal diameters, intersecting at a 55° angle. Where, (a) is the 3D model of the intersection of the fittings; (b) is the actual interface surface of the two fittings obtained by the surface intersection method; (c) is the calculation of the neutral layer curve by the interface surface, and the red bolded curve in the figure is the neutral layer curve.

In order to further verify the effect of the unfolding correction method on the promotion of welding quality, the industrial robot offline programming software RobotStudio is used to simulate and verify the welding path, and the collision detection function in the software is used to monitor the collision of the entire welding process of the robot to ensure that no collision occurs during the entire welding process. Therefore, the above-mentioned welding path can generate the corresponding Rapid program, which can be imported into the welding robot control cabinet to be programmed on site.

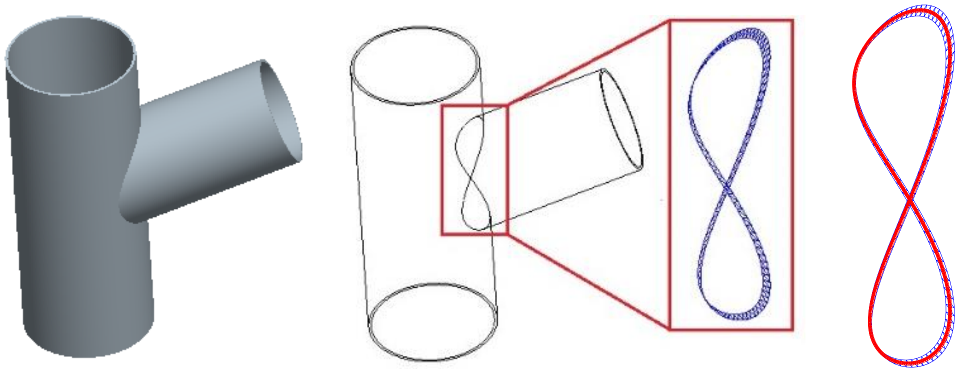

(a) Three-dimensional model of the intersection of the tubes (b) Theoretical intersection curve. (c) Neutral layer intersection curve.

**Figure 4:** Arbitrary fillet butt welding of unequal diameter circular pipe parts.

### 4.2 Weld test of unequal diameter pipe

In order to more intuitively verify the rationality of the welding path calculation method proposed in this paper, the OTC FD-B6 welding robot is now used to physically weld the unequal diameter pipe weldments in Figure 4. As shown in Figure 5, the size of welded parts: the diameter of pipe 1 is 50 mm, the wall thickness is 4 mm; the diameter of pipe 2 is 40 mm, the wall thickness is 4 mm; two pipes fittings are 55 ° intersecting connection, the joint surface using V-bevel design. The relevant welding parameters are as follows: welding current is 150A; voltage is 17V; welding speed is 25mm/s; welding wire type is ER50-6.

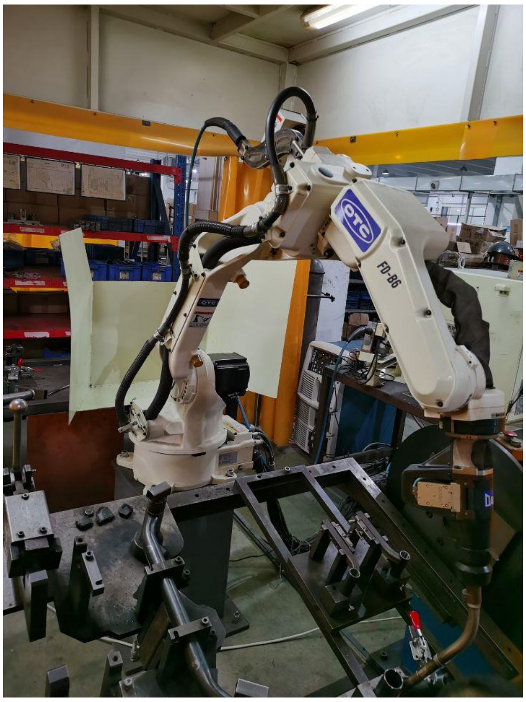


(a) Welding robot.

(b) Tooling turntable.

**Figure 5:** Welding robot welding example.

In order to facilitate comparative testing, this example uses two sets of round pipe parts of the same material and size combination, choose the same welding parameters for welding and forming. As shown in Figure 6, the automatic welding results obtained by using the manual teach-in method for welding path planning can be seen from the two different poses of the tube forming (a) and (b): the residual height of the weld is obvious and the quality of the weld is poor. As shown in Figure 7, the automatic welding results obtained by using the graphical calculation method for weld path planning can be found from its two different poses (a) and (b): the weld residual height is better and the weld quality is also significantly better than that of the teach-in method.

(a) Attitude 1 (b) Attitude 2

**Figure 6:** Example of welding by manual demonstration method.

(a) Attitude 1 (b) Attitude 2

**Figure 7:** Example of welding by this method.

## 5 CONCLUSION

A graphical computational method of the robot welding path planning problem is studied, which abstracts the welding path planning as a surface intersection problem of the welded parts. Using the advantages of the three-dimensional point cloud model, the high-dimensional calculation of complex three-dimensional graphics is simplified to the one-dimensional calculation of geometric elements, which greatly reduces the complexity of the calculation, reduces the time for manual demonstration of the planning path, avoids the chance of random errors easily generated by the manual demonstration method, and improves the accuracy of the welding path calculation. Combined with the industrial robot off-line programming software RobotStudio for welding path planning, and the welding of unequal diameter pressure pipes as an example was experimentally verified. The test results show that: the welding process is smooth, no collision phenomenon, good quality weld forming, no weld collapse, weld through, edge biting and other phenomena occur, the proposed welding path calculation method can effectively improve the accuracy of welding forming.

**FUNDING**

This study was supported by the Domestic Visiting Engineers Project of Zhejiang Education Department in 2020, China (Grant No.FG2020196).

**REFERENCES**

1. Xuewu Wang, Yixin Yan, Xingsheng Gu. Spot welding robot path planning using intelligent algorithm [J].Journal of Manufacturing Processes, 2019(42):1-10.

2. Jiansheng Zhang, Qiuyun Wang, Guiqian Xiao, et al. Filling Path Planning and Polygon Operations for Wire Arc Additive Manufacturing Process [J].Mathematical Problems in Engineering, 2021(2021):6683319.

3. Peng Zhou, Rui Peng, Maggie Xu, et al. Path Planning With Automatic Seam Extraction Over Point Cloud Models for Robotic Arc Welding[J].IEEE ROBOTICS AND AUTOMATION LETTERS,2021,3(6):5002-5009.

4. Tao Wang, Zhilong Xue, Xiaoqing Dong, et al. Autonomous Intelligent Planning Method for Welding Path of Complex Ship Components [J]. Robotica, 2012(39):428-437.

5. HC Fang,SK Ong,AYC Nee. Robot path planning optimization for welding complex joints [J].Int J Adv Manuf Technol, 2017(90):3829-3839.

6. Yan Liu, Xincheng Tian. Robot path planning with two-axis positioner for non-ideal sphere-pipe joint welding based on laser scanning [J].The International Journal of Advanced Manufacturing Technology,2019(105):1295-1310.

7. H. Ghariblu, M. Shahabi. Path Planning of Complex Pipe Joints Welding with Redundant Robotic Systems [J]. Robotica, 2019(37):1020-1032.

8. Xinyu Zhou, Qingjie Zhao, Dongxu Zhang. Discrete Fireworks Algorithm for Welding Robot Path Planning [J].Journal of Physics, 2019(1267):012003.

9. Pengfei Zheng, Qing Liu, Dajun Lin, et al. An Algorithm for Computing Intersection of Complex Surface Parts and Its Application [J].IEEE, 2019:304-310.

# INTERPRETING PARAMETRIC-BIOMIMICRY DESIGN FROM CAD TO BIM SOFTWARE: DIGITAL MODELLING BASED ON A SKETCH OF NANDI FLAME

Biljana S. Jović[1,*], Aleksandar Čučaković[2], Anđela D. Mitić[1], Vesna Golubović Ćurguz[1] and Benjamin Chemarum[1]

[1] Department of Landscape Architecture and Horticulture, Faculty of Forestry, University of Belgrade, Belgrade, Serbia

[2] Department of Mathematics, Physics and Descriptive Geometry, Faculty of Civil Engineering, University of Belgrade

* Corresponding author: biljana.jovic@sfb.bg.ac.rs

**ABSTRACT**

*This research represents an application of two digital modelling softwares, first digital modelling software, chosen as representative of Computer-Aided Design – CAD modelling tool was Fusion 360. The representative of Building Information Modelling (BIM) as second digital modelling software was ArchiCAD. The aim of the research was to translate the same parametric-biomimicry design methodology used in CAD process modelling into BIM environment. African species Spathodea campanulata P. Beauv, whose common name in Kenya is Nandi flame, has been selected for the purpose of this digital modelling processes. As one of the most spectacular flowering plants, Nandi flame is indigenous to the tropical dry forests in Kenya. The decorative flower of this species was the basic model, more precisely the botanical sketches of the flower. This sketches were implemented into digital modelling softwares and used for parametric modelling. The results of this processes were represented as urban models or installations (landscape-architectural elements) in open space. This approach of digitally generating conceptual solutions from nature elements has capability to boost the formulation of new creative inventions in the different fields. The unique geometric patterns found in the flower of Spathodea campanulata P. Beauv served as a good example of how we may transform these ideas into actual design installations– using CAD or BIM software tools. This research has been carried out with the aim to find the position of BIM tools in parametric-biomimicry design.*

**Keywords:** Parametric-biomimicry design; Computer-Aided Design (CAD); Building Information Modelling (BIM); digital modelling; Spathodea campanulata P. Beauv (Nandi flame)

## 1. INTRODUCTION

Nature is an inexhaustible inspiration resource for any design profession and also for various other fields like medicine or engineering. In areas of art and design, nature patterns are recognized as a forms of visual harmony and they are studied primarily through different geometrical principles and models. The frequency of their repetition is characterized by the nature patterns itself, but each pattern is inclined to changes and modifications in order to achieve the flexibility. This is why results and solutions, obtained from nature patterns, are sustainable and timeless. Famous examples of nature patterns can be recognized in DNA structure, nervure of the leaf or interesting print of the bodies of some animals. Nature’s geometric patterns (often seen in flowers, leaves, forms and colors in nature) may be one of the first natural rules which are recognizable.

The integration of natural patterns into design processes and methods could be achieved with the help of different digital tools. With advances in using different digital softwares based on parametric modelling, the uses of various nature patterns were enabled. This method of using different nature patterns found in our environment in modelling process to acquire different results and solutions is known as biomimicry approach. Biomimicry, as the name says, means imitating different nature elements (form, structure, process, function) in process of gaining the desired result.

This research looks into a two examples of the boundless potentials which geometric patterns in nature may offer to us, as a source of inspiration for applying biomimicry approach in landscape architectural design projects. The different ideas obtained from nature could be best explored through digital modelling. Though the biomimicry design approach we may mimic either the natural forms in nature, the natural processes in nature, or the natural ecosystems in nature. In this research the mimicry was focused on natural forms found in nature, specifically from the spectacular flame-like flower and the simply beautiful seeds of the African species *Spathodea campanulata* P. Beauv, whose common name in Kenya is Nandi flame. The unique geometric patterns found in the flower and other plant parts (heart shaped seed) of *Spathodea campanulata* P. Beauv served as a simple and good example of how we may transform these nature forms into actual design solutions of varying complexities in landscape architecture design. This approach of digitally generating conceptual solutions for the design of various landscape-architectural elements represents original and very interesting way of representing various nature elements and integrate them into urban environments, it is a new creative invention in the field of landscape architecture. The research was carried out with the aim to find and observe what new digital tools could be used with regard of applying biomimicry in landscape architecture field.

## 2. BIOMIMICRY AND PARAMETRIC MODELLING

Natural patterns organize and define different relations in nature. They include symmetries, trees, spirals, meanders, waves, foams, tessellations, cracks, stripes and many different occurrences. Visual patterns in nature could find explanations in different forms like- chaos theory, fractals, logarithmic spirals, topology and other geometrical patterns. Imitating nature patterns – mimesis, could be seen first from the Platonic forms. The most perfect forms were considered to be the sphere, the circle, the cube and the square. And these initial bases were considered as basic for all other forms and structures. That could also be seen and in the use in landscape design process [1].

Biomimicry, as a process of imitating different levels of nature, finds its starting point in three bases: natural forms, processes, and ecosystems [2, 3]. Biomimicry is basically a design that is inspired by nature [4]. Biomimicry is an approach that seeks for sustainable solutions to human challenges by imitating natural patterns and strategies. Biomimicry, also known as biomimetic, refers to the direct exploration of nature, its organisms, ecosystems and processes in order to find inspiration and proper base models for solving anthropogenic problems. This type of approach was used to create the first flying machine, inspired by eagles and owls. This paved the way for complex technologies such as jets and airplanes. Biomimicry offers an understanding of how life works and where we fit in, so we could understand better how we should construct our environment. It is a practice that learns from and mimics the strategies used by all plant and animal species [5–9].

*"Nature never relies on just one solution. Complexity and diversity are essential for flexibility. Diversity is built into nature to provide opportunities, and complexity provides many ways to get there.*"
(Macnab, M. 2012) [5].

By creating and designing different elements and models based on biological materials or processes (nature patterns), we could find ad see a possible balance and harmony with nature. The various designs, that are present in nature, are elegant, biodegradable and durable, and these are the characteristics that we seek for, in order to create better sustainable world. Biomimicry is the practice of looking to nature for inspiration to solve different problems in our urban environment. Circularity, sustainability and regenerative designs and solutions— they all represents the design models that could become some very significant elements for restoring air, water, and soil instead of degrading them [10–14].

Nature patterns can be integrated into design with the use of different digital technologies-softwares. Modelling represents a creative process in which we could create a desired model of our imagination. Softwares based on parametric modeling are using different parameters and defined values of selected parameters to describe the model. Parametric models, as a results of parametric modelling process, are easy and flexible to operate with. They become new mediums of experience and exploration of endless possibilities of modelling of nature patterns. These access of changing parameters represents form finding design process of exploring the nature of parametric modelling [15, 16].

Parametric modelling has become an integral part of the landscape-architectural design process. It contributes to design process as the process becomes more interactive, complex and with innovative results. Designing according to natural patterns seeks to use the properties of living structures, forms and natural processes. Parametric modelling is the appropriate geometric tool for reading, generating and modelling of natural patterns and converting them into the desired structures and elements that could be presented in the physical world [17–19].

## 3. METHODS

The methods of this research included exploration of biological material or selected plant species *Spathodea campanulata* P. Beauv (Nandi flame), generation of a geometric pattern through two different digital softwares: *Fusion 360* (CAD software type) and *ArchiCAD* (BIM software type) using the same parametric-biomimicry design methodology, and modeling the desired urban 3D models. The aim of this research was to obtain ideas from geometric patterns present in *Spathodea campanulata* P. Beauv species, and to use them to come up with innovative and unique design solutions in the field of landscape architecture.

### 3.1 Parametric-Biomimicry Design Methodology

The biomimetic approach consists of 3 basic steps: biological (selecting proper model form of nature), geometric (generate geometric form in computer environment) and technical (physically represent the 3D model by using 3D printing methods or some other designing methods).

For the biological step, it is important to choose a proper base model from nature. For this research, selected plant species was *Spathodea campanulata* P. Beauv, widely known as Nandi flame. Geometric analysis in this research focuses on a geometric patterns of selected plant species. By applying a separate geometric pattern of the selected plant species to the geometry of conceptual landscape/urban design elements, original solutions were proposed. Initial sketch of flower and some other parts like seeds of *Spathodea campatulata* P. Beauv. was used as conceptual model for designing landscape architectural elements like bench and bench-fountain. Inspired by the geometric structure of the flower of Nandi Flame, the outside form of the flower was drawn and scanned so it could be used in adequate software for parametric modelling—like ArchiCAD and Fusion 360. Modelling process, as main part of geometrical analysis, allows to automatically generate heights, sections and 3D views based on scanned sketch which was imported, by using basic computational drawing tools. When creating objects and details that are multi-store and multi-layered, like in this research, minor flaws in the design were simply corrected through a 3D viewer, which makes this tool perfect for use in finding possible errors. In this research, the main focus was on 2 basic steps of biomimetic approach: biological – finding proper plant species and generate adequate base for further step, and geometric – use of parametric modelling approach. This two steps made the parametric-biomimicry design methodology of this research.

### 3.2 Biological Step - Sketch of Nandi Flame (*Spathodea campanulata* P. Beauv.)

African species *Spathodea campanulata* P. Beauv, whose common name in Kenya is Nandi Flame (Fig. 1), has been selected for this research. Nandi Flame is an indigenous specie in Kenya, with very decorative flame-like flower which represented basic model for the design of 3D models in this research.

*Spathodea campanulata* P. Beauv. is one of the most spectacular flowering plants that is indigenous to the tropical dry forests of West Africa. Belongs to the family Bignoniaceae and the order is Lamiales. The plant is popularly known as the fountain tree, the African tulip tree or the Nandi Flame [20-23]. The flowers bloom in great abundance and at such time the tree can be seen from a great distance. It is widespread in the tropics in large gardens and parks and has numerous healing properties. This woody species is rarely affected by diseases or pests, but can temporarily shed its leaves during periods of severe drought. In landscape architecture of this type of plant is recommended as a shade tree for parks and yards. It is also valuable as a barrier plant or a wind breaker. This species, either planted or growing naturally, is often used for hedges. Parts of this plant species are used for food, medicine and various products that are used typically. It is planted during afforestation, for soil protection and as a plantation crop for the production of plywood. This specie is native to Angola, Ethiopia, Kenya, Sudan, Tanzania, Uganda and Zambia. In

Kenya, Nandi Flame is concentrated in Western and Central parts of the country [24]. The African tulip tree is an evergreen or semi-deciduous tree with a dense, bushy oval crown. This tree can grow from 10 to 35 meters in height.

**Figure 1:** Decorative tree of Nandi Flame (*Spathodea campanulata* P. Beauv.). Source: https://tropical.theferns.info/viewtropical.php?id=Spathodea+campanulata


(a) (b)

**Figure 2:** (a) Flower Source: Brayan David and (b) Heart shaped seeds Source: https://keyserver.lucidcentral.org/weeds/data/media/Html/spathodea_campanulata.htm

Description of some plant parts used in this research: The leaves grow about one to two meters and have a bronze color. Horn-shaped buds, which appear in large clusters, are formed on the tops of the branches. The lowest layers of buds become red-orange (in some varieties yellow) bell-shaped like tulips. The leaves are deciduous, opposite leaflets, with 13–17 elliptical lamina. The large, compound leaves are dark green on the upper surface, and lighter below. On the stems the leaves are opposite. The leaves are bright green and pinnately arranged with an odd number of elliptical leaves. As invasive species, reproduces aggressively and creates winged seeds that are scattered by wind and water. Fruit, in the form of pods, are capsules, spears or in the shape of a boat on thick stems. Large about 75 cm elliptical pods are held upright, full of winged seeds that are easily scattered by the wind. The flowers are accompanied by an upright, brown, ship-shaped spear, up to 25 cm long, within which are woody seed capsules with paper, winged, wind-scattered seeds [25, 26]. The most spectacular element of this specie is its flower. The flowers of Nandi Flame grow about 10 centimeters long. The tree blooms all year round (flowering period: from March to December), but the peak of the flowering season is spring. The flower is a hermaphrodite, in the shape of a bell, claw-shaped with wrinkled orange-red to crimson-yellow petals, with 4 pale yellow anthers and dark brown anthers (Fig. 2). Horn-shaped buds, which appear in large clusters, are formed on the tops of the branches. The lowest layers of buds become red-orange (in some varieties yellow) bell-shaped like tulips. Large flowers are grouped in large clusters.

### 3.3 CAD Modelling Process

The CAD modelling process of this research represents the parametric design methodology based on biomimetic approach. The biomimetic approach and its integration into parametric modelling process with help of different digital softwares, mostly CAD types of softwares, was analyzed in some previous researches. The biological step of this research methodology was included process of selecting proper model from nature, which was very decorative plant species Nandi Flame (*Spathodea campanulata* P. Beauv.). The geometrical step was included parametric modelling process in Online based CAD software – *Fusion 360*.

Fusion 360 is a CAD / CAM tool based on the principle that combines modeling of organic shapes, mechanical design and production in one comprehensive software package. In this digital software, one can easily master how to realize an idea, by moving on to modeling parts and assembly, and as a last step, creating, rendering and preparing for use on a CNC machine or 3D printer. Some of the advantages of this online based software are removing barriers to interacting with team members and get back to creating innovative design models and products, designing using intuitive parametric, freeform, direct, and surface modeling tools, and reducing the impact of design changes and ensure manufacturability of the models with rapid prototyping tools all in one digital software. The basic tools of this software, in 3D Design and Modeling field, could be grouped in few groups: sketching, direct modelling, surface modelling, parametric modelling, mesh modelling, freeform modelling, and for the end rendering and design integration. This software is good also for data management field, team collaboration, additive manufacturing, generative design and simulation.

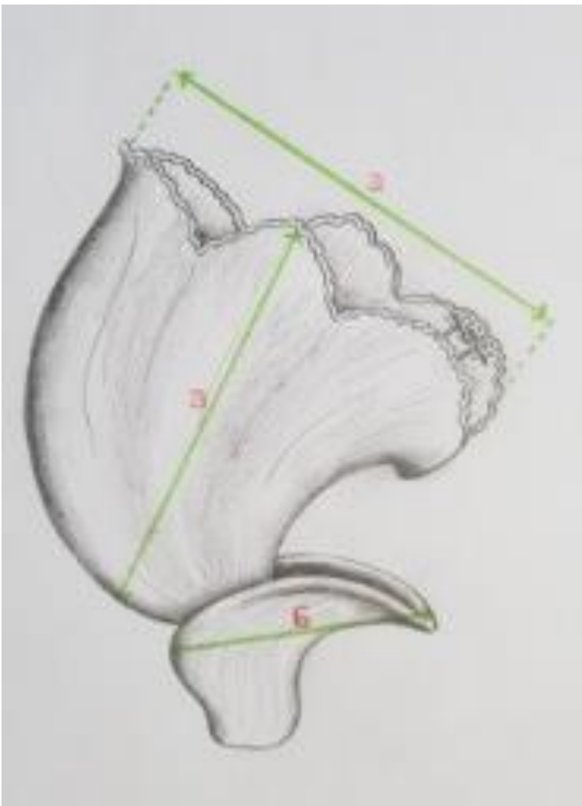


**Figure 3:** Hand drawing of flower Nandi Flame. Source: Benjamin Chemarum.

In this research, two visualization technics were used, one traditional–sketch, and one contemporary—computational modeling.

The best way to describe and explore some plant species was through drawing process. This method was effective for the purpose of delineate and detail descriptions of different plant species, and all drawings made are known as very significant botanical illustrations. Botanical illustration is the art of depicting the form, color and very small and significant details of plant life. Prior today’s contemporary visualizations tools, botanical illustration was the only way of visually recording many plant species.

For this research, the first visual technic used was hand drawing of flower Nandi Flame (Fig. 3). The aim of this sketch was to capture outside form of the flower so further it could be used in computation modeling. Only one drawing was selected for further modelling process. The second step was to import hand sketch of the flower into chosen CAD and BIM software. The drawing was scanned and the obtained picture was then imported into CAD and BIM environment.

Computational modelling process in CAD based digital software included importing sketch of selected plant and using software tools first to draw 2D frame of plant form of the flower and then, by giving volume to 2D form, modelling 3D structure of future 3D model (Fig. 4). The first tools used in this process was from free sketching group for creating and editing sketches with sketch constraints and dimensions. Next step was using tools for adding surfaces into extracted 2D form to create 3D base model for further designing process. The process of adding meshes and volumes into 3D model of bench and removing freeform errors occurred in first step, was the second step of parametric modelling. The third was checking the printability of the 3D model of bench. The result of this two steps of the parametric-biomimetic modelling approach was 3D model of bench with garbage cans near bench (Fig. 5).

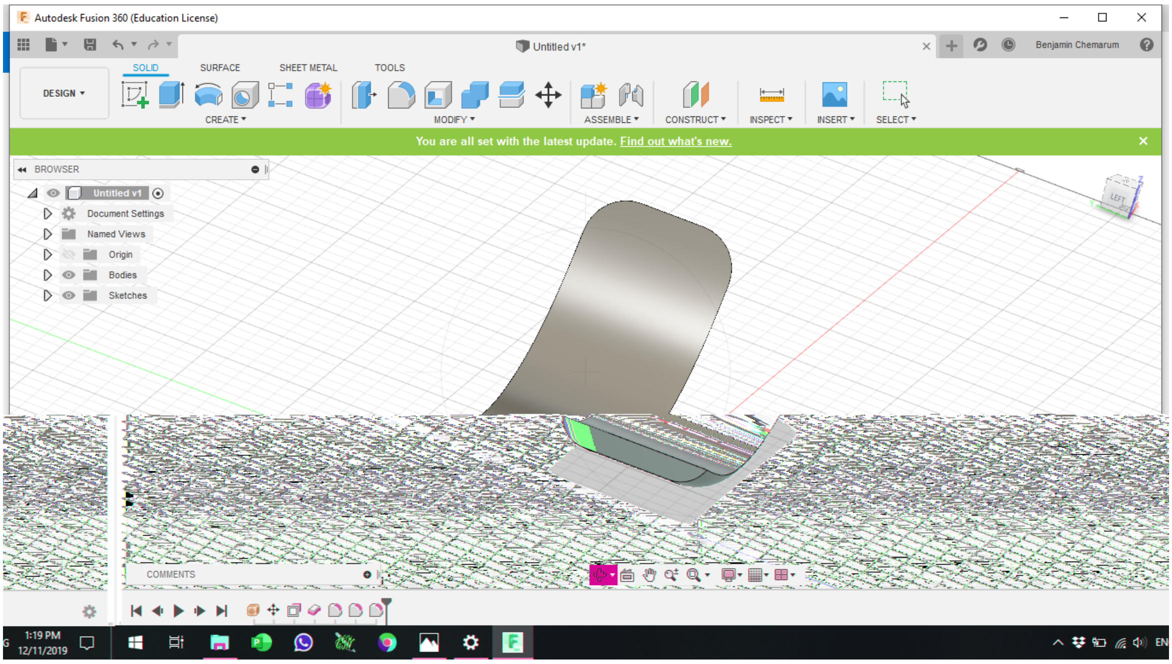


**Figure 4:** Modelling process in CAD software – Fusion 360. Source: print screen Benjamin Chemarum.

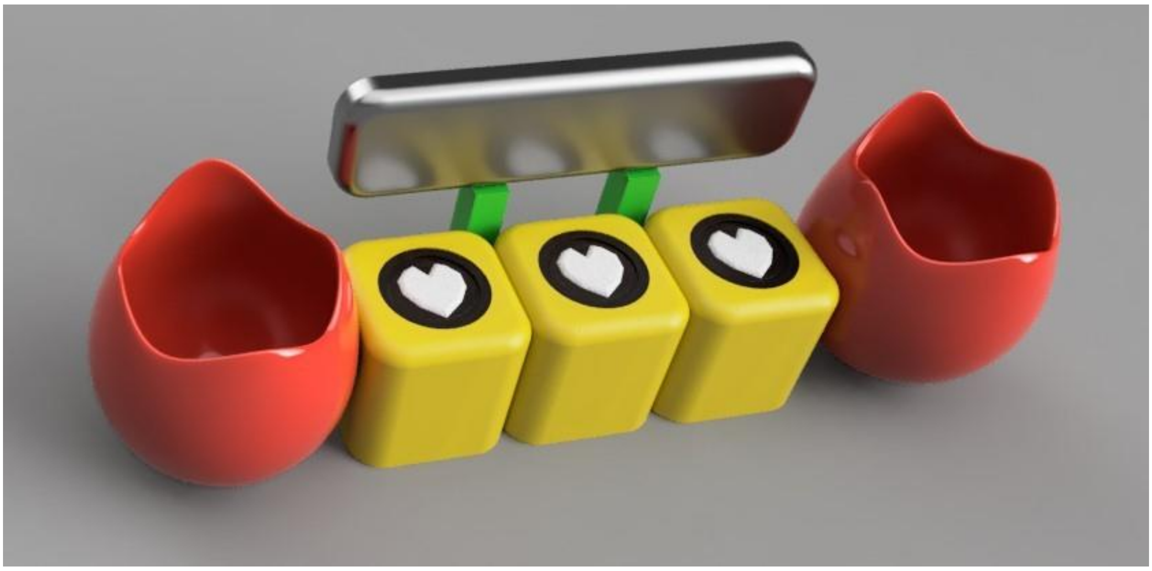

**Figure 5:** 3D model of bench designed in CAD software – Fusion 360. Source: final rendering Benjamin Chemarum.

### 3.4 Interpreting Parametric-Biomimetic Modelling Approach from CAD to BIM Software

For interpreting parametric-biomimetic modelling methodology used in CAD digital software – Fusion 360 into a new software – BIM software ArchiCAD, we were using the same sketch which were the base in previous modelling process. Also we were using the plain element for importing the sketch in BIM environment. The difference was in used tools of the ArchiCAD software. The result of modelling process in ArchiCAD was bench-fountain 3D model - bench and small fountain as one urban landscape architecture element.

The ArchiCAD software is one of the most innovative BIM platforms available [27]. It is a very powerful software that can meet the design needs of many different fields. In this research, a 2D sketch (chosen botanical illustration) was imported in ArchiCAD and it was converted into a 3D model. Even though the name of the software has “CAD” in it, ArchiCAD is most definitely a BIM software. Some of the users call ArchiCAD the real—original BIM software, as it was the first one to reach the market in year 1987. At its launch, it was considered revolutionary for being able to store large amounts of information within the 3D model. This software still remains one of the strongest solutions for data-heavy models. He also has the 2D functionality for producing documentation from the BIM, and a very strong interface for linking between 2D and 3D different elements of the model. There are many other BIM softwares on the market now, so it is also important that software could import different file types, especially important for this research approach as it was needed to import drawing file into software so modelling process could start. ArchiCAD supports a wide range of file formats for import and export. He supports ArchiCAD DWG and DXF file formats, Microstation DGN, Navisworks NWC, Solibri SMC, Sketchup SKP, OpenBIM formats IFC and BCF, and many more. The also great BIM software on the market is REVIT software – a BIM software from Autodesk software family. Revit and ArchiCAD are both great pieces of BIM software and widely used by architects around the world. Revit is mainly used in North America but also in the other parts. Models can be linked for live collaboration in BIM 360, which is very good option for many users today. It is customizable with a wide range of Add-ins and it represents strong support for structural & MEP design. ArchiCAD, is on other hand, easy to use with intuitive design libraries out of the box, it can manage large models in a single file, has strong 2D / 3D interface and has strong OpenBIM / IFC support. For the purpose of this research, the ArchiCAD software has been chosen, based on its supports a wide range of file formats for import and export.

The modelling process covers several steps: importing chosen picture into BIM environment using Plan mode option so sketch was used as 2D plane object, using available tools in software so the flower form could get outside form, giving freely chosen parameters according to some often used measurements in landscape architectural field for bench model and finalize the 3D model by giving it a thickness and colors (Fig. 6 and 7). It is important to single out that this 3D model—urban installation represents innovative and original design model so most of measurement used are according to author’s creative aspects [28, 29].

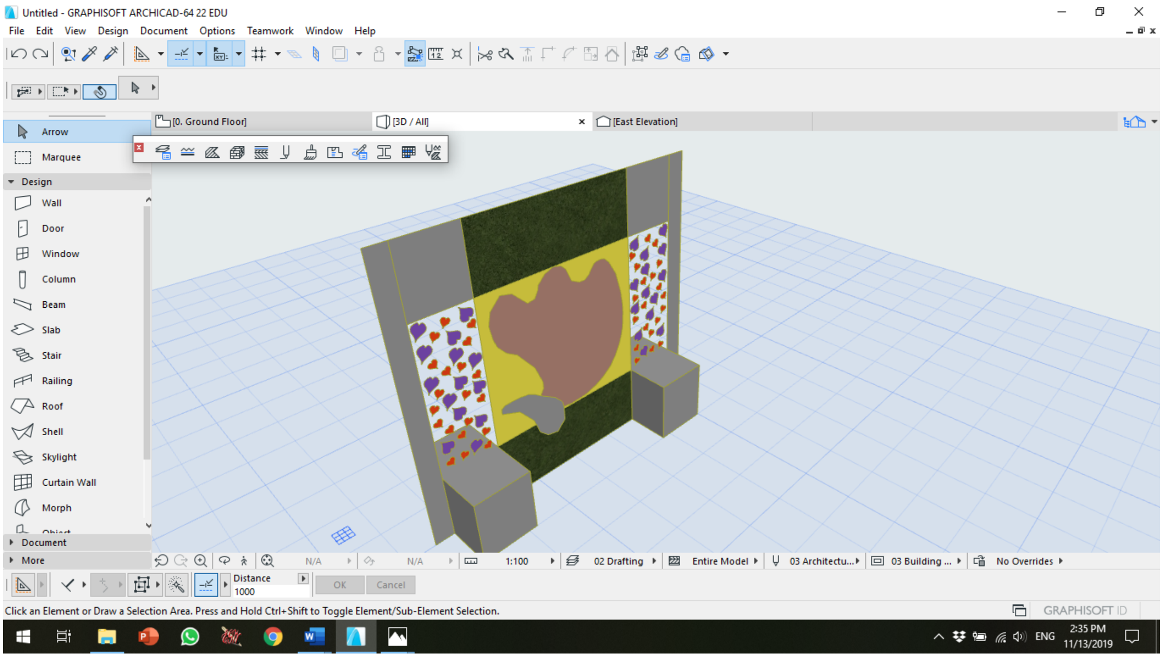


**Figure 6:** Modelling process in BIM software – ArchiCAD. Source: print screen Benjamin Chemarum.

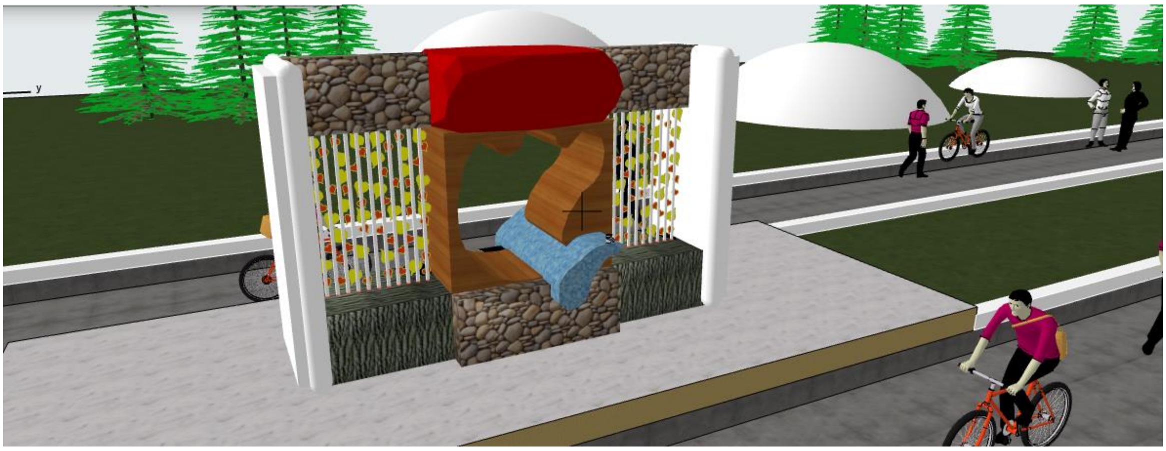

**Figure 7:** 3D model of bench-fountain designed in BIM software – ArchiCAD. Source: final rendering Benjamin Chemarum.

Starting with the import of sketch drawing into BIM environment as Plane object, the modelling process begins with using Element Parameters in ArchiCAD software. In this software there are some libraries with defined parametric objects like door, windows and others, mostly used in architecture and building design field. For purposes of this research, these elements were not needed. We used general parameters in the modelling process. First, we adjusted the 2D view of the plane object for further using of parametric tool–in this case a shell option to draw an external form of the flower of Nandi Flame. The desired design was drawn in 2D view as front view of the imagined future urban furniture. We defined some parameters like length and area, and then started to work in 3D view environment, to add a volume, thickness and surfaces to the model. The 3D modelling process of the bench-fountain model included defining surface area that follows the external flower form. The desired design was imaged so the users of the open space could set in the flower structure, more precisely in external flower form of Nandi Flame. So the external flower form could be found in rectangle structure so sitting part and near fountain small element could be designed as one urban model. After defining surfaces, the next step was to adjust parametric elements as volume and thickness of the model. The fountain element was modelled as lower bud which is near the flower sit. In this way, all users could sit on the ‘’Flame’’ bench, and drink water to lower their body temperature. This is why this urban model was imaged to be in one open fitness space, where people actively exercise and run. The special element of this urban model represent the net design which is located on right and left side of the flower sit form. On the net, small objects were modelled based on the heart like seeds of Nandi Flame plant. They are modelled like plane objects with very small thickness parameter. The results of this research was urban bench-fountain 3D model in imaged environment for this model to be implemented.

## 4. DISCUSSION AND CONCLUSIONS

Nature is full of wonderful inspirations through which we as designers can add beauty to the artificial inventions that we are constantly creating. Observing natural structures, it is important to notice their forms and processes and devise how to apply them as easily as possible in technology and design. In nature, each element is multifunctional and functions in conjunction with other elements, transferring action to each other. In nature, elements are constructed so that they have more characteristics or the composition of several elements fulfills a certain function. The morphological structure is the result of the harmonization of the natural world and its unique environment.

Digital modeling is one of the contemporary ways of generating different nature patterns. Natural patterns organize and define relationships in nature and they could be integrated into biodesign models with the help of digital technologies. Thanks to the permanent development of digital technology, the process of designing and modeling various shapes and forms has been greatly facilitated today. Modeling is a creative process that results as the creation of an appropriate model. Today, digital modeling, as parametric process, is an integral part of every 3D modeling software. Digital modeling is also called 3D modeling software because it uses three dimensions: length, width and height, so involves defining and manipulating certain parameters. Each complex model or shape could be constructed and modified using simple geometric models and changing various parameters. Thanks to these features, parametric models are flexible to operate. Parametric-biomimetic models as a result of this modeling process was innovative and original models. The model built in the software is based on the flow and modification of various information from a base model to a physically defined object. Different Digital modeling programs, such as ArchiCAD, Fusion 360, 3Ds Max, Maya, Cinema 4D, Blender, Rhinoceros and others, have various tools that enable shape transformation.

The aim of the research is to emphasize the importance and explain the possibility of applying the parametric-biomimetic modelling approach through the analysis and the procedure of digital modeling of urban installation. This paper included the research of the application of the nature-geometric pattern of the species *Spathodea campatulata* P. Beauv., more precisely, the geometric pattern of flowers. A geometric pattern is, in known parametric modeling softwares— ArchiCAD and Fusion 360, generated to obtain an appropriate geometric form which further finds its application in the design.

The result of this parametric-biomimetic modeling method were conceptual urban design models – bench modeled in CAD software and bench-fountain modeled in BIM software. This 3D models represents possible urban installations that could be 3D printed and someday installed in some open space in our urban environment.

The conclusion of this research was that the parametric-biomimetic modelling methodology used in CAD software could be easily applied in BIM software. Using similar tools of the CAD and BIM software, it was possible to generate 3D model using parametric modelling and biomimetic approach. The possibility of modelling nature patterns in BIM software was confirmed by this research.

Driven by parametric modeling tools, the landscape architectural designs are pushing boundaries of form, customization and construction in all aspects of the profession. Integration of parametric modeling into designing process could be a promising direction for the further development of landscape architecture. The positive effects of including this design methodology in landscape architectural profession are, first of all, new and innovative design methodology that has the big potential for exploring design on some completely new ways. Developing innovative solutions and design-based research based on inspirations found in nature also represents a natural connection between biology and design that gets its form in landscape architecture. There are many ways in which nature could influence design and its end models and forms. These free-flowing forms are new and innovative and could represents an attractive elements of urban space. Creating new urban environments that strengthens the connection between people and nature is a new challenge in designing an urban spaces. This new and original urban design model of public space could be new direction towards naturally inspired urban design.

## ACKNOWLEDGEMENT

The authors are supported by the Ministry of Education, Science and Technological Development of the Republic of Serbia, (451-02-68/2020/14/2000169 and 200092).

## REFERENCES

1. Garden Visit. https://www.gardenvisit.com/history_theory/library_online_ebooks/architecture_city_as_landscape/imitation_nature (accessed on 25. 8. 2020.)

2. AIouguina, A., Dawson, J.W., Hallgrimsson, B., Smart, G.: Biologically informed disciplines: A comparative analysis of bionics, biomimetics, biomimicry, and bio-inspiration among others. Int. J. Des. Nat. Ecodynamics 197–205 (2014).

3. Agkathidis, A.: Implementing Biomorphic Design. In: eCAADe. The 34th International Conference on Education and Research in Computer Aided Architectural Design, Oulu, Finland, 24–26 August (2016).

4. Benyus, J.M.: Biomimicry: Innovation Inspired by Nature. Harper Perennial, New York, NY, USA 1-308 (2002).

5. Macnab, M.: Design by Nature Using Universal Forms and Principles in design, New Riders, Berkeley, CA, USA 1-313 (2012).

6. Biomimicry. https://biomimicry.org/what-is-biomimicry/ (accessed on 25. 8. 2020.)

7. Whitesides, G.: Bioinspiration: Something for Everyone. The Royal Society Publishing, London, UK (2015).

8. Gruber, P.: Biomimetics in Architecture: Architecture of Life and Buildings. Springer, Wien New York, USA, 1-276 (2011)

9. Critchlow, K.: The Hidden Geometry of Flowers Living Rhythms, Form and Number. Floris Books, Edinburgh, UK, 1-448, (2011).

10. Nestorović, M., Čučaković, A., Jović, B.: Geometric correlation of folded spatial structures in the function of bionics. In: Conference UNGIG, Proceedings moNGeometrija, pp 199-208, Niš, Serbia (2008).

11. Jović, B., Tripković, M., Čučaković, A.: Geometric correlation of cultural landscape patterns and Prunus domestica L. species leaf. Bulletin of the Faculty of Forestry, pp 29–40 (2011).

12. Nuraliev, M.S., Sokoloff, D.D., Karpunina, P.V., Oskolski, A.A.: Patterns of Diversity of Floral Symmetry in Angiosperms: A Case Study of the Order Apiales. Symmetry 473 (2019).

13. Fisch, M.: The Nature of Biomimicry: Toward a Novel Technological Culture. Sci. Technol. Hum. Values 795–821 (2017).

14. Jović, B.S., Čučaković, A.A., Grbić, M.N.: Circle in Space—Space in Circle: A Study of Ratio between Open Space and Built-Up Area in Historical Circular Objects. Sustainability 4662 (2021).

15. Čučaković, A., Jović, B., Komnenov, M.: Biomimetic Geometry Approach to Generative Design. Periodica Polytechnica Architecture, pp 70–74 (2016).

16. Čučaković, A., Obratov- Petković, D., Jović, B., Mitić, A.: Parametric Modelling as Geometric Tool for Designing Urban Model of Biomorphic Form Inspired by Flower of Bell Flower (Campanula Persicifolia L.). In: Proceedings of the 6th International Conference on Geometry and Graphics moNGeometrija 2018, pp117-125, Novi Sad, Serbia, 6th – 9th June (2018).

17. Jović, B., Čučaković, A., Tomićević Dubljević, J., Mitić, A.: Examination of the visual experience of biomorphic form materialized in urban design. In: electronic Proceedings of The 18th International Conference on Geometry and Graphics, Italy, Milano, AISC 809, full paper no. p. 798 ff, 3–7 August (2018).

18. Jović, B. Biomimetic principles in landscape architectural design. In: Symposium "Landscape Horticulture 2018'', Association for Landscape Horticulture of Serbia and the University of Belgrade - Faculty of Forestry, pp 104 – 114, Belgrade, Serbia (2018).

19. Jović, B., Čucakovic, A., Obratov-Petković, D., Ždímalová, M., Komnenov, M.: Transposition of Biomimetical Principles into Generative Design: Example of the Species Campanula patula L. In: Faces of Geometry, Springer Nature, II Edition pp 139-158, Cham, Switzerland (2020).

20. Acevedo-Rodríguez, P., Strong, M.T.: Catalogue of seed plants of the West Indies. Smithsonian Research Online, Washington, DC, USA (2012).

21. African Tuliptree—Spathodea campanulata. Available online: https://candidegardening.com/ZA/plants/eaabf98455d9bdfef9c454fdb2ea58cd (accessed on 25.8.2020).

22. Bärtels, A.: Guide des Plantes tropicales: Plantes ornementales, plantes utiles, fruits exotiques. Editions Eugen Ulmer, Paris, France, 1-384, (1993).

23. Connor, K.F., Francis, J.K.: Spathodea campanulata P. Beauv. Part II—Species Descriptions, Spathodea campanulata P. Beauv. Available online: https://www.srs.fs.fed.us/pubs/ja/2002/ja_2002_connor_001.pdf (accessed on 24.8.2020).

24. Nandi Flame—Infonet Biovision. Available online: https://infonet-biovision.org/EnvironmentalHealth/Trees/Nandi-flame (accessed on 25.8.2020).

25. Spathodea campanulata, Spathodea nilotica, African Tulip Tree, Flame-of-the-Forest. Available online: http://www.flowersinisrael.com/exoticSpathodeacampanulata_page.htm (accessed on 25.8.2020).

26. Labrada, R., Medina A.D.: The invasiveness of the African Tulip Tree, Spathodea campanulata Beauv. Journal Biodiversity 79–82 (2009).

27. ArchiCAD. Available online: https://myarchicad.com/ (accessed on 25. 8. 2020.).

28. Jović, B., Mitić, A.: Introduction of nature forms through urban design: Biomimetic method in the process of designing candelabra model. In: Proceedings of 12th Asian Forum on Graphic Science, electronic Proceedings full paper no. ID 32, pp 1-6, Kunming, China, 9–12 August (2019).

29. Jović, B., Čucakovic, A., Marković, M., Cvijic, K.: Biomimetic Approach to Parametric Flower Modeling. In: Proceedings of 19th ICGG 2021, pp. 244–251, International Society for Geometry and Graphics, Sao Paulo, Brazil, 18–22 January (2021).

„8th International Conference moNGeometrija, focused on the research about geometry, graphics and application to science, engineering and art“

Belgrade, 10.-12. September, 2021.

# ORGANIC MESH AND RIGID BODY UV UNWRAPPING AND MAPPING TAUGHT IN THE SUBJECT TEXTURE AND LIGHT DESIGN

Ivana Vasiljević[1*], Filip Mirčeski[2], Nikola Milinković[3], Ratko Obradović[4]

[1-4]University of Novi Sad, Faculty of Technical Sciences, Computer Graphics Chair, 21000 Novi Sad, Serbia

[1]ivanav@uns.ac.rs, [2]filip.mirceski@uns.ac.rs, [3]nikolam@uns.ac.rs, [4]obrad_r@uns.ac.rs

**ABSTRACT**

*Unwrap is a well-known process in the computer graphics field and represents the first step in texture design for 3D models. Unwrapping is the process of developing a mesh into a plane and the seams by which the model is "cut" must be placed properly. That means that a 3D model is unfolded in a plane without stretching and creasing components and that the seams are not visible after gluing the texture to the model, especially textures that contain characteristic elements repeated according to a pattern. This is the main goal of the unwrapping process. Textures can be created manually or in software that specializes in creating textures.*

*This paper presents a teaching process of unwrapping and texture design for different types of 3D models: rigid, organic, developable, and undevelopable through the contents of the undergraduate subject of the Computer Graphics study program at the Faculty of Technical Sciences, at the University of Novi Sad. The paper presents examples of unwrapped and textured models created by the first-year students, as the supervised project, done through the subject Texture and Light Design of the Computer Graphics study program. This subject is being studied for the first time since this school year (2020/2021) according to the new accreditation cycle. In addition, the paper highlights the differences between unwrapping rigid form, organic form, developable and undevelopable surfaces.*

**Keywords:** unwrap, texture, mapping, texture design, lighting, computer graphics

## 1. INTRODUCTION

Undergraduate study program Engineering Animation was established at the Faculty of Technical Sciences, University of Novi Sad in 2011. This is an interdisciplinary study program combining electrical engineering and mathematics [1], [2], [3].

The aim of this paper is to present the content of the First assignment in one undergraduate subject (namely, Texture and Light Design) of the Computer Graphics study program at the Faculty of Technical Sciences, at the University of Novi Sad. Undergraduate Academic Studies last four years and comprise 48 subjects, of which 39 are compulsory subjects and nine electives [4]. The paper presents examples of unwrapped and textured models created by the first-year students, as their supervised project. This subject has been introduced for the first time in the 2020/2021 school year according to the new accreditation cycle. According to the old accreditation from 2013, the students had a 3d modeling course in the second year of study where they learned proper modeling, topology, and different way of modeling rigid and organic models, as well as unwrapping and texturing [4]. Now the goal is, for students, to acquire, as much as possible, the skills and knowledge necessary for the preparation of models for animated films in the first year. The need for visualization is necessary in all spheres of life because it is the most natural way of seeing the world and an excellent choice to render objects – a visual representation for learning and teaching and for spreading information [5]. In order for the obtained rendered image to be convincing and realistic, the key elements that contribute to realism are textures and lights. For this reason, the students begin to study and deal with the mentioned topic already in the first year.

## 2. STUDY COURSE TEXTURE AND LIGHT DESIGN

Study course Texture and Light Design is an undergraduate subject of the Computer Graphics study program at the Faculty of Technical Sciences. In this course, students learn how to prepare 3D models for texturing, how to create textures and how to properly illuminate a scene. This subject is studied for the first time starting from 2020/2021 academic year according to the new accreditation cycle. In addition, the paper highlights the differences between unwrapping rigid form, organic form, developable and undevelopable surfaces. First, examples were made on geometric primitives such as a sphere, a cylinder, a box, a pyramid, a fish (an example of a simple organic form), and later it was necessary to apply the acquired knowledge and skills to more complex shapes in the project done for evaluation.

### 2.1 Unwrap process

Unwrapping is the process of developing a mesh into a plane which means that a 3D model is unfolded in a plane without stretching and creasing components and that the seams are not visible after gluing the texture to the model [6]. Irregularities and mistakes made during unwrapping are most visible and noticeable in textures that contain elements repeated according to a pattern. This process is the first step in preparing a model for texturing and can be done in a 3D software specialized for 3D modelling like 3ds Max [7], Maya [8], or Blender [9]. The aim of the First assignment in the course Texture and Light Design is to learn how to properly unfold 3D models into a plane. Also, students need to learn the differences between unwrapping rigid form, organic form, developable and undevelopable surfaces.

Before starting the unwrapping process, in the case of organic form, it is very important to explore character anatomy and find good texture references so as to know how and where to put seams. Good texture reference means that we know in advance which shapes and according to which pattern are repeated on the texture. In the case of a rigid form, it is important to know which surfaces are developable and undevelopable because the procedure of unwrapping depends on the surface type. Good texture reference is also required. Developable surfaces can be flattened into a plane without distortion (stretching, compressing or tearing) [10]. That means that unwrapping procedure is done after putting seams and cutting the model according to the assigned seams. In a small number of cases additional settings are required. In the case of undevelopable surfaces, it is necessary to resolve the distortion that arises. The distortion occurs in the form of stretching, compressing or tearing geometry and overlapping parts of the geometry of a 3D model developed into a plane. These problems must be solved with additional settings before gluing the texture to the 3D model.

The result of the Unwrap process is stored in the form of a 2D image, the so-called Unwrap Template, exported from 3D software in the format .jpg, .png, .tiff or other. This Template is actually the basis for the next step, which is creating texture. This means that it is necessary to import the unwrap template into the software where the textures will be created. Adding colors and patterns which the texture will contain is performed in a new layer which fills parts of the image only where the geometry of the 3D model is present. Figure 1 shows an Unwrap Template.

As mentioned, for the First assignment the students were required to create a base of 3D models that needed to be unfolded into a plane, i.e., for each model to do the Unwrap process, and then create textures for these models. The models that needed to be created and unfolded were Rubik's cube (the base is a cube), Djoser's pyramid (the base is a pyramid), a cardboard coffee cup (the base is a cylinder), an ice cream cone (the base is a cone), a pan or pot (example from exercises: teapot), lizard (an example from exercises: fish). Figures 2, 3, and 4 show the mentioned 3D models unfolded in a plane (students' works).

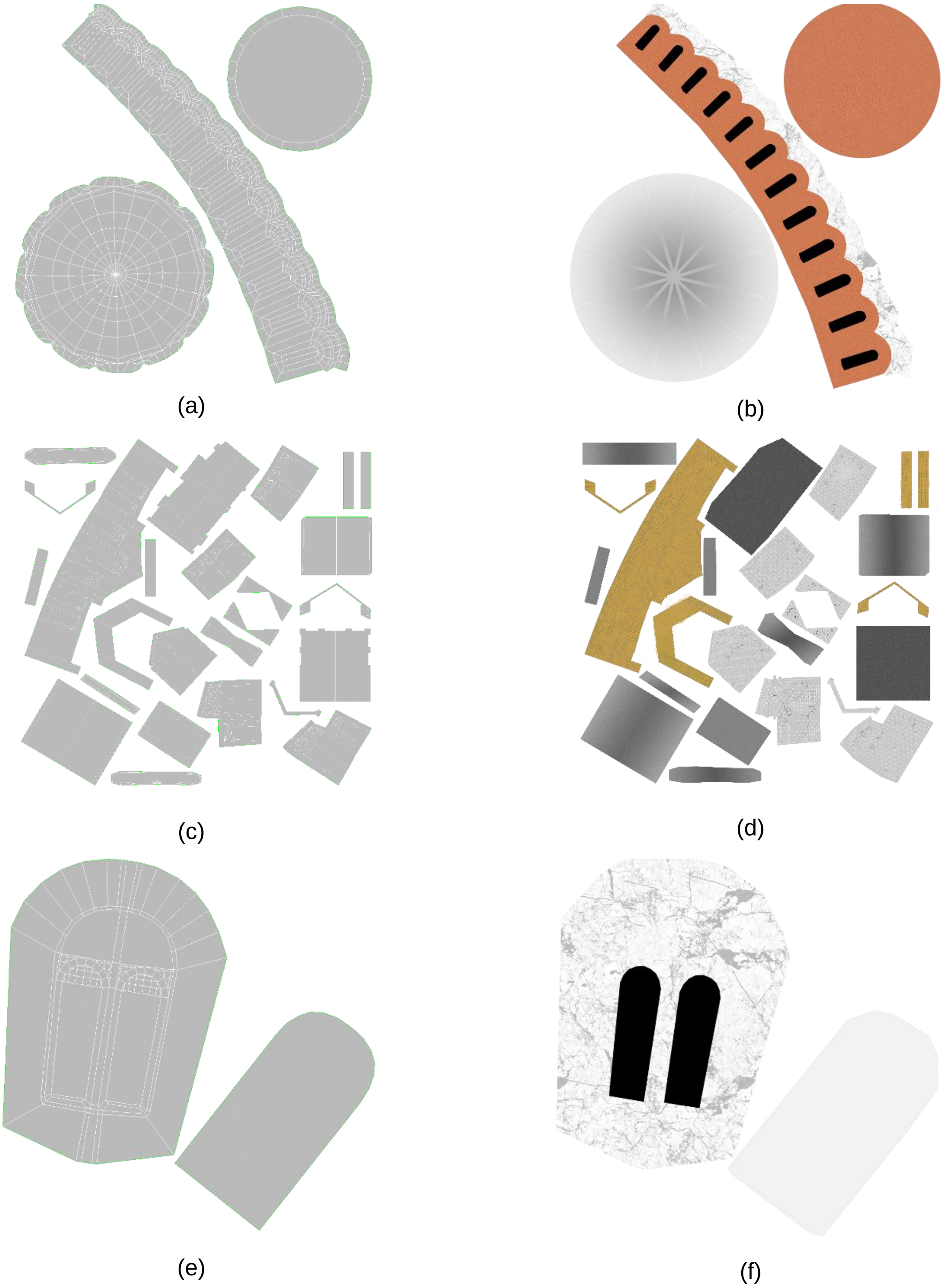

**Figure 1:** Example of an Unwrap Template, done by student Petar Vučetić: a), c), e) Unwrap Template without designed texture; b), d), f) Unwrap Template with designed texture

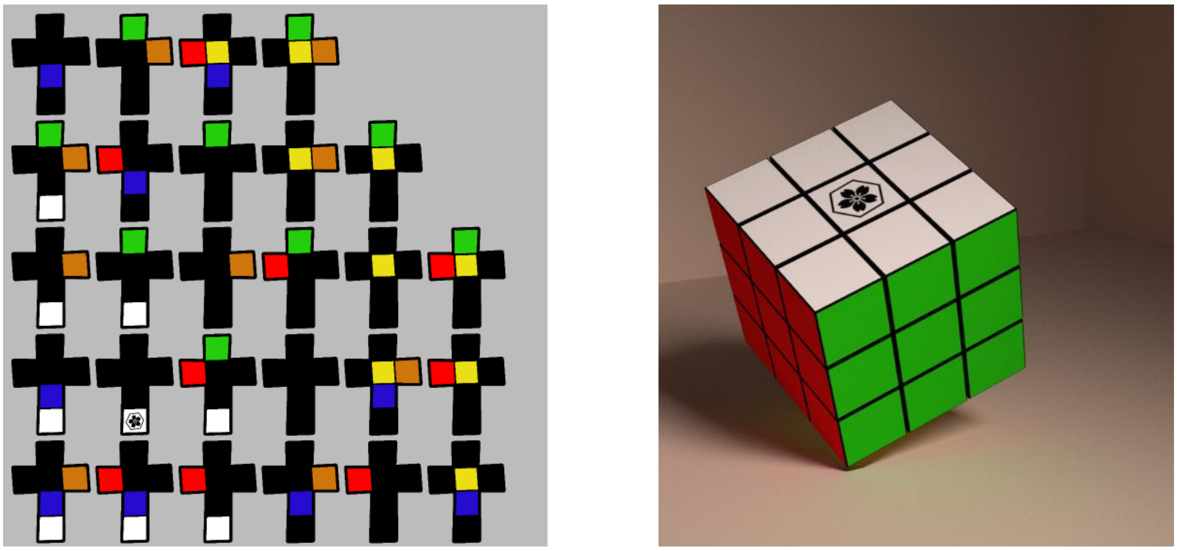

(a) (b)

**Figure 2:** Example of the developable surface, Rubik's Cube, done by student Ivana Lilić: a) Unwrap Template with designed texture; b) textured 3D model

(a) (b)

**Figure 3:** Example of the undevelopable surface, pot, done by student Jovana Pešić: a) Unwrap Template with designed texture; b) textured 3D model

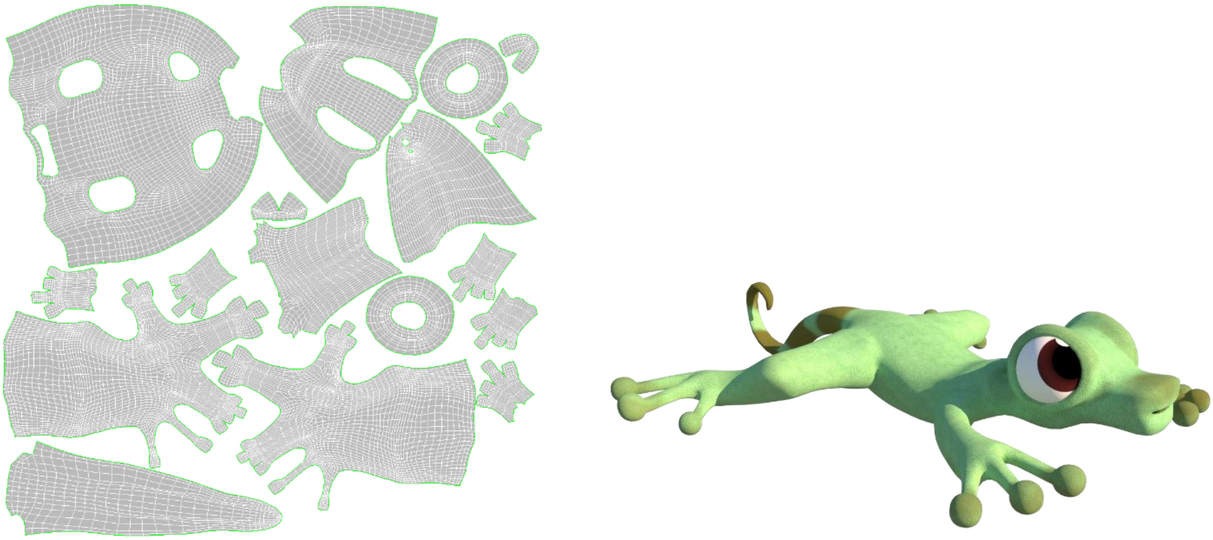

(a) (b)

**Figure 4:** Example of an organic form, lizard, done by student Nataša Orešković: a) Unwrap Template without designed texture; b) textured 3D model

### 2.2 Texture design

Texture creation, i.e., texture design was done in software programs such as Adobe Photoshop [11] or Substance Painter [12]. The difference between the mentioned software is that in Adobe Photoshop software, the user creates all textures and maps (Bump, Diffuse, Normal, Height, Roughness, etc.) manually which is not the case with Substance Painter. Depending on the material you create and the parameters you enter for the Metalness property of the material or the Roughness property, Substance Painter automatically creates the appropriate folders and offers the possibility to export the mentioned folders in the appropriate format. Also, within Substance Painter, there are libraries of ready-made materials that students could use by adapting them to the propositions of the task, while it was necessary to manually add damages to materials (rust, cracks in wood, stains on fabric, etc.). Within this software, there are also so-called Smart Materials, which is actually a library of materials with additional damages. However, the students were not allowed to use the mentioned group of materials, as the teaching goal was to master and go through all the steps in creating materials and textures manually. Additionally, during the manual creation and creation of textures, the students had the opportunity to show their creativity. This manual mode of operation has a positive effect on understanding the operation of automatic options and algorithms offered by some other programs specialized in creating textures in general, and when it comes to another process. Namely, once you have thoroughly mastered and learned a work process in one software, you will easily adapt to other software for 3D modeling, digital sculpting, unwrap, texturing, lighting creation, and the like.

Figures 5, 6, 7, and 8 show the textured models of arbitrarily selected subjects chosen by the students as examples of a complex form.

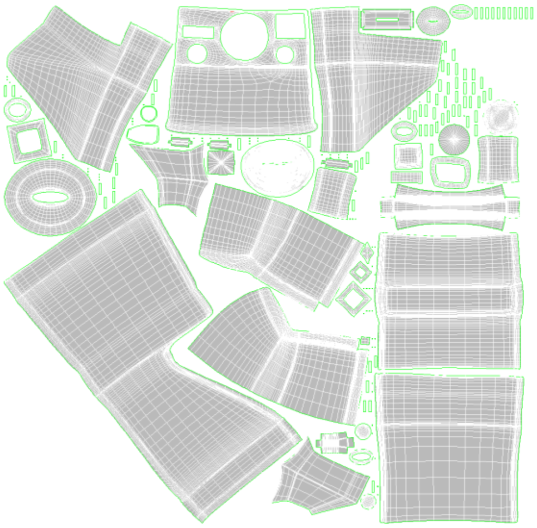

(a)


(b)

**Figure 5:** Example of the complex form, polaroid, done by student Isidora Popović: a) Unwrap Template without designed texture; b) textured 3D model

(a)

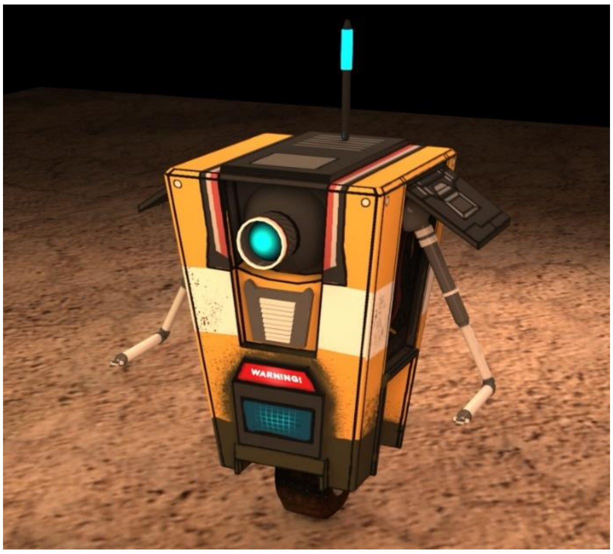


(b)

**Figure 6:** Example of the complex form, robot, done by student Luka Marković: a) Unwrap Template with designed texture; b) textured 3D model

(a) (b)

**Figure 7:** Example of the complex form, old TV, done by student Jovana Pešić: a) Unwrap Template with designed texture; b) textured 3D model

By the end of the semester, the students have another subject task where they learn how to illuminate characters for different genres of film, and within the subject project, they create night and day scenes of interiors and exteriors. This means that in this subject they learn the whole process of preparing models for texturing process, texturing, and creating lighting.

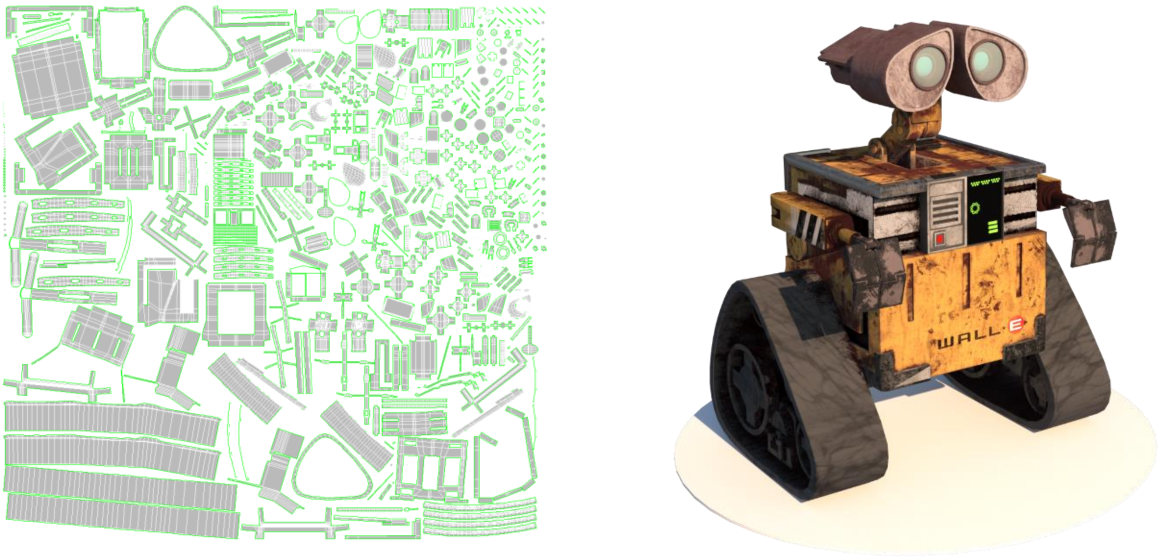

(a) (b)

**Figure 8:** Example of the complex form, Wall-E, done by student Nataša Orešković: a) Unwrap Template without designed texture; b) textured 3D model

## 3. CONCLUSION

We can conclude that the students of the first year of the study program Engineering Animation already after the first year of study acquire all the knowledge necessary for the preparation of 3D models for rendering, i.e., the preparation of models for a 3D animated film. During two semesters, students go through the introduction of 3ds Max software and 3D modeling software in general to creating a final product (3D model) fully ready for use in animated film scenes. This methodology of the courses is well accepted by the students, and they are motivated to engage in the task which is interesting for them. The students' projects are successfully completed and they are also very interesting, which can be seen from the examples shown in the paper. We hope that the majority of students will successfully complete the courses.

## REFERENCES

1. Computer Graphics - Engineering Animation. Available online: http://www.racunarska-grafika.com (accessed on 20 June 2021).

2. Faculty of Technical Sciences, Undergraduate Academic Studies Engineering Animation. Available online: http://www.ftn.uns.ac.rs/2028806618/engineering-animation (accessed on 20 June 2021).

3. Obradovic, R., Vujanovic, M., Popkonstantinovic, B., Ivetic, D., & Sidanin, P. (2019). COMPUTER GRAPHICS-ENGINEERING ANIMATION STUDY PROGRAM AT THE FACULTY OF TECHNICAL SCIENCES IN NOVI SAD. Journal of Industrial Design and Engineering Graphics, Volume 14(1), pp. 319-326.

4. Stajić, B., Šunjka, N., Mijatov, J., Perišić, A., Obradović, R. 3D modeling course at the computer graphics—engineering animation studies. In Between Computational Models and Performative Capacities 4th eCAADe International Regional Workshop, pp. 124-138.

5. Obradović, R., Vujanović, M., 2012. New curriculum at the faculty of technical sciences: computer graphics—engineering animation. In: Obradović, R. (ed.) 3rd International Scientific Conference moNGeometrija 2012, pp. 481–486. University of Novi Sad, Faculty of Technical Sciences, Novi Sad, Serbia

6. Autodesk. Available online: https://knowledge.autodesk.com/support/3ds-max/learn-explore/caas/CloudHelp/cloudhelp/2017/ENU/3DSMax/files/GUID-EA10E59F-DE7F-497E-B399-6CF213A02C8D-htm.html (accessed on 21 June 2021).

7. Autodesk 3ds Max. Available online: https://www.autodesk.com/products/3ds-max/overview?panel=buy&term=1-YEAR (accessed on 21 June 2021).

8. Autodesk Maya. Available online: https://www.autodesk.com/products/maya/overview?term=1-YEAR (accessed on 21 June 2021).

9. Blender. Available online: https://docs.blender.org/manual/en/2.93/index.html (accessed on 23 June 2021).

10. Obradović, R., Beljin, B., & Popkonstantinović, B. (2014). Approximation of Transitional Developable Surfaces between Plane Curve and Polygon. Acta Polytechnica Hungarica, 11(9).

11. Adobe Photoshop. Available online: https://www.adobe.com/products/photoshop.html (accessed on 23 June 2021).

12. Substance Painter. Available online: https://www.substance3d.com/products/substance-painter/ (accessed on 23 June 2021).

# 3-SPHERE IN A 4-PERSPECTIVE

Mgr.Jakub Řada[1], Mgr. Michal Zamboj, Ph.D.[2]

[1] Charles University, Faculty of Mathematics and Physics, Mathematical Institute of Charles University, Prague, Czech Republic

[2] Charles University, Faculty of Education, Department of Mathematics and Mathematical Education, Prague, Czech Republic

rada@karlin.mff.cuni.cz, michal.zamboj@pedf.cuni.cz

***ABSTRACT***

*A classical sphere (2-sphere) is naturally embedded in a 3-dimensional Euclidean space. Analogically, in a higher dimension, a 3-sphere might be embedded in a 4-dimensional Euclidean space. Computer visualizations and constructive methods of examining properties of a 3-sphere and quadric sections of hypercones have already been studied in a double orthogonal projection of a 4-space onto two mutually perpendicular 3-spaces. Based on its double orthogonal projection, a synthetic construction of a 3-sphere in a 4-dimensional perspective is proposed in this contribution. The method of visualization is a 4-dimensional generalization of linear perspective. Instead of the picture plane, the image is a 3-dimensional model in the modeling 3-space, and the use of a double orthogonal projection of a 4-space onto two mutually perpendicular 3-spaces is an analogy to Monge's projection. We discuss a perspective construction of a section of a 3-sphere with a 3-space in various positions. Consequently, we provide a construction of shades of a 3-sphere in central and directional lighting using polar properties of quadrics. The boundary of a shade of a 3-sphere is a 2-spherical intersection of the 3-sphere and its polar 3-space, with the pole being the proper or improper source of light. The perspective image of a shade is a quadric embedded in the 3-dimensional modeling space. Our virtual 3-D models and synthetic constructions are created in the interactive environment of the dynamic geometry software GeoGebra. The results are supplemented with visualizations in Wolfram Mathematica based on analytic representation.*

**Keywords:** Fourth dimension, 3-sphere, central projection, lighting

## 1. INTRODUCTION

Rapidly emerging dynamic 3-D geometry software tools have redrawn the border of precision in geometric constructions beyond its previous limitations. With an interactive 3-D virtual modeling environment, we are now able to carry out synthetic geometric constructions similar to those drafted on paper. Consequently, classical descriptive geometry using planimetric (2-D) methods to visualize spatial (3-D) objects might be easily generalized to visualize 4-D objects in a 3-space. The four-dimensional descriptive geometry method using double orthogonal projection of a 4-space onto two mutually perpendicular 3-spaces (4DDOP) was introduced in (Zamboj, 2018a) and construction of shades and shadows in (Zamboj, 2018b).

While two images in orthogonal projections are often suitable for measurements, there are more interpretative ways of visualization in one representative image; leastwise, in 3-D to 2-D projections. The 4DDOP method is applied to construct a 3-dimensional perspective image and lighting of a 3-sphere embedded in a 4-space in this paper. Where the 3-sphere is a 4-dimensional analogy of a classical (2-)sphere, i.e., a 3-sphere is the set of all points in the same distance from a fixed point in a 4-space. Projections and intersections of a 3-sphere with 3-spaces, planes, and lines in 4DDOP are described in (Zamboj, 2019).

Previously, central projections of four-dimensional hypercubes in computer graphics were discussed in the pioneering work by (Noll, 1967). Analytically treated description and visualization of central and orthogonal images of various curves and surfaces are, for example, in (Banchoff, 1990; Zacharias et al.., 2000). Particularly animations and interactive methods of multidimensional visualization were used by (Black, 2010; Bosch, 2020; Chu et al.., 2009; Hanson et al.., 1993; Matsumoto et al.., 2019; Miwa et al.., 2018; Zhang et al.., 2007).

### 1.1 Double orthogonal projection of a 4-space onto two mutually perpendicular 3-spaces – 4DDOP

Let us briefly introduce the 4DDOP method used to construct perspective images of points in the next section. A double orthogonal projection of a 3-space onto two mutually perpendicular planes is known as Monge's projection. 4DDOP method is a natural generalization of Monge's projection in a higher dimension. Let us have a 4-space with reference axes $\boldsymbol{x}, \boldsymbol{y}, \boldsymbol{z}$ and $\boldsymbol{w}$. A point $\boldsymbol{P}(\boldsymbol{p_x}, \boldsymbol{p_y}, \boldsymbol{p_z}, \boldsymbol{p_w})$ in the 4-space is projected orthogonally to its two conjugated images in the 3-spaces $\boldsymbol{\Xi}(\boldsymbol{x}, \boldsymbol{y}, \boldsymbol{z})$ and $\boldsymbol{\Omega}(\boldsymbol{x}, \boldsymbol{y}, \boldsymbol{w})$. One of the 3-spaces, say $\boldsymbol{\Xi}$, is rotated about the plane $\boldsymbol{\pi}(\boldsymbol{x}, \boldsymbol{y})$ to the second (modeling) 3-space $\boldsymbol{\Omega}$ such that $\boldsymbol{z}$ and $\boldsymbol{w}$ have opposite orientations ($\boldsymbol{w}$ upwards, $\boldsymbol{z}$ downwards in this paper). As a result, the point $\boldsymbol{P}$ has two conjugated images in the modeling 3-space – the $\boldsymbol{\Xi}$-image $\boldsymbol{P_3}(\boldsymbol{p_x}, \boldsymbol{p_y}, \boldsymbol{p_z})$ and $\Omega$-image $\boldsymbol{P_4}(\boldsymbol{p_x}, \boldsymbol{p_y}, \boldsymbol{p_w})$. The conjugated images $\boldsymbol{P_3}$ and $\boldsymbol{P_4}$ lie on their common ordinal line perpendicular to the plane $\boldsymbol{\pi}(\boldsymbol{x}, \boldsymbol{y})$ in the modeling 3-space. In Monge's projection, conjugated images of a 2-sphere are two equiradial disks. In 4DDOP, conjugated images of a 3-sphere $\boldsymbol{\Sigma}$ are two equiradial 2-balls $\boldsymbol{\Sigma_3}, \boldsymbol{\Sigma_4}$.

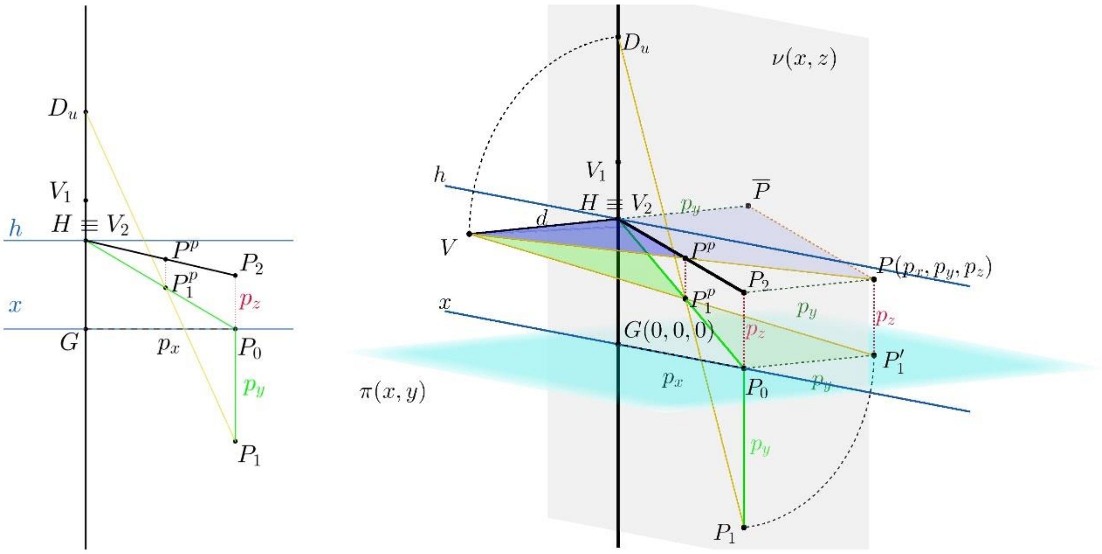


(a) (b)

**Figure 1**: (a) The principle of the 3-perspective construction of a point with associated Monge's projection. The 3D-image is projected in orthographic projection. (b) The perspective image from the perspective center.

## 2. FOUR-DIMENSIONAL PERSPECTIVE

To start with, we describe the generalization of linear perspective in a four-dimensional setting.[1] The 3-perspective is a central projection, in which each point is projected from a fixed center (viewpoint, entrance pupil of an eye or camera) into a picture plane. The resulting intersection of the projecting ray and picture plane is called the perspective image of the point. Classical linear perspective should satisfy certain conditions appropriate for human vision (degree limit for vision cone, minimal distance of the viewpoint from picture plane). In the context of four-dimensional generalization, no human will (hopefully) argue if we do not take them into account while keeping our figures illustrative. Furthermore, basic elements of 3-perspective are generalized in 4-perspective as follows (Figures 1 and 2). In the 4-perspective, a point is projected from a fixed perspective center into a modeling 3-space instead of a picture plane. In both cases, we label $\boldsymbol{D}$ the distance between the perspective center and the picture plane or modeling 3-space, i.e., the focal length. And in both cases, the orthogonal projection of the perspective center into the picture plane or modeling 3-space is the principal (vanishing) point $\boldsymbol{H}$. Assuming the surrounding 3-space in 3-perspective, the

[1] To simplify the language, we will refer to linear perspective in three dimensions as 3-perspective and its four-dimensional generalization as 4-perspective.

picture plane is in the vertical position, and we assume the ground (or base) plane in the horizontal position. The orthogonal projection of the principal point $\boldsymbol{H}$ into the ground plane (chosen not through $\boldsymbol{H}$) is the ground point $\boldsymbol{G}$. Let us rather use the Cartesian coordinate system $(\boldsymbol{x},\boldsymbol{y},\boldsymbol{z},\boldsymbol{w})$ in the four-dimensional case. Instead of the ground plane assume ground 3-space $\Xi(\boldsymbol{x},\boldsymbol{y},\boldsymbol{z})$ and the modeling 3-space is $\boldsymbol{\Omega}(\boldsymbol{x},\boldsymbol{y},\boldsymbol{w})$. The orthogonal projection of the principal point $\boldsymbol{H}$ into the ground 3-space is the ground point $\boldsymbol{G}$. In 3-perspective, the intersection of the ground plane with the picture plane is the ground line. In 4-perspective, the intersection of the ground 3-space $\Xi(\boldsymbol{x},\boldsymbol{y},\boldsymbol{z})$ with modeling 3-space $\boldsymbol{\Omega}(\boldsymbol{x},\boldsymbol{y},\boldsymbol{w})$ is the ground plane $\boldsymbol{\pi}(\boldsymbol{x},\boldsymbol{y})$. In 3-perspective, the horizon plane is parallel to the ground plane through the perspective center, and its intersection with the picture plane is the horizon line, i.e., the line of vanishing points in horizontal planes. In the four-dimensional case, we have the horizon 3-space through the perspective center and totally parallel to the ground 3-space $\Xi(\boldsymbol{x},\boldsymbol{y},\boldsymbol{z})$ Its intersection with the modeling 3-space $\boldsymbol{\Omega}(\boldsymbol{x},\boldsymbol{y},\boldsymbol{w})$ is the horizon plane $\boldsymbol{\eta}$.

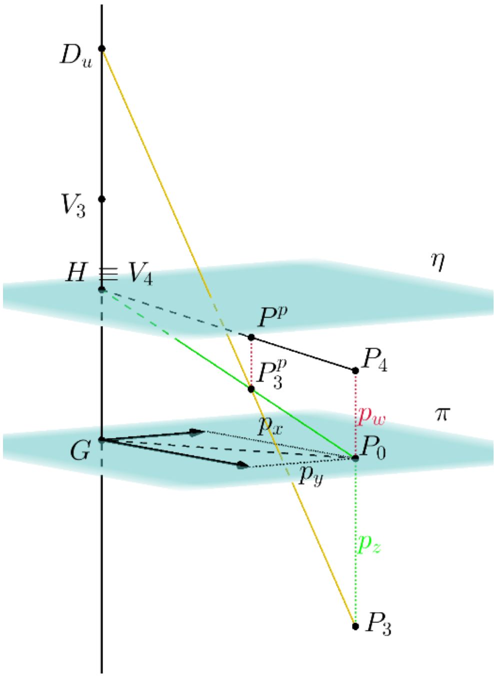


**Figure 2:** The principle of the 4-perspective construction of a point with associated 4DDOP in the modeling 3-space.

One way of constructing perspective images of points in 3-perspective is to use associated Monge's projection with the same picture plane, in which the ground plane $\pi(x,y)$ is rotated onto the picture plane $(x,z)$ about the ground line ($x$-axis) (Figure 1a). We will use similar construction in the 4-perspective associated with 4DDOP.[2] Consider the situation in the 4-space $(x,y,z,w)$, the ground 3-space $\Xi(x,y,z)$ is rotated around the ground plane $\pi(x,y)$ onto the modeling 3-space $\Omega(x,y,w)$ (Figure 2). The perspective image $P^p$ of a point P is the intersection of the projecting line $VP$ of the point P from the perspective center V with the modeling 3-space. Let $P_3'$ and $P_4$ be the orthogonal projections of the point P into $\Xi(x,y,z)$ and $\Omega(x,y,w)$, respectively. Moreover, label $P_3^p$ the perspective image of the point $P_3'$ and $P_3$ the image of the point $P_3'$ after the initial rotation of $\Xi$ onto $\Omega$. The orthogonal projection of $P_3'$ into the modelling 3-space is labeled $P_0$. The lines $P_0H$ and $P_3P_0$ are, respectively, the perspective image and the $\Xi$-image in 4DDOP of the line $P_3'\,P_0$ orthogonal to the modeling 3-space. Furthermore, let $D_u$ (upper distance point) be the image of the viewpoint $V$ rotated about the horizon plane $\eta$ into $\Omega(x,y,w)$.[3] Note that the triangles $VHP_3^p$ and $P_3'P_0P_3^p$ are homothetic with center $P_3^p$ (from initial construction). Furthermore, the triangles $VHP_3^p$ and $D_uHP_3^p$ are congruent (due to rotation). Also $P_3'P_0P_3^p$ and $P_3P_0P_3^p$ are congruent (due to rotation). Hence $D_uHP_3^p$ and $P_3P_0P_3^p$ are similar. Since $HP_3^pP_0$ are collinear, then also $D_uP_3^pP_3$ are also collinear. Consequently the triangles $D_uHP_3^p$ and $P_3P_0P_3^p$ are homothetic with the center $P_3^p$ and coefficient $\frac{|VP|}{|P_3'P_0|} = \frac{|D_uP|}{P_3P_0} = \frac{d}{p_z}$, where $d$ is the perspective distance and $p_z$ is the $z$-

[2] In 3-perspective (Figure 1a), points $P_1, P_2$ play the same role as $P_3, P_4$ in the 4-perspective (Figure 2), respectively. Similarly for other points with the same indexes.

[3] To shorten the construction, the rotation has the same orientation as the initial rotation of the ground 3-space $\Xi$ onto the modeling 3-space $\Omega$.

coordinate of the point $P$. These are the key relations for synthetic construction between the perspective image and Ξ-image in 4DDOP images and vice versa. The Ω-image $P_4$ is the orthogonal projection of $P$ into the modeling 3-space Ω, and so it lies on the perpendicular through $P_0$ to $\pi$ and also on the line through $P^p$ and the principal vanishing point $H$. The distance $|P_0P^p| = p_w$ is the $w$-coordinate of $P$. The triangles $VP^pH$ and $PP_4P^p$ are also homothetic with the center $P^p$ and the same coefficient $\frac{d}{p_z}$. For further constructions note that the Ω-image of the viewpoint $V$ is equal to the principal point, $V_4 \equiv H$, in the modeling 3-space, and the Ξ-image $V_3$ lies on the ray $GH$ such that $|GV_3| = d$.

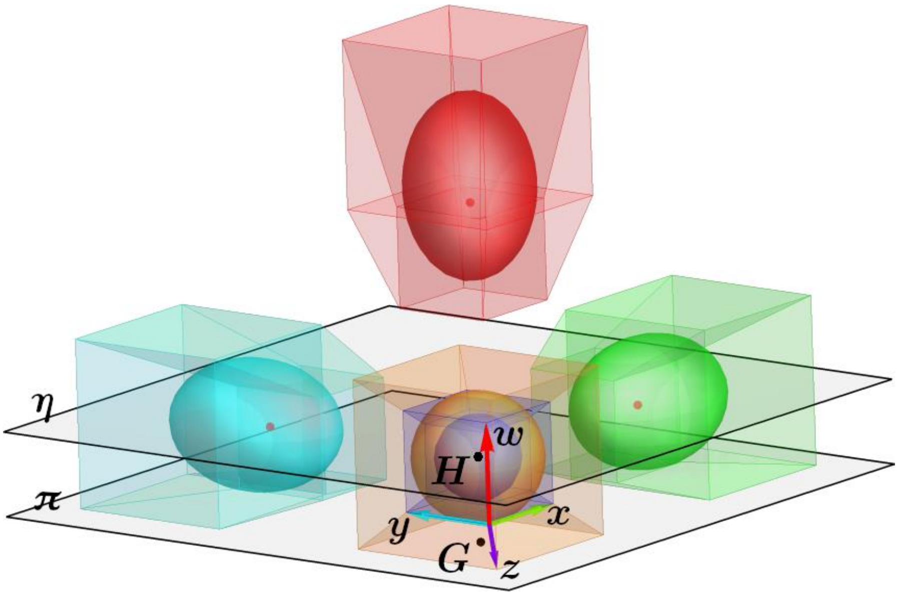


**Figure 3**: A perspective image of a system of 3-spheres inscribed into hypercubes in the modeling 3-space. Assuming the orange 3-sphere to be the center of an arbitrary reference system, the green, cyan, blue, and red 3-spheres are translated in $x, y, z$ and $w$-direction, respectively.

For analytic representation, it is convenient to translate the origin of the 4-space into the viewpoint $V(0,0,0,0)$ by vector $\overrightarrow{GV}$. In such case, the modeling 3-space has the equation $z = d$, where d is the perspective distance and a point P has newly acquired coordinates $(p'_x, p'_y, p'_z, p'_w)$. Let $\bar{P}$ be the orthogonal projection of the point $P$ into the z -axis (similarly in the 3-perspective in (Figure 1), where $\bar{P}$ is the projection into $y$-axis), then the triangles $VP\bar{P}$ and $VP^pH$ are homothetic with the center $V$. Thus, the coordinates of the perspective image of the point $P$ are given by the scaling factor $\frac{d}{p'_z}$, and so, omitting the $z$-coordinate in the modeling 3-space Ω, we have $P^p\left(\frac{d}{p'_z}p'_x, \frac{d}{p'_z}p'_y, \frac{d}{p'_z}p'_w\right)$.

The apparent contour of the 3-sphere in the 4-perspective is the projection of its contour generator. The contour generator is the intersection of the 3-sphere and the polar 3-space of the viewpoint (pole) with respect to the 3-sphere. Therefore, the contour generator is a 2-sphere and its perspective image is an unruled regular quadric (assuming the center of the projection is not incident with the 3-sphere). Figure 3 shows a 4-perspective image of a system of 3-spheres inscribed into hypercubes for better control. Figures 3 – 5 are created in *Wolfram Mathematica 11* with the use of analytic representation. In this case, we use homogeneous coordinates (with the homogenizing coordinate at the end) in the projective extension of the real space. Hence the viewpoint has coordinates $V(0,0,0,0,1)$, the equation of the modeling 3-space becomes

$$x_3 = dx_0. \qquad \text{(Eq. 1)}$$

A 3-sphere Σ with a radius $r$ and proper center $S(s_1, s_2, s_3, s_4, 1)$ has the equation

$$(x_1 - s_1x_0)^2 + (x_2 - s_2x_0)^2 + (x_3 - s_3x_0)^2 + (x_4 - s_4x_0)^2 - r^2x_0^2 = 0. \qquad \text{(Eq. 2)}$$

The matrix of the quadratic form of the 3-sphere is

$$\Sigma = \begin{pmatrix} 1 & 0 & 0 & 0 & -2s_1 \\ 0 & 1 & 0 & 0 & -2s_2 \\ 0 & 0 & 1 & 0 & -2s_3 \\ 0 & 0 & 0 & 1 & -2s_4 \\ -2s_1 & -2s_2 & -2s_3 & -2s_4 & s_1^2+s_2^2+s_3^2+s_4^2-r^2 \end{pmatrix} \quad \text{(Eq. 3)}$$

Therefore the polar 3-space $\Theta$ of the pole $V$ with respect to $\Sigma$ is (matrix multiplication on the left side)

$$\Theta: V^T\,\Sigma(x_1,x_2,x_3,x_4,x_0) = s_1x_1+s_2x_2+s_3x_3+s_4x_4-(s_1^2-s_2^2-s_3^2-s_4^2+r^2)x_0 = 0 \quad \text{(Eq. 4)}$$

The intersection of the 3-sphere $\Sigma$ and 3-space $\Theta$ is the contour generator – 3-sphere $\phi$. Finally, to obtain the perspective image $\phi^p$ of the 3-sphere $\Sigma$, we apply the above-mentioned transformation of coordinates.[4]

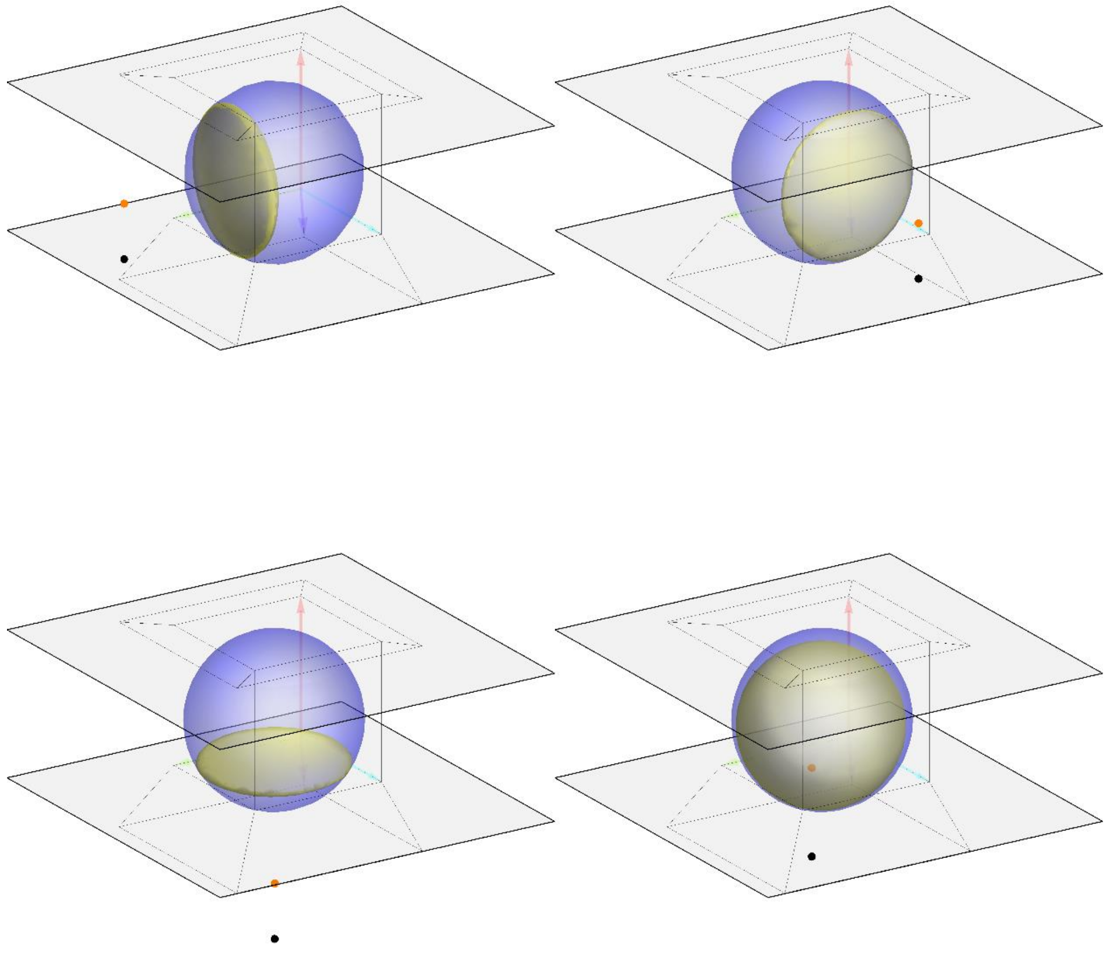

**Figure 4**: Perspective images of shades of a 3-sphere with respect to point light sources represented by orange points in various positions. Black points are the orthogonal projections of the light sources into the ground 3-space used to locate the sources in the 4-space.

Similarly, if we use arbitrary point $P$ instead of the viewpoint, we can create the edge of the shade of the 3-sphere from either point (Figure 4 or directional Figure 5) light source (proper or improper pole $P$ in the projective

[4] Alternatively, we could construct the intersection of the modeling 3-space and the tangent hypercone with the base 2-sphere $\phi$ and vertex $V$, obtaining the same collinear mapping.

extension). The shade is a 2-sphere – the intersection of the polar 3-space of the light source with respect to the 3-sphere and the 3-sphere. Its perspective image becomes, again, an unruled regular quadric.

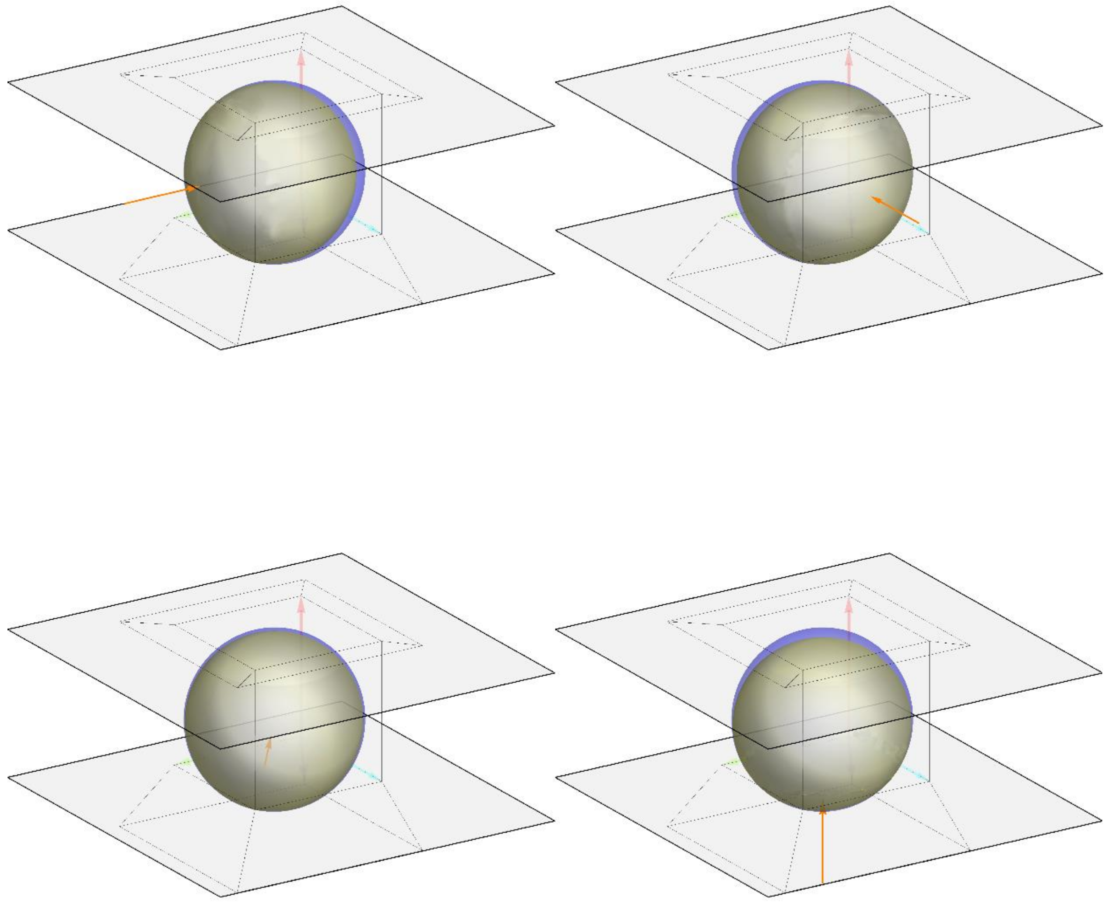

**Figure 5**: Perspective images of shades of a 3-sphere with respect to directional light sources represented by orange arrows in various positions. The sources are in the directions of the reference axes $x, y, z$ and $w$.

### 2.1 Construction of a perspective image of a 3-sphere in 4-perspective

Let us first realize a similar problem in the 3-perspective (Figure 6). A 2-sphere $\sigma$ is given by its conjugated images in Monge's projection (equiradial disks $\sigma_1, \sigma_2$). The conjugated images $c_1$ and $c_2$ of the contour generator $c$ are in ellipses (circles, or segments in special positions) constructed in Monge's projection as the intersections of $\sigma$ with the polar plane $\theta$ of the pole V. The perspective image $c^p$ is the intersection of the picture plane and the tangent right cone $\kappa$ with the vertex $V$ and circular base $c$. The perspective image $c^p$ is a conic section constructed classically via foci using Quetelet-Dandelin theorem (Piska et al..,1972, pp.302-303), or projectively through the 5-point construction.

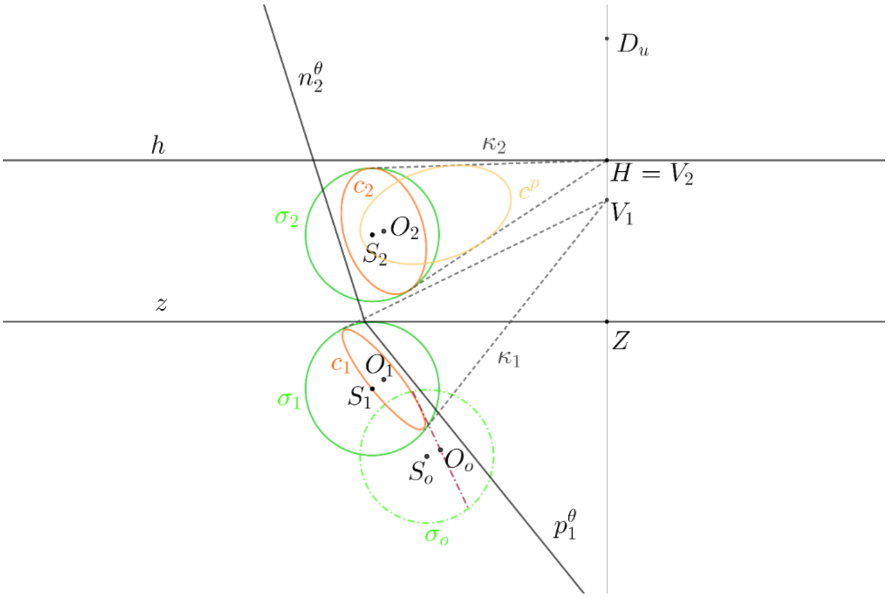


**Figure 6:** 3-perspective image $c^p$ of a 2-sphere $\sigma$, with the construction in associated Monge's projection.

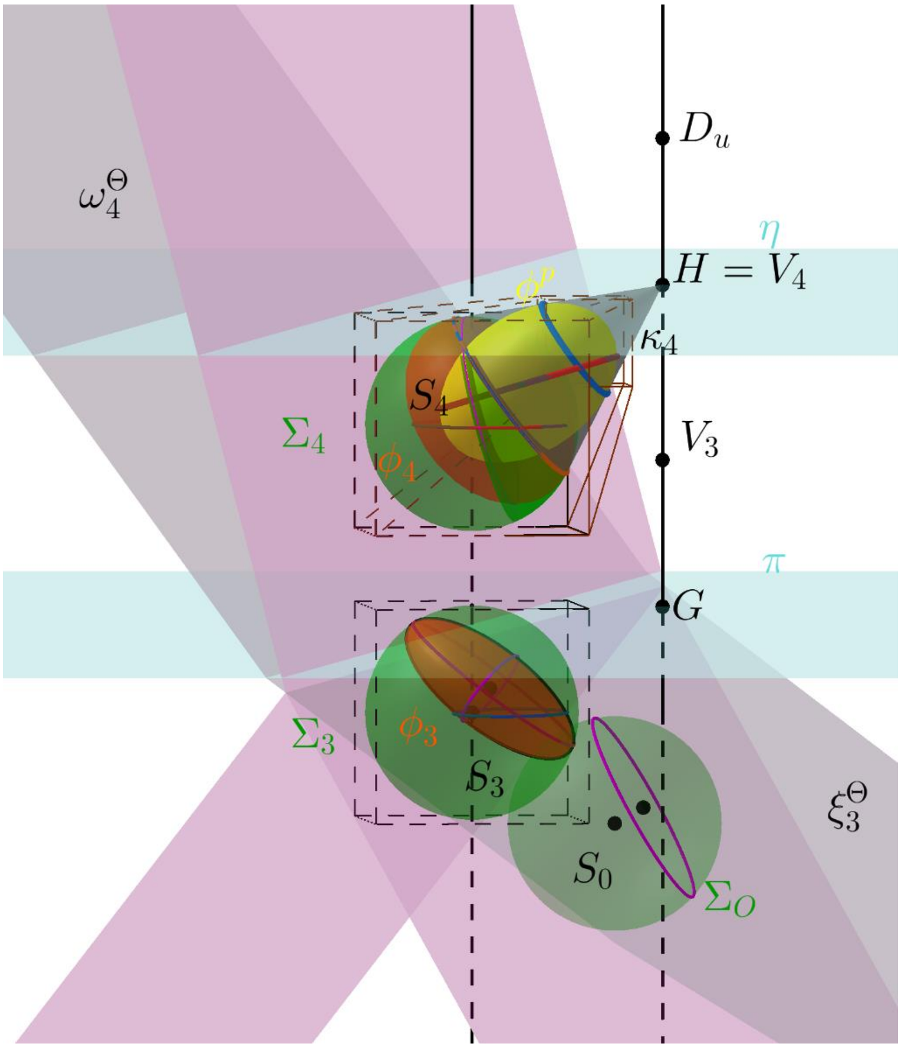


**Figure 7**: 4-perspective image $\phi^p$ of a 3-sphere $\Sigma$, with the construction in the associated 4DDOP projection.

By analogy in the 4-space, the contour generator $\phi$ of the 3-sphere $\Sigma$ is a 2-sphere, and its perspective image $\phi^p$ is an unruled quadric. Instead of the 5-point construction of a conic, we can use the 9-point construction of a quadric (see Korotkiy, 2018; Blossier 2019).

Let us have a 3-sphere $\Sigma$ with center $S$ in the 4-space given by its $\Xi$ and $\Omega$-images --- 2-balls $\Sigma_3$ and $\Sigma_4$ in the associated 4DDOP (Figure 7). The 4-perspective is given with the horizon plane $\eta$ with principal point $H$, ground plane $\pi(x,y)$ with ground point $G$ and principal distance $d$ with the upper distance point $D_u$. See also step-by-step construction in (Řada, 2021).

1. Construct the 4DDOP conjugated images $V_3, V_4$ of the viewpoint $V$ such that $V_3 \in \overrightarrow{GH}, |V_3G| = d = |D_uH|$ and $V_4 \equiv H$.
2. In 4DDOP, construct the trace planes $\xi_3^\Theta$ and $\omega_4^\Theta$ (intersections with $\Xi$ and $\Omega$) of the polar 3-space $\Theta$. The 3-space $\Theta$ is perpendicular to $VS$ and contains the tangent points of the tangent cone to $\Sigma$ with vertex $V$.
3. In 4DDOP, find the quadric $\phi$ of intersection of $\Sigma$ and $\Theta$. For example, with the use of the rotated image $\Sigma_0$ (see Zamboj, 2019). It is also sufficient to find 9 suitable points.
4. From the conjugated images in the 4DDOP, construct the perspective images of points on $\phi$ (Figure 2).
5. Use the 9-point construction to obtain the perspective image $\phi^p$.

In addition, we have constructed a hypercube circumscribed around $\sigma$ with its perspective image (see also Rada, 2021).

## 2.2 Construction of a section of a 3-sphere with a 3-space in 4-perspective

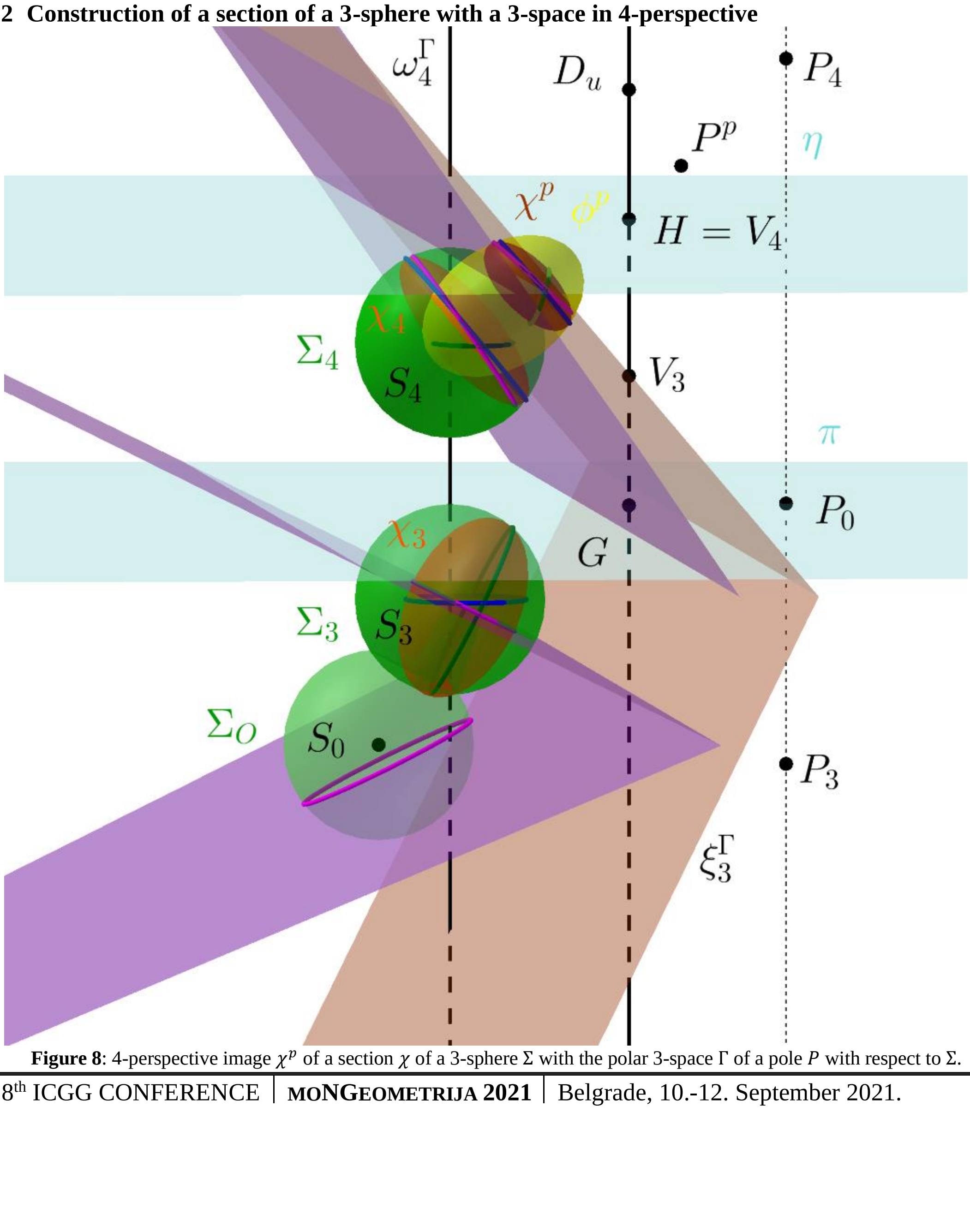


**Figure 8**: 4-perspective image $\chi^p$ of a section $\chi$ of a 3-sphere $\Sigma$ with the polar 3-space $\Gamma$ of a pole $P$ with respect to $\Sigma$.

Let us continue the previous construction with the construction of a section $\chi$ of the 3-sphere $\Sigma$ with the polar 3-space $\Gamma$ of an arbitrary point $P$ given by its conjugated images $P_3, P_4$. The construction is similar to the construction of the perspective image $\phi^p$ of $\Sigma$. Instead of the polar 3-space $\Theta$ of the viewpoint $V$, the polar 3-space $\Gamma$ of the pole $P$ must be constructed. The intersection of $\Gamma$ and $\Sigma$ is the 2-sphere $\chi$ constructed first in the 4DDOP as $\chi_3, \chi_4$ and consecutively with the use of the 9-point construction in the 4-perspective as $\chi^p$ (Figure 8), which is again an unruled quadric.

Additionally, the section $\chi$ is also the shade of light from the source $P$. Assuming the position of the point $P$ in the 4-perspective, we can choose P to be proper (not in $\eta$) or improper (in $\eta$), defining central or directional lighting, respectively.

## 3. CONCLUSION

We have described the synthetic construction of a perspective image of a 3-sphere in a generalized perspective projection of a 4-space to a three-dimensional modeling space. The construction is based on the associated double-orthogonal projection of the 4-space onto mutually perpendicular 3-spaces. Furthermore, we have provided a construction of a 2-sphere-section of 3-sphere with a 3-space, using polar properties of quadrics. The provided construction might also serve as a construction of a shade of a 3-sphere with respect to a point or directional source of light. Our interactive synthetic constructions in *GeoGebra* are available for readers online.

Throughout the work on this contribution, we have opened some further issues. By creating the models in Wolfram Mathematica based on the analytic representation, we have obtained a tool to visualize any set of points in the 4-perspective. Such 4-perspective mapping is opened for interactive elements (e.g., motion of the object or viewpoint, or manipulable parts of the object). Moreover, the problem of lighting of a 3-sphere might be easily generalized for any algebraic hypersurface.

## ACKNOWLEDGEMENTS

Jakub Řada was supported by the grant SVV No. 260580.

## REFERENCES

1. Banchoff, T. F., 1990. *Beyond the third dimension*. New York: Scientific American Library.

2. Black II, D. V., 2010. *Computational techniques to enable visualizing shapes of objects of extra spatial dimensions*. University of California, Irvine.

3. Blossier, M., 2019. Quadric through 9 points, https://www.geogebra.org/m/xqkwgcan [accessed 1st July 2021].

4. Bosch, M. T., 2020. *N-dimensional rigid body dynamics*. ACM Transactions on Graphics (TOG), 39(4), 55-1.

5. Chu, A., Fu, C. W., Hanson, A., Heng, P. A., 2009. *GL4D: A GPU-based architecture for interactive 4D visualization*. IEEE transactions on visualization and computer graphics, 15(6), 1587-1594.

6. Hanson, A. J., Cross, R. A., 1993. *Interactive visualization methods for four dimensions*. In Proceedings Visualization’93 (pp. 196-203). IEEE.

7. Korotkiy, V. A., 2018. *Construction of a Nine-Point Quadric Surface*. Journal for Geometry and Graphics, 22(2), 183-193.

8. Matsumoto, K., Ogawa, N., Inou, H., Kaji, S., Ishii, Y., Hirose, M., 2019. *Polyvision: 4D Space Manipulation through Multiple Projections*. In SIGGRAPH ASIA Emerging Technologies (pp. 36-37).

9. Miwa, T., Sakai, Y., Hashimoto, S., 2017. *Learning 4-D spatial representations through perceptual experience with hypercubes*. IEEE Transactions on Cognitive and Developmental Systems, 10(2), 250-266.

10. Noll, A. M., 1967. *A computer technique for displaying n-dimensional hyperobjects*. Communications of the ACM, 10(8), 469-473.

11. Piska, R., Medek, V., 1972. *Deskriptivní geometrie I*., Nakladatelství technické literatury, Prague.

12. Řada, J. 2021, *Geogebra kniha: 3-sphere in a 4-perspective*, https://www.geogebra.org/m/qw297dfd [accessed 1st July 2021]

13. Řada, J. Zamboj, M., 2020. *3D printed models of a tesseract in the double orthogonal projection and 4D perspective*, Proceedings of Slovak-Czech Conference on Geometry and Graphics 2020, volume 40, pp 153-158, Pardubice. Vydavatelský servis, Plzeň.

14. Zachariáš, S., Velichova, D., 2000. *Projection from 4D to 3D*. Journal for Geometry and Graphics, 4(1), 55-69.

15. Zamboj, M., 2018a. *Double Orthogonal Projection of Four-Dimensional Objects onto Two Perpendicular Three-Dimensional Spaces*. *Nexus Network Journal*, 20. pp. 267–281.

16. Zamboj, M., 2018b. *Sections and Shadows of Four-Dimensional Objects*. *Nexus Network Journal*, 21. pp. 475–487.

17. Zamboj, M., 2019b. *1-2-3-sphere in the 4-Space. In Proceedings of Slovak-Czech Conference on Geometry and Graphics*, pp. 217-222.

18. Zhang, H., Hanson, A., 2007. *Shadow-driven 4d haptic visualization*. IEEE Transactions on Visualization and Computer Graphics, 13(6), 1688-1695.

„8th International Conference moNGeometrija, focused on the research about geometry, graphics and application to science, engineering and art“

Belgrade, 10.-12. September, 2021.

# DIMENSIONING A PTC SYSTEMS USING PARABOLA PROPERTIES

Miša Stojićević[1], Branislav Popkonstantinović[1] ,Zorana Jeli[1], Ivana Cvetković[1], Boris Kosić[1]

[1]University of Belgrade, Faculty of Mechanical Engineering, Department of Theory of Mechanisms and Machines, 11000 Belgrade, Serbia

mstojicevic@mas.bg.ac.rs

***ABSTRACT***

*Out of many geometric curves, parabola stands out in usage in concentrated solar power (CSP). Its reflective properties allow reflecting light into one single point. This paper gives insight into the geometry of parabolic trough concentrators from the point of designing a size of a collector regarding two inputs. The first input is a parameter of the parabola which, provides the shape and size of the reflecting surface. A second input is a deviation of the angle of incoming light. Usually, this angle is perpendicular to the parabola's directrix, but the sizing of the collector tube must consider that because manufacturing or any other inaccuracy reflected ray might disperse from the focal point of the parabola. A detailed view of this dissipation of reflected rays depending on the entering ray's angle will be explained in the paper. A geometrical and algebraic display will be given, and a formula for sizing collector will be derived. In this equation two input values will be combined: parameter of parabola and value of the deviation of entering ray of light. This gained formula can later be used to show dependence between these two inputs and provide the answer to a question: is there a way to construct a mechanism that will move the focal point in accordance to changing entering angle and parameter of a parabola?*

**Keywords:** parabolic trough collector; parabola; concentrated solar power; focal point; applied geometry, accuracy; design

## 1 INTRODUCTION

In geometry of concentrated solar power (CSP) parabola is one of the most used curve. Its property to concentrate ray into one focal point is used in several types of CSP installations (Stojicevic et al.., 2019). One of those installation is parabolic trough solar thermal power (PTSTP) system. In core of this system is parabolic trough collector (PTC), shown in Fig 1a and Fig. 1b, which is made out of parabolic-shaped mirrors with a tube as receiver placed in focal point. Principle of work is very simple: Sun rays are reflected from parabolic shaped long mirrors and reflected into one point were collector is placed. PTC is the most proven and lowest cost large-scale solar power technology available today (Price¨ et al.., 2002) and this concept has been proven in many countries (Fernández-García, A. et al.., 2010). In 1870, the first practical experience with PTCs belonged to John Ericsson (a Swedish engineer immigrant to the United States), who designed and constructed a collector with an aperture area of (3.25 m2) to produce steam for drive a small (373 W) engine. He also built (from 1872 to 1875) seven similar systems with air as working fluid (Abdulhamed, A.J. et al.., 2018) (Pytilinski, J. T. et al.., 1978).There are several directions of research in this area described in many research papers. One direction of research in this area is usage of different materials for better effectiveness of system (Liang, H. et al..,2015) and other is geometry design. Authors in (Jebasingh, V.K. et al.., 2016) have given an insight in performance of PTC and it applications in industrial and domestic utilizations. Two similar technologies, Fresnel and PTC, are compared in (El Gharbi, N. et al.., 2011) where authors give a better performance characteristics to PTC in aspect of optical quality and thermal efficiency. Three different models were analyzed for PTC by authors (Liang, H. et al.., 2016) from aspect that solar flux is not evenly distributed on the absorber. Research of geometry of parabola is done in (Ada, Tuba et al.., 2015) and (Glaeser G. et al.., 2016) in aspect of definition of Euclidean and Taxicab geometry. Papers (Hoseinzadeh, H. et al.., 2018) and (Cheng, Ze-Dong et al.., 2015) have done research in aspect of optimization of design of PTC which gave result in decreasing size of collector’s tube. Step by step design of designed parabolic trough is given in (Masood, R. et al.., 2016) where it can be seen its basic geometry.

One more concept will be shown in this paper. Design of PTC, will be done in regard of entering rays of sunlight in angle that is not perpendicular in directrix of parabola. By changing this angle it will be show how collector's tube can be sized so that it can compensate errors that are produced from changing angle of entering ray. Similar subject is mentioned in (Macedo-Valencia et al.., 2014) where the dimensions of the collector can be seen with calculus.Aim of this paper will be on dimensioning parabolic trough collector starting with assuming that entering ray of light will deviate from its track that usually is used in designing PTC systems. Depending of angle of deviation a receiver tube will be dimensioned so it can absorb errors that are made during this deviation process.

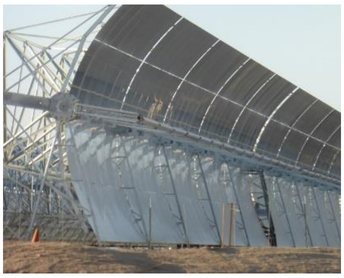

(a) (b)

**Figure 1:** (a) Parabolic trough collector and receiver tube and (b) Field of PTC in work
(Source: Z22 - Own work, CC BY-SA 3.0, https://commons.wikimedia.org/w/index.php?curid=27881587 and ArséniureDeGallium - United States Department of Energy: http://www.nrel.gov/solar/parabolic_trough.html, Public Domain, https://commons.wikimedia.org/w/index.php?curid=671862

## 2. REFLECTING PROPERTIES OF PARABOLA

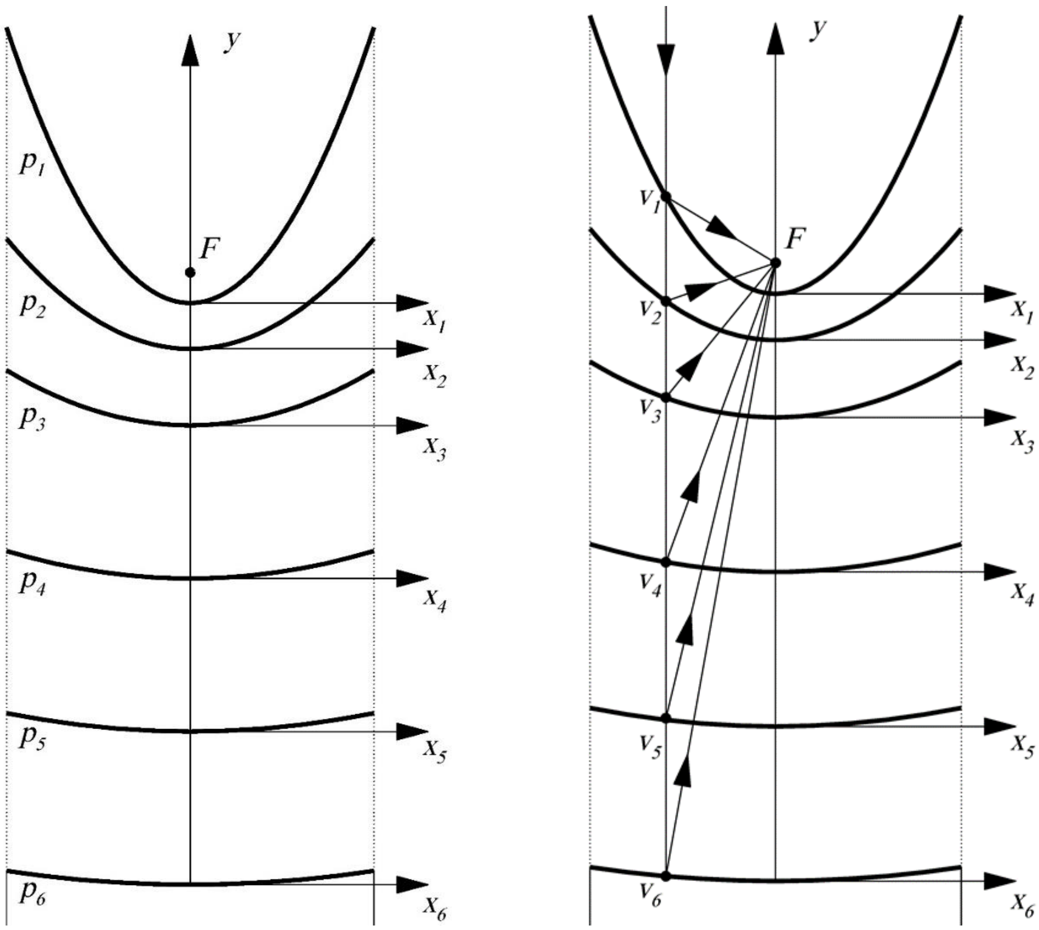


(a) (b)

**Figure 2:** (a) Virtual model of the location, and (b) An image example of different nature

In core of all this research is parabola. A parabola is a non-central second-order curve where any point on that curve is at an equal distance from the focus of parabola (F) and a fixed straight line called the directrix. Equation of parabola can be presented as: $x^2 = 2py$.

Considering that p is parameter of parabola and when p is large number parabola become narrow and steep, and when it gets smaller it flattens a parabola and distances it of its focus point F. This is shown in Fig. 2a where $p_1>p_2>p_3>p_4>p_5>p_6$. For fixed point, focal point F, parabola is flattening for same width of parabola.

To see this problem graphically dependence between shape of parabola and parameter of parabola a Fig 1b is given. Here, an entering ray passes trough points on parabola labeled with V. When hits reflecting surface in certain point a ray is redirected into focal point F.

When designing PTC systems a parameter of parabola is very important. All six parabolas are receiving a same amount of light it can be noted that 5th and 6th parabola are giving a potential trouble for design for its focal point is much more distanced from mirror surface.

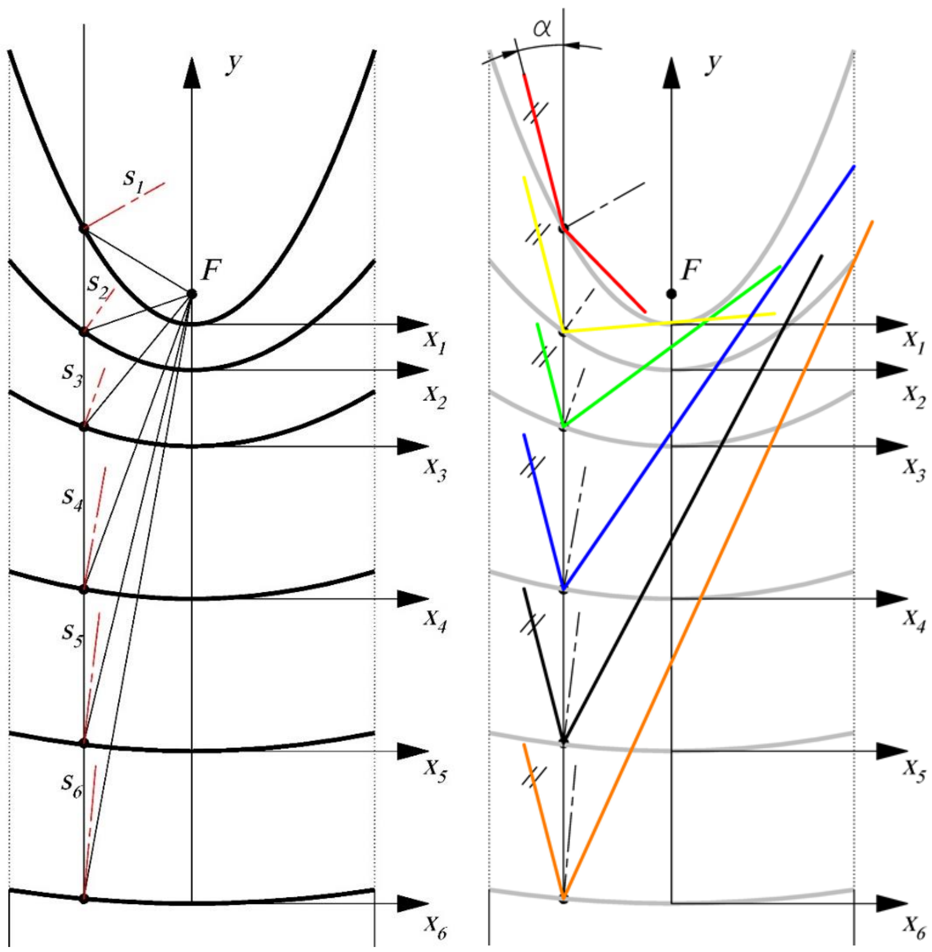


(a) (b)

**Figure 3:** (a) Virtual model of the location, and (b) An image example of different nature

Assumption is that every point V, where ray is reflected of surface, there must be a line that passes trough point V and which is a symmetry for entering and exiting ray. For all 6 parameters of parabola, a symmetry line can be seen of Fig 3a. With rise of parameter a symmetry line will be steeper and steeper. This symmetry will remain even if entering ray is deviates by angle $\alpha$ as can be seen in Fig3b. In parabolic trough CSP systems a collector is placed in center of focal point F. All rays that are reflected from surface must at least be tangent to collector's diameter. This way, collector tube will absorb all reflected ray within allowed angle $\alpha$. All this point to a conclusion that there must be a formula that binds parameter of parabola, position of point V and entering angle $\alpha$ in order to gain a diameter of collector tube for parabolic trough.

## 3. EQUATIONS OF PARABOLA

Parabola can be represented as set of vertices that are on an equal distance from directrix and focus point ($d_P$: $y = \frac{p}{2}$), p>0 where p is parameter of parabola with coordinates:

$$F = (0, \frac{p}{2}) \quad \text{(Eq. 1)}$$

Equation of parabola shown in Fig. 2 can be described using equation:

$$x^2 = 2py \quad \text{(Eq. 2)}$$

For any line, represented with general equation as $= kx + n$ , that passes through parabola $x^2 = 2py$ as a tangent of that parabola, in point V($X_v$, $Y_v$), equation 2 must be satisfied:

$$p = 2kn \quad \text{(Eq. 3)}$$

Then a tangent in point V($X_v$, $Y_v$) on parabola can be described as:

$$y_t \cdot y_v = p(X_t + X_v) \quad \text{(Eq. 4)}$$

For a point V on parabola it can be said that a tangent line can be represented as

$$Y_t = \frac{p}{Y_v} X_t + \frac{pX_v}{Y_v} \quad \text{(Eq. 5)}$$

For line $y = kx + n$ to be rotated for 90 degrees it can be presented as:

$$y = -\frac{1}{k} x + n \quad \text{(Eq. 6)}$$

Then Equation 5 becomes:

$$y_s = -\frac{Y_v}{p} x_s + \frac{pX_v}{y_v} \quad \text{(Eq. 7)}$$

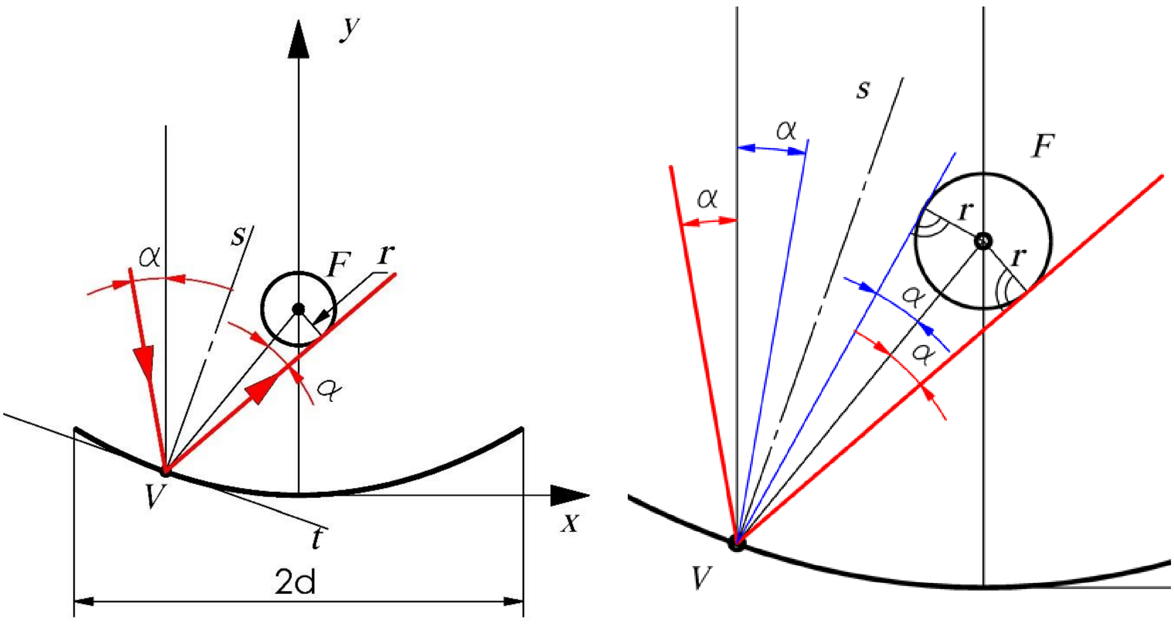


(a) (b)

**Figure 4**: (a) Virtual model of the location, and (b) An image example of different nature

Equation 6 is a line that passes through point V on parabola and represents a symmetry between input and output ray on reflective surface. Changing angle of input ray, for some alpha, will change output ray by same angle alpha.

When a symmetry can be established for certain parabola

$$r = L\,sin\ \alpha \qquad \text{(Eq. 8)}$$

Where L is distance between point $V(X_V, Y_V)$ on parabola and focal point $F(X_F, Y_F)$

$$L = \sqrt{(X_F - X_V)^2 + (Y_F - Y_V)^2} \qquad \text{(Eq. 9)}$$

For a point on parabola V, which is furtherd from focal point F, it can be considered that

$X_V$ = d (or -d) and $Y_V$= $d^2/2p$

Equation 8 become:

$$L = \sqrt{(0 - d)^2 + \left(\frac{p}{2} - \frac{d^2}{2p}\right)^2} \qquad \text{(Eq. 10)}$$

Further solving this equation:

$$L = \sqrt{d^2 + \left(\frac{p^2 - d^2}{2p}\right)^2} \qquad \text{(Eq. 11)}$$

$$L = \sqrt{\frac{4p^2d^2 + p^4 - 2p^2d^2 + d^4}{4p^2}} \qquad \text{(Eq. 12)}$$

$$L = \sqrt{\frac{p^4 + 2p^2d^2 + d^4}{4p^2}} \qquad \text{(Eq. 13)}$$

$$L = \sqrt{\left(\frac{p^2 + d^2}{2p}\right)^2} = \frac{p^2 + d^2}{2p} \qquad \text{(Eq. 14)}$$

Formula for calculating a radius of collector depending from parameter of parabola, maximum distance point from y axis and value of deviation angle entering ray becomes:

$$r = \frac{p^2 + d^2}{2p} \sin \alpha \qquad \text{(Eq. 15)}$$

## 4. EXAMPLE

Equation 15 shows that angle $\alpha$ is sine function and its value can vary from 0 to 1 where for value of 1 angle $\alpha$ is 90 degrees. Considering this as a maximum that entering ray can deviate in most distant point on parabola equation 15 become dependent only on remaining two factors: parameter p and size of parabola d., radius of collector for few values of p and d is presented in Table 1.

| p \ d | 10 | 20 | 30 | 40 | 50 | 60 | 70 | 80 | 90 | 100 |
|---|---|---|---|---|---|---|---|---|---|---|
| 10 | 10 | 13 | 17 | 21 | 26 | 31 | 36 | 41 | 46 | 51 |
| 20 | 25 | 20 | 22 | 25 | 29 | 33 | 38 | 43 | 47 | 52 |
| 30 | 50 | 33 | 30 | 31 | 34 | 38 | 41 | 46 | 50 | 55 |
| 40 | 85 | 50 | 42 | 40 | 41 | 43 | 46 | 50 | 54 | 58 |
| 50 | 130 | 73 | 57 | 51 | 50 | 51 | 53 | 56 | 59 | 63 |
| 60 | 185 | 100 | 75 | 65 | 61 | 60 | 61 | 63 | 65 | 68 |
| 70 | 250 | 133 | 97 | 81 | 74 | 71 | 70 | 71 | 72 | 75 |
| 80 | 325 | 170 | 122 | 100 | 89 | 83 | 81 | 80 | 81 | 82 |
| 90 | 410 | 213 | 150 | 121 | 106 | 98 | 93 | 91 | 90 | 91 |
| 100 | 505 | 260 | 182 | 145 | 125 | 113 | 106 | 103 | 101 | 100 |

**Table 1**: Maximum size of r relative to p and d

Graphical representation of this is shown in Fig. 5 where a size of collector is on y axis and d is on x axis.

On this graph it can be seen that for a parameter p=10, maximum size of collector will rise much faster than case where parameter is larger. For three parameters equal to 150, 200 and 250 growth of collector's size is nearly same relative to much lower parameter of 10. Collector size will be better scaled if parameter of parabola is larger and it will absorb more errors that are made from changing angle of entering ray.

Table 1 and Fig 5 shows a values for a size of collector when part of equation 15 is at its maximum. This maximum is when entering angle is 90 degrees which is very large angle to be taken in consideration during design of PTC. In order to grasp a relative angle that can be considered an angle of entering ray is show it graphically. Fig. 6 shows a parabola with 11 equidistant points on it. For all this points, a symmetry line is drawn accordant to Equation 7. This can be visually confirmed as entering rays and reflected rays are symmetrical to each other relative to symmetric line.

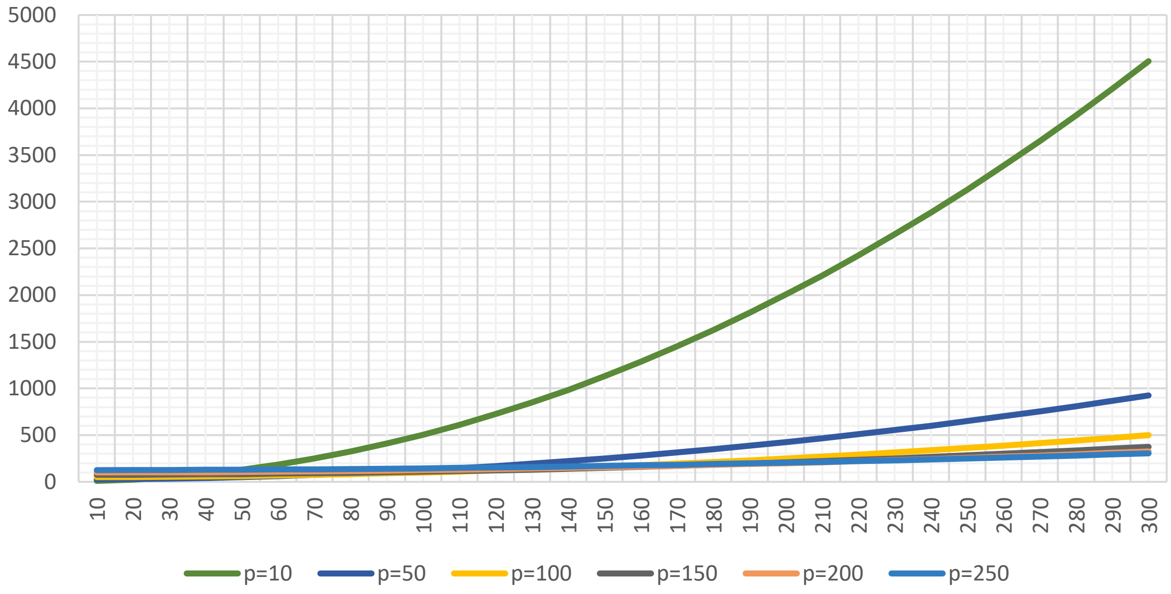


**Figure 5:** Size of collector depending of parameter p and distance d when $\sin\alpha = 1$

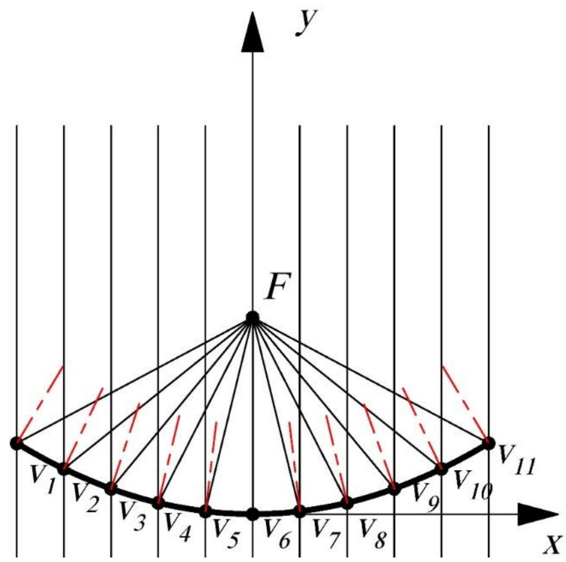


**Figure 6:** Parabola with symmetries in 11 points.

Fig. 7a to Fig. 7d is showing what is happening when angle $\alpha$ have four different values of this angle and it can be seen how a potential diameter of collector is growing and for angle large as much of 30 degrees. Most distant points will reflect entering ray back to parabola (Fig. 7c). For value of 45 degrees (Fig. 7d) dimension of collector that will absorb all errors is impossible.

Example can be made if values of parameter of parabola and most distant point are taken from Table 1. For values of p=100 and d= 50 a maximum radius size is r=125. In order to absorb all angles lesser than 10 degrees a size of collector is r=22. If a parameter of parabola is changed to be 3 times larger a size of collector will slightly change to r= 27.

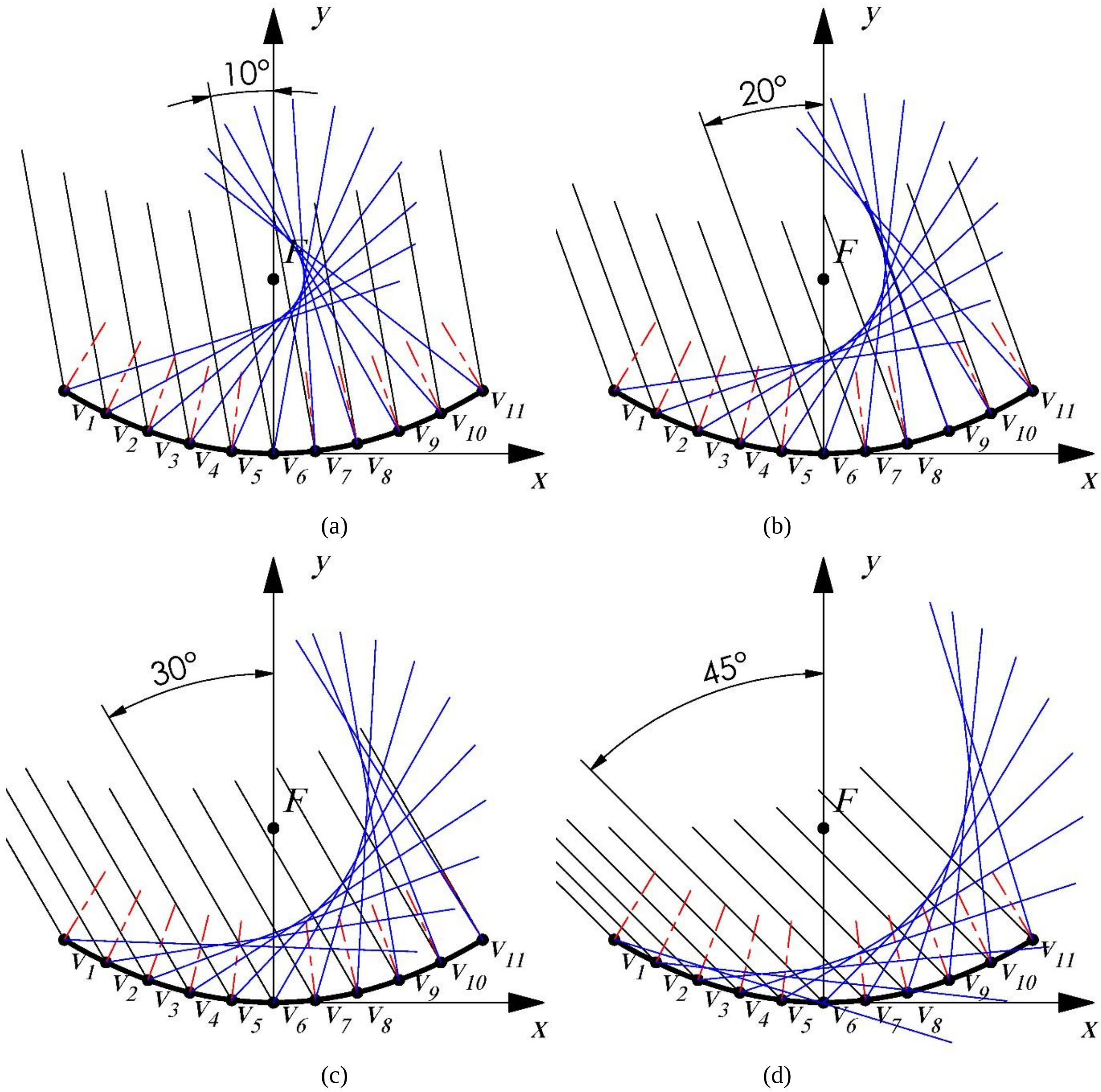


**Figure 7:** (a) Reflection of ray when $\alpha = 10$ deg (b) Reflection of ray when $\alpha = 20$ deg (c) Reflection of ray when $\alpha = 30$ deg (d) Reflection of ray when $\alpha = 45$ deg

## 5. CONCLUSION AND FURTHER RESEARCH

The parabolic trough solar thermal power (PTSTP) system has, among all other CSP systems, a lowest cost of exploration (Price¨ et al.., 2002), (Grena, Roberto et al.., 2010) but at this moment it is more expensive than fossil fuel plants of same capacity (Price¨ et al.., 2002, Cheng, Z.D. et al.., 2014, Cheng, Z.D. et al.., 2015). As a prices of using

CSP systems drops, more interest will be shifted into green and renewable energy sources. Aim of this paper is to bring a small contribution in geometry of renewable technologies. It gives an insight in one seemingly insignificant problem that can be described as dimensioning a collector in PTC but it provides a start point for further research in this area. Algebra is provided so a potential user can check results in some software program for mathematical representations.

Further research, which will be based on this paper, can be best described as finding optimum size of collector and to do a thermodynamic calculations to see a heat transfer. Size of collector have a giant impact of efficiency of entire system in term of capacity of future plant. In this case collector will be static. Second path of research will be to look for a possible way to keep a size of collector as small as it can be in order to heat it up fast. In order to do so hypothesis is that a parabola will have a moving focal point that moves in way to absorb all reflected rays. Idea here is that a heavy large parabolic mirror will stay still or have a least possible movement. Meanwhile a much lighter and smaller collector will move by previously given trajectory. In overall this system should be in theory much more energy efficient than systems which required for movement of entire parabolic mirrors.

## REFERENCES

1. Stojicevic, M., Jeli, Z., Obradovic, M., Obradovic, R. and Marinescu, G.C., 2019. Designs of solar concentrators. FME Transactions, 47(2), pp.273-278.

2. Price, H., Lu¨ pfert, E., Kearney, D., Zarza, E., Cohen, G., Gee, R. and Mahoney, R., 2002. Advances in parabolic trough solar power technology. J. Sol. Energy Eng., 124(2), pp.109-125.

3. Fernández-García, A., Zarza, E., Valenzuela, L. and Pérez, M., 2010. Parabolic-trough solar collectors and their applications. Renewable and Sustainable Energy Reviews, 14(7), pp.1695-1721.

4. Abdulhamed, A.J., Adam, N.M., Ab-Kadir, M.Z.A. and Hairuddin, A.A., 2018. Review of solar parabolic-trough collector geometrical and thermal analyses, performance, and applications. Renewable and Sustainable Energy Reviews, 91, pp.822-831.

5. Pytilinski, J. T. (1978). Solar energy installations for pumping irrigation water. Solar energy, 21(4), 255-262.

6. Liang, H., You, S. and Zhang, H., 2015. Comparison of different heat transfer models for parabolic trough solar collectors. Applied energy, 148, pp.105-114.

7. Jebasingh, V.K. and Herbert, G.J., 2016. A review of solar parabolic trough collector. Renewable and Sustainable Energy Reviews, 54, pp.1085-1091.

8. El Gharbi, N., Derbal, H., Bouaichaoui, S. and Said, N., 2011. A comparative study between parabolic trough collector and linear Fresnel reflector technologies. Energy Procedia, 6, pp.565-572.

9. Liang, H., You, S., & Zhang, H. (2016). Comparison of three optical models and analysis of geometric parameters for parabolic trough solar collectors. Energy, 96, 37-47.

10. Ada, Tuba, Aytaç Kurtuluş, and H. Bahadır Yanik. "Developing the concept of a parabola in Taxicab geometry." International Journal of Mathematical Education in Science and Technology 46.2 (2015): 264-283.

11. Glaeser, Georg, Hellmuth Stachel, and Boris Odehnal. The Universe of Conics: From the ancient Greeks to 21st century developments. Springer, 2016..

12. Hoseinzadeh, Hamed, Alibakhsh Kasaeian, and Mohammad Behshad Shafii. "Geometric optimization of parabolic trough solar collector based on the local concentration ratio using the Monte Carlo method." Energy Conversion and Management 175 (2018): 278-287.

13. Cheng, Ze-Dong, Ya-Ling He, Bao-Cun Du, Kun Wang, and Qi Liang. "Geometric optimization on optical performance of parabolic trough solar collector systems using particle swarm optimization algorithm." Applied energy 148 (2015): 282-293.

14. Masood, R., Gilani, S.I.U.H. and Al-Kayiem, H.H., 2016. A simplified design procedure of parabolic trough solar field for industrial heating applications. ARPN J. Eng. Appl. Sci, 11, pp.13065-13071.

15. Macedo-Valencia, J., Ramírez-Ávila, J., Acosta, R., Jaramillo, O.A. and Aguilar, J.O., 2014. Design, construction and evaluation of parabolic trough collector as demonstrative prototype. Energy procedia, 57, pp.989-998.

16. Grena, Roberto. "Optical simulation of a parabolic solar trough collector." International Journal of Sustainable Energy 29, no. 1 (2010): 19-36.

17. Cheng, Z.D., He, Y.L., Wang, K., Du, B.C. and Cui, F.Q., 2014. A detailed parameter study on the comprehensive characteristics and performance of a parabolic trough solar collector system. Applied thermal engineering, 63(1), pp.278-289.

18. Cheng, Z.D., He, Y.L. and Qiu, Y., 2015. A detailed nonuniform thermal model of a parabolic trough solar receiver with two halves and two inactive ends. Renewable Energy, 74, pp.139-147.

# ORTHOPEDIC HIP REVISION ASSEMBLY WITH FRAGMENTED GRAFT AND RECONSTRUCTION NET - AN EXPERIMENTAL AND VIRTUAL APPROACH

D.L. Popa[1], G. Buciu[2*], D.D. Vintilă[3], A. Duță[1], I.L. Petrovici[4], C.D. Călin[5]

[1]University of Craiova, Faculty of Mechanics, Department of Automotive, Transportation and Industrial Engineering, 200512 Craiova, Romania

[2]Titu Maiorescu University, Faculty of General Health Care, 210106 Targu Jiu, Romania

[3]University of Craiova, Faculty of Mechanics, Department of Applied Mechanics, 200512 Craiova, Romania

[4]University of Medicine and Pharmacy of Craiova, Faculty of Medicine, 200349 Craiova, Romania

[5]Slatina County Emergency Hospital, Orthopedics and Traumatology Section, 230008 Slatina, Romania

buciugabriel@yahoo.com

***ABSTRACT***

*Primary and revision hip arthroplasty are considered today the life-saving solution in hip joint damage. Over time, prosthetic wear occurs, resulting in prosthetic loss. This is a complication that must be carefully managed as certain aspects must be anticipated related to: the present implant which will be removed, the instrumentation, how to restore existing bone defects, and the patient's characteristics (osteopenia, osteoporosis, comorbidities). The use of the "Bone Packing" technique in the recovery of acetabular defects is based on a study of the results of at least 10 years, but also numerous internships carried out in our country and Europe. Initially, the devices and methods needed for experimental testing were identified. Also, a device for fixing the orthopedic orthopaedic assembly was designed and modelled, which was practically made. Using this device through which the orthopedic assembly with the reconstruction net and the fragmented graft made on a hip taken from the cow was fixed on a universal test machine and the forces to which this system has a mechanic failure were obtained. For the virtual analysis, the main methods by which virtual bone components can be obtained from CT images have been identified. Through various software techniques, these primary geometries have been transformed into virtual solids. These virtual models were imported into a finite element analysis software. Finally, for the integer human hip and for the orthopedic assembly with the fragmented graft, the applications were run, result maps were obtained and important conclusions were drawn.*

**Keywords:** virtual reality, medical imaging, orthopedic hip revision, virtual test, 3D reconstruction

## 1. INTRODUCTION

Primary hip arthroplasty is considered, today, the saving solution in hip joint damage. Undoubtedly, we can say that the appearance of these implants has radically changed the quality of life of patients with joint pain. Therefore, the number of these interventions has greatly increased. The new implants created allow the prosthesis of even younger patients, the immediate results being spectacular. Over time, prosthetic wear occurs, resulting in prosthetic loss. This is a complication that must be carefully managed as certain aspects must be anticipated related to: the implant present and to be removed, the instrumentation, how to recover existing bone defects, as well as the patient's characteristics: elderly, deficient bone bed (osteopenia, osteoporosis), comorbidities (Popa et al., 2014).

Prosthesis loosening is an alteration of the function and position of a total hip prosthesis with reference to the initial surgical moment. In the natural evolution of an arthroplasty, loosening is a real phenomenon, which can appear sooner or later being influenced by a multitude of factors. It has been observed that often the loss mechanisms intertwine, sometimes even potentiating by altering the bone-prosthesis / bone-cement interface and more rarely, the cement-prosthesis interface (Ciunel et al., 2014).

The fragmented graft proved to have a predictable integration. Numerous studies show very good results (cup migration <5 mm at 7 years, full integration according to CONN criteria and CT examination) in the case of the impacted bone graft. The most common source is fresh-frozen allograft of the femoral head, 1/3 distal femur or 1/3 proximal tibia (Buciu et al., 2014).

The acetabular reconstruction net can be used in all acetabular defects except pelvic discontinuity. It must be associated with a fragmented and impacted bone graft. It can be modelled and adjusted intraoperatively to the existing bone defect. The attachment to the host bone is made with screws, ensures a good primary stability, usually the chosen cup is a cemented polyethylene one (Petrovici et al., 2019).

## 2. CONSTRUCTION OF AN ORTHOPEDIC ASSEMBLY WITH MORCELATED BONE GRAFT AND RECONSTRUCTION NETWORK. EXPERIMENTAL TESTING

A segment of the femur and pelvic bone were taken from an animal (cow). Figure 1 shows these bone components that were analyzed and after the analysis establishing the surgical procedures and performing the orthopedic assembly.

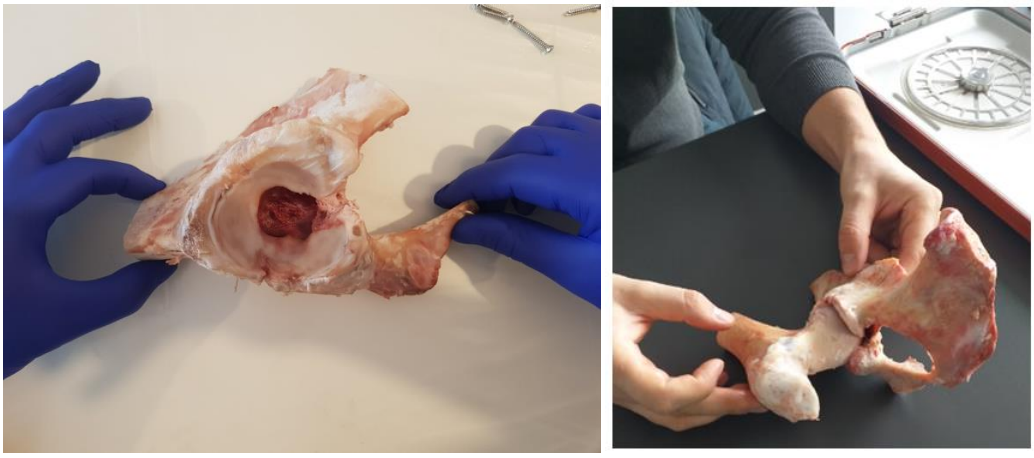

**Figure 1**: The two bone components taken from the animal (cow)

To obtain this assembly, a fragmented bone graft was created as shown in Figure 2.

**Figure 2**: Obtaining the fragmented graft

The areas to be removed were marked on the bone taken from the animal and removed using the specific instrumentation and the positioning of the polyethylene cup was tested (Figure 3).

**Figure 3**: Remove marked areas and position the cup

The fragmented bone graft was placed in the acetabular cavity and adjusted in the areas with bone loss using the specific instrumentation. Next, the reconstruction mesh was prepared, cut and adjusted to the necessary dimensions so as to completely cover the fragmented bone graft, the reconstruction net was fixed using orthopedic screws and the positioning of the polyethylene cup was checked, as shown in Figure 4.

**Figure 4**: Steps for locating the fragmented graft and the reconstruction net

Finally, the acetabular cavity was covered with orthopedic cement and the assembly was obtained with a fragmented bone graft and reconstruction mesh, as shown in Figure 5.

**Figure 5**: Final assembly with fragmented graft and reconstruction mesh

The orthopedic assembly with fragmented bone graft and reconstruction net was placed in the fixing device. The prosthesis stem was also attached to the upper device of the fastening system so that the action of the force was vertical. Figure 6 shows the assembly with fragmented bone graft and reconstruction net on the EDZ 20 test machine.

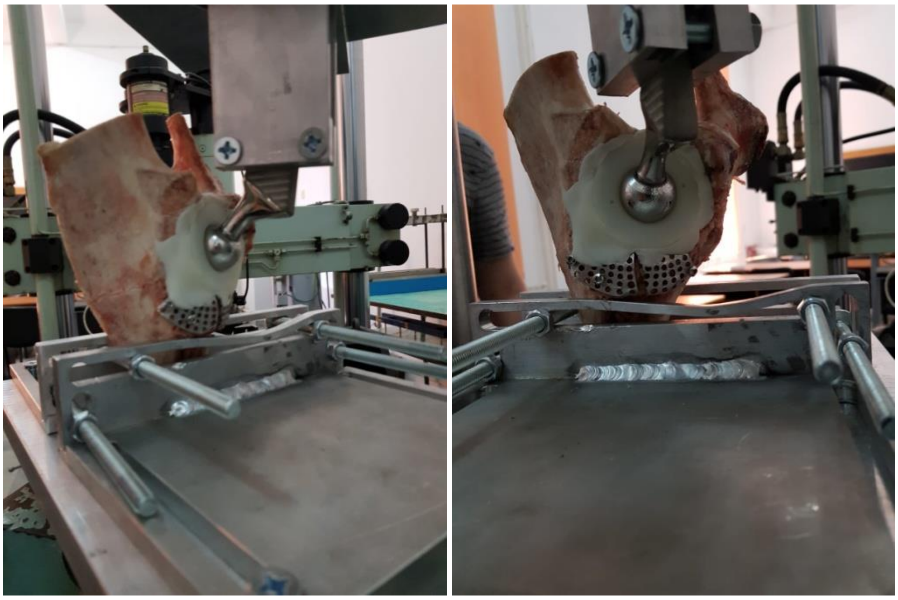

**Figure 6**: Assembly with fragmented bone graft and reconstruction mesh attached to the EDZ 20 test machine

The force was gradually amplified until the orthopedic assembly with a fragmented bone graft and reconstruction net failed. On the panel of the universal machine EDZ 20 was read the value of 1790 Kgf, ie 17559 N. After the failure of the assembly, it was studied and analyzed with the digital stereomicroscope INSIZE ISM-PM200SB, a series of images being presented in Figure 7.

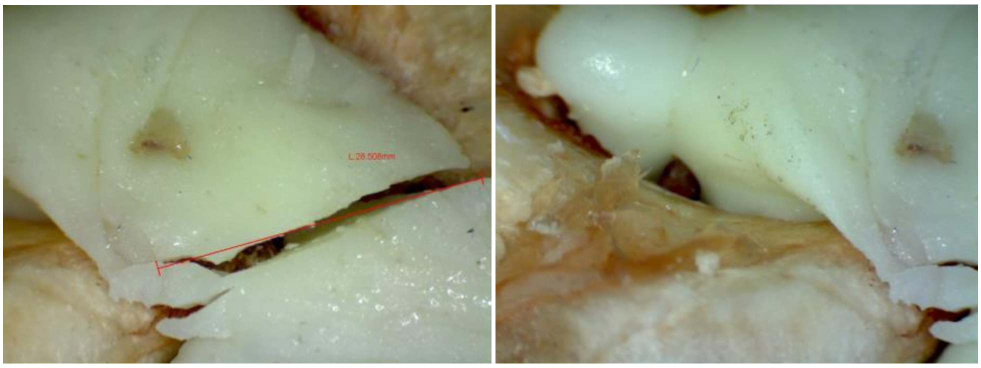

**Figure 7**: Images and measurement realized using the digital stereomicroscope

## 3. THE THREE-DIMENSIONAL MODEL OF THE INTEGER HIP JOINT

### 3.1 3D Model Of The Pelvic Bone

Six sets of CT scans performed on various patients were used to obtain the geometry of the human hip joint. These CT scans were analyzed and, finally, we studied the set that was considered to be as close as possible to an ideal hip joint. Figure 8 shows the interface of the InVesalius program after uploading DICOM files obtained from the CT scanner.

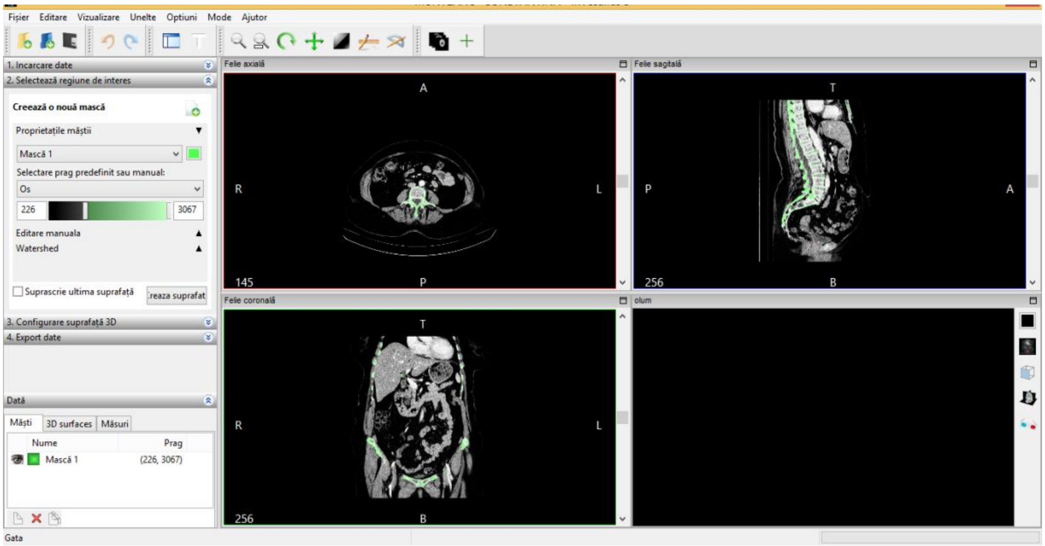


**Figure 8**: InVesalius program interface.

Through specific commands that involve the choice of a template that allows identification based on the shades of gray corresponding to bone tissue, a primary model was obtained for the tomographic area on the patient. Obviously, this primary model, presented in Figure 9, there are also elements that are not of interest in this study, including geometries due to X-ray reflection and refraction.

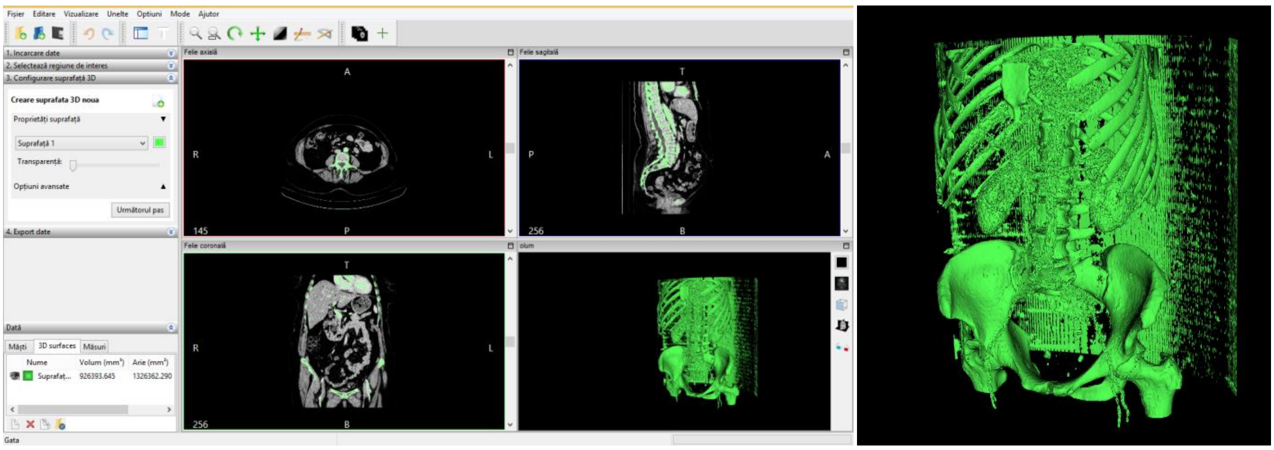

**Figure 9**: Primary geometry obtained with the InVesalius program

To process this model in a .stl format similar to three-dimensional scanning, this geometry was loaded into the Geomagic program. Figure 10 shows the interface of the Geomagic program after loading the model.

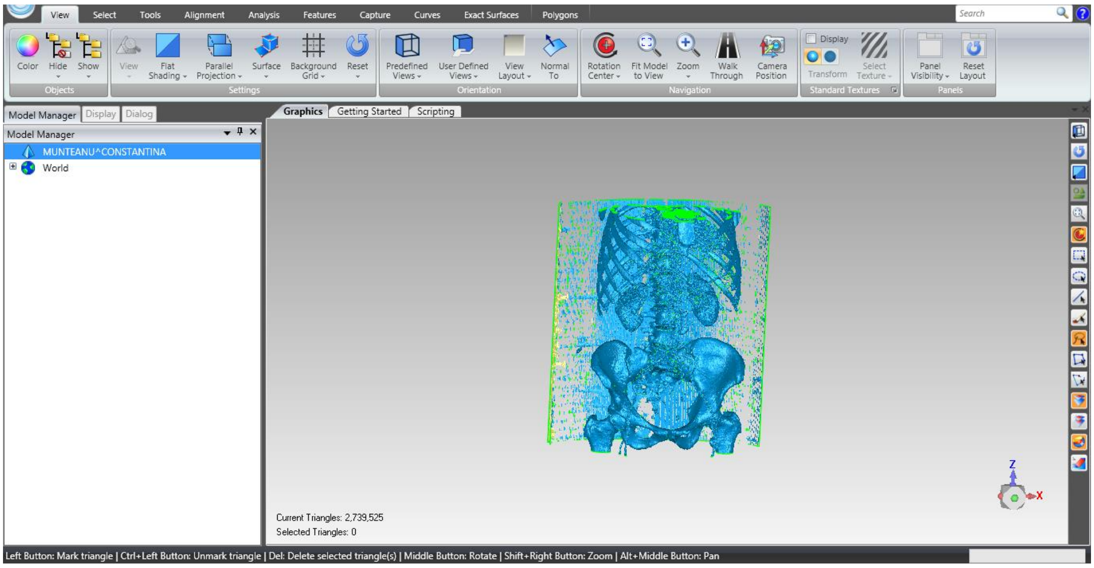


**Figure 10**: Geomagic program interface

Obviously, the model also contained elements that were not of interest, such as other bone components or elements of the computer tomograph support. These items were removed manually, in several steps, using a lasso-type selection, as shown in Figure 11.

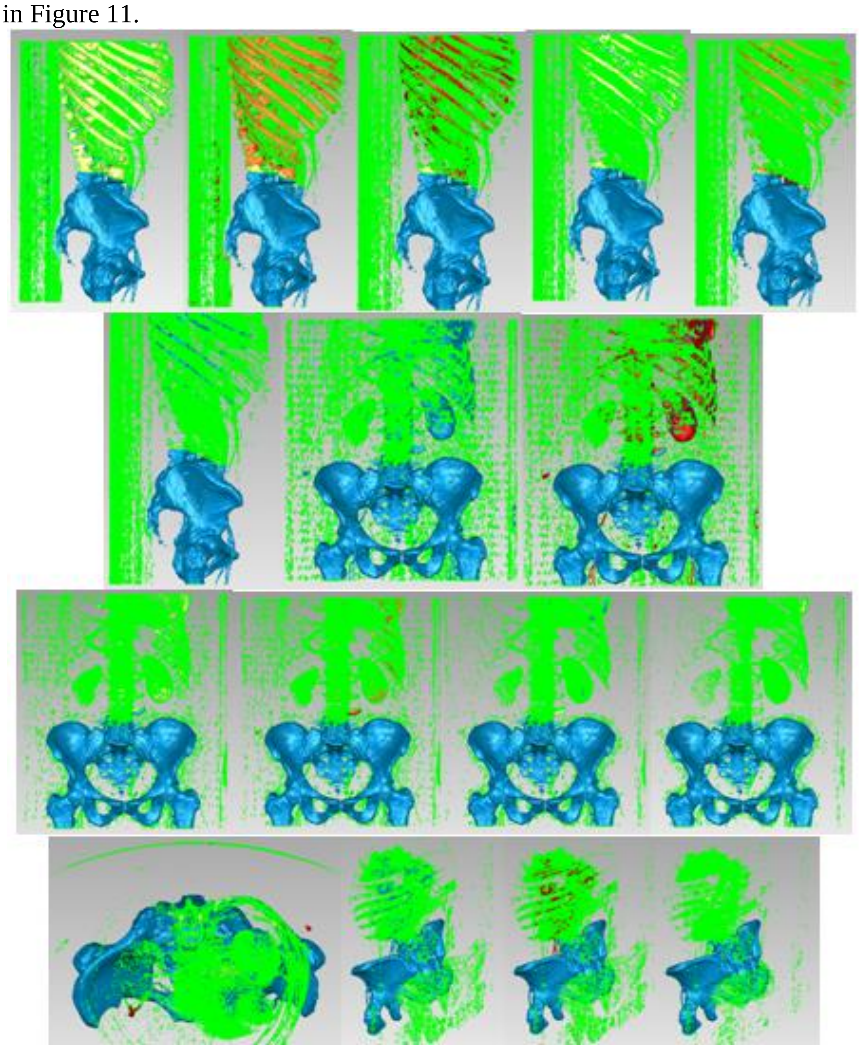

**Figure 11**: Steps to remove additional items

Several removals and finishing techniques were applied. The model had at that time 234,830 triangular elementary surfaces. It is known that a model that has more than 200,000 surfaces cannot be transformed into a virtual solid. To decrease this number, the Decimate command was used, which reduces the quality of the model. In this case, the Smooth command that finishes the model was later used. This model was exported to SolidWorks where it was automatically transformed into a virtual solid (Calin et al.., 2016). Figure 12 shows the model after loading and after applying smoothing and visualization commands.

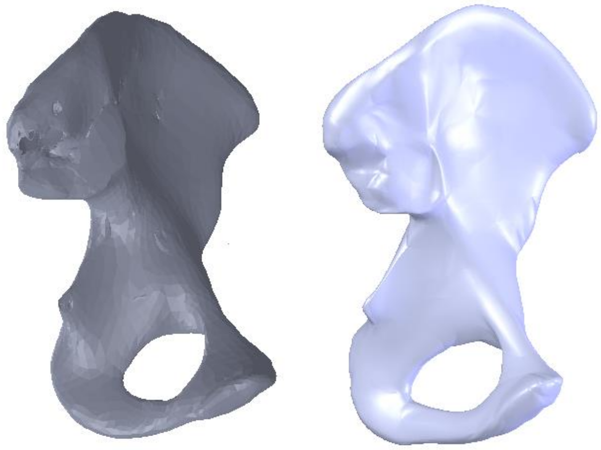

**Figure 12**: Virtual model of the left iliac bone in SolidWorks

### 3.2 3D Model Of The Sacrum Bone

To obtain the virtual model of the sacrum, we started from the same model obtained from the set of tomographs that was processed using similar CAD techniques used in both the Geomagic program and SolidWorks. The final model from Geomagic was imported into Solidworks and automatically transformed into a virtual solid, as shown in Figure 13.

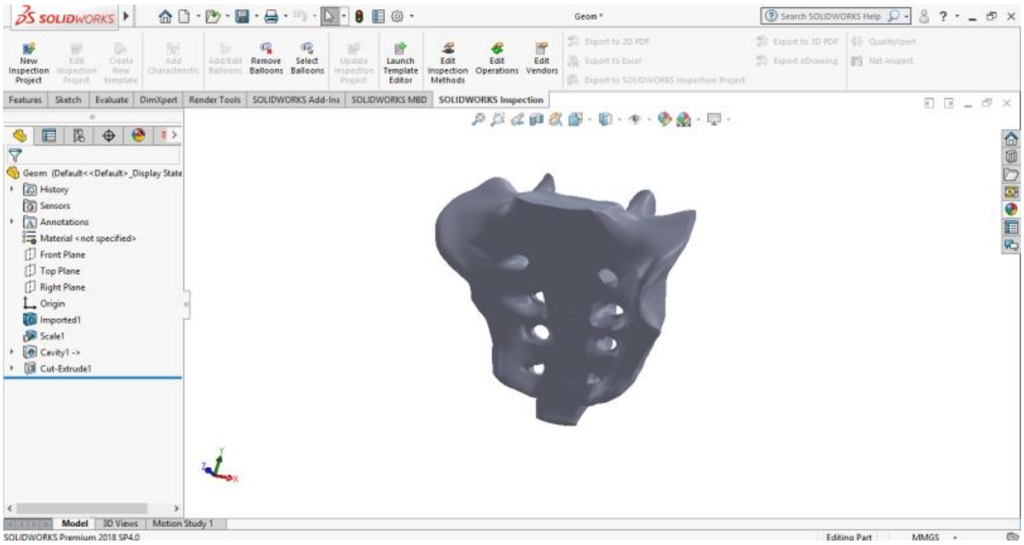


**Figure 13**: The virtual model of the sacrum in SolidWorks

### 3.3. 3D model of a femur

To obtain the virtual model of the femur, a tomography of a femur taken from a corpse was used. Figure 14 shows this femur before it is scanned at the CT scan.

**Figure 14**: Femur taken from a corpse

The set of tomographs obtained was taken from the InVesalius program where a primary geometry of the femur was generated, as shown in Figure 15.

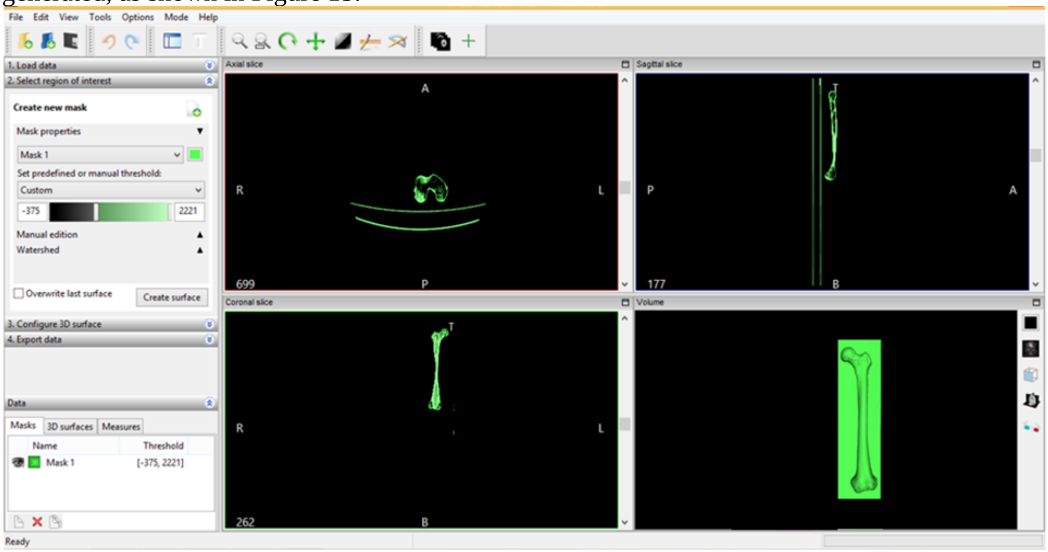


**Figure 15**: Primary geometry of the femur in the InVesalius program

This primary geometry in .stl format was loaded into the Geomagic program for processing and adaptation. At that time the model contained 1,092,725 triangular primary surfaces. The model was processed similarly, using different CAD techniques and methods in the Geomagic program. Finally, when the model had 37,919 elementary surfaces, it was exported to SolidWorks where it was automatically transformed into a virtual solid (Vatu et al., 2019), (Tarnita et al., 2010). Figure 16 shows the final virtual model of the femur in different viewing settings.

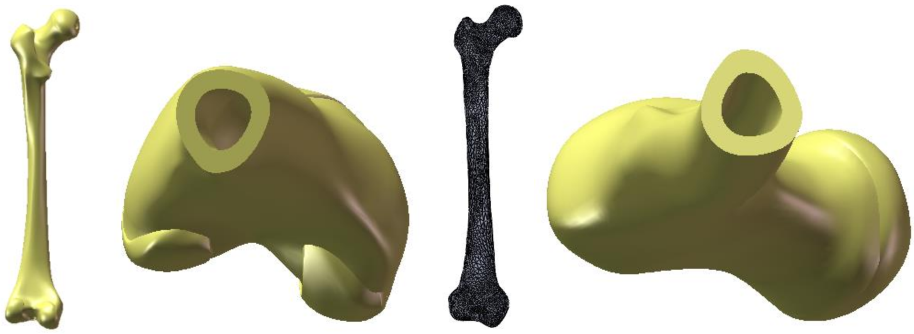

**Figure 16**: The final model of the femur in SolidWorks

### 3.4. 3D Model Of A Hip Joint

Virtual bone models were loaded into SolidWorks Assembly mode. Based on anatomical data these components were positioned and attached to each other using specific commands and CAD techniques. Also, the pubic symphysis was created directly using various data from the bibliography. Figure 17 shows the final model of the intact hip joint.

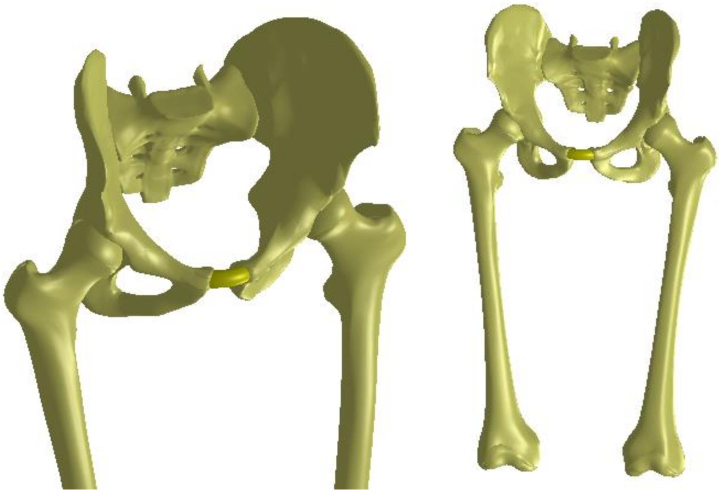

**Figure 17**: The final model of the intact hip joint

## 4. VIRTUAL EXPERIMENTAL TESTING OF THE HIP JOINT WITH REVIEW ORTHOPEDIC ASSEMBLY WITH FRAGMENTED BONE GRAFT AND RECONSTRUCTION NETWORK FOR NORMAL LOAD LOADING

The orthopedic assembly with the fragmented graft and the reconstructive net was modelled and created in SolidWorks starting from the model of the whole hip joint to which the real surgical techniques were applied, but in the virtual environment (Tarnita et al., 2018), (Popa et al., 2019). The following simplifying hypotheses were used in these analyzes:

- knowing that the orthopedic cement, used in these orthopedic assemblies, ensures the stability and fixation of the components, it was not geometrically modelled,and its behaviour was replaced with the use of Bonded finite elements, which practically ensures the binding of the components.
- it is known that, during human walking, the variation of the force that appears in the hip joint varies between the values 0 N and approximately 2300 N. We considered that, it is a cover, to use an equivalent force that has a linear variation between the values of 800 N (characteristic of orthostatic position) and 2300 N (maximum value of force during walking).
- for the revision assembly using a fragmented bone graft, the study was considered to have been performed after the osseointegration of this graft when it acquires the appearance and physical-mechanical properties of the trabecular bone.

The model of the hip joint with orthopedic revision assembly with fragmented bone graft and reconstruction net was loaded in Ansys Workbench, and the interface of this program is presented in Figure 18.

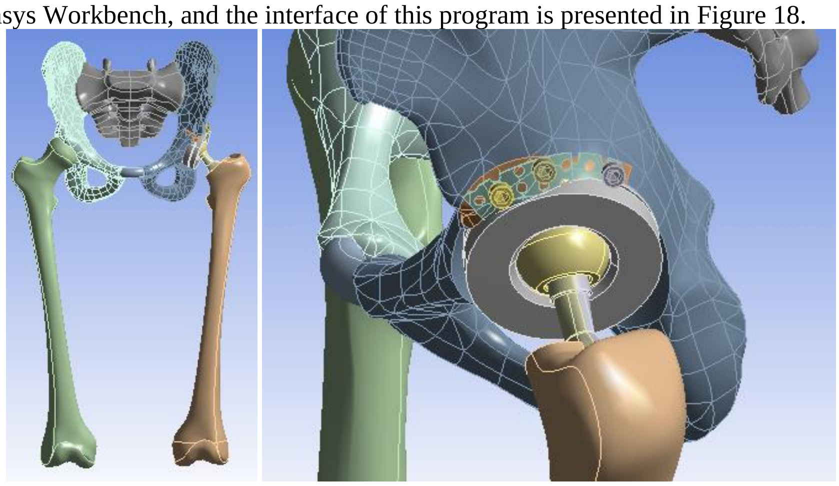

**Figure. 18**: Ansys Workbench program interface after loading the analyzed model

First of all, the division into finite elements was performed and 343,182 elements with a maximum size of 2 mm and a tetrahedral shape were obtained (Mercut et al., 2020). Figure 19 shows the finite element structure of the analyzed system.

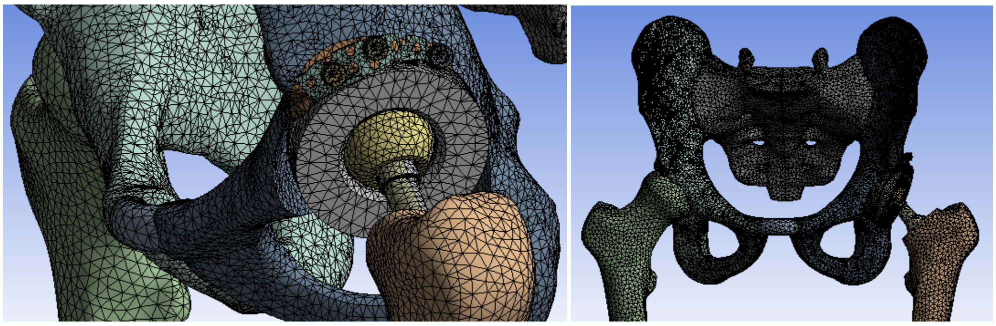

**Figure 19**: The finite element structure of the analyzed system

In order to perform a Static Structural analysis, it was considered that the system has fixation surfaces in the condylar area of the femoral bones, and a variation of the force between 800 and 2300 N during a second and positioning on the sacrum bone was considered.

The Ansys program has a module that stores the materials used, but also their characteristics, called Engineering Data. It was considered that the fragmented graft is already osseointegrated and can be considered similar to the trabecular bone. In this Engineering Data module, the materials presented in Table 1 were defined and activated. The materials and their properties were activated after analyzing a series of works (Cicciù et al., 2015), (Hsu et al., 2010), (Keulemans et al., 2015), (Benazzi et al., 2016), (Baciu 2019), (Laflamme et al., 2013), (Ambrosio et al., 2010), (Witvoet 1990), (Kirkendall et al., 2002).

| *Component* | *Material* | *Density (kg/m3)* | *Young's module (Pa)* | *Poisson's ratio* | *Transverse modulus (Pa)* |
|---|---|---|---|---|---|
| *Femur, pelvis* | *Bone* | *1400* | *1 E+10* | *0.3* | *8.3331 E+9* |
| *Fragmented graft* | *Trabecular bone* | *2140* | *1.76 E+10* | *0.25* | *7.04 E+9* |
| *Pubic symphysis* | *ligament* | *955* | *1.2 E+9* | *0.42* | *2.4 E+9* |
| *Reconstruction net* | *Stainless steel* | *7750* | *1.93 E+11* | *0.31* | *1.693 E+11* |
| *Polyethylene cup* | *Polyethylene* | *950* | *1.1 E+9* | *0.42* | *2.291 E+9* |
| *Metal spherical head* | *Stainless steel* | *7750* | *1.93 E+11* | *0.31* | *1.693 E+11* |
| *Orthopedic screw* | *Stainless steel* | *7750* | *1.93 E+11* | *0.31* | *1.693 E+11* |
| *Femoral stem* | *Stainless steel* | *7750* | *1.93 E+11* | *0.31* | *1.693 E+11* |

**Table 1**: Materials with mechanical-physical properties used in simulation

After running the application, result maps were obtained. Figure 20 shows the displacement map of the analyzed system.

Figure 21 shows the strain map.

Figure 22 shows stress maps.

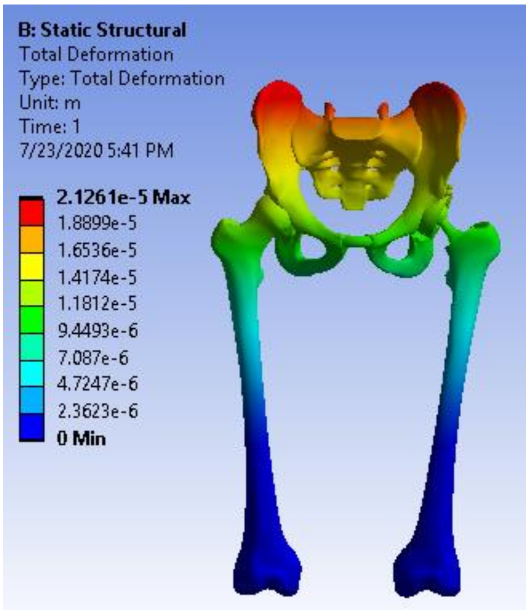


**Figure 20**: Deformation map

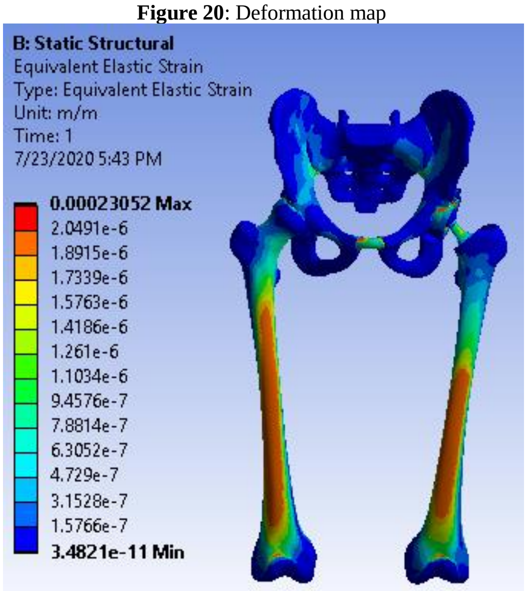


**Figure 21**: Strain map

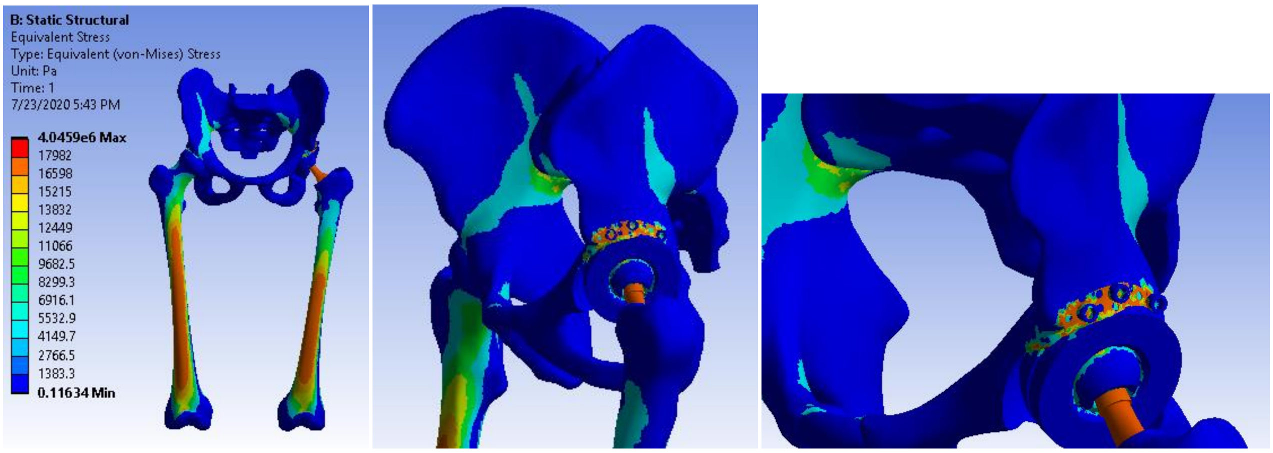


**Figure 22**: Stress maps

## 5. CONCLUSIONS

Analyzing the techniques, methods and models obtained, the following observations were highlighted:

- The components of prostheses and revision systems are parameterized, so that they can be adapted to various anthropological dimensions;
- These models can be used in various tests or real or virtual experiments;
- By attaching these revision systems to virtual bone components, various "in vitro" analysis can be obtained.

By studying and analyzing the results obtained for an orthopedic revision installation, the following conclusions and observations can be outlined:

- Analyzing the more stressed areas and surfaces from the overhaul assembly, the maximum stresses are found on the prosthesis elements, and the bone components that are in contact with them are less stressed;
- using CAD and FEM methods, very complicated biological systems can be modeled and simulated;
- the virtual models proposed in this paper were experimentally validated;
- finite element analysis methods, coupled with virtual reconstruction of CT or MRI images and reverse engineering methods, pave the way for innovation in customized orthopedic systems for each patient.

The analysis of the content of this paper highlights, at least, the following original elements:

- study, analysis and practical realization of orthopedic hip revision assemblies using animal bone elements;
- design, modeling and practical realization of an original device that allows fixing and orientation of revision assemblies for experimental testing;
- the use, in an original way, of experimental devices and techniques used in engineering to obtain experimental data for overhaul assemblies;
- the use of methods and techniques specific to engineering, in an original way, for obtaining three-dimensional models of the revised assemblies studied and analyzed;
- coupling, in an original way, medical imaging techniques with methods of reconstruction and three-dimensional modeling;
- the use of high performance equipment and programs for three-dimensional modeling and for the analysis with the finite element method of orthopedic revision assemblies;
- coupling the experimental methods with the virtual-experimental ones for mutual validation.

From the analysis of the orthopedic systems for revision of the hip prosthesis, it was found that the orthopedic assembly with fragmented bone graft and reconstruction net ensures both a good primary resistance and a durability of the assembly. It also ensures the reconstruction of the acetabural cavity and the total integration of the graft by restoring the local anatomy, the integrated bone tissue being viable and thus able to withstand daily demands. These conclusions were validated, both by experimental testing and by the finite element analysis method, using the load specific to normal human gait.

## REFERENCES

1. Ambrosio, L., A. Gloria, and F. Causa, 2010. Composite materials for replacement of ligaments and tendons, *Biomedical Composites*, L. Ambrosio, Editor 2010, Woo dhead Publishing. pp. 234-254.

2. Baciu, C. C., 2019.Reconstruction of the anterior cruciate ligament using a synthetic-biological mixed graft - experimental model on the study animal (in Romanian), *PhD Thesis*, University of Medicine and Pharmacy Carol Davila, Bucharest.

3. Benazzi, S., Nguyen, H. N., Kullmer, O. and Kupczik, K., 2016. Dynamic Modelling of Tooth Deformation Using Occlusal Kinematics and Finite Element Analysis, *PLOSONE*, pp. 1-17.

4. Buciu, G., Tarnita, D.N., Popa, D.L., Lungu, M.A., Miritoiu, C. and Ungureanu, A., 2014. Virtual and Experimental Studies about Human Walking-Virtual Lower Leg Environment-Innovative Design of Tibia Nail. *Applied Mechanics and Materials*, vol. 657, pp. 770-774.

5. Calin, D., Tarniţă, D., Popa, D., Calafeteanu, D. and Tarnita, D., 2016. Virtual Model and Simulation of the Normal and Affected Human Hip Joint. *Applied Mechanics and Materials*, vol. 823, pp. 167-172.

6. Cicciù, M., Cervino, G., Bramanti, E., Lauritano, F., LoGudice, G., Scappaticci, L., Rapparini, A., Guglielmino, E. and Risitano G., 2015. FEM Analysis of Mandibular Prosthetic Overdenture Supported by Dental Implants: Evaluation of Different Retention Methods, *Hindawi Publishing Corporation, Computational and Mathematical Methods in Medicine*, pp. 1-16.

7. Ciunel, S., Popa, D.L., Gherghina, G., Bogdan, M.L. and Tutunea D., 2014. Human Head-Neck System Behavior During Virtual Impact Automotive Simulations. *Applied Mechanics and Materials*, vol. 659, pp. 177-182.

8. Hsu, M.-L. and Chang, C.-L., 2010. Application of finite element analysis in dentistry. Finite Element Analysis, *InTech*, pp. 43-66.

9. Keulemans, F., Shinya, A., Lassila, L.V.J., Vallittu, P.K., Kleverlaan, C.J., Feilzer, A.J. and DeMoor R. J.G., 2015. Three-Dimensional Finite Element Analysis of Anterior Two-Unit Cantilever Resin-Bonded Fixed Dental Prostheses, *Hindawi Publishing Corporation, Scientific World Journal Volume*, pp. 1-10.

10. Kirkendall, D. T., and W. E. Garrett, J., 2002. Muscle, tendon, and ligament: Structure, function, and physiology, *Orthopaedics*, R. H. Fitzgerald, H. Kaufer, and A. L. Malkani, eds., Elsevier, St. Louis, MO, pp. 177-178

11. Laflamme, M., J. Lamontagne, and R. Guidoin, 2013. Anterior cruciate ligament prostheses using biotextiles, *Biotextiles As Medical Implants*, M.W.K.S.G. Guidoin, Editor 2013, Woodhead Publishing. pp. 590-639.

12. Mercut, M.F., Dumitrescu, D., Craitoiu, Ș., Mercut, R., Stefanescu Dima, A., Tanasie, A. and Popa, D.L., 2020. Three-Dimensional Model of the Human Eye Development based on Computer Tomograph Images. *Current Health Sciences Journal*, vol. 46, no. 1.

13. Petrovici, I.L., Tenovici, M.C., Vaduva, R.C., Tarnita, D.N., Vintila, G. and Popa, D.L., 2019. About Three-Dimensional Models of Osteosynthesis Systems. *Journal of Industrial Design and Engineering Graphics*, vol. 14, no. 1, pp. 159-162.

14. Popa, D.L., Buciu, G., Calin, D.C., Popkonstantinović, B. and Poenaru, F., 2019. CAD, CAE and rapid prototyping methods applied in long bones orthopaedics, *FME Transactions*, vol. 47, no. 2, pp. 279-286, 2019

15. Popa, D.L., Duta, A. and Pitru A.R., 2014. The Modeling of Some Types of Implants and Prostheses Used for Osteointegration. *SDÜ Mühendislik Bilimleri ve Tasarım Dergisi*, vol. 2, no. 3, pp. 273-281.

16. Tarnita, D., Boborelu, C., Popa, D. and Tarnita, D.N.,2018. Design and Finite Element Analysis of a New Spherical Prosthesis-Elbow Joint Assembly. *New Advances in Mechanism and Machine Science*, pp. 127-135.

17. Tarnita, D., Tarnita, D.N., Bizdoaca, N., Popa, D., Tarnita, C.E. and Cismaru, F., 2010. Modular Orthopedic Devices Based on Shape Memory Alloys. *SYROM 2009*, pp. 709-721.

18. Vatu, M., Vintila, D., Mercut, R., Popescu, S.M., Popa, D.L., Petrovici, I.L., Vintila, G. and Pitru, A., 2019. Three-dimensional modeling of the dental-maxillary system. *Journal of Industrial Design and Engineering Graphics*, vol. 14, no. 1, pp. 207-210.

19. Witvoet, J., 1990. Technique de pose d’une prothese totale de hanche a cotyle visse, *Encyl. Med. Chir.*, Ed. Techniques, Ortopedie, Paris, pp. 1-14.

# ABOUT THE METHODS FOR VIRTUAL RECONSTRUCTION OF DIFFERENT HUMAN TISSUES BASED ON CT IMAGES

D.L. Popa[1], G. Buciu[2*], D. D. Vintilă[3], A. Duță[1], I.L. Petrovici[4], C.D. Călin[5]

[1]University of Craiova, Faculty of Mechanics, Department of Automotive, Transportation and Industrial Engineering, 200512 Craiova, Romania

[2]Titu Maiorescu University, Faculty of General Health Care, 210106 Targu Jiu, Romania

[3]University of Craiova, Faculty of Mechanics, Department of Applied Mechanics, 200512 Craiova, Romania

[4]University of Medicine and Pharmacy of Craiova, Faculty of Medicine, 200349 Craiova, Romania

[5]Slatina County Emergency Hospital, Orthopedics and Traumatology Section, 230008 Slatina, Romania

buciugabriel@yahoo.com

***ABSTRACT***

*Medical imaging was an important step that greatly improved medical diagnosis. Medical imaging methods are related to computed tomography, which combines the X-rays technique and magnetic resonance imaging with computerized imaging methods. Recently, software techniques have appeared for three-dimensional reconstruction of CT or MRI images based on the transformation of shades of gray into three-dimensional geometric structures, using programs such Mimics or InVesalius. These primary geometries could be identified with the tissue structures in the human body. Thus, ranges of shades of gray specific to different tissues such as cortical bone, spongy bone, fat tissue, muscle tissue or tooth enamel were determined. Based on them, the structure of a human body, scanned by CT or MRI, can be reconstructed in a virtual environment, with considerable precision. These processes are similar to those already known by reverse engineering where the external geometry of an object can be determined by 3D scanning. Thus, using programs such as Geomagic, these structures from a patient's body can be recomposed in the virtual environment. These structures, which are initially in the form of "point clouds" (identical to those in 3D scanning) can be transformed into surfaces or virtual solids geometries using CAD techniques or reverse engineering methods. From here, these personalized structures can be 3D printed, can be loaded in a CAD environment, analyzed by FEM methods or loaded into a virtual reality system. These techniques, which are currently laborious to apply, open the way for medical diagnosis in virtual reality.*

**Keywords:** virtual reality, medical imaging, virtual tissues, medical diagnosis, 3D reconstruction

## 1. INTRODUCTION

Three-dimensional reconstruction of human tissues is important because:

- The geometric structure of the tissues can give important information about specific human pathology and can lead to a better medical diagnosis (Calin et al., 2016), (Popa et al., 2014);
- Different medical devices such as prostheses can be attached to the virtual structure of human tissues and, thus, new surgical techniques adapted to the pathology and customized morphology for each patient can be determined (Ciunel et al., 2014), (Buciu et al., 2014);
- Once obtained, the three-dimensional geometry of the tissues can be analyzed with CAD specific methods, finite element method or techniques specific to reverse engineering or rapid or virtual prototyping (Tarnita et al., 2018), (Popa et al., 2019).

Several methods are known by which, starting from tomographic images, virtual solids can be obtained to reconstruct in a virtual environment the structure of some portions of the human body. But the method that most accurately reproduces these geometries is based on automatic reconstruction based on different shades of gray of human body tissues. There are two known programs that do this in an automatic way and these are Mimics and InVesalius. InVesalius is a program developed as a free source and is dedicated to research. The result obtained after using such programs is in the form of a "point cloud" similar to the usual three-dimensional scan (Vatu et al., 2019), (Tarnita et al., 2010).

In order to be able to transform these "point clouds" into surface or virtual solid geometries, the reverse engineering methods included in Geomagic type programs are used. In these programs, in a first phase, a primary geometry based on numerous triangular surfaces can be obtained. Often, this geometry is discontinuous and cannot be immediately transformed into a virtual solid. This is, however, possible after the use of certain specific techniques and methods. Also, the number of these surfaces is very large and often it must be reduced without affecting the geometry and general shape (Petrovici et al., 2019).

## 2. THREE-DIMENSIONAL GEOMETRY OF THE DIFFERENT TISSUES OF A HUMAN HEAD

To obtain different tissues of a human head, a set of tomographic images was used, which underwent a first processing using the InVesalius program. For starters, the set of tomographic images obtained in DICOM format was loaded into the program. The primary interface of this program is shown in Figure 1.

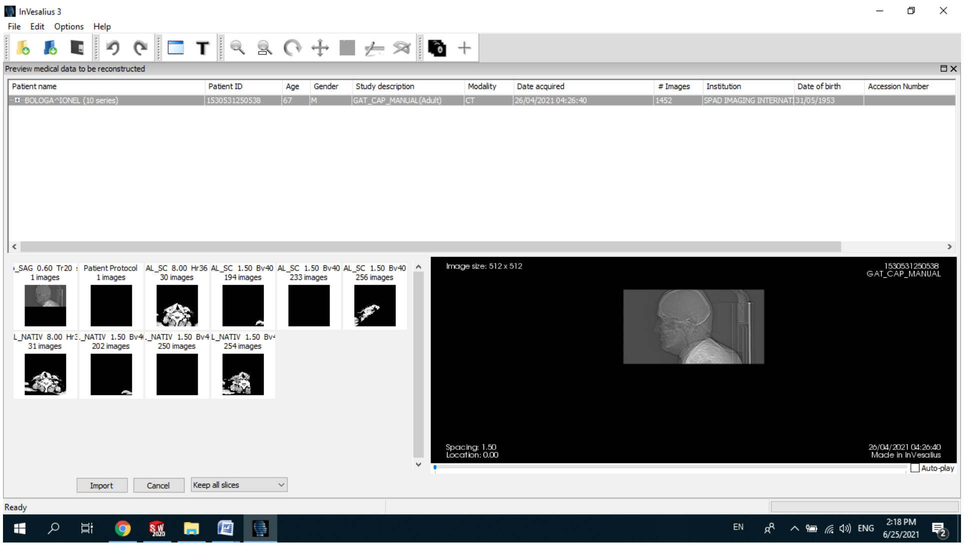


**Figure 1**: The primary interface of the InVesalius program

After the tomography set has been loaded, the program interface displays the tomographic images in three anatomical planes. You can also select the type of tissue you are interested in such as Skin, Compact Bone, Enamel, Fat Tissue, Spongial Bone a.s.o. In the fourth image the program displays the three-dimensional geometry of the selected tissue. For example, Figure 2 shows the interface of the Skin tissue program.

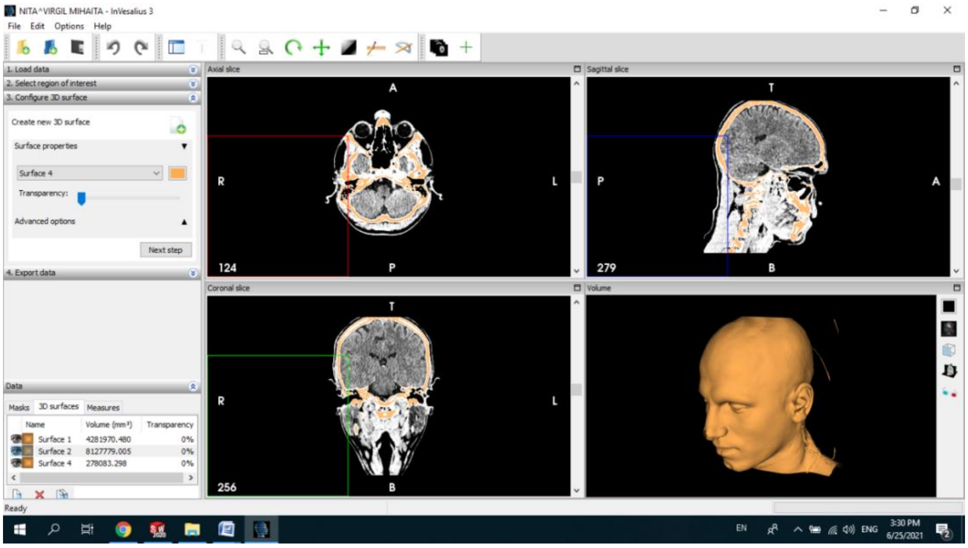


**Figure 2**: Interfata programului InVesalius pentru tesut de tip Skin

We were interested, in a first phase, in the bone structure of the human head. For this, the Compact Bone (Adult) tissue type was selected. Figure 3 shows the primary structure of bone tissue for the analyzed patient.

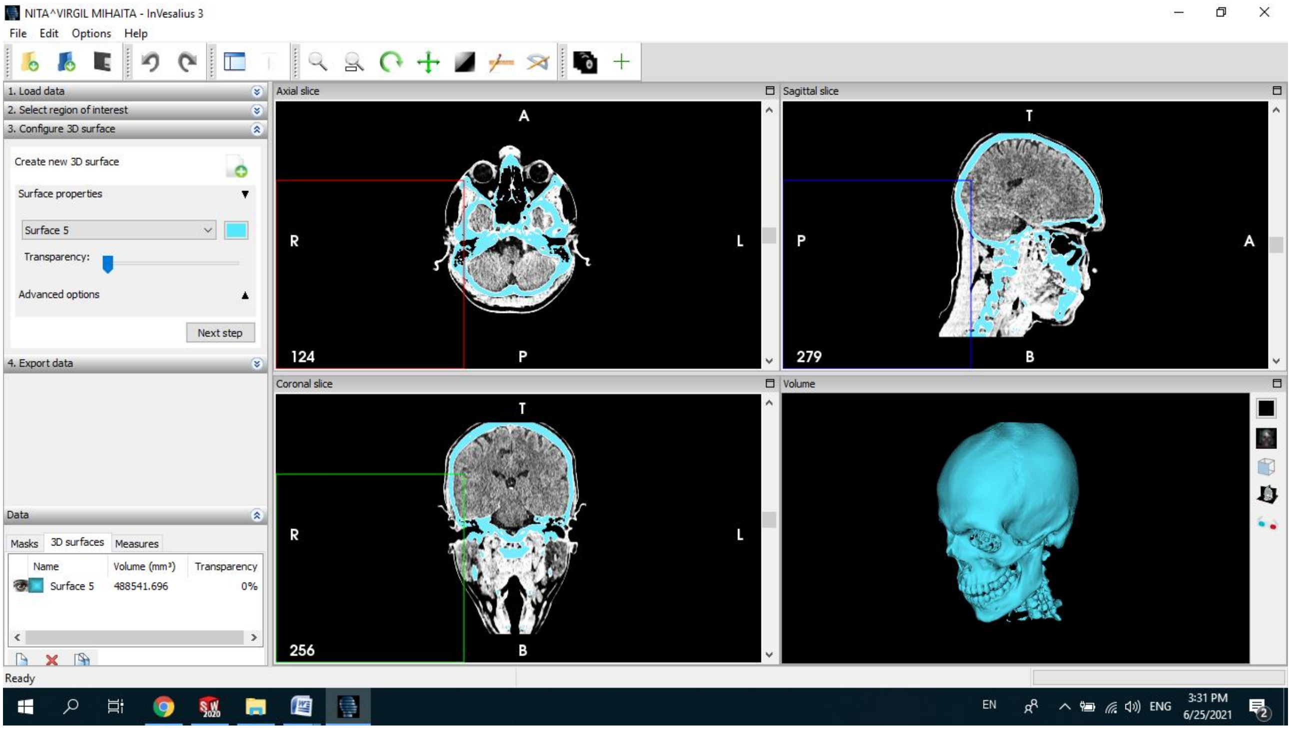


**Figure 3**: InVesalius Compact Bone Tissue Interface (Adult)

This structure is composed of a "point cloud" and can be saved in .stl (Stereolithography) format and does not contain surface or virtual solid structures, but can be 3D printed. This "point cloud" has been loaded into the Geomagic program that allows further processing. Figure 4 shows the interface of the Geomagic program with the file containing the bone structure.

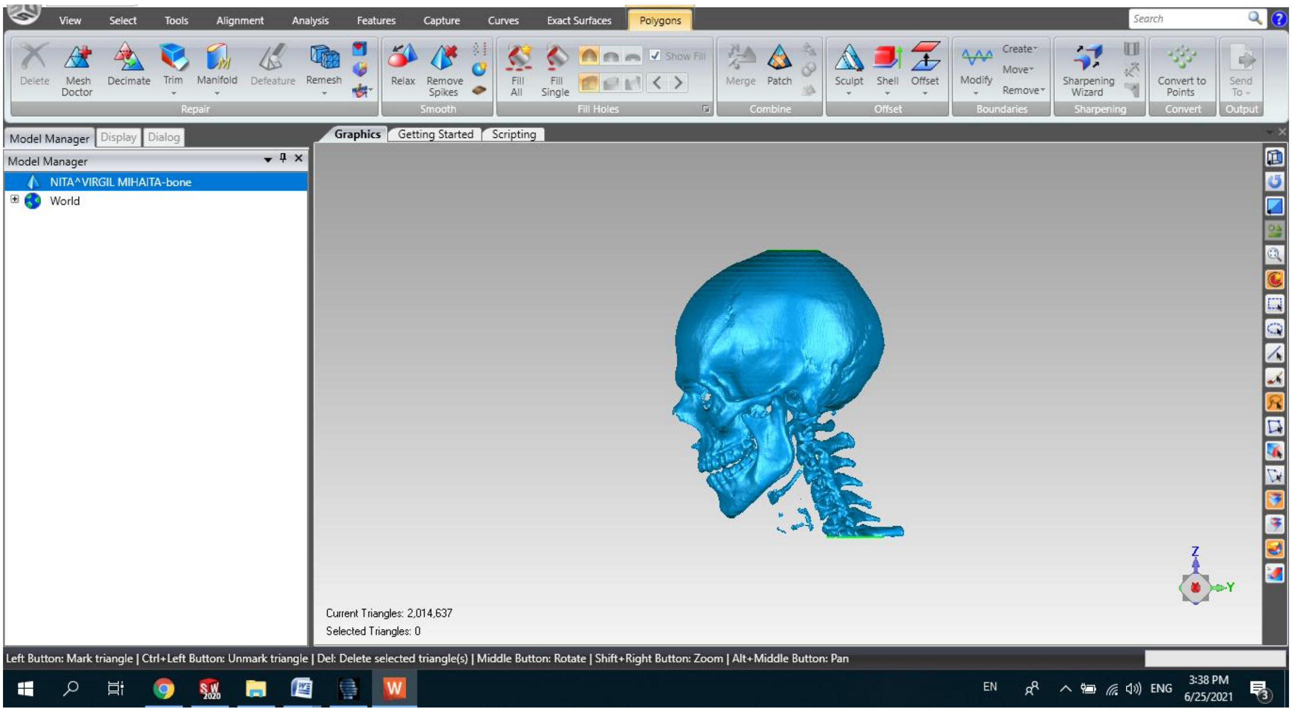

**Figure 4**: Geomagic program interface

In the following, it was intended to obtain the two bone components separately, namely, the jaw and the mandible. At this time, the structure was automatically transformed into 2,014,637 triangular elementary surfaces. Also, the vertebrae of the cervical spine will be removed. Steps of this operation are shown in Figure 5.

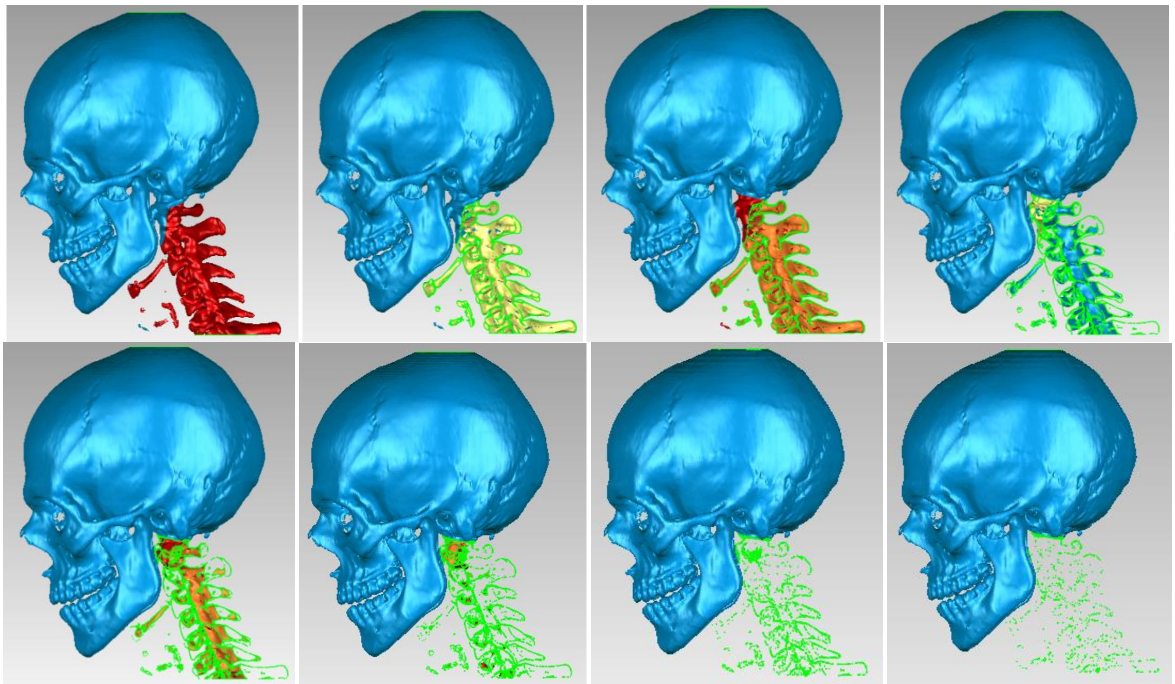
**Figure 5**: Stages of elimination of the cervical spine

Next, we will get, separately, the mandible and the jaw. In the following steps, shown in Figure 6, the jaw is removed first.

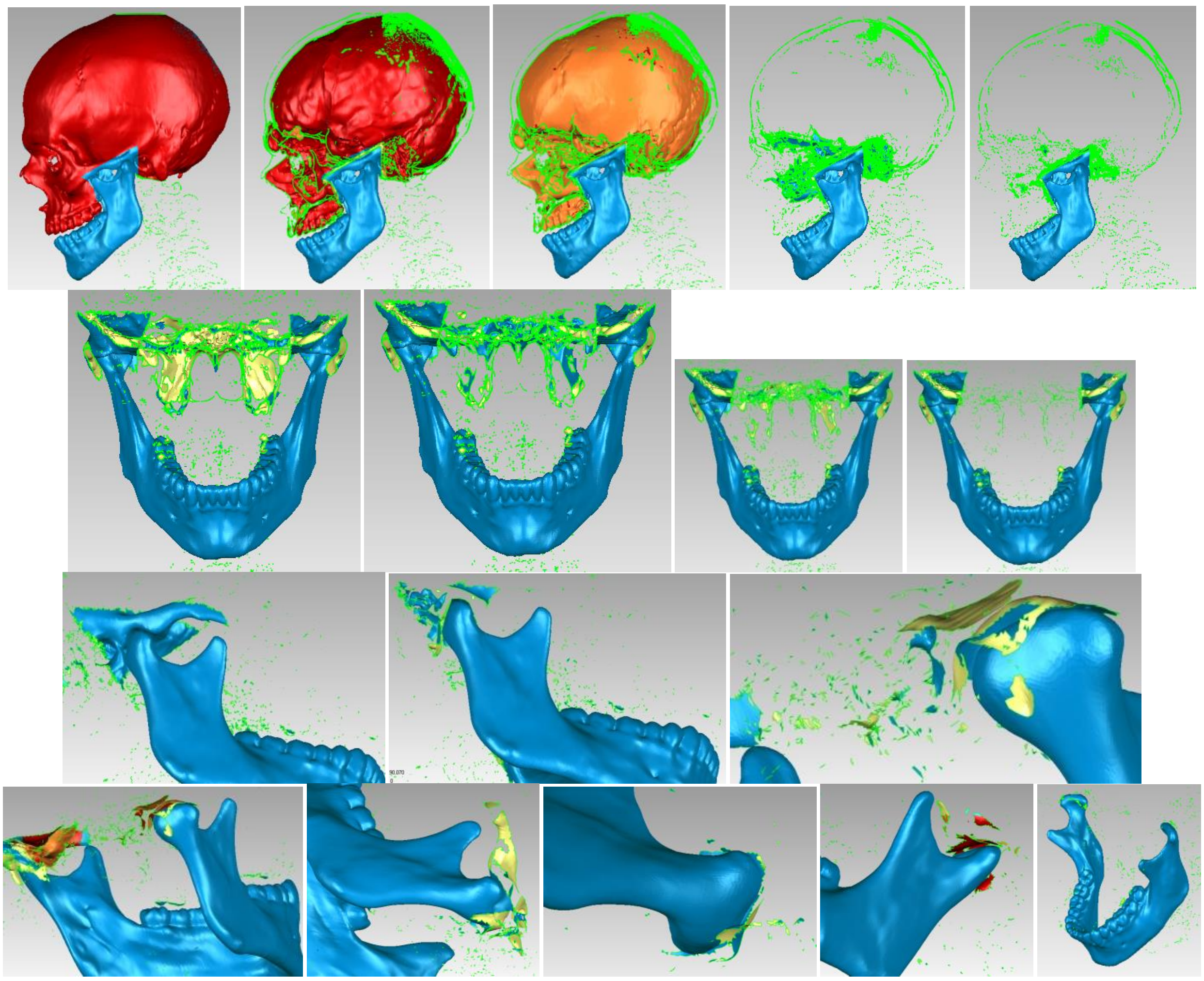

**Figure 5a**: Stages of jaw removal

It is very possible that, during the procedures for removing the surfaces that do not belong to the mandible, gaps will appear in the structure. To "fill" these gaps, the Fill command was used. Figure 6 shows an area before and after applying this command.

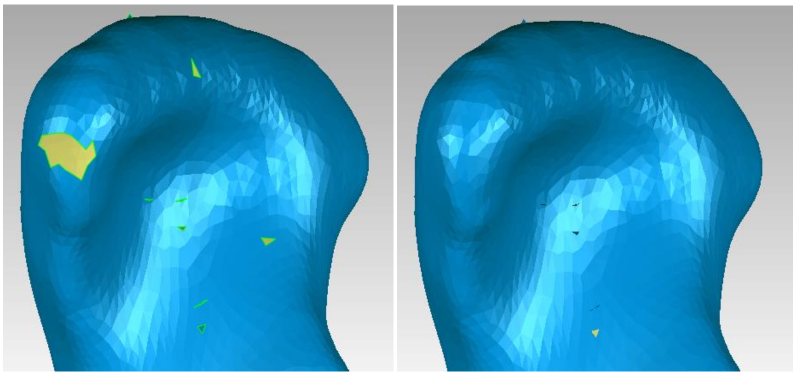

(a) (b)

**Figure 6**: (a) Before Fill command, and (b) After Fill command

Other commands were used to finish the surface and the final model is shown in Figure 7. At that time the model contained 161,012 elementary surfaces, but also some surfaces that are not part of the mandible model. The template has been saved in .stl format.

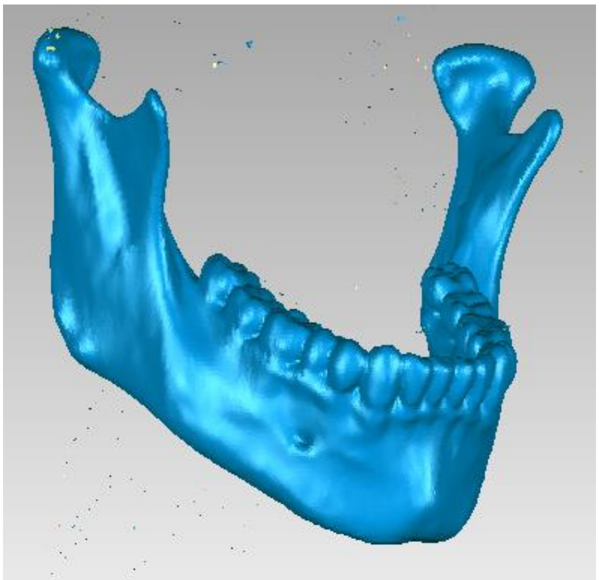

**Figure 6a**: Final model of mandible in Geomagic

The model was imported into SolidWorks where it was automatically transformed into a virtual solid. The additional components in the definition tree have also been removed. Figure 7 shows the final model of the mandible.

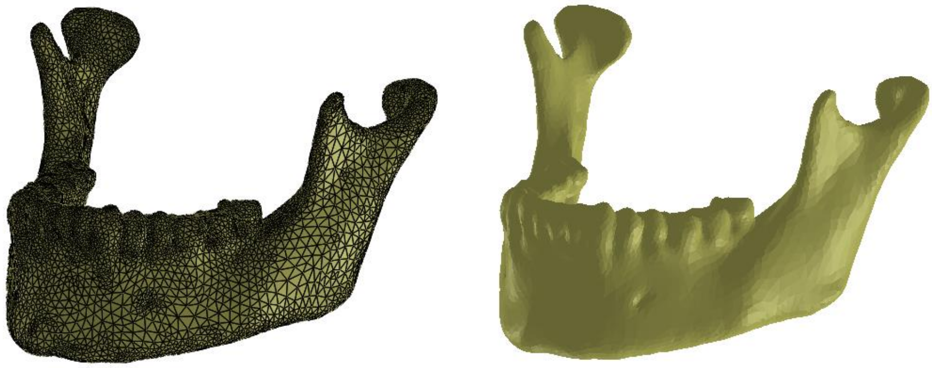

**Figure 7**: Final model of mandible in SolidWorks

Using similar methods and techniques, the jaw model was obtained, as shown in Figure 8.

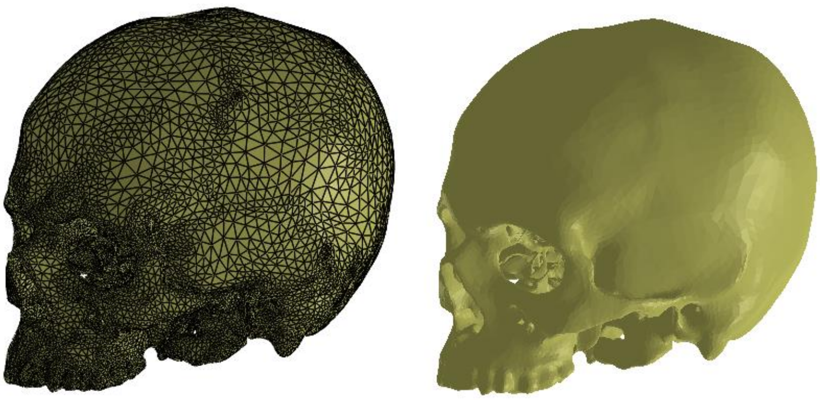

**Figure. 8**: Final model of jaw in SolidWorks

These models were loaded into the Assembly module of SolidWorks where, using the basic plans of each model, the dentomaxillary apparatus was obtained in the position in which the tomography operation was performed. Figure 9 shows this model.

**Figure 9**: Final model of dentomaxillary system in SolidWorks

In order to be able to make a more complex analysis, we were also interested in the muscles of the face that act on the mandible. For this, InVesalius selected the Muscle Tissue mode as shown in Figure 10 and the model was exported in .stl format.

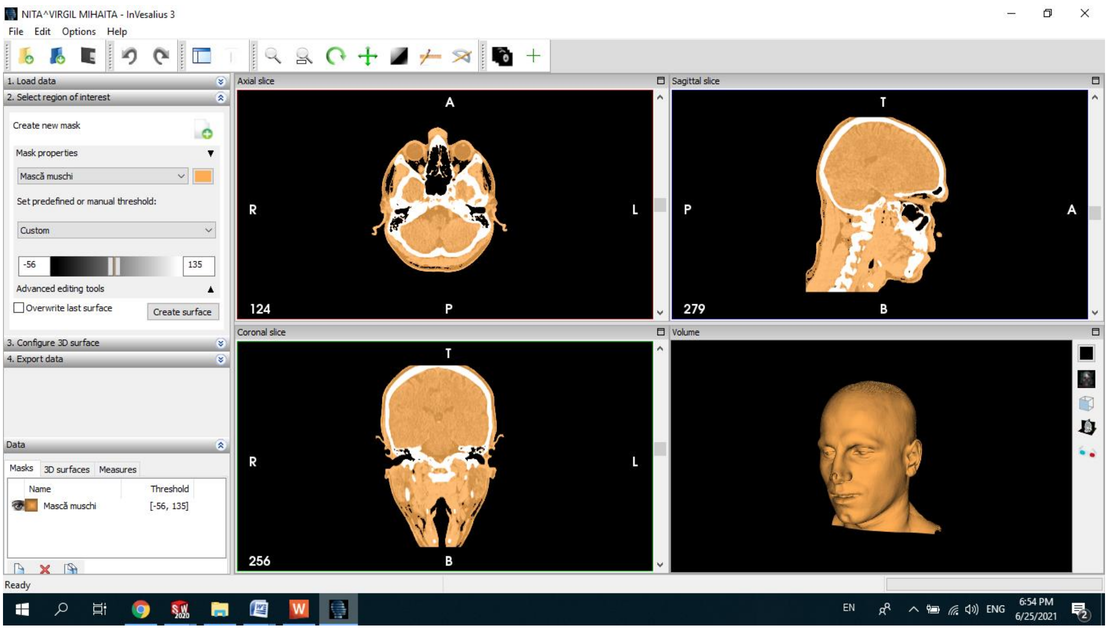


**Figure 10**: Invesalius interface with Muscle Tissue mode activated

The obtained model was saved in .stl format and was imported into Geomagic for further processing. The Geomagic model is shown in Figure 11.

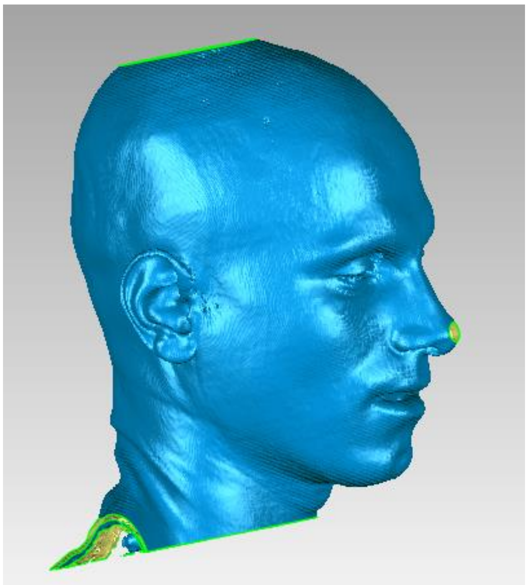

**Figure 11**: Muscle tissue model in Geomagic

Because human skin also contains muscle tissue, in a first phase, two layers of the obtained geometry were removed. The model obtained after this operation is presented in Figure 12.

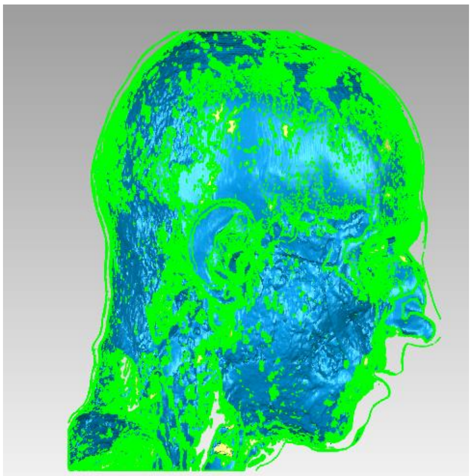

**Figure 12**: Muscle tissue model after removing two layers in Geomagic

Due to the fact that we were only interested in obtaining the muscle tissue that acts on the mandible, other areas of the obtained geometry were removed. Figure 13 shows the final model loaded into SolidWorks.

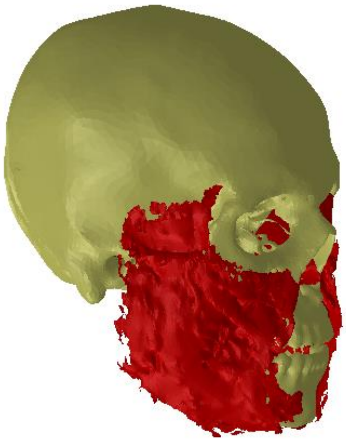

**Figure 13**: The final model of muscle tissue in SolidWorks

## 3. THREE-DIMENSIONAL GEOMETRY OF THE DIFFERENT TISSUES OF A HUMAN EYE. KINEMATIC ANALYSIS

To obtain virtual-experimental simulations of the functioning of the human eye in normal and pathological conditions. it is necessary, in a first phase, to model the main components of this important biomechanical system. In other words, a method must be found to obtain the 3D geometry of the main elements of the system to obtain the entire biomechanical behavior.

Thus, the main components of this simplified system were identified:

- the human eye, in which the following important components have been identified:
  - cornea;
  - sclera;
  - iris;
  - the lens;
  - ciliary body;
  - vitreous body.

- the bone component in which the human eye functions;

- muscular components that allow eye movements:mușchiul drept superior;
  - lower right muscle;
  - the right internal muscle;
  - external right muscle;
  - the superior oblique muscle;
  - the lower oblique muscle.

Several sets of tomographies were used to obtain these geometries. Figure 14 shows the interface of the InVesalius program with the Skin mode activated.

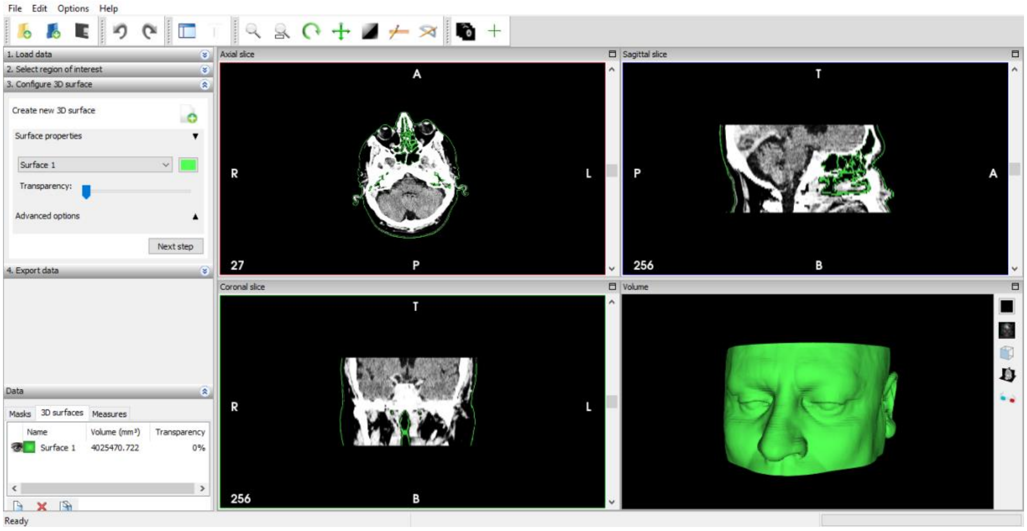


**Figure 14**: Interfata InVesalius with Skin mode enabled

Using the same methodology for virtual reconstruction, a human eye was modeled in which it was intended to obtain a kinematic simulation for the main movements of the human right eye, the initial model was subjected to virtual cutting operations. The final model of the bone component is shown in Figure 15.

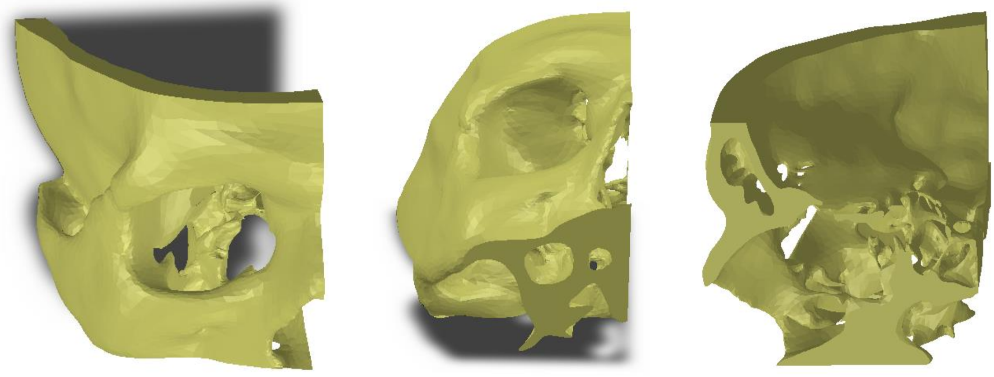

**Figure 15**: Bone component obtained for the right eye

Using specific modeling and geometric identification commands, the main components of the human eye were defined and, finally, the model presented in Figure 16 was obtained (Mercut et al., 2020).

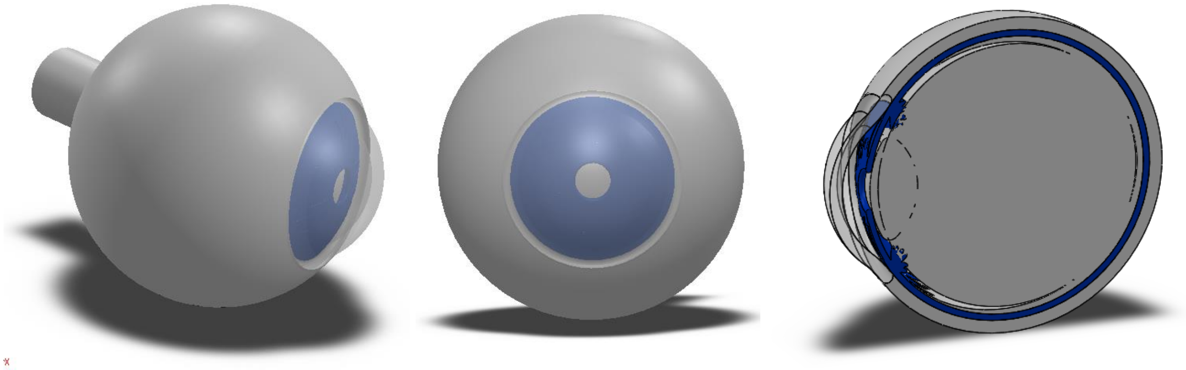

**Figure 16**: The model of the human eye

In the Assembly module of the SolidWorks program were loaded the two main elements of the biomechanical system of the human eye, for positioning using tomographic images, but also anatomical information as can be seen in

Figure 17. Muscle models were generated which contributes to the main movements of the human eye (upper right muscle, lower right muscle, internal right muscle, external right muscle, upper oblique muscle and lower oblique muscle) (Mercut et al., 2020).

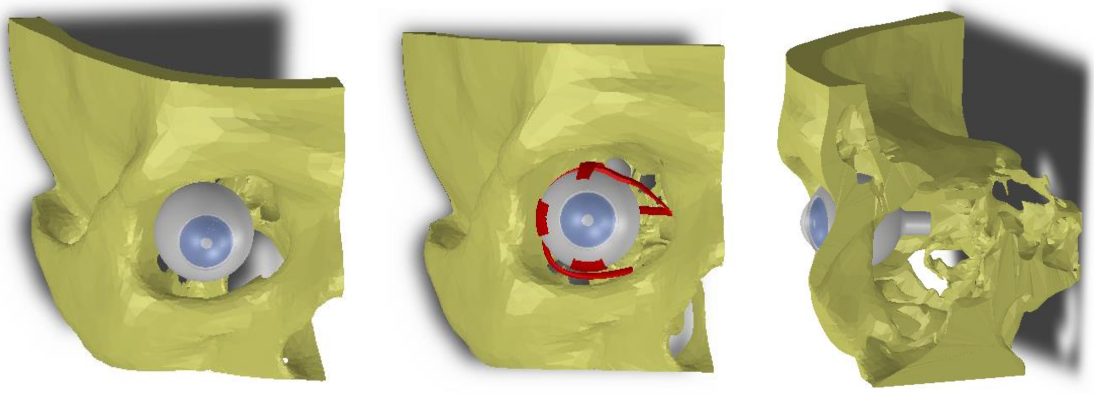

**Figure 17**: The final model of the human eye

Obviously, the purpose of kinematic analysis is to determine the forces acting on the human eye during the four main movements. Because the previously defined system is particularly complicated, the six main muscles acting on the eye have been replaced with six virtual springs (springs) in which the forces acting in the system will develop, similar to the muscular forces. These springs were considered as devices that record the forces during each movement. It is logical that, once these forces have been determined (as a temporal evolution), the virtual engine can be eliminated and, put into action in the system, produce the four main movements of the human eye. These virtual springs used as insertion points exactly the insertion points of the extraocular muscles (Figure 18) (Mercut et al., 2020).

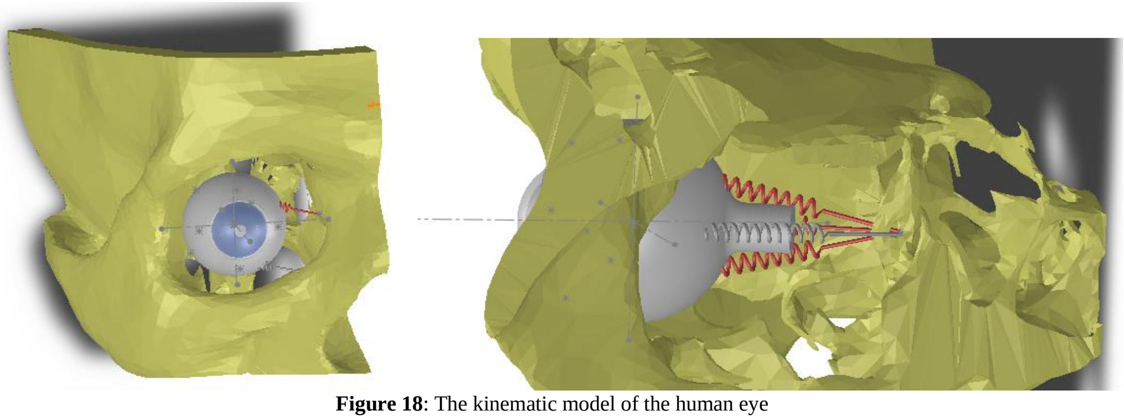

**Figure 18**: The kinematic model of the human eye

Considering that all six muscles have a similar internal structure, then it can be considered that all virtual springs have the same constant **k**. This value was attached to all six virtual springs for all four kinematic simulations. It was also considered that each movement lasts one second.

Very important are the physical-mechanical characteristics of the materials of the components of the human eye that can be attached to the virtual models created. For this, an extensive bibliography was analyzed which, either by "in vivo" determinations or by mathematical models, conducted studies to determine these properties (Aloy et al., 2017), (Stitzel et al., 2002), (Morita et al., 2012), (Luce et al., 2005). The most important results are numeric, because the program exports the entire kinematic behavior of the virtual biomechanical system to the Microsoft Office Excel program. Thus, the evolution of the forces that appear in the six virtual springs and that simulate the movement of the extraocular muscles is shown in Figure 19.

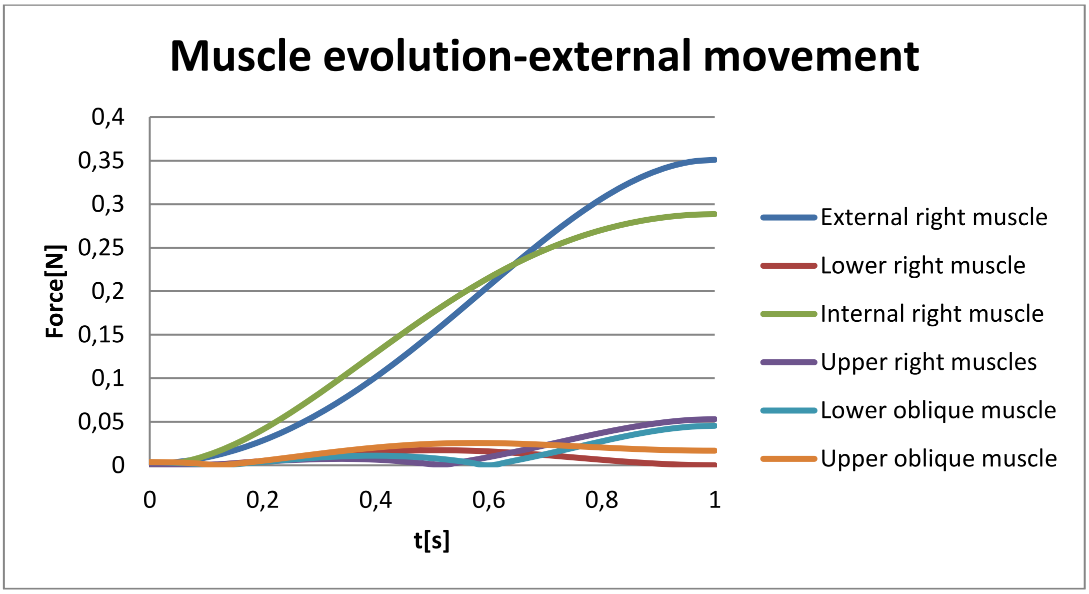


**Figure 19**: Evolution of muscle forces for internal movement

## 4. CONCLUSIONS

The paper presents a methodology that allows obtaining tissues from the human body in a virtual environment. This methodology consists of a series of techniques that combine medical imaging methods, CAD methods or reverse engineering methods. These methods and techniques were exemplified on two complex models: a human head and an eye. This paper demonstrates that, starting from tomographic images, the geometry of each tissue in the human body can be obtained.

However, the following conclusions can be highlighted:

• the method of transferring information of geometric nature from tomographic images is viable and leads to concrete results;

• the results obtained by applying the technology given by programs such as InVesalius can produce, through visual techniques, a better medical diagnosis;

• the transfer of complex geometries, such as tissues from the human body, from tomography to CAD or FEA programs is an important step in analyzing customized geometries or adapting implants;

• the methods and techniques presented and exemplified in this paper, give a good chance for medical diagnosis in virtual reality.

## REFERENCES

1. Aloy, M. A., Adsuara, J. E., Cerda-Dura, P., Obergaulinger, M., Esteve-Taboada, J. J., Ferrer-Blasco, T. and Montes-Mico, R., 2017. Estimation of the mechanical properties of the eye through the study of its vibrational modes. *PLOS ONE*, September 18, pp. 1-19.

2. Buciu, G., Tarnita, D.N., Popa, D.L., Lungu, M.A., Miritoiu, C. and Ungureanu, A., 2014. Virtual and Experimental Studies about Human Walking-Virtual Lower Leg Environment-Innovative Design of Tibia Nail. *Applied Mechanics and Materials*, vol. 657, pp. 770-774.

3. Calin, D., Tarniţă, D., Popa, D., Calafeteanu, D. and Tarnita, D., 2016. Virtual Model and Simulation of the Normal and Affected Human Hip Joint. *Applied Mechanics and Materials*, vol. 823, pp. 167-172.

4. Ciunel, S., Popa, D.L., Gherghina, G., Bogdan, M.L. and Tutunea D., 2014. Human Head-Neck System Behavior During Virtual Impact Automotive Simulations. *Applied Mechanics and Materials*, vol. 659, pp. 177-182.

5. Luce, D., 2005. Determining in vivo biomechanical properties of the cornea with an ocular response analyzer. *J Cataract Refract Surg*.

6. Mercut, M.F., Dumitrescu, D., Craitoiu, Ș., Mercut, R., Stefanescu Dima, A., Tanasie, A. and Popa, D.L., 2020. Three-Dimensional Model of the Human Eye Development based on Computer Tomograph Images. *Current Health Sciences Journal,* vol. 46, no. 1.

7. Morita, T., Shoji, N., Kamiya, K., Fujimura, F. and Shimizu, K., 2012. Corneal biomechanical properties in normaltension glaucoma. *Acta Ophthalmologica*.

8. Petrovici, I.L., Tenovici, M.C., Vaduva, R.C., Tarnita, D.N., Vintila, G. and Popa, D.L., 2019. About Three-Dimensional Models of Osteosynthesis Systems. *Journal of Industrial Design and Engineering Graphics*, vol. 14, no. 1, pp. 159-162.

9. Popa, D.L., Buciu, G., Calin, D.C., Popkonstantinović, B. and Poenaru, F., 2019. CAD, CAE and rapid prototyping methods applied in long bones orthopaedics, *FME Transactions*, vol. 47, no. 2, pp. 279-286, 2019

10. Popa, D.L., Duta, A. and Pitru A.R., 2014. The Modeling of Some Types of Implants and Prostheses Used for Osteointegration. *SDÜ Mühendislik Bilimleri ve Tasarım Dergisi*, vol. 2, no. 3, pp. 273-281.

11. Stitzel, J.D., Duma, S.M., Cormier, J.M. and Herring, I.P.,2002. A Nonlinear Finite Element Model of the Eye with Experimental Validation for the Prediction of Globe Rupture. *Stapp Car Crash Journal*, Vol. 46, pp.1-23.

12. Tarnita, D., Boborelu, C., Popa, D. and Tarnita, D.N.,2018. Design and Finite Element Analysis of a New Spherical Prosthesis-Elbow Joint Assembly. *New Advances in Mechanism and Machine Science*, pp. 127-135.

13. Tarnita, D., Tarnita, D.N., Bizdoaca, N., Popa, D., Tarnita, C.E. and Cismaru, F., 2010. Modular Orthopedic Devices Based on Shape Memory Alloys. *SYROM 2009*, pp. 709-721.

14. Terai, N., Raiskup, F., Haustein, M., Pillunat, L.E. and Spoerl, E., 2012. Identification of Biomechanical Properties of the Cornea: The Ocular Response Analyzer. *Current Eye Research*., 37(7), pp. 553–562.

15. Vatu, M., Vintila, D., Mercut, R., Popescu, S.M., Popa, D.L., Petrovici, I.L., Vintila, G. and Pitru, A., 2019. Three-dimensional modeling of the dental-maxillary system. *Journal of Industrial Design and Engineering Graphics*, vol. 14, no. 1, pp. 207-210.

„8th International Conference moNGeometrija, focused on the research about geometry, graphics and application to science, engineering and art“

Belgrade, 10.-12. September, 2021.

# EXAMINATION OF DIFFERENT CROSS SECTION OF DRAIN PIPES IN DISTILATION COLUMN

Rodoljub Milicevic,[1] Danilo Miljkovic[1], Branislav Gajic[1], Boris Kosic[1]

[1]Faculty of Mechanical Engineering, University of Belgrade, Republic of Serbia

rmilicevic@mas.bg.ac.rs, dmiljkovic@mas.bg.ac.rs, bgajic@mas.bg.ac.rs, bkosic@mas.bg.ac.rs

***ABSTRACT***

*In this paper, we will be discussing various shapes of drain pipes for tray columns for distillation (rectification). Drain pipes are used for distribution of liquid from upper trays to next trays and it is important to respect some guidelines about geometry. Three different solutions have been presented and the conclusion about the results have been made. By adopting the optimal solution for drain pipes, engineers manage to obtain constant flow through tray columns as well as safe and reliable operation, as a result. Different standpoints have been mentioned, from various authors having worked in engineering for many years.*

**Keywords:** drain pipes, geometry, distillation, tray columns, liquid.

## 1.INTRODUCTION

Engineers in their work face many challenges that they need to overcome. One of the problems that engineers face daily in their calculation are the pressure drops and the impact that geometry has on it. In almost all industrial plants or factories, there are pipes which transport either air or water. Other than geometry, some of the factors that affect the pressure drop are the type of flow (laminar or turbulent), the state of the pipe whether it has irregularities or not, the type of fluid, local impacts like bends, valves, and many other factors. The type of flow in a pipe is determined by the relationship between the inertial forces and viscous forces that engineers call Reynolds number (Re). Depending on the geometry of the pipe, the critical number for determining the flow type has a different numerical value (for circular pipes the value is 2320 or 2300 depending on the author, for square shapes, it is around 1600 [1]). There are numerous guidelines and recommendations given by different engineers that work in the field. In this paper, we will see the effect that geometry has on the velocity of the fluid, and consequently, the impact it will have on the pressure drop. In our calculation, we used the “Navier – Stokes” equation, and the law of the conservation of mass. Mathematically, the equation is written in this form[3]:

$$\rho \cdot \frac{D\vec{V}}{Dt} = -\nabla p + \rho \cdot \vec{g} + \mu \cdot \nabla^2 \vec{V} \qquad \text{(Eq.1)}$$

Where:
$\rho$ is density
$\vec{V}$ is the velocity vector
$t$ is time
$p$ is pressure
$\vec{g}$ is the gravitational acceleration
$\mu$ is viscosity.

What is important about the theory of turbulent flow is that the results are mostly generated with the use of experimental data, given that the equations aren’t yet solvable. Coefficients that are given in the equations like Bernoullies serve as an example in favour of this statement. Nowadays, the production of ethyl alcohol is one of the most important parts of the process industry. The main part of distillation process are tray columns. The number of needed trays is calculated for every distillation process separately. There are some elements such as drain pipes, bells, holes, nozzles etc. These elements are used for the distillation process. The mixture of alcohol and water flows through trays where the liquid part is flowing downward, due to gravity, while the steam part is flowing on the tray above it. For the liquid to fall down on the tray below it and not cause a clog, the design of the drain pipe must be done carefully and correctly. The thickness of the drain pipe is usually not that big since the operating pressure isn’t that high. A guideline recommended by most engineers is that the inlet area is a similar size as the outlet area. The drain pipe must be made in such a way for it not to cause an overflow, and that the liquid part must flow constantly [2]. Drain pipes used in a distillation plant have different shapes and cross section geometry. Another way of illustrating the work of the technical system is the formation of the prototype and its analysis in the laboratory. This method is one of the closest ways to check the functionality of the real technical system, but economically, very challenging, since it is expensive. With the development of computer and software techniques, the method of analysis of the 3D model has appeared. This method is affordable, quite close to the real system, and allows a large number of changes on the spot, without a lot of unnecessary elements [4].

## 2. GEOMETRY AND VISUAL CHARACTERISTICS

In our model, K-omega model was used and the fluid used was ethyl alcohol-water. The pipe was made of solid steel. Inlet speed used was 2 m/s, the number of iterations used was around 200. For different parameters, the results may differ but they should look similar to the ones that are shown in the pictures below. Something that needs to be mentioned is that the results also change depending on the tray position in the distillation tower. The models in this study was designed in SolidWorks 2020 software tool (pictures 1, 2,3) and passed through a simulation tool flow ANSYS 2021. [5].

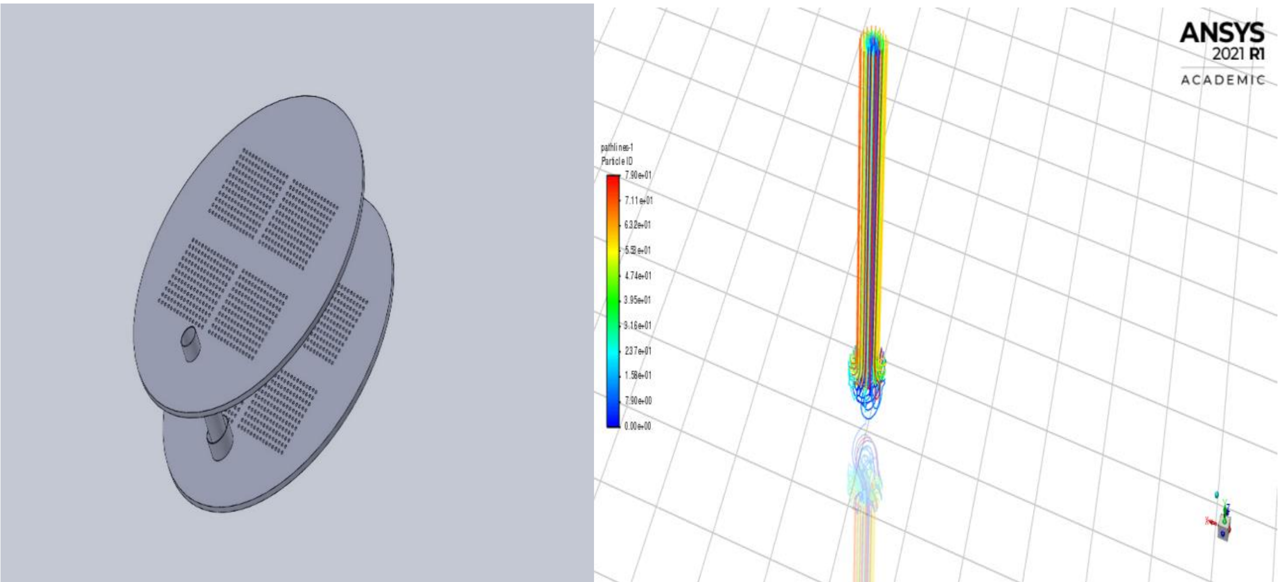


**Figure 1:** Fluid velocity in a circular shape pipe

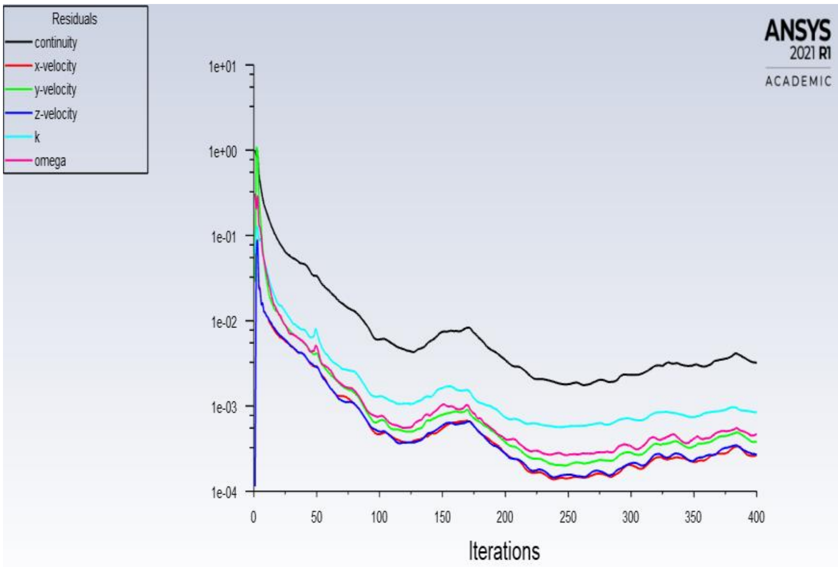


**Figure 2:** Graphic view Fluid velocity in a circular shape pipe

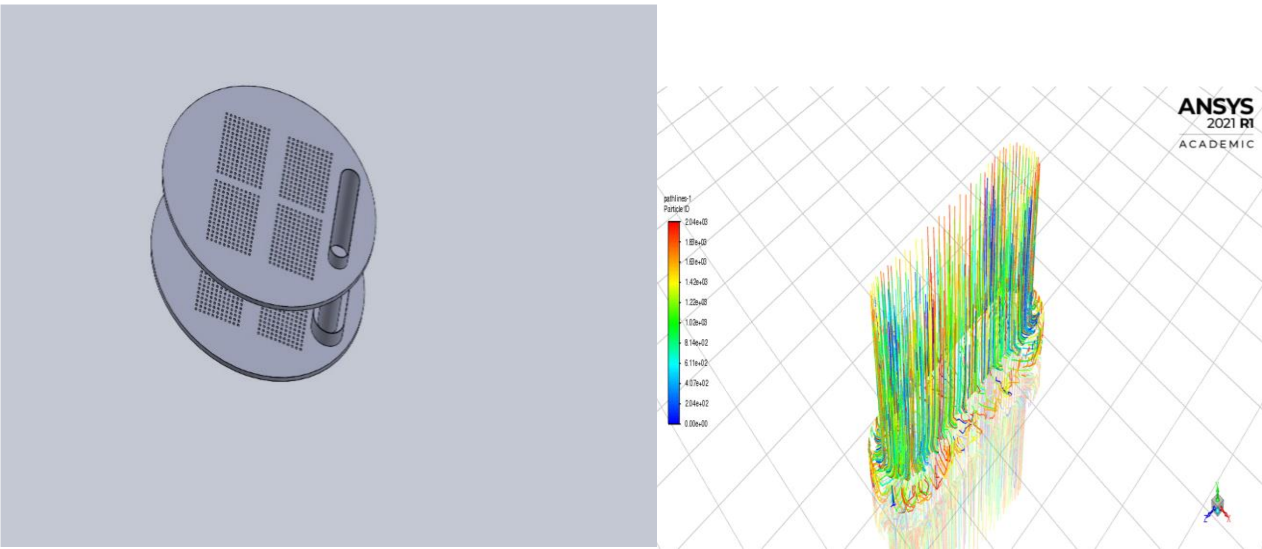


**Figure 3:** Fluid velocity in a square pipe with rounded corners

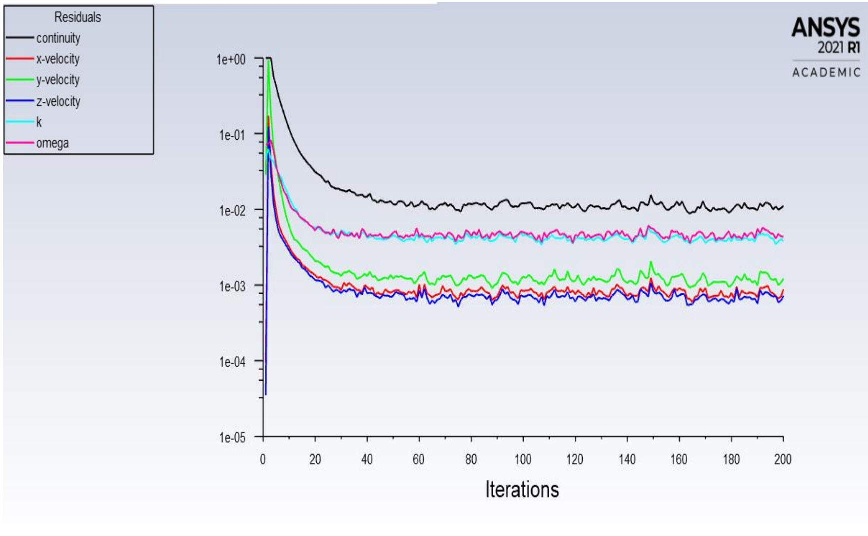


**Figure 4:** Graphic view fluid velocity in a square pipe with rounded corners

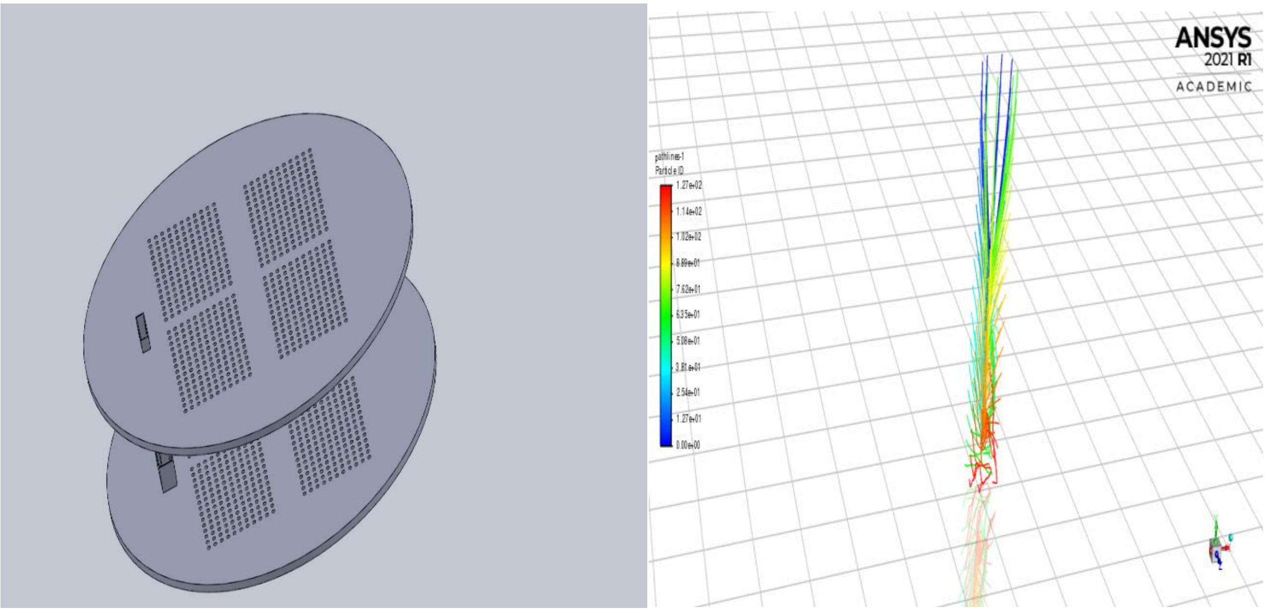


**Figure 5:** Fluid velocity in a square shaped pipe

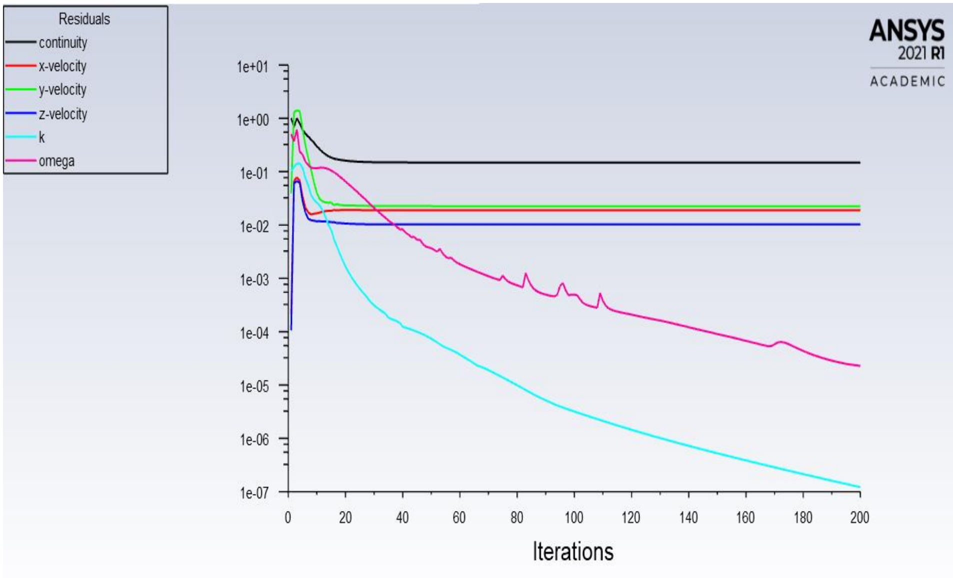


**Figure 6:** Graphic view Fluid velocity in a square shaped pipe

### 3. RESULTS

In distillation, the problem that arises is due to both liquid and steam phases flowing simultaneously. As we can see in the pictures, there are different fluid velocities depending on the geometry, the best dispersion is given when a pipe has circular geometry, second best is square geometry with a rounded corner, and lastly, the square pipe geometry. The reason lying behind this phenomenon is a uniform distribution obtained in a circular pipe. As a result of this, a circular pipes cross section will be relatively pressure resistant. Another thing worth mentioning about circular pipes is that the temperature increase will not result in geometry change (the pipe will spread or retract depending on the temperature, but the shape will stay circular). For the square geometry fluid streamline will bend causing vortexes to appear. Also, the liquid will not flow evenly and there are “dead zones” in which the liquid doesn’t flow. There isn’t a smooth transition when the geometry changes, and this causes the fluid flow to be uneven. If two trays are too close to each other (meaning that the drain pipes are too short), it can cause the process to overflow. Therefore, the solution that is most commonly used is the square geometry with rounded corners [6]. The reason why this is used more commonly than the circular pipe is that during the flow in a circular pipe, the liquid phase flowing can drop all at once, which may lead to the distillation process operating in modes that aren’t recommended.

### 4. CONCLUSION

Geometry makes a big impact on the working condition of the plant whether it is on the tray design or the pipe shape. In this paper, the results for the three most commonly used geometry shapes are shown. It can be seen that there are many different factors and effects that need to be taken into account while designing a distillation plant. A poorly chosen geometry shape can have a dramatic influence on the working condition of the process. Due to this, numerous engineers have given their recommendations and advice on how to choose an adequate tray/pipe shape. While these recommendations are given, they are not set in stone, their purpose is to act more like guidelines rather than a rule. This method is affordable, quite close to the real system, and allows a large number of changes on the spot, without a lot of unnecessary elements.

## REFERENCES


1. Voronjac D., Mehanika fluida
2. Jacimovic B., Genic S., Beograd 2010, Difuzione operacije i aparati
3. Crnojevic C., Mehanika fluida, Masinski fakultet Univerziteta u Beogradu.
4. Jeli Z., Stojicevic M., Cvetkovic I.,Duta A.,Popa D., A 3d Analysis of Geometrical Factors and Their Influence on Air Flow Around a Satellite FME Transactions VOL.45, No2, 2017.
5. Krister Z.K.,McGraw-Hill 1992, Distillation design

# APPLICATION OF 3D SCANNING AND MODELING IN THE PROTECTION OF CULTURAL HERITAGE

Aleksandra Joksimović[1], Emil Veg[1], Ivana Medojević[2], Mladen Regodić[1]

[1]Department of Theory of Mechanisms and Machines, University of Belgrade-Faculty of Mechanical Engineering, Republic of Serbia

[2]Department of Agricultural Engineering, University of Belgrade-Faculty of Mechanical Engineering, Republic of Serbia

ajoksimovic@mas.bg.ac.rs, eveg@mas.bg.ac.rs, imedojevic@mas.bg.ac.rs, mregodic@mas.bg.ac.rs

***ABSTRACT***

*In order to preserve our culture, customs and history, the protection of cultural heritage comes to the fore. Cultural heritage represents tangible and intangible cultural heritage, as well as movable and immovable property. The topic of the paper is a part of cultural heritage that includes monuments, figures and objects of historical significance. Depending on the initial condition, the material of the production, the method of storage and maintenance, there may be wear and tear of materials, damage due to negligence and, in the end, completely impairment of monuments, figures and objects of historical significance. To prevent any damage on the one hand, and again the availability of objects of historical importance to those interested on the other hand, 3D scanning and modeling technology is applied. 3D scanning technology aims at credible analysis, imaging and scanning monuments, figures and objects of historical significance. 3D modeling technology aims to create virtual 3D models of monuments, figures and objects of historical significance,as well as preparation for making them from different materials. 3D scanning and modeling can be applied in the preparation of the mold for already existing objects of historical significance,and thus ensure their re-creation and reconstruction.*

*This paper will present the importance of introducing new technologies with the aim of preserving existing monuments, figures and objects of historical significance, and yet their accessibility to human curiosity and tourists, without fear of harm. Also, one of the goals is to combine the historical and the modern and increase the interest of young people in history and cultural heritage, with the nurturing of existing and preserved monuments, figures and objects of historical significance.*

**Keywords:** 3d scanning, 3d modeling, history, figures

## 1. INTRODUCTION

The cultural heritage is inherited by the current society and it is necessary to be preserved in the most optimal conditions for the next generations. It is very importance of introducing new technologies with the aim of preserving existing monuments, figures and objects of historical significance.

With the new technologies, there is a possibility to record images of cultural assets as monuments, figures, and objects of historical significance and then process them to obtain virtual or physical items, and all of that with respect for their physical integrity. Representative cultural heritage sites have been lost or damaged by natural disasters, human conflicts, and deterioration. This can be prevented by using three-dimensional (3D) modeling techniques and in that way enables to ensure access to preserved models for future generations. 3D digital recording technologies have become increasingly popular for rapid, cost-effective, and accurate archaeological documentation in the field. [3].

Lately all over the world, scanning these heritage objectives has become a priority, in order to preserve in the smallest details the used monuments, figures, architecture and objects of historical significance. The evolution of technologies in the last half of the 21st century has led to huge advances in electronics, IT, graphics (digital three-dimensional (3D) models), making it possible to develop laser, terrestrial (TLS - Terrestrial Laser Scanning and MMS—Mobile Mapping System), and aerial (UAV Unmanned aerial vehicle) scanning technology. Thus, the possibility of processing dense points clouds in an efficient and cost-effective manner has facilitated a multitude of applications concerning the acquisition of 3D data in areas such as, topography, environmental protection, water management, the completion and preservation of cultural heritage, forest resources, etc. [4]. This paper has an exclusively theoretical review on the topic of application of 3d scanning and modeling in the protection of cultural heritage.

## 1. ABOUT 3D SCANNING

3D Laser Scanning is a non-contact, non-destructive technology that digitally captures the shape of physical objects using a line of laser light. 3D laser scanners create “point clouds” of data from the surface of an object. In other words, 3D laser scanning is a way to capture a physical object’s exact size and shape into the computer world as a digital 3-dimensional representation.

3D laser scanners measure fine details and capture free-form shapes to quickly generate highly accurate point clouds. 3D laser scanning is ideally suited to the measurement and inspection of contoured surfaces and complex geometries which require massive amounts of data for their accurate description and where doing this is impractical with the use of traditional measurement methods or a touch probe.

3D Laser Scanning Process An object that is to be laser scanned is placed on the bed of the digitizer. Specialized software drives the laser probe above the surface of the object.

Laser scanning is the fastest, most accurate, and automated way to acquire 3D digital data for reverse engineering. Again, using specialized software, the point cloud data is used to create a 3D CAD model of the part’s geometry. The CAD model enables the precise reproduction of the scanned object, or the object can be modified in the CAD model to correct imperfections. Laser Design can provide a surface model or the more complex solid model, whichever results are needed for the application. [5].

### 1.1 From Physical to Digital

One of the biggest challenges people encounter when converting physical objects to digital is a major incompatibility between two different types of 3D models: **meshes** and **solids**.

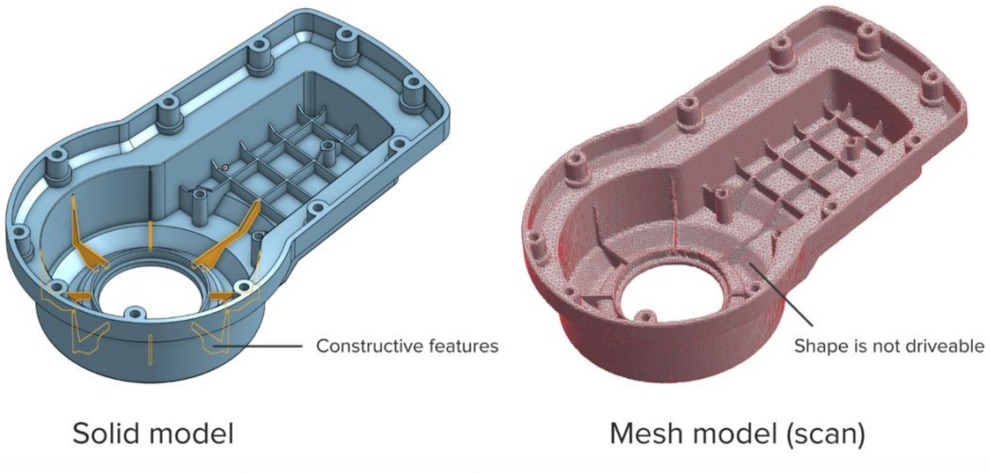


**Figure 1**: A 3D scanner outputs a mesh, rather than a constructive “solid” model. Meshes need to be reverse engineered to be made editable (Source: https://formlabs.com/blog/how-to-use-3d-scanning-and-3d-printing-for-reverse-engineering/)

**Meshes** are the main output of all 3D scanners, and the format commonly understood by 3D printers (STLs). A mesh represents the surface of a shape with a large number of triangles, connected edge to edge. Mesh models don’t contain any information about the object, besides the position of the triangles that define the shape. On the other hand, engineers are trained to work with **solid models**. Solid models hold information about how an object is designed, and this information is explicitly encoded into the model as features in a 'stack' of logical steps. In solid CAD, it's possible to change the dimensions for a single feature, and the rest of the model will update to accommodate the change. Since meshes lack information about the construction of the object, the ways you can alter a mesh model are limited—CAD software like Solidworks and Onshape can't directly modify meshes. [6].

## 2. ABOUT 3D MODELING

3D modeling is the process of creating a 3D representation of any surface or object by manipulating polygons, edges, and vertices in simulated 3D space. You can see the results of 3D modeling in movies, animations, and video games filled with fantastical and imaginative creatures and structures. 3D modeling is achieved manually with specialized 3D production software that lets an artist create and deform polygonal surfaces or by scanning real-world objects into a set of data points used to represent the objects digitally. there are some clear problems that specialists face regarding 3D modelling of cultural heritage objects, such as: proper selection of technology for image acquisition and post-processing, automation of the image-matching procedure, visual and metric quality of the final product, and proper documentation. [7]. The 3D modelling of cultural heritage objects is a challenging task, from the data acquisition and gathering of all possible input data through to the final phase of visualisation. The final accuracy is directly related to the image resolution and the success of web visualisation directly depends on the number and quality of the images used.Whe CAD drawings were used as the main source of information, the accuracy is related to the geometrical quality of the 3D model which has been shown to be at centimetre level.

## 3. EXAMPLES FROM PRACTICE

### 3.1 The Church of St. Peter and Paul

The studied area corresponds to the exterior façades of the Church of St. Peter and Paul, located in the center of the historical city of Calw. [2] The availability of such models can increase interest in visiting the facility, especially young people, which is one of the goals.

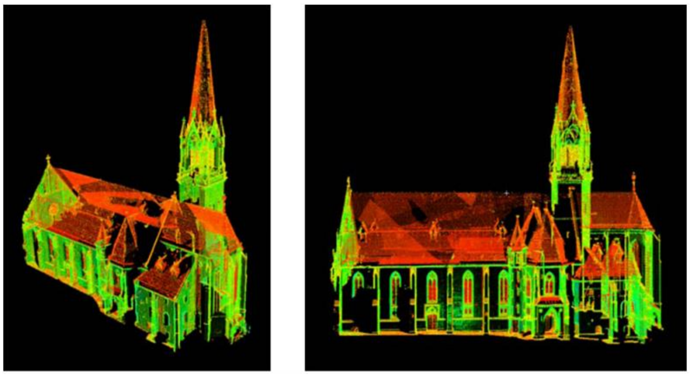

**Figure 2**: Point cloud obtained using TLS systems (Source: Paper Methodology for digital preservation of the cultural and patrimonial heritage: generation of a 3D model of the Church St. Peter and Paul (Calw, Germany) by using laser scanning and digital photogrammetry)

**Figure 3**: Different oblique perspectives of the 3D photorealistic model obtained (Source: Paper Methodology for digital preservation of the cultural and patrimonial heritage: generation of a 3D model of the Church St. Peter and Paul (Calw, Germany) by using laser scanning and digital photogrammetry)

In this research paper [2], an approach for the reconstruction of 3D photorealistic models by utilizing data obtained using laser scanning and photogrammetry are shown. The combination of both data sources offers an efficient and optimized solution for the generation of 3D models of buildings and monuments with high historical value. Embedding 3D models into virtual globes and software applications results in a powerful tool for digital preservation of cultural and patrimonial heritage and for ensuring knowledge to next generations.

### 3.2 Nefertiti

The berlin egyptian museum has produced a detailed scanned digital version of the famous bust of nefertiti with 6.4 million polygons in full color. Thanks to a three-year lawsuit, this file is now available for free download by a court decision in germany, based on free access to information from public institutions. [8]

**Figure 4**: 3D model of Neferiti
(Source: https://solfins.com/blog/3d-print-scan-6/post/primena-3d-stampe-i-3d-skeniranja-u-arheologiji-oblasti-kulture-i-zastite-spomenika-340)

### 3.3 Making a replica of the tombstone of Franjo Tahy using 3D technologies

The ever-increasing application of 3d technologies has enabled another successful reproduction and contributed to the preservation of cultural heritage. The museum of peasant revolts in gornja stubica exhibits a tombstone of the croatian nobleman franjo tahy as part of a permanent exhibition. [9]

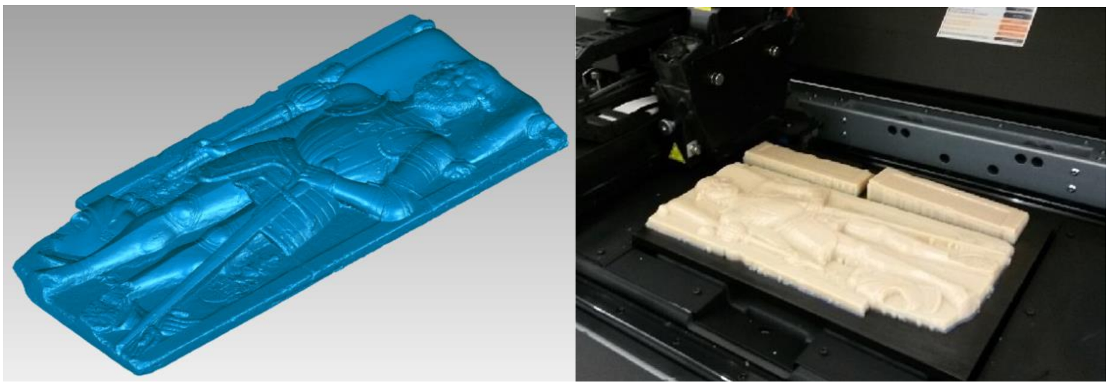

**Figure 5**: 3D scanning model and process of making
(Source: https://izit.hr/primjeri-iz-prakse/izrada-replike-nadgrobnog-spomenika-franje-tahyja-koristenjem-3d-tehnologija/)

The finishing was done in collaboration with an expert in the restoration of works of art. After that, the three-part model was glued to a wooden base and the display was achieved as in the original form, as it is shown on the figure 6.

**Figure 6**: Model of Franjo Tahy using 3D technologies
(Source: https://izit.hr/primjeri-iz-prakse/izrada-replike-nadgrobnog-spomenika-franje-tahyja-koristenjem-3d-tehnologija/)

### 3.4 Church of Saint Sava

The church of saint sava in belgrade is the largest serbian orthodox church. The height of the top of the dome is 70 m, while the main gilded cross is another 12 m high, which gives the temple a total height of 82 m. The 3d model of the temple was made at the faculty of mechanical engineering in belgrade. The 3d model is a scaled-down but credible version of the temple with all the details.

**Figure 7:** Original picture and 3d model of church of Saint Sava

## 4. CONCLUSION

Digitalization of industrial heritage, cultural monuments, objects, buildings, did not arise only because today we have the opportunity to do it, but it will have an increasing real significance in the coming decades. Significance of application of 3d scanning and modeling in the protection of cultural heritage is as follows:

- Secure storage of complete heritage information even in the event of loss of the original
- Possibility of detailed reconstruction based on available information
- creating interactive presentations of heritage that can be exchanged via the Internet or used in education
- 3D scanning and modeling can be applied in the preparation of the mold for already existing objects of historical significance, and thus ensure their re-creation and reconstruction.
- The increase of the interest of young people in history and cultural heritage

The study of the 3D printing materials and their suitability for the physical restoration of heritage might become an innovative field of research. 3D printing and 3D scanning can be used in countless ways and successfully applied in almost all activities from industry through medicine to art.

## REFERENCES

1. María Higueras, Ana Isabel Calero, Francisco Jose Collado-Montero, *Digital 3D modeling using photogrammetry and 3D printing applied to the restoration of a Hispano-Roman architectural ornament,* Digital Applications in Archaeology and Cultural Heritage 20, (2021), number e00179.

2. bdalmenem Owda, José Balsa-Barreiro and Dieter Fritsch, *Methodology for digital preservation of the cultural and patrimonial heritage: generation of a 3D model of the Church St. Peter and Paul (Calw, Germany) by using laser scanning and digital photogrammetry*, Faculty of Aerospace Engineering and Geodesy, Stuttgart, German, Emerald Publishing Limited [ISSN 0260-2288] [DOI 10.1108/SR-06-2017-0106], Volume 38, Number 3, 2018, 282–288.

3. Marina Gavryushkina, *The potential and problems of volumetric 3D modeling in archaeological stratigraphic analysis: A case study from Chlorakas-Palloures*, Cyprus, Digital Applications in Archaeology and Cultural Heritage 21 (2021), Number e00184.

4. Adrian S, muleac, Laura S, muleac,, Teodor Eugen Man, Cosmin Alin Popescu, Florin Imbrea, Isidora Radulov, Tabita Adamov and Raul Pas, *Use of Modern Technologies for the Conservation of Historical Heritage in Water Management,* Water 2020, 12, 2895; doi:10.3390/w12102895.

5. https://www.laserdesign.com/what-is-3d-scanning [Accessed: 1st August 2021].

6. https://formlabs.com/blog/how-to-use-3d-scanning-and-3d-printing-for-reverse-engineering/ [Accessed: 2nd August 2021].

7. Mila Koeva, *3D Modelling and Web-based Visualisation of Cultural Heritage objects*, The International Archives of the Photogrammetry, Remote Sensing and Spatial Information Sciences, Volume XLI-B5, DOI:10.5194/isprs-archives-XLI-B5-297-2016.

8. https://solfins.com/blog/3d-print-scan-6/post/primena-3d-stampe-i-3d-skeniranja-u-arheologiji-oblasti-kulture-i-zastite-spomenika-340 [Accessed: 3rd August 2021].

9. https://izit.hr/primjeri-iz-prakse/izrada-replike-nadgrobnog-spomenika-franje-tahyja-koristenjem-3d-tehnologija/ [Accessed: 3rd August 2021].

# GAMIFICATION OF MARKETING MATERIAL USING AUGMENTE REALITY

Igor Sabo[1*], Petar Pejic[2]

[1]Belgrade Metropolitan University, Faculty of digital arts, 11000 Belgrade, Serbia

[1]Belgrade Metropolitan University, Faculty of information technologies, 11000 Belgrade, Serbia

igor.sabo@metropolitan.ac.rs, petar.pejic@metropolitan.ac.rs

***ABSTRACT***

*Technological development and new digital tools bring additional opportunities for promotion and marketing. One such technology is augmented reality (AR) which can be used to present additional digital information's on top of traditional printed marketing materials. Gamification of marketing involves the incorporation of gaming elements into a non-gaming context to improve engagement levels and encourage users to take specific actions.*

*This paper analyses existing approaches in gamification of marketing materials using AR. The complete process of AR experience creation for marketing purposes with elements of gamification is presented in the case study. We create an AR experience for brochures that promote Bachler studies of Game development at Metropolitan University. Brochure cover is used as a marker for AR experience on the top of which small labyrinth game is presented. The user needs to find a way through the labyrinth, using the mobile application (the actual game).*

**Keywords:** Gamification; Augmented Reality, Marketing, Game, Brochure

## 1. INTRODUCTION

Technological development and new digital tools bring additional opportunities for promotion and marketing. One such technology is augmented reality (AR) which can be used to present additional digital information's on top of traditional printed marketing materials (Pejic, et al., 2017). Augmented Reality is an emerging computer technology where the perception of the user is enhanced by the seamless blending between a realistic environment and computer-generated virtual objects coexisting in the same space (Pejic, et al., 2015). The resulting mixture supplements reality, rather than replacing it (Pejic, et al., 2015). According to Azuma (Azuma, 1997), Augmented Reality represents a variation of Virtual Environments, or Virtual Reality as it is more commonly called. In these so-called Virtual Reality, the user is completely surrounded by a synthetic environment. In that state, the user can not perceive the real world and the real environment that surrounds him. On the contrary, the Augmented Reality allows the user to perceive the real world while the virtual elements are superimposed upon or composited with the real world (Ivan, 1968).

Gamification describes the enrichment of non-playful tasks with elements from video games, to give a normal real-world task a playful character. This can create motivation, foster fun and increase the overall user experience. Ultimately, this leads to a better (or at least a faster) performance of the gamified task (Korn, et al., 2019). In the area of education, gamified solutions called "serious games" have already proven to work well (Backlund & Hendrix, 2013). When game consoles with movement controllers like the Nintendo Wii (2007) and Microsoft Kinect (2010) came up, gamification also was applied more frequently in the health sector as application like "VI-Bowling" (Morelli, et al., 2010), or "motivation60+" (Brach, et al., 2011) show.

Gamification of marketing involves the incorporation of gaming elements into a non-gaming context to improve engagement levels and encourage users to take specific actions. The main objective of marketing is the satisfaction of consumer needs (Ferrell & Hartline, 2012). In order to maximize sales, marketing has made use of the Augmented Reality as a tool of promotion. All this has shown that marketing adapts to the constant changes that have arisen as technology continues to evolve. Although marketing strategies have been studied extensively and are directly oriented to traditional methods, the inclusion of various methods based on technological advances facilitates the promotion of new products in a more interactive way (Gallardo, et al., 2018).

In this paper, we present the historical development of Augmented Reality with a focus on existing AR games. The complete process of AR experience creation for marketing purposes with elements of gamification is presented in the case study. We create an AR experience for brochures that promote Bachler studies of Game development at Metropolitan University. Brochure cover is used as a marker for AR experience on the top of which small labyrinth game is presented. The user needs to find a way through the labyrinth, using the mobile application (the actual game).

## 2. AUGMENTED REALITY IN MARKETING

AR-based product visualization can be used to deliver interactive advertising experiences that connect with customers on a deeper level than traditional advertising. Opportunities are available for marketers to connect with potential customers using technology that allows customers to try out products from the safety and comfort of their own homes. Without the limitations of more mainstream advertising models, Augmented Reality finally come of age for marketing (Clark, 2021).

A recent report from Futurum Research and sponsored by SAS revealed significant pandemic-induced shifts in consumer behaviour and opinions including the acceptance of immersive tech. According to the report, 69% of those polled expect to use AR and VR to sample products in 2021, and 63% are willing to use AR and VR to visit remote locations.

An April 2020 report from ThinkMobile indicated that over 50% of smartphone owners already use AR apps when shopping, and IBM puts that figure at 32%. The numbers may be off due to the fact that many consumers are not even aware that they are using AR. Apps such as Google Translate using AR via their smartphone’s camera to see any text in 40 foreign languages as the user’s native language. Google SkyMap enables users to overlay their smartphone with the sky to see the names of the stars, planets, and constellations, all through the use of AR.

### 2.1 History of augmented reality

Over the last 50 years, Augmented Reality technology has reshaped the way we consume content in the real world (Poetker, 2019). The most important moments in the history of Augmented Reality are presented in the figure 1.

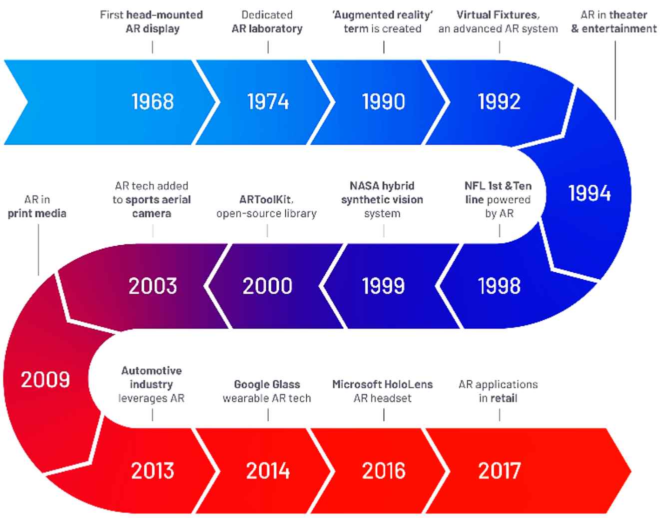


**Figure. 1**: History of Augmented Reality (Source: (Poetker, 2019))

1968: Ivan Sutherland, a Harvard professor and computer scientist, created the first head-mounted display called “The Sword of Damocles”. The user experienced computer-generated graphics that enhanced their sensory perception of the world. Within these walls, projection and camera technology was used to emit onscreen silhouettes which surrounded users for an interactive experience.

1990: Tom Caudell, a Boeing researcher, coined the term ‘augmented reality’.

1992: Louis Rosenberg, a researcher in the USAF Armstrong's Research Lab, created ‘Virtual Fixtures’, which was one of the first fully functional augmented reality systems.

1994: Julie Martin, a writer and producer, brought augmented reality to the entertainment industry for the first time with the theater production titled Dancing in Cyberspace. The show featured acrobats dancing alongside projected virtual objects on the physical stage.

1998: Sports-vision broadcasts the first live NFL game with the virtual 1st & Ten graphic system – aka the yellow yard marker. The technology displays a yellow line overlayed on top of the feed to that views can quickly see where the team just advance to to get a first down.

This system is still used today, although admittedly more advanced than it was in the late ‘90s. Viewers have become accustomed to the yellow line marker and other additional graphics – most don’t even know that this is a form of AR technology.

1999: NASA created a hybrid synthetic vision system of their X-38 spacecraft. The system leveraged AR technology to assist in providing better navigation during their test flights.

2000: Hirokazu Kato developed an open-source software library called the ARToolKit. This package helps other developers build augmented reality software programs. The library uses video tracking to overlay virtual graphics on top of the real world.

2003: Sport-vision enhanced the 1st & Ten graphic to include the feature on the new Skycam system – providing viewers with an aerial shot of the field with graphics overlaid on top of it.

2009: Esquire Magazine used augmented reality in print media for the first time in an attempt to make the pages come alive.

2013: Volkswagen debuted the MARTA app (Mobile Augmented Reality Technical Assistance) which primarily gave technicians step-by-step repair instructions within the service manual.

2016: Microsoft starts shipping its version of wearable AR technology called the HoloLens, which is more advanced than the Google Glass, but came with a hefty price tag. It’s definitely not an everyday type of accessory.

2017: IKEA released its augmented reality app called IKEA Place that changed the retail industry forever.

### 2.2 Augmented Reality games

One of the most popular Augmented Reality game is Pokémon GO. It is one of the most successful mobile games of all time, breaking records like fastest to earn $100 million and most-downloaded in its first month of release. To date, it has grossed almost $2 billion in revenue and been downloaded 800 million times. Although no longer the global phenomenon,  it was in 2016, the game remains incredibly popular. Pokémon GO is the world's most important game. Thanks to its success, it will almost certainly influence the design of future AR experiences for years to come. But the game could also have a broader impact on society through its potential health benefits (Chamary, 2018).

The game involves catching pocket monsters (Pokémon) at specific places via your phone (Figure 2). You also need to visit “Poké stops” check-in points at landmarks to collect items like the “Poké balls“ needed to capture those creatures. A tracker shows Pokémon at nearby stops and the weather at your position determines which kinds are available, enticing you to rush out and catch them. Your collection of creatures can also be used to battle other monsters in “gyms“ that earn rewards such as coins, which are used to purchase useful items (Skipper, 2016).


**Figure 2**: Pokemon GO screenshots (Source: (Skipper, 2016))

Another successful AR game is Angry Birds AR. In addition to appearing in tons of different video games (for both mobile devices and home consoles), the Angry Birds have their own merchandise (toys, clothing, etc.), multiple web series, and even feature films. The original Angry Birds mobile game was released on iOS in December 2009 and on Android in October 2010. It had a simple premise: Green pigs had stolen the Angry Birds' eggs, and players needed to help the birds retrieve them by launching their new feathered friends out of a slingshot toward the pigs' towers and defenses. While some Angry Birds games have different gameplay (for instance, Angry Birds Dream Blast is a mobile puzzle game that asks players to tap on blocks to remove them from the screen), the next game in the franchise takes the series back to its roots, albeit with an interesting twist (Berthelson, 2019).

Angry Birds AR: Isle of Pigs will use augmented reality (AR) technology on iOS or Android devices to cause the slingshot, birds, pigs, and the towers to appear as though they're in front of the player in the real-world (Figure 3). As a refresher, AR technology uses a device's camera to display the real-world environment on the device's screen so that in-game elements appear as though they're in front of players.


**Figure 3**: Angry birds screenshots (Source: (Berthelson, 2019))

### 3. CASE STUDY: AR MAZE BROCHURE

The complete process of AR experience creation for marketing purposes with elements of gamification is presented in the case study of the AR maze brochure. AR experience for brochure promote Bachler studies of Game development at Metropolitan University. Brochure cover is used as a marker for AR experience on the top of which small labyrinth game is presented. The user needs to find a way through the labyrinth, using the mobile application (the actual game). The mobile application is created using the Unity game engine and Vuforia Engine for AR component. Brochure cover (Figure 4) is used as a marker that trigger AR experience.


**Figure 4**: Brochure cower (Source: Metropolitan University)

The goal is to present small maze game on the top of brochure back cover. In the game, the user is guided small ball through the maze by physically moving the brochure, with the goal to find a way out of the maze. The project started with a 3D model of a maze, which was created in Autodesk Maya (Figure 5). It was created with polygon sorting, making it one big object in the end, that was exported as an FBX file prepared for Unity 3D.

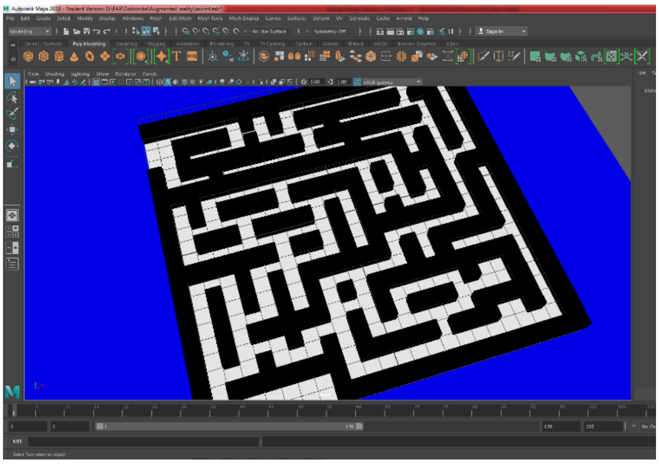

**Figure 5**: Maze 3D model (Source: authors)

Brochure cover photo (Figure 4) was converted to AR image target using Vuforia and imported in Unity. Maze 3D model (Figure 5) is also imported in unity and positioned on the top of image target (Figure 6). Blue ball was created as a simple 3D sphere. The script was created and attached to the ball that add physical parameters (gravity) which allow the possibility of movement by rotating marker. Final version of the application is built and exported for Android smart devices (Figure 7).

## 4. CONCLUSION

Gamification using Augmented Reality is currently gaining popularity in the academic and research world. Although there is little discussion and application in the commercial world about AR system and gamification combination, it is possible to make it happen since AR games have existed for a long time. This research was about mixing new technologies, art, gaming and marketing into one experience. Our case study proves that gamification of marketing material using augmented reality is possible and relatively easy to create using available and widely adopted Unity game engine and Maya 3D modelling software. Future research should measure the impact of created the AR experience and student’s opinion.

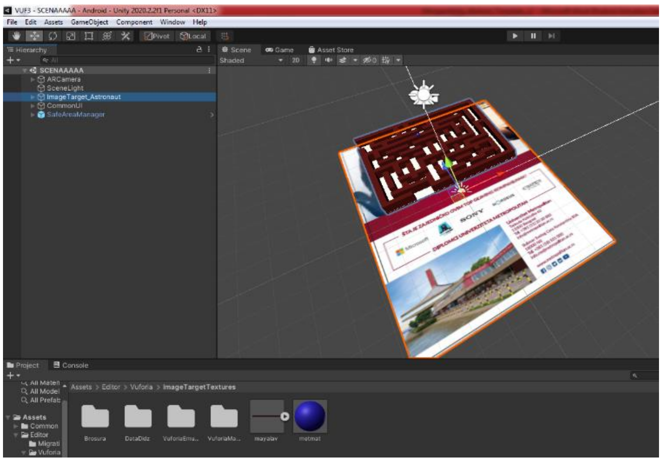

**Figure 6**: Unity (Source: authors)

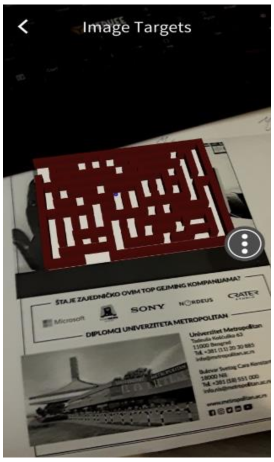


**Figure 7:** Final application (Source: authors)

## REFERENCES


1. Azuma, R., 1997. A Survey of Augmented Reality. Teleoperators and Virtual Environment, pp. 335-385
2. Backlund , P. & Hendrix, M., 2013. Educational games - Are they worth the effort? A literature survey of the effectiveness of serious games. 5th International Conference on Games and Virtual Worlds for Serious Applications (VS-GAMES), pp. 1-8.
3. Berthelson, B., 2019. Angry Birds AR: Isle of Pigs Lets You Defeat Pigs in Augmented Reality. Super Parent
4. Brach, M. et al., 2011. Modern principles of training in exergames for sedentary seniors: Requirements and approaches for sport and exercise sciences. International Journal of Computer Science in Sport, 11(1), pp. 1-13.
5. Chamary, J., 2018. Why 'Pokémon GO' Is The World's Most Important Game. Forbs.
6. Clark, S., 2021. Has Augmented Reality for Marketing Finally Come of Age? CMS WiRE.
7. Ferrell, C. & Hartline, D., 2012. Marketing Strategy. s.l.:Cengage Learning Editors.
8. Gallardo, C. et al., 2018. Augmented Reality as a New Marketing Strategy. Lecture Notes in Computer Science, Augmented Reality, Virtual Reality, and Computer Graphics, pp. 351-362.
9. Ivan, E. S., 1968. A head-mounted three dimensional display. Proceedings of the December, fall joint computer conference, part I. ACM,, pp. 757-764.
10. Korn, O. et al., 2019. Using Augmented Reality and Gamification to Empower Rehabilitation Activities and Elderly Persons. A Study Applying Design Thinking. Advances in Artificial Intelligence, Software and Systems Engineering, pp. 219-229.
11. Morelli, T., Foley, J. & Folmer, E., 2010. Vi-bowling: A Tactile Spatial Exergame for Individ-uals with Visual Impairments. Proceedings of the 12th International ACM SIGACCESS Conference on Computers and Accessibility, p. 179–186..
12. Pejic, P., Krasic, S., Petkovic, D. & Veljkovic, M., 2015. Application of augmented reality in facade redesign presentation. Journal of Industrial Design and Engineering Grapphics, 10(4), pp. 45-49.
13. Pejic, P., Krasic, S., Veljkovic, M. & Sakan, S., 2017. Augmented and virtual reality application in traditional architectural project presentation: Case study of MH Petra house. FME Transactions, pp. 227-231.
14. Pejic, P., Rizov, T., Krasic, S. & Tasevski, R., 2015. Presentation of Existing Architectural Objects Using Augmented Reality: Case study - Ada Bridge, Belgrade, Serbia. South East European Journal of Architecture and Design, pp. 1-4.
15. Poetker, B., 2019. A Brief History of Augmented Reality (+Future Trends & Impact). [Online] Available at: https://www.g2.com/articles/history-of-augmented-reality [Accessed 2021].
16. Skipper, B., 2016. Pokemon Go review: Nostalgic joy fuels Niantic's free-to-play catch 'em all simulator.

# TOPIC 2: APPLIED GEOMETRY AND GRAPHICS

# THE ABILITY OF UNREAL ENGINE TO CREATE AN INTERACTIVE SPACE FOR IMMERSIVE AND NON-IMMERSIVE TYPES OF VR SYSTEMS

Miloš Obradović, Assistant - Master[1], Jelena Kićanović, Assistant - Master[1]

[1]University of Novi Sad, Faculty of Technical Sciences, Department of Architecture and Urbanism, 21000 Novi Sad, Serbia

milos_obradovic@uns.ac.rs, kicanovicj@uns.ac.rs

**ABSTRACT**

*In the world of architecture, visualization has always been a central part of architectural design, and any project can be presented in many ways - using orthogonal drawings, 3D rendering, photorealistic renders, animation, real models, Augmented Reality, Virtual Reality, etc. Virtual Reality is increasingly present as an integral part of any architectural project. Also, any project can be created as an interactive visualization by using game engine like Unreal Engine. Projects designed in Unreal Engine can be created as an immersive, non-immersive, or semi-immersive system. The aim of this paper is to inspect the ability of Unreal Engine to create an interactive space for immersive and non-immersive types of VR systems. Also, a comparison of the software usage, for the given two systems, was made, as well as a parable of a different approach in a creation process of projects within the UE, for the given systems. As a result, the advantages and disadvantages of these types of system creations were highlighted, as well as the possibilities for improving the obtained results. By a presented research, it has been compared which type of system has a wider application in an interactive visualization. On the basis of everything analyzed, the conclusion has been made in order to define how, and to what extent, it is possible to simplify and equalize the way of creating both types of projects, so that the final result can be used for both systems, depending on the user will.*

**Keywords:** Virtual Reality; Interactive Visualization; Architectural Visualization

## 1. INTRODUCTION

Virtual Reality (VR) can be defined as a computer-generated environment with scenes and objects that appear to be real, making the users feel they are immersed in their surroundings (Virtual Reality: another world within sight, 2021). Also, VR is a term used to describe a computer-generated three-dimensional environment that a person can explore and interact with (Donovan A., 2019). The possibilities of user interaction with the virtual scene are based on moving through space and interacting with objects by changing them, lifting or capturing them, as well as using it as a way of reviving cultural heritage (Ferdani D. et al., 2020; Gaitatzes A. et al., 2001; Whyte J. et al., 1999; Gaoliang P. et al., 2010, Obradović M. et al, 2020).

With VR, the user is transported to a different space in which he/she interacts with digital objects, using assets in his/her virtual environment. In this way, the users change the way they look at a particular event, place and space, by participating in it (Zhanga Y. et al., 2019). 3D presentation has become the main tool of architectural representation. One of the ways how visualization and the experience of space are dramatically developing is Virtual Reality. Nowadays VR technology has a lot of potential for application in architecture (TMD STUDIO LTD, 2017; Šiđanin et al., 2017).

The aim of this paper is to inspect the ability of Unreal Engine software to create VR space for an immersive and non-immersive system. The advantages and disadvantages of immersive and non immersive system creations were highlighted, as well as the possibilities for improving the obtained results. By a presented research, it has been compared which type of project has a wider application in an interactive visualization. Finally, it has been analyzed whether, and to what extent, it is possible to simplify and equalize the way of creating both types of projects, so that the final result can be used for both systems, depending on the user will.

## 2. METHODS USED TO CREATE AN INTERACTIVE SCENE

Interactive visualization in architecture is used to allow the user to interact with a space, in which, for some reason, he/she is unable to reside, as well as to interact with a space that has not yet been built. It is a good tool for the real estate market, because it allows buyers to see the space as it should be in a future, before it is built.

### 2.1 Presentation of a Multi-Family Residential Building In a Row Using Virtual Reality

Interactive presentation in architecture can be observed through two examples, where the type of interaction differs, depending on the user's wishes. The first example is the creation of a virtual walk through space, where the user has the ability to move through a certain space, which is predefined so that his/her flow of movement is limited to a certain extent. For example, a door through which he/she can pass is open, while one through which he/she cannot pass is locked. The point of this type of interactive display is based on the fact that the user can experience the space by walking through it, either using a computer, or a VR headset and controllers. The degree of interaction is much smaller than in the example that follows, but the process of creating this type of project is much shorter and simpler.

**Figure 1:** View from the balcony (Screenshot - Unity Game Engine)

### 2.2 Interactive Presentation of a Single-Family Residential Building Using Virtual Reality

In addition to the ability to move through space and observe it, there is the ability to introduce certain interactions, which can be created using the programming language for a specific Game Engine. Interactions created in a specific engine, which are closely related to the interior and exterior, are moving through space, changing materials, changing furniture elements, interacting with individual elements in the form of opening or closing doors, turning on lights, and lifting certain elements. The process of creating this type of project takes more time than the previous example, which is only the basis of what can later be upgraded to the necessary interactions, using the various features of a given Game Engine.

**Figure 2:** View of the living room (Screenshot - Unreal Game Engine)

### 3. IMMERSIBLE, NON-IMMERSIVE AND SEMI-IMMERSIVE SYSTEMS

One of the differences between the immersive and non-immersive system is that the non-immersive is available to a larger number of users, because, in addition to computers, it does not require the possession of additional equipment (Kundalakesi M. et al. 2017). The immersive type of system, in addition to computers, requires the possession of equipment, headsets and controllers, which increase the degree of immersion of the user. CAVE (Computer automated virtual environment) is an environment created from projection surfaces, where the immersion of users into the virtual world takes place. The HMD (Head-mounted display) provides the same capability, but when using the equipment, the user does not see their physical environment around them. In this paper, both systems are analyzed on the example of Unreal Engine software. In the non-immersive system, when starting a project, the character has a rifle, as well as the possibility of firing bullets from a rifle. These segments can be removed, which is most often removed during interactive visualization in architecture. The possibility of interaction with objects, after the removal of the mentioned segments, has not been reduced. In the immersive system, the character has hands, which can be replaced by another model of hands, and the possibility of interaction with space is based on them, which the user moves using controllers.

### 4. USER INTERACTION WITH VIRTUAL SPACE

User interaction with virtual space can be observed through several basic stages, and they are related to the way of creating a scene, the possibility of user interaction with space, the way of moving through space, interaction with objects, and the ability to change elements and materials (Obradović M. et al. 2020). In interactive architectural visualization, the focus is on changing the elements and materials of the interior and exterior, moving through space, as well as on interactions with light and animated 3D models.

#### 4.1 The Way of Creating a Scene

Unreal Engine offers the ability to create several types of projects, while this paper analyzes FirstPerson and VirtualReality, that are used in an interactive architectural visualization. Segments of the first project can be implemented in the second, and vice versa, but not completely. Therefore, it is important to decide which type of project is the final product and accordingly choose the appropriate type at the very beginning.


**Figure 3:** Project types (Screenshot - Unreal Game Engine)

In the FirstPerson project, the user explores the space by using a computer, moves through the virtual space, and realizes all interaction by using the mouse and keyboard, as well as he/she does in video games. VirtualReality type of project is created on a computer, just like the previous one, but its application is tested with the help of headset and controller, and without the appropriate equipment it is impossible to test the created project as a whole. For this paper, a 3D model of the interior was used, in which all types of interactions were compared in both types of projects.

### 4.2 Moving Through Space

The difference in moving through space is that in the non-immersive type of project the user uses the keyboard to move on a predefined ground, which must have the appropriate collision, while in the case of using the immersive type of project, the user uses controllers for teleportation through space, taking into consideration in which direction his gaze will be directed, after teleportation. There is a possibility to implement the way of moving in the FirstPerson type of the project to the VirtualReality type of the project, where the user could move through the space without teleportation, but with a virtual walk. This way of moving through space can easily cause nausea and dizziness, because a large amount of images changes in front of the user's eyes, while he/she is physically standing in one place.

**Figure 4:** Movement through space (Screenshot - Unreal Game Engine)

**Figure 5:** Moving through space in an immersive system (Screenshot - Unreal Game Engine)

### 4.3 Interactive Objects

The programming system in Unreal Engine is based on Blueprint. The Blueprints Visual Scripting system in Unreal Engine is a gameplay scripting system based on the concept of using an interface based on interconnected nodes to create specific gameplay elements. By connecting nodes, events, functions and variables with the help of strings, it is possible to create complex gameplay elements. Blueprints work by using node charts for a variety of purposes — object construction, individual functions, and general game events — that are specific to each instance of Blueprint in order to implement behavior and other functionality (Thomsen M. 2010; Unreal Engine). When programming the interaction with objects in a non-immersive system, two CustomEvents were created, one related to picking up and the other to dropping elements. In the code itself, it is possible to set limits regarding the weight that can be lifted, as well as the way of lifting, rotating and lowering that element. The code binds to the character, which can then pick up any element in the scene, which fits the parameters written in the code, and it is not necessary to apply the code to each element in the scene, which significantly speeds up the work process.

In a non-immersive system, the interaction with objects is created in a different way. A variable to raise the element is created and a button is selected over which the element is held, or not held. A string of events is created, just as in the immersive system there are PickUp and Drop, so that the given CustomEvents can be linked to a predefined control. Using LineTraceForObject, a list of input parameters is generated, where it is possible to choose the type of object, the way in which the virtual line from the mouse will be displayed, as well as other tools based on input nodes. The location of the object that the user is holding is set so that it is in front of him/her, and the Grab Location and Physics Handle components have been created for a given function. Also, an event is created that is called (Event Tick) in each frame, so that it can recognize the location from which the user interacts. As the PickUp is connected to the lifting component, the Drop is connected to the Release component, which is used to drop objects. The logic of dropping and raising the element is based on the created loop. If the user does not hold a pre-programmed button, he/she does not hold the object, and the goal of the same is to lift the given object. If he/she holds the object, the output parameter is correct, and the user's goal is to drop the object. The variable, created at the beginning, is associated with PickUp and Drop events, where the boolean operation will be correct in case of object lifting, and in case of dropping, the same variable will be incorrect. It is necessary to adequately prepare the collision, so that the player is not blocked by the object he/she is carrying, but also not to create a situation to go through it. In order to prevent the object from rotating during holding it in the air, Angular Dumping was created. Finally, it is possible to choose how fast the object falls to the ground, or is there a possibility that it will fall under the influence of gravity. Also, there is an option to choose whether the user can lift each element, or only those that are heavier than a predefined value. With the immersive system, the whole procedure is simpler. The lifting of the elements is based on two CustomEvents, one related to the lifting and the other to the dropping of the object. It is necessary to add a physics simulation to both Events, where, if a given command is activated, the object is attached or detached from the user's virtual hand, using a specific button on the controller.

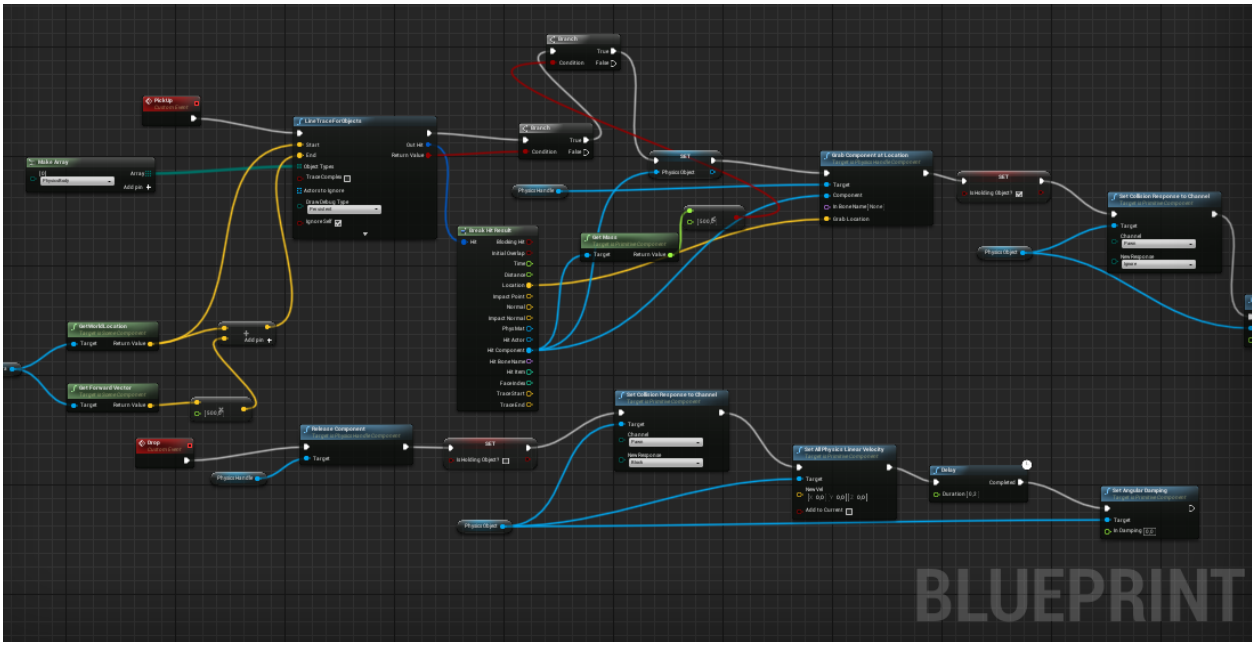


**Figure 6:** Blueprint for raising elements in a non-immersive system (Screenshot - Unreal Game Engine)

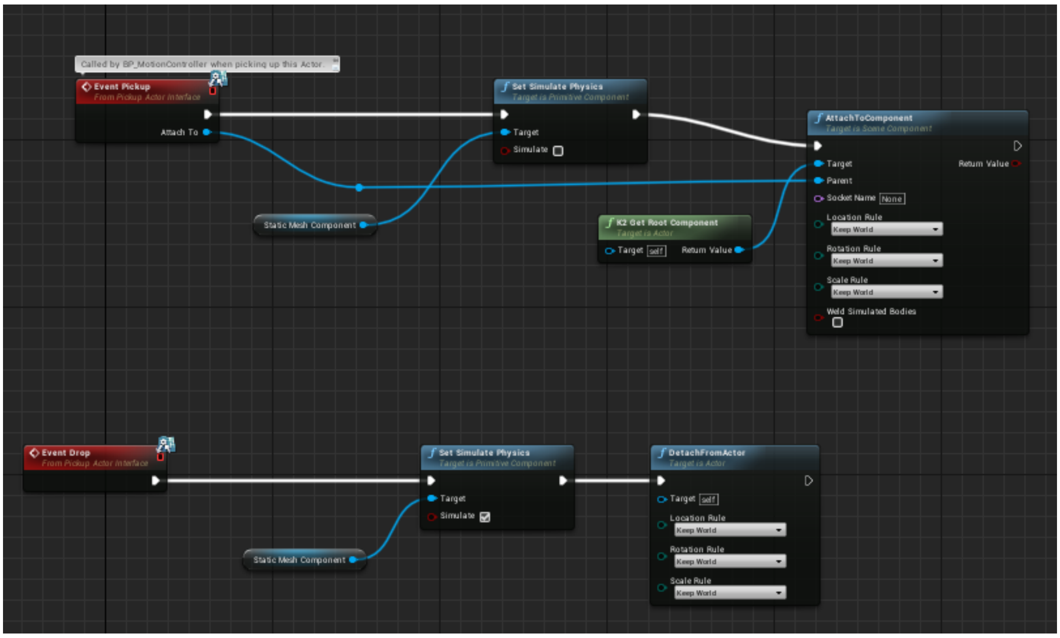


**Figure 7:** Blueprint for raising elements in an immersive system (Screenshot - Unreal Game Engine)

**Figure 8:** Picking up elements using both systems (Screenshot - Unreal Game Engine)

Interaction with models in the immersive type of project is simpler, because there is a pre-programmed Blueprint that can make any asset in the space interactive, ie. allow it to be picked up and dropped by the user. It is necessary to take into account the collision, because the interaction of the object is based on the contact of the virtual hand and the collision of the object, and it must be complex. The problem of applying Blueprint to each asset separately requires a lot of time when creating a project, so it is necessary to think in advance which models on the scene will be interactive, add a given Blueprint to them, and form a complex collision. Also, all assets must have appropriate physical properties, which directly affect how it is possible to interact with objects on stage.

#### 4.4 The Way of Interaction With Virtual Space

When creating an interactive space, it is necessary to take into account the elements that will be interactive (Obradović M. et al. 2020). This means lights, which can be turned on or off by applying a specific command. Also, it is possible to introduce interaction in the form of opening doors, windows, as well as other furniture elements, which imply preliminary analysis of 3D models into several segments, based on which an animation is created, which simulates a certain movement. Thus, the door is divided into a frame and a central part, where the central part rotates around the z axis so that the door opens towards the interior of the building. The animation can be activated with a command, which needs to be programmed. In both the immersive and non-immersive type of project, it is necessary to create a Collision Box, which is activated at the moment when the user of the space accesses that predefined range. At a given moment, it is possible to activate the command to perform a certain function, where in a non-immersive system a certain button on the keyboard is used, and in an immersive system, a certain button on the controller is used. The button selection can be changed at the user's request, and when the user goes outside the Collision Box, the given controls are disabled, so that it is not possible to turn on the light, if he/she is not near the switch for the same, nor to open the door, if he/she is not in front of it. The entire code can be applied to both types of systems, and the only difference is which button is used to activate it.

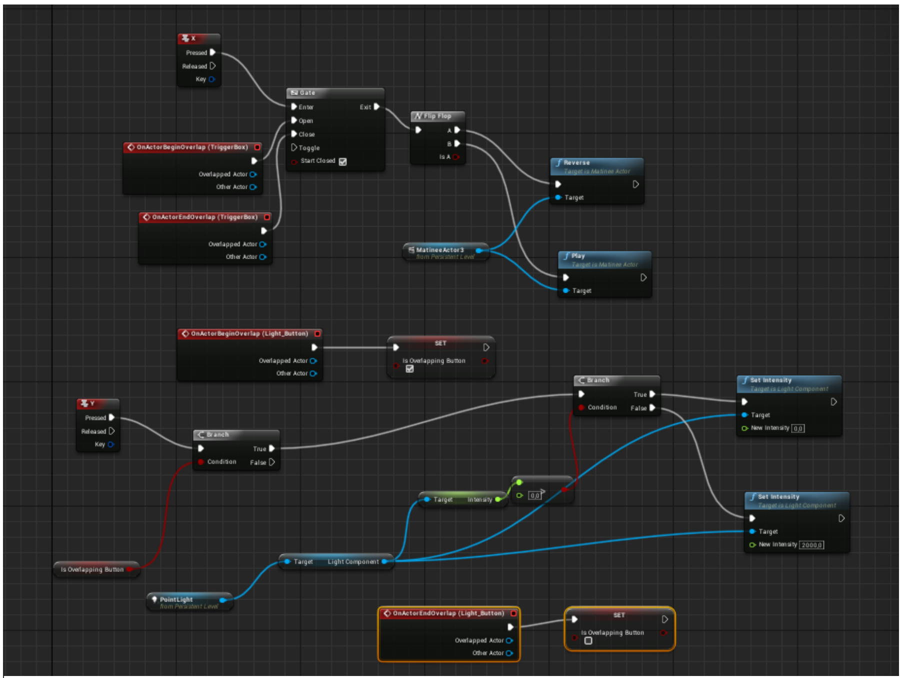


**Figure 9**: Blueprint for user interaction with elements in virtual space (Screenshot - Unreal Game Engine)

**Figure 10:** Opening the door (Screenshot - Unreal Game Engine)

Interaction with objects that change position is based on animation. A door opening animation was created via Add Matinee component, where it has been taken into account that the model that is moving must be physically separated from the one that will remain static. For example, the drawer will be pulled out, and the dresser will remain fixed in place. A Collision Box has been formed which will be activated when the user steps into it, while there is also an EndOverlap, which is switched off when the user goes outside the given frame. The Gate tool is used, which is followed by FlipFlop, which enables two outputs. A connection is established with something from the scene, in this case, with animation, which needs to be played back and forth so that the door can open and close.

In the case of light, Blueprint was made, which is a switch for turning on the light, where it is desirable to use the model of the light switch, as well as the Collision Box. The light is set to the desired location, and the intensity is set to zero. A variable has been created, and there should be two light intensities, one is zero, while the other is determined as desired. At the end of the code, there is an output value from the loop when the light is zero intensity, as well as when it has an intensity greater than zero.

### 4.5 Changing Elements and Textures

When a user finds himself/herself in a virtual space, it is likely that he/she will want to see what that space would look like with certain changes. Changes can be reflected in the form of material changes, but also certain geometries, by replacing certain 3D models. The replacement of the 3D model is based on the program code which consists of the creation of the Collision Box, in which, when the user accesses, he/she can replace the given furniture element with an appropriate command. When he/she goes out of that box, that option is disabled. It is necessary to think in advance which elements of the furniture can be changed, as well as which elements would be replaced. The selection of the interaction button can be changed, as in chapter 4.4, where, in the non-immersive system, the button on the keyboard is used, and in the immersive system, the button on the controller is used. Changing the material takes place independently of the geometry, with the help of a widget. Widgets can be seen constantly, only when the gaze is directed towards them, or when the user steps into a predefined space, by which they are activated. Also, when changing the material, it is necessary to take into account how the geometry is grouped, because it is not possible to change only the materialization of a certain segment of the 3D model, but the whole model, and in that case there should be unwrapped textures for the same. In a non-immersive system, the option to activate them when the user steps into a certain space showed a good degree of immersion, because at a given moment the entire gameplay is paused, the user has a mouse on the desktop, as well as widgets shown, and the user can use the mouse to choose which material he/she wants for the appropriate geometry. At that particular moment, he/she is disabled from all the other options, except from one to choose the material, as well as to interactively observe the changes in the current model. This way of changing the material is not cost-effective with an immersive system, because it is not possible to transfer options from the controller to another device, just as with a non-immersive system, the options are temporarily transferred from the keyboard to the mouse. The immersive system can use widgets that are activated when the user points the laser at them, and it is cost-effective to have them directly next to the object where the material needs to be changed. This type of material replacement is also possible with a non-immersive system. Also, there is the possibility of connecting two codes, where the user could change the model of the furniture with a certain button, and through the widget change the material of each of these 3D models. This way of interacting with objects in the scene is good because it gives the user the opportunity to influence the space to a great extent. Using the widget, it is possible to activate other, pre-programmed tools, and one of them can be teleporting to another space/level. Also, it is necessary to take into account that the interaction in the immersive system must be based on a virtual hands, and it is necessary to create a laser, through which the user can interact with widgets. The same laser can be applied to a non-immersive system, and at the touch of a button, the laser can be hidden or visible on stage.

**Figure 11:** Changing the color and 3D model (Screenshot - Unreal Game Engine)

In an immersive system, a laser is created and a Widget Interaction component is added to the BP_MotionController to be able to interact with the widget, which must be part of the Motion Controller in order to function. There is a possibility to adjust the laser colour, visibility and distance of interaction. There is also a laser disappearance code, where it is possible to choose whether the laser will be visible or not, by pressing a certain button. The initial value is also determined, so that the given laser is invisible. When the user presses the texture widget, the Blueprint created to change the material is called. The For Each Loop tool can be used when the same command is executed for multiple objects from an array, and this would be useful if, instead of one material replacement model, there were more than one. At the end of the code itself, the appropriate material is selected for each widget.



**Figure 12:** Blueprint for interactively changing models and materials (Screenshot - Unreal Game Engine)

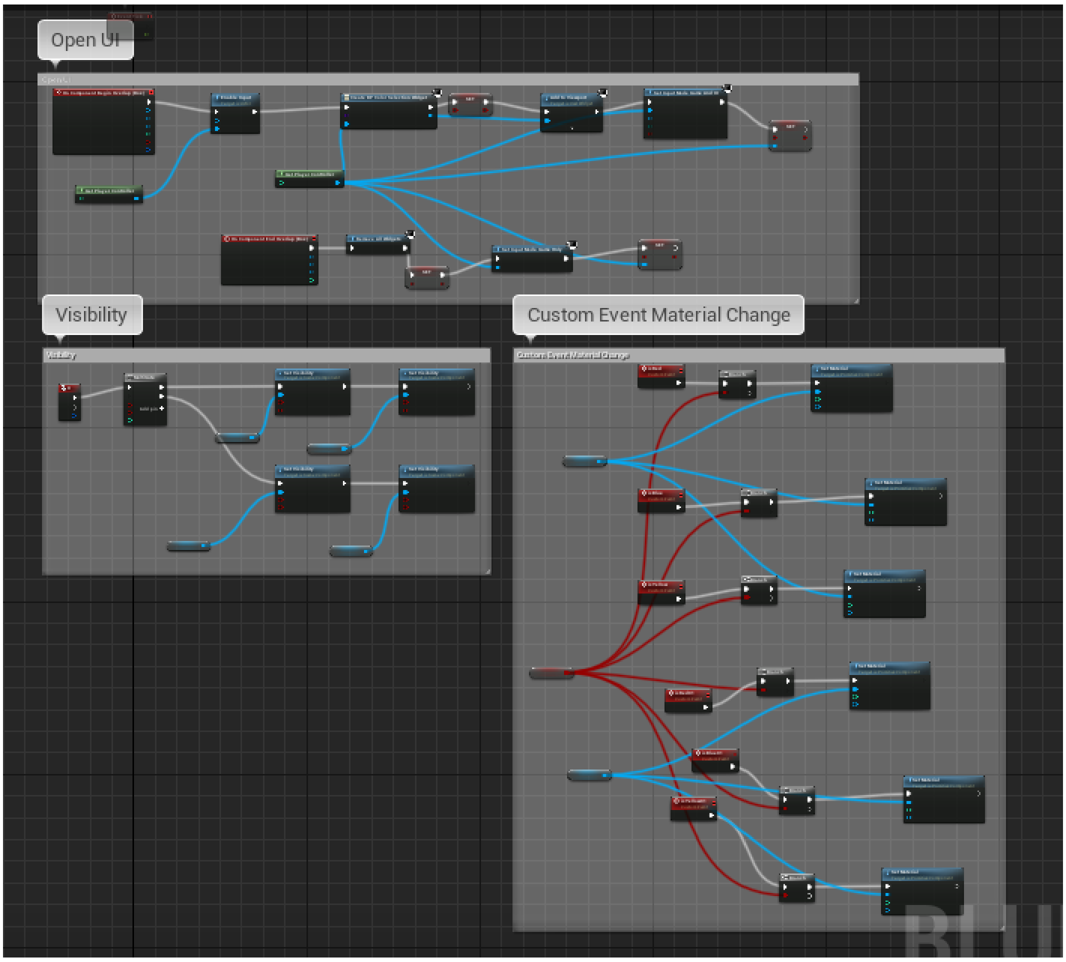


**Figure 12.** Blueprint for interactively changing models and materials (Screenshot - Unreal Game Engine)

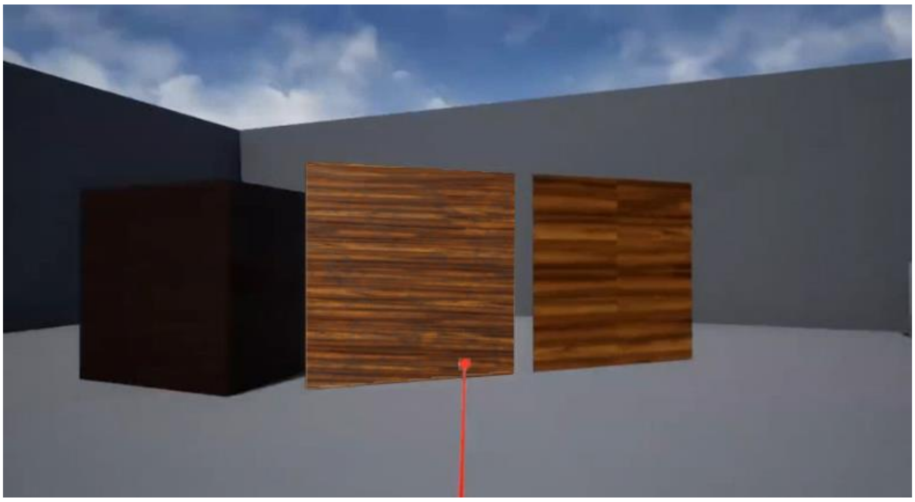

**Figure 13:** Laser interaction - Unreal Game Engine)

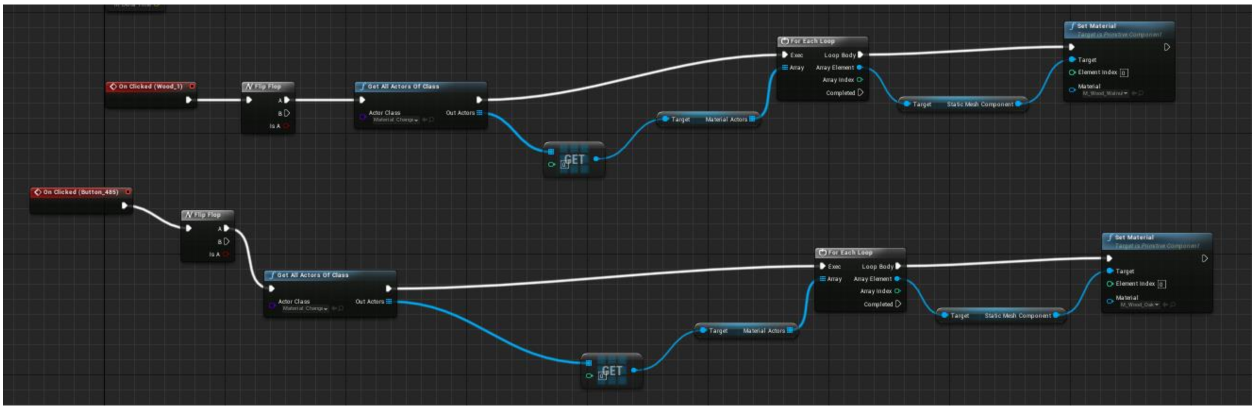


**Figure 14:** Blueprint for material change in immersive system (Screenshot - Unreal Game Engine)

For the immersive system, Blueprint was created, which consists of two components, which alternate so that one is visible and the other is not. A Collision Box has been implemented around the 3D model, on which the interaction takes place. The On Component Begin Overlap event refers to the moment a user steps into the scope of a given Box Collision. With MultiGate, it is possible, by selecting the button as desired, to change the model, influencing whether it will be visible or not. Asset was then connected with MultiGate, in order to be able to replace the two models. In a non-immersive system, widgets are created to change the material, which appear when the user steps into a given space, then a mouse appears and the image freezes. At a given moment, widgets are created and added to the viewport. On Component End Overlap decides that when exiting that space, the commands cease to be valid, and then the Remove All Widgets option is used. The Input Mode Game And UI set is the part where the user interface receives input and builds on the Add To Viewport. In the remove node, Set Input Mode Game Only is added, and then only the player receives inputs. A variable has been added, depending on whether the widget has been created or deleted. Finally, an event is added where the materials for both objects are adjusted. Then on the Blueprint Widget, when the user clicks the button, it is possible to invite all participants in the class of that Blueprint. An event created earlier, related to the material, is invited. Finally, by clicking on a specific widget, there is a possibility to change exactly that material.

**Figure 15:** Interactive model change

### 4.6. Advantages and Disadvantages of Immersive and Non-Immersive System

In order to be able to distinguish between the two systems, it is necessary to single out their advantages and disadvantages. One system has not completely supplanted the other, nor can it be more dominant and easier to use in all parameters. Also, not all users experience the degree of immersion in the same way, so to a certain extent the subjective opinion about which system has a more efficient application in the world of architecture is retained.

#### 4.6.1. Advantages

The advantage of the non-immersive system is that it is more accessible to everyone, as well as the fact that it is possible to find a lot of material on a given topic online, as well as in the professional literature. It is possible to create a project and export it so that it is available to anyone who owns a computer, regardless of whether they have an Unreal Engine installed. Codes related to the elements of interaction in sections 4.3. and 4.4. can be duplicated and used for multiple elements in the scene, meaning it is not necessary to write code from the beginning every time. Also, the codes can be implemented in another project. The advantage of the immersive system is that the user is in a virtual environment in which he/she is not physically present at a given moment (Kontos D. et al. 2020), where he/she is fully focused on it, has the ability to see and feel something that may be in the real world he/she couldn't. Everything that can be created for a non-immersive system can also be applied to an immersive system, with minor or major modifications. In this way, it is possible to experience a space that has not yet been created, or a space that is not physically available to the user at a given time. Also, interactive change of elements and materials is not possible in real space, and in that way the user can most easily decide on the appropriate solution.

#### 4.6.2. Disadvantages

With a non-immersive system, one of the disadvantages is the lack of immersion, because the user interacts with the space via a monitor, but is not in a given virtual space. If the user owns the equipment and uses an immersive system, it is necessary to calibrate it and take care that the sensors function adequately, there is a possibility of dizziness and nausea, because the user physically stands still, while in the virtual space, the user moves. Also, the project is more difficult to transfer to another computer, because that would mean having adequate VR equipment to run it. No matter how much immersion is in the immersive system, the use of the non-immersive system is more accessible and thus more widespread.

### 4.7. Possibilities to Improve the System

In order for the systems to be improved, it is necessary to establish the closest possible relationship between the two systems, so that anyone who aims to create an immersive project can work on non-immersive, but during testing would switch to immersive, using appropriate equipment. Writing codes for an immersive system differs in some segments from writing codes for a non-immersive system, and the optimal solution should be chosen, whenever possible, that can be used in both systems. Blueprint related to raising elements is simpler in an immersive system, because there are virtual hands there, and there is a possibility of creating a similar Blueprint system for a non-immersive system. Conversely, Blueprint can be used to lift elements from non-immersive to immersive, but it is an unnecessarily long process. In the non-immersive system, when navigating through the Collision Box, the user should choose one of the offered options, in order to change the material, and then other functions are disabled, and the same principle should be applied to the immersive system, where the immersion could be even higher. Both systems can be enhanced by adding individual asset, which users need to use to perform some functions, for example, to use a key to unlock the door. In every project, it is possible to use sound, in order to have a higher degree of immersion.

## 5. CONCLUSION

In the world of architecture, the non-immersive system is more widely used, due to its accessibility, multitude of available materials, and the need to have additional equipment, so users can easily opt for it and thus avoid nausea, dizziness, and everything that the immersive system has. It is necessary to simplify and equalize the work in both systems, so that the project is easily portable from immersive to non-immersive, and in non-immersive widgets that correspond to the immersive system should be used, a laser should be used, because communication between the two systems is easier The interaction needs to be feasible in both, and the only thing that changes is the character, depending on whether it is a FirstPersonCharacter or an VRPawn character. A compromise should be found for the way of raising the asset, more precisely, it is possible to use non-immersive program code in an immersive system, but the question arises to what extent it facilitates the work process, and whether it is profitable, which may be the subject of another research. Then the meaning of the Blueprint that already exists disappears and a double procedure is made. This interaction is not possible in the opposite direction, because in a non-immersive system there are no hands that would react to the collision. The goal is to find a compromise and use what could be used in both systems, and if the user decides on one from the very beginning, then it is possible to deviate from a solution that is suitable for both systems, but focus on one. If the user is not sure in which system he/she would like to work, it is necessary to create a project so that it can be used for both, depending on what the user will decide later.

## REFERENCES


1. Ferdani D. et al. 2020. 3D reconstruction and validation of historical background for immersive VR applications and games: The case study of the Forum of Augustus in Rome. Journal of Cultural Heritage 2020, Volume 43, 2020. pp. 129-143.

2. Gaitatzes A. et al. 2001. Reviving the Past: Cultural Heritage Meets Virtual Reality. Proceedings of the 2001 conference on Virtual reality, archeology, and cultural heritage 2001. pp. 103-110.

3. Gaoliang P. et al. 2010. A desktop virtual reality-based interactive modular fixture configuration. Computer-Aided Design. Vol. 42, pp. 432-444.

4. History of the Unreal Engine, 2012. *https://www.ign.com/articles/2010/02/23/history-of-the-unreal-engine* [Accessed: 15th March 2021]

5. How VR Technology Is Changing the Way Architects Design Your Home, 2019. *https://interestingengineering.com/how-vr-technology-is-changing-the-way-architects-design-your-home* [Accessed: 15th March 2021]

6. Introduction to Blueprints, *https://docs.unrealengine.com/en-US/Engine/Blueprints/GettingStarted/index.html* [Accessed: 25th March 2021]

7. Kontos D. et al. 2020. Performing 3D measurements in a VR environment. The International Archives of the Photogrammetry. Remote Sensing and Spatial Information Sciences, Volume XLIII-B2-2020. pp. 863–870.

8. Kundalakesi M. et al. 2017. A Study of Virtual Reality. International Journal of Trend in Research and Development, Volume 4(3), ISSN: 2394-9333. pp. 374-377.

9. Obradović M. et al. 2020. Implementation of the 3D model complexity in VR environment in the case of Novi Sad city center. FME Transactions ISSN (print version) – 1451-2092; ISSN (online version) – 2406-128X

10. Obradović M. et al. 2020. Interactive presentation in architecture by Virtual Reality. FME Transactions ISSN (print version) – 1451-2092; ISSN (online version) – 2406-128X

11. Obradović M. et al. 2020. Virtual Reality Models Based on Photogrammetric Surveys - A Case Study of the Iconostasis of the Serbian Orthodox Cathedral Church of Saint Nicholas in Sremski Karlovci (Serbia). Applied Sciences, 2020, Vol. 10, No 8, ISSN 2076-3417.

12. Šiđanin P. et al. 2018. Virtuelna i proširena realnost, koncepti, tehnike, primene. Novi Sad, Srbija

13. Virtual Reality Uses in Architecture and Design, 2017. *https://medium.com/studiotmd/virtual-reality-uses-in-architecture-and-design-c5d54b7c1e89* [Accessed: 10th March 2021]

14. Virtual Reality: another world within sight, *https://www.iberdrola.com/innovation/virtual-reality* [Accessed: 24th March 2021]

15. Whyte J., et al. 1999. From CAD to virtual reality: modelling approaches, data exchange and interactive 3D building design tools. Automation in Construction. Vol. 10, pp. 43–55.

16. Zhang Y. et al. 2019. User-centered interior finishing material selection: An immersive virtual reality-based interactive approach. Automation in Construction. Vol. 106, 10288

# TILINGS WITH DIAMOND, STAR AND PINEAPPLE SHAPES BASED ON THE GEOMETRY OF THE REGULAR PENTAGON

Marija Đ. Obradović[1]

[1]University of Belgrade, Faculty of Civil Engineering, Department for Mathematics, Physics and Descriptive Geometry, Bulevar kralja Aleksandra 73 11000 Belgrade, Serbia

marijao@grf.bg.ac.rs

***ABSTRACT***

*This paper presents a gallery of tessellations created by combining the following equilateral shapes: diamonds and stars, which can be further assembled into a pineapple shape. These three shapes can be decomposed into simpler shapes: an isosceles triangle and a rectangle. The triangle is formed by a subdivision of the regular pentagon into five equal sections, so that each have a base of length* $\boldsymbol{a}$ *and legs of length* $\boldsymbol{b}$*. The rectangle is created by having the same* $\boldsymbol{a}$ *and* $\boldsymbol{b}$ *for its sides. The diamond is formed by two such triangles and one rectangle, while the star is formed by a radial arrangement of five triangles back into the pentagon onto which five more triangles are added (elevated). Using these two shapes, we can tile the Euclidean plane without overlaps and gaps in different ways, including the pentagonal matrix. They can be further assembled into a "pineapple" shape, which can also tile the plane arranged in different ways, using only one shape (tile). We present several examples that include: periodic, non-periodic, rotational, radial and free-form tessellations. These shapes, in addition to their visual attractiveness and decorativeness which can be used in design, also hide the connection with patterns that can be found in nature, similar to Turing patterns.*

**Keywords:** pentagon, star, tiling, isosceles triangle, rectangle.

## 1. INTRODUCTION

Tilling the plane is one of the oldest problems in geometry, and yet it is still relevant in modern days. Both in the theoretical and in the practical sense, solving the fitting of congruent or incongruent planar figures, captures the attention of both scientists and designers. Nowadays, with the advent of graphics software, generating geometric patterns based on the division of the Euclidean plane has been greatly facilitated compared to earlier epochs when the tool for solving these problems was restricted to classical accessories: ruler, compass and knowledge of trigonometry. However, in addition to the computer aided approach, this problem is especially addressed by scientists from the aspect of group theory.

In this paper, we treat the problem purely from the aspect of constructive geometry, 2D transformations and CAD, which facilitates the construction and generation of identical regular or irregular polygons. The emphasis is on the possibilities and diversity of pattern creation, so a gallery will be displayed as an overview of the assorted solutions. To obtain them, in addition to geometric thinking, there is also a merit of spatial understanding and some creativity, which still offers solutions that escape algorithms.

The starting point of the research is the shape of a regular pentagon. This polygon is the first in a series of single-digit-sided polygons that "detaches" in its geometry from the polygons that surround it: equilateral triangle, square and hexagon. These polygons, including the octagon, appear in many convex regular-faced polyhedra, while in the Euclidean, *k*-uniform tillings (Grünbaum et al., 1977) they partake with only one other polygon: dodecagon. However, the regular pentagon appears in a number of regular-faced polyhedra, for example in the Platonic solid, dodecahedron, and also in Archimedean and Johnson solids (Johnson 1966), although it does not participate in 2D tilings with regular polygons (Grünbaum et al., 1977). Trigonometrically, no other regular polygon complements the pentagon to the point of assembling even a local patch without gaps and overlaps, let alone the entire plane. Therefore, this shape has been a challenge for solving the tiling problem from antiquity to the present day. It is well known that progenitors of many geometric settings, such as Dürer (1525) or Kepler (1619) dealt with this problem. Each of them gave their own solutions which, in addition to the regular pentagon, included other forms (Lück, 2000). In Dürer's solution, it was a radial tilling that included rhombuses in addition to the pentagon. In Kepler’s, a more complex one, the forerunner of later solutions in the domain of symmetric groups, in addition to the pentagon we encounter a "star" polygon (pentagram, pentagon stelation), a decagon, and another form merging two decagons, which he named a "monster." The pentagon, as unsolvable for tiling with other regular polygons, remained a problem not only as a shape of the tile, but also as a shape of the base to be tiled. Many mathematicians dealt with this problem after Kepler, but it was not before the 20th century that the satisfactory solution was found. Robert Penrose (1074) gave his result that met the requirements of 5-fold symmetry. His solutions appears in three variations and only in one of them does the regular pentagon take place. Along with the pentagon, two more shapes appear in this solution: the “boat” and the rhombus. In the other two solutions, Penrose reduced the number of shapes to only two, and neither of them is a regular polygon. In one of the variations the shapes are "darts" and "kites", and in the other they are "thick" and "thin" rhombus.

Guided by these examples, the solutions in this paper are given, using the geometry of the pentagon and its angular measures, while the pentagon itself does not appear as such. Actually, in the presented solutions, the pentagon-based field can be tiled in 5-fold symmetry using the proposed tile shapes, namely: “diamond” (in fact: elongated rhombus), “star” (not a stelation of the pentagon as in Kepler’s solution, but its elevation) and “pineapple” (a shape formed as a conglomerate of two diamonds and one star). All these shapes are equilateral and made up of two primary shapes: an isosceles triangle and a rectangle. The ratios of their sides correspond to the ratio of the side $\boldsymbol{a}$ of the pentagon and the radius $\boldsymbol{R} = \boldsymbol{b}$ of its circumscribed circle. The procedure for obtaining these shapes and the tilings themselves will be described below.

## 2. DEFINING TILE SHAPES AND THEIR CONFIGURATIONS

This paper is a continuation of the research presented in the paper (Obradović et al., 2021) (in print). As explained in the aforementioned source, the inspiration for the presented solution(s) of a pentagon based tiling, and consequently for the shapes of the tiles, came from the spatial covering of a specific polyhedral composition. The polyhedra that constitute it are: concave cupolae of the second sort (Obradović et al., 2008) with the pentagonal base, minor type (*CC-II- 5.m*). The covering itself consists of equilateral triangles and squares that fit exactly on the triangular faces of *CC-II-5.m*, thus building a complex corrugated polyhedral surface. Orthogonally projected onto the plane of the cupolas’ bases, we obtain shapes: an isosceles triangle and a rectangle, whose sides have a ratio corresponding to the ratio of the side of the regular pentagon ($\boldsymbol{a}$) and the radius of the circle circumscribed around it ($\boldsymbol{b}$). Thereby: $a\colon b = 1\colon \frac{\varphi}{\sqrt{(1+\varphi^2)}}$. As is well known, when it comes to a regular pentagon, $\varphi$ represents the golden ratio. In other hand, the triangles are created by radially subdividing pentagons into five equal sections, while rectangles can be seen as polygons inserted between them within a regular decagon (Fig. 1 a). Such a disposition of shapes can also be identified as an orthogonal projection of the Johnson solid J5 (Johnson 1966), a pentagonal cupola.

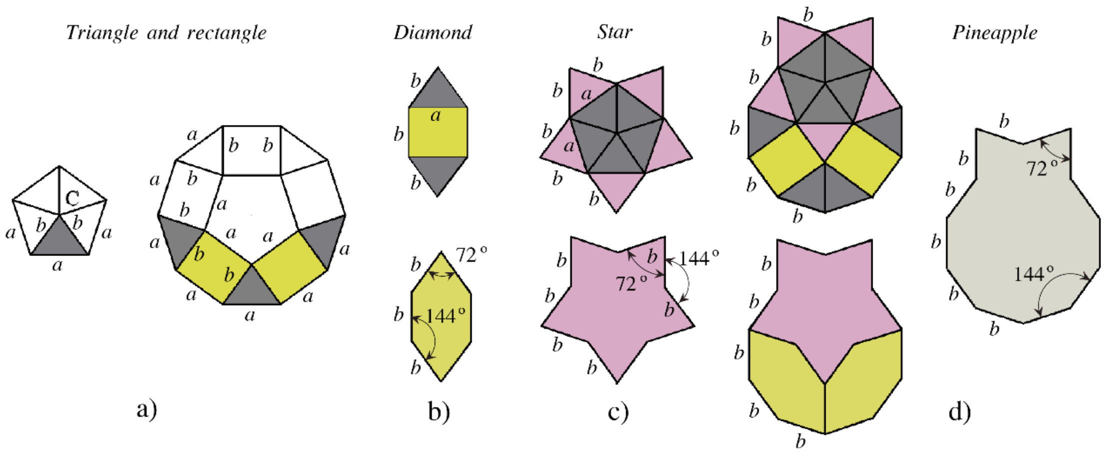


**Figure 1**: Shapes of the tiles used for tiling: a) triangle and rectangle, b) diamond, c) star, d) pineapple

By combining these two shapes, we get shapes of "diamond" and "star". The diamond is actually an elongated rhombus composed of two isosceles triangles reflexively symmetrical across the sides of triangle $a$, between which a rectangle is placed (Fig. 1 b). The star is a shape created by elevation (augmentation) of a pentagon, by adding a new isosceles triangle onto each of its sides, reflexively symmetrical across the side $a$ itself (Fig. 1 c). These two shapes, thus, always contain starting triangles and rectangles, so they can be substituted by such elementary shapes in another form of the solution. Just as the diamond and the star are made up of triangles and rectangles, we can create new shape out of them as well. Such a shape is named a "pineapple" (Fig. 1 d), and it contains one star and two diamonds, reflexively symmetrical in relation to the axis of the star overlapped with the side of the diamond itself. (This shape is named “shield” in (Li et al., 2017), but we keep the name already used in Obradović et al., 2021.)

We can manipulate this shape easier than the composition of the star and the diamonds, and even tile a whole plane solely by this single shape. Therefore, in the illustrations given in the paper, we will encounter the shape of pineapple along with diamonds and stars, although it can be reduced to more and more elementary shapes: first to diamonds and stars, and then to triangles and rectangles. Hence, the method of creating tilings, and the rule we use to generate them is the substitution rule.

### 2.1 Tile grouping and forming the aggregations of tiles

In order to form a tiling, it is necessary to arrange the tiles next to each other without overlapping and gaps. Such fitting of the chosen tiles is enabled by their angular coordinates. As we can see in Fig. 1, angles of 72$^o$ and 144$^o$ (216$^o$) appear as the angular measured of the tiles, which easily complement each other to $2\pi$ angle. This ensures that, with the given shapes, we can continue arraying the tiles in an arrangement that may be geometrically determined, but also arbitrary, even generative. To facilitate the tiling generation, instead of individual sequence of tiles, we can use their grouping into aggregates that we can use either as new tiles, or as a kind of “core” from which we proceed in arranging the tiles.

In Fig. 2, some of such shapes are given, as an illustration of the aggregation of tiles that we use to expedite pattern establishing.

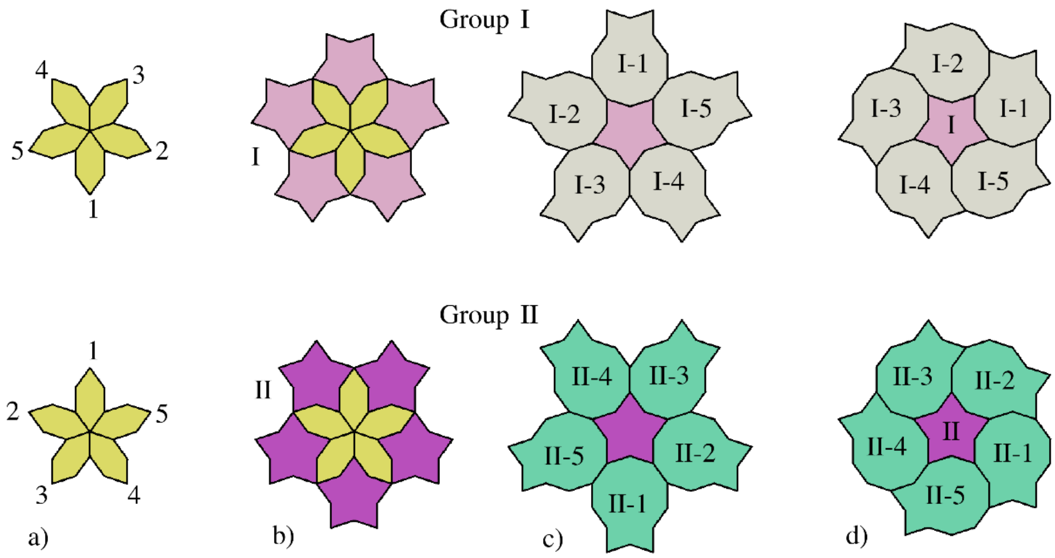


**Figure 2:** Grouping the tiles into aggregations: a) diamonds, b) stars of Groups I and II, c) pineapples of Groups I and II, s) tiles of Group I and II aggregated in the new “lettuce” formation

We see that diamonds can be arranged in the positions rotated by 72$^o$ in relation to the adjacent one, establishing 5-fold symmetry. Whether placed with a vertical diamond "up" or "down" in such an arrangement, their five possible positions remain the same (1, 2, 3, 4 and 5). However, this will not apply to stars and pineapples. Thus, if we rotate a star around its centroid by 180°, we get two different positions: “I” and “II”. Position "I" is shown with the star point on the vertical axis "down", and position "II" with the star point "up".

The pineapple can have positions as in Fig. 2 c, and 2d. If the "star" section of the pineapple is set in position “I”, we have a pineapple tile of Group I in which five different positions of the tile itself are possible (shown in light gray). We also have another five positions of pineapple tiles in Group II (shown in green), so there are a total of 10 positions of pineapple tiles.

**Note:** In order to make it easier to follow the resulting patterns, the different positions of the tiles from Groups I and II are shown in different colors.

In the following examples, we will see how these tiles can be arranged in different types of tiling: from periodic, non-periodic, rotational, radial to free form.

## 3. PERIODIC TILING WITH DIAMONDS, STARS AND PINEAPPLES

Periodic tiling implies such an arrangement of tiles (prototiles), or regions (fundamental region, composed of several prototiles), where they are transformed by translation. If we can establish a relation of translation to the entire tiling, then we have a periodic sequence of tiles. K-uniform tilings are actually all periodic tilings.

In Fig. 3 we see pineapple tiles of Group II-1 forming a periodic tiling (Fig. 3 a). We can break them to diamonds and stars (Fig. 3 b), and then to triangles and rectangles (Fig. 3 c). It is clear that in an identical way we can form a periodic tiling using any of the remaining 9 positions of pineapple tiles, just as we can convert a given solution into any of them by a simple rotation for $n \cdot 36^o$, where $n \in \{1, 2, 3, 4, 5, 6, 7, 8, 9\}$.

By combining tiles of Group I and Group II, we can also obtain periodic tiling. Tile I-1 and II-1 adhere to each other without overlapping or gaps, so that they can be arranged in rows, as shown in Fig. 4 a. Also, using the feature that the pineapple tiles of the same numbers from Groups I and II adhere perfectly onto each other, we can form different zigzag repetitive tilings, as shown in Fig. 4b and c, where we have an alternating series of tiles I-2 and I-3 with II-2 and II-3. Depending on the number of tiles in a row $(2, 3, 4, \dots n)$ and the multiplicity of rows of tiles from the same group, we can get an infinite number of different solutions based on this same scheme.

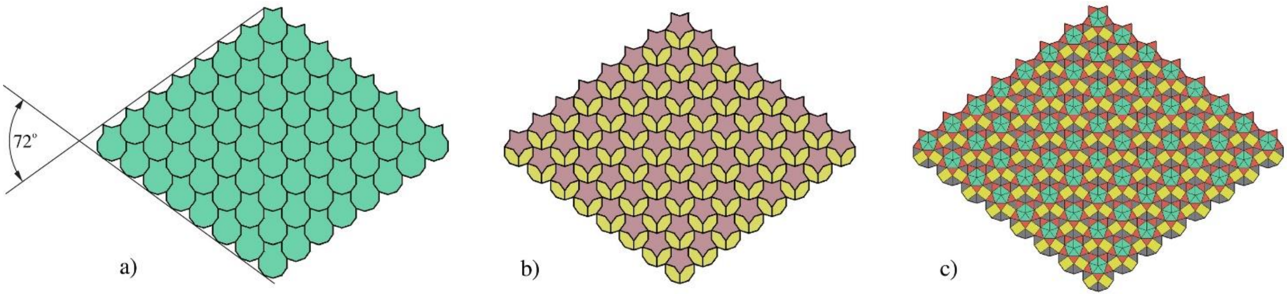


**Figure 3**: Periodic tilings with: a) pineapples, b) stars and diamonds, c) triangles and rectangles

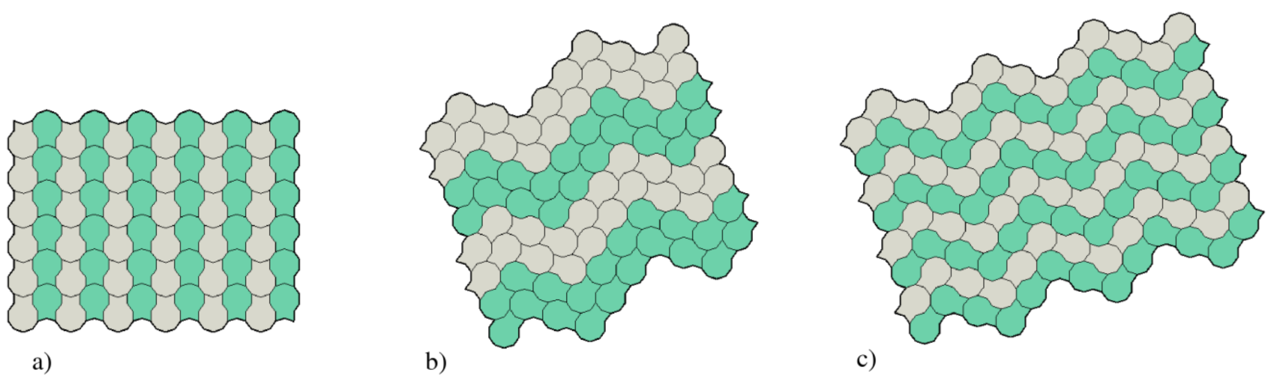


**Figure 4**: Periodic tilings with combinations of the tiles from Groups I and II arranged in rows

In Fig. 5 we see the tiling obtained using an aggregation of pineapple tiles of Group II, as in Fig. 2 d. In addition to this shape, pineapple tiles: II-4, I-4 and I-2 are used, together with star tiles both of I and II position and diamond tiles, in order to "clog" the gaps between these aggregations. Such tiling is named "garden" because the shapes used are reminiscent of vegetable shapes: leaf, flower, pineapple, lettuce.

This surely does not exhaust all the possibilities of creating periodic tilings with these shapes of tiles. Also, combinations of different "patches" of periodic arrangements are possible, i.e. with locally organized tiles in periodically tiled regions that complement each other. The layout of these regions and the way the tiles are arranged within them depend on the designer's intention, creativity and the geometric needs of the tiling surface itself, so they can have a decorative and even artistic role along with the geometric one.

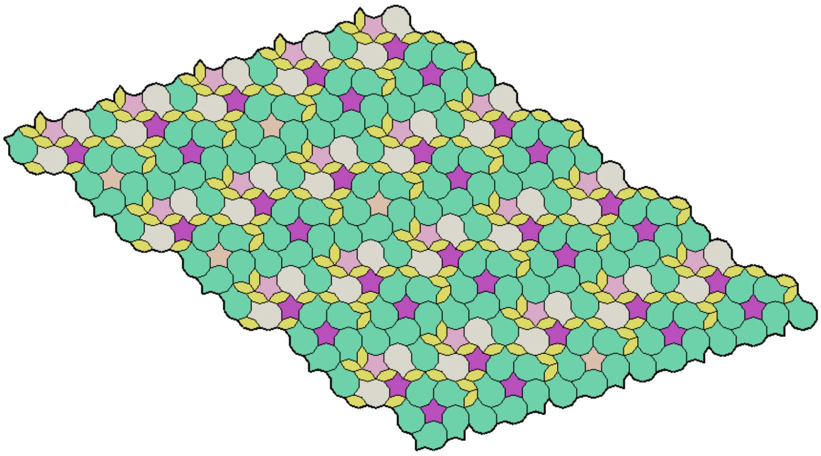

**Figure 5:** The "garden" tiling composed of tiles and the aggregations of tiles from both Groups I and II

Fig. 6 shows two examples of crossing two or more periodic pineapple tillings into one, supplemented by diamond and star tiles.

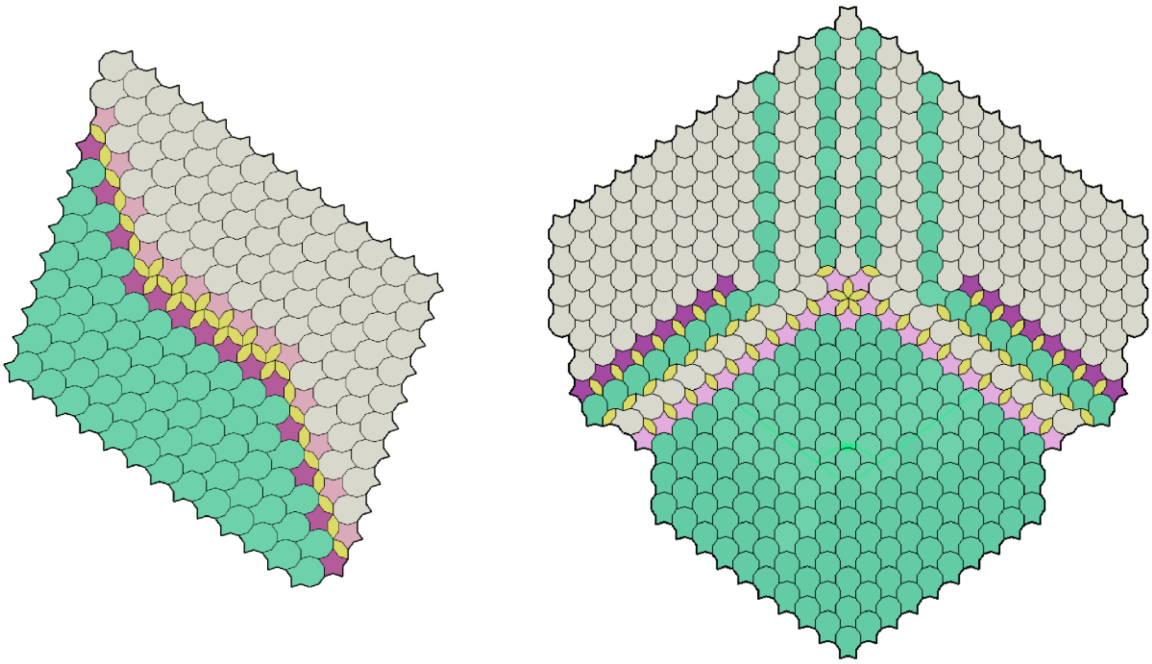

**Figure 6**: Tiles obtained by combining regions periodically tiled by the pineapple tiles from Groups I and II

## 4. NON-PERIODIC TILING WITH DIAMONDS, STARS AND PINEAPPLES

Non-periodic tilings, as their name suggests, cannot occur by applying (only) translation. The presence of local translation is possible in these arrangements of tiles, but in general, they occur by using other transformations or procedures. For example, they can be created by dividing the tiles of a periodic tiling, so that we get a non-repeating pattern. More demanding to create, especially for n-fold symmetries where seamless fitting of adjacent regions is required, are tilings obtained by rotation (perhaps most common for polygonal, and thus pentagonal bases). Such tilings can be radial, displaced radial (Shawcross, 2012) or aperiodic. Aperiodic tiling excludes translation and we do not find it even in local regions. The problem of aperiodic tiling is one of the most challenging in the whole subject of tiling the Euclidean plane and is relatively recent (solved in 20th century by R. Berger, R. M. Robinson and R. Penrose). The most famous among them is Penrose tiling, based on the geometry of a regular pentagon, as well as the cases considered in this paper. However, unlike Penrose tilling where rotational symmetry can be established locally in multitude of different centers, in the given solutions there is one center only.

Here, we present a several examples of tilings with rotational symmetry, created by rotating planar regions within a sector of 72 degrees, using a polar array of 5 such elements within a range of $2\pi$. The differences between them are mainly reflected in the organization of tiles within a given region.

The tiles can be arranged by applying translation alone, and by using a single tile (pineapple), with the exception of one, the star, in the center of rotation, as shown on Fig. 7. This is exactly the tiling that emerges as a projection of the spatial "covering" (Fig. 7 d), presented and explained in Obradović et al. (2021). Such an arrangement of tiles within a pentagonal base that can be spread to infinity. It is actually a radial tiling, because all tiles are arranged in rows that radiate from the center of rotation onwards to infinity.

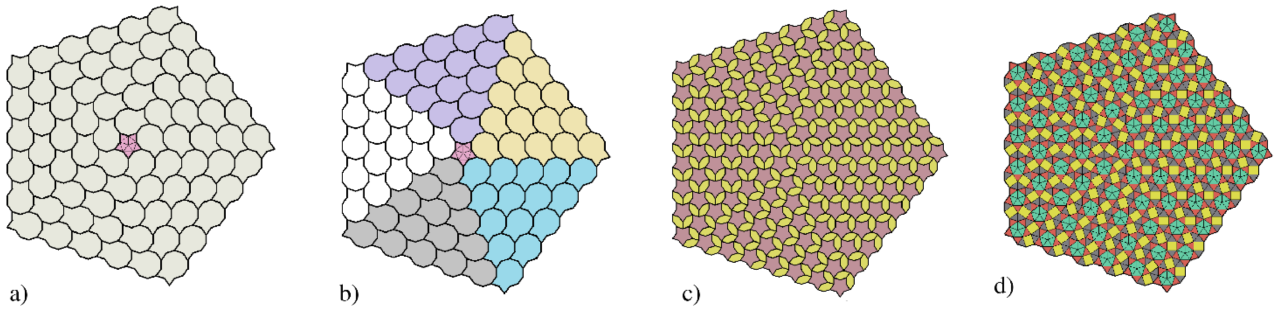


**Figure 7**: Radial, pentagon based tiling with a) pineapples, b) pineapples in periodic regions, c) the tiling reduced to diamonds and stars, d) the same tiling reduced to triangles and rectangles

### 4.1. Radial and rotational tilings

Radial tiling can be obtained in many different ways, and one of them is shown in Fig. 8 a, where clusters of diamond tiled fill the zones between rows of pineapple ones.

If we place the rows of tiles so that their main directions do not cut across the center of rotation but past it, we encounter the so-called "displaced" radial tiling (Shawcross, 2012), but it is still a rotational tilling with a periodic and predictable arrangement of tiles, which can be spread to infinity with an evident pattern of further sequence.

In some of the examples (Fig. 8 a, c) we see that diamond tiles play the role of independent factors that form entire local regions without the presence of other tiles. They can also form tiling independently, as shown in Obradović et al. (2021) (see Fig. 6 a). Also, we notice that in such solutions, we start from the "core" in the center of rotation, defined by a rotationally symmetrical arrangement of tiles. In the examples given in Fig. 8 a-c, these solutions corresponds to the group of tiles shown in Fig. 2b, Group I, while in the solutions in Fig. 8 e-f in the "core" we find the groups of tiles shown in Figure 2 d (or their variation, in Fig. 8 d).

Further sequence of tiles, starting from the given "core", can be quite diverse, almost arbitrary, but certainly with respect to the rules of tile fitting. What we have to keep in mind is the fit of two adjacent regions rotated by 72° (in the polar array of 5 items in the $2\pi$ range), which reflects on the definite layout of the tiling.

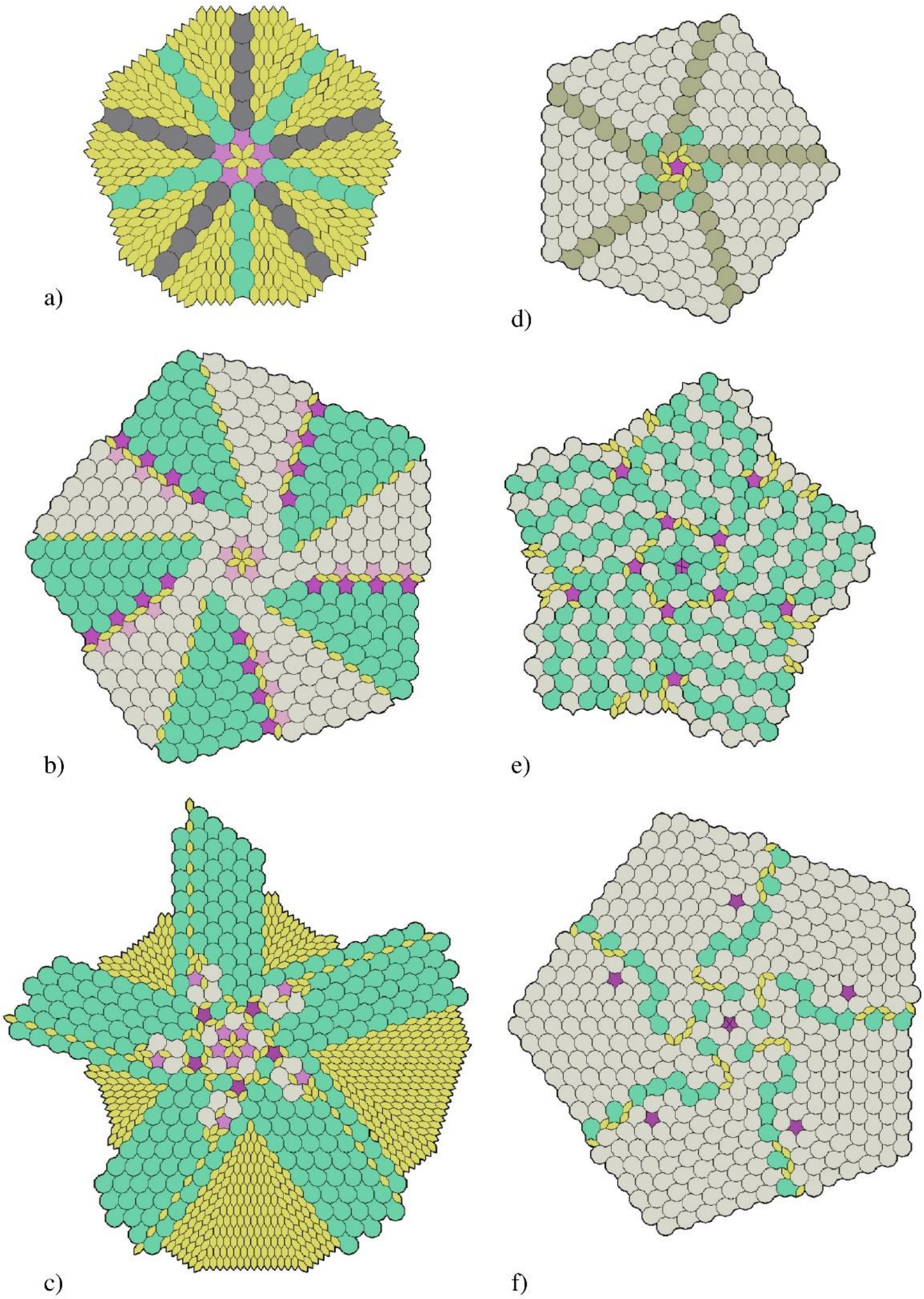


**Figure 8**: Some examples of radial tilings

If the tiles do not respect the stringing within the selected region, i.e. a radial arrangement in relation to the center of rotation, but form distinct patterns with possible new centers of rotation, as in Fig. 9 a, b, c, and e, it is a simple rotational tiling. Although these solutions may be seemingly similar, they actually differ not only in the selection of tiles from different Groups I and II, but also in their disposition. It is important to note that even a slight change in the position of a single tile, leads to a completely different arrangement of the subsequent tiles. Thus, we can create a multitude of different solutions.

The solution in Fig. 9 d could almost be treated as (displaced) radial or even spiral, but still, due to the irregular change of the tiles' directions from the different groups (Groups I and II) and their formation by rotation, it is placed among the rotational tilings.

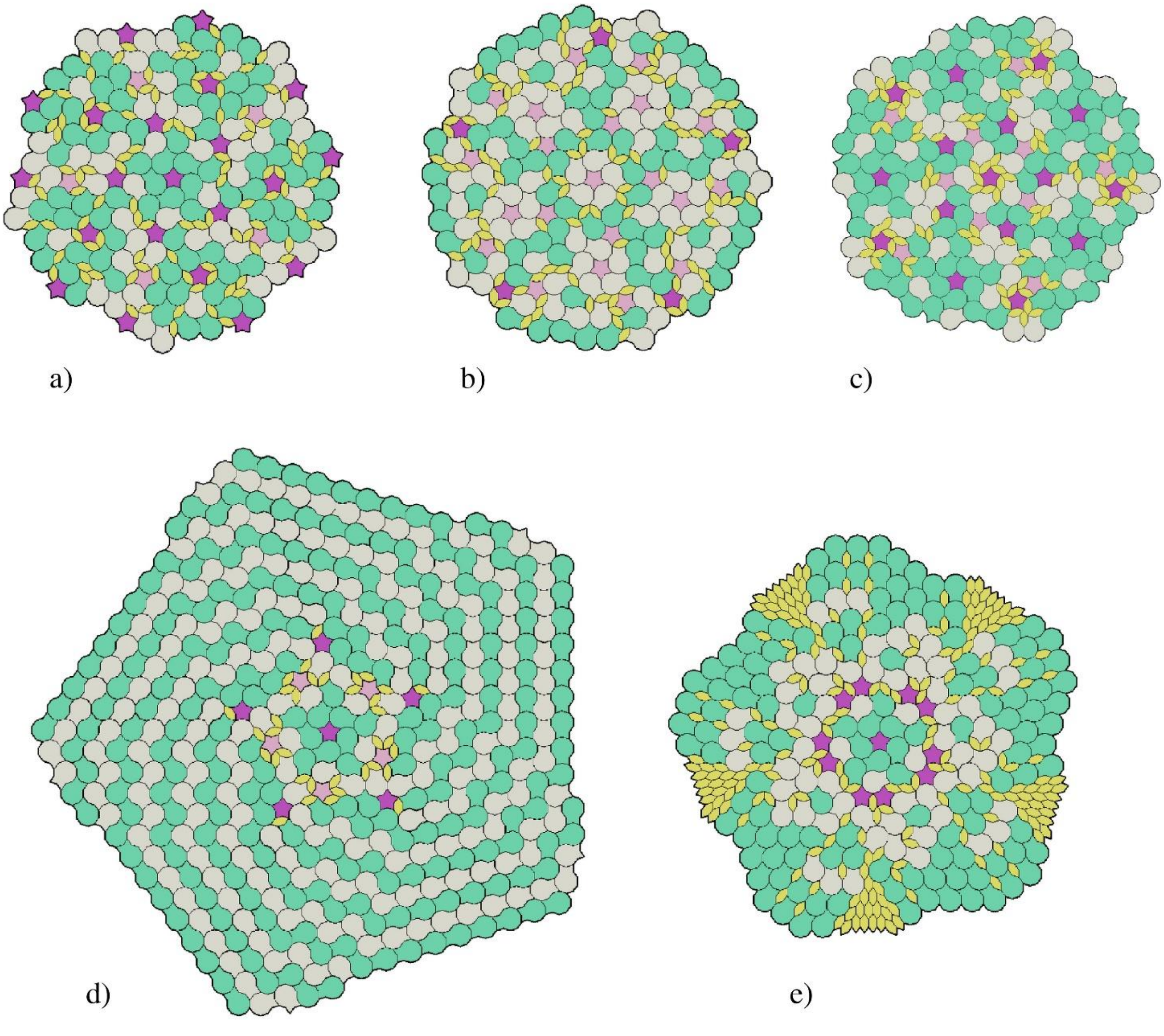


**Figure 9:** Some examples of rotational tilings

### 4.2 Tilings with single (central) decagon

The solutions given in Fig. 10 represent a certain anomaly among the solutions formerly shown, because another, fourth shape of tile appears here: a decagon. It is present as a single tile in the center of the tiling, but despite of disrupting the established set of tiles, an arrangement obtained by its introduction gives a fairly orderly disposition of tiles, moreover, with a lesser number of different tile shapes.

In the examples shown in Fig. 10 a, c and d, we see that, in addition to the central decagon, only diamonds and pineapples appear, and the stars appear in the case given in Fig. 10 b, only in the first ring around the decagon. Such solutions often give spiral arrangements of tiles, or concentric, as in Fig. 10 d. In this example we can see that, as in the case given in Fig. 4, the number of rows in which the tiles of Group I and Group II alternate can be taken arbitrarily.

In all these examples of rotational tilings, we can notice that the regularities are more noticeable the closer to the center of rotation the observed region is. As the distance increases, the number of tiles within the unit region becomes larger and their positions may be more diverse. Hence, their arrangement can produce conflicts with the adjacent unit region after rotation, but also within the region itself. These conflicts can be resolved by more suitable arrangement of the given three shapes of tiles. Yet, the further we move away from the center, the more reflection is needed to resolve the fitting of the tiles. The author takes the liberty of saying that solving these tillings can be just as much fun and challenging as solving enigmatics or computer games (similar to Tetris). This means that the solutions shown are valid only in the zone close to the center of rotation, but their further expansion can have several different solutions.

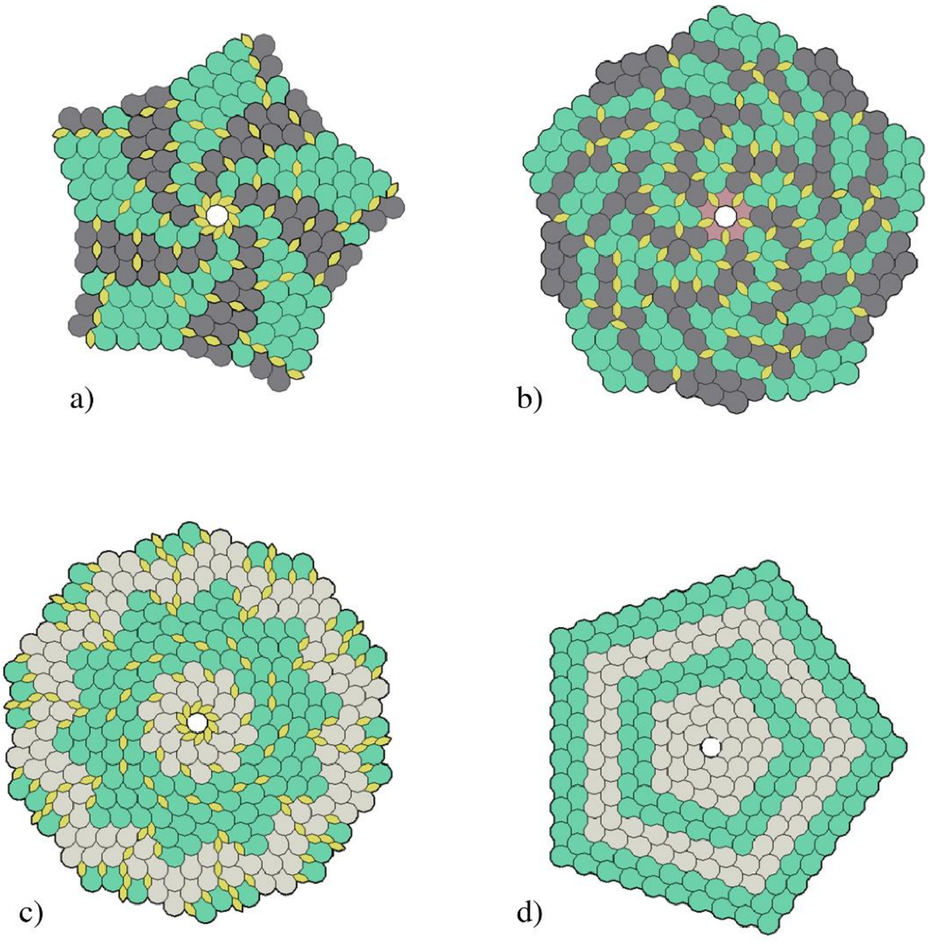


**Figure 10**: Examples of rotational tilings with a central decagonal tile

### 4.3 Combined and free-form solutions

The tiles can be combined and arranged in much complex ways. We can create tillings using previously formed aggregations of tiles, e.g. the one given in Fig. 2 d (Group II). Such a new shape, reminiscent of a flowering plant is named "lettuce", as in one of the previous solutions (see Fig. 5). We start with the given aggregations of pineapple tiles of Group II and array them in two parallel rows, starting from the position of the same shape in the center of the tilling (Fig. 11). Filling the gaps between them is performed with new pineapple and diamond tiles. After the rotation by 72°, we get zones that are not covered with tiles. To facilitate the “patching” of these empty zones, we also use parts of the "lettuce" aggregation, made of 3 pineapple tiles arranged around the central star. As we can notice, only the tiles from Group II are present in this solution.

For a clearer picture, they are shown in different colors: the pineapple tiles that make up the "lettuce" formation are colored green, and the tiles that fill the gaps are colored red. The diamonds that can only have their five positions, regardless of group, are given in yellow. In this way we get a solution that can be reduced to only two shapes: diamonds and stars, but also to another two: triangles and rectangles, as elementary shapes. The solution itself also belongs to rotational tilings.

As mentioned above, with these tiles we can play and create all kinds of different patterns, including free-form, and even generative. One of such free-form solutions is given in Fig. 12. Here we can see that, for such solutions, also some ready-made aggregations of tiles can be used. For easier tracking of solutions and eventually for achieving decorative patterns, we can display the tiles and aggregations by using different colors. Laying the tiles further on, in order to tile the entire plane, now is much simpler, since it is not conditioned by the fitting with the adjacent region after rotation.

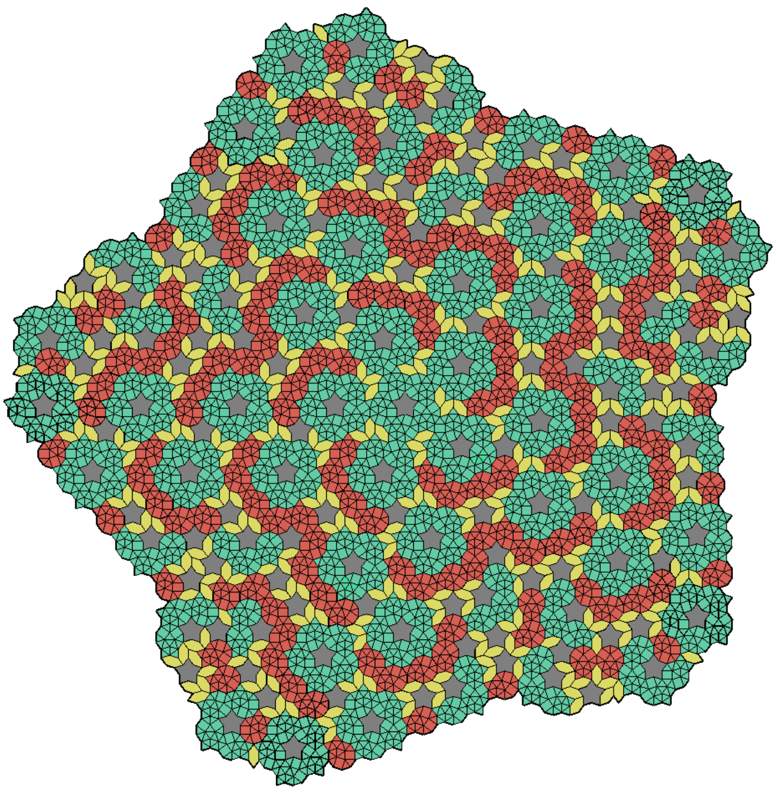

**Figure 11**: Tiling obtained by using “lettuce” aggregations of Group II tiles

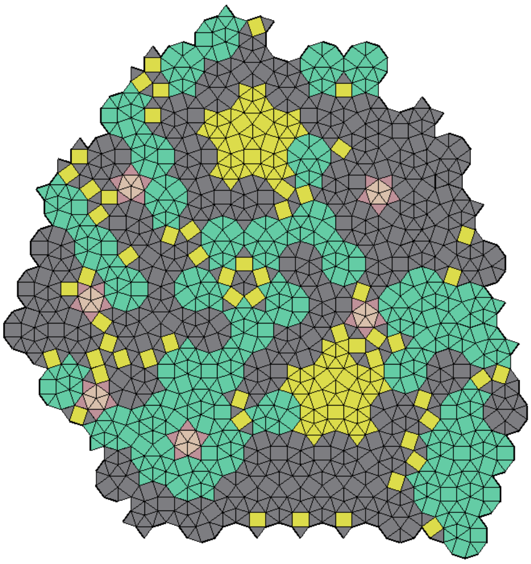

**Figure 12**: Free-form tiling using pineapples, stars and diamonds, broken into triangles and rectangles

Finally, we give some of the presented solutions, reduced to the shapes of triangles and rectangles. As we can see in Fig. 13, the arrangement of these elementary shapes results in patterns that are quite reminiscent of the Turing patterns. We can encounter them in marine organisms such as corals, sea urchins (which also have 5-fold symmetry), or even some species of fish (Ellison, 2019). In this way, we can try to decipher and link the formation of these bionic patterns with geometric ones.

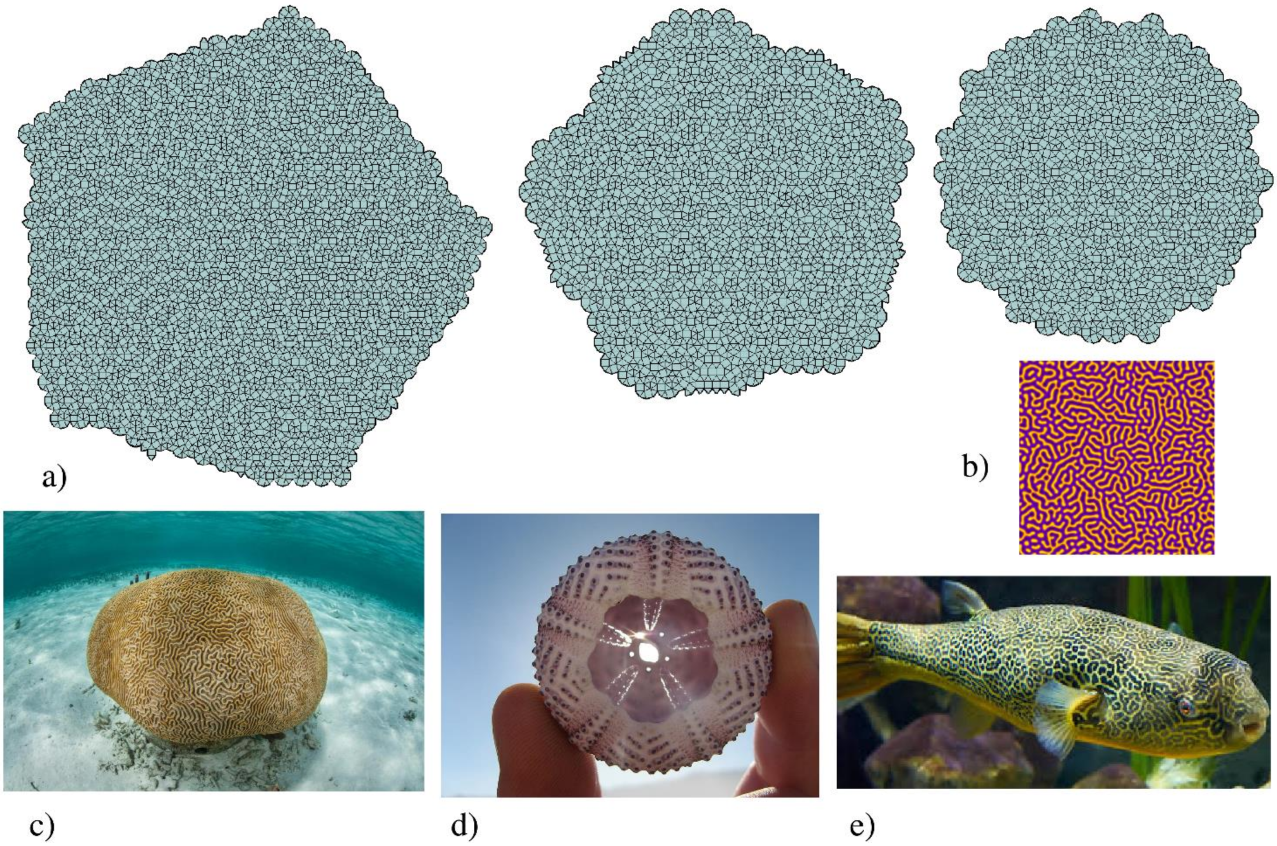


**Figure 13**: a) Patterns that emerge by reducing some of the above solutions into triangles and rectangles and their resemblance to b) Turing patterns (Source: see reference 10), and patterns from nature: c) “brain coral” Diploria labyrinthiformis (Source: see reference 12), d) sea urchin shell (Source: see reference 13) and e) Puffer fish, Tetraodon mbu (Source: see reference 11)

## 5. CONCLUSIONS

Based on all the above, the following conclusions can be drawn:

1. “Diamond” and “star” shapes, formed of isosceles triangles and rectangles originating from the ratio of the side and the radius of the circumscribed circle around the regular pentagon, can tile the whole Euclidean plane without overlapping and gaps.
2. These shapes, as well as the third, "pineapple" shape formed by combining them (two diamonds and one star), can tile the plane in several different ways, including periodic and non-periodic tiling.
3. Among the non-periodic tilings, a special variety of patterns can be obtained by applying radial and rotational arrangement of tiles.
4. Applying the rule of substitution, we can get larger aggregations of tiles and also use them in tiling the plane. We can always reduce the obtained solutions to more elementary forms.
5. The obtained solutions, in addition to their geometric curiosity, can also have a decorative role in design.
6. By reducing the presented solutions to triangles and rectangles, we obtain patterns similar to those we find in nature, especially in those where 5-fold symmetry appears.

From all the presented we conclude that, although it is probable that there are infinitely many different solutions, the way of forming them can still be examined and researched in terms of understanding the rules of their formation and thus a better knowledge of the world around us.

## ACKNOWLEDGEMENT

This paper is part of the technological development of project No. 200092 funded by the Ministry of Education, Science and Technological Development.

## REFERENCES

1. Dürer, A., 1525. *Unterweysung der messungmitdem Zirckel und Richtscheyt*, 1st Edition, 1525, 2nd Edition, 1538, Hieronymus Formschneyder, Nürenberg, cited after Peltzer, A.,1908. (Ed.), Albrecht Dürer’s Unterweisung der Messung, Munich.

2. Grünbaum, B. and Shephard, G. C., 1977. “Tilings by regular polygons”, *Mathematics Magazine* 50/5, pp. 227-247.

3. Johnson, N. W., 1966. Convex Solids with Regular Faces. *Canadian Journal of mathematics* 18 (1): pp.169-200.

4. Kepler, J., 1619. *Harmonices mundi. Libri V.* 1619, Reprint Bruxelles: Culture et Civilisation, (1968).

5. Li, H., Ma, H., Hou, L., Guo, M. and He, Z., 2017. Shield-like tile and its application to the decagonal quasicrystal-related structures in Al-Cr-Fe-Si alloys. *Journal of Alloys and Compounds*, *701*, pp. 494-498.

6. Lück, R., 2000. "Dürer–Kepler–Penrose, the development of pentagon tilings" *Materials Science and Engineering: A* 294, pp. 263-267.

7. Obradović, M. and Mišić, S., 2008 “Concave Regular Faced Cupolae of Second Sort”, In: *Proceedings of 13th ICGG, Dresden, August 2008*, ed. G. Weiss, El. Book, ISGG/ Technische Universität Dresden, pp. 1-10.

8. Obradović, M. and Mišić, S., 2021. Pentagon-Based Radial Tiling with Triangles and Rectangles and its Spatial Interpretation, SmartArt 2021 (in print).

9. Penrose, R., *1974.* “The role of aesthetics in pure and applied mathematical research”, *Bulletin of the Institute of Mathematics and Its Applications 10, pp.* 266-271.

***Online:***

10. Degenerate State, Turing patterns: http://www.degeneratestate.org/posts/2017/May/05/turing-patterns/ (Accessed June 13 2021).

11. Ellison N., Alan Turing: how the world’s most famous codebreaker unlocked the secrets of nature’s beauty, The Conversation (2019) https://theconversation.com/alan-turing-how-the-worlds-most-famous-codebreaker-unlocked-the-secrets-of-n atures-beauty-119425 [Accessed: 13th June 2021].

12. Oceana: Grooved Brain Coral https://oceana.org/marine-life/corals-and-other-invertebrates/grooved-brain-coral (Accessed June 13 2021).

13. Pixabay: Sea Urchin https://pixabay.com/photos/sea-urchin-shell-beach-sun-round-1794323/ (Accessed June 13 2021).

14. Shawcross Graham: Periodic and Non-Periodic Tiling, Order, rhythm and pattern. https://grahamshawcross.com/2012/10/12/periodic-and-non-periodic-tiling/ (Posted October 12. 2012, Accessed June 6. 2021.)

„8th International Conference moNGeometrija, focused on the research about geometry, graphics and application to science, engineering and art“

Belgrade, 10.-12. September, 2021.

# 3D PRINTING LARGE SCALE CURVED FORMS USING HEAT FORMED CORAL REEF TILES

Marko D. Jovanović[1*], Marko P. Vučić[2], Radovan B. Štulić[3], Maja M. Petrović[4]

[1, 2, 3] University of Novi Sad, Faculty of Technical Sciences, Department of Architecture, 21000 Novi Sad, Serbia

[4] University of Belgrade, Faculty of Transport and Traffic Engineering, Chair of Technical Sciences, 11000 Belgrade, Serbia

[1] markojovanovic@uns.ac.rs, [2] vucic.marko@uns.ac.rs, [3] stulic@uns.ac.rs [4] majapet@sf.bg.ac.rs

***ABSTRACT***

*The use of additive manufacturing has found its way into architectural fabrication. Besides the conceptual use for printing on extraterrestrial soil by mobile autonomous vehicles, 3D printing on Earth is used in printing houses by using robotic fabrication or large gantries. However, desktop printers have been used to fabricate small tiles, which are then assembled into a larger structure. The notion of printing the tiles flat and then forming then into shape for the final assembly has been researched through the use of gravity, tension and heat. In this paper, the goal is to develop a workflow for fabricating large scale 3D printed structures. The phases of this workflow entail the generation of a desired form, its conformal mapping into a flat plane and desired tessellation. The flat pieces are then printed on a desktop 3D printer, after which the tiles are heat formed into the desired shape by using a mould and then assembled and fused together into a final structure. The main design idea is to use coral reef patterns to design the tiles. In this research, the emphasis is placed on the exploration of various design parameters such as pattern shape, width and height, the variations that are produced as a result and their heat forming on a waffle type mould.*

**Keywords:** additive manufacturing; heat forming; dynamic optimization; mapping

## 1. INTRODUCTION

Architects have always found innovation in their design approaches by observing the world around them or exploring other disciplines. One example can be seen in using shapes and processes found in nature and implementing them in architectural forms and functions - like biomimicry (Knippers et al, 2012). Another example shows how methods in aviation industry have influenced the architectural design approach through modelling and fabricating curved structures. Similar to the implementation of nature and aviation, the 3D printing industry has also found its footing in architecture, inspiring the fabrication process on a much larger scale.

Its most notable use is seen as a method of constructing protection structures on extraterrestrial soils, such as the surface of Mars (Sawantt, 2021) or the Moon (Ceccanti et al, 2010). In this case, the use of heavy machinery is scarce, which is why the basic method of printing in layers is taken as a guiding trope, with smaller mobile robotic vehicles. This process is prone to unforeseen circumstances. By exploring problems and caveats, the field of large scale 3D printing expands. On extraterrestrial soil, the time is in abundance. However, given that time on Earth is not a commodity; the use of heavy machinery for 3D printing is welcomed. One way of solving the scale issue is to use large gantries, imitating the desktop 3D printers (Hager et al, 2016). This approach requires a box-like construction enclosing the future structure, which can be too rigid, and time demanding to setup. In order to save the time and effort in constructing a gantry, the entire large scale 3D printing approach has to be refined. This is seen in the use of use of industrial robots (Soto et al, 2018, Anton et al, 2018, Ko et al, 2018), or crane-mounted extruders (Jordahn, 2019).

Their advantages can be seen in more flexibility during the fabrication process and less setup time. This allowed for the design process to become an integrated part of fabrication. Furthermore, industrial robots are made mobile (Tiryaki et al, 2019), allowing for the fabrication process to be more independent of the scaffolding and be done in teams (Zhang et al, 2018). Even though the industrial robots made the fabrication process more accessible and flexible, the problem of their implementation on one large task proved to be labour intensive. In order to compartmentalize the fabrication process and make it more task independent, novel approaches are developed that utilize specific processing route (Gosselin et al, 2016) or prefabrication through function representation (Bhooshan et al, 2018). The introduction of parameters guides the infill design approach to be integrated with structural stability (Kontovourkis et al, 2020), thus making a structurally informed model (Mostafavi et al, 2016). However, all these approaches treat the use of industrial robots as end effectors without the feedback from the structure being fabricated.

This is why it became necessary to upgrade the industrial robot application on multiple levels. First approach is to equip the robot with sensors to monitor the structure as it is being printed (Sutjipto et al, 2018). The shift from classical 3D printing is not only highlighted through visual monitoring loops but also though innovative use of robots. The horizontal layer by layer approach of printing is scrapped in order to ascend from the usual approach to printing (Lim et al, 2016). This can be seen in a setup where the extruder is no longer perpendicular to the print-bed or platform, but is instead used to fabricate 3D structures as spatial lattices (Peng et al, 2018) or to print directly on a 3D model underneath (Tam et al, 2016). Further departure from the norm is seen when the robots are not used as end effectors but as systems that changed the orientation of the print-bed platform (Keating et al, 2013) or navigate a 3D model in reference to a fixed extruder head (Anton et al, 2018). The combination of the robotic printing for both model orientation and navigation and the multi axis printing process is seen in Zaha Hadid's Thallus project (Schumacher et al, 2017). It highlights the extent to which the exploration and integration of different approaches and disciplines can carry the architecture design process. However, the process also shows the dependence of the structure's scale to the volume of the industrial robot's work area or better yet the restrictions. This is why the compartmentalization section, mentioned previously, is important i.e. the tessellation of large scale structures into parts that can be printed individually and assembled later on.

Projects that utilize a classical desktop 3D printer configuration and the multipart assembly process are the Silky Concrete Project (O'Neal, 2015) and The VULCAN (Santos, 2015), which is also named for being the largest 3D printed structure at the time. The 3D printing process is very time consuming, taking into consideration the tile's volume and the fact that the support also needs to exist to print the exact shape of the tile. This is why flat printing of cable nets (McGee et al, 2017), curve ups (Guseinov et al, 2017) or 4D Meshes (Wang et al, 2018) can be beneficial, since the 3D printing process is used to flat print an unrolled part, without support, after which the shape takes place under gravity, tension or heat forming, respectively. Since these approaches require additional preparation and limitations due to the nature of their design forming, simple unrolling and use of moulds can be an option as well. Moulds can be expensive, especially if they are custom made for each element. However, use of waffle structures, which can be fabricated cheap and easily and in a time efficient manner, can suit a large number of doubly curved surfaces, albeit with some discretization present (Mitov et al, 2019). Further improvement can be seen with adjustable moulds (Larocque, 2017) that can accommodate a large number of elements, by changing some of the physical properties of a single mould configuration. In order to unroll the part correctly, even doubly curved surfaces, approaches, such as conformal mapping exist that can aid in such an endeavour (Crane, 2013).

All the aforementioned approaches are different, each exploring a part of the large scale implementation of 3D printing in architecture. Regardless of each individual approach, a tendency to go beyond the status quo and use the tools in a more innovative fashion can be noticed. The thing that connects most of the state of the art examples is a heavy dependence on industrial robots or case-specific printing configurations. In order to mitigate the fabrication setup time, preparation load and mechanization cost, as the large scale 3D printed structures have shown, it is prudent to utilize desktop style 3D printers and assembly process. The notion of printing flat unrolled pieces of a larger structure and then morphing them into shape is another example of making the process more time-effective and straightforward with regards to material waste reduction.

In this research the aim is to explore the application of desktop 3D printers for a time-effective, low cost and low setup fabrication process of a piecewise assembled large scale curved architectural form. The main goal is to fabricate a structure made out of mutually connected linear ribbon patches that resemble a coral pattern. The application of coral reef patterns in architecture and design is connected to the biomimicry mentioned at the start of the paper. In nature, form follows function and in that notion, the structural stability of the coral reef is secured (Chen, 2015), while the pattern provides an adequate natural and biophilic appearance. In this case, the accent is placed on the form, perforations and the generated spatial flow, given its linear depiction and less impact is placed on its structural stability. The structure fabrication approach utilizes piecewise unrolled patches that are printed on a desktop 3D printer, morphed into shape by heat and a mould and then assembled into its final form. The criteria that are used for evaluation are the print time, material amount, pliability and sturdiness. The print time should be low in order to speed up the printing process. The material amount should be minimal, with a shape that can cover the tile in a continuous curved path. The pliability refers to the ability of the tile to conform to the mould without distortions or long periods of heat forming, while sturdiness refers to the ability of the tile to remain in the newly formed shape. The workflow and the methods are explained in the following chapter.

## 2. METHODS

As with most architectural projects the architectural form is the starting point that is used for other phases of the research such as analysis or fabrication. In this case, the emphasis is placed on fabricating physical prototypes first and then using the acquired data to drive the design process accordingly. Rhinoceros and Grasshopper is used for the algorithmic modelling part and Ultimaker S5 is used for 3D printing. Given the mentioned procedure, the approach needs to integrate both fabrication and design parameters. With the specificity of this approach, which is comprised of several joined approaches, the research is divided into the analytical part and the practical design workflow part..

### 2.1 The Analytical Design Part

The analytical part is divided into several phases. First, the design parameters need to be explored - the linear ribbon pattern, its width and height. Hence, a 10cm x 10cm boundary is determined for generating various parametrically driven geometrical solutions. Since these parameters rely on practical testing, the second phase entails the generation of several prototypes, with varying patterns, widths and heights and their fabrication through 3D printing. In the third phase, the fabricated parts are placed in a doubly curved mould - a hyperbolic paraboloid approximated through interconnected waffle parts. The waffle parts can be added or removed to check the sagging due to the 3D printed element being pliable. Upon placing the prototypes on the mould, they are heated with a constant temperature fan air varying exposure times to conform into shape. The fourth phase is used to analyze the data and draw conclusions based on important criteria. These phases are repeated iteratively, since information is procured for a certain dataset which is improved upon in the later iteration.

As mentioned before, the main design parameters are the linear ribbon pattern, its width and height. The end goal is to use a coral reef pattern as a very intriguing pattern for biophilic architecture. However, the intricacies surrounding the more complex coral reef pattern can be explored by following the information derived from heat forming simpler shapes such as straight lines (Figure 1a) and wavy lines (Fig 1b), before moving to the coral reef pattern.

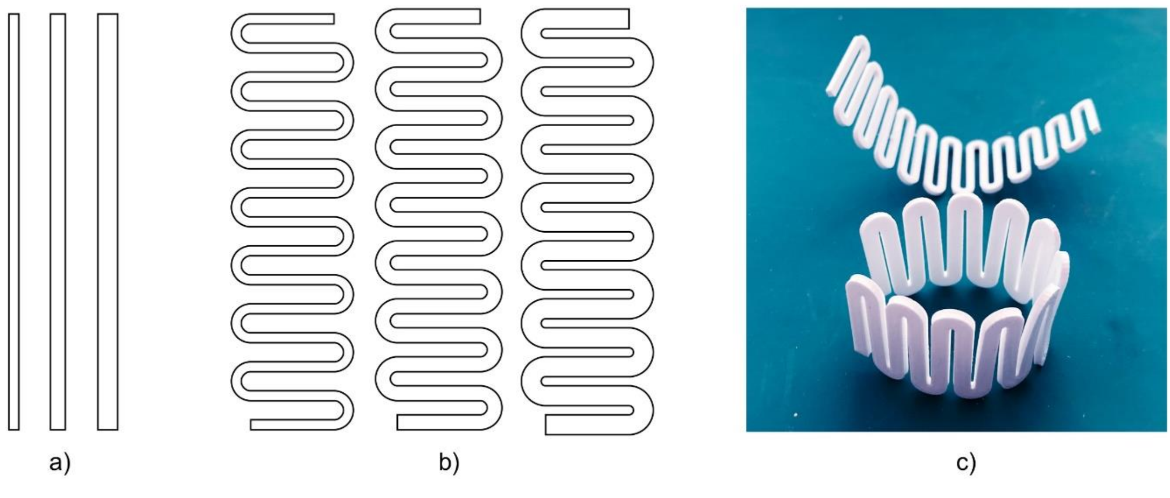


**Figure 1**: The shapes chosen for initial rapid prototyping (a) Shape 1 - Straight lines of varying width (b) Shape 2 - Small wavy lines of varying width (c) a heat formed Shape 2 that is pliable but also flexible

The shapes 1 and 2 shown in Figures 1a and Figure 1b respectively are not interconnected, since a starting line width and height has to be determined first. Using samples this small speeds up the rapid prototyping phase, where an assortment of samples need to be printed before the information is acquired for the optimal set of parameters. Widths that were used are in accordance with the nozzle extrusion width of 0.4mm, meaning that the chosen widths have 0.4mm as a factor. The chosen height is done in a similar manner, where the heights have a 0.2mm factor. Small values are chosen - widths of 1.2mm to 3.6mm and heights of 0.8mm to 3.2mm, with a hypothesis that the parts are sturdy enough before and after heat forming. However, all the parts were extremely pliable and flexible, needing between 5 to 10 seconds to heat bend and even distort, given the varying exposure times (Figure 1c). Shapes 1 and 2 are used to verify the initial hypothesis regarding the width and height values and are excluded from the subsequent analysis.

A more elaborate shape, Shape 3, consisting of interconnected wavy lines is used (Figure 2a) with the height values upped to 4mm, 6mm, 8mm and 10mm. All test pieces are made to fit in a 10cm x 10cm boundary, as stated before to accommodate for the mould of the same size later on. The arc radius and subsequently the distance between the straight lines differ, as can be seen in Figure 2b.

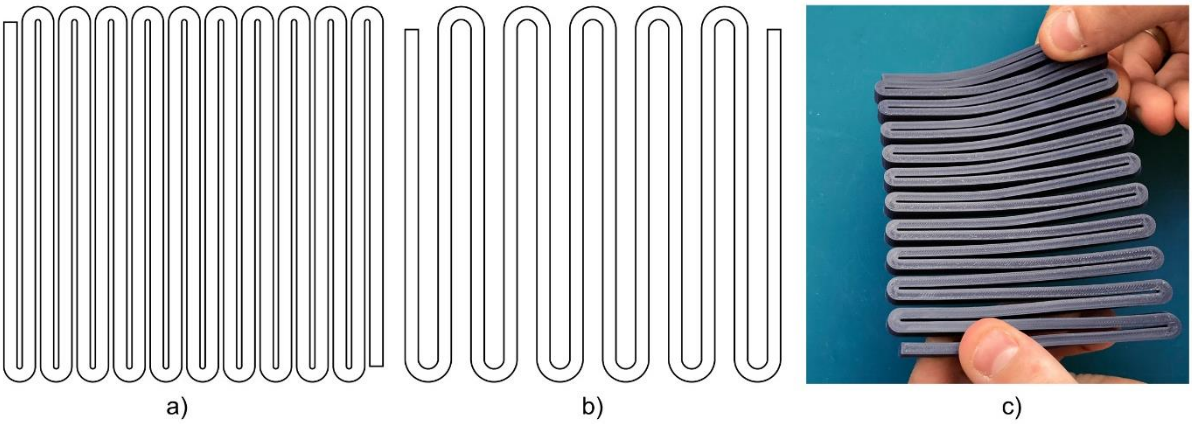


**Figure 2:** The differences in width and radii in Shape 3 (a) Radius is 1.5 times the width of the shape (b) Radius is 3 times the width of the shape (c) 3D printed pieces with a present flexibility due to pattern

Regardless of the parameters for the width, height and arc radius, due to the nature of the shape, even the 10mm height parts, with small radii (Figure 2c) are high in flexibility i.e. flimsy. This means that generating shorter continuous parts that are cantilevered can lead to a decrease in flexibility. Also, the width of the lines does not influence the sturdiness hence, smaller widths up to 5mm are used. Larger height values increase the print time much more than an increase in the width, given the same volume to print. With the data for height and width, a more complex shape is chosen to prototype, a coral reef pattern - Shape 4.

A coral reef pattern has a profound randomness to its shape, one that cannot easily be replicated by a manual input. Digital tools provide the possibility of simulating coral reef growth in an accessible and easy manner. This is why a dynamic optimization approach is chosen to procure a valid testing shape sample. By using a dynamic optimization approach, mere changes in the initial set of parameters i.e. forces, can procure different results with unique design shapes. Hence, this approach provides the ability to get the coral reef pattern each time, but with differences in shape and flow, providing the growth randomness effect that exists in nature. The basic idea is to draw a curve, approximate it through smaller lines, and gradually increase their length, while allowing for the chunks to bend around their kinks in a random fashion. In order to model this, first, a boundary of 10cm x 10cm is drawn as a square inside which a circle is placed (Figure 3a). The circle is chosen to be placed in the centre, with a diameter half that of the edge length i.e. 5cm, however the radius and the position can be chosen by user input. Even the circle can be replaced by a single line going across the square shape or multiple lines or curves. The circle is approximated as a polyline (in this case a polygon) i.e. by a large number of straight line segments. The number of segments has to be determined optimally, since oversampling can increase the dynamic optimization time unnecessarily and cause a sluggish interface, while undersampling can lead to intertwining or self intersections, with very basic shapes. The main idea behind the optimal number is to calculate the longest curve with a desired width that can fit inside the tile area and approximate it with line chunks of the same length. Following this logic, no self-intersection can occur and the sampling is proper. In order to calculate the optimal number of samples [n] i.e. line chunks, an equation (Equation 1) is introduced, which takes into account the area of the tile [A] and the desired width of the pattern [w]

$$n = \frac{A}{w^2} \quad \textbf{(Eq. 1)}$$

Once the number of segments is calculated, a certain thickness is added to the line segments, which is the width of the shape path. A force enlarging the length of the line chunks is introduced inside a dynamic optimization engine (Kangaroo inside Grasshopper and Rhino), which gradually enlarges the line segments but also randomly bends them in reference to the adjacent ones (Figure 3b). By increasing the length value more, the polyline reaches the boundary and starts to deform to accommodate for the shape (Figure 3c), eventually making its way through the centre of the square and filling the entire boundary up (Figure 3d).

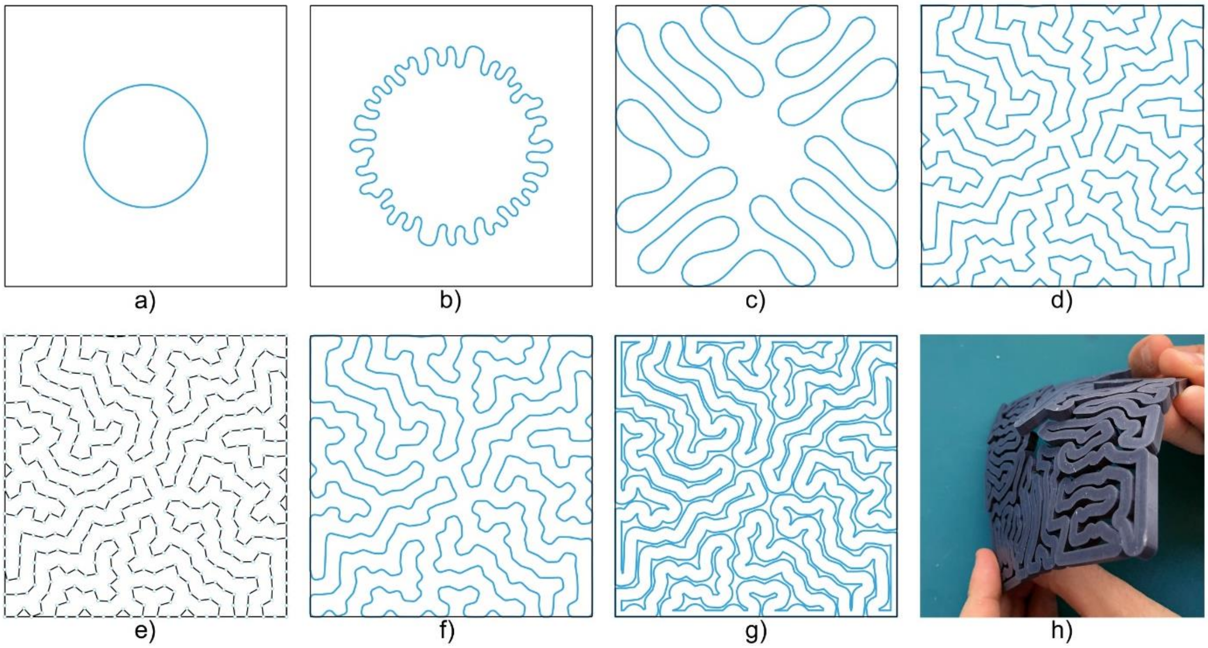


**Figure 3**: The coral reef generation process (a) generating any curve inside the tile (b) Using the dynamic optimization forces to enlarge the length of the polyline chunks (c) The lines reaching the boundary start to conform to it (d) The final coral reef shape (e) Visible control points for local curve modification (f) filleting the sharp corners of the shape (g) offsetting the shape according to the desired width (g) Trimming the shape according to the tile boundary

The end points of each line segment i.e. the control points are visible and can be interactively moved to satisfy user preferences in this manner (Figure 3e). These control point movements can only occur locally, given the strong forces that push the entire polyline in a state of equilibrium. After the main path is generated, the sharp angles are filleted with a radius equal to half that of the desired width (Figure 3f). The path is then offset on both sides, making sure that the desired offset amount i.e. the width does not cause an overlap of the shapes or self-intersection that would negate the creation of a planar region later on. Finally, the shape is trimmed according to the boundary (Figure 3g) and after adding the height, is printed.

Before and after the prototype is heat formed, the same problem remains - the larger cantilevered segments tend to be more flexible, but far less than the Shape 3 example (Figure 3h). The control over the cantilever excessive length is hard to control in this case, given that the entire process is self contained. There are no restrictions placed on the larger coral reef cantilevers that form, given that their generation is post introduction of the forces and the commencement of the entire dynamic optimization process. Inserting some way of reducing the large cantilevered parts could be beneficial in solving the issue. For example, placing circles with the same width (diameter equals the width) at the start of critical cantilevered parts can reduce their length and potentially solve the issue (blue circles in Figure 4a). However, performing manual corrections on a larger number of tiles can be tiresome, time-consuming and prone to errors. Also, a larger problem becomes more evident, which is that these types of shapes can be laser cut out of polycarbonate sheets of plastic, with far less time, albeit with a strict choice of material and height. In order to solve the cantilevering problem and utilize the full potential of 3D printers, cross lamination is introduced.

### 2.1.1 Cross lamination With Different Shapes

The first approach to cross lamination entails that each pattern is generated, on top of another pattern in the modelling phase, joining them into a cohesive geometry, with small height values for each. This process is applied a desired number of times, making this type of geometry only possible to fabricate on a 3D printer. The additional pattern shapes can originate from any new curve or curves. For the second cross lamination layer, a rectangle (Figure 4b) is used, which generates another coral reef pattern (Figure 4c), in this case with a smaller width than the first one, which is then joined on top of the first one (Figure 4d).

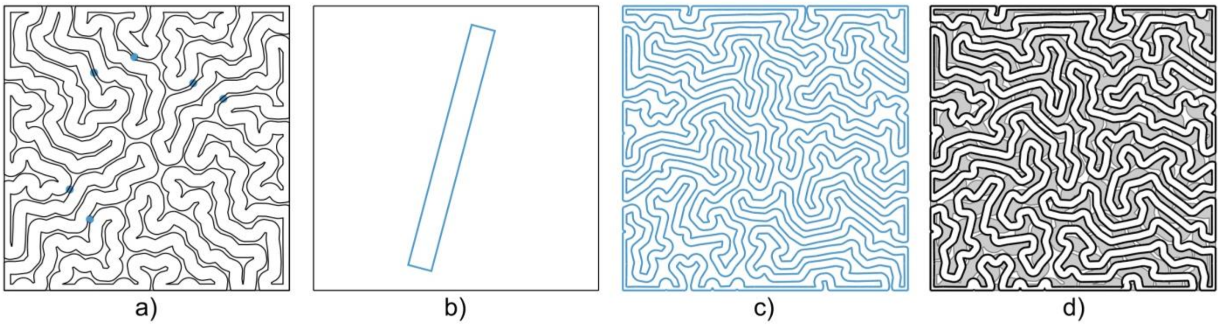


**Figure 4**: The first cross lamination approach (a) the possible positions of additional geometry to prevent large cantilevering elements (b) a new initial shape for the coral reef pattern generation (c) a new coral reef pattern after the dynamic optimization process (d) the first and the second coral reef shape one on top of another

Given that these layers are fused together while printing, and the small gap bridging does not require support, a piece that is less flexible but more pliable is produced. However, the transition from one shape to another is abrupt, even though the flexible large cantilevering problem is solved. In order to have a much smoother transition, the cross lamination process is refined.

### 2.1.2 Cross Lamination With Identical Shapes

The second approach to cross lamination is imagined by making the pattern larger and rotating it in smaller increments, moving them upwards to fuse the cantilevering parts together and provide a much smoother transition in the cross lamination procedure, since all the shapes originate from one. In the end, the shape is just trimmed to the tile size. In order to achieve this, the initial tile shape is chosen (for testing purposes still a square), and a circle is circumscribed around it. The pattern is generated inside of the circle, as described previously (Figure 5a). Afterwards, the final rotation angle is determined, the desired height and the number of layers. These parameters are interconnected so that once the number of layers is determined, the height of each layer is set, as well as incremental rotation angle for each layer. The path is given the offset and the extrusion after which the rotation and movement are applied as described previously (Figure 5b). Finally, the layers are joined together and trimmed according to the tile size (Figure 5d).

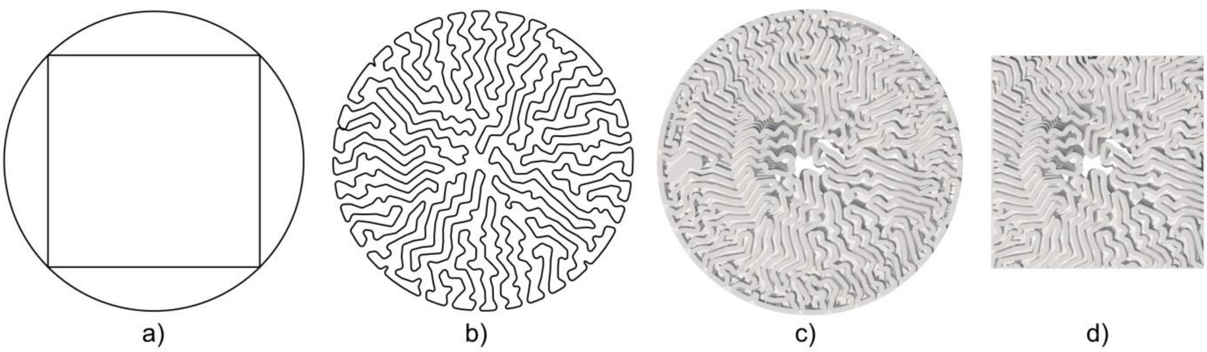


**Figure 5**: The second cross lamination approach (a) Circumscribing the circle around the square tile (b) generating a coral reef shape with circular boundaries (c) rotating the thickened shape one on top of the other (d) joining and trimming the shape according to the tile boundaries

An important note here is that the desired rotation angle should be higher, to avoid overhanging parts and enable bridging and cross lamination (Figure 6a). However, the large rotation angle value has the highest impact the furthest the geometry is from the center of rotation. So, even though the outskirts are overlapping adequately, the parts near the centre of rotation do exhibit overhanging problems (Figure 6b). Accordingly, this approach is improved in the following manner.

If the pattern seen in Figure 5b is used for rotation and movement only (without offset and extrude), the rotational set of these pattern shapes can be lofted into a surface. The main consideration in this case is the final rotation angle, since large rotations can create an inclination surface under 45° that is not possible to print without support on the 3D printer, due to overhanging. Equation 2 is introduced to calculate the limitation angle [α], under which it would become difficult to print out the piece without support, taking into consideration the radius of the circumscribed circle [r] and the height of the final piece [h].

$$\alpha = \frac{180*h}{r*\pi} \quad \textbf{(Eq. 2)}$$

This equation takes into consideration the worst case scenario that can occur on the furthest parts of the print, given that there the rotated parts travel the most. The lofted surface is made into a mesh, and given thickness (offset on both sides as a solid) and smoothed out by using Catmull-Clark subdivision algorithm (Figure 6c). While this refinement emphasizes the coral reef motif of the pattern, and provides a change in experience while viewing from different angles, it does not cause as strong cross lamination as the previous example. This is due to each successive layer not connecting to any new shape parts in the layer underneath. Also, the parts near the centre of rotation do not have as pronounced inclination angle as the ones further away from it which still causes cantilevering parts in that area (Figure 6d). Even though the inclination surface prevents excessive movement of the cantilevered parts, they still exist, but provide a fair compromise between smooth transition and cantilever prevention as opposed to the first cross lamination approach. However, the second approach causes a larger problem, though - by trimming the excessive parts outside of the tile, the pattern ceases to be a whole and breaks up into smaller parts. Multiple alignment and joining issues would arise for a single tile even before the assembly process of the tiles into a single structure would have commenced. Hence, further upgrade is introduced in the following manner. Given the problem that is presented - losing the uniform geometry by trimming - one of the solutions would be to generate a boundary geometry that binds everything together. This binding piece would be fairly visible in the final structure and diminish the coral reef pattern that should be dominant. Instead of trying to fix the problem, the approach is to avoid it altogether.

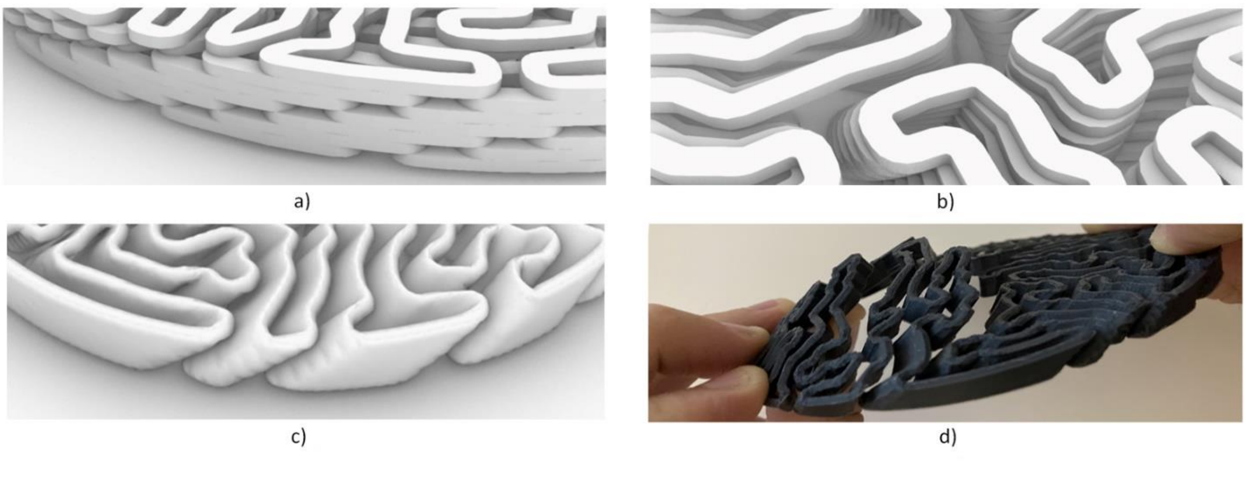


**Figure 6**: The overhanging issue (a) Large angle rotation ensures overlapping away from the centre of rotation i.e. the tile boundary (b) large angle rotation does not ensure proper overlapping near the centre of rotation - overhang problem (c) generating a loft surface from the rotated path shapes (d) giving thickness to the lofted surface to generate a printable 3D volume

### 2.1.3 Cross lamination with evolving shapes

The main idea of third cross lamination approach is to record iterative states of the coral reef pattern during the dynamic optimization process, move it upwards in incremental values and generate volume around it. However, in order to make the whole process more random, voxels (volumetric pixels) are used to fill out the form and create a mesh out of it, which is faster to compute and provides a more natural looking piece. Hence, a square tile is chosen and a circle inside it, as before. The dynamic optimization algorithm is adjusted to record the shape states during the process. In order to have a more elaborate form, states near the converged (final) state are chosen. These states are chosen to be those that develop from the one contacting the tile boundary (Figure 7a). In this state and the subsequent ones, the length is almost fully developed, while subtle protrusions and modifications of the shape are formed causing deviations from the original (Figure 7b). Adding the volume to follow this shape is the next step. The method applied in the second approach produces results that are straightforward, inorganic and without randomness present in the volumetric interpretations of the form. In order to improve on this, a Grasshopper add on is used - Dendro - which takes the shapes as input, voxel size and desired thickness and generates a mesh that is aesthetically pleasing, natural looking and done with far less computational demand than the previous one (Figure 7c). It even allows for the thickness definition for each part of the shape, meaning the volume can be thicker in the center to fuse the cantilevers and thinner near the boundary(Figure 7d).

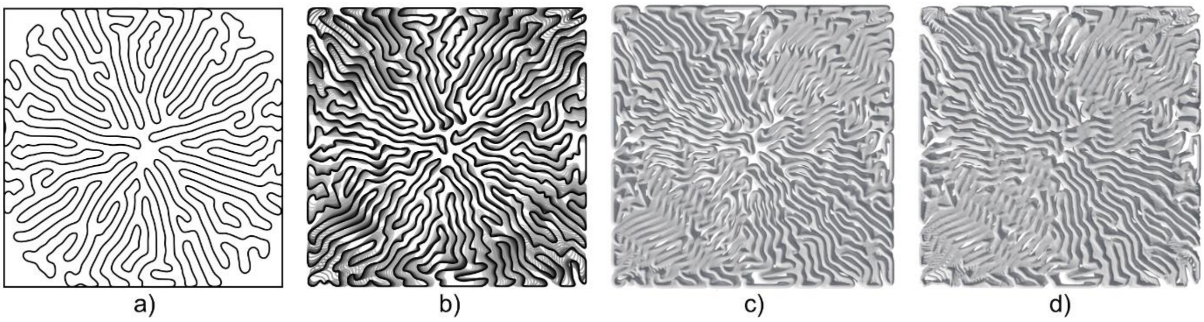


**Figure 7**: The third cross lamination approach (a) near convergent state of the shape from the dynamic optimization process (b) 15 shapes prior to the convergent shape, set one on top of another (c) the generation of the volume using voxels and thickness values with Dendro (d) using additional Dendro features that allow for localized thickness of the shapes portions

Since the third cross lamination approach generates an organic looking volumetric piece with a smooth transition i.e. a simulated differential growth appearance, without large cantilevering parts, it is the chosen method for the design phase of the large scale structure to fabricate. The overall height is set to a maximum of 1cm, given that the print time increases much more as opposed to the increase of the width for the same volume of material. Regarding the width, it is determined that between 5 and 10mm is the optimal value for fast prints and decent 3D printed pieces - sturdy but pliable. Next, all the information gathered from the analytical part are used to design a large scale 3D structure for printing via a desktop 3D printer.

### 2.2. The practical design part

In the design part, first a doubly curved surface is generated. Second, the surface is unrolled using a conformal mapping approach. Third, the unrolled surface is used as a basis for tiling, making sure the size of the tiles does not exceed the work area of the 3D printer. Fourth, the tiles are populated with coral reef patterns as explained in section 2.1. Fifth, the tile patterns are mapped back from the unrolled surface onto the original surface to render the final output. Sixth, the mould is made out of waffle parts for the original surface. Finally, the printed parts are placed on the mould, heated to conform into shape making sure to join adjacent tiles by heating the plastic and fusing them together. For the purposes of this research, only a small portion of the surface is made as a proof of concept.

The surface chosen for this test is a doubly curved surface that serves a purpose of a partitioning wall or decoration on existing walls or facades (Figure 8a). It is modelled to fit inside a bounding box of 200cmx200cmx20cm. The depth of 20cm is kept low, since larger protrusions from a vertical wall would be noticeable, hard to manoeuvre around and prone to damage from outside factors. A surface is generated in this case, however, the model can be any brep or mesh model, which is then converted into a triangular mesh by using an add-on - Mesh Machine (Figure 8b). A 'boundary first flattening' add-on is applied, where the mesh is flattened out by using conformal mapping and tiled using customized Voronoi cells (Figure 8c). The boundary of each cell can fit inside of a printer’s print bed, whose area is 300mm x 240mm. Instead of using circles for the initial curves - the same curves that are used to 'grow' the coral reef pattern from, parts of a larger continuous curve are used to test whether it is possible to generate a continuous form from smaller tileable patches (Figure 8d). The end points of these chunks are anchored to the tile boundary to ensure the continuation.

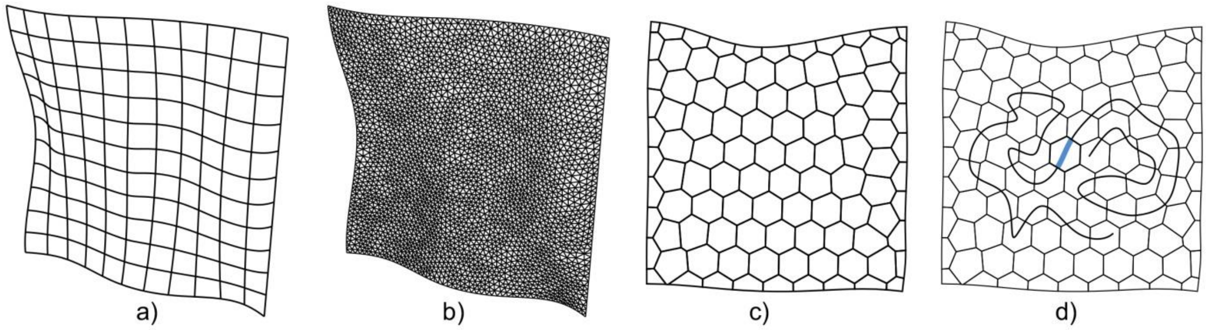


**Figure 8**: The design workflow (a) The generation of a doubly curved surface (b) the surface approximation by triangles using Mesh Machine (c) a flat developed surface using conformal mapping with Voronoi based tiles (d) a curve connecting adjacent cells in order to test the continuity aspect of coral reef tiles on a larger scale

By using mapping functions, all flat tiles generated on a layout like the one seen in Figure 8c are mapped back to the original doubly curved geometry and rendered. For testing purposes, only 15 cells near the centre are used.

## 3. RESULTS

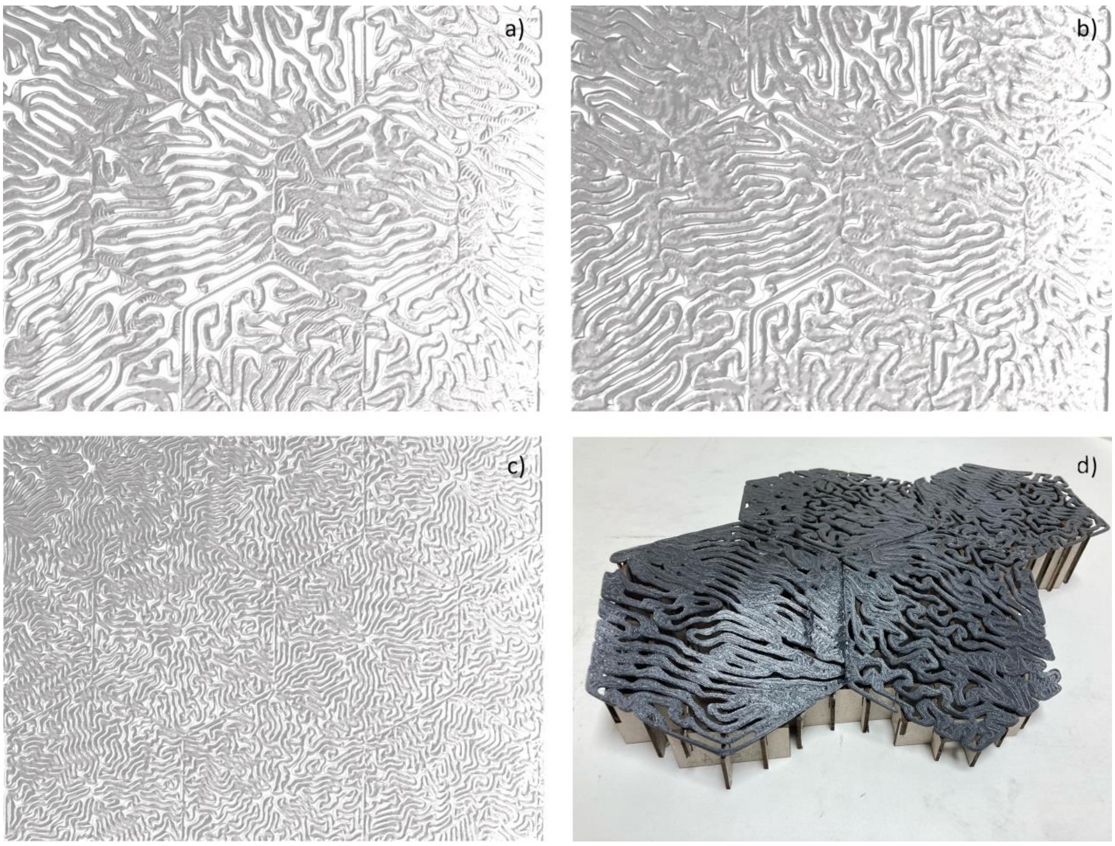


**Figure 9**: The rendered results of the applied workflow (a) the use of continuous curve chunks to emphasize the fluidity of the final overall shape, with the appropriately modelled width (b) width the increased width (c) the use of circles as initial curves with reduced visibility of cantilevering shapes towards the centre, but more noticeable tile seam (d) the final portion after 3d printing and heat forming in a mould

The choice of using continuous curve chunks as initial curves proved to be intriguing and an improvement, since the tile seams were less noticeable and the continuation of the pattern from one tile to another seemed to be more dominant (Figure 9a). The results tend to get worse if a larger thickness is used like in Figure 9b.

For a partitioning decorative wall with a small mass that carries the load vertically or is suspended from the ceiling, large cantilevering parts are not so much of a problem, if only observed aesthetically. For comparison purposes, a circle is also used as an initial line (Figure 9c). Given the smaller path width, the protrusions and the shapes are more profound, with the cantilevering parts becoming negligible, but the tile boundary is more visible. Finally, the parts are 3d printed flat and then heat formed with a waffle structure mould to conform to shape (Figure 9d). The process of heat forming took between 10s to 30s seconds with the temperatures mediated to allow the shape to set and then be cooled down. Regardless of the exposure time and the temperature, the parts failed to fuse together solely based on adhesion, which is why a soldering iron had to be applied to get the final result. Only a small portion of the entire surface was fabricated as a proof of concept, in order to gather relevant information and improve the workflow for future work.

## 4. CONCLUSION

In this paper the main goal is to explore the possibilities of using a desktop 3D printer to fabricate a large scale 3D printed curved structure. This is imagined by using flat printed tiles that are heat formed on a mould to conform into shape. Using the Mesh Machine and Boundary First Flattening add-ons for Grasshopper allowed for a quick mapping function between the desired doubly curved form and its flattened out counterpart. The tessellation procedure can be performed according to user preference and used as the tile boundaries for coral reef pattern generation. Performing the analytical part first i.e. rapid prototyping different linear shapes and pieces with varying widths and heights proved to be extremely important in the subsequent design workflow. It is noticed that the increases in the height value do not reduce the flexibility of the pieces in a more significant way, related to shapes 1,2 and 3. The same can be concluded for the width - even though a larger width generates a thicker piece, the flexibility is only reduced slightly and not removed completely. Heat forming the initial shapes 1, 2 and 3 provided information as to the pliability of the printed pieces and the material behaviour. It is noticed that thicker parts take longer to bend, but the time consumption is negligible when compared overall. The flexibility of shape 4, before and after heat forming, is lessened due to the coral reef pattern presence and a 1cm height. The larger problem is presented with cantilevering parts that have a significant length when compared to the overall size of the tile. Cross lamination is introduced to try and solve the issue. The first approach is successful in reinforcing the cantilevered parts but provides a non-smooth transition between the joining shapes. The second approach of using a rotational set of patterns proved to be inefficient, since the transition portion is solved, but the cantilevering is only slightly lessened and not removed. The third cross lamination approach is a more refined version of the previous two. The use of coral reef dynamic optimization process and state recording of the shapes proved to be an excellent manner of generating a volume that has an organic looking transition, but with random fuses of cantilevering parts, removing them completely or mitigating their influence significantly. The use of portions of a continuous curve for the initial coral reef curve is shown to procure a more fluent looking form, with less visible seams between the tiles and a more pronounced continuation of the coral reef pattern. Special attention needs to be paid to the thickness of the final shape tile, since a large increase in the thickness can diminish the coral reef look that should be the main motif. Heat forming the parts is not accentuated in this paper, but it is noticed that heated parts do not adhere to one another and the application of a soldering iron is necessary to bring it together.

## REFERENCES


1. Anton, A. and Abdelmahgoub, A., 2018. Ceramic components-computational design for bespoke robotic 3D printing on curved support.

2. Anton, A., & Abdelmahgoub, A., 2018, Ceramic components-computational design for bespoke robotic 3D printing on curved support.

3. B.G. Soto, I. Agustí-Juan, J. Hunhevicz, et al., Productivity of digital fabrication in construction: cost and time analysis of a robotically built wall, Autom. ConStruct. 92 (2018) 297–311,

4. Bhooshan, S., Ladinig, J., Van Mele, T. and Block, P., 2018, September. Function representation for robotic 3D printed concrete. In Robotic Fabrication in Architecture, Art and Design (pp. 98-109). Springer, Cham.

5. Ceccanti, F., Dini, E., De Kestelier, X., Colla, V. and Pambaguian, L., 2010, August. 3D printing technology for a moon outpost exploiting lunar soil. In 61st International Astronautical Congress, Prague, CZ, IAC-10-D3 (Vol. 3, pp. 1-9).

6. Chen, D.A., Ross, B.E. and Klotz, L.E., 2015. Lessons from a coral reef: Biomimicry for structural engineers. Journal of Structural Engineering, 141(4), p.02514002.

7. Crane, K., 2013. Conformal geometry processing. California Institute of Technology.

8. Gosselin, C., Duballet, R., Roux, P., Gaudillière, N., Dirrenberger, J. and Morel, P., 2016. Large-scale 3D printing of ultra-high performance concrete–a new processing route for architects and builders. Materials & Design, 100, pp.102-109.

9. Guseinov, R., Miguel, E. and Bickel, B., 2017. CurveUps: Shaping objects from flat plates with tension-actuated curvature. ACM Transactions on Graphics (TOG), 36(4), pp.1-12.

10. Hager, I., Golonka, A., & Putanowicz, R., 2016, 3D printing of buildings and building components as the future of sustainable construction?. Procedia Engineering, 151, 292-299.

11. Knippers, J. and Speck, T., 2012. Design and construction principles in nature and architecture. Bioinspiration & biomimetics, 7(1), p.015002.

12. Jordahn, S., 2019, 3D-printed Gaia house is made from biodegradable materials, https://www.dezeen.com/2019/02/27/gaia-wasp-3d-printed-house-biodegradable-video/

13. Keating, S. and Oxman, N., 2013. Compound fabrication: A multi-functional robotic platform for digital design and fabrication. Robotics and Computer-Integrated Manufacturing, 29(6), pp.439-448.

14. Ko, M., Shin, D., Ahn, H., & Park, H., 2018, InFormed ceramics: multi-axis clay 3D printing on freeform molds. In Robotic Fabrication in Architecture, Art and Design, pp. 297-308, Springer, Cham.

15. Kontovourkis, O. and Tryfonos, G., 2020. Robotic 3D clay printing of prefabricated non-conventional wall components based on a parametric-integrated design. Automation in Construction, 110, p.103005.

16. Larocque, J.O., 2017. Digital Mould: Hybridizing Digital-Analogue Fabrication Techniques (Doctoral dissertation, Carleton University).

17. Lim, S., Buswell, R.A., Valentine, P.J., Piker, D., Austin, S.A. and De Kestelier, X., 2016. Modelling curved-layered printing paths for fabricating large-scale construction components. Additive Manufacturing, 12, pp.216-230.

18. McGee, W., Velikov, K., Thun, G. and Tish, D., 2017. Infundibuliforms: kinetic systems, additive manufacturing for cable nets and tensile surface control. Fabricate 2017: Rethinking design and construction, pp.84-91.

19. Mitov, D., Tepavčević, B., Stojaković, V. and Bajšanski, I., 2019. Kerf Bending Strategy for Thick Planar Sheet Materials. Nexus Network Journal, 21(1), pp.149-160.

20. Mostafavi, S. and Bier, H., 2016. Materially informed design to robotic production: a robotic 3D printing system for informed material deposition. In Robotic Fabrication in Architecture, Art and Design 2016 (pp. 338-349). Springer, Cham.

21. O’Neal, B., 2015, Silky Concrete Project: Massive Concrete Installation Built by KUKA Robot & Ten 3D Printers, https://3dprint.com/80490/silky-concrete-project/

22. Peng, H., Briggs, J., Wang, C.Y., Guo, K., Kider, J., Mueller, S., Baudisch, P. and Guimbretière, F., 2018, April. RoMA: Interactive fabrication with augmented reality and a robotic 3D printer. In Proceedings of the 2018 CHI conference on human factors in computing systems (pp. 1-12).

23. Saili Sawantt, Mars: Life Enhancing Architecture on the Red Planet, © Hassell Studio, https://parametric-architecture.com/mars-life-enhancing-architecture-on-the-red-planet/, April 29, 2021, Accessed June 24 2021

24. Santos, M., 2015, Meet The World’s Largest 3D-Printed Structure, https://futurism.com/meet-the-worlds-largest-3d-printed-structure

25. Schumacher,P.,ZahaHadidArchitects,ZHACode.Thallus for White in the City. 3D Printed Installation .Italy, Milan: Accademia di Belle Arti di Brera, 2017: http://www.zaha-hadid.com/2017/04/05/thallus-for-white-in-the-city/

26. Sutjipto, S., Tish, D., Paul, G., Vidal-Calleja, T. and Schork, T., 2018, September. Towards visual feedback loops for robot-controlled additive manufacturing. In Robotic fabrication in architecture, art and design (pp. 85-97). Springer, Cham.

27. Tam, K.M.M., Coleman, J.R., Fine, N.W. and Mueller, C.T., 2016. Robotics-enabled stress line additive manufacturing. In Robotic Fabrication in Architecture, Art and Design 2016 (pp. 350-361). Springer, Cham.

28. Tiryaki, M.E., Zhang, X. and Pham, Q.C., 2019, November. Printing-while-moving: a new paradigm for large-scale robotic 3D Printing. In 2019 IEEE/RSJ International Conference on Intelligent Robots and Systems (IROS) (pp. 2286-2291). IEEE.

29. Wang, G., Yang, H., Yan, Z., Gecer Ulu, N., Tao, Y., Gu, J., Kara, L.B. and Yao, L., 2018, October. 4DMesh: 4D printing morphing non-developable mesh surfaces. In Proceedings of the 31st Annual ACM Symposium on User Interface Software and Technology (pp. 623-635).

30. Zhang, X., Li, M., Lim, J.H., Weng, Y., Tay, Y.W.D., Pham, H. and Pham, Q.C., 2018. Large-scale 3D printing by a team of mobile robots. Automation in Construction, 95, pp.98-106.

# SOME ASPECTS OF ALGEBRA OF COLOR

Bojan D. Banjac[1*], Lidija S. Krstanović[2], Branko J. Malešević[3], Luka B. Milinković[4]

[1]University of Novi Sad, Faculty of Technical Sciences, Computer graphics chair, 21000 Novi Sad, Serbia

[1]bojan.banjac@uns.ac.rs

[2]University of Novi Sad, Faculty of Technical Sciences, Computer graphics chair, 21000 Novi Sad, Serbia

[2]lidijakrstanovic@uns.ac.rs

[3]University of Belgrade, School of Electrical Engineering, Department of Applied Mathematics, 11000 Belgrade, Serbia

[3]malesevic@etf.bg.ac.rs

[4] lukaui@yahoo.com

***ABSTRACT***

*Color is one of the most important elements of computer graphics and computer image processing. Engineers developed many different models for the pixel color representation, but most of them were developed purely for solving single problem. Even though there are many practical applications, it is rare to find mathematical analysis of those models. In this paper will be presented some mathematical properties of most common color representation models. Some additional applications of these properties will also be presented and practical implementations will be discussed.*

**Keywords:** Color model, mathematical analysis, algebra of color

## 1. GENERAL INFORMATION

Importance of color to humans is undeniable. It was one of the most important aspects of vision, as it allowed us to recognize the state of food sources and to detect predators hiding in surroundings with complicated textures. Even in animal kingdom color vision is preferred (Kelber et al. 2010), and grayscale vision is mostly present in special surroundings such as the aquatic animals, or with the nocturnal animals and reptilians. Among humans colors today are used for many different purposes, from signalling and making some distinctions, to simply esthetical purposes.

While colors are definitely important to us, we made the models for defining colors only recently. Most precise way of handling this issue would be to define color by frequency and intensity of light emitted and received by the eye, but this model of color representation is very hard to use in technical sciences and creates many limitations, as well as not being very intuitive to use. One of the first color models was Munsell color model (Ibrageem et al. 2012), created 1913. as atlas of colors. While this model is very simplistic it was adopted by United States of America agriculture department, as they found practical applications for it. It is still present in some industries where color examples are used. After that, International Commission on Illumination (authority for the light, color and color systems) has created CIE XYZ color model. This model offered much better way of defining color through three parameter function, which would later become standard. After this model many other appeared, as was shown in papers of Ibraheem et al. (2012) and Kour (2015).

As there are currently many different color models, they can be classified based on several different factors which will determine for which application they are best suited for:

- Additive or substractive model : Some models such as the RGB are made to represent addition of light of different wavelength to achieve selected color, while some such as CMYK are defined to be used in the printing industry where different pigments are applied to the white paper to reduce reflection of some wavelengths from printing medium.

- User oriented, device dependant, device independant: Some models such as RGB or YUV are created to best serve electronic devices for recording, transmission or storage of images. While these models are easy enough to understand, humans have much harder time defining color in these models without prior training, as they are not intuitive. Other models, such as HSL, are more similar to our comprehension of color, and while more complicated for image processing operations, allow people to quickly determine exact color that they wanted. There are also models that are device independent and while they are not suited nether for humans or machines, they have some industrial applications.
- Which aspects of color are used for definition: While all models are used to define color, different aspects of color will offer different capabilities for image processing. RGB color model is easiest to implement as it is very closely related to way image is obtained from digital sensors. HSL, HSV and other models of this type allow for quick hue change, or easy desaturation of image. YUV is great for computer vision, as its Y component can be used as grayscale image of surrounding without unnecessary color information.

While there are many other aspects in which these color models differ, it is important to know that all of them are interchangeable. Image can be received in one color model, and using some simple mathematical formulas we can quickly change between two models. For example, transformation from the RGB to HSI according to Ibraheem et al. (2012) can be done as:

$$I = \frac{R+G+B}{3}$$
$$S = 1 - \frac{3}{R+G+B} \cdot [\min(R,G,B)]$$
$$H = \arccos\left(\frac{0.5\cdot((R-G)+(R-B))}{\sqrt{(R-G)^2+(R-B)\cdot(G-B)}}\right)$$
$$if\ B > G\ then\ H = 360° - H$$

(RGBHSI transformation)

Many researchers today focus primarily on different applications of color models, and which model best suits which purpose. For example Bueno et al. (2008) researched which color models are best suited for the analysis of microscopic images. Bora et al. (2015) discussed different color models and their application for image segmentation. Some researchers, such as Rasras et al. (2007), are working on new models that could have some applications in technology. Mathematical foundations of these models are identical between most of them, but they are rarely researched. In this paper we present some properties of algebra of color and limitations that are related to most common system of component values. These properties can be applied to the most common color models such as RGB, CMYK, YUV, Grayscale. For HSL, HIS, HSV models Hue component behaves differently than those in other models, as it is represented as angle instead of numerical value in range.

## 2. MATHEMATICAL FOUNDATIONS OF COLOR MODELS

One of common engineering problems with image representations, independently of color model, is in which way to represent values of different channels – components of color model. Most common solutions are as decimal value between 0 and 1, and as integer value. Depending of sampling frequency of values, when using integer values we will get value between 0 and 256 (when using 8bit representation), 1024 (10bit representation), 4096 (12bit representation) or more. While integer operations are generally faster to run, compared to decimal ones, overhead with introducing checks on how big value range is may throttle performance. Thus, it is common to convert integer representation to decimal. Decimal representation is independent of sampling frequency, and thus it can combine values between different formats. For purposes of this paper, we will consider only decimal representation. We will also show operations only on single channel, as all operations are done in same manner on per channel basis.

### 2.1. Addition and multiplication with range limitations

As the basis for most operations in image processing we use addition and multiplication. Still, it is important to impose limitations, as values out of range (either (0,1) or integer value range) cannot be represented on display devices. Let us first observe the most common way of introducing these limitations, and what mathematical properties follow from these.

a⊕b=min(1,max(0,a+b) ) (standard addition)

a⊙b=min(1,max(0,a·b) ) (standard multiplication)

For operation of addition defined in this way, and $a, b \in \mathbb{R}$, following properties were observed:

- Is operation algebraically closed: addition is algebraically closed

$$a, b \in \mathbb{R} \Rightarrow a \oplus b \in \mathbb{R}$$

- Is operation associative: addition is not associative as there is the counter example of that

$$(\forall a, b, c \in \mathbb{R})$$
$$a \oplus (b \oplus c) = (a \oplus b) \oplus c$$
$$a, b, c > 0$$

$$a \oplus (b \oplus c) = \begin{cases} 1, b + c \geq 1 \\ \min(1, a + b + c), b + c < 1 \end{cases}$$

$$(a \oplus b) \oplus c = \begin{cases} 1, a + b \geq 1 \\ \min(1, a + b + c), a + b < 1 \end{cases}$$

$$b + c \geq 1$$
$$a + b < 1$$
$$a \oplus (b \oplus c) = (a \oplus b) \oplus c = 1.$$

$$b + c < 1$$
$$a + b \geq 1$$
$$a \oplus (b \oplus c) = (a \oplus b) \oplus c = 1.$$

$$a = b = c = 0$$
$$a \oplus (b \oplus c) = (a \oplus b) \oplus c = 0.$$

$$a, b, c < 0$$
$$a \oplus (b \oplus c) = (a \oplus b) \oplus c = 0$$

In case of

$$c < 0 \text{ and } a, b > 0.$$
$$a + b < 1$$

we can find the counter example where associativity doesn't hold

$$a = 0.5$$
$$b = 0.6$$
$$c = -0.3$$
$$a \oplus (b \oplus c) = 0.8 \neq 0.7 = (a \oplus b) \oplus c$$

- Does operation have neutral element: addition doesn't have neutral element as there is the counter example of that

$$0: (\exists 0 \in \mathbb{R})(\forall a \in \mathbb{R})$$
$$a \oplus 0 = 0 \oplus a = a$$

$$a \in (0,1)$$
$$0 \oplus a = a = a \oplus 0$$

But in case where

$$a > 1$$
$$0 \oplus a = a \oplus 0 = 1 \neq a$$

as

$$a > 1$$

and in case where

$$a < 0$$
$$0 \oplus a = a \oplus 0 = 0 \neq a$$

as

$$a < 0$$

- Does operation have inverse element: addition doesn't have inverse element

$$-a: (\exists -a \in \mathbb{R})(\forall a \in \mathbb{R})$$
$$a \oplus (-a) = (-a) \oplus a = 0$$

as there is no neutral element.

- Is operation commutative: addition is commutative as it holds for addition of real values

$$(\forall a, b \in \mathbb{R})$$
$$a \oplus b = b \oplus a$$

For operation of multiplication defined in this way, and $a, b \in \mathbb{R}$, following properties were observed:

- Is operation algebraically closed: multiplication is algebraically closed

$$a, b \in \mathbb{R} \Rightarrow a \odot b \in \mathbb{R}$$

- Is operation associative: multiplication is not associative as there is the counter example of that

$$(\forall a, b, c \in \mathbb{R})$$
$$a \odot (b \odot c) = (a \odot b) \odot c$$

$$a, b, c \in (0,1)$$
$$a \odot (b \odot c) = (a \odot b) \odot c = a \cdot b \cdot c$$

$$a, b, c > 1$$
$$a \odot (b \odot c) = (a \odot b) \odot c = 1$$

$$a = b = c = 0$$
$$0 \odot (0 \odot 0) = (0 \odot 0) \odot 0 = 0$$

$$a = b = c = 1$$
$$1 \odot (1 \odot 1) = (1 \odot 1) \odot 1 = 1$$

$$a, b, c < 0$$
$$a \odot (b \odot c) = (a \odot b) \odot c = 0$$

$$c < 0$$
$$a, b < 0$$
$$a \odot (b \odot c) = (a \odot b) \odot c = 0$$

In case of

$$a, b < 0$$
$$c > 0$$

we can find the counter example where associativity doesn't hold

$$a = -0.3$$

$$b = -0.1$$
$$c = 0.2$$

$$-0.3 \odot (-0.1 \odot 0.2) = 0 \neq 0.006 = (-0.3 \odot -0.1) \odot 0.2$$

- Does operation have neutral element: multiplication doesn't have neutral element as there is the counter example of that

$$1: (\exists 1 \in \mathbb{R})(\forall a \in \mathbb{R})$$
$$a \odot 1 = 1 \odot a = a$$

$$a \in (0,1)$$
$$1 \odot a = a$$

But in case where

$$a > 1$$
$$1 \odot a = 1 \neq a$$

as

$$a > 1$$

and in case where

$$a < 0$$
$$1 \odot a = 0 \neq a$$

as

$$a < 0.$$

- Does operation have inverse element: multiplication doesn't have inverse element

$$1/a: (\exists 1/a \in R)(\forall a \in R \backslash \{0\})$$
$$a \odot \frac{1}{a} = \frac{1}{a} \odot a = 1$$

as there is no neutral element.

- Is operation commutative: multiplication is commutative as it holds for multiplication of real values

$$(\forall a, b \in \mathbb{R})$$
$$a \odot b = b \odot a$$

### 2.1. Addition and multiplication based on hyperbolic tangent function

While previous solution is commonly used in image processing and computer graphics, it has limited properties in mathematical sense, and thus it is not open to many optimizations that steam from them. In this paper we propose use of function based on the hyperbolic tangent, as it has much better properties for optimization. Let us first observe the family of functions and its inverse function

$$f_a(x) = \frac{tanh\left(a \cdot x - \frac{a}{2}\right) + 1}{2}$$
$$f_a^{-1}(x) = \frac{arctanh(2 \cdot x - 1)}{a} + \frac{1}{2}$$

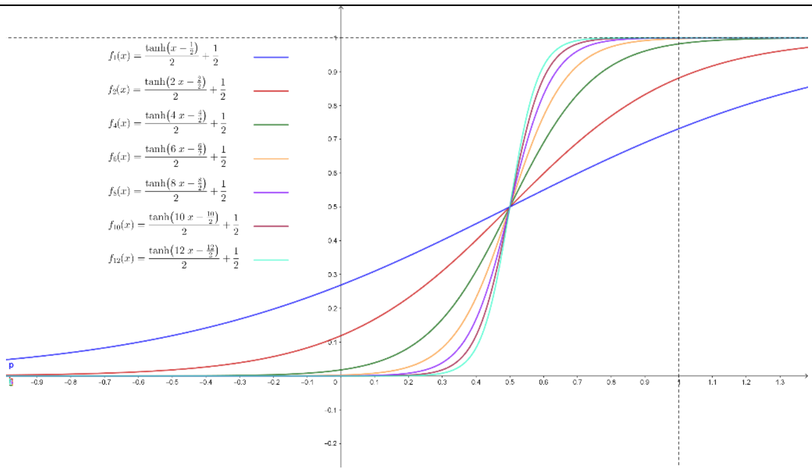

**Figure 1**: Different members of family $f_a(x)$

This family of functions doesn’t approximate the linear function directly as it introduces certain error. Error distribution and the maximum value can change with the parameter $a$. As shown on Figure 1. higher values of parameter $a$ give smaller error at borders, but produce steeper incline, which introduces greater error in approximating linear function. While for $a = 2.82 \ldots$ function has the smallest maximum value of error of 0.056…, error in border cases is too great. Most systems use 8bit color coding per channel. This makes for error allowance of $\Delta = \frac{1}{256}$ at $x = 0$ and $x = 1$ which we would like to achieve. This can be achieved by use of members of the function family that have $a > 5.54$ (see Figure 2).

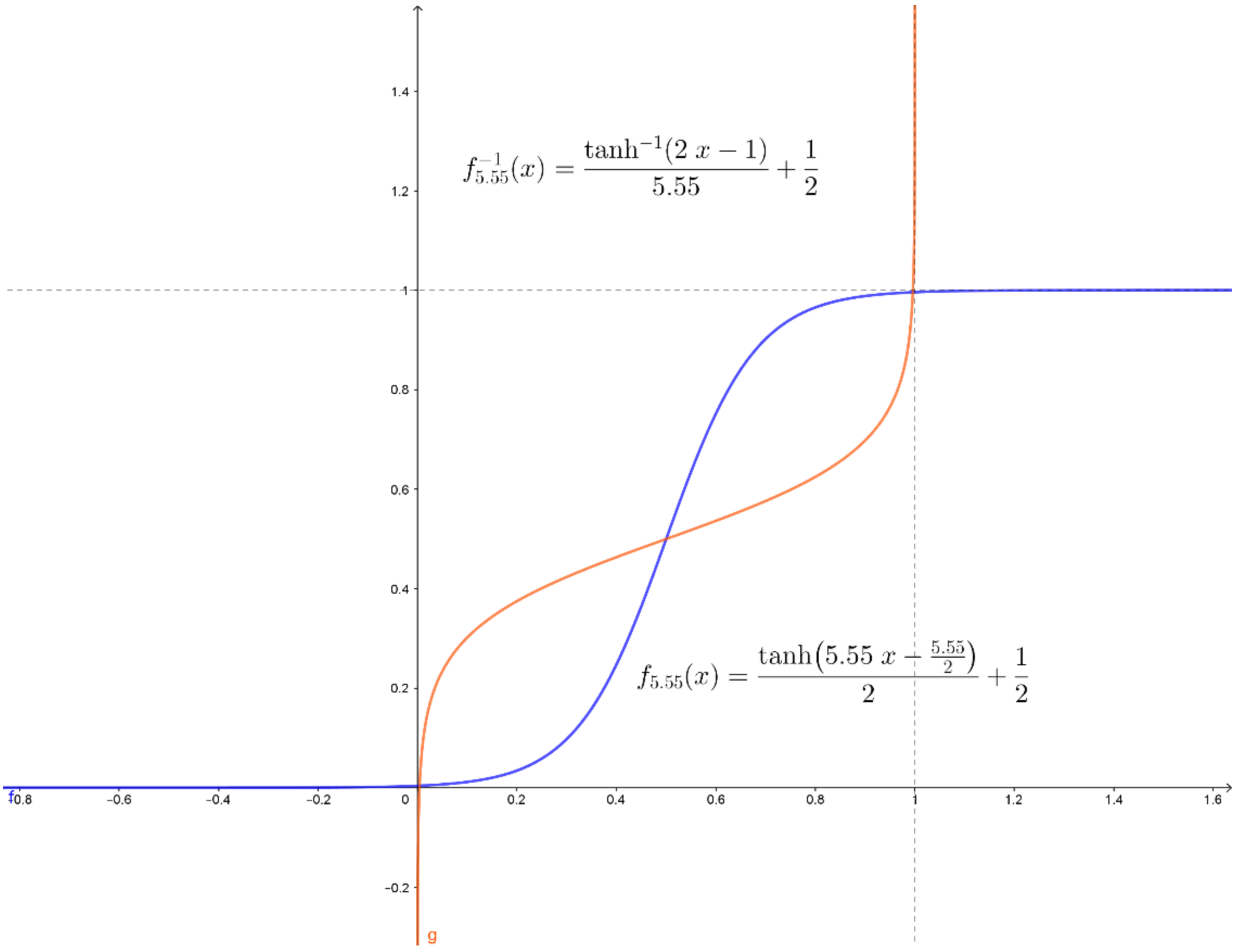


**Figure 2**: Function $f_{5.55}(x)$ and its inverse function

Relaying on our family of the functions $f_a(x)$ let us define addition and multiplication in following way

$$a \oplus b = f\left(f^{-1}(a) + f^{-1}(b)\right) \qquad \text{(new addition)}$$

$$a \odot b = f\left(f^{-1}(a) \cdot f^{-1}(b)\right) \qquad \text{(new multiplication)}$$

One of main differences between the functions defined in this way, and the standard addition and multiplication is that instead of $a, b \in \mathbb{R}$ in this case $a, b \in (0,1)$. Let us observe some properties of the addition and multiplication defined in this way. For new version of operation of addition and $a, b \in (0,1)$, the following properties were observed:

- Is operation algebraically closed: addition is algebraically closed

$$x \oplus y = f\left(f^{-1}(x) + f^{-1}(y)\right) \in [0,1]$$
$$f^{-1}(x) \in [0,1]$$
$$f^{-1}(y) \in [0,1]$$

as for

$$(\forall x \in \mathbb{R})$$
$$f(x) \in [0,1]$$

- Is operation associative: addition is associative

$$\begin{aligned}(x \oplus y) \oplus z &= f\left(f^{-1}(x \oplus y) + f^{-1}(z)\right)\\ &= f\left(f^{-1}\left(f\left(f^{-1}(x) + f^{-1}(y)\right)\right) + f^{-1}(z)\right)\\ &= f\left(f^{-1}(x) + f^{-1}(y) + f^{-1}(z)\right)\\ &= f\left(f^{-1}(x) + f^{-1}\left(f\left(f^{-1}(y) + f^{-1}(z)\right)\right)\right)\\ &= f\left(f^{-1}(x) + f^{-1}(y \oplus z)\right)\\ &= x \oplus (y \oplus z)\end{aligned}$$

- Does operation have neutral element and inverse: addition has both of these elements

$$f(x) = \frac{\tanh\left(a \cdot x - \frac{a}{2}\right)}{2} + \frac{1}{2}$$

$$(\forall x)(\exists y)$$

$$x \oplus y = y \oplus x = e$$

where $e$ is neutral element and $y$ is inverse for addition

For inverse element we find that:

$$(\exists e)(\forall x)$$

$$x \oplus e = e \oplus x = x$$

$$x \oplus e = f\left(f^{-1}(e) + f^{-1}(x)\right) = f\left(0 + f^{-1}(x)\right) = f\left(f^{-1}(x)\right) = x$$

We seek such $e$ that

$$f^{-1}(e) = 0$$

$$f^{-1}(e) = \frac{1}{2} - \frac{1}{a} \cdot \tanh^{-1}(1 - 2e) = 0$$

$$e = \frac{1}{2} - \frac{\tanh\left(\frac{a}{2}\right)}{2}$$

as

$$\tanh\left(\frac{a}{2}\right) \in [0,1] \Rightarrow e \in [0,1]$$

From here for inverse element $y$

$$(\exists y)(\forall x)$$

$$x \oplus y = y \oplus x = e$$

we find element $y$ which is inverse for addition to $x$

$$x \oplus y = f\left(f^{-1}(x) + f^{-1}(y)\right) = \frac{1}{2} - \frac{\tanh\left(\frac{a}{2}\right)}{2}$$

$$f^{-1}(y) = \frac{1}{2} - \frac{\tanh\left(\frac{a}{2} + \tanh^{-1}(-1+2x) + \tanh^{-1}\left(\tanh\left(\frac{a}{2}\right)\right)\right)}{2}$$

$$f^{-1}(y) \in [0,1]$$

$$y = f\left(f^{-1}(y)\right)$$

$$y \in [0,1]$$

- Is operation commutative: addition is commutative

$$x \oplus y = f\left(f^{-1}(x) + f^{-1}(y)\right) = f\left(f^{-1}(y) + f^{-1}(x)\right) = y \oplus x$$

For new operation of multiplication and $a, b \in (0,1)$, following properties were observed:

- Is operation algebraically closed: multiplication is algebraically closed

$$x \odot y = f\left(f^{-1}(x) \cdot f^{-1}(y)\right) \in [0,1]$$

$$f^{-1}(x), f^{-1}(y) \in [0,1] \Rightarrow f^{-1}(x) \cdot f^{-1}(y) \in [0,1] \Rightarrow f\left(f^{-1}(x) \cdot f^{-1}(y)\right) \in [0,1]$$

- Is operation associative: multiplication is associative

$$\begin{aligned}(x \odot y) \odot z &= f\left(f^{-1}(x \odot y) \cdot f^{-1}(z)\right) \\ &= f\left(f^{-1}\left(f\left(f^{-1}(x) \cdot f^{-1}(y)\right)\right) \cdot f^{-1}(z)\right) \\ &= f\left(f^{-1}(x) \cdot \left(f^{-1}(y) \cdot f^{-1}(z)\right)\right) \\ &= f\left(f^{-1}(x) \cdot f\left(f^{-1}\left(f^{-1}(y) \cdot f^{-1}(z)\right)\right)\right) \\ &= f\left(f^{-1}(x) \cdot f^{-1}(y \oplus z)\right) \\ &= x \odot (y \odot z)\end{aligned}$$

- Does operation have neutral element: multiplication has neutral element

$$(\exists e)(\forall x)$$

$$x \odot e = e \odot x = x$$

$$x \odot e = f\left(f^{-1}(x) \cdot f^{-1}(e)\right) = e$$

We seek $e$ such that

$$f^{-1}(e) = 1$$

$$f^{-1}(e) = \frac{1}{2} - \frac{1}{a} \cdot \tanh^{-1}(1 - 2e) = 1$$

$$e = \frac{1}{2} + \frac{\tanh\left(\frac{a}{2}\right)}{2}$$

- Does operation have inverse element: multiplication has inverse element

$$(\exists y)(\forall x)$$

$$x \odot y = y \odot x = e$$

we seek $y$ which is inverse of $x$ for multiplication

$$x \odot y = f\left(f^{-1}(x) \cdot f^{-1}(y)\right) = \frac{1}{2} + \frac{\tanh\left(\frac{a}{2}\right)}{2}$$

$$f^{-1}(y) = \frac{1}{2} + \frac{\tanh\left(\frac{4\cdot\tanh\left(\tanh\left(\frac{a}{2}\right)\right) - 2\cdot\tanh(-1+2x) + a}{4\cdot\tanh(-1+2x) + 2a}\right)}{2} \in [0,1]$$

$$y = f\left(f^{-1}(y)\right)$$

as

$$\tanh(z) \in [0,1]$$

- Is operation commutative: multiplication is commutative as it holds for multiplication of real values

From all previous properties we can determine that for $A = (0,1)$ and the operations $\oplus$ and $\odot$ we have two Abelian groups. Group theory has already done much for computer vision, and transformation of standard operations to Abelian groups could lead to many optimizations. As many current computer systems operate based on group theory, there is already much research to introduce to color models.

It should be noted that while approximation function presented here is not approximating linear function as well as some others would, its properties give it the much higher value, while it is better approximating human vision which is by its nature not linearly dependent of the light intensity. Most computer systems today relay on some form of exponential function for the signal processing, and it is done on hardware level. Thus, computational weight, while it seem much larger at the first glance, could be easily circumvented by use of such hardware. By use of some other members of family of function or similar function with more parameters even better approximation of human vision could be achieved, as example from this paper was selected because of its symmetry and flexibility.

## 3. CONCLUSION

In this paper were presented some mathematical basics of new addition and multiplication functions that could be applied in the color models to achieve even better properties than current ones. While retaining all good properties of previous methods for describing values in color models, we have improved them to have the properties such as inverse value and neutral for two most common arithmetic operations in image processing. In the future research authors of this paper plan to focus on beneficial properties of models with these operations and to find optimization opportunities that rise from its application. Additionally, authors plan to research some new definitions of the arithmetical operations over color with different choices of functions *f* that are closely related to the hyperbolic tangent function. For these new functions we shall also consider application to the new fields such as image reconstruction.

## ACKNOWLEDGMENTS

This research was supported by the Science Fund of the Republic of Serbia, #6524560, AI-S-ADAPT, by the Serbian Ministry of Education, Science and Technological Development through the project no. 451 03-68/2020-14/200156: “Innovative Scientific and Artistic Research from the Faculty of Technical Sciences Activity Domain” and by the Serbian Ministry of Education, Science and Technological Development, under Projects ON 174032 & III 44006, which are realized at the School of Electrical Engineering

## REFERENCES

1. Kelber A. and Osorio D.,2010. From spectral information to animal colour vision: experiments and concepts, *Proceedings of the royal society B*, 277, pp. 1617–1625

2. Bora D. J., Gupta A. K., Khan F. A., 2015. Comparing the Performance of L*A*B* and HSV Color Spaces with Respect to Color Image Segmentation, *International Journal of Emerging Technology and Advanced Engineering*, 5(2)

3. Bueno G., González R., Déniz O., González J., García-Rojo M., 2008. Colour model analysis for microscopic image processing, Proceedings of 9th European Congress on Telepathology and 3rd International Congress on Virtual Microscopy, Toledo, Spain, Diagnostic Pathology 2008, 3(Suppl 1):S18

4. Rasras R. J., El Emary I. M. M., Skopin D. E., 2007. Developing a New Color Model for Image Analysis and Processing, *ComSIS*, 4(1), pp 43-55.

5. Kour H., 2015. Analysis on Image Color Model, *International Journal of Advanced Research in Computer and Communication Engineering*, 4(12), pp 233-235

6. Ibraheem N. A., Hasan M, M., Khan R. Z., Mishra P. K., 2012., Understanding Color Models: A Review, *ARPN Journal of Science and Technology*, 2(3), pp 265-275

# SHAPES, COLORS AND LINES IN LANDSCAPE DESIGN

Radenka Kolarov, Milena Lakićević

University of Novi Sad, Faculty of Agriculture, Department of Fruit growing, Viticulture, Horticulture and Landscape architecture, 21000 Novi Sad, Serbia

kolar.rada@gmail.com

***ABSTRACT***

*Urban green areas have numerous ecological and social functions, and many papers discuss their importance in terms of providing and maintaining diverse ecosystem services. Urban green space is an important part of the urban ecosystem of parks, urban gardens, streets and other human inhabited places because it promotes mental health by reducing stress and recovery from mental and physical fatigue. It can also support biodiversity growth and provide forest products and services, besides offering recreational opportunities. Therefore, visual quality is an important part of the experience. The visual and aesthetic features of any landscape are defined by color, form, line, texture, proportion and spatial topographies. This paper focuses on social functions of urban landscapes, first of all, their psychological and visual functions which are interrelated. Among visual and aesthetics features, the analysis focuses on using different shapes, colors and lines, and provides the examples from historic gardens, but also proposals for a new landscape design.*

**Keywords:** landscape architecture, shapes, colors, line, psychological impact

## 1. INTRODUCTION

Landscape is always an essential component of urban environment. Its multifaceted functions primarily include controlling soil erosion, enhancing water filtration to soils thereby cooling the cities and reducing urban heat island effect. Furthermore, it improves air quality and promotes positive physiological, psychological and economical responses in people. A healthy lifestyle is not necessarily only physical well-being rather it also includes mental calmness and restoration as well. Instinctively, it seems that responding to the changing seasons and climate is equally essential for survival. Plant color could be a cue to such changes. With the increase in urbanization, there in a growing concern about future generations' exposure to nature. Research had already proved that adult preferences and attitudes to plants were strongly influenced by their childhood interaction with nature. The interaction between landscape design and human psychology is important, but it is still largely ignored or even neglected inside and outside the design industry. In addition, the relationship between landscape design and psychology is not only resultant, but also two-way. Successful design has been proven to have obvious physiological effects; on the other hand, psychology, human experience, and the function of our nervous system all play an important role in what we believe to be successful design. This paper is dedicated to understanding how this complex relationship has evolved and how it works in today's world. It first explores the structure and function of the urban areas, how this structure and function benefited our human ancestors, and how functionality of green areas affects modern society.

## 2. MATERIAL AND METHODS USED

The aim of this paper is to analyze urban landscape design from the perspective of social impact of shapes, colors and lines as a basic instrument of creative expresson of a landscape architect based on a collected literature.

## 3. RESEARCH FUNDAMENTALS

Landscape styles have evolved over time as the preferences of the general public have changed, and as new materials and building processes have been discovered. Some styles have been fads that have quickly come and gone, while others have stood the test of time and been around for centuries, even influencing some modern architecture today. Although the word “beautiful” is fundamentally subjective, the feeling associated with it is universal. Seeing something we define as beautiful causes us to feel pleasure. The feeling of pleasure is a result of oxytocin, endorphins and DHEA being released inside our brain. If the sole purpose of buildings is form, or a place where humans can simply gather for some specific purpose, why then would they have the ability to positively impact us physiologically? Again, the answer has its basis in evolution (Ulrich, 1979).

## 4. DISCUSSION

Color in plant material and hardscape adds interest and variety to the landscape. Color is the most conspicuous element in the landscape and is usually the focus of most homeowners; however, it is also the most temporary element, usually lasting only a few weeks a year for individual plants. The use of color is guided by color theory (use of the color wheel) to create color schemes (**Figure.** 2). A simple description of the color wheel includes the three primary colors of red, blue, and yellow; the three secondary colors (a mix of two primaries) of green, orange, and violet; and six tertiary colors (a mix of one adjacent primary and secondary color), such as red-orange. Color theory explains the relationship of colors to each other and how they should be used in a composition. The basic color schemes are monochromatic, analogous, and complementary. Colors can be used to visually change distance perspective. Warm colors and light tints like red, orange, yellow and white advance an object or area toward the observer. These colors and tints placed near the foundation of a house would make the house appear closer to the street. Cool colors and deep shades like blue, green and black recede and can be used to make the house appear farther from the street. Cool colors are restful while warm colors express action and are best used in filtered light or against a green or dark background. Color can be used to direct attention in the landscape. Due to this strong characteristic, color should be used carefully. When color is used for this purpose, consideration must be given to year-round color not just to seasonal color. Consideration may also be given to the time of day when this color will be enjoyed. White or light tints could be used to create interest on a patio. Dark colors would add little to family enjoyment of this area as the daylight hours passed. Color can also be used to capture attention and direct views. Focal points can be created with bright colors. For example, bright yellow, which has the highest intensity, also has a high contrast with all other colors (often described as a "pop" of color) and should be used sparingly (**Figure.** 1). A small amount of intense color has as much visual weight as a large amount of a more subdued or weaker color. Color schemes in the garden can change with the seasons. Summer colors are usually more varied and bright with more flowers, while winter colors tend to be monochromatic and darker with more foliage. Color is also affected by light quality, which changes with the time of day and time of year. Brighter, more intense summer sun makes colors appear more saturated and intense, while the filtered light of winter makes colors appear more subdued.

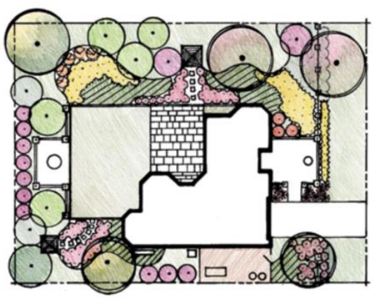

**Figure 1:** Colour sheme

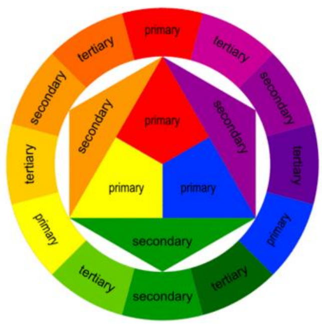


**Figure 2:** Colour wheel

Line in the landscape is created by the edge between two materials, the outline or silhouette of a form, or a long linear feature. Lines are a powerful tool for the designer because they can be used to create an infinite variety of shapes and forms, and they control movement of the eye and the body. Landscape designers use lines to create patterns, develop spaces, create forms, control movement, establish dominance, and create a cohesive theme in a landscape. Landscape lines are created several ways: when two different materials meet on the ground plane, such as the edge of a brick patio meeting an expanse of green turf; or when the edge of an object is visible or contrasts with a background, such as the outline of a tree against the sky; or by the placement of a material in a line, such as a fence. Figure 1 shows common landscape lines, including bedlines, hardscape lines, path lines, sod lines, and fence lines. Lines can have one or more characteristics, such as those described below, but they typically serve different purposes. Line is related to eye movement or flow. The concept and creation of line depends upon the purpose of the design and existing patterns. In the overall landscape. Line is also created vertically by changes in plant height and the height of tree and shrub canopies. Line in a small area such as an entrance or privacy garden is created by branching habits of plants, arrangement of leaves and/or sequence of plant materials. Straight lines tend to be forceful, structural and stable and direct the observer's eye to a point faster than curved lines. Curved or free-flowing lines are sometimes described as smooth, graceful or gentle and create a relaxing, progressive, moving and natural feeling. Plant forms include upright, oval, columnar, spreading, broad spreading, weeping, etc. Form is basically the shape and structure of a plant or mass of plants. Structures also have form and should be considered as such when designing the area around them (Fig 1.). Straight lines tend to be forceful, structural and stable and direct the observer’s eye to a point faster than curved lines. Curved or free-flowing lines are sometimes described as smooth, graceful or gentle and create a relaxing, progressive, moving and natural feeling (Hansen, 2010).

Straight lines tend to be forceful, structural and stable and direct the observer's eye to a point faster than curved lines. Curved or free-flowing lines are sometimes described as smooth, graceful or gentle and create a relaxing, progressive, moving and natural feeling (**Figure.** 3).

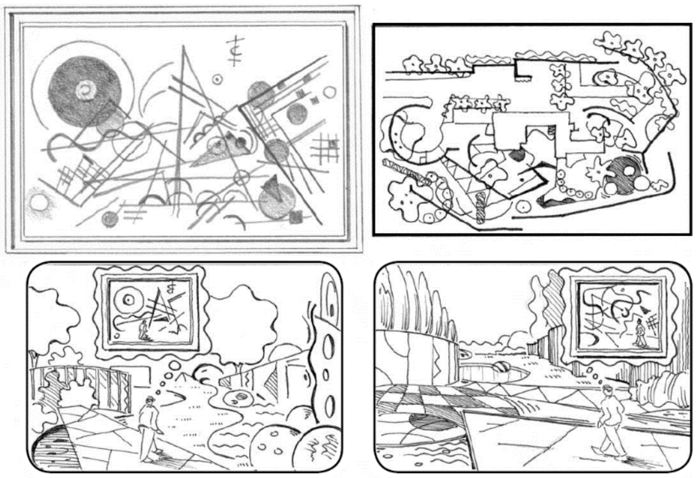

**Figure 3:** Line as a tool in a design

Patterns, have long been a subject of human curiosity, and we have successfully adapted them for use in our ability to plan ahead. There are several different ways in which our brain recognizes patterns. The first, known as feature matching, is when incoming pattern information is broken down by the brain into parts which are then compared and contrasted one by one with parts of a previously stored pattern. Prototype matching is similar to feature matching except rather than our brain matching an incoming pattern to a stored pattern, it attempts to link the incoming information with certain characteristics of a known prototype. This would be equivalent to identifying an apple as a fruit, rather than an apple as an apple (the latter being an example of feature matching). The last method of matching is template matching, in which only certain aspects of the incoming pattern are matched to a template or prototype, rather than the entire incoming pattern.

Shape is created by an outline that encloses a space, and form is the three-dimensional mass of that shape. Form is found in both hardscape and plants, and it is typically the dominant visual element that spatially organizes the landscape and often determines the style of the garden (Ingram, 1991). The form of structures, plant beds, and garden ornaments also determines the overall form theme of the garden. Formal, geometric forms include circles, squares, and polygons. Informal, naturalistic forms include meandering lines, organic edges, and fragmented edges. Plants create form in the garden through their outlines or silhouettes, but form can also be defined by a void or negative space between plants. Organic path forms, 'pendula' forms and cooler colors have a calming effect while straight lines, topiary forms and intense colors increase concentration and alertness (**Figure.** 4). Accordingly, a combination of different elements achieves a different effect within a landscape design. It is recommended that organic forms are applied in those spaces that are intended for longer stays, such as hospital complexes and parks. While more dynamic forms are necessary where we need to maintain our attention, in which case the application of such greenery would find application along roads or other transit points.

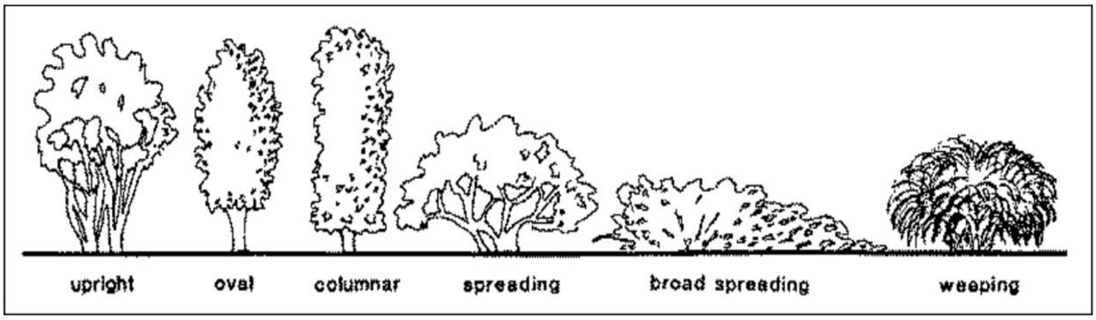


**Figure 4:** Dynamic of habitus shape

Symmetrical balance has been overdone in residential landscape design. This approach seems formal and monotonous. Asymmetrical balance is often more desirable for residential landscapes as balance is created without monotony. Size is balance by mass and texture in this example. Architectural style may dictate the use of symmetry or asymmetry. Driveways, parking and walks must be functional. They must be positioned to provide easy access from points of entry onto the property to the entrance of the house (**Figure.** 5). Too often walks are placed from the street to the front door with no consideration of access from the driveway to the front door. Many times a walk dividing the front yard is not necessary and may detract from the house.

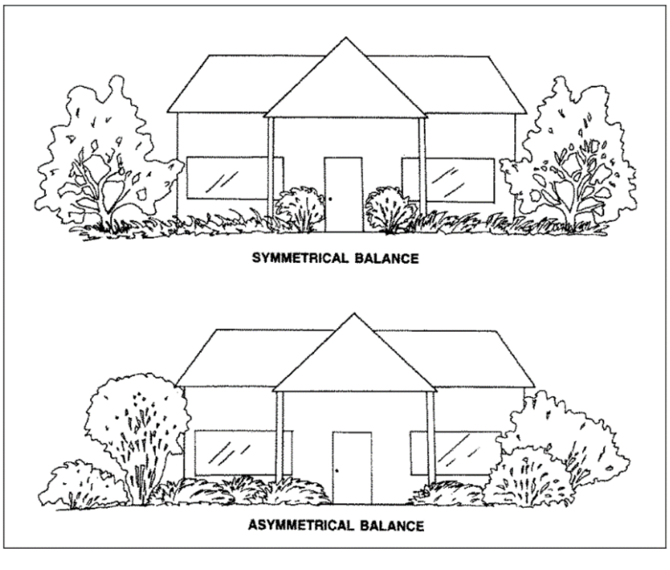


**Figure 5:** Visual impact of different vegetation height

Patterns represent consistency and organization; a lack of chaos. When our ancestors were able to identify a pattern and predict what came next, their chances of survival were improved. Today, patterns in our built environment that the brain recognizes from nature as having been advantageous to our ancestors evoke the same physiological reaction. It makes intuitive sense that chaos or unpredictability, the opposite of pattern, can negatively impact us physiologically. The human brain has used pattern recognition as a form of survival for so long, it has become something we do subconsciously daily. Although your conscious mind might not realize the feelings it is experiencing are due to a pattern, or lack thereof, our physiological system does resulting in the same sympathetic or parasympathetic response our ancestors experienced. The importance of pattern goes beyond the ability to recognize something literal like familiar landscape or a house. It is also important due to its aesthetic impact on beautiful architecture. Pattern in landscape architecture is often referred to as rhythm; it is what causes the eye to flow from one focal point to the next. Not only does it work to grab one's attention, but it also contributes to the beauty of the observed object. There are four categories of rhythm in the architectural world that also apllyies to the landscape architecture: Alternation, the repetition of a contrasting pair; Progression, either increasing or decreasing the size of the element in the pattern; Repetition, continuously repeating a single element; and Transition, the use of a line that the eye is able to continuously follow from one point to the next. Buildings and surrounding landscape that incorporate certain aesthetically pleasing patterns or rhythm are considered more beautiful because our brains are conditioned by evolution to associate those patterns with safety, security, well-being and survival. As noted previously, that perception results in the release of oxytocin, endorphins and DHEA, and throttles back the fight or flight sympathetic nervous system, all resulting in a sense a pleasure. This in turn works to restore our body, immune system, telomeres, etc., which is beneficial for both our mental and physical health.

A long low house (ranch style) can be made to appear taller in relation to its length by proper placement of plant materials. Larger trees planted as a background break the horizontal roof line. Smaller trees spaced a few feet from the ends or corners of the house would also help the house seem taller in relation to its length. A tall slender house seems longer when few or no trees are placed in the background but medium-sized, rounded trees are positioned on either side of the house. Plants placed near these trees should be shorter and decrease in height the farther from the house they are positioned. This planting design effectively created a sloping line to replace the strong vertical line of the house. The house then appears longer in relation to its height.

The contemporary style of the building, its soft rounded curves, and its use of neutral earth-like tones are intended to exemplify rocks in their natural setting. The Eden Project in Cornwall, England, consists of several transparent domes that house a wide variety of plants. The architect Nicholas Grimshaw found his inspiration from bubbles, making it easy for the translucent domes to effortlessly coexist with the surrounding nature.

Color, line, form, texture and scale are tools which are used in combinations to adjust design principles. Design principles include unity, balance, transition, focalization, proportion, rhythm, repetition and simplicity. All these principles interact to yield the intended design.

## 5. CONCLUSIONS

The fundamental concept of landscape design is problem solving through the use of horticultural science, artful composition, and spatial organization to create attractive and functional outdoor "rooms" for different uses. The elements (visual qualities)—line, form, texture, color, and visual weight, and principles (guidelines) —proportion, order, repetition, and unity of design are used to create spaces, connect them, and make them visually pleasing to the eye. Landscape design that contain certain patterns or rhythms are considered more beautiful because our brains are constrained by evolution, linking these patterns to safety, security, well-being, and survival. As mentioned earlier, this perception leads to the release of oxytocin, endorphins and DHEA, and inhibits the fight or flight of the sympathetic nervous system, all of which produce a sense of pleasure. This in turn helps to restore our body, immune system, telomeres, etc., which are good for our physical and mental health.

## REFERENCES

1. Boults, E. and Sallivan, C., 2010. Illustrated History of Landscape Design. John Wiley & Sons, Inc.
2. Hansen, G. (2010). Basic Principles of Landscape Design. Horticulture, July, 12.
3. Ingram, D. L. (1991). Basic Principles of Landscape Design 1. June, 1–19.
4. Ulrich, R. S. (1979). Visual Landscapes and Psychological Weil-Being. Landscape Research, 4(1), 17–23. https://doi.org/10.1080/01426397908705892

# AESTHETICS THROUGH THE GEOMETRY OF STRUCTURAL ELEMENTS ON BYZANTINE CHURCHES

Jovana Vukanić

Department of Architecture, University of Nis, Nis, Republic of Serbia, student

jovanavukanic96@gmail.com

**ABSTRACT**

*For the design of sacral buildings, buildings of great spiritual importance for a nation, the solution should be sought in science and, above all, in truth and faith. Geometry as a language of architecture is one of the main guidelines in the design of church buildings. By transformation, combination and mutual position of the primary solid, cube, sphere and roller, an internal space is created that directly affects the external appearance of the object. The relation between structure and form, that is, the connection between interior and exterior space, is an inexhaustible source of inspiration. The aim of this paper is to point out the ability of Byzantine builders to, in addition to a perfect architectural structure, their architectural edifice, by applying knowledge in the field of geometry and arithmetic, get a good aesthetic solution. The geometry of shapes and irrational numerous relations emphasize the beauty of Byzantine forms of architecture. The starting element of the Byzantine builders is the dome, the structure which was preceded by the analytical idea of the apparent boundary between the sky and the earth's surface. This proves that architecture is basically an unbreakable connection of three components, primarily function, construction and form, and that an object should always be viewed from all three aspects, regardless of the fact that sometimes only one dominates.*

**Keywords:** geometry; aesthetics; construction; form; church

## 1. INTRODUCTION

Every architectural work is based on a solid scientific basis and that is its main component for such a work to survive. Apart from the scientific, the aesthetic component is also very important, which is the product of scientific analyzes, evidences and conventions with the architect's ability to create an impressive final model of the building, showing artistic freedom and leaving personal mark. The choice of material for the final process of an architectural work also goes through an analysis from a scientific aspect in order to see all the physical and mechanical properties of a particular material, its durability, quality, but ultimately perform an analysis of the aesthetic effect. When creating an architectural work, in addition to the creator's personality, his individuality and affinity, his konwladge and skills are also important and how he transfers it to the work. It is possible to see and experience an architectural work, it is possible to separate certain elements from nature or the environment, but it is a part of the universe that is complex and we feel it with the mind.

The architectural form corresponds to the emphasized hierarchy of the church as a circle of spiritual and architectural orientation upwards, towards heights. The already realized form provoked a sign interpretation. The builder overcame the existing technical problems and the function of the space. The simbolically shaped form conditioned by the construction proved to be suitable to get its conceptual solution, that is, the symbolism.

The dome stands out in the Byzantine ideas of the spatial solution and its place is in the center of the horizontal plan. The beauty of Byzantine architectural forms is explained by the geometry of forms and technical solutins in the notion of space that permeates irrational numerous relations.

## 2. BYZANTINE CURCHES

In the field of architecture, the transformation of the Eastern Roman Empire into the Byzantine Empire was relatively peaceful. The center of the development of Byzantine architecture extends to the middle part of the Balkan Peninsula and the area of Asia Minor, the Caucasus and Russia. During the formation of the Byzantine society, the architect continued to have the status of an educated gentleman well informed about technical theory and practice. Byzantine architects did not have the freedom to express their creativity in designing churches in the way they might have wanted, there were limitations in functional, economic, stylistic and intellectual terms, the real success was to give an innovative solution by adhering to all conventions. In the 6th century, after the collapse of the Western Roman Empire, the eastern part, Byzantium, experienced expansion, the mass construction of sacral buildings of the Byzantine-early Christian type began, where the sacral buildings of the basilica and central plan merged.

Spiritual buildings were realized mainly as centric buildings covered with a dome with zoned wall surfaces covered with paintings and mosaics.

Orthodox and especially Byzantine churches became smaller and darker in the mature and late Middle Ages, the light in them became more and more dim. The churches were mostly illuminated through the dome, the most protruding part along the height of the building, so the image of Christ Pantocrator was always painted there.

The most important monuments of early Byzantine art are located in Ravenna, Italy, which was the center of Byzantine rule in Italy during the reign of Emperor Justinian.

- San Vitale 526. - 547. Ravenna

The church of San Vitale in Ravenna has the base of an octagon above which central part is the dome. Through a series of semicircular niches, the central nave of the church is connected to the side nave (Figure 1). Churches with such a dome have been predominant in Orthodoxy since Emperor Justinian representing a link between ancient and Byzantine structures.

- Hagia Sophia 532-537. Constantinople

It is the most famous building of Byzantine art. It was built during the reign of Emperor Justinian in 532 on the site of a church previously built by Theodosius II, which burned down. Saint Sophia was the church where the coronation of Byzantine emperors took place. After the fall of the Byzantine Empire in 1453, Sultan Mehmet ordered turning church into the mosque (Figue 2.).

**Figure 1**: The curch of San Vitale in Ravenna

**Figure 2**: Hagia Sophia in Constantinople

## 3. THE RELATION BETWEEN THE FUNCTION, CONSTRUCTION AND FORM

The architectural form in the process of analysis, design and construction can be observed through three orthogonal projections, regardless of its complexity, it is always special and makes a unique composition. In one of the architectural compositions, each shape has its own characteristics that do not always coincide with the other parts of the composition, but affect each other through their connection within the structure. Therefore, the outer wall is basically also the side of the belonging facade, the horizontal parts of the section are the parts of the floor, and the contour of the section represents the shape of the facade. This spatial relation of two-dimensional drawings determines a three-dimensional shape (Figure 3.).

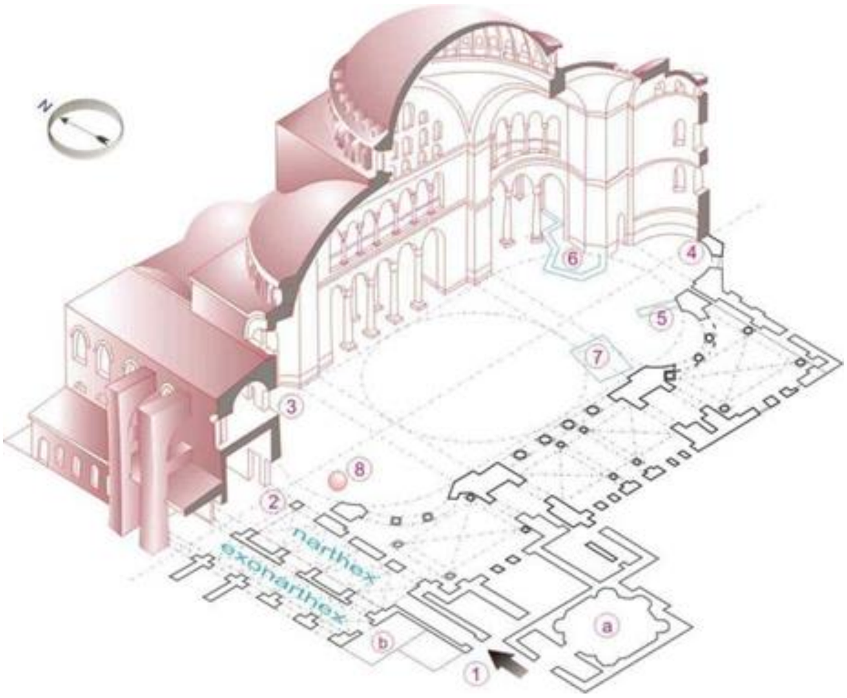


**Figure 3**: Floor plan, section and 3d model of the building

The diversity of architectural works is reflected in the different cultural and historical specifics of one area, the way of creating these works as a process is subject to certain rules. In the 5th and 6th centuries, diversity in the exterior design and structure was noticed, while the original type of design prevailed in the interiors of the churches. retained when it comes to the interior of the church. The architectural form corresponds to the emphasized hierarchy of the church as a circle of spiritual and architectural orientation upwards, towards heights.

- San Vitale 526. - 547. Ravenna

The church of SanVitale was built on the model of the church of St. Sergius and Bacchus in Constantinople. The building has a central plan and differs from the churches in the west, which are mostly of the basilica type. The base has the shape of an octagon, above the center of which rises a dome. The central nave is connected to the side nave by eight semicircular pylons connected by exedra (Figure 4.).

By supporting the main naves over the vaulted structures of large naves, on the church San Vitale in Ravenna, where the large naves are multi-storey so that the vaults on the ground floor and at the gallery ensure greater rigidity of the large nave and thus support the dome structure. Each niche on the ground floor has a gallery above. The narthex is to the west but is displaced in relation to the axis of the altar apse. The interior of the church is richly decorated with mosaics, using a large number of golden decorations, and the proctor is filled with a glow of yellow light (Figure 5). The facade is of simple brickwork, full wall with a large number of openings.

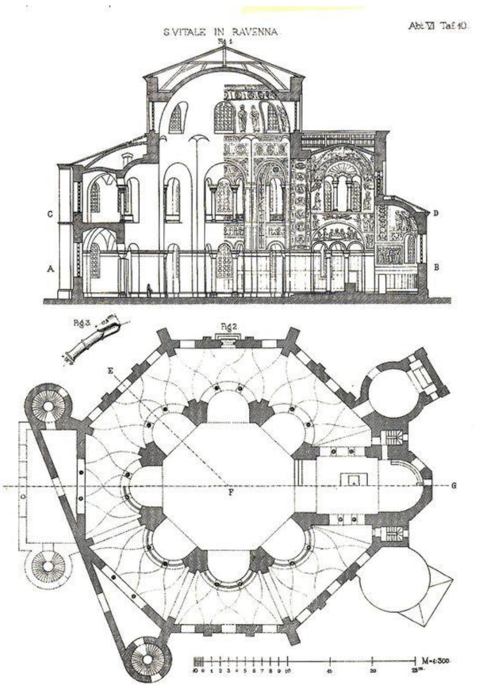


**Figure 4**: The curch of San Vitale in Ravenna, the floor plan and section **Figure 5**: The curch of San Vitale in Ravenna, the interior

- Hagia Sophia 532-537. Constantinople

The most significant work of early Byzantine architecture is the Church of St. Sophia in Constantinople, built in the period 532-537. years, during Justinian's great renewal of the city. Before that, there were two smaller churches from the epoch of Constantine and Theodosius in the same place, which were swallowed by fires (the last during the famous Rebellion of Nick, an uprising against Emperor Justinian in 531. year). The designers of this monumental building were Anthemius of Tralles and Isidorus of Miletus, who managed every day for five years with ten thousand workers who raised St. Sophia.

The base of the Church of St. Sophia is approximately square in shape, formed by a combination of a basilica and a central core, with a dome above the central part supported by two hemispheres, so that the central part takes on an oval shape (Figure 6). At the base of St. Sophia, we find a unique combination of two types of Christian structures, the basilica type and the concept of central core with a dome. The load is transferred onto four strong columns, and to the bulky walls over the transverse arches.

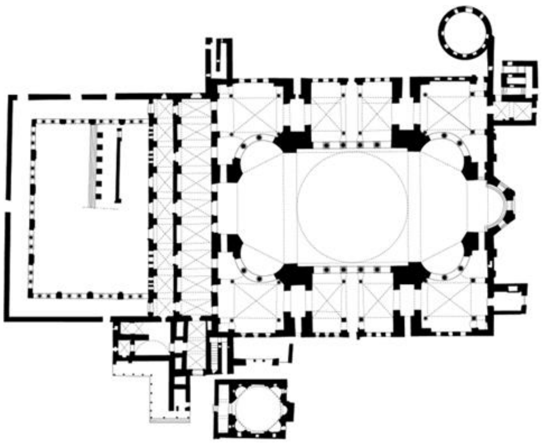

**Figure 6:** Hagia Sophia in Constantinople, floor plan

The main dome was supported by four pendants (Figure. 7). It is a sliced dome with 40 radial ribs between which the shallow vaults are made of brick. The space under the dome with 40 radial arches and 40 windows gives the impression of an airy, weightless space.

The pillars are made of the most valuable marble from the Sea of Marmara, Nicaea, South Africa. Four huge pillars carry a 32-meter-diameter dome at a height of 55 meters. The interior of the church is large, 70 x 75 meters. In the exterior, the volume is closed with flat geometric surfaces (Figure. 8), while in the interor, the wall is completely dematerialized with marble artwork and mosaics, giving it a painting character.

**Figure 7:** Hagia Sophia in Constantinople, the main dome

**Figure 6:** Hagia Sophia in Constantinople, exterior

The original central dome was shallow, with inadequate curvature, so due to a large load it collapsed in 558. In the overhanging form, the dome was repaired by Isidorus the Younger. Later, semi-calottes collapsed one after another due to poor calculations and earthquakes. The western hemisphere was repaired by the Armenian architect Tiridit, and in the 13th century the eastern hemisphere was rebuilt (Figure. 9).

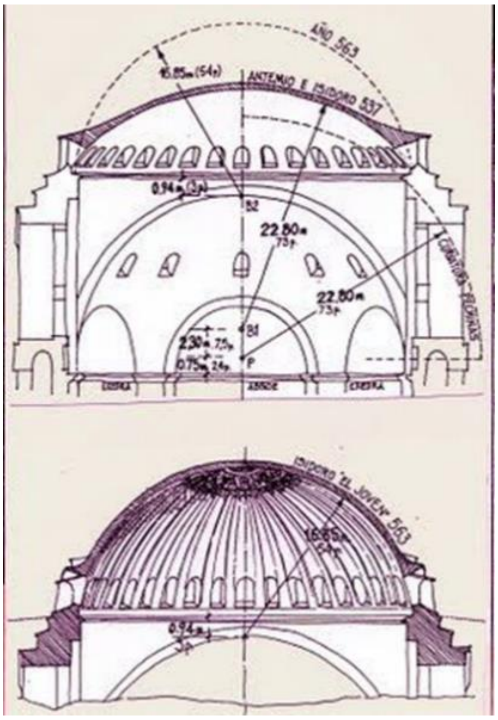


**Figure 9**: Hagia Sophia in Constantinople, the main dome

The use of vaulted structures was of the great importance in the designing of Orthodox churches. Beginning with the reign of Emperor Justinian, the domed churches of the central plan in Byzantium prevailed over the basilical solutions.

In a large number of Byzantine domed churches of the central plan, different types of structures existed depending on whether they followed a developed or concise inscribed cross shape, or they had the other characteristics of a triconch, a large nave with several domes.

The tendency for designing elements that are symmetrical or applying the pairs of elements in sacral objects is justified by the fact that similar elements give pleasure to the human eye. Any irregularity and inequality would distract a person and ask questions to which he as an observer would not be able to give an answer. In Byzantine churches, we can notice the uniformity of the domed arches, which contribute to the beauty and at the same time the stability of the construction. With the harmonious geometry of the structure elements, a master builder primarily contributes to its stability and security, while creating  harmonious whole through which the beauty of the shape of the object stands out. Not every constructive element on the temples has to be beautiful itself, it is important that in combination with the others it is harmoniously connected and together they form a beautiful unit.

In Byzantine architecture, churches of larger dimensions acquire with a very wide base and a narrower dome in relation to the base. In the buildings of the central plan, due to the use of arches and vaults in the lower levels of the spatial assembly, it is much easier to suppress lateral stresses and the expansion of supports than it is in buildings of the basilica type with longitudinal walls. Byzantine builders, relying on their construction skills, used a large number of arches and vaults in such buildings, which supported the construction of the dome. Besides the justification from the aspect of construction, a large number of arched elements were used to represent Christ, the Mother of God, martyrs, saints and angels, and they also had a symbolic meaning.

The authors of this paper had in mind such approach while addressing this research to the aesthetics through the geometry of structural elements on byzantine churches.

## 4. APPLICATION OF GEOMETRIC SHAPES IN THE CONSTRUCTION OF BYZANTINE CHURCHES

Geometry is a surreal creation of ideal shapes that helps us recognize in the real world shapes as a simple or complex geometric configuration and then describe it in geometric terminology and rules before we can say anything else about them.

Geometric elements are, if we do not delve into all the details and specifics, a point, a straight or curved line, a straight and horned or round shape. Each of these elements has its own definition that makes it uniquely permanent and unchangeable. The definition speaks only about it, and not about its relation to the real world, nor about its application.

Geometric elements, by being introduced into the real material world, get the stamp of that world, materialization, specificity, imperfection and dependence on the characteristics of the builder, that is, on the subjective.

Among the geometric entities are those that have the greatest degree of similarity. An example is a triangle, a square and a circle, whose perfection grows gradationally and intertwines with each other. If an equilateral triangle is the most beautiful among triangles because of the equality of the sides, it is more beautiful than it is a square that is axially symmetric, the distance from the center to the vertices to the midpoints of the edges is not equal. The points on the circle are share equal distance from the center. Due to its beauty, the Byzantine builders derived the shapes of arches and vaults from the circle. The sphere and the circle have a symbolic value in sacral architecture, since they are geometric shapes that have no beginning and no end, symbolizing the continuity of eternity, and thus immortality. It is a common opinion that, for these reasons, they symbolize heavens.

The harmony of the interior architecture of the Byzantine churches is largely achieved by the vault.

Although the vault as an independent element does not have as much significance as the dome, their harmonious relation emphasizes the beauty of the dome, so it can be said that the shape and position in the composition are carefully chosen for each of the elements. Behind the mutual harmonious relation of elements in Byzantine churches is the use of proportion, through which the shapes of arches, vaults and domes are defined, their position and connection with other elements of structure.

The earliest form of the vault in the Middle Ages was the groin vault, which influenced Roman and Byzantine architecture. By interpenetrating geometric shapes, semi-circular entities, several types of arches were obtained. The symbolism and meaning of the vault is not determined by its shape. Such a groin vault appears in the church of San Vitale in Ravena with a characteristic positioning in the apse above the altar space (Figure. 10).

**Figure 10.** : The curch of San Vitale in Ravenna, groin vault

## 5. INFLUENCE OF GEOMETRY ON AESTHETICS

Before the form was generated through geometry, a unit of measurement was chosen as a module for the design of a building, Architects of Christian churches used such method to transmit messages of faith.

In the VI century, which is considered transitional for Byzantine architecture, the designer of the great church of St. Sophia in Constantinopole, Anthemius of Tralles, is the last architect of the Roman imperial tradition. He knew the properties of cones, he was the first to describe the construction of an ellipse with the help of a rope fixed in two points. He studied and interpreted geometry of Euclid.

The churches of the central plan, with a dome, corresponded to the spiritual needs of the Byzantines.

In order to analyze the shape, we must first experience, experience and feel it, because that also affects the properties of the shape and determines them. Geometric shapes are part of the real world, but we are subjects with our own world, our own feelings and thoughts, so it seems that the real world is eluding us. In fact, it exists, but we cannot catch it as it is because it exists beyond our interests. We are interested in when a geometric or any real element becomes an aesthetic architectural element, when the message of its essence as an ethical determinant turns into an aesthetic message, because it seems to us that this is less manifested in things and more in the established relation between them.

In addition to practical reasons, the application of proportion significantly influenced the aesthetics of the building.

Good knowledge of the geometry and arithmetic of Byzantine builders is reflected in dimensioning of the spatial elements of the building through the application of proportion. By applying the ratio implied by the proportion, harmony was achieved between various structural elements or the whole. In order to see the beauty of the vaults from the outside, the roof covering was placed directly on the back of the vault instead of on the board substructure.

## 6. CONCLUSION

In Byzantine churches, shapes are a material and integral part of the building. Observing the object, we start from the basic geometric solids and single out the walls as a church envelope, lines as its contour or a place of change of material, shape, structure, color. In architectural drawing, these basic elements have technical and aesthetic properties. The shape is not enough to see, it needs to be recognized. Recognition is the process of matching / identifying with some familiar shape and configuration. A shape can be represented by the essential elements that make it up, rather than by drawing or rendering all the parts of which it actually consists. These parts are important because they send us messages about the whole that we feel but it does not exist. We experience the whole because it is correct and simple and we have seen it many times, so only certain knowledge allowed us to form it in our heads, so the Byzantine architects divided the space into three naves with a colonnade of pillars inside the church, separated the choirs and apse, although there is no real division it is felt.

In order to achieve a certain effect or convey a message, we often view the church as a complex set of forms. By merging geometric entities, rectangles and squares, prisms and cubes or other geometric shapes, an assembly is created in which all the elements act as one whole and on the other hand the initial, basic shape can be recognized. Thus, in Byzantine churches, domes, vaults, pillars, window openings, walls represent separate elements of the building and with their relation they create a stable whole in a constructive and aesthetic sense. In considering the architectural work, the phenomenon of the predominance of shapes is known, which means that in the composition of curves, curved volumes, a simple rectangular shape is first noticed, but also vice versa. In church buildings with mostly rectangular layouts, the dome stands out in the architectural structure as the most impressive element of the composition. These examples show that we do not experience shapes as they are, but as we see them and how they fit into the context, and that this relation significantly affects the vision and experience of the object.

## REFERENCES


1. Bjelić I.: Tipološke I konstruktivne karakteristike lukova I svodova sakralnih objekata na tlu srednjovekovne Srbije, Doktorska disertacija, Univerzitet u Nišu, Građevinsko-arhitektonski fakultet, 2016.
2. Folić Lj.: Arhitektura hrama. Svetigora Cetinje, Eparhijska radionica za umetničko projektovanje i oblikovanje Beograd, FTN Univerzitet u Prištini Kosovska Mitrvica, Beograd 2012/13.
3. Folić N.: Obrazovanje i stvaralačke mogućnosti graditelja u kasnorimskom i ranovizantijskom period, Univerzitet u Nišu, 2011.
4. Martinović U.: Svet arhitekture, Univerzitet u Beogradu, Beograd 1980.
5. Protođakon Simić P.: Crkvena umetnost, Sv. Arhijerejski sinod Srpske pravoslavne crkve, Beograd, 1994.
6. Anthony Cutler: Structure and Aesthetic at Hagia Sophia in Constantinople, The Journal of Aesthetics and Art Criticism, Vol. 25, No. 1 (Autumn, 1966), pp. 27-35 (9 pages) Published By: Wiley https://doi.org/10.2307/428881 https://www.jstor.org/stable/428881
7. Nadine Schibille: Hagia Sophia and the Byzantine Aesthetic Experience, November 2014, DOI:10.4324/9781315586069, Publisher: AshgateISBN: 978-1-4724-3758-7
8. Bogdanović J.: The Domed Canopy in Byzantine Church Design, The Institute for Sacred Architecture, Spring 2020.
9. Wassim Jabi, Iakovos Potamianos: First Geometry, Light, and Cosmology in the Church of Hagia Sophia, Published June 1, 2007 Research Article, https://doi.org/10.1260/1478-0771.5.2.3

# VISUALIZATION OF GEODYNAMIC CHANGES OF TERRAIN USING GOOGLE EARTH PRO AND QGIS

Anastasija B. Martinenko[1*], Marija Đ. Obradović[2]

[1]University of Belgrade, Faculty of Civil Engineering, Department Geodesy and Geoinformatic, 11000 Belgrade, Serbia

[2]University of Belgrade, Faculty of Civil Engineering, Department for Mathematics, Physics and Descriptive Geometry, 11000 Belgrade, Serbia

amartinenko@grf.bg.ac.rs , marijao@grf.bg.ac.rs

***ABSTRACT***

*The paper presents a way of visualizing terrain changes in the observed time period, caused by natural disasters such as landslide. The application of the Google Earth Pro application for generation of DSM (Digital Area Model) data is presented, and the software package Qgis with accompanying tools was used for analysis, modelling and visualization of the obtained data. The settlement of Umka in the city municipality of Čukarica in Belgrade was adopted as an area of interest. Part of Umka territory is a landslide, a geodynamic process which is considered a natural disaster. Thus, as such, it is interesting to monitor changes in the terrain over time period. Changes were monitored within intervals of 8 years, for a period of 2011 to 2019. In Google Earth Pro, DSM was generated via isohypses. Data were generated for different dates using Historical imagery option and compared over time. Obtaining DSM through isohypses in this manner is an efficient and cheap way to obtain terrain data. Therefore, despite certain inaccuracies compared to standard practice, it can be applied in cases where a high level of accuracy is not required, and it is necessary to prepare data in a short time. The method presented in this paper is suitable for a preliminary review of the condition of the terrain, without the need for more demanding procedures.*

*The processing of the generated DSM was performed with Qgis software application. For the selected area of interest, the DSM data was exported from Google Earth Pro and loaded into Qgis. By applying the existing tools, additional terrain analyzes of the area were performed. As a result, terrain models are presented, showing clearly visible changes that occurred within a given time period. The described procedure itself provides several important advantages compared to standard procedures: the use of freeware, rapidity of obtaining results, simultaneous visualization of changes, simplicity of the procedure and obtaining results accurate enough for immediate evaluation of the situation on site. In addition, due to its illustrative nature, this method can be used for educational purposes.*

**Keywords:** DSM, isohypses, Qgis, Google Earth pro, landslide

## 1. INTRODUCTION

The surface of the planet Earth is constantly changing due to the action of various atmospheric and geodynamic processes, such as erosion, volcanism, tectonic disturbances, etc. Since these processes have been active, practically since the formation of the Earth as a planet, there is a need to register changes, learn and understand their tendencies, in order to prevent possible catastrophes.

Topographic bases and Digital Surface Model (DSM) usually represent input data for analysing geodynamic processes (landslides, floods, etc.). However, such information has its limitations and most users rely on official topographic bases and ready-made digital surface models, most often by state institutions. In the last decade, images obtained from satellite images are more and more used as topographic bases. The development of computers and high-performance computer systems has contributed to the increasing use of high-resolution images and geographic information systems that are used as security intelligence, marketing products, but also in scientific research (Gorelick et al., 2017).

Google Earth Pro has positioned itself at the forefront of this wave of spatial information by providing free access to high-resolution images through a simple, user-friendly interface (Fisher et al., 2012; Mutanga et al., 2019). The use of high-resolution images is very common in search of tourist places, education and space visualization. However, studies that use high-resolution images to gain quantitative insight into the processes and mechanisms that act on the Earth's surface over time, are not abundant. When it comes to the accuracy of satellite imagery used by Google Earth Pro, (ANATUM, 2019; Goudarzi et al., 2017) state that the accuracy of aerial imagery in urban areas could average about 0.5 m. In rural areas, the accuracy could be on average 1 to 1.5 m, or even lower. In Gorelick et al. (2017) examine the accuracy, which examines the accuracy of Google Earth Pro images across the city of Montreal, Canada, and the authors found that the accuracy in some parts of the city is about 0.1 m, but in other parts of the city even 2.7 m. Also, in research Zomrawi et al. (2013) shows Root Mean Square Error (RMSE) which is calculated by comparing the measured coordinates of points with the geodetic Global Positional System (GPS) receiver coordinates that provide accurate coordinate measurement on the same ellipsoid as Google Earth. This information can be used to verify the accuracy of Google Earth. RMSE was computed for horizontal coordinates and was found to be 1.59 m. For height measurement RMSE was computed to be 1.7 m.

This paper presents a research on a zone of the settlement of Umka, which belongs to the Belgrade municipality of Čukarica and represents a zone of pronounced landslide that endangers the infrastructure and built facilities of this place. Therefore, as such, it is an interesting area to monitor and track changes that are taking place. The changes were monitored in an interval of 8 years, for the period from 2011 to 2019. Based on previously conducted research (Erić et al., 2015; Samardžić-Petrović et al., 2020; Abolmasov et al., 2017; Abolmasov et al., 2020) in the area of the Umka landslide, permanent GNSS monitoring shows horizontal and vertical displacement. During the first time period (March 2010 - December 2013), the total 2D shift was 84 cm to the northwest, and the vertical shift was almost -30 cm. During the second time period (September 2014 - December 2018), the point of the object moved 63 cm to the northwest, and the vertical movement was almost -16 cm. In general, the Umka landslide moves continuously and significantly towards the northwest, ie towards the Sava River. The average annual 2D displacement was approximately 22 cm and 15 cm, for the first and second time periods, with the same direction of movement.

This paper proposes an alternative method of obtaining DSM data for a wide area as opposed to traditional geodetic methods that involve time-consuming and expensive work. The application of Google Earth Pro for generating DSM data is presented, and the software package Qgis with accompanying tools was used for analysis, modelling and visualization of the obtained data. The advantage of this application is reflected first of all in the facility of its usage, and also in its public availability.

## 2. METHODOLOGY

The Umka landslide (*Fig 1*) was chosen as the study area due to its geodynamic nature, and for many years the landslide flow has been monitored by various geodetic methods. Traditional geodetic methods include terrestrial data collection methods, but also include the processing of aerial and satellite images.

In recent years, the landslide has been monitored using high-resolution digital terrain models obtained by processing aerial images. One of the methods of visualizing geodynamic changes in the terrain is the generation of DSM based on satellite images from which data on the height of the terrain are collected and loaded into the appropriate CAD or GIS software.

The Umka landslide is a very old landslide and its origin and development is related to the geological structure of the terrain and the centuries-old evolution of the Sava River. It is positioned between two cities in Serbia: Belgrade, the capital city, and Obrenovac, of just over 70,000 inhabitants, settled along the right bank of river Sava. The speed and magnitude of terrain deformation is complex and closely related to the shapes and depths of the landslide body, the depth of the Sava riverbed, and the groundwater and surface water regime. As a rule, the largest and fastest deformations follow the parts of the coast where the depth of the Sava riverbed is about 20 m (Mitrović et al., 2006).

This area includes the settlement of Umka, which is dominated by built and agricultural land. Also, a state road of the first order passes through this settlement, which connects Belgrade with Podrinje and, further, with Sarajevo in Bosnia and Herzegovina. The effects of landslides on this area rich in agricultural land are of great importance for monitoring the direction in which the landslide is moving. For the selected area in this study, it was necessary to collect terrain elevation data based on Google Earth Pro images for the mentioned period.

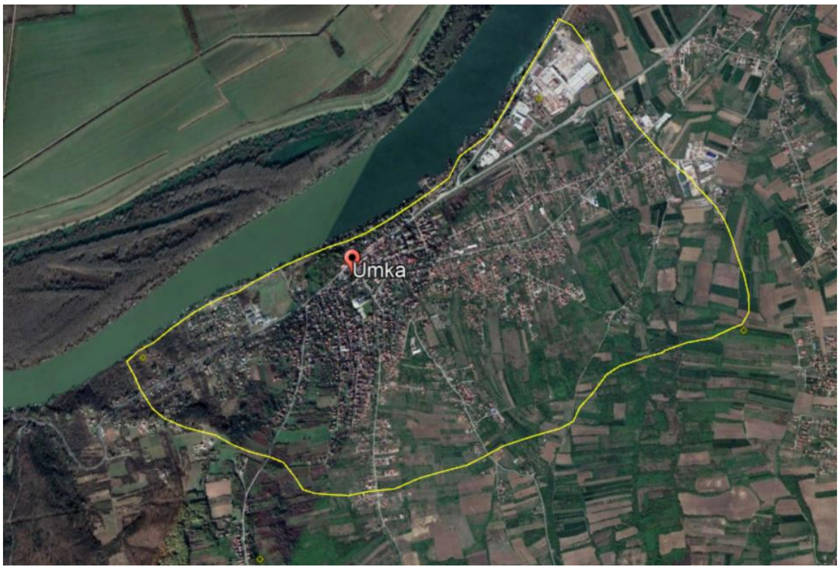


**Figure 1**: Boundary of the Umka area

Landslides can be observed through developed landslide identification criteria from Google Earth Pro and a method for estimating accuracy has been introduced (Rabby et al., 2019), this paper presents a similar approach that has an advantage in the availability of high-resolution images in Google Earth Pro allows visual interpretation, but also alternative collection of terrain data.

The basic principle of this method is the identification of landslides and the collection of data on the height of the terrain. Terrain identification was done by forming a polygon that includes a landslide and drawing a dense network of nets through the terrain profile, in order to collect terrain height data. Changes in the field can be tracked based on satellite images for specific periods. There is a *Historical Images* option in Google Earth Pro that allows one to view older satellite images (at one-month intervals). Data is generated for time period 08/2011 (*Fig 2a*) and 08/2019 (*Fig 2b*), to monitor changes in terrain height based on DSM and terrain isohypses.

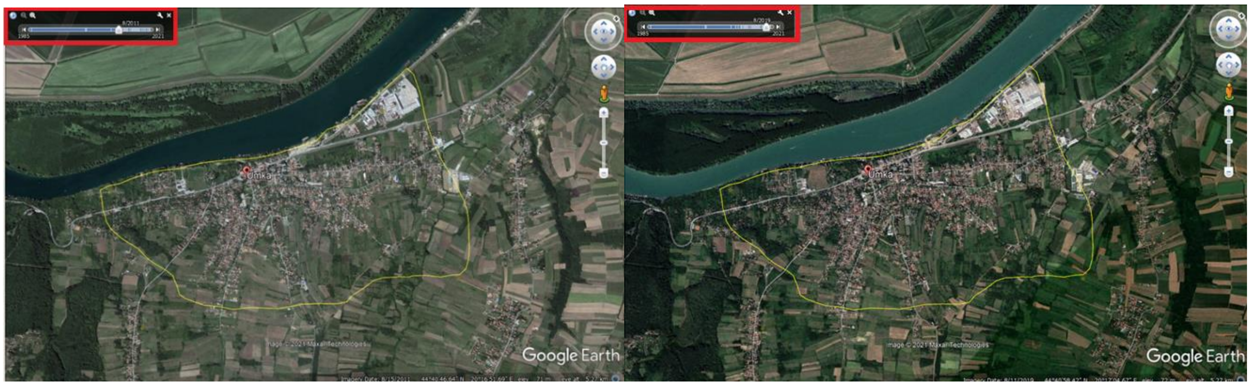


(a) (b)

**Figure 2**: (a) Area of Umka landslide from 08/2011 (b) Area of Umka landslide from 08/2019

The plot profile was drafted by drawing lines (*Path* command) approximately parallel to the boundaries of the chosen landslide area, so that the entire area of interest is covered with a grid, in order to achieve as much detail as possible. The denser the grid, the greater the accuracy of the collected data for the DMS formation is obtained. For each plotted profile within Google Earth Pro, a display with data on altitude, distance (from the starting point of the trajectory), maximum slope and averaged terrain slope is automatically obtained (*Fig 3*).

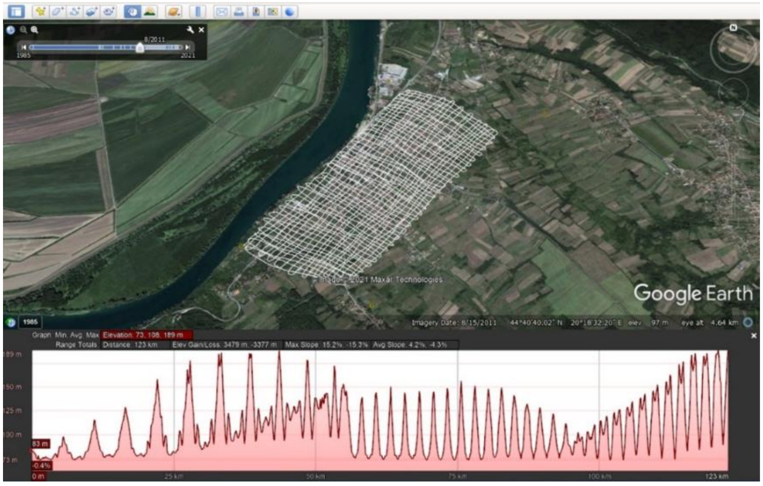


**Figure 3**: Histogram with data from 08/2011 on terrain height, distance and slope

The generated data is saved within a *.kml* file and then loaded into the Qgis software as characteristic terrain profile points. Each of the points has position and altitude coordinates and as such is used as input data to create the DSM (*Fig 4*).

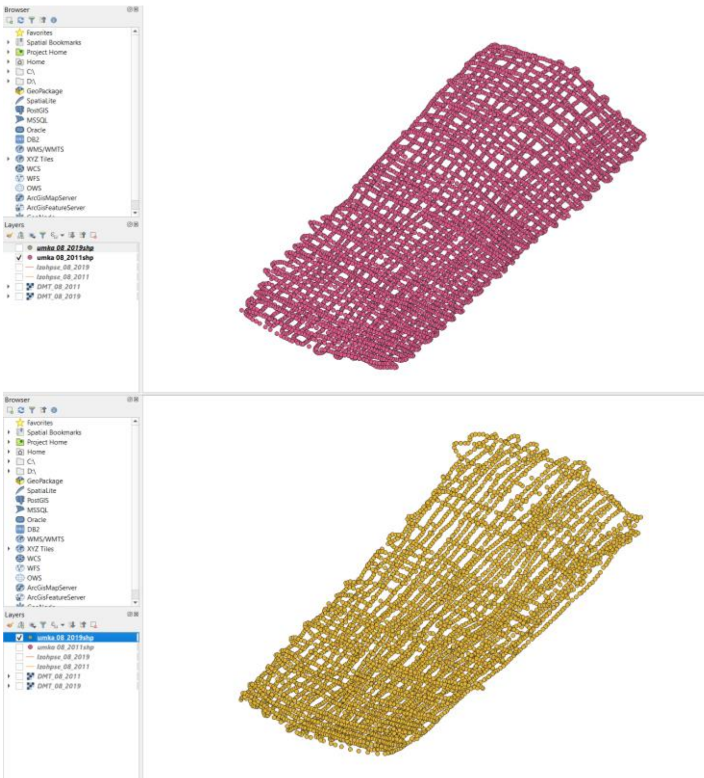

**Figure. 4:** Characteristic profile points for 08/2011 (top) and 08/2019 (bottom)

To create DSM in Qgis software, the *Natural Neighbour* [5] function was used (*Fig 5*), where the input data is a *.shp* file with characteristic profile points, an attribute by which interpolation is performed (terrain height) together with the size of the output cell (*Fig 6*).

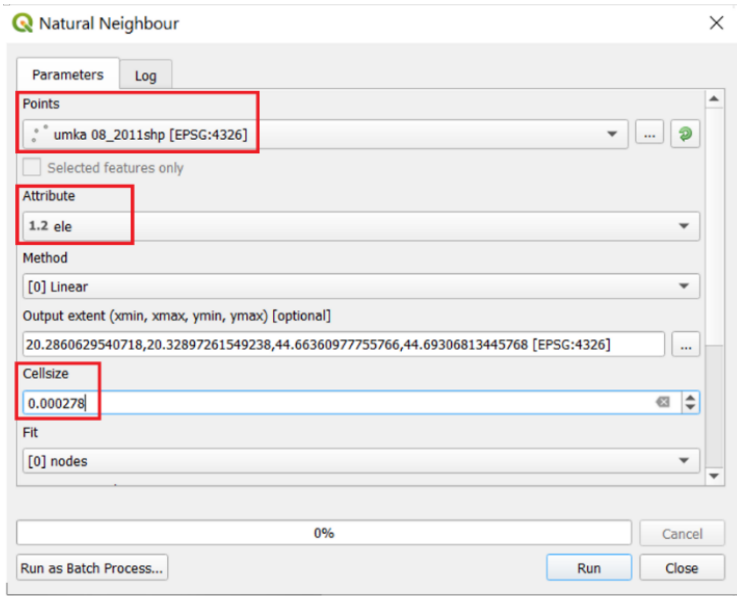


**Figure 5:** Natural Neighbour

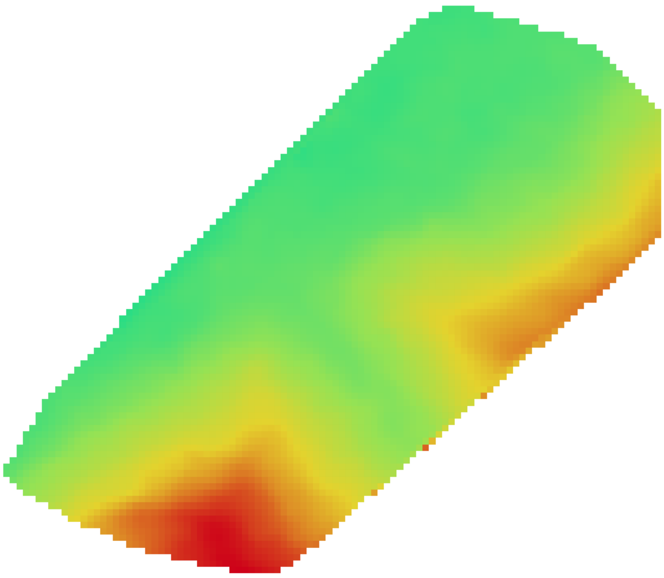

**Figure 6:** Generated DSM 08/2011

*Fig 7* shows the generated DSM for the 08/2011 time period, which resulted in a range of terrain heights from 67.12 m to 187.66 m. Also, the DSM generated for the 08/2019, resulted in an identical terrain height range. The DSM served as a basis for extracting the isohypsis of the terrain, which allows a clearer idea of the height of the terrain.

[5] Natural Neighbour method for grid interpolation from irregular distributed points.

Extraction of terrain isohypses was performed using the *Contour* function, which requires DSM and isohypsis equidistance as input data (*Fig 8*).

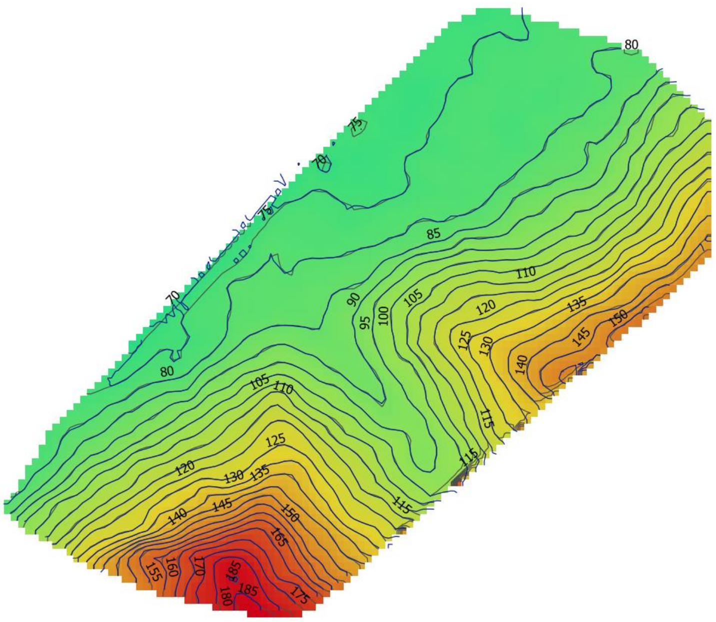


**Figure 7:** DSM and isohypses

## 3. RESULTS

The extracted isohypses for both periods are shown on the DSM base. Isohypses are different because they are generated on the basis of DSM which has different height values at identical points of different periods. Thus, it can be concluded that in certain parts of the area there is a mismatch of isohypses (*Fig 8*), which can be interpreted as a consequence of moving the landslide itself, but it should be borne in mind that the results are burdened by path creation error in Google Earth Pro and DSM generation error.

The difference between isohypses can be approximated by the minimum distance between the same isohypses for the two periods 08/2011 and 08/2019. *Fig 9* shows an example of a possible displacement of the terrain, from which we can see globally that in this part there was a displacement of the terrain at the meter level (specifically, 1.798 m was measured). Such data must be taken with a grain of salt because, depending on the input data, the accuracy of the DMS development also depends. Certainly, we see that the aberrations exist and that such large deviations surely signal the movement of the soil and consequently the shift of isohypses that describe it.

The advantage of the applied methodology is that in a short time interval we get information on whether there are terrain changes in an area, which is of great importance due to the disturbance of terrain morphology, and it affects the construction potential of the area, agricultural development, and many possibilities of such terrain.

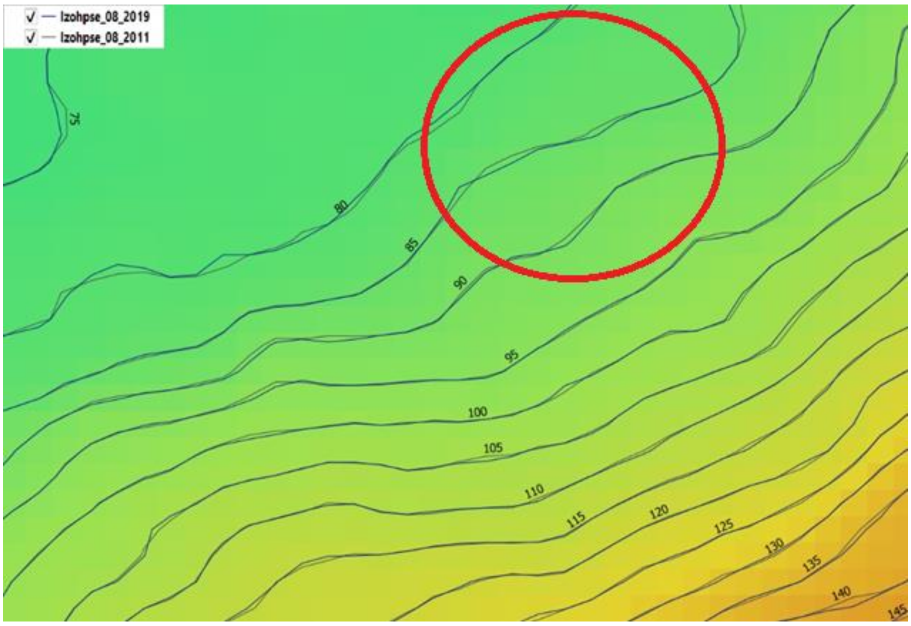


**Figure 8:** Isohypses from the periods 08/2011 and 08/2019 overlapped


**Figure 9:** Minimum distance between the same isohypses from the periods 08/2011 and 08/2019

By applying the described methodology, satisfactory results were obtained. Terrain models with clearly visualized changes in topography due to landslide shifts are displayed, observed within a given time period.

## 4. CONCLUSIONS

Based on the obtained results, it can be concluded that the use of Google Earth Pro in combination with Qgis software has a number advantages over standard procedures, when it comes to visualizing and presenting changes that occur in the field. The use of open source / freeware, high speed of obtaining results, simultaneous visualization of changes, as well as the simplicity of the procedure itself make this methodology acceptable and competitive for the mentioned purpose. In addition, due to its illustrative nature, this methodology can also be applied for educational purposes. On the other hand, the limiting factor in the application of this method is the somewhat lower accuracy of DSM generation.

Visual interpretation of the landslide using images taken from Google Earth Pro shows that the development of such a landslide in the future leads to great damage to human society, which is reflected in the infrastructure, then in arable land and roads. Applying this methodology, many professions can very quickly and efficiently have an insight into the areas affected by natural disasters, which is of great importance for companies that want to invest in an area.

Due to slightly lower accuracy compared to geodetic measurements, this method can be used as a preliminary testing phase, where only the landslide is determined and to what extent, which could be useful to the casual, non-professional user when choosing a location for their activity, e.g. construction, agriculture or similar without hiring expensive experts (for example, if you are just deciding to buy, in order to reduce the investment risk).

## ACKNOWLEDGEMENT

This paper is part of the technological development of project no. 200092 funded by the Ministry of Education, Science and Technological Development.

## REFERENCES

1. Abolmasov, B., Marjanović, M., Milenković, S., Đurić, U., Jelisavac, B. and Pejić, M., 2017. *Study of Slow Moving Landslide Umka Near Belgrade, Serbia (IPL-181). Advancing Culture of Living With Landslides*, Vol 1: Isdr-Icl Sendai Partnerships 2015-2025. pp 419-427.
2. Abolmasov, B., Đurić, U., Popović, J., Pejić, M., Petrović, M.S. and Brodić, N., 2020. *Results of Recent Monitoring Activities on Landslide Umka, Belgrade, Serbia—IPL 181. In Workshop on World Landslide Forum*. pp 225-234.
3. ATATUM, 2019. https://www.agsgis.com/Advanced-Mobile-Mapping-Series-Why-Does-My-GPS-Data-and-Imagery-Not-Line-Up_b_1062.html [Accessed: 31 st July 2021].
4. Erić, V., Božić, B., Pejić, M., Abolmasov, B. and Pandžić, J., 2015. Permanent geodetic monitoring of the Umka Landslide using GNSS technology and GeoMoss system. Abstract book / 2nd Regional Symposium on Landslides in the Adriatic-Balkan Region : 2nd ReSyLAB 2015. Vol. 1 University of Belgrade, Faculty of Mining and Geology, Belgrade. pp 39-39.
5. Fisher, G. B., Amos, B. C., Bookhagen, B., Burbank, W. D., and Godard, V., 2012. *Channel widths, landslides, faults, and beyond: The new world order of high-spatial resolution Google Earth imagery in the study of earth surface processes. Geological Society of America Special Papers 492*, no. 01. pp 1-22.
6. Gorelick, N., Hancher, M., Dixon, M., Ilyushchenko, S., Thau, D. and Moore, R., 2017. *Google Earth Engine: Planetary-scale geospatial analysis for everyone. Remote sensing of Environment 202*. pp 18-27.
7. Goudarzi, M. A., and Landry, R. J., 2017. *Assessing horizontal positional accuracy of Google Earth imagery in the city of Montreal, Canada. Geodesy and Cartography*, 43(2). pp 56-65.
8. Mitrović, P. and Jelisavac, B., 2006. *Sanacija klizišta 'Duboka'. Materijali i konstrukcije,* 49(1-2). pp 46-59.
9. Mutanga, O. and Kumar, L., 2019. *Google Earth Engine Applications. Remote Sensing*, 11(5). pp 591.
10. Rabby, Y. W., and Yingkui, L., 2019. *An integrated approach to map landslides in Chittagong Hilly Areas, Bangladesh, using Google Earth and field mapping*. *Landslides 16*, no. 3. pp 633-645.
11. Samardžić-Petrović, M., Popović, J., Đurić, U., Abolmasov, B., Pejić, M. and Marjanović, M., 2020. Permanent GNSS monitoring of landslide Umka. XIV International Conference On Contemporary Theory And Practice In Construction XIV Stepgrad XIV Proceedings, 2020. University of Banja Luka Faculty of Architecture, Civil Engineering and Geodesy.
12. Zomrawi, N., Ahmed, G. and Eldin, M., 2013. *Positional accuracy testing of Google Earth. International Journal Of Multidisciplinary Sciences And Engineering*, vol. 4, no. 6. pp 6-9.

# IMPLEMENTATION OF WOODEN CURVE BENDING IN CELL-BASED PAVILION DESIGN

Pejic Stefan[1] , Radjenovic Nikola[2] , Jovanovic Marko[3]

[1]University of Novi Sad, Faculty of Technical Sciences, Department of Architecture and Urban Planning, 21000 Novi Sad, Serbia

[1]stefanpejic74@gmail.com, [2]nradjenovic.office@gmail.com, [3]markojovanovic@uns.ac.rs

***ABSTRACT***

*The implementation of pavilion structures in architecture has always served as testing grounds for novel materials, forms, and fabrication techniques. Mostly, pavilions are depicted as encased entities that create a distinct boundary between the inner and outer space. However, with the use of modern-day technology the limits of pavilion envelopes are pushed to new territory. These pavilions require proficient methods and fabrication tools such as industrial robots, CNC milling machines, and custom-made molds to fabricate. The main problem with the aforementioned approaches is a very complex fabrication process. The complexity is seen through high production expenses and slow assembling time due to project specifics. However, with regards to linear elements, 2D lasers, and circular saws are shown to be time-efficient and versatile tools to apply. Hence, this paper aims to explore a design workflow for fabricating pavilions out of curved wooden elements by using the kerf bending technique which includes laser cutting and circular saws as fabrication tools. The design process entails the use of a faceted design pavilion that can be approximated through wooden planks as bendable elements and developable metal strips as joints. Applied methods include the generation of the desired pavilion form, approximation by larger irregular polygon shapes similar to Voronoi, while the exploration of bending curved surfaces is tested empirically through the fabrication of series of different patterns in order to find the best one in terms of strength and pliability. To significantly simplify the construction of the pavilion and speed up the assembly process, the joints, which are usually very complex to fabricate are generated as developable strips of metal that can be welded alongside a joining edge. In addition to the above, through empirical research of a scale model, the results would be verified.*

**Keywords:** algorithm, curve bending, wooden, pavilion, fabrication

## 1. INTRODUCTION

Since advanced computational technology is giving unlimited possibilities in the process of architectural design, architectural designers are bringing engineers up to a very challenging point to successfully fabricate complex shapes and structures. During the design process, it is necessary to think about less demanding fabrication methods in terms of material consumption, sustainability, people involved in constructing that model, and time spent preparing the constructional elements and joining them. Modern materials used on such projects as titanium, aluminum, iron, copper can bring the cost of fabrication to mind-blowing sums especially when they are deformed to make curved surfaces. Therefore, using sustainable materials such as wood, adapted through software-generated algorithms for processing surfaces by reducing strength on certain parts of wooden planks can increase the bending, leading to cost-effective and less time-consuming methods for making structures using bent wooden elements.

Considering long experience in wood bending that lasts since ancient craftsmen first started bending wood to make boats, sailing ships, barrels, furniture, tools, till this day methods have significantly advanced. Of the several methods commonly used to produce curved wooden parts, traditional bending is still the most economical of material, the most productive of members of high strength, and perhaps the cheapest (Peck, 1957). The only problem when it comes to using traditional wooden bending in commercial operations often results in serious losses because of breakage during bending operation or in the second process while fixing the wood in place and certain shape for drying.

The most important point in bending is the wood itself, as not every type of wood is suitable for bending. Frequently used types of wood are oak, beech, yew, ash, elm, and walnut as these types have a certain elasticity (according to new research, 2021).

When bending a small piece of wood by hand, the piece of wood compresses on the concave side and stretches on the convex side of the bend. The distortion that is formed from the stresses tends to bring the wooden piece back into its original shape with the original straightness. To restrict the development and affection of these stresses on the bent wooden piece, it is necessary to soften the wood either with plasticizing chemicals or heat and moisture.

Traditionally bending large wooden surfaces includes steaming wood in large steam chambers for several hours and can be very difficult especially with larger wooden elements as a process in fabrication. To properly make wood pliable, it is necessary to expose it to high heat and steam as moisture steams through wood fibers which soften the wood, stretches its cellulose fibers that compose the major structure, and makes wooden planks pliable. After cooling down, wood forms and holds its new shape, and remains structurally stable even though some wooden species get slightly stressed which can cause breakage over time. To prevent breakage, it is recommended to clamp the wood to a solid mold, reinforcing the bends made to the wood during the drying process. This also prevents the wood from straightening until it is fully dried. The process can take a long time to prepare the wood, steam it, shape it and properly dry it to have it fully ready as a construction element and in the desired shape.

Another method that is most advanced and modern as a woodworking technique in bending wood is microwave bending. This technique is very similar to traditional steam bending but is more manageable and much quicker when it comes to getting desired results. To generate steam while microwaving wooden elements, it is necessary to wrap each piece of wood in a wet paper towel or blanket properly soaked in water and put it in the microwave. The heating varies depending on the size of the wood as well as its thickness.

**Figure 1:** Kerf Pavilion made by MIT Department of Architecture (source:https://www.tylercrain.com/projects_kerfpavilion#2)

The quickest method for bending wooden surfaces is called kerf bending. This technique refers to the removal of material at strategically located areas on a wood surface, to weaken the material locally to bend it. (Gillkvist et al., 2016; Mitov et al., 2019) Removing material can be done approximately but the angle of the curvature of the bend cannot be precisely determined. Therefore generating an algorithm that will determine the necessary intervention and locally define positions where the wooden surface has to be weakened to get the proper angle of the bend would be a helpful tool in new woodworking industries for making simple and fast bending of such surfaces. The researcher that pioneered wood bending through this technique is Aaron Porterfield who researched different patterns through empirical experiments with laser kerf bent wood after parametrically generating those patterns and simulating them throughout software Rhino with help of a plugin for visual programming called Grasshopper (Aaron Porterfield, 2017). By changing variables, such as distance between slots, the scale of the pattern, the directions of the elements that form the pattern, and converting the linear elements into curved or dotted lines, a variety of conclusions can be drawn, that is useful for further developments of the application of the technique. (Kalama et al., 2021).

One of the greatest examples of a structure made out of wood using the kerf bending technique was made by graduate students from the MIT Department of Architecture. The Kerf Pavilion (Figure 1) is the result of an old technique reinvented using digital strategies and tools. The research made by the students combined the material logic of kerfing with the flexibility of parametric modeling and the accuracy of a CNC route.

Contemporary and modern-day architecture has not developed through large and complex projects as much as through much smaller projects in form of pavilions. The advantage of small projects can be seen through a straightforward scientific approach to a specific idea, problem, and performance as they can be easily processed on a much smaller grade through pavilions. Conclusions derived from the fabrication process of those pavilions can later be used on everyday problems seen on the construction site to simplify complex ways of fabricating demanding structures and elements that modern architecture is bringing regularly. Besides pavilion structures, this principle can be used for fabricating formwork for developing concrete constructions. Making bent kerf surfaces as support for outpouring concrete can help engineers form very complex shapes and objects. Therefore, it is very important to reach the desired angle, deflection of the wood without significantly breaking its natural stability and balance in structure.

This research aims to explore an advanced method for the existing principle of kerf bending where wooden planks are relieved on certain spots to get reasonable bending of such planks and tested through pavilion generation. The research is divided into several phases. the first one is the generation of the desired pavilion form. Next, the pavilion is approximated by larger irregular polygon shapes, similar to Voronoi. These shapes are used as the basis for generating the fillet edge look of each cell. Finally, as a proof of concept, one cell is chosen and unrolled, with a parametric kerf pattern in specific locations to physically produce a prototype and verify the flexibility and pliability.

## 2. METHODS

The first step towards generating a pavilion is to select the starting base on which the pavilion form will develop during the process. The assembly of several surfaces into one causes the complexity of the shape of the future pavilion (Figure 2a). The next step would be the separation of the initial form into segments. When dividing into pieces with the rebuild command in the Rhinoceros program, it is necessary to pay special attention to the number of components as it has to be the same in both directions for each set area to form the correct division principle (Figure 2b).

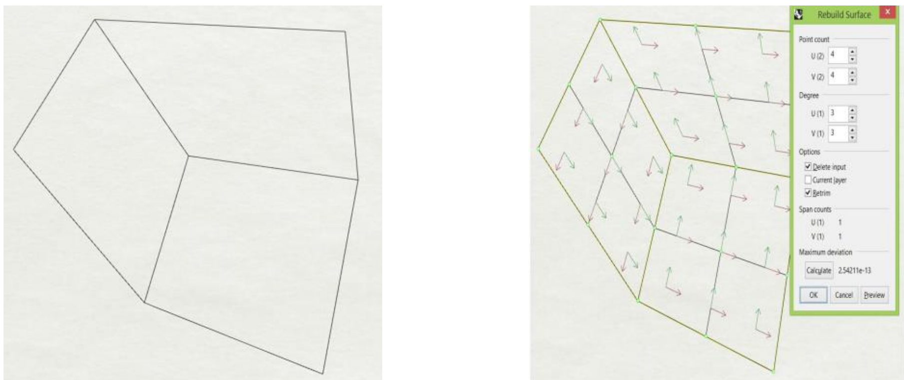


(a) (b)

**Figure 2**: (a). Forming the starting base of the pavilion, and (b). Separation of the initial form into segments

It is possible to move the control points by activating them. This process corrects the initial shape of the pavilion as well as to emphasizes the supports and heights. (Figure 3a) The newly created modified surface converts into the Mesh, which is the starting point for the further stages of generating the pavilion. (Figure 3b).

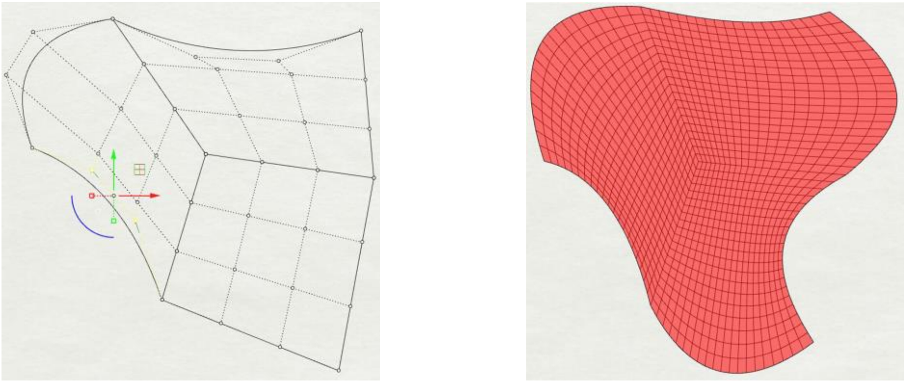

(a) (b)

**Figure 3:** (a) Correction of the initial form with control points, and **(b)** Conversion of the obtained area into Mesh

By doubling the curves, three new concave curves are generated which have a role of supports. Also, three other convex curves represent heights in the process of forming the pavilion. (Figure 4a) All the forces that act on this structure are precisely calculated using the tools from the Kangaroo addon. After correctly entering data into the solver tool from the same addon, a new mesh form is generated according to the given parameters that can be modified until the desired appearance of the future structure is obtained. (Figure 4b).

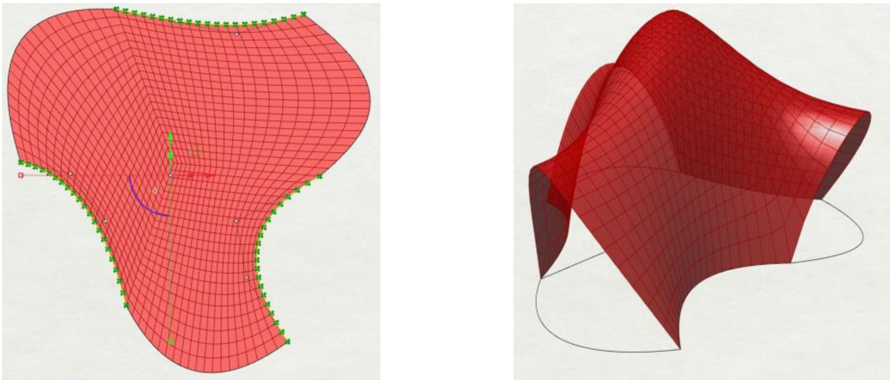

(a) (b)

**Figure 4:** (a) Forming the 3D structure of the pavilion, and **(b)** Selection of supports and heights:

The next step in generating a pavilion is to randomly place points on the Mesh whose number is directly conditioned by the radius selected in the SphereCollide function used to obtain a cleaner and more uniform structure. (Figure 5a) By correcting the parameters used to form the newly formed structure, optimized points are obtained and distributed. It should be emphasized that the points on the extreme curves (supports and heights) have the greatest value in this optimization, which is the essence of this step. (Figure 5b).

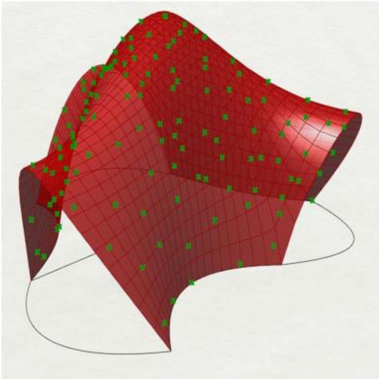
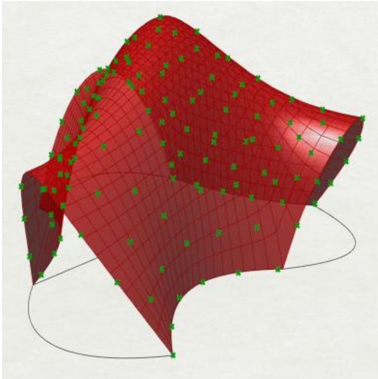

(a) (b)

**Figure 5:** (a) Adding points to the mesh, and **(b)** Optimization of points

The formation of a grid is obtained by using the tool 3DVoronoi where, based on the formed mixture, a set of cells is obtained, conditioned by the set parameters. To make the newly created set of cells more uniform, and at the same time the shape of the pavilion cleaner and more harmonious, the tool for SphereCollide is used again. (Figure 6a) This step seeks to solve the problem of previous research stages that occur at the junctions of several different cells. Two points that are too close to each other have to either move away or merge. Some of the solutions are to use the Magnetic Snap command, which does not give good results because it forms irregular/deformed cells, in this case. After reusing the SphereCollide tool, uniform and cleaner cells are obtained together with connectors with the required number of points. (Figure 6b).


(a) (b)

**Figure 6:** (a) Formation of a set of Voronoi cells, and **(b)** Optimization of Voronoi structure:

The position of the cells that make up the structure of the pavilion was generated using Voronoi cells on the surface of the newly formed structure. After that, they were modified into evolving curved surfaces by using the Fillet option which creates filleted angles. Each cell needs to be assigned the dimensions for the material of the structure. For this research, MDF 3 mm thick and 10 cm wide was selected. The position of maximum stresses during bending was tested, wherein this way the wood was "weakened" using the Kerf method with the help of a previously prepared algorithm. To connect cells, each contains a flat part that is an interconnection.

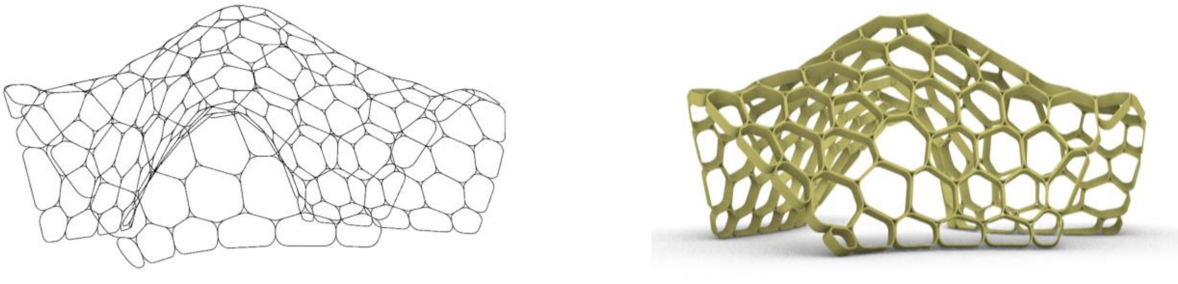

(a) (b)

**Figure 7:** (a) Structure formed from filleted Voronoi cells, and (b) Pavilion with final dimensions

The pattern that was used for the fabrication of evolving boards was designed by Aaron Porterfield and consists of horizontal parallel lines, which present discontinuity at two or three points. As Kalama said in their paper (Kalama et al., 2021), this pattern is the most common pattern that has been applied to structures that use this bending method. It is observed that the specimen reaches a high degree of curvature and strength. Therefore, by optimizing gaps and distance between dashes, several different boards were fabricated and tested to find the most adequate pattern settings in terms of bending and strength. (Figure 8).

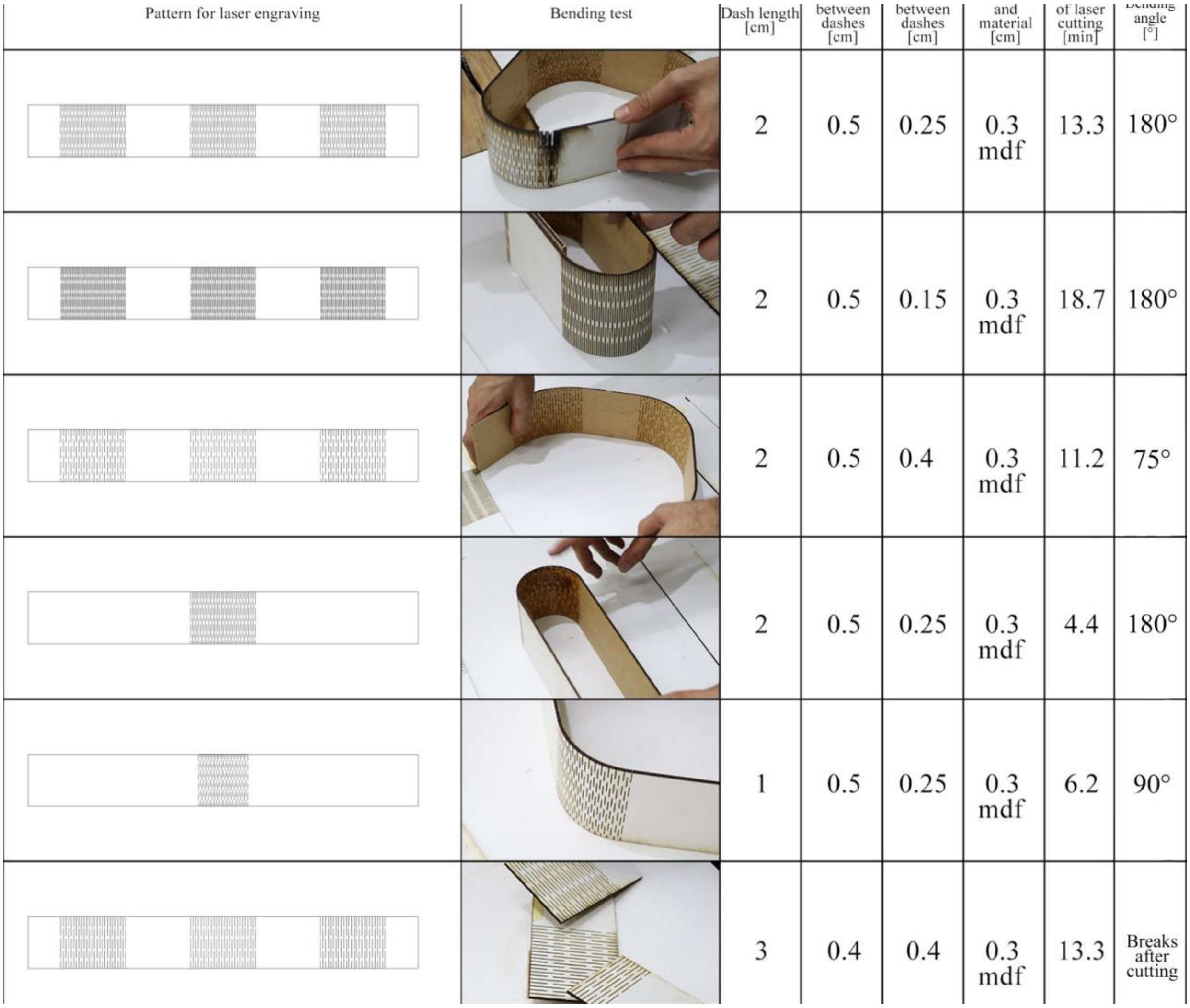

| Pattern for laser engraving | Bending test | Dash length [cm] | between dashes [cm] | between dashes [cm] | and material [cm] | of laser cutting [min] | angle [°] |
|---|---|---|---|---|---|---|---|
| | | 2 | 0.5 | 0.25 | 0.3 mdf | 13.3 | 180° |
| | | 2 | 0.5 | 0.15 | 0.3 mdf | 18.7 | 180° |
| | | 2 | 0.5 | 0.4 | 0.3 mdf | 11.2 | 75° |
| | | 2 | 0.5 | 0.25 | 0.3 mdf | 4.4 | 180° |
| | | 1 | 0.5 | 0.25 | 0.3 mdf | 6.2 | 90° |
| | | 3 | 0.4 | 0.4 | 0.3 mdf | 13.3 | Breaks after cutting |

**Figure 8:** Table with a comparison of patterns with different settings

## 3. RESULTS

The bending of the fabricated boards gave satisfying results and as boards did successfully bend to the desired shape without breaking apart. Unlike the bending, boards were not expected to be as flexible and limber as supposed. After the fabrication of each successive board, the problem was keeping them together and stable, which was not possible without additional clamps, bolts, or screws. Therefore, panels that were previously cut in the cell's required shape were added inside the evolving boards to shape them and keep them stable and strong. By using a small metal board and four screws, two sides of the board were connected as well as two boards by putting them next to each other. The combination of panels inside and connecting metal panels with screws gives the future panels the desired strength and shape.

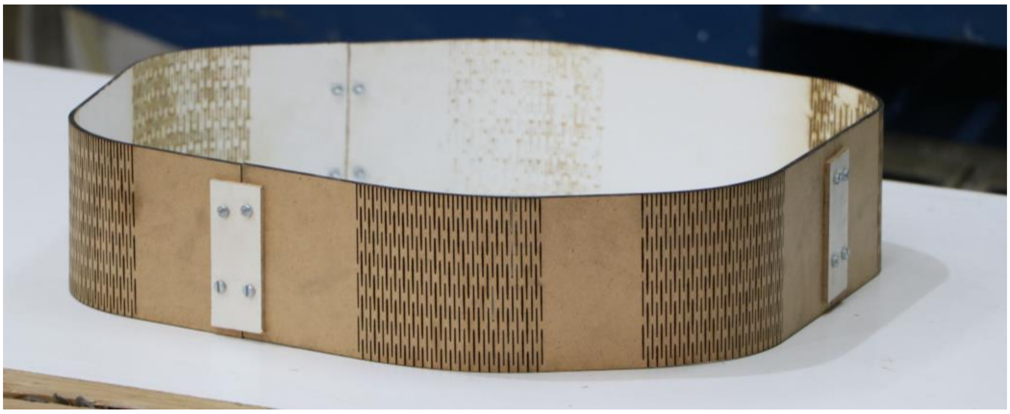

**Figure 9:** Fabricated cell

**Figure 10:** Visualisation of the pavilion

## 4. CONCLUSION

The implementation of parametric design can contribute to the very rapid creation of pavilion forms that mimic curved objects. It has been found that if the spacing between gaps is wider, then the surface bends less. If the distance is smaller, then it bends more. It is best to use some universal relationship that is reached empirically. The best solution obtained based on tests is shown in Figure 8 under the first position. To preserve the shape of the cell due to the pressure of others, it cannot carry itself and it is necessary to insert a plate inside it to make it tenser.

Engraving wooden surfaces which weaken those wooden elements in some spots does lead to natural wooden bending but on the other hand, does make those constructional elements fragile and can lead to the collision of the structure. Therefore, by generating this algorithm that provides a concrete solution with an exact formula for weakening specific parts of wood by laser, it is possible to keep the strength of wooden elements as well as provide the necessary bend to a certain angle. Kerf bending is one of the quickest and easiest ways to form stable, strong, and self-sustainable structures from bent wooden boards. The next step would be fabricating a real-life model of the pavilion.

**REFERENCES**

1. Gillkvist, O., Henriksson, V., Poulsen, E., 2016. Digital Wood - Design & fabrication of a full-scale exhibition structure in plywood [WWW Document]. Issuu. URL https://issuu.com/v.henriksson/docs/digitalwood (accessed 10.20.19).

2. Mitov, D., Tepavčević, B., Stojaković, V., Bajšanski, I., 2019. Kerf Bending Strategy for Thick Planar Sheet Materials. Nexus Netw J 21, 149–160.

3. Kalama, A. M., Tzoni, D., & Symeonidou, I. (2021). Kerf Bending: A Genealogy Of Cutting Patterns For Single And Double Curvature. International Conference moNGeometrija, focused on the research about geometry, graphics, and application to science, engineering, and art, Belgrade, Serbia. URL https://www.researchgate.net/publication/345391743

4. Peck, E. C. (1957). Bending solid wood to form: Vol. No. 125 (Agriculture Handbook ed.). U.S. Department of Agriculture. https://www.fpl.fs.fed.us/documnts/usda/ah125.pdf

5. S. (2021, May 10). How to Bend Wood [Best Methods]. Start Woodworking Now. https://startwoodworkingnow.com/how-to-bend-wood/

6. A Dimitar. (2014). COMPARATIVE ANALYSIS OF METHODS FOR PLASTIFICATION OF SOLID WOOD. Journal of International Scientific Publications: Materials, Methods, and Technologies. Volume 8.

7. Aaron Porterfield. (2017, September 29). Curved Kerf Bending Part 2. Instructables. https://www.instructables.com/Curved-Kerf-Bending-Part-2/

8. Harding, J., Pearson, W., Lewis, H., and Melville, S., 2015. The ongreening pavilion. In Advances in architectural geometry 2014 (pp. 295-308). Springer, Cham.

9. Harris, R., Haskins, S., and Roynon, J., 2008. The Savill Garden gridshell: design and construction. The Structural Engineer, 86(17), pp.27-34.

10. Vucic, M., Tepavcevic, B., Stojakovic, V., Jovanovic, M., Mitov, D. and Bajšanski, I., 2018. Topology design of form- active gridshell structures.

11 .Naicu, D., Harris, R. and Williams, C., 2014, August. Timber gridshells: Design methods and their application to a temporary pavilion. In World Conference on Timber Engineering (pp. 10-14).

12 Larsen, O.P., 2014. Reciprocal frame (RF) structures: real and exploratory. Nexus Network Journal, 16(1), pp.119-134.

13 Dörstelmann, M., Knippers, J., Koslowski, V., Menges, A., Prado, M., Schieber, G. and Vasey, L., 2015. ICD/ITKE research pavilion 2014–15: Fibre placement on a pneumatic body based on a water spider web. Architectural Design, 85(5), pp.60-65.

14 Knippers, J., La Magna, R., Menges, A., Reichert, S., Schwinn, T. and Waimer, F., 2015. ICD/ITKE research pavilion 2012: coreless filament winding based on the morphological principles of an arthropod exoskeleton. Architectural Design, 85(5), pp.48-53.

15 Pizzigoni, A., Micheletti, A., Ruscica, G., Paris, V., Bertino, S., Mariani, M., Trianni, V. and Madaschi, S., 2019, October. A new T4 configuration for a deployable tensegrity pavilion. In Proceedings of IASS Annual Symposia (Vol. 2019, No. 9, pp. 1-6). International Association for Shell and Spatial Structures (IASS).

# RATIONALIZATION OF CYLINDERS AND CYLINDROIDS ON THE FRANK GEHRY OBJECT - CASE STUDY WALT DISNEY CONCERT HALL

N. Kocić[1*], M. Nikolić[2], S. Krasić[1], J. Stanković[1]

[1]University of Niš, Faculty of Civil Engineering and Architecture, Department of Visual Communications, 18000 Niš, Serbia

[2]University of Niš, Faculty of Civil Engineering and Architecture, Department of Public Buildings, 18000 Niš, Serbia

nadja93.al@hotmail.com

***ABSTRACT***

*The development of technology enables the construction and design of various shapes and forms of buildings. Among the most attractive objects today, the most common is the use of curved surfaces that highlight the shape of the object itself, while the function can be solved later. That idea was applied on the buildings of American-Canadian architect Frank O. Gehry. Timeless and unique, Gehry made sure that his architectural expression was not easy to imitate. From curved surfaces, he most often uses cylinders and cylindroids for his objects. Cylindroids are very attractive twisted, ruled surfaces with one system of generatrices and their application in architecture was in expansion at the end of the 20th century.*

*Many of Frank Gehry's buildings have cylindroids for basic form, but that does not exclude the combination with prismatic shapes. In some examples, cylindroids are used only for wall canvases, and in some cases both for wall canvases and roof surfaces. Subject of geometry analysis in this paper will be discretizing and rationalizing these geometries into smaller, prefabricated parts on the example of Walt Disney Concert Hall in Los Angeles. This would make these complex surfaces easier to perform, and thus contribute a greater application in architecture.*

**Keywords:** cylindroids, geometric surfaces, discretizing, rationalizing, Frank Gehry

## 1. INTRODUCTION

The twentieth century brought with it a wave of application of free forms and structures of high geometric complexity [1] Post-modern architecture has seen different types of architectural styles and movements, including the deconstructivism movement. Frank Gehry uses curved forms on his objects and is a representative of deconstructivism [2] Through his works, from Gehry's residence to present day buildings, his fascination with chaotic masses can be seen. This brings him to the forefront of the deconstructivist movement in "no rules architecture" [3].

Although nowadays the creation of digital models of complex structures is somewhat simple, their fabrication and construction are still a challenge. In recent years, architects are increasingly using mathematical theories and concepts to characterize architectural products, but also as methods in planning [4].

Geometry can be seen as a bridge between mathematics, abstract science and architecture, concrete art [2] Geometric configurations are applied to the design of surfaces, shapes and spaces that strive to achieve beauty using materials and manufacturing methods [17] The complex architectural design and application of digital three-dimensional modeling emphasizes the role of geometry in current architecture. Therefore, the rationalization of geometric form plays a crucial role in modern advanced practice. It translates irregular, sculptural architectural forms into constructs that can be built [5].

One of the motivations for rationalization efforts is primarily the cost of the project and the time required for construction [6] In this paper, architectural rationalization is applied to Frank Gehry’s Walt Disney Concert Hall, a building whose façade planes are constructed of developable and double curved surfaces. The Walt Disney Concert Hall encountered a number of different problems during construction, including a sharp rise in construction prices from what was originally expected, as a result of Gehry’s complicated design [3] This paper aims to simplify the shape of the structure by discretization, while retaining the visual effect. It focuses on the method of geometric rationalization of curved surfaces by planarization.

## 2. RATIONALIZATION OF CURVED SURFACES

Construction activities remain subject to economic constraints. Accordingly, the rationalization criteria include a reduction in the number of different types of building elements for serial production, and a reduction in the cost of building and assembling the elements (time and material required). During the design process, it must be determined which criteria are relevant and what their relative priority is. For example, rationalization to reduce material waste can be abandoned in favor of rationalization for logistics and construction order, or a reduction in the number of different elements can be discarded in favor of a smoothly curved overall shape. Although the priorities among the rationalization criteria are largely determined by economic and time considerations, they were also chosen in accordance with their ability to support the building of innovation [5] Rationalization for the purpose of construction can be seen on the example of the Sydney Opera House (1957-73). The building was designed before the advent of digital geometric modeling, and has therefore undergone significant design changes. The parabolic geometry of the shell has been replaced by spherical elements. With the same radius, the shells could be divided into individual elements, pre-manufactured and mounted on site. With the advent of digital modeling of curved surfaces, such limitations have been reduced, but still exist [6].

Frank Gehry's objects are characterized by complex, curved forms, volumes captured at the moment of movement. The search for breaking down the barriers between art and architecture, going beyond the grid and experimenting with zoomorphic shapes are also visible in the project of the Concert Hall in Los Angeles. Both pre-rationalization and post-rationalization were used for the Walt Disney Concert Hall. Gary limited the surfaces he applied to the surfaces that could be developed, which guaranteed the load-bearing capacity of the sheet metal cladding. The results were later streamlined into systems that could be built [2].

Gehry used developable surfaces-cylinders and double-curved cylindroids for the facade metal elements of the hall. Single-curved or developable surfaces can be unfolded into a plane without stretching, cutting or wrinkling the material [7] This makes them easy to cover with metal planes. These surfaces contain straight lines, along which each has a constant tangent plane, which in turn has the advantage of making a substructure [1].

More recently, the free Grasshopper plugin for the Rhinoceros software offers the ability to model complex geometric shapes. This approach to geometric modeling is gaining momentum, especially in architectural education [5] In Grasshopper, a method can be applied to approximate the initial shape of a curved surface to obtain planar elements [8].

## 3. CASE STUDY - WALT DISNEY CONCERT HALL

It can be said that the "deconstructivist" architectural style requires a complete architectural education in order to evaluate the philosophy behind it [9] Frank Gehry was one of the first architects to incorporate surfaces of complex geometric shapes into his projects, such as the Guggenheim Museum in Bilbao (1991-1997) (Figure 1), the Museum of Pop Culture in Seattle (1999-2000) and Walt Disney Concert Hall in Los Angeles (1989-2003), and thus encourage research into architectural geometry [1] Going beyond the usual ways of designing and using materials, Gehry's works change the way architecture is experienced [3] The case study used is Frank Gary’s Walt Disney Concert Hall, which was built from 1999 to 2003. (Figure 1). The method was performed in the Rhinoceros software with the Grasshopper plug in. Using the method, we present the rationalization of the architectural geometry of the building. This method is defined using geometric discretization by planarization of a double-curved cylindroid shape. The optimization method allows objects to be built from simplified planar elements, but while maintaining the visual features of the object, and facilitates the process of construction and fabrication of prefabricated elements [10].


**Figure 1:** Walt Disney Concert Hall (source: https://www.laphil.com/)

### 3.1. Modelling in Rhinoceros

The geometry of the building is defined in the Rhinoceros. This software has options that allow you to easily get developable and double curved surfaces [8] The building has single-curved developable surfaces-parts of cylinders and double-curved surfaces-parts of cylindroids. They are shown in Figure 2 in different colors and marked with numbers in order to recognize them during the rationalization process. The cylinders are shown in red color and 5 of them are set aside for planarization. The cylindroids are shown in blue color and 6 of them are selected.

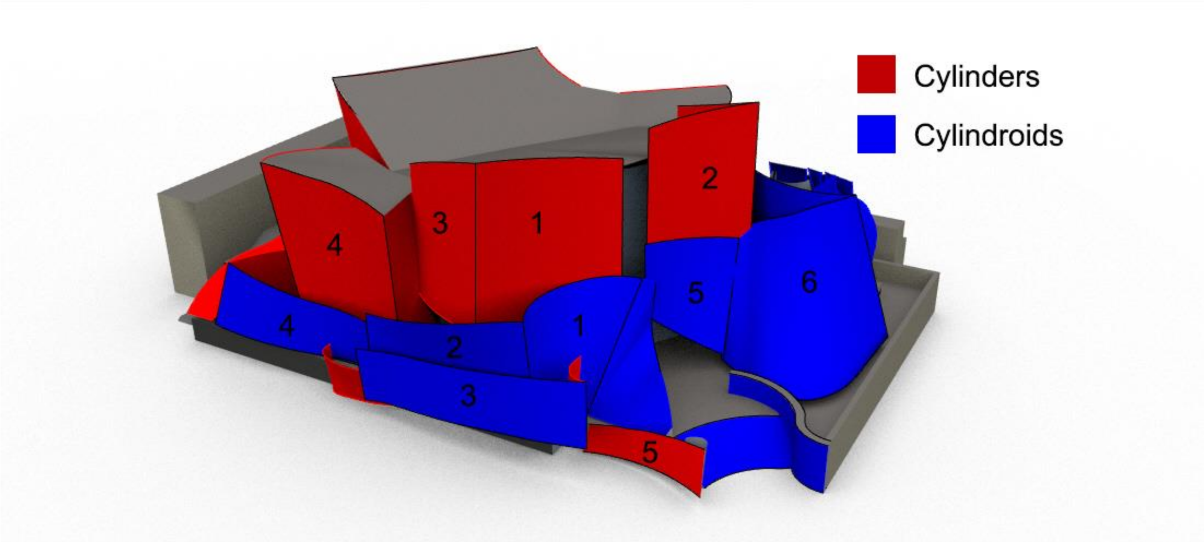


**Figure 2:** Model of an object with marked surfaces; cylinders are marked in red, and cylindroids in blue (source: author's team N. Kocić et al.)

### 3.2. Optimization With Grasshopper

In Grasshopper, the planarization of curved surfaces was performed and the structure of planar elements was obtained (Figure 3). This optimization of geometry is shown on the example of cylinder number 1 and cylindroid number 6.

The curved surfaces in the Grasshopper are discretized by planarization, where the number of divisions in both directions (U and V) can be easily changed and the most suitable solution can be chosen. On the given example of the cylinder, the division into 19 parts in the V direction was choosen in order to maintain the similarity between the curve and the polygonal line and the initial visual effect. Then, the division in the U direction into 9 parts was chosen (Figure 4). On the example of a cylindroid, the division into 15 parts in the V direction and 9 parts in the U direction was choosen (Figure 5). The resulting surfaces consist of planar elements of quadrangular shape.

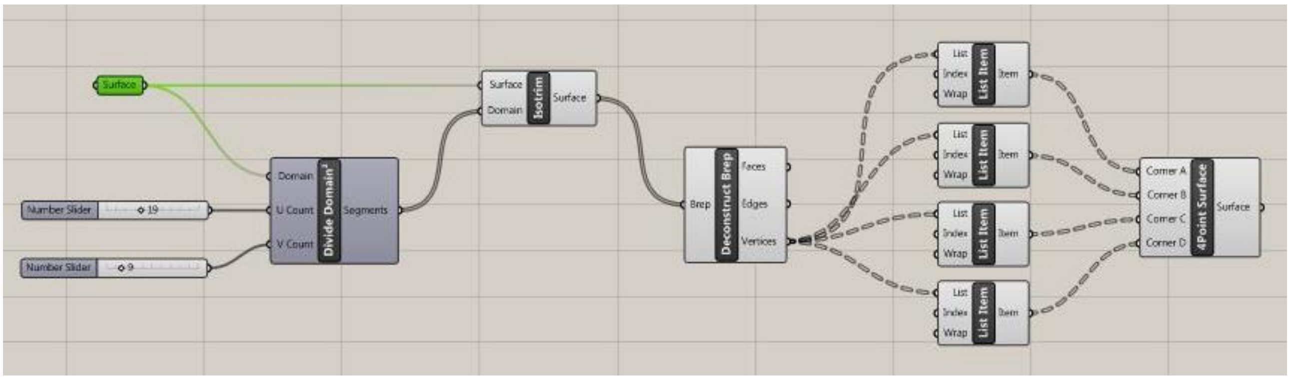


**Figure 5:** Scheme in Grasshopper (SOURCE: AUTHOR'S TEAM N. KOCIĆ ET AL.)

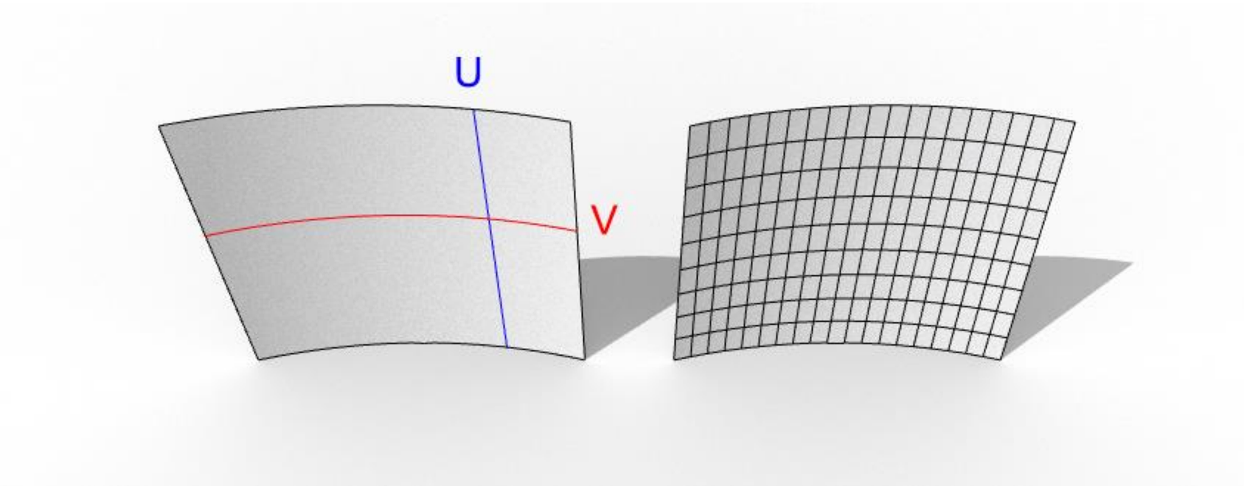


**Figure 3:** CYLINDER SURFACE DIVIDED INTO PLANAR ELEMENTS IN U AND V DIRECTION (SOURCE: AUTHOR'S TEAM N. KOCIĆ ET AL.)

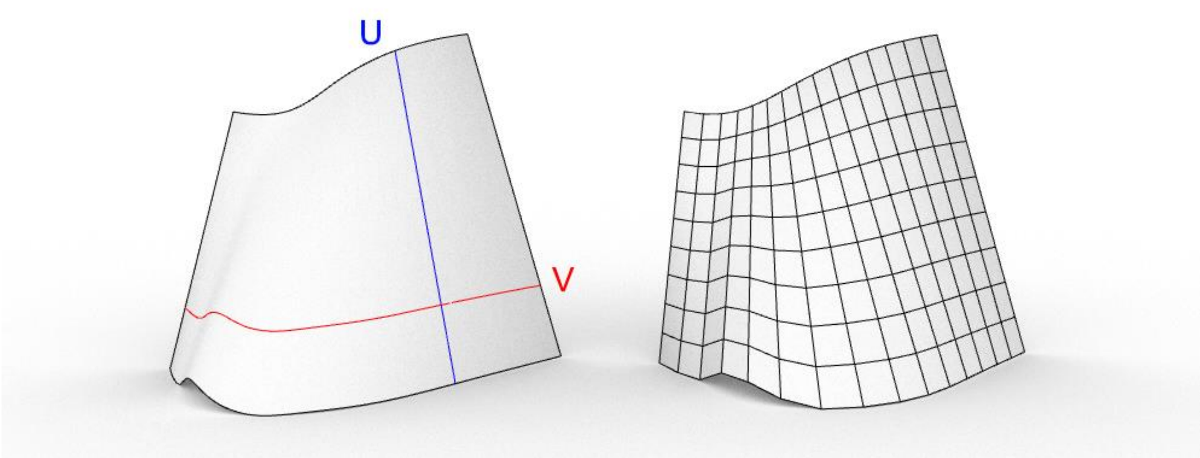


**Figure 4:** CYLINDROID SURFACE DIVIDED INTO PLANAR ELEMENTS IN U AND V DIRECTION (SOURCE: AUTHOR'S TEAM N. KOCIĆ ET AL.)

The procedure was repeated for the other selected cylinders and cylindroids on the front facade of the building. They are shown in Figure 5. The number of divisions in the U and V directions for each surface is shown in Table 1.

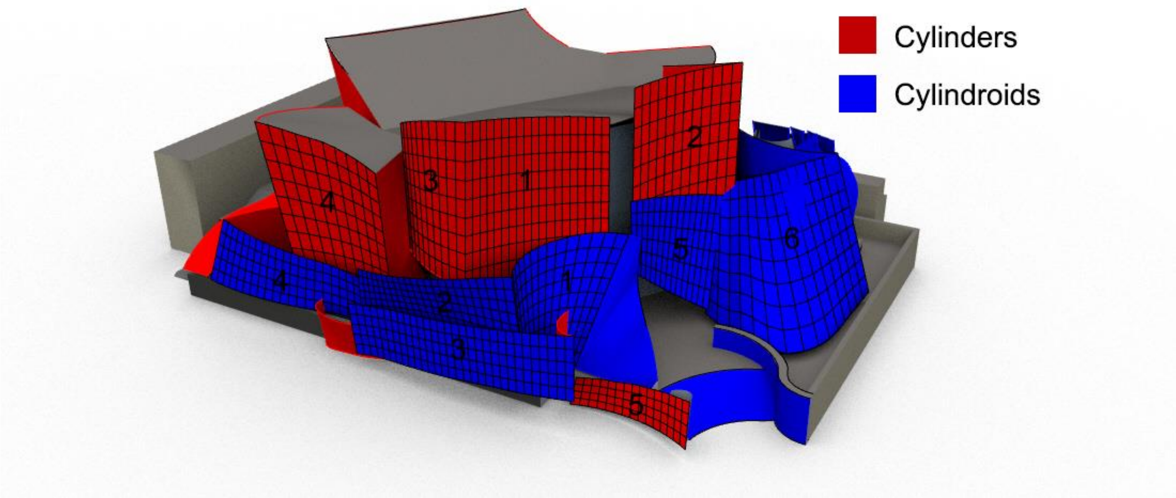


**Figure 6:** Appearance of the building with planarized surfaces (source: author's team N. Kocić et al.)

| CYLINDERS | | |
|---|---|---|
| Number of surface | division in U direction | division in V direction |
| 1 | 9 | 19 |
| 2 | 9 | 12 |
| 3 | 9 | 10 |
| 4 | 9 | 10 |
| 5 | 4 | 15 |
| CYLINDROIDS | | |
| Number of surface | division in U direction | division in V direction |
| 1 | 9 | 14 |
| 2 | 9 | 23 |
| 3 | 5 | 30 |
| 4 | 5 | 10 |
| 5 | 6 | 15 |
| 6 | 9 | 15 |

**TABLE. 1:** Division of surfaces in U and V direction for selected cylinders and cylindroids (source: author's team N. Kocić et al.)

When selecting the number of divisions in both directions, the division into different numbers of elements was tested. The division given in the tables was chosen as the most optimal with the smallest deviations from the initial curvature of surfaces.

The obtained elements enable the construction of the building from various materials, including concrete, which was the original intention of the Walt Disney Concert Hall building. The division into triangular elements can also be choosen, where the third system of lines would be the diagonals of quadrilateral elements.

## 4. CONCLUSION

In addition to digital evolution, the use of geometry enables the design and construction of the most complex architectural forms. The application of mathematical theories greatly contributes to this. Rationalization of complex structures implies their simplification, while reducing the time frame and construction costs. Besides that, the rationalization of geometry provides opportunities to bridge the gap between architectural and engineering practices. Simplification of elements and their prefabrication facilitate the process of building complex structures. When choosing the shape and number of elements, it is important that in addition to the constructive, they also meet the visual criteria.

The method of geometric optimization helps to define the shape and dimensions of the elements, and provides opportunities for the analysis of their constructive features. This paper presents a case study, using the Walt Disney Concert Hall as an example of an object of complex geometry.

Frank Gehry has produced a large number of buildings with the support of the CATIA software. Nevertheless, their performance was not at all simple, and relied heavily on the skills of the masters builders who performed the works. Therefore, different solutions can be explored and the principle of geometric rationalization applied. The method described in this paper offers a solution for different shape and size of planar elements, which are used for the curved shape of the object. For application of different materials, using a different type of rationalization than the one used in the design of this building, which would greatly facilitate the construction process. That is why rationalisation is important, not only for existing buildings, but also for new architectural projects and for education on architecture academic courses. For the selected surfaces the number of elements was choosen in order to keep the shape with minimum deviation from the original curvature of surface.

After analyzing the geometry, optimizing and determining the shape and number of elements, the next step is the digitization of the construction project.

## REFERENCES


1. Pottmann, H. Architectural Geometry and Fabrication-Aware Design. Nexus Netw J 15, 195–208 (2013).

2. Srinivasan, Urmila (2009). Approaches to the Use of Geometry in Architecture: A study of the works of Andrea Palladio, Frank Lloyd Wright, and Frank Gehry. Master's thesis, Texas A&M University

3. Osman, Y. (2001). The Use of Tools in the Creation of Form: Frank (L. Wright & O. Gehry). The Association for Computer Aided Design in Architecture, pp.44-51

4. İnceköse, Ü. (2007). Geometrical Transformation: A Method for the Creation of Form in Contemporary Architecture, pp.415-422

5. Fischer, T. (2012). Geometry Rationalization for Non-Standard Architecture. ARCHITECTURE SCIENCE, No. 5, pp.25

6. Shelden, Dennis. (2005). Digital surface representation and the constructibility of Gehry's architecture. Thesis (Ph. D.), Massachusetts Institute of Technology, Dept. of Architecture

7. Krasic, S. (2012). Geometrijske površi u arhitekturi, Građevinsko-arhitektonski fakultet, Niš

8. Kocić N., Krasić S., Tošić Z., Stanković J.: Applying of Grasshopper in Geometry Optimization of Torus Shell, Proceedings International scientific conference on Geometry and Graphics, MoNGeometrija 2020, Belgrade 2020, pp. 621-626

9. Hegzi, Y.S. and Abdel-Fatah, N.A. (2018). Quantifying students' perception for deconstruction architecture. Ain Shams Engineering Journal, 9(4), pp.2745-2754

10. Tošić, Z. et al. (2019). Geometry and Construction Optimization: An example using Felix Candela's Church of St. Joseph the Craftsman in Mexico. Nexus Netw J 21, 91–107

# SPATIAL CONFIGURATIONS OF FLOATING SETTLEMENTS – PARAMETRIC METHOD

J. Stanković[1*], S. Krasić[1], M. Nikolić[2], N. Kocić[1]

[1]University of Niš, Faculty of Civil Engineering and Architecture, Department of Visual Communications, 18000 Niš, Serbia

[2]University of Niš, Faculty of Civil Engineering and Architecture, Department of Public Buildings, 18000 Niš, Serbia

jovana__stankovic@hotmail.com

***ABSTRACT***

*The beginning of the 21st century brings with it a lot of problems for the urban atoll islands as a consequence of climate change. Many research studies have shown that these problems can be solved by building on the water, i.e. applying floating architecture: very large floating structures and modular floating structures. In this way, new settlements can be built on the water surface. The approach to designing floating structures and settlements brings with it new principles that need to be adhered to because building on the water surface and land is not the same. Methods of parametric design can help in this process, whereby it is necessary to take into account terms of stability, the purpose of the building, properties of locations and sustainable design.*

*Spatial configurations of floating settlements for urban atoll islands are the topic of the research in this paper. By studying the characteristics of urban atoll islands, floating structures and parametric design, geometric parameters, conditions and constraints of floating settlement can be defined in parametric design software and then incorporated into existing floating settlement configurations. The aim is to find out which spatial configuration is suitable for these islands according to its advantages and disadvantages in terms of physical and architectural comfort, i.e. implementation of all geometric parameters in the parametric design process.*

**Keywords:** floating structures; floating settlements; parametric design; spatial configuration; urban atoll islands

## 1. INTRODUCTION

The modern world is facing the problems of the consequences of climate change (El-Shihy & Ezquiaga, 2019; Moon, 2011). The trend of rising temperatures, the number of warm days, the amount of annual, seasonal and extreme precipitation, erosion of coral reefs, increasing acidity of the oceans, etc., directly affects island and coastal areas by increasing sea levels in the form of localized floods to the full immersion predicted in the next few decades. According to Oppenheimer et al. (2019), these areas can be divided into resource-rich coastal cities, urban atoll islands, large tropical agricultural deltas and arctic communities. Urban atoll islands are particularly vulnerable due to low altitude (<4 m above mean sea level, <1.8 m in elevation), mainly composed of reef-derived unconsolidated material, small land areas and exposure to extreme weather and climate change. The consequences are coastal and land erosion, salinization, loss of homes, crops and drinking water, migration and various diseases. This situation imposes a new term ‘refugees due to climate change’ (Balesh, 2015). Countries that are facing this problem are the Maldives in the Indian Ocean, Marshall, Tuvalu, the Kiribati islands in the Pacific Ocean, etc.

Researchers around the world try to offer solutions through the disciplines of architecture and civil engineering, considering the limiting parameters and new possibilities for critical design thinking as well as environmental, economic, living, socio-cultural and social and geopolitical factors (Moosa et al., 2020). According to Moosa et al. (2020), three key strategies are defense, isolation or relocation of affected people. Defense techniques are also largely unsustainable, so according to El-Shihy & Ezquiaga (2019), relocation to an artificial island is imposed as a solution with moderate to high financial resources, high durability and lifespan, moderate to longer construction time, positive impact on the environment and with the highest performance of 72.5%.

This problem can be solved by floating architecture, i.e. by building structures, settlements and entire cities on the water. The approach to designing such architectural structures brings with it new principles that need to be adhered to because building on water and land is not the same. Today, parametric design is increasingly used in the world due to its advantages in the process of designing any type of building. In a previous paper, the author team Stanković et al. (2021) concluded that the principles of parametric design and regular tessellation can be used to quickly and economically design a sustainable floating settlement for Kiribati residents, as a representative of the urban atoll islands, with the hexagon proving to be an adequate form of the basis of a floating housing and public purpose module, because of maximum area and minimum perimeter. By multiplication of these modules according to certain parameters and constraints/conditions of physical and architectural comfort (Stupar, 2017), a floating house for a family of four (as the average minimum of household members on the atolls of this island) can be created, and then a sustainable floating settlement with 12 houses for about 50 inhabitants. At the end of the paper, the authors point out that in the case of family expansion, it is possible to add an appropriate housing module to the existing floating house. The question is whether this module will be suitable for a larger number of household members within the defined spatial configuration of the floating settlement or it must be changed.

The aim of this research is the application of parametric design, i.e. set parameters and constraints in the design and thus define an algorithm/scheme/spatial configuration by which a floating settlement can be designed as an alternative to urban atoll islands.

## 2. LITERATURE REVIEW

Before defining the research methodology, it is necessary to investigate the characteristics of urban atoll islands, floating structures and parametric design and, finally, to connect them with the subject of research.

### 2.1. Characteristics of Urban Atoll Islands

Urban atoll islands are the Maldives in the Indian Ocean, Marshall, Tuvalu, Kiribati islands in the Pacific Ocean, etc. Their common characteristics are (National Statistics Office of Ministry of Finance in Bairiki, 2015; Secretariat of the Pacific Community, 2012; National Bureau of Statistics of Ministry of Finance and Treasury in Male, 2014; Central Statistics Division (CSD) of the Government of Tuvalu, 2012):

**Nature:** Low altitude (<4 m above mean sea level, <1.8 m in elevation), mainly composed of reef-derived unconsolidated material, small land area and exposure to extreme weather and climate change (Oppenheimer et al., 2019);

**Man-made environment:** The problem of drinking water supply to the population and agricultural crops; damaged critical infrastructure;

**Culture, society and demography:** High population density (147 inhabitants/km$^2$ in Kiribati - 1812 inhabitants/km$^2$ in the Maldives; the average number of household members (6 in the Maldives, Kiribati, Tuvalu - 7 in Marshall islands); fishing and local crops are a primary food resource for almost every household;

**Economy:** Tourism, agriculture, fishing, shellfish farming, seafood collection;

**Technical and technological development:** Brick, wood, sheet metal, local materials, etc.

### 2.2. Floating Structures

The term ‘aquatecture’ refers to the architecture associated with the element of water. It implies awareness of the architectural qualities that water can provide, as well as respect for the element of water in its architectural context (Wylson, 1986). Taking into account a different approach to architectural design, mobility and spatial relationship to water, Piatek (2016) points out that floating structures are buoyant, movable, partly submerged structures, kept in place by a variety of systems such as mooring or stopping piles, anchors, and mooring lines; they include structures of different functions, applications, and sizes, comprising a singular unit or multiple interconnected floating units; depending on the number of units and their dimensions, they can form very large floating structures (VLFS) - artificial floating islands: floating breakwaters, bridges, airports, storage or military facilities, wind and solar power plants, parks, mobile offshore structures, floating cities and living complexes (Wang and Tay, 2011) or small floating structures (Adnan, 2020) – (floating houses, etc.).

In recent years, studies of floating structures have attracted architects and urban planners, as well as civil engineers, and have emerged as an effective solution to the challenges of sea-level rise (El-Shihy & Ezquiaga, 2019; Danilescu, 2020; Endangsih, 2020). With the advancement of floating technologies, floating houses become energy-efficient, sustainable, ecological and independent, because they have systems of all installations necessary for the self-sufficiency of a household based on the use of renewable energy sources. The characteristics of floating houses are (Moon, 2011; Moon, 2015; Danilescu, 2020; El-Shihy & Ezquiaga, 2019):

- resilience to the effects of climate change (rising sea levels, floods, etc.) thanks to a single floating system;
- modernization of the vulnerable population of the coastal area and island countries;
- encouraging ecotourism;
- contribution to the health of the population and visitors thanks to the natural environment;
- mobility, i.e. possibility to move from one location to another;
- conservation of the marine/river/ocean ecosystem;
- without negative impact on the port, tides and sea waves;
- the possibility of using recycled, local and natural materials;
- use of renewable energy sources (sun, water, wave, wind) for solar heating panels and solar photovoltaic cells, hydrothermal heating/cooling system, heat recovery system, water purification, desalination system, etc. and
- possibility of application of modular design and construction system.

The application of modularity in floating architecture has resulted in a new typology of objects called modular floating structures (MFS). Modular floating structures are a type of system of several floating structures assembled into a large group so that they can be described as a series of relatively small floating elements (Adnan, 2020). Therefore, if the floating house is identified with a small floating element, i.e. module, its multiplication can create a system of modular floating objects. The advantages of applying such a system of facilities are (El-Shihy & Ezquiaga, 2019; Lister & Muk-Pavic, 2015; Czapiewska et al. 2013; Adnan, 2020; Kizilova, 2019; Simovic et al., 2019):

- flexibility and convenience in disassembling/subtracting/adding an element/module from/in the structure/system;
- passive mobility (easy to move from location to location due to small module dimensions);
- the possibility of expanding the island area following urban needs and population growth;
- creation of ordered spatial configurations (system of modular floating objects);
- multifunctionality of modules (modules of all purposes - public, residential, commercial, etc.);
- integration of sustainable systems into the design and constructive system of modules leading to energy independence;
- the simplicity of current module maintenance (damage to one module does not affect other system modules)
- fast and economical construction of floating houses due to prefabrication of modules and
- flexibility in design (changing housing requirements, different use of the building, etc.).

Modular floating structures, as a type of aquatecture, represent an adequate way to solve the problem of the consequences of rising sea levels in urban atoll islands.

### 2.3. Floating Structures

According to Karle and Kelly (2011), parametric design is a way of connecting tangible and intangible systems into a conceptual solution and establishes a relationship between properties within the system. This type of design initiated a new way of thinking in the design process itself called parametric design thinking (PDT) (Oxman, 2017), which is associated with abstract, mathematical and algorithmic thinking. It refers to the understanding of parametric structures that can be formulated and presented as a generic parametric scheme. Therefore, parametric design is an approach that is symbolically based on parameters. It should be emphasized that the architect must include social, historical, environmental problems, functional and program requirements and psychological needs of users (Oxman and Gu, 2015; Zawidzki and Szklarski, 2020) in the parametric scheme, i.e. apply multi-objective optimization in order to form a quality architectural solutions. The characteristics of the parametric design process are (Oxman and Gu, 2015):

- architects design rules and define their logical relationships in creating models;
- architects can change and modify their design at any stage of design, because all procedures and activities are interconnected, which makes the design process open and flexible and
- alternative possibilities can be developed in parallel at any stage of design and this changes the way of thinking and contributes to research processes.

Floating settlements have become an alternative to future urban development due to the problem of rising sea levels. The design of such a settlement is complex because many requirements need to be considered at the same time. Therefore, parametric design methods can be very useful for solving these problems and creating the spatial configuration of floating settlements (Cubukcuoglu et al., 2016).

## 3. RESEARCH METHODOLOGY

This research has the following methodology:

**Stage 1: Defining the purpose of the area**

The average number of household members is 6, so it is necessary to design a floating house for a family of 6. The floating house must contain an entrance area, a kitchen and a bathroom, a living room and a dining room, a minimum of 3 bedrooms, a vegetable garden and shelter for animals.

Taking into account the public spaces, it is necessary to provide space for gathering people (2 $m^2$ per inhabitant), walkways and greenery. Note: The floating settlement must have a connection with the mainland due to other public facilities.

For each space for public and residential purposes, a prefabricated module of a regular hexagonal prism with an area of 10 $m^2$ will be used (Stanković et al., 2021).

**Stage 2: Floating house parameters in parametric design software**

Rhinoceros and Grasshopper software was chosen for the parametric design process.

**The first parameter** (Figure 1a) that is set is the central position of the auxiliary zone module, i.e. bathroom and kitchen, because then the maximum collection of rainwater is achieved, which is later purified and used in a floating house and for watering the vegetable garden. Therefore, **the second parameter** (Figure 1b) will be the position of the open spaces module-vegetable garden to the position of the auxiliary zone module due to the need to water the crops. **The third parameter** (Figure 1c) is the position of the open spaces module-vegetable garden to the position of the open spaces module-shelter for animals due to the related purpose of the space. The position of the other modules of the floating house is not conditioned by the parameters.

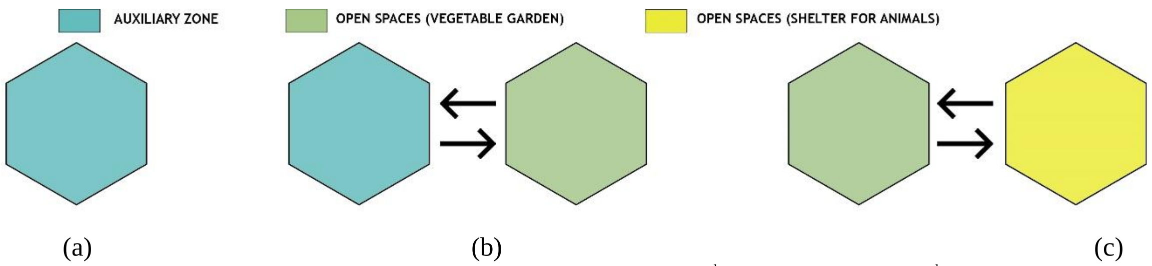


**Figure 1**: Floating house parameters: (a) The 1st parameter, (b) The 2nd parameter and (c) The 3rd parameter

**Stage 3: Setting conditions/constraints: The solution with the smallest perimeter of a floating house**

By evaluating a large number of possible combinations of floating houses, it is necessary to choose the solution with the smallest perimeter. There were 4 solutions with the same perimeter, but a solution in which all bedrooms have an exit to the common area was chosen (Figure 2).

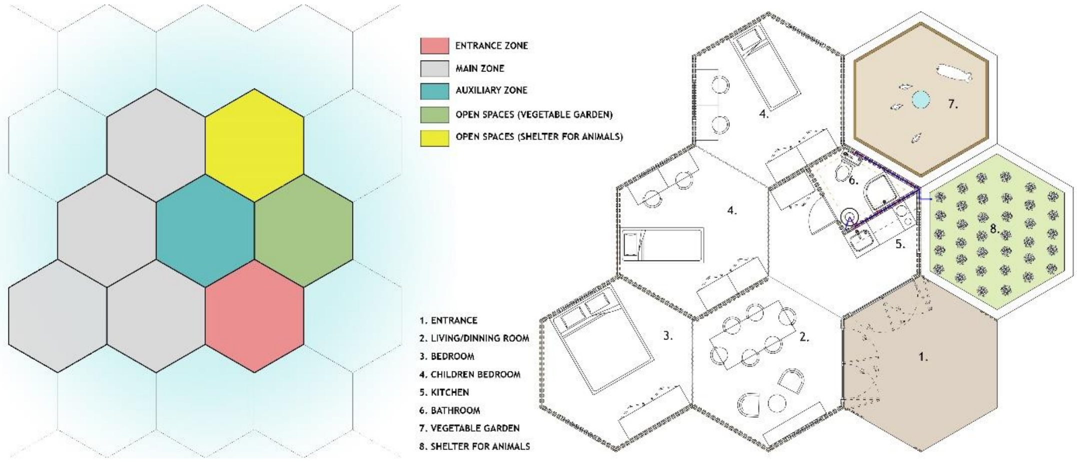


**Figure 2**: A floating house with the smallest perimeter

**Stage 4: Floating settlement configurations according to Czapiewska et al. (2013)**

According to Czapiewska et al. (2013), the system of floating houses can be created in the form of islands (Figure 3a), branch (Figure 3b), composite structure (Figure 3c) and single large structure (Figure 3d). The islands and branch configuration will be used for the floating settlement in question for about 100 inhabitants (16 houses). The islands spatial configuration is a scheme in which each floating house is located on one platform, where they are connected by walkways and other public areas, while in the branch spatial configuration several floating houses are located on one platform.

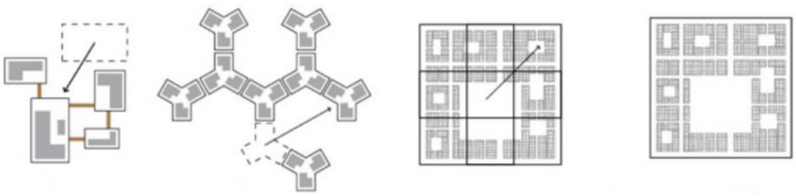

(a) (b) (c) (d)

**Figure 3**: Types of floating settlement configurations: (a) islands, (b) branch, (c) composite structure and (d) single large structure (Czapiewska et al., 2013)

**Stage 5: Floating settlement parameters in parametric design software**

Before the process of designing a floating settlement, it is necessary to set the parameters. **The first parameter** (Figure 4a) is the central position of the space for gathering residents because this space should be equally distant from all floating houses. **The second parameter** (Figure 4b) is to connect the floating houses with the space for gathering residents by walkways/greenery, whereby the walkways must make a connection via the module of the entrance zone of the floating house. **The third parameter** (Figure 4c) is the position of the animal shelter, as a module of the open spaces of the floating house, towards the open sea due to a possible unpleasant smell. **The last fourth parameter** (Figure 4d) is to omit at least one module between the floating houses and the public purpose module due to the realization of physical and architectural comfort.

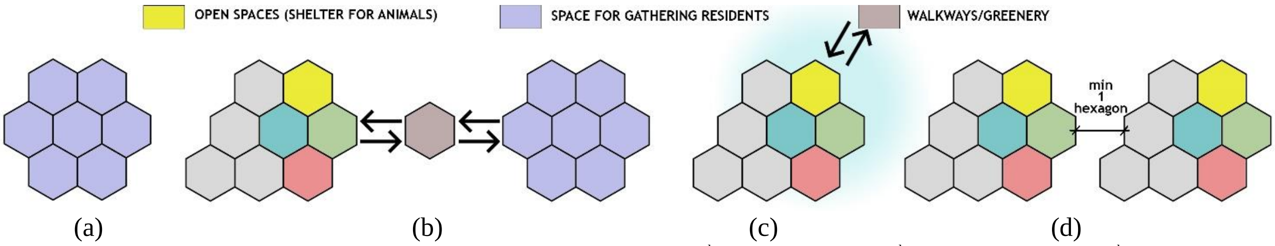


**Figure 4**: Floating settlement parameters: (a) The 1st parameter, (b) The 2nd parameter, (c) The 3rd parameter and (d) The 4th parameter

**Stage 6: Setting conditions/constraints: The solution with the smallest perimeter of a floating settlement - the islands spatial configuration**

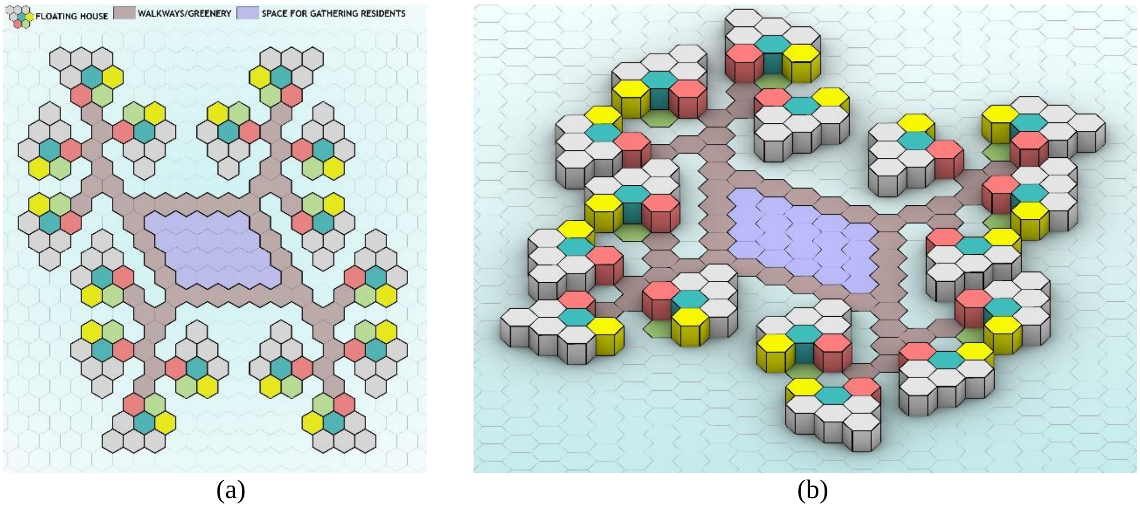


**Figure 5**: Floating settlement configuration islands: (a) 2D model and (b) 3D model

After selecting the islands spatial configuration, the process of designing a floating settlement for urban atoll islands is approached. The parameters can be used to create a spatial configuration on the water surface. By evaluating a number of combinations and setting the condition-solution with the smallest perimeter of the floating settlement, an adequate way of grouping modular floating houses with the smallest perimeter and modules of public purpose is chosen (Figure 5a, b).

**Stage 7: Setting conditions/constraints: The solution with the smallest perimeter of a floating settlement - the branch spatial configuration**

After selecting the branch spatial configuration, the process of designing a floating settlement for urban atoll islands is approached. The parameters can be used to create a spatial configuration on the water surface. By evaluating a number of combinations and setting the condition-solution with the smallest perimeter of the floating settlement, an adequate way of grouping modular floating houses with the smallest perimeter and modules of public purpose is chosen (Figure 6a, b).

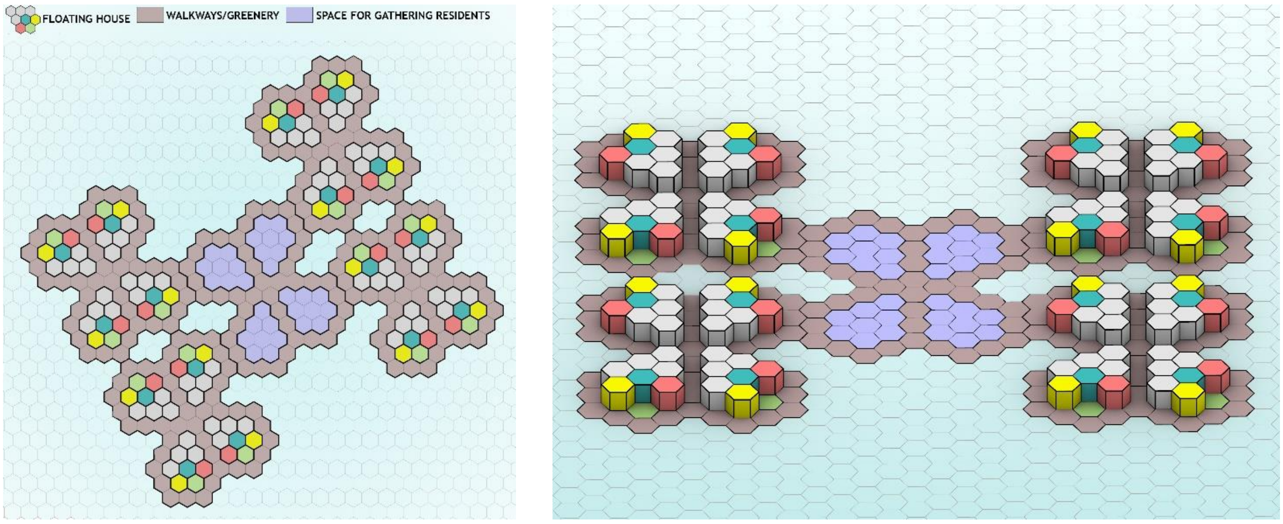


(a) (b)

**Figure 6**: Floating settlement configuration branch: (a) 2D model and (b) 3D model

## 4. RESULTS AND DISCUSSION

Based on the research results, the following can be concluded:

With the islands spatial configuration, all set parameters were respected and all types of comfort were achieved. Floating houses are independent of each other, so any module of the housing unit can be moved/subtracted/added (Figure 7a, b). This is very important in case of a module failure or family expansion. However, it is impossible to add a new floating house to the spatial configuration in question, so the number of houses is limited to the adopted number 16. According to Czapiewska et al. (2013), the disadvantages of this solution are a large number of connections, the need for a large number of moorings and a large swell.

In the branch spatial configuration, not all set parameters were met and all types of comfort were not achieved. There must be a walkway around each floating house, as a module of public purpose, so that the privacy of the residents is violated and the previously stated condition in the design process is not fulfilled. The animal shelter is positioned towards the open sea within one platform, but when connecting with others it comes into contact with other contents so that the condition of parametric design is not met again. Floating houses depend on each other, so it is impossible to move/take away/ add any housing unit module which is very important in case of failure of any floating house module and family expansion. According to Czapiewska et al. (2013), the disadvantages of this solution are no possibility to move a single house, the need for uniform structures to be able to fit together and a large number of mooring constructions. The advantage of this solution is that an unlimited number of floating houses can be added, which is not the case with the previous spatial configuration.

Finally, a more suitable spatial configuration is the islands scheme due to all the above-mentioned advantages. However, the question arises of how to make a floating settlement for an unlimited number of people for urban atoll islands by applying parametric design and the islands spatial configuration. This problem will be the topic of research on the future work of the author team.

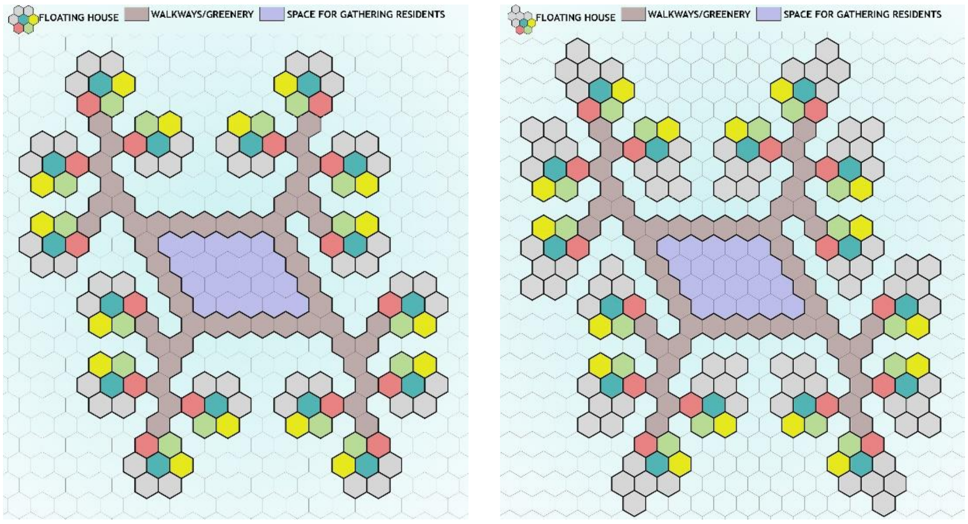


(a) (b)

**Figure 7:** Floating settlement configuration islands: (a) For a family of 4 and (b) For a family of 8

## 5. CONCLUSION

Floating architecture is a solution to the problem of rising sea levels in urban atoll islands. Modular floating structures have proven to be suitable for the formation of floating house systems, i.e. floating settlement from the aspect of the speed of implementation and cost. Parametric design can help the design process by defining the parameters, conditions and constraints of the functional zones of residential and public spaces, which must be achieved. The islands spatial configuration has proven to be an adequate floating settlement scheme with hexagon modules and also can be used as an algorithm/template to design a floating settlement for a maximum of 100 inhabitants of any urban atoll island. The advantage of this solution is the possibility of subtracting/adding housing modules so that a floating house for 4 and 8 family members can be obtained.

## REFERENCES

1. C Adnan, A., 2020. Floating cities from concept to creation: a discussion of the challenges that are pending the floating city through literature review (doctoral dissertation). University of British Columbia.

2. Balesh, R., 2015. Submerging Islands: Tuvalu and Kiribati as Case Studies Illustrating the Need for a Climate Refugee Treaty. Earth Jurisprudence & Envtl. Just. J., 5, 78.

3. Cubukcuoglu, C., Chatzikonstantinou, I., Tasgetiren, M. F., Sariyildiz, I. S. and Pan, Q. K., 2016. A multi objective harmony search algorithm for sustainable design of floating settlements. Algorithms, 9(3), 51.

4. Czapiewska, K., Roeffen, B., Zanon, B. D. B. and de Graaf, R., 2013. Seasteading Implementation Plan, Final report. Delft, The Netherlands.

5. Danilescu, I. C., 2020. Study on the Architectural Projects of the Floating Structures for Housing and Leisure, along the Danube. Journal of Danubian Studies and Research, 10(2).

6. Endangsih, T., 2020. Floating houses technology as alternative living on the water. In IOP Conference Series: Materials Science and Engineering (Vol. 797, No. 1, p. 012020). IOP Publishing.

7. El-Shihy, A. A. and Ezquiaga, J. M., 2019. Architectural design concept and guidelines for floating structures for tackling sea level rise impacts on Abu-Qir. Alexandria Engineering Journal, 58(2), pp 507-518.

8. Karle, D. and Kelly, B., 2011. No title given, Proceedings of ACADIA 2011.

9. Kizilova, S., 2019. Form and functional features of modular floating structures. In E3S Web of Conferences (Vol. 91, p. 05013). EDP Sciences.

10. Lister, N. and Muk-Pavic, E., 2015. Sustainable artificial island concept for the Republic of Kiribati. Ocean Engineering, 98, pp 78-87.

11. Moon, C., 2011. Sustainable Characteristics of Floating Architecture. In Proceedings, IAPS International Network Symposium (p. 1).

12. Moon, C., 2015. Architectural characteristics of floating building. In World architects congress (pp. 1-6).

13. Moosa, A., Do, K. and Jonescu, E., 2020. Design response to rising sea levels in the Maldives: A study into aquatic architecture. Frontiers of Architectural Research, 9(3), pp 623-640.

14. Oppenheimer, M., Glavovic, B., Hinkel, J., van de Wal, R., Magnan, A. K., Abd-Elgawad, A.,… Sebesvari, Z., 2019. Sea level rise and implications for low lying islands, coasts and communities.

15. Oxman, R. and Gu, N., 2015. Theories and Models of Parametric Design Thinking. Proceedings of eCAADe 2015, Vienna, pp. 477-482.

16. Oxman, R., 2017. Thinking difference: Theories and models of parametric design thinking. Design studies, 52, pp 4-39.

17. Piątek, Ł., 2016. Displacing architecture? From floating houses to ocean habitats: Expanding the building typology. Education for research, research for creativity. Ed. J. Słyk, L. Bezerra. Warsaw. Wydział Architektury Politechniki Warszawskiej, pp 273-280.

18. Simovic, M., Krasic, S., Nikolic, M.: Floating Solutions: The New Meaning of Mobility. In WCFS2019 (pp. 411-426). Springer, Singapore (2020).

19. Stanković, J., Krasić, S., Mitković, P., Nikolić, M., Kocić, N and Mitković, M., 2021. Floating modular houses as solution for rising sea levels - A case study Kiribati island. Proceedings of eCAADe 2021, Novi Sad.

20. http://papers.cumincad.org/cgi-bin/works/paper/ecaade2021_264

21. Stupar, D., 2017. Arhitektonički komfor u predškolskim ustanovama, doktorska disertacija. Univerzitet u Beogradu, Arhitektonski fakultet, Beograd.

22. Wang, C. M. and Tay, Z. Y., 2011. Very large floating structures: applications, research and development. Procedia Engineering, 14, pp 62-72.

23. Wylson, A., 1986. Aquatecture, Water in landscape and Architecture.

24. Zawidzki, M. and Szklarski, J., 2020. Multi-objective optimization of the floor plan of a single story family house considering position and orientation. Advances in Engineering Software, 141, p. 102766.

25. National Statistics Office of Ministry of Finance in Bairiki, 2015. http://www.mfed.gov.ki/statistics/documents/2015_Population_Census_Report_Volume_1final_211016.pdf [Accessed: 15th April 2021].

26. Secretariat of the Pacific Community, 2012. https://spccfpstore1.blob.core.windows.net/digitallibrary-docs/files/db/db673b9b910843576e39d9ec6c4408e0.pdf?sv=2015-12-11&sr=b&sig=S8fIZi7%2BRUzP907QSHS91aDvSYWtqqanuF1Tat2ty2w%3D&se=2021-12-20T12%3A48%3A16Z&sp=r&rscc=public%2C%20max-age%3D864000%2C%20max-stale%3D86400&rsct=application%2Fpdf&rscd=inline%3B%20filename%3D%22Marshall_Islands_2011_Census_Report.pdf%22 [Accessed: 3rd May 2021].

27. National Bureau of Statistics of Ministry of Finance and Treasury in Male, 2014. http://statisticsmaldives.gov.mv/nbs/wp-content/uploads/2016/07/Statistical-Release-IV-Housing-FINAL.pdf [Accessed: 3rd May 2021].

28. Central Statistics Division (CSD) of the Government of Tuvalu, 2012. https://spccfpstore1.blob.core.windows.net/digitallibrary-docs/files/1a/1a4ebc34e9aa569d07c9efc67b6b9100.pdf?sv=2015-12-11&sr=b&sig=SDNy0EV03dJhgocXaL93tdESkcuAo3dn1N92R2vKODA%3D&se=2021-11-14T04%3A21%3A01Z&sp=r&rscc=public%2C%20max-age%3D864000%2C%20max-stale%3D86400&rsct=application%2Fpdf&rscd=inline%3B%20filename%3D%22Tuvalu_2012_Census_Analytical_Report_Vol_1.pdf%22 [Accessed: 15th April 2021].

# TOPIC 3: GEOMETRY, GRAPHICS EDUCATION AND TEACHING METHODOLOGY

# TWO POINTS A LINE

Maja Glavaš – Trbić

Civil Engineering School, 11000 Belgrade, Serbia

mglavas6@gmail.com

***ABSTRACT***

*After years of presenting and teaching geometry in secondary school and monitoring how students perceive geometry and graphics, I have got an idea to give some new meaning, viewpoint, in words, as epic and lyric poems inspired by geometry. Probably Paul Klee famous quote "A line is a dot that went for a walk" inspired me to dedicate poem to lines, combining their multipurpose use in geometry and life on several levels, including social, educational and aesthetic components. Few samples performed in the classroom will be analyzed. After years of geometry exploitation in descriptive geometry and technical drawing, it deserves some kind of gratitude and appreciation.*

**Keywords:** geometry; line; poem; social, educational and aesthetic component

## 1. INTRODUCTION: NO DAY WITHOUT A LINE

Continuously thinking of issues of descriptive geometry and technical drawing to get closer to students, to intrigue, to interest, to touch, to move, to involve them, to connect abstract and real, we become narrators and poets, we expand the story, compose rhymes, glorifying ordinary, dull terms, putting it in new relations, linking them unexpectedly, following wordplay, imputing multiply meanings and additional possible interpretations…

It is notable lower knowledge of geometry terms as well as poor comprehension of space relations, hardly perception and adopting of geometric images with students then other mathematic terms. Insufficient paying attention to geometric issues in elementary school could be seen at initial exam of 1st grade students in impossibility of constructing equilateral triangle or square, sketching parallel/normal lines and planes, making no distinction in geometric solids and shapes and their names. It is shown the geometry as the main problem at final math exam of last grade elementary school students.

'Great amount of pupils cannot see the role of geometry in everyday life what is a reason for low motivation on math classes', I would add, descriptive geometry classes too, although 'teaching geometry holds important part in school curriculum of all educational systems', (Šiljić, 2015).

COVID pandemic has moved teaching remarkably into online spaces, separated us for months to two metres like kilometres, where a word has become only available mean, with explanations hard to be followed without that line, sketch drawn into student's notebook during lesson in classroom. Each student has been an island for a year where many cultures are to grow and bear fruits of work and knowledge. Everybody seats at its own place in the classroom, with no possibility of glance at friend's notebook and get affirmation of his own good work, the most valuable and most effective age-mate support alive has been excluded, mobile phones and picture transfers have entered to the scene.

So an attempt starts to animate examples, to transform not much interesting issues, to enlarge importance of a dot or a line, everything in order to glorify geometry and drawing. Famous Paul Klee saying 'A line is a dot that went to a walk' or 'No day without a line', and our school 'One line a day takes mischief away!' remind us and induce every day. Euripides quote and moNGeometrija motto 'Mighty is geometry; joined with art, resistless' is the heart of all aspirations.

## 2. TWO POINTS A LINE

Playing with words and ratio 2:1, it conduced to the poem about lines and friendship. Cases of mutual relations of lines has become a metaphor of social relations, fellowships or disregards, meetings and departures, misalignments, disagreements and differences, common acts, adventures, way to school, time, ideas, hopes and horizons. Geometric terms have been transferred to social sphere, came to life and played a show. At the same time, whole range of terms, expressions, objects, means and relations in geometric space has been spread out in front of young people in order to intrigue and inspire them to find, study and learn about it.

Two points a line

Two points a line
Two friends a line to friendship
A line that connects
Two infinities

Lines that meet
Lines that are a pair
Lines that pass by
Lines that overlap
Lines that touch
Lines that derive
Lines that transform to a circle
Lines that appear as a point
Lines that define a slope
Lines that loose length due to no weight
Lines that reflect map
Lines that walk
Lines that rule
Lines that hatch
Lines that direct
Lines unreachable and close at the same time
Lines that count
Lines that play music
Lines that dictate
Lines that are half right
Lines that divide all into equal parts
Lines that have broken to reach the school
There are normal too
A bunch
A trace
A beam
A horizon
A line, a line that connects
Two infinities

## 3. FRIENDSHIP LINE, KNOWLEDGE LINE, FRIEND – COLUMN

### 3.1. Friendship line

Since we had met point in general and special cases trough places in the classroom (x number of desks from windows, y number of desks from blackboard, height – lay down, sit down, stand up), arms in x and y direction and head and neck in z, it was time for lines and segments. First question referred to prepared template of their classroom, something known, in all three views. It took times to recognize space, not all did it, but with some help we solved step one. In preparation of exercise, instead of data lot, students were placed around the classroom, excluding places of same x and y values, they have been asked for his best friend among present. Depending on answers, someone has been moved too, for the diverse lines layout. It was very pleasant to see students turning each to other from around classroom, referring to distant classmate, looking for, checking; more pleasant was fact there were no excluded D-P, P-Ve, B-Ve, Ve-Vu, Vu-B.

Students marked their places/ points by own initials or syllable and wrote it in (x; y; z) form, after we have done first point together for one who needed help at most. We checked all places/points and wrote at blackboard. On their templates, students „found“ themselves, as it is always important to know where we are and to determine position in space and life, and marked "own" point in 3 projections. Adding the friend into drawing, with the turning to him, checking at the same time, and the other point is in drawing with the name of the friend. It is the moment to trace friendship line connecting two of "our" points in top view, from friend to friend, from desk to desk, Fig.1 (a). At that very moment, balls were missing to be thrown within students and tighten presented relations; it would stay for next school year! We found 2nd and 3rd projections, staying at same level of desk and colors. Horizontals bridged over the distance between students placed across the classroom. It is interesting there were no return links among students, so all five lines are different, Fig.1 (b).

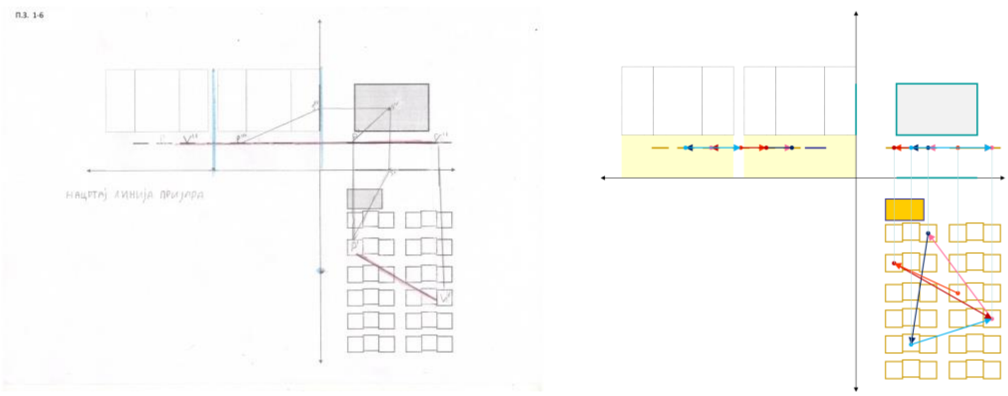

(a) (b)

**Figure 1**: (a) Student work, and (b) Friendship lines

Time (shortened classes) did not allowed us to draw friendship lines to other present classmates, it could stay for homework. The example could be connected with mathematic, combinatorics and mapping, vectors too. If we do teamwork drawing, and everyone draws his friendship lines, how many different lines would be? Better to draw first or last? How many lines last student should draw or who could not have pencil and ruler? At technical drawing lessons earlier we divided a circle into 32 pieces and connected circumference points each to another. We could remind of that on this occasion.

### 3.2. Knowledge Line

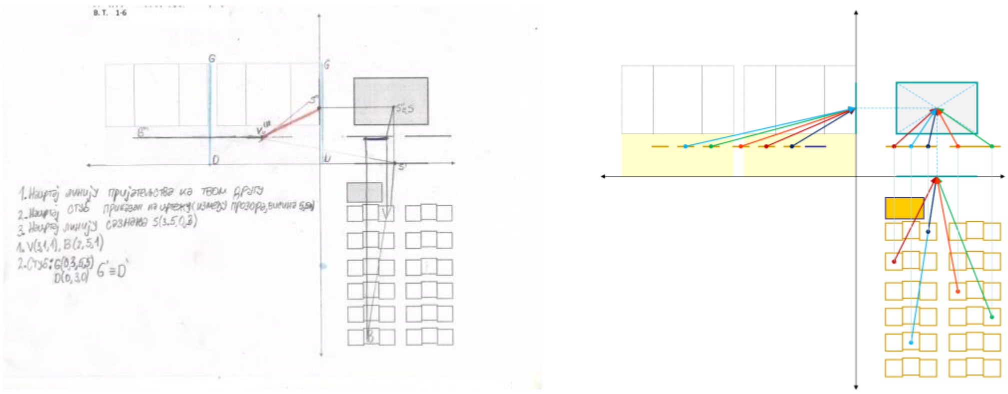

(a) (b)

**Figure 2**: (a) Student work, and (b) Knowledge lines

It is imagined as a line from student to blackboard as the knowledge place, cradle of cognition. It is a line in general position with a special point on frontal plane. We drew given point S (3.5; 0; 3), approximately centre, blackboard mass centre, in all projections and connected to our point, Fig.2 (a). So we have drawn another important life line as continuous, tick line. It should not be dashed, what happens sometimes during a class!

The point could be given as centre or mass, centre of rectangular blackboard that should be graphically found in the drawing in next version of exam. It would be linked to terms of statics and physics in that way. The teamwork drawing of all knowledge lines would be interesting as a bunch of lines from centre point after adding of all single knowledge lines in drawing. The knowledge point would shine like sun in frontal view sending power beams to those who are ready to learn and prosper, Fig.2 (b).

### 3.3. Friend – Column

Column, pillar, supporter, post, stud, stanchion, reliance, abutment, archetype, mainstay, anchor, world axis, power and many, many other nice words are literal and figurative meanings for the same term. It is building element of z direction, one of three special lines which are perpendicular to projection planes. Three directions most exploited in architecture, vertical column, beams of x and y directions, usually building frame. In saying woman is a column of house, home and family. At teenage the support is important, friend has role of column. In example we observed same column at profile wall, between windows. We dematerialized it, defined upper G and lower D points according to its position and height in drawing. We drew it in all views and marked it, vertical line in profile plane has been presented, Fig.3 (a). Example which would strengthen bonds of friendship and knowledge can be presentation of column at the friend's place, next year maybe. In teamwork drawing we would have forest, multiplied verticals, reliances, aspirations and supports. Each student is a mainstay to other and he himself stands upright, Fig.3 (b).

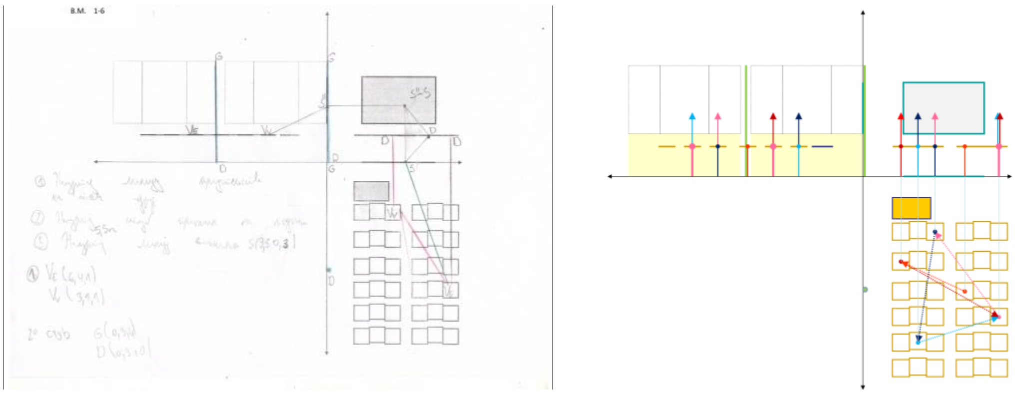

(a) (b)

**Figure 3**: (a) Student work, and (b) Friends – columns

### 3.4. Overview and Further Steps

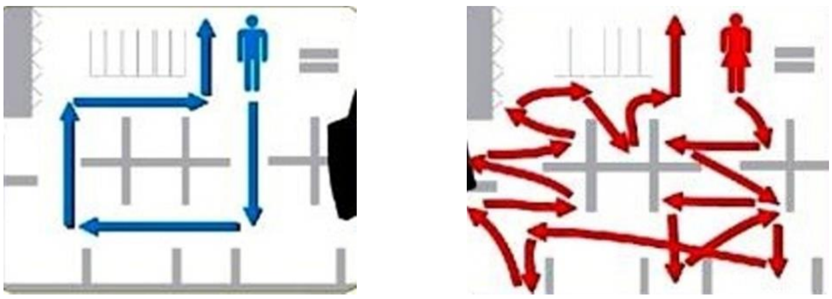

(a) (b)

**Figure 4**: (a) Desired track, and (b) My track

In this entire walk around my "point" got tired at most, visiting and checking drawings of each student. It would be interesting to have colored soles and GPS to save track and mileage! Difference between desired and real tracks during lessons can be noticed in Fig. 4, but gain and pleasure were more important. Student's comments were positive, easygoing lesson (80%) and 20% without comment – student who had difficulties to recognize classroom template.

Digital technology should back up and support this exercise, teacher assistant as well:

- Layout of the classroom for easier recognition and orienting in drawing and space presented, with desk numbering
- Input of points, mine, yours, at the same time view of whole group of students
- Layout of all friendship lines with gradually input in different colours and projections
- Colorful relations – net of friendship lines – fellowship, summary, Fig.1 (b)
- Views of all knowledge lines from central point to each student, gradually input in different colours, Fig.2 (b)
- Views of all vertical lines – columns at student’s points with gradually input in different colours, Fig.3 (b).

## 4. ODE TO GEOMETRY

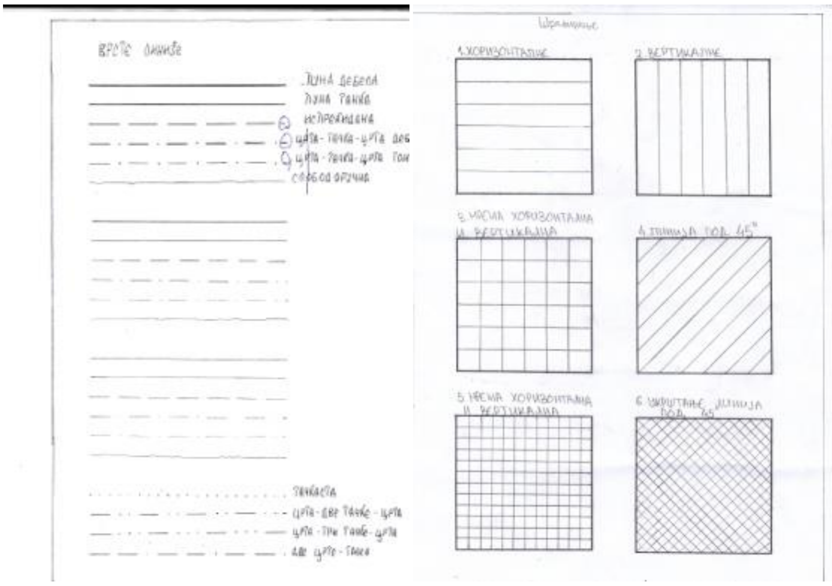

(a) (b)

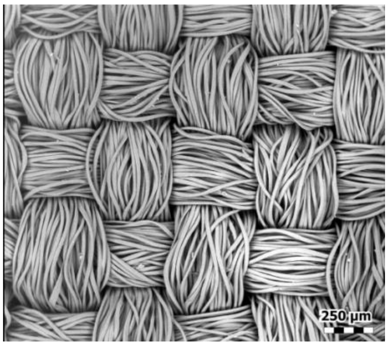

(c)

**Figure 5**: (a) Types of lines, (b) Hatches, and (c) Mask detail

Lines types and hatches at the beginning of technical drawing course are just drafting exercises. Group of lines repeats few times but in different thickness, Fig.5 (a). Six squares should be filled by various regular hatches changing angle and density of hatch lines, Fig.5 (b). It happens sometimes that hatch looks uncombed, but rarely, Fig.5 (c)! Repeating in exercise sounds like musical or speech fugue. Memories of fantastic fugue “Serbia” by composer Aleksandar Vujić have awoken. First lines of Ode to Geometry have arisen, which could grow into rhythmic audio record for School days celebrations. From types of lines in technical drawings the clue moved on to the lines used in geometry, space relations and positions we consider in descriptive geometry. Over the geometric shapes, solids and their properties presented in courses, generalization has followed up to the geometry authors, not held in school curriculum but of course worth mentioning.

At the same time, the Ode signifies constant presence and development of geometry in human society, an unavoidable discipline today as well as it has been for ages. Inseparable from human, geometry continues to live and to develop forever. Speech fugue would be performed in 4 voices, each repeats own term until all include when common term at the end of stanza should be repeated by all. In periods of COVID pandemic and social distance lot of music performances appeared with help of IT devices, participants recorded own part, then single records have been mixed in a group audio visual digital performance. Preparing the Ode is possible in digital way too, which could be even more interesting to students, everyone has own scene and play but would fit in the whole. A rhythm matrix is key requirement for good beginning and whole project. However I prefer live work, choired and scenic training and doing. It is immeasurable pleasure of achieving group performance, harmony, consent formed by coaptation, listening, following the other, fitting into group project for common welfare and joy of participants and public.

Ode to Geometry

Point line curve
Solid thick
Solid thin
Dashed
Freehand

Dash dot
Dash 2 dots
Dash 3 dots
Double dash dot
Dotted

Basic
Contour
Hidden
Construction
Sketch

Horizontal
Vertical
Perpendicular
Bisector
Axis

Parallel line
Profile line
Frontal line
Diagonal
Midline

Inscribed
Circumscribed
Triangle
Square
Circle

Ellipse
Parabola
Arc
Chord
Centre

Face
Shape
Figure
Polygon
Surface

Cube
Cone
Prism
Sphere
Solids

Lateral surface
Base Base
Trunk
Cylinder
Roller

Pyramid
Roof
Plane
Section
Intersection

Length
Width
Area
Hight
Volume

View
Top
Front
Side
Oblique

Projection
Rotation
Transformation
True size
Monge

15 years
Guarded
Secret
Geometry
Descriptive

Euclid
Riemann
Lobachevsky
Geometry
Forever


**Figure 6**: Nulla dies sine linea, Raša Todosijević

It is important: no day without a line, as conceptual artist Raša Todosijević sais with his set of twelve pictures ironically about artwork, Fig. 6, long time after antic painter Apelles said and worked 'Nulla dies sine linea', all about necessity of continuous improvement in art and craft, drawing, painting.

To give meaning to lines, to explain existing, to learn the language of lines, to give them new, additional meaning familiar to students, known from life, real situations, to insert association, metaphor, humor, playing with words and pictures, to dignify teaching, educational and pedagogic process.

## 5. THREAD THAT CONNECTS US

### 5.1. Egg Curve

Lecture on egg curve at moNGeometrija 2008 conference, in part 'Construction of an egg curve using the method of mathematician Fritz Hügelschäffer, is based on the construction of ellipse by method of concentric circles, with radii a and b that respond to the parameters of the ellipse', (Obradović et al, 2008) inspired me to expand technical drawing lessons and construction of curve lines with construction of egg curve using appropriate power point presentation, considering it would attract and be further interesting to students because it is a form so well known and familiar from everyday life and home. Construction of ellipse by concentric circles served as a base for construction of oval with moved centres of circumscribed and inscribed circle. Then Easter workshops followed where we constructed, mapped, painted, made collage or ovaloids.

(a) (b)

**Figure 7**: (a) Painted artworks, and (b) Cut artworks

### 5.2. Thread That Connects Us

This year we were lucky to be in school before Easter holiday after a period of online teaching. Still serious epidemic situation caused prolonged, linear character of the workshop, day by day, through all my classes, during seven days of April 2021 in order to avoid gathering. Name „Thread that connects us“ has symbolic meaning of upcoming holidays that connect us together as well as art, beauty, joy of creation, association on linear character of this 9$^{th}$ Easter workshop and line in our professional subjects, a curve line this time.

Students have been offered two possibilities, to paint with felt pen surface of 2d paper model (envelope recycling), Fig.7 (a), or to make some kind of collage cutting egg shaped form, Fig.7 (b). We painted and cut „eggs“ with minimal resources and accessories in minimal time limit. Four colours used for work also connected all pieces in a line, cycle and period but by different authors.

Additional request was to name artwork, linking form and idea, enriching it; this was well accepted by students. It was very interesting watching student's efforts and creation of work, looking for corresponding name, combining artistic expression and words. Showing an example is necessity but it carries risk for students not to move far enough away from the example in own work, particularly in very limited conditions we worked.

It is worth to mention the most interesting names which correspond to the most successful artworks as well, Colourful valley, Jolly stream, Hero, Landscape, River of life, Cross, Colourful egg, Chopped egg etc. I have to explain The Hero as an egg in wounds and cuts but it has survived all challenges of Easter traditional knocking of boiled painted eggs. Results and photos of artworks were notified on FB page Грађевинска, МОЈА школа that I run.

### 5.3. Calligram

Apollinaire's visual poetry, 'lyrical ideograms' as he called them, a perfect blend of poetry and artistic elements to my opinion, influenced my modest attempt, providing another dimension to our Easter gathering. Workshop is described in the poem enclosed here as a *Word* calligram.

Oval,

is it alive?

Its field

colourful,

four colours

make wonders.

Its body

twisted,

each pattern

creates magic.

Oval,

it is alive, WITH US!

## 6. CONCLUSION

Education sometimes looks like the cartoon by Nedeljko Ubović, Yugoslav artist, Fig.8. It is a metaphor but sometime it happens that someone act like policeman in picture, supervisor, disciplining ideas and creativity, not allowing diversity, a different view, a new method.

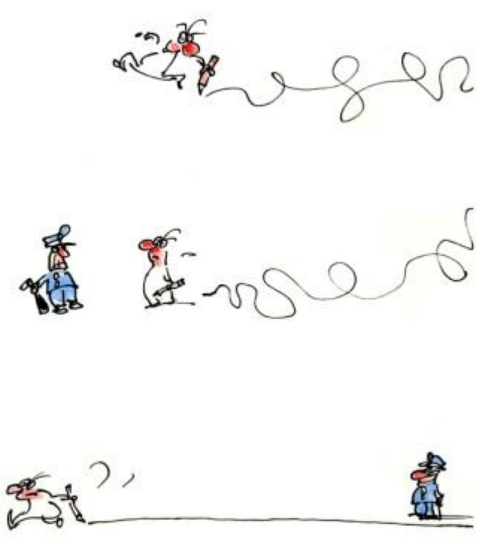

**Figure 8**: No comment, Nedeljko Ubović

However, if we are led or guided by Paul Klee quote, taking dot walk and line as a research, way to new ideas and art forms, not withdrawing from internal restlessness so characteristic to mankind, naturally given, innovating and positioning familiar into new relations, even unexpected, infinity point will become finite, we shall achieve the power glorifying by Euripides saying, so well emphasized at moNGeometrija site.

Creative thinking walk through geometric and physical spaces will contribute. Inwrought with play and challenges, seeking for Schiller's ideal of beauty in the most perfect possible union and equilibrium of reality and form, it will play role of aesthetic education, affecting and cultivating young people. So let's keep trying!

## REFERENCES

1. Obradović, M. and Petrović, M., 2008. The spatial interpretation of Hügelschäffer's construction of the egg curve. Proceedings of moNGeometrija 2008, Niš, Serbia. pp. 222-232.
2. Faculty of Mathematics, University of Belgrade, 2015. http://elibrary.matf.bg.ac.rs/bitstream/handle/123456789/4225/Siljic_Jovan.pdf?sequence=1 [Accessed: 1st Feb 2021.
3. 2018. https://www.youtube.com/watch?v=EqjjIbXF1O0&ab_channel=AndjelkoDuplancic [Accessed: 21st Feb 2021

„International Conference moNGeometrija, focused on the research about geometry, graphics and application to science, engineering and art“

Belgrade, 10.-12. September, 2021

# ADVANCED SIMULATION IN ANIMATION COURSE AT THE FACULTY OF TECHNICAL SCIENCES

Ana Perišić[1], Marko Lazić[2], Lidija Krstanović[1]

[1]University of Novi Sad, Faculty of technical sciences, Department of fundamentals sciences, 21000 Novi Sad, Serbia

[2]University of Novi Sad, Faculty of technical sciences, Department of architecture and urban planning, 21000 Novi Sad, Serbia

anaperisic@uns.ac.rs

**ABSTRACT**

*This paper presents the overview of the new course that is lectured at the Faculty of technical sciences in Novi Sad. The name of the course is Advanced simulation in animation and it is obligatory subject for all students of master academic study program of Engineering Animation. Simulations are an integral part of the validation of geometric characteristics of 3D models and they are important part of solving engineering problems using computer animation. Depending on the type of 3D object and its behaviour in specific time, specialized types of simulations are performed. Computational fluid dynamics software is used in practical classes, but different types of engineering simulations are presented in the lectures. The aim of the practical part of the course is a validation of a design based on an aerodynamic characteristics of the geometry and the visualization of the flow results around different aeronautical and non-aeronautical objects using computer graphics. Structure of the course is presented through chapters about lectures, practical classes and assignments. At the end of the paper student results are shown with the commentary of their progress during the semester. The course is integral part of master education programme of Computer Graphic Engineering students and it is helping them to test their designs in a practical way so they can be better at designing overall.*

**Keywords:** Computer simulation, Education, Computer graphics, Computational fluid dynamics.

## 1. INTRODUCTION

Computer simulations is a contemporary and highly developing field in science, engineering and education. Computers and publicly available cloud services are able to perform very complex calculations in a short period of time overcoming the initial hurdles of simulation computing in the early phase. This technology offers its users efficient prediction and validation of various products or processes especially in the field of situational training and risk assessment. Also, it is possible to spot problems on existing solutions in design with insight into detailed reports on their causes.

Integrating simulation in education is diverse and depending on the professional field the students are preparing for. Most disciplines have specialized tools for performing simulations. Examples of effectively used simulation processes in education are: simulation of the structural system and fracture of structural elements in construction (AbouRizk, et al., 1998, McKenna, 2011), then the use of an air tunnel in aeronautics (Spalart, et al., 2016) or simulation of the complete production process of manufacturing and / or distribution of products in engineering management (Ameli, et al., 2019; Ingalls, et al, 2008). They all require completely different approach and methods in performing simulations. Training students for different types of simulations enhance their problem-solving motivation, understanding of complex environments and processes and also their analytical and deductive capabilities. Also in the research (Prauzner, 2016, Rutten, et al., 2012) it was noticed that groups of students who master the material using simulation software have better results in the final exams.

Computational fluid dynamics (CFD) is one of the most utilized simulation environments in education. It has been adopted in both undergraduate and graduate level courses in many universities. This type of simulation analysis and solve problems involving fluid flows (primarily water and air) in different conditions. Estimating fluid movement relative to solid geometry can serve as an effective tool for validating micro designs (Jones, 2013) to urban areas and cities (Gros, et al., 2016). CFD simulations can be applied in various disciplines, primarily those that use 3D modelling or geometry scanning techniques. The introduction of *Advanced simulation in animation* course and implementing CFD simulation techniques in engineering education can increase the quality of similar university study programs containing the basics of 3D modelling.

## 2. GOALS AND METHODOLOGY

The aim of the research is to present the *Advanced Simulation in animation Course* in the study programme of Engineering Animation at the Faculty of Technical Sciences in Novi Sad. For the first time in this course, students of the Animation in Engineering encounter computer simulations used in various fields, which have not been applied exclusively for the purpose of visualization. It is meant for design evaluation and performance enhancement study primary. The course is performed in master's academic studies, at a time when all participants are trained in complex 3D modeling and animation in undergraduate studies. The experiences presented in this paper can help define other courses in which participants have prior knowledge in the fields of design, 3D modeling, animation, and applied mathematics and physics.

The paper presents the entire scope of the course, including the manner and content of lectures, exercises and tasks that are assigned to students during the semester. The results achieved by the participants are presented in this paper, as well as a discussion of the challenges that arose during the work on this course.

The course was held for the first time according to the new accreditation of the school year 2020/2021 and at the time of writing, only one generation of 8 students attended. The achieved results in the course were analyzed on a small sample, but the results are sufficient to draw conclusions about minor changes and improvements in the course in future work.

## 3. STRUCTURE OF THE COURSE

The structure of the course in this paper is divided into three main units: conducting lectures, performing exercises and reviewing student assignments. The material is synchronized so that most of the same content is processed through all three parts. There are also significant differences between the three main units. The lectures are focused on the coverage of computer simulations in a broad sense, while the exercises are applied to a selected segment of simulations in practice. One part of the assignments is formulated in a way that students are referred to more detailed research in various areas mentioned in the lectures. The second part presents a synthesis of the practical application of the methods learned in the exercises in personal projects.

The approximate connection of the material is shown in Figure 1 where it can be seen that 30% of the connected material is present between lectures and exercises. Also that about 60% of the materials in the exercises are directly necessary for work on the tasks and that 50% of the materials can be used for the same. The rest of the task, of about 20%, is the independent work of students in relation to the specifics of the tasks assigned to them. Percentages do not represent the time required for work, but the methodology and resources covered by lectures and exercises.

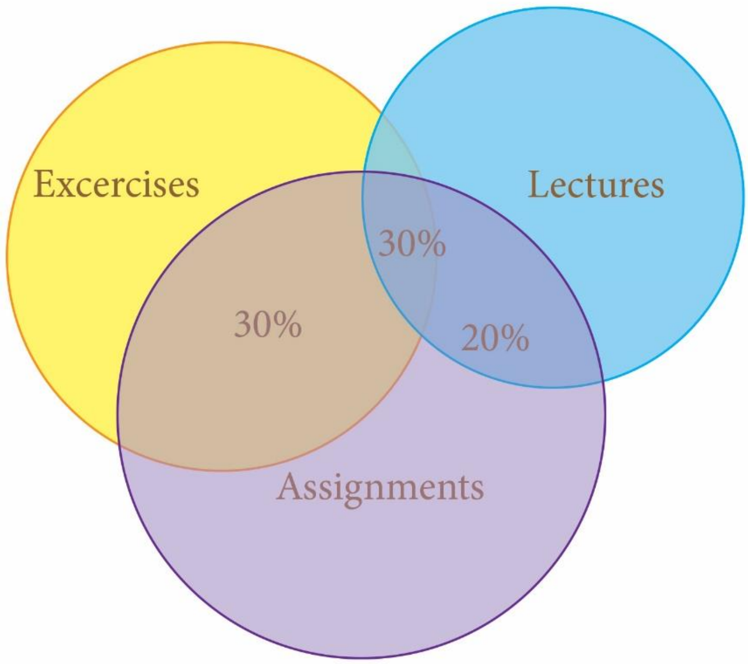


**Figure 1**: The relationship of the total material on the subject between the Assignments, Exercises and Lectures

### 3.1 Lectures overview

Since students encounter the topic of problem solving for the first time with the help of computer simulations, a wide area with specifics of application in the profession is initially presented. In the introductory part of the course, students get answers to the questions: What types of simulations exist? The way they came about? How have they evolved over time? The aim is to gain a clear insight into the history of the development of computer simulations in order to be able to show off current methods and tools.

The principles that emerged at an early stage of development in this area are applied today and serve as a basis for a large number of software. An important task is to present the subject with a comprehensive approach that aims to broaden their horizons and understanding of the area from different angles. Students get a structure that is the basis for their own research that they will perform as part of the work on the course. They involve linking existing software tools and algorithms to key figures, the history and circumstances of the emergence of specific scientific and technological innovations and their impact on industry and the engineering profession.

A significant part of the lecture has a topic from the field of CFD simulations, which are the main topic of performing exercises on the subject. CFD simulations involve a system of work that gives results by analyzing the geometric characteristics of objects whose design is tested in a predefined environment. In addition to the history of simulations and CFD systems, the following topics were covered: simulation of catastrophic events, simulations in architecture, simulations for the construction industry, simulations and climatology, simulations in medicine, simulations in astronomy, simulations of neural networks, simulations of production systems and technology, process simulations and industry, simulations in aeronautics, simulations in the film industry, simulations in the video game industry, simulations in education and simulations for the military industry. After presenting the different areas of application of simulations, students had a lecture on the impact of AI technology from the point of view of simulations as well as on the most important parameters on the basis of which simulations are evaluated. The program also includes a lecture focused on current trends in the profession and the future development of the field of computer simulation. Table 1 shows the schedule of topics, with key terms by week.

| Week | Lecture topic |
|---|---|
| 1. | Introductory lecture (overview of course topics, task explanation, work plan) |
| 2. | General history of using simulations as a scientific method - beginnings and influences |
| 3. | History of computer simulations |
| 4. | General classification of computer simulations and definition of basic concepts |
| 5. | CFD simulation - theoretical foundations |
| 6. | CFD simulation - classification of different scenarios |
| 7. | CFD simulation - analysis of software tools and application in practice |
| 8. | CFD simulation - discussion on the topic of the exercise task |
| 9. | Discussion and selection of topics for seminar work, research methodology and paper writing |
| 10. | Software environments for computer simulations |
| 11. | Computer simulations applied in architecture |
| 12. | Application of simulations in the entertainment industry |
| 13. | Influence of AI on the development of computer simulations |
| 14. | Current situation in practice and development of simulations in the future |
| 15. | Presentation of seminar paper and practical assignments from exercises |

**Table 1**: Schedule of topics in lectures on the course Advanced simulations in animation

At the end of the theoretical lectures, examples of the application of different software and software companies that influenced the development of the environment needed for virtual testing and simulation of different scenarios depending on the type of simulation and the model on which the simulation is performed are presented. The program provides 3 terms for discussion, evaluation and presentation of the finished research of students. In this way, students learn to apply the scientific apparatus and formulate their research through interaction with colleagues and the subject teacher. Table 1 shows the schedule of topics, with key terms by week.

### 3.2 Practical classes overview

The focus of the exercises is on the field of CFD simulation. It is defended as the most suitable for the professional profile for which engineering animation students are educated. It has the most points of contact with previously mastered areas that students studied during their undergraduate studies. CFD not only involves the analysis of geometric models but also the visualization of simulations in the form of animating the results through the time component of design valorisation. The software used in the exercises is Autodesk CFD (ACFD, 2021). The most important reason for this decision is the fact that it belongs to the Autodesk software family along with software like 3Ds-max or Maya which are environments in which students, who attend this course, are well acquainted. Autodesk CFD is accessible to students through an educational free license, and the interface and tools have similarities to other Autodesk software.

The initial exercises are dedicated to the correct preparation of geometry in the 3D modeling software Autodesk 3DS Max (A3DS, 2021). After that, the work in CFD software on a model of a cooling system is presented, as an example on a system that has a fluid geometry closed by solid objects. After this type of task, an example of simulating the aerodynamics of an airplane as a CFD air tunnel system where the fluid is not directly surrounded by solid objects was examined. Autodesk Simulation works in a specific way where the input is the geometry of the object that must be optimized and reduced to key design components that affect performance. The work process itself is divided into three main phases: pre-processing, processing and post-processing.

Pre-processing is the first phase in CFD simulations and involves defining the input parameters of the simulation. Students mastered the basics of geometry preparation, meshing, defining the material characteristics of 3D models as well as setting the boundary layer and defining the conditions of the environment in which the model is tested (conditions). The success of this phase depends on testing and checking the geometric model of the vehicle or 3D model that is tested for errors such as: Open geometry, edges and vertices, missing or folded faces that can contribute to the occurrence of errors in numerical calculation during simulation. The model should be of the closed type solid. After preparing the model, a phase of problem analysis is performed, which is to be simulated on a 3D model. It involves defining the attributes of the model on which the simulations are performed.

In the examples presented, the preparation and analysis of 3D models from the aspect of aerodynamics in the Autodesk CFD software environment was done. After defining the attributes of the 3D model, the Meshing procedure is performed, which implies defining the physical domain of the environment in which the 3D model is tested and dividing it into defining the region-cell (control volumes). These cells are defined by the equations of fluid dynamics. At this stage, the goal is to refine the model by reducing the dimensions of the cells and thus provide greater precision and accuracy of the simulation analysis results. Setup Solver is a phase of analysis in which the conditions for the problem to be solved through the simulation are defined.

| Week | Exercise topic |
|---|---|
| 1. | Introduction to the program of subjects and necessary tools for work |
| 2. | Introduction to the interface and basic tools |
| 3. | 3D Modeling for simulation purposes - basic principles |
| 4. | 3D Modeling for simulation purposes - testing of 3D models and corrections |
| 5. | Introduction to the interface and basic tools in CFD software |
| 6. | CFD analysis of cooling system examples - pre-processing phase |
| 7. | CFD analysis of cooling system examples – processing i post processing |
| 8. | CFD analysis of examples of cooling systems - processing and post processing |
| 9. | CFD analysis of the air tunnel - processing and post processing |
| 10. | Work on different vehicle models, application of learned principles |
| 11. | Work on student vehicle models, corrections and discussions |
| 12. | Types of result visualization in CFD software |
| 13. | Fundamentals of engineering animation and visualization of simulation results |
| 14. | Creating an animated sequence of simulation results and interpreting CFD simulation results |
| 15. | Consultative exercises |

**Table 2**: Schedule of topics for exercises in the subject Advanced simulations in animation

For example, turbulence model for aerodynamic analysis or fluid type and boundary conditions. Knowledge of the physical aspects of the problem being researched is crucial because the numerical solutions are reconfigured in the software. In this phase, the method of the analysis procedure and the number of iterations of the verification of the results are defined. After defining the stated parameters, a processing phase is performed, which implies solving (Solve) simulation based on predefined values. In this phase, the student determines the duration of the simulation as well as the type of presentation of the simulation results. This part of the procedure requires special attention as it has an impact on the way the results will be read. This phase also involves the creation of an animated sequence showing the behavior of the 3D model in predefined conditions through the aspect of time. In this way, students of engineering animation create engineering animation of simulation results. The post-processing phase of the work involves checking and validating the results that can be achieved by comparative analysis and predefined parameters based on which the expectations of the 3d simulation are timed. If it turns out that a higher percentage of error returns to the pre-processing phase and checks the geometry (CAD clean-up) or meshing (Mesh generation) as well as checking all the above steps in that phase. Students were shown examples in exercises and were given 3D models for situational training, where they have the task to first detect errors and then correct the simulation procedure. In this way, their progress is checked in several steps and it is ensured that they understand the working principle in Autodesk CFD. The schedule can be seen in the following table2.

### 3.3 Assignments overview

Tasks are structured so that students apply the knowledge gained in exercises and lectures on practical examples. The tasks are divided into two parts, the first is theoretical research and it involves writing a seminar paper, the second is the creation of simulations on practical examples and their analysis.

The seminar paper is written from the topics covered in the theoretical lectures. Students were asked to write a brief historical overview of the selected type of simulation (from the analogue version to the digital version). They are expected to list the names of key inventors and scientists who have contributed to the development of the field they are researching. They analyse technology development and innovation. Answer the questions: How has the scientific approach changed depending on software development and industry requirements and what have been the key innovations in these fields? Students researched and reviewed commercially available software related to the field and their development throughout history (when they appeared and how they changed). By analyzing the characteristics of 1 to 3 simulation software in the field, students gained insight into their work procedures (model definition, model type, model preparation, duration, procedures within analysis, data processing procedures, procedures / results / final outcome / scenario) as well as the method placement and comparison of results. Also, thanks to the comparative analysis of software packages, they developed critical thinking through tabulation of advantages and disadvantages of available software, as well as problems that occur during application in the profession.

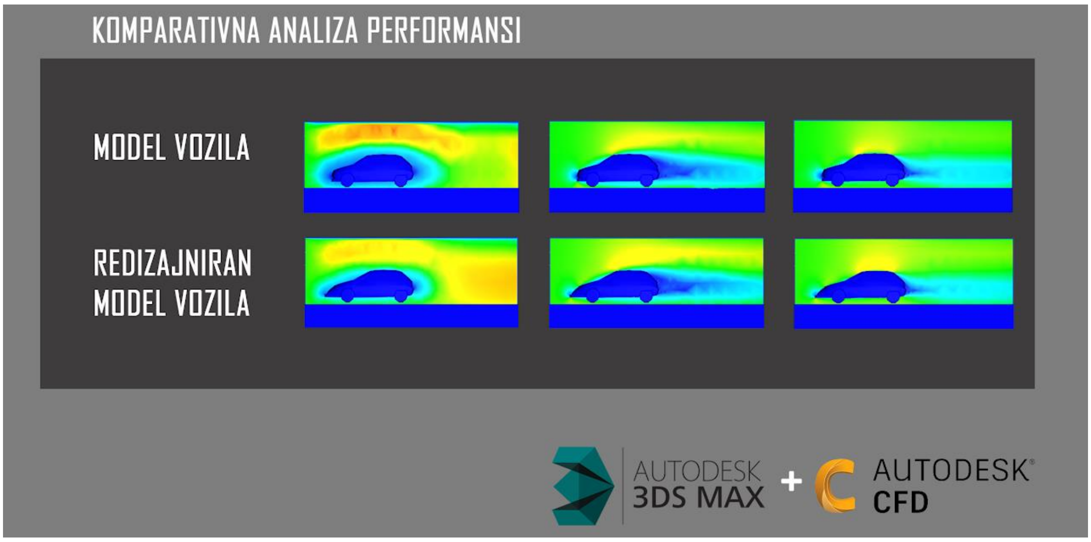


**Figure 2**: The graphical representation of the comparative performance analysis of the existing and corrected design of the 3D vehicle model by student Aleksa Paunović

In addition to seminar work, students also worked on a practical project. It was expected to apply the methods they had mastered during the exercises. Students did a comparative simulation of the aerodynamic performance of a 3D vehicle model. They could choose whether to do the simulation on 3 models of complex geometry vehicles or 5 models of simple geometry vehicles. The task envisages doing at least 100 iterations of model testing. Based on the results of the simulation, the students were asked to perform an analysis of which form and design solutions have the best aerodynamic performance. Based on the comparative analysis, it is planned to make a hierarchy of vehicle models from the one with the most favorable aerodynamic characteristics to the one with the lowest results. After that, as a test of their understanding of the work in the software, it is planned to make a correction of the geometry of one vehicle model in order to improve its aerodynamic performance. When this step is done, a comparative performance analysis of the existing and corrected design of the 3D vehicle model is performed (Fig.2).

All results are presented both in the form of an animated sequence of sequences and in the form of numerical results in the form of a table. At the end of the semester student have 3 levels of passing the exam, the first one is the oral and public discussion of their seminal work and thesis discussion, they can exchange with their peers the experience and research and have a feedback from the professor and fellow students on the topic. After the theoretical work they present the results of the experimental practical project and passing that phase they can complete the theory based written exam. The questions on the written exam are based on the lectures students attended too during the semester. Students have the possibility of correcting the final grade by working on additional tasks or correcting the seminal work according to the professor comments in the paper.

## 4. WORKING IN VIRTUAL ENVIRONMENT

In the school year 2020/21, all classes at the Faculty of Technical Sciences in Novi Sad were conducted online with the help of the MS Teams platform. Teachers and associates had all the communication exclusively in digital format. This circumstance greatly influenced the environment off the classes in both positive and negative ways.

Positive experiences are primarily the comfort that students had at work. There was no need to travel to the place of teaching, this gave them more time to focus on work and tasks. Digital communication through a single platform facilitated work when exercise materials and lecture references were posted.

The negative aspects are largely related to performing the exercises. The software necessary for teaching the subject is demanding and in combination with the communication platform, it was necessary to have more powerful computers for uninterrupted work. Not all students were able afford computers in the range of necessary capacities. The network connection was also unstable in one part of the students, which is a rule of work problems. File size for CFD simulations has proven to be a challenge on computers that did not have adequate hard disk space to store them. Such problems would not occur in the conditions of physical work in the laboratory. The equality of work conditions was lacking in that sense for some of the attendants. If a student has a problem with the software, solving it took much more time than physically teaching the subject. It was greatly challenging for the teaching stuff from the technical point of view.

Also, teaching on the new platform required the preparation period by the Faculty of technical sciences, which caused a reduced number of working weeks in relation to the total fund that is planned to work in Tables 1 and 2. For this reason, the scope of tasks is reduced compared to the planned realization, but the results showed that the challenges that arose when working in a virtual environment were successfully overcome. Eventually all students regularly attending the course were able to finish the practical projects and tasks with success that surpassed initial expectations.

## 5. RESULTS

The results of the seminar papers showed that the students successfully researched the topics they chose. Students chose topics based on their affinities from different areas. In terms of selection, papers were submitted in the field of simulations in medicine, simulations for the needs of the film industry, simulations of catastrophic events, simulations in video games, military simulations and simulations of neural networks. Students have shown in their works that they are able to explore complex topics and to master the basic methods of using different methods of computer simulations.

The results of the graphic works showed that the students successfully mastered the work in the software for CFD simulations. The modifications of geometry they made contributed to the aerodynamic shape of the redesigned vehicle models. They also showed that they can perform comparative analyses and recognize in the graphical representation the critical points in the geometry of the 3D model, the modification of which results in better model performance. Examples of works are illustrated in Figures 2, 3, 4 and 5.

The topics chosen by the students were comparing cars (Fig.3 and 4), trucks, planes (Fig.5) and aircraft from the Star Wars movies (Fig.6). Interesting results were obtained in all cases and after the submission of papers, a discussion was held on key points for improving the design in terms of aerodynamic performance on the analyzed examples. Students showed great interest in this type of analysis in their later work. The examples are shown in the following.

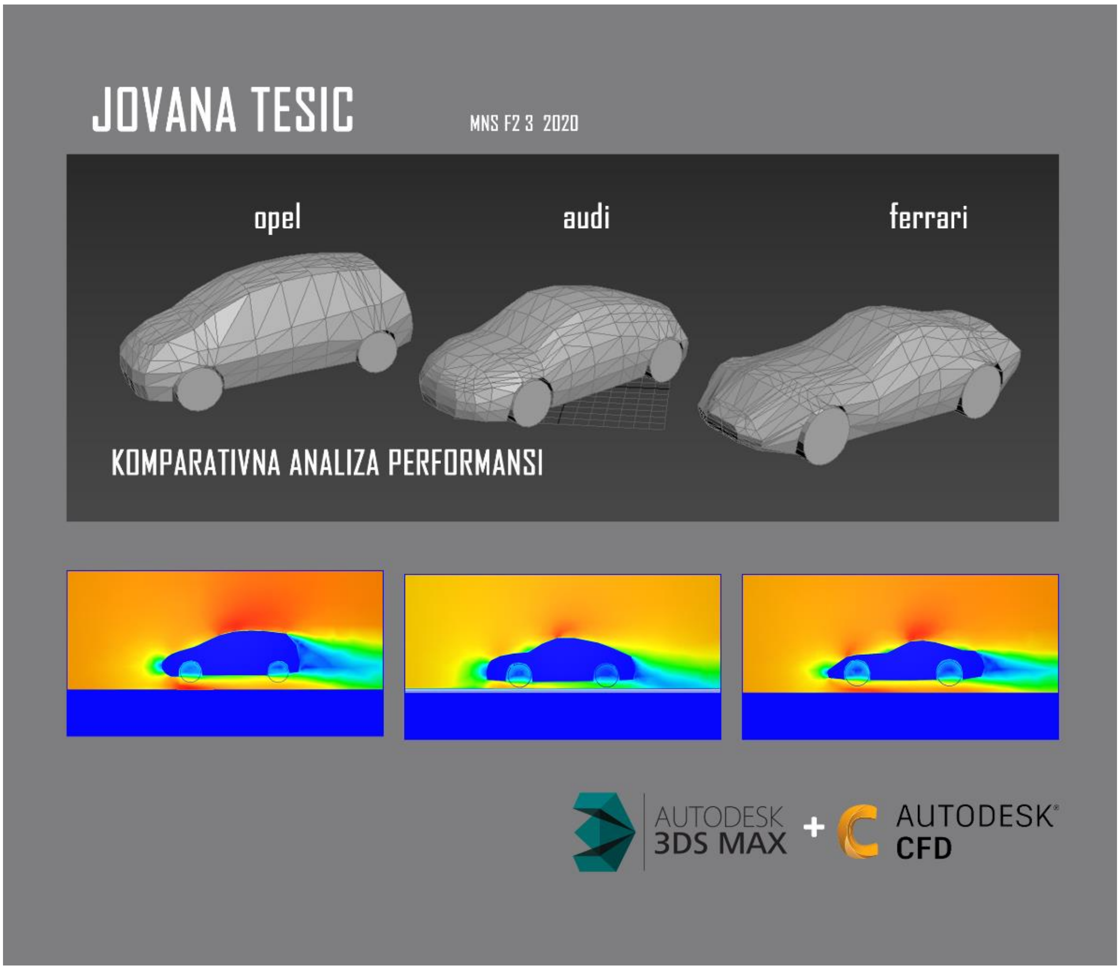


**Figure 3**: The graphical representation of the aero-dynamical performance analysis of 3D car models of the car brands Opel, Audi and Ferrari by student Jovana Tešić

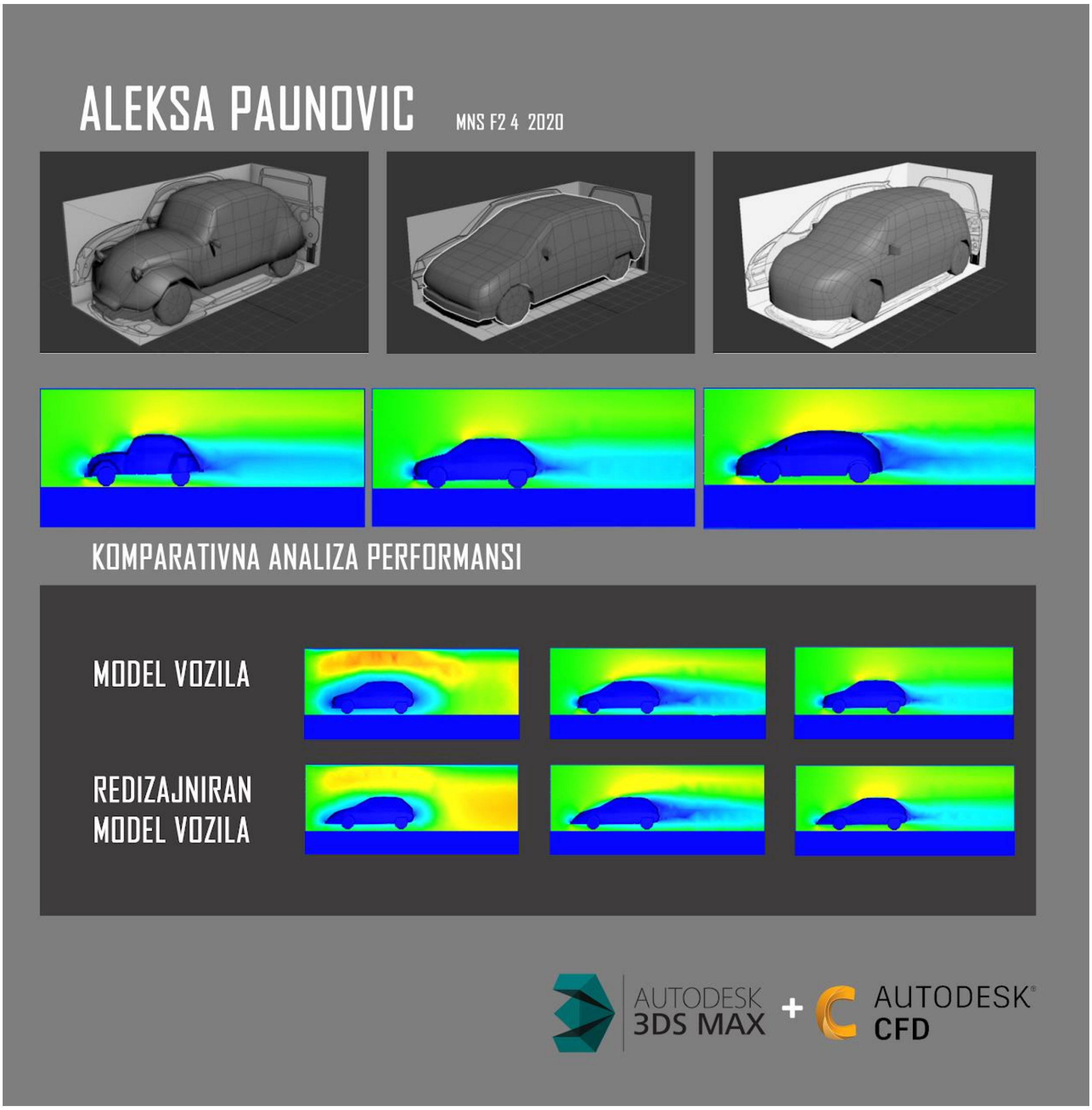


**Figure 4**: The graphical representation of Example of comparative analysis and design correction based on aerodynamic performance by Aleksa Paunović

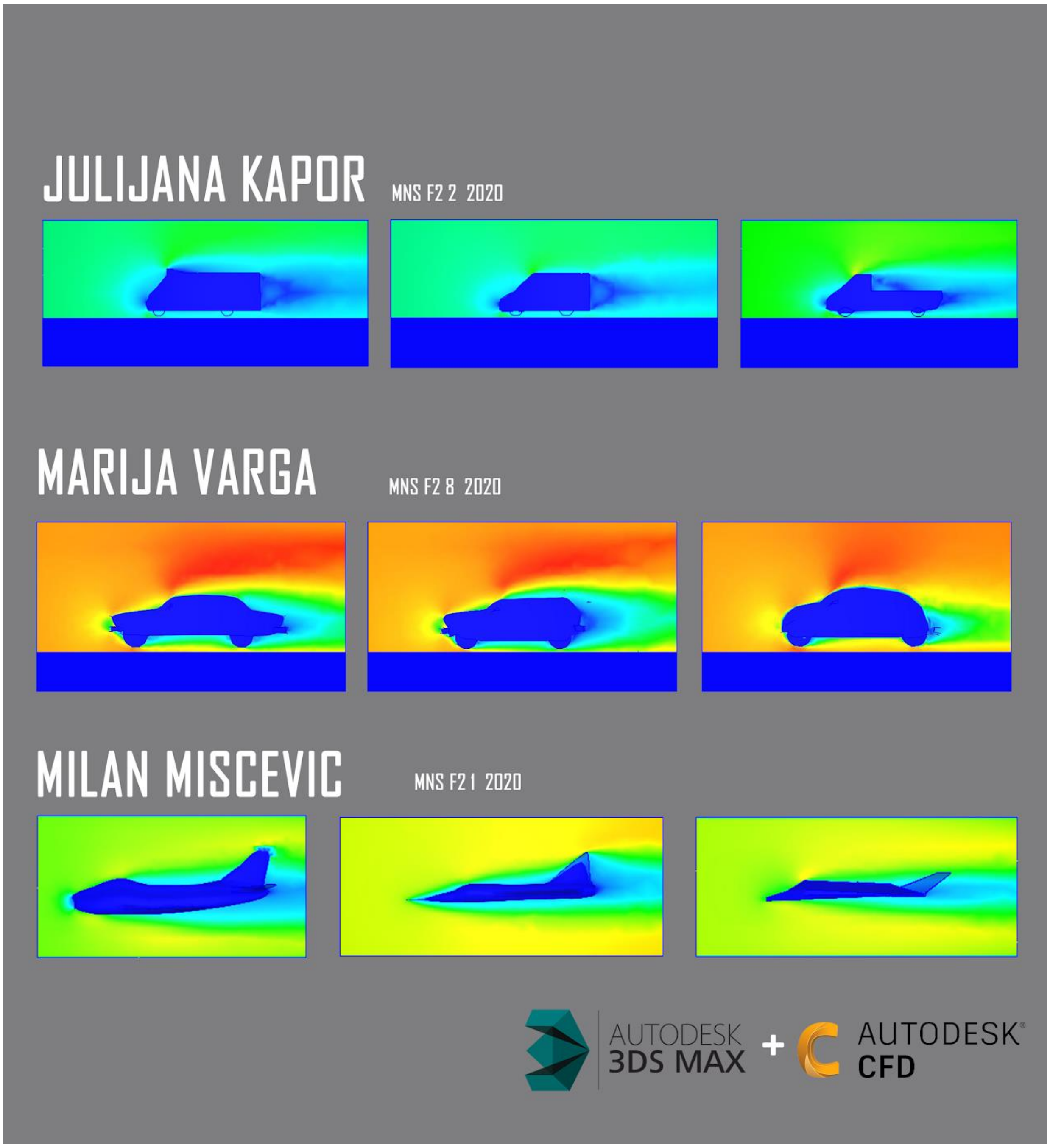


**Figure 5**: The graphical representation of aerodynamic analysis of design for different types of vehicles by Marija Varga, Milan Miščević and Julijana Kapor.

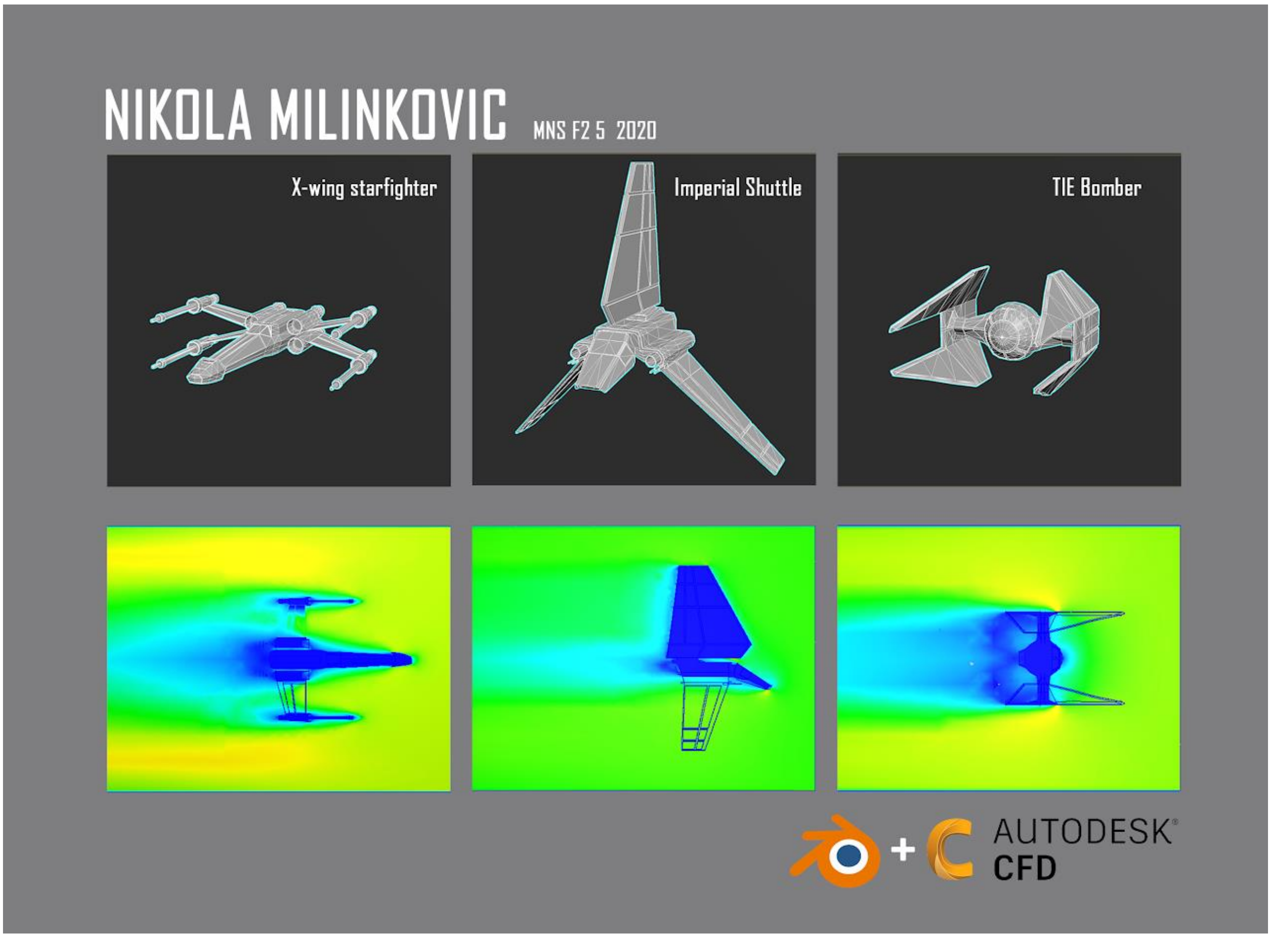


**Figure 6**: The graphical representation of aerodynamic analysis of science fiction vehicle design-aircraft from the Star Wars movies by Nikola Milinković

The results show that the program of this course, our master students attended, has successfully prepared them for design performance assessment by simulation. They are able to recognize and upgrade the design of various 3D models of vehicles according to the environment and situational assessment in the software Autodesk CFD.

## 6. CONCLUSION

Computer simulations are an important area that is becoming increasingly popular in various scientific disciplines. Work on simulations in education has shown significant results in terms of understanding the design process and complex systems.

In the previous section on Results, the projects illustrated show that students achieved the anticipated results and beyond when working with the proposed program. They prove that it is possible to successfully apply the proposed methodology of work with a general overview of different simulations in lectures and with work in CFD software in exercises. This format of combining experimental and deductive methodology in education has proven the right choice for master students of Engineering Animation.

The observations in this paper can help to specify similar courses in studies for students who are previously acquainted with the basic principles of 3D modeling and design. In future work, we plan an expansion in the form of various other simulation tools and software environments testing the limits of current technologies from the aspect of performance design. In order to test different scenarios students will be able to adapt their projects even more to their professional field of interest.

## REFERENCES


1. AbouRizk, S.M. and Hajjar, D., 1998. A framework for applying simulation in construction. *Canadian journal of civil engineering*, 25(3), pp 604-617.

2. Ameli, M., Mansour, S. and Ahmadi-Javid, A., 2019. A simulation-optimization model for sustainable product design and efficient end-of-life management based on individual producer responsibility. *Resources, Conservation and Recycling*, 140, pp 246-258.

3. ACFD, 2021. https://www.autodesk.com/products/cfd/overview [Accessed: 1st June 2021].

4. AMAX, 2021. https://www.autodesk.com/products/3ds-max/overview [Accessed: 1st June 2021].

5. Gros, A., et al., 2016. Simulation tools to assess microclimate and building energy–A case study on the design of a new district. *Energy and Buildings* 114, pp 112-122.

6. Ingalls, R. G., Cornejo, M., Methapatara, C., and Sittivijan, P. 2008. Integrating simulation and optimization research into a graduate supply chain modeling course. Proceedings of Winter Simulation Conference Miami, USA. pp. 2527-2533.

7. Jones, M.A., 2013. CFD Analysis and Design Optimization of Flapping Wing Flows (Doctoral dissertation, North Carolina A&T State University).

8. McKenna, F., 2011. OpenSees: a framework for earthquake engineering simulation. *Computing in Science & Engineering*, 13(4), pp 58-66.

9. Prauzner, T., 2016. Interactive computer simulation as a response to contemporary problems of technical education. Proceedings of the International Scientific Conference in Society. Integration. Education, Rezekne, Latvia. Vol. 2, pp. 579-588.

10. Rutten, N., Van Joolingen, W. R., and Van Der Veen, J. T. 2012. The learning effects of computer simulations in science education. *Computers & Education*, 58(1), pp 136-153.

11. Spalart, P. R. and Venkatakrishnan, V., 2016. On the role and challenges of CFD in the aerospace industry. *The Aeronautical Journal*, 120(1223), pp 209-232.

# ONLINE PRACTICE CLASSES AT THE ACADEMIC COURSE GEOMETRIC SURFACES IN ARCHITECTURE AT THE FACULTY OF CIVIL ENGINEERING AND ARCHITECTURE IN NIS

S. Krasić[1], Z. Tošić[1], J. Stanković[1], N. Kocić[1]

[1]University of Nis, Faculty of Civil Engineering and Architecture, Department of Visual Communications, 18000 Nis, Serbia

krasic.sonja@gmail.com

***ABSTRACT***

*Practical classes at the academic course Geometric Surfaces in Architecture (furher GSA) at the Faculty of Civil Engineering and Architecture (further FCEA) in Nis are conducted in the second year of the study program Architecture, with a fund of 45 minutes, in software Rhinoceros. In practical classes students model architectural objects, from geometric surfaces, that they learned in the theoretical part, in the computer software Rhinoceros. For practical classes, the authors prepared templates for exercises, in which students have explanation in text and drawings how to model a given surface. In live practical teaching, the explanations for solving the tasks are repeated until all the students have completed the entire model of the object.*

*In online practice classes, conducted using the Microsoft Teams platform, the academic hour is shortened to 30 minutes. Each class is recorded and placed on a platform, with repeated explanations, so that students can complete the exercise task. In addition, the author team prepared video instructions for exercises in Web Launch Recorder Software. In the video recorded in this software, the process of making a model of the object is clearly indicated, the image and sound are of good quality. Since the video lasts 15 minutes, the commands are not repeated when modelling. It took two videos to make some tasks. The aim of the paper is to show how, with the help of modern software, it is possible to organize practice classes that are conducted online, to help students more easily master the course program at FCEA in Nis.*

**Keywords**: Geometric Surfaces in Architecture, online practical classes, video instructions

## 1. INTRODUCTION

The application of geometric and free-form surfaces for the design of buildings in modern architecture is expanding. Therefore, it is necessary for architects to get acquainted with the basic characteristics and the way of modeling geometric surfaces while studying. To design the architecture under its various forms, a student in architecture needs to know the geometry of these forms [3]. Whereas the variety of shapes that could be treated by traditional geometric methods has been rather limited, modern computing technologies have led to a real geometry revolution [9]. This was noticed by the authors of the paper and already in the academic year 2009/10 it was introduced into the curriculum, in the study program Master of Architecture, course Geometric Surfaces in Architecture (furher GSA) at the Faculty of Civil Engineering and Architecture (further FCEA) in Nis. Students could use the knowledge they gained in this academic course only for the preparation of final master's works. After that, from the academic year 2016/17, the GSA course is foreseen in the curriculum of the second year of integrated academic studies of architecture, with a fund of 1 + 1 hour (1 – 45 minutes). From this academic year, students were able to use the acquired knowledge of geometric surfaces not only for the final project in this course, but for all final projects within other courses in the study of architecture. The GSA course program increases students' creativity, which can be seen in their final projects. The GSA academic course at FCEA in Nis consists of theoretical and practical part.

## 2. THEORETICAL CLASSES ON THE GSA COURSE

In the theoretical part of the GSA course, students are introduced to the types and characteristics of geometric surfaces and examples of derived architectural objects. (Table 1.). Theoretical classes are conducted in 12 units, of which the first two are introductory. In the first unit, students are introduced to the content and goals of the GSA course, using examples of derived architectural objects and the best final projects, of students of previous generations, on the subject. Surface classification and historical development are represented in the second unit. From the third unit, students learn about geometric surfaces according to the classification given in the second unit. Lectures are conducted orally with the help of PowerPoint presentations (fig. 1 and 2). Figures 1 and 2 show representative slides from the presentation for unit 8 – Conoids, cylindroids and tetroids and for unit 9 – Revolving and Elliptical hyperboloids of one sheet and Hyperbolic paraboloids. Each unit contains slides on the method of constructing a given surface (fig. 1(a), 2(a)), then slides with planar sections and breakthroughs (fig. 1(b), 2(b)) and examples of derived architectural objects from a given surface.

| | | | |
|---|---|---|---|
| Unit 1 | Introduction in course | Unit 7 | Helicoids |
| Unit 2 | Classification of the surfaces | Unit 8 | Cylindroids, Conoids and Tetroids |
| Unit 3 | Regular polyhedra, Platonic and Archimedean solids | Unit 9 | Revolving and Elliptical hyperboloids of one sheet and Hyperbolic paraboloids |
| Unit 4 | Pyramids and prisms | Unit 10 | Double curved surfaces - Sphere |
| Unit 5 | Cones and cylinders | Unit 11 | Ellipsoids, Paraboloids and Hyperboloids of two sheets |
| Unit 6 | Twisted surfaces | Unit 12 | General surfaces of revolution, Torus and Sliding surfaces |

**Table 1.** Content of lectures in course GSA on FCEA in Niš, (Source: Krasic et al. 2018)

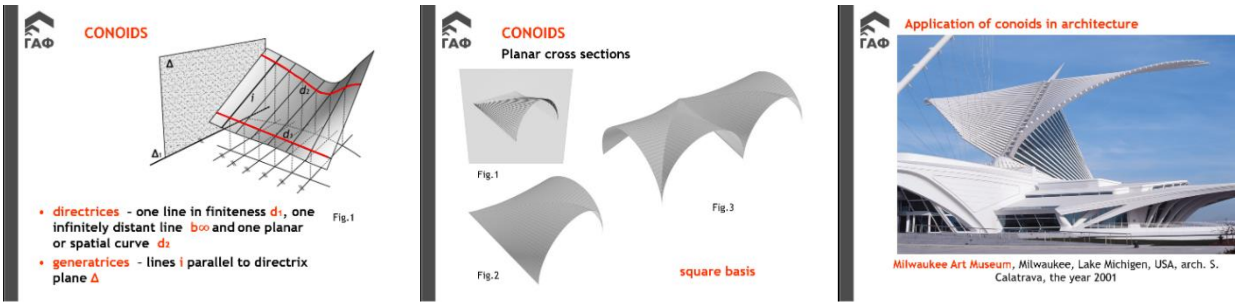


(a) (b) (c)

**Figure 1.** Presentation for unit 8 – Conoids, cylindroids and tetroids (a) method of constructing a given surface, (b) planar sections, (c) derived architectural objects (Source Krasic 2012)

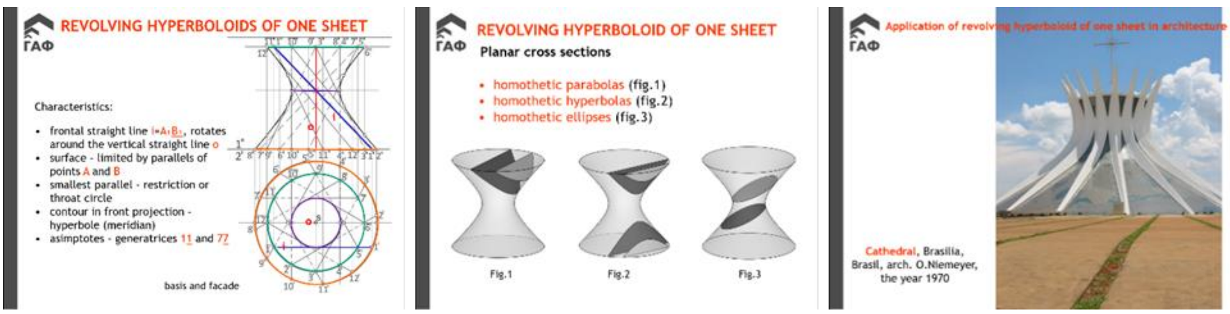


(a) (b) (c)

**Figure 2.** Presentation for unit 9 – Revolving and Elliptical hyperboloids of one sheet and Hyperbolic paraboloids (a) method of constructing a given surface, (b) planar sections, (c) derived architectural objects

Powerpoint presentations help students to better master the course, and examples of derived architectural objects from geometric surfaces serve as inspiration for their final project on the course, which carries 35 points (35%). The final project in the GSA course is the design of an architectural object from one geometric surface given by professor, which should be presented through perspective images, orthogonal projections and steps by which the object is designed.

## 3. PRACTICAL CLASSES ON THE GSA COURSE

In the practical part of the GSA course, students learn to model architectural objects, from the geometric surfaces they have mastered in the theoretical part of the course. (Table 2.). The didactic principle of gradual problem solving is represented in the preparation of practical classes which are performed in 12 units, in the CAD software Rhinoceros. Modern teaching aids, computer and software for drawing and modeling, Rhinoceros, were introduced, and the didactic principle applied in the classical teaching method was retained. In this software simply models architectural objects created from geometric surfaces. Since students are encountering the computer CAD software Rhinoceros for the first time, the first three units explain the basic commands for manipulating the software, then the commands for drawing points, lines, polygons, planar and spatial curves and options for modeling geometric surfaces and solids.

From the fourth to the twelfth unit, geometric surfaces are modeled according to the classification, which is given in the theoretical part of the teaching. Considering that there is a small fund of practice classes (45 minutes), and students should get acquainted with the way of modeling as many geometric surfaces as possible, the practical part of the classes is created so that one geometric surface is done in an exercise (fig. 3(a)), and the other as homework (fig. 3(b)). Examples of architectural objects that are attractive and for whose modeling it was possible to use a number of different options offered in the Rhinoceros CAD software were selected for the practical classes. Thus, for example, for unit 9 was chosen to model the „Chapel St. Vicente de Paul, Mexico City, Mexico, arch. F. Candela” (fig. 4(a) and 5(a)), and for unit 10 was chosen to model the „Cathedral Brasilia, Brazil, arch. O. Niemeyer” (fig. 4(b) and 5(b)). The author's team decided to create a templates for exercises and homework in which the "step by step" method explains how to model an architectural object from a given surface. The steps for solving the tasks are explained textually and with the help of drawings, so that the students can more easily follow the way of modeling in the exercises and do their homework on their own (fig. 8). Exercise tasks are designed so that they can be completed in class, with the help of an assistant. The architectural objects that are done in the exercise class are more complex than the architectural objects that are done for homework. All exercises and homework are evaluated and thus pre-examination points are achieved, 65 (65%).

| | | | |
|---|---|---|---|
| Unit 1 | Rhinoceros – points, lines and polygons | Unit 7 | Rhinoceros – Oblique helical staircase and normal helical staircase (homework) |
| Unit 2 | Rhinoceros – free form curves, conics and spatial curves | Unit 8 | Rhinoceros – Conoidal canopy and cylindroid (homework) |
| Unit 3 | Rhinoceros – surfaces and geometric solids | Unit 9 | Rhinoceros – Hyperbolic paraboloid object and spherical canopy (homework) |
| Unit 4 | Rhinoceros – Pentagonal dodecahedron and icosahedron (homework) | Unit 10 | Rhinoceros – Revolving hyperboloid of one sheet object and spherical slice (homework) |
| Unit 5 | Rhinoceros – Pyramidal folds and prism’s folds (homework) | Unit 11 | Rhinoceros – Triaxial ellipsoid object and paraboloid object (homework) |
| Unit 6 | Rhinoceros – Conical folds and cylinder’s object (homework) | Unit 12 | Rhinoceros – Torus object and sliding surface (homework) |

**Table 2.** Content of exercises in course GSA on FCEA in Niš,
(Source: Krasic et al. 2018)

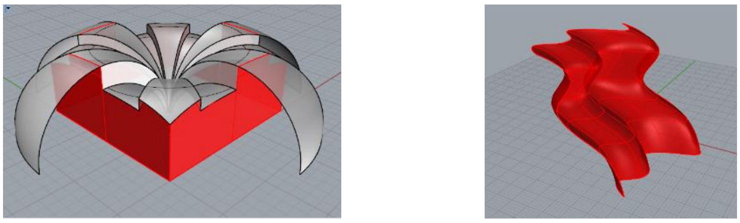

(a) (b)

**Figure 3.** Final models (a) Torus object – exercises 12, (b) Sliding surface – homework 12

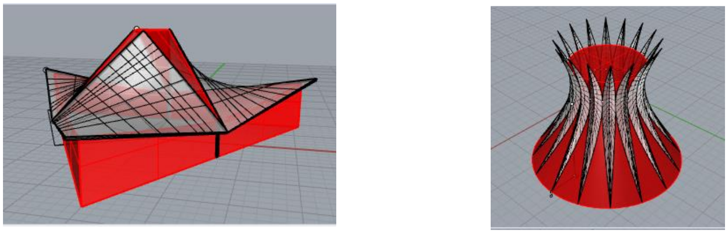

(a) (b)

**Figure 4.** Final models (a) Chapel St. Vicente de Paul, Mexico City, Mexico, arch. F. Candela – exercise 9, (b) Cathedral Brasilia, Brazil, arch. O. Niemeyer – exercise 10

(a) **(**b)

**Figure 5.** Photographs (a) Chapel St. Vicente de Paul, Mexico City, Mexico, arch. F. Candela – exercise 9, (b) Cathedral Brasilia, Brazil, arch. O. Niemeyer – exercise 10

### 3.1 Live Practice Classes at The Course GSA

Live practice classes are organized so that the assistant solves the task, following the steps in the exercise templates, on his computer, and the desktop of the CAD software Rhinoceros is projected onto the canvas using a video beam. Each student monitors the work of the assistant on their computer. The practical lesson lasts 45 minutes and is performed in groups of max 15 students. At the exercise class assistant has enough time for explanation for all units. In addition, it is possible to move back and forth when working in the program, so that all students can complete the modeling of the architectural object in class. When conducting practical classes live, assistants can also dedicate themselves to individual work with students, thanks to the exercises templates, "step by step". Modeling architectural objects in exercises, for units 1, 2, 3, 4, 5, 6, 8 and 11 is simpler, and for units 7, 9, 10 and 12 is more complex. For homework were selected architectural objects which can be modeled in a shorter time than objects in exercises, that is individual for each student.

**3.. Online Practice Classes at The Course GSA**

Due to the measures implemented due to the Corona virus epidemic, which did not allow the presence of students in the premises of the Faculty, online teaching was organized. Online classes are organized through the business communication platform Microsoft Teams, which is used to all higher education institutions in Serbia for this type of teaching.

Each leson is organized according to the principle of video conference. The assistant invites to class and shares with the present students his screen, on which is the desktop of CAD software Rhinoceros. During the exercise class, the assistant solves the task on his/her computer, following the steps in the templates. Each student models the object independently on his/her computer, following the work of the assistant. The practical class hour lasts 30 minutes and is performed in groups of max 15 students. Due to the fact that the class is shortened in relation to live teaching, the assistant does not have enough time to move back and forth during work and there is no possibility to dedicate individually to each student. Exercise classes are recorded and posted on the platform as video instructions, so that each student can finish the task from the exercise. However, the quality of the video obtained using the Microsoft Teams platform is not always the best, because there are occasional interruptions in the sound, and occasionally the image loses clarity.

Therefore, the author team was hired to make video instructions in other software Web Launch Recorder 2.0. This software can be downloaded for free from the Internet and is suitable for education. The advantages of this software are that the picture and sound quality in the recorded video is better than in the recording made via the Microsoft Teams platform. The process of making videos in this software is simple. The disadvantage of the software is that the video lasts a maximum of 15 minutes, so for more complex exercises, two videos had to be made. In addition, there is no repetition of steps in the video, but it is possible to stop and return during the review, so software Web Launch Recorder 2.0 was chosen to record a video instruction for exercises from the GSA subject. Since there are templates step-by-step for exercises, with video instructions recorded via the Microsoft Teams platform and via Web Launch Recorder 2.0, all students were able to complete the exercise tasks and get the maximum number of points for it. So far, no video instructions for homework have been created, but in the next period, it will be the task of the author's team.

**4. CASE STUDY – VIDEO INSTRUCTION FOR EXERCISE 8**

The case study will show a video for one of the exercises in the course Geometric Surfaces in Architecture, recorded in Web Launch Recorder 2.0 software. Exercise 8 – modeling conoid was chosen, which is one of the simpler (fig. 6 and 7). This video lasts 13:26 minutes, which shows that the modeling of the conoid canopy from figure 8 is one of the exercises, for which one video was enough. Figure 6 shows what the template for exercise 8th looks like with an explanations in steps, textually and by using drawings. The video instruction for the 8th exercise will be accompanied by pictures of characteristic steps, which will be highlighted in the video, whereby during the presentation of the work the picture can be shown together with the sound. Figures 8 - 10 show the final appearance of steps 1 - 8 from the 8th exercise pad (fig. 8) in the Rhinoceros CAD software. Figures 11 and 12 show the initial appearance of steps 9 and 10 with a drop-down menu and the final appearance of the same steps from the exercise 8 (fig. 7) in the Rhinoceros CAD software. The final model of the conoid canopy is shown in all four views in figure 13.

**EXERCISE 8 – Rhinoceros: Conoid**

Procedure for constructing conoidal canopy in figure 7:

1. In **Top** view, draw square of 6x6m with **Curve / Rectangle / Corner to corner** option;
2. In **Front** view, draw semicircle above one of the square sides using the options **Circle**, **Line**, **Trim**;
3. In **Perspective** view, using the option **Surface / Loft** connect semicircle with the opposite side of square (*if square is polyline separates lines with* **Explode** *option*);
4. Using the option **Surface / Plane / Plane Cutting** in **Top** view set vertical intersection plane along the diagonal of square;
5. Use **Trim** option to remove lower part of conoid;
6. Using the option **Cut** or **Delete** on keyboard delete vertical plane;
7. Using the option **Transform / Mirror** in **Perspective** view mirror part of conoid in relation to diagonal of square;
8. In **Perspective** view, give thickness of conoid to inside (*down*) using the option **Solid / Offset, 0.2m,** take care of direction of vector (*direction of vector changes by left clicking on surface*);
9. In **Perspective** view make a pillar using the option **Solid / Box / Corner to Corner 0.2x0.2, Height 4m** and using the option **Transform / Copy** copy pillars in corners of the square in basis as supports for conoids;
10. Using the option **Transform / Array / Polar, Number of items 4, angle 360$^0$** rotate and copy conoids with pillars;


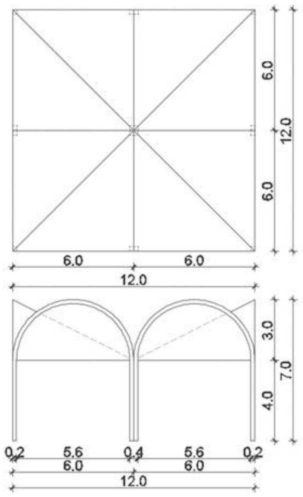


**Figure 6:** Template for exercise 8 – modelling conoidal canopy (left) and top and front view (right)

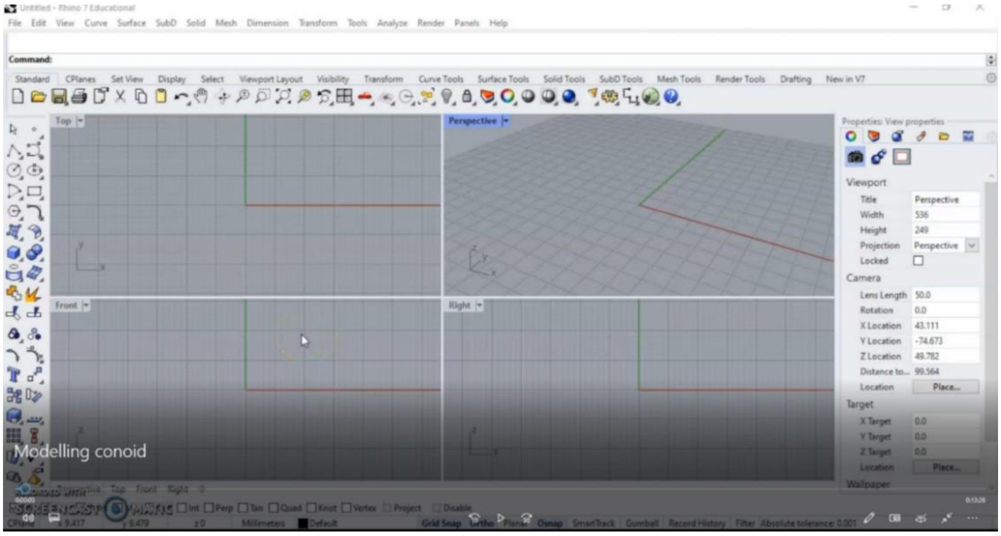


**Figure 7**. Desktop Rhinoceros software in Web Launch Recorder 2.0

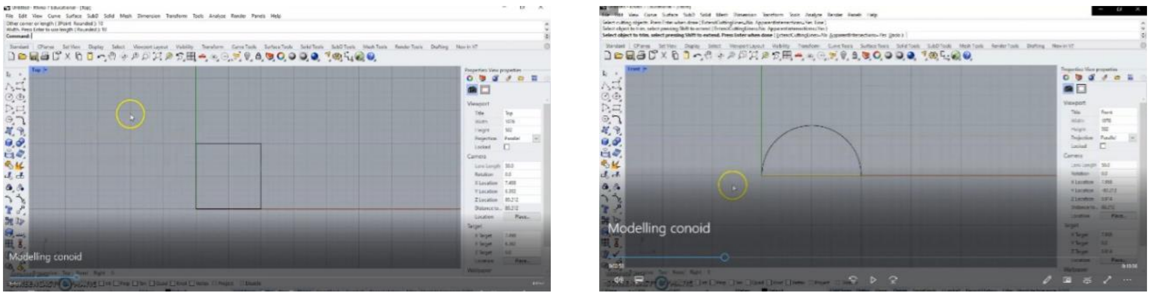


(a) (b)

**Figure 8.** Modelling conoid – video instruction, (a) step 1, (b) step 2

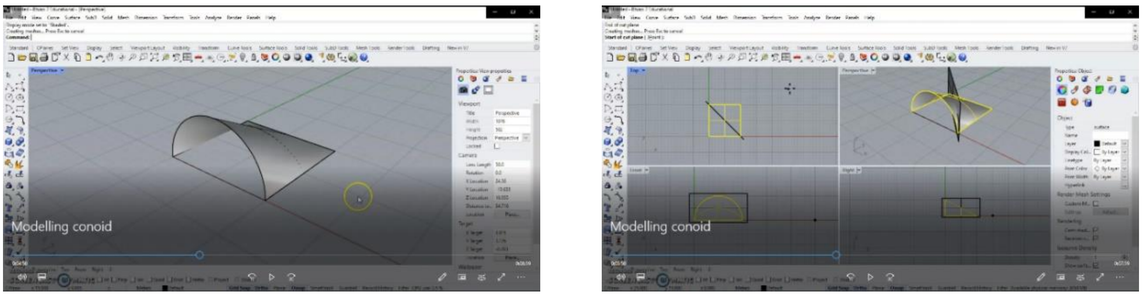


(a) (b)

**Figure 9.** Modelling conoid – video instruction, (a) step 3, (b) step 4

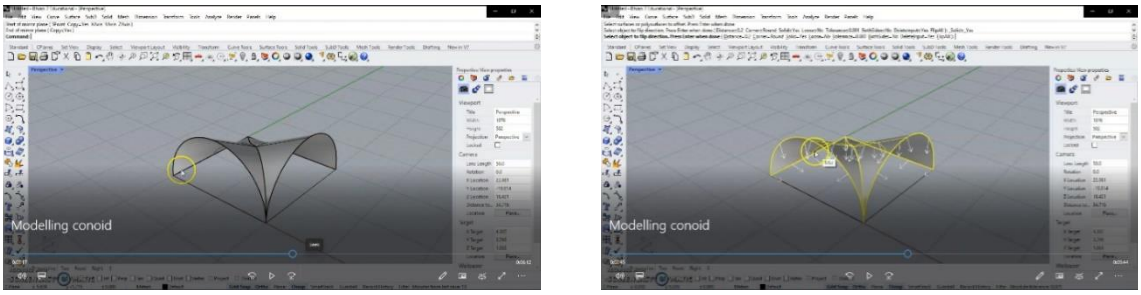


(a) (b)

**Figure 10.** Modelling conoid – video instruction, (a) step 7, (b) step 8

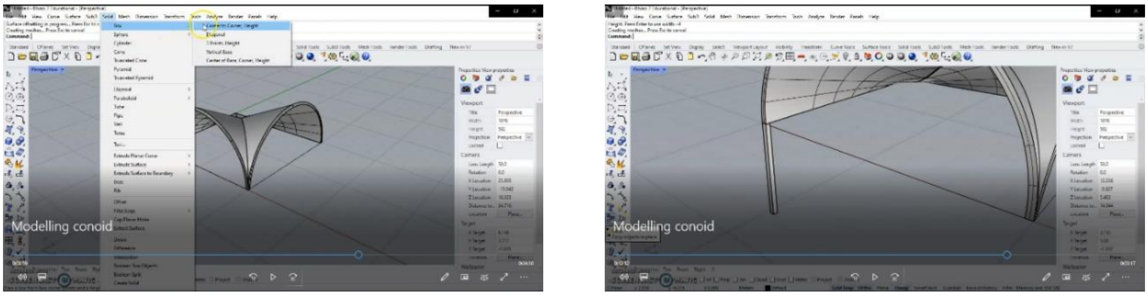


**Figure 11.** Modelling conoid – video instruction, (a) step 9, (b) step 9

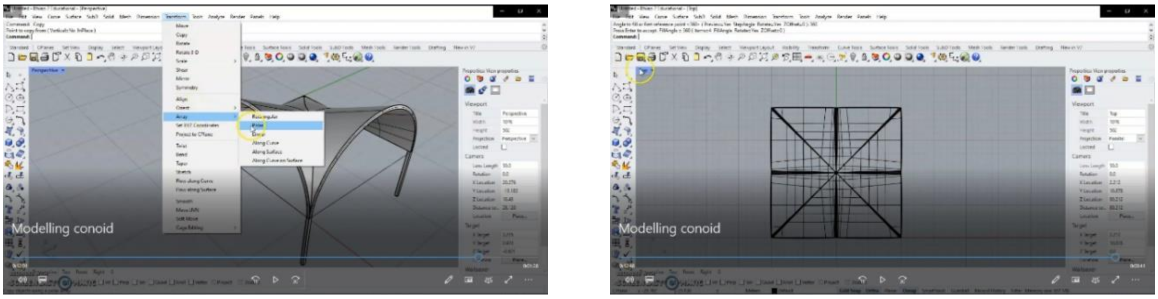


(a) (b)

**Figure 12.** Modelling conoid – video instruction, (a) step 10, (b) step 10

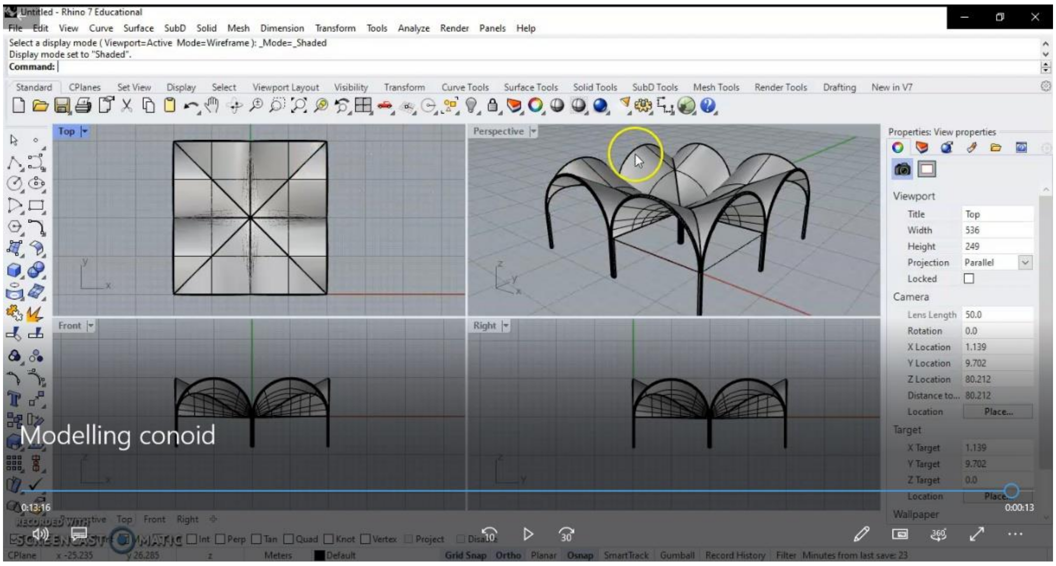


**Figure 13.** Modelling conoid – video instruction final appearance of conoidal canopy

## 5. EVALUATION

Obligatory conditions for students to fulfill during semester is to submit all 12 exercises and 12 homework and fulfill 50% of the prescribed pre-exam points, which are 30 points. In the academic year 2020/21, 76 students attended the GSA course, which were divided into 5 exercise groups. From that number, 68 students (89,5%) fulfilled the condition for submitting the final project. The maximum number of pre-exam points, 65, was achieved by 27 (35,5%) of students. No survey was conducted among students on opinion on the: course organization and their improvements in mastering engineering skills and geometric knowledge. In the conversation with the students during the classes, we found out that, video instructions and templates with steps for making exercises and homework is very useful for them.

The video instructions were also of great benefits for student's improvements in mastering engineering skills and geometric knowledge.

## 6. CONCLUSION

The video instruction for the 8th exercise from the GSA course is one of 12 recorded in Web Launch Recorder 2.0 software and posted on the Microsoft Teams platform. All video instructions, along with recorded exercise classes conducted through the Microsoft Teams platform, are of great use to students in mastering the GSA course material. Since mastering the modelling of geometric surfaces in the CAD software Rhinoceros is necessary to do the final project on this academic course, students in this way received the necessary information, which remains permanently written down. All video instructions are of great help to students for their future work on other design academic courses at the FCEA in Niš.

## REFERENCES


1. Asensi F.I., 1975. *Geometria descriptiva superiory aplicada*, Editorial dossat. S.A. Madrid, Spain

2. Brauner H., Kickinger W., 1980. *Geometrija u graditeljstvu*, Školska knjiga, Zagreb, Croatia

3. Graur A. M., Marza C., Corsiuc G., 2018. The helical surfaces and their application in students' works, Proceedings of Mongeometrija 2018, Novi Sad, Faculty of Technical Science, University of Novi Sad, pp. 575-584.

4. Krasić S., 2012. *Geometrijske površi u arhitekturi*, Građevinsko—arhitektonski fakultet, Univerzitet u Nišu, Niš, Serbia

5. Krasić S., Ando N., Pejić P., Tošić Z., 2018. Comparative Analysis of Teaching in Geometric surfaces at Architectural Faculties in Niš and Tokyo, Part of Advances in Intelligent Systems and Computing, book series (AISC, volume 809), Springer, Tiergartenstraße 17, 69121 Heidelberg, Germany, www.springer.com, pp. 1611-1623.

6. Krasić S., Ando N., Pejić P., Tošić Z., 2019. Teaching of Geometric Surfaces for Architectural Students at the Faculty of Engineering and Design, of Hosei University in Tokyo, Japan, FME Transactions, VOL.47, No.2, pp.293-298.

7. Krasić S., Tošić Z., Pejić P., 2019. Introduction of Rhinoceros software for exercises of subject Geometric Surfaces in Architecture, Journal of industrial Design and Engineering Graphics, number 14, Issue 1, Section 5, pp. 303-309.

8. Pottman H., Asperl A., Hofer M., Kilian A., 2007. *Architectural geometry*, Bentley Institute Pres, Pennsylvania, USA

9. Veljković M., Krasić S., Pejić P., 2016. Use of the torus in the design of modern architectural structures, Book of abstracts, International scientific conference on Geometry and Graphics, MoNGeometrija 2016, pp. 125-126.

10. Veljković M., Krasić S., Pejić P., Tošić Z., 2017. A case study of modeling a torus in different modeling softwares, Journal of industrial Design and Engineering Graphics, number 12, Issue 1, Section 1, pp. 37-40.

# HOW DO CHILDREN LEARN ABOUT TRAFFIC SAFETY IN A GEOMETRICALLY MODELED ENVIRONMENT?

Aleksandar Trifunović[1a]*, Dalibor Pešić[2b], Dragan Lazarević[3c], Maja Petrović[4d]

[1] University of Belgrade - The Faculty of Transport and Traffic Engineering, 11000 Belgrade, Serbia,

[a] PhD, Assistant Professor, a.trifunovic@sf.bg.ac.rs

[b] PhD, Associate Professor, d.pesic@sf.bg.ac.rs

[c] PhD, Assistant Professor, d.lazarevic@sf.bg.ac.rs

[d] PhD, Assistant Professor, majapet@sf.bg.ac.rs

***ABSTRACT***

*The application of geometric modelling in many scientific fields (engineering, educating, etc.) has made it possible to solve a problem, which by then seemed unsolvable, and it has opened new opportunities for improving and linking different fields. Connecting interactive tests and computer-assisted education in the field of traffic safety enables geometric modelling. Creating a virtual traffic environment, using computers, is a powerful tool for testing and educating children. The flexibility, economy, safety, and attractiveness, which is enabled by the application of geometric modelling, for experimental purposes, in the field of child traffic safety, represents a great potential for improving this area and creating a safe traffic system for children. In the field of child traffic safety, this tool is very sparingly used and presented in professional and scientific literature. Educational material, that can be shown to children using geometric modelling, brings traffic safety closer to children's thinking, while on the other hand, through play and education, enable to safe participation of children in traffic. For these reasons, an experimental study was conducted on educating children about traffic safety, in a virtual (computer) and real (traffic playground) environment. The experiment involved 48 subjects, aged between 8 and 10 years. The results showed that children achieve better results when solving tasks in a virtual environment.*

**Keywords:** geometric modelling, education, traffic safety, children, virtual and real environment.

## 1. INTRODUCTION

According to the World Health Organisation, each year in the world 75 million people suffer from injuries, and 23% of trauma victims die or suffer permanent disability (Goniewicz et al., 2017). A road traffic accident is a leading cause of death among infants and children in both developed and developing countries (Park et al., 2018). Children are more likely to be injured from road traffic accidents than adults and are more susceptible to intracranial injury, which is one of the most common fatal injuries (Park et al., 2018). According to Global Burden of Disease data estimates, about 34 thousand children ages between 5 and 14 died from road traffic accident in 2017, whilst about 25,000 (74%) of those deaths were child pedestrians (Wang et al., 2021). In the Republic of Serbia, 39 children were killed and another 4,446 children were injured in traffic accidents, when the period from 2017 to 2019 is observed (ages of 0 to14). After 2010, a stable downward trend is observed, which was interrupted in 2015 and 2017 (ABS, 2018). In 2015, there was an increase in the number of children killed, when 14 children died. In 2016, 12 children died, while in 2017, 17 children died, which is the highest in the last six years (Traffic Safety Agency, 2020).

One prominent risk factor is children’s cognitive-perceptual skills. Since children’s cognitive-perceptual skills naturally develop through the early and middle childhood years, they demonstrate inadequate knowledge about road safety rules and practices (Koekemoer et al., 2017), misperceive risk from oncoming traffic (Poudel-Tandukar et al., 2007), and demonstrate inadequate attention and visual searching abilities amidst traffic (Tabibi and Pfeffer, 2007). Deficits in these cognitive-perceptual skills increase risk for traffic-related injuries (Wang et al., 2021).

Pedestrian-oriented educational measures may change children's behavior when crossing the street, but it is still unknown whether they effectively reduce the risks of motor vehicle-pedestrian collisions. Thoughtful and age-appropriate road safety instructions within the context of family, school and community is required. An early, presentation of road safety will also influence the belief in system and mind-set of current and future road users and their attitude toward safety (Trifunović et al., 2017).

*- Children Education*

Education, which is regularly conducted on children of preschool and school age, has always been the best measure for improving the safety of children in traffic (Dragutinovic and Twisk, 2006). Although education is a key measure in preparing children for independent participation in traffic, its effects are limited (Twisk et al., 2007, Trifunović, 2020). Teachers often adopt passive lecture format and attempts to teach all of the content from the literature. Therefore, it is difficult that students develop a genuine interest in learning about any area, and even about traffic. This method of learning is dull and monotonous, and too much emphasis tends to be placed on the training of theoretical knowledge. Consequently, it is easy for children to lose interest in learning (Li, 2011; Sun, 2018). Also, educators can create an environment in which children are eager to explore and learn about traffic safety (Trifunović et al., 2017; Trifunović et al., 2018). In contrast, a better way for children is to integrate traffic education explicitly with new technologies. In support of this view, Pešić et al. (2019a) showed that active learning, with the application of new technologies, opportunities provide a fertile ground for the application of concepts beyond theory, and consequently, children learners can better understand traffic safety, and thus be safer road users.

It is the application of geometric modeling that can connect children's education about traffic safety and new technologies. Geometric modeling is a discipline that studies the methods of constructing geometric and natural forms by means of computer graphics and enables the creation of these forms in a real environment (Lieu and Sorby, 2015). Graphic communication is a universal tool for accurately describing the size, shape, and interrelationships of the physical components that make up some systems (Lieu and Sorby, 2015). Creating a traffic environment in the virtual world, using computers, is a powerful tool for testing and educating children. In the field of child safety in traffic, this tool is very sparingly used and presented in the professional and scientific literature.

For these reasons, an experimental study was conducted on educating children about traffic safety, in a virtual and real environment. The virtual environment is showed on the computer, while the real environment is showed on the traffic playground. The aim was to examine whether there are differences between the two environments, as well as to examine potential gender differences in the education of children in the field of traffic safety.

## 2. METHODOLOGY

*- Participants*

The experiment involved 48 subjects, aged between 8 and 10 years. 24 respondents are female and the same number of respondents are male. The respondents are from primary schools located in Belgrade and Rača Kragujevačka. There is parental consent for all respondents. The experiment was conducted in compliance with all ethical principles and regulations.

*- The design of an experimental environment*

For the purposes of this research, four traffic situations were geometrically modeled, on a traffic playground and identical situations on a computer. The traffic playground was created in the AutoCAD software, and it is made of colored canvas, size 7x8 meters. For traffic situations in a virtual environment, some situations were created in free software packages for mobile applications, and the application of the Traffic Safety Agency was also used. The appearance of traffic situations is shown in Table 1 and Table 2. The task of the children was to cross the street safely at the traffic lights, as pedestrians (Table 1) and as cyclists (Table 2).

| ***Traffic situations*** | ***Virtual Environment*** | ***Traffic Playground*** |
| --- | --- | --- |
| Red light at a traffic light (pedestrian) | 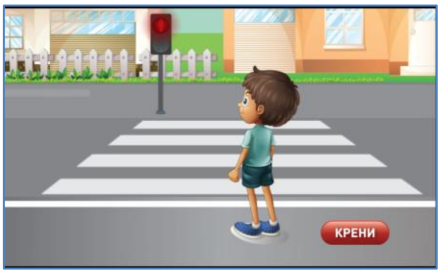 |  |
| Green light at a traffic light (pedestrian) | 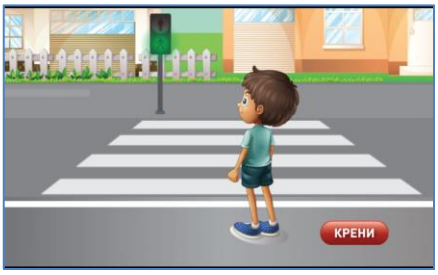 |  |

**Table 1** Traffic situations presented to children (pedestrian)

| ***Traffic situations*** | ***Virtual Environment*** | ***Traffic Playground*** |
|---|---|---|
| Red light at a traffic light (cyclists) | 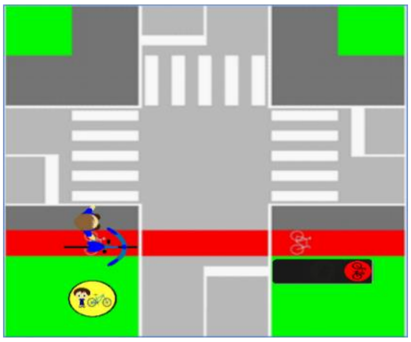 |  |
| Green light at a traffic light (cyclists) | 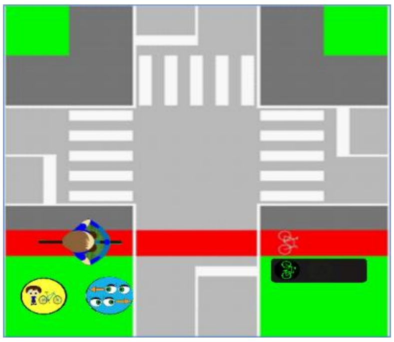 |  |

**Table 2** Traffic situations presented to children (cyclists)

*- Data processing*

The results were recorded in an online questionnaire on a mobile phone and stored directly in an MS Excel database. Statistical analysis was performed by the statistical software package IBM SPSS Statistics v. 23. Based on the results of descriptive statistics and cross tabulation it was presented the basic statistical analysis of data obtained in the experiment. Normality distribution was tested by inspection of histograms and the Kolmogorov-Smirnov test (Pešić et al., 2019a, Pešić et al., 2019b). As the Kolmogorov-Smirnov test has determined that results do significantly deviate from a normal distribution, the decision was to use Mann-Whitney Test. The threshold of statistical significance (α) is set at 5% (Pešić et al., 2019a, Pešić et al., 2019b).

## 3. RESULTS

*- Pedestrian traffic light*

When analyzing the behavior of children when the red light was on at the pedestrian traffic light, all children gave the correct answer for both environments (virtual and real environment) (Figure 1). However, when the green light for pedestrians appeared at the traffic light, children show better knowledge when solving the task on the computer (virtual environment – female 83%, male 67%; traffic polygon – female – 42% ,male 33%), which is confirmed by statistically significant differences between these two environments (Z = -2.591; p=0.010). There are no statistically significant gender differences for the mentioned traffic situations.

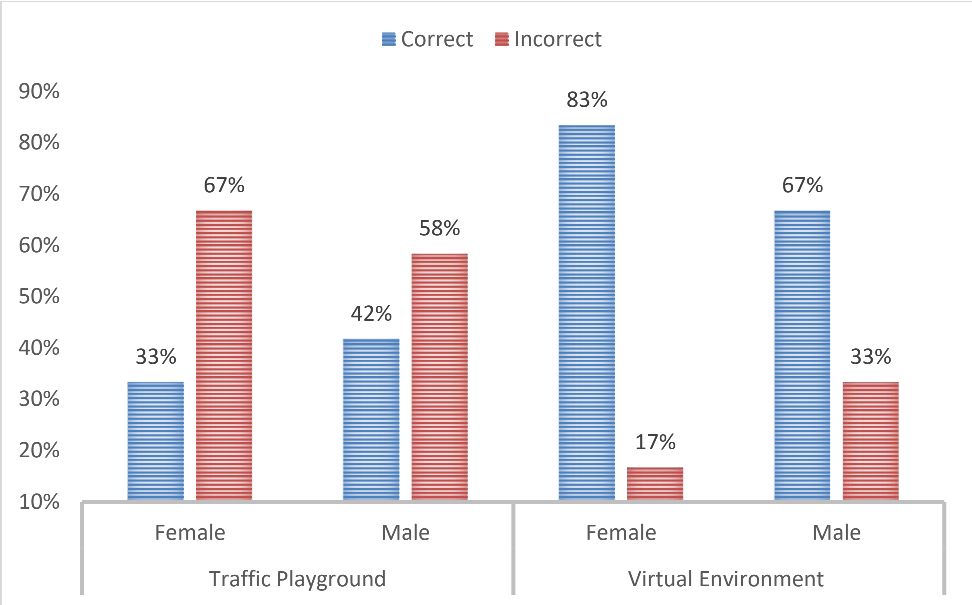


**Figure 1:** Results of children's achievements when the pedestrian traffic light is on with a red / red light - by gender and environment

*- Cyclists traffic light*

As with the traffic lights for pedestrians, and with the traffic lights for cyclists, all the children gave all the correct answers for the red light, for both environments (virtual and real environment) (Figure 2). The results of the chi-square test show statistically significant differences between the results of children in a virtual and real environment, when they cross the street by bicycle, when the traffic light is green for cyclists. Children have better results for this task in a virtual environment (Figure 2). As for the previous task, there are no statistically significant gender differences.

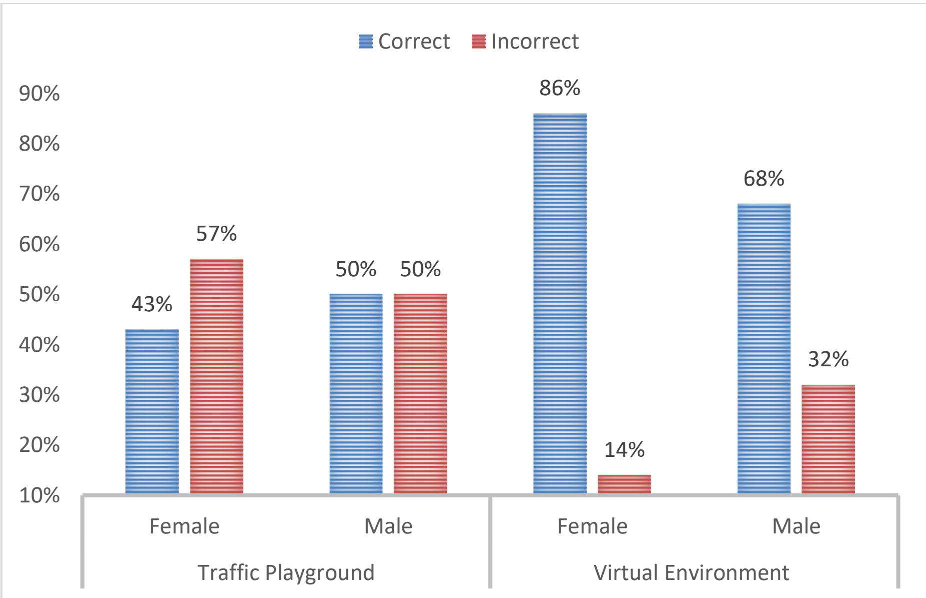


**Figure 2:** Results of children's achievements when the cyclists traffic light is on with a red / red light - by gender and environment

*- Pedestrian and cyclist traffic light*

Figure 3 shows the overall results of children's behavior at the traffic lights for pedestrians and cyclists. It can be concluded that children have better results when they solve the task on the computer, which was shown by statistically significant differences. Although it can be noticed on the same chart that men have better results in both environments, there are still no statistically significant gender differences.

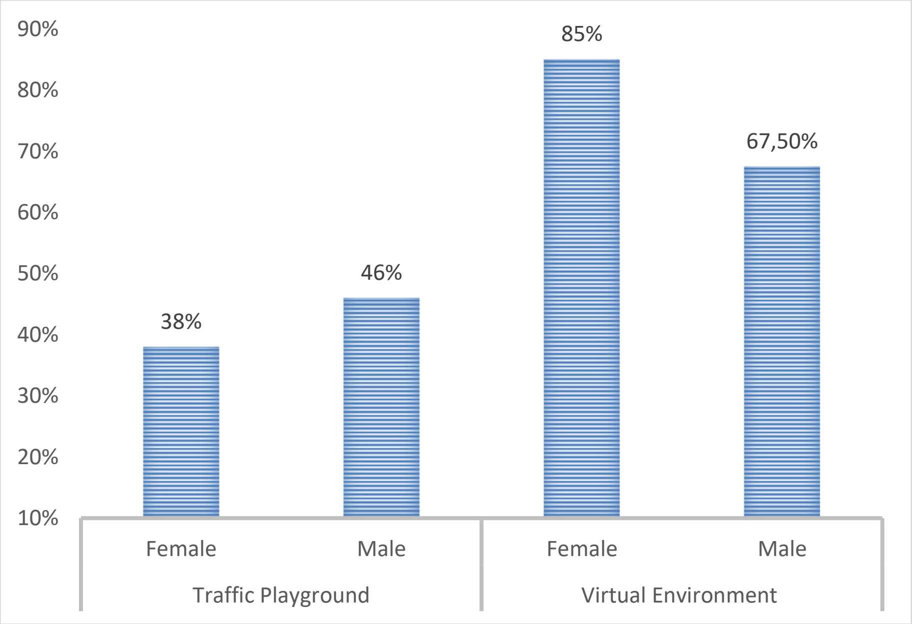


**Figure 3:** Overall results of children's behavior at traffic lights for pedestrians and cyclists

## 4. CONCLUSION

Based on the data collected and analyzed in our research, it can be derived general conclusions:

- Children have all the correct answers for behavior at a red light at a traffic light for pedestrians and cyclists. These results show that children are careful and know that we must not cross the street at a red light, neither when they are pedestrians, nor when they are cyclists.

- When it comes to children's behavior in the green light at the traffic lights for pedestrians and cyclists, children record a larger number of correct answers when solving a task in a virtual environment. These results can be explained by the fact that children have the theoretical knowledge, while they lacking practical knowledge and experience.

- There are no statistically significant gender differences for any of the tasks. This result confirms that children of both genders solve the stated tasks equally and no special approach is needed for either gender.

It is the application of geometric modeling that has enabled children to be tested and educated in the field of traffic safety in a simple, safe and practical way. At the same time, the virtual and real environment, which was created with the application of geometric modeling, children gladly accept and have additional motivation to master the field of traffic safety and thus become able to participate safely in traffic as pedestrians and cyclists (Pešić et al., 2019a; Trifunović et al, 2017; Trifunović, 2020). The directions of future research should be directed towards a larger number of respondents of different ages, as well as through a larger number of different geometrically modeled traffic situations.

**REFERENCES**


1. Dragutinovic, N. and Twisk, D., 2006. The effectiveness of road safety education: A literature review. *SWOV Institute for Road Safety Research*.
2. Goniewicz, K., Goniewicz, M., Pawłowski, W., Fiedor, P. and Lasota, D., 2017. Risk of road traffic accidents in children. *Medical Studies/Studia Medyczne*, *33*(2), pp.155-160.
3. Koekemoer, K., Van Gesselleen, M., Van Niekerk, A., Govender, R. and Van As, A.B., 2017. Child pedestrian safety knowledge, behaviour and road injury in Cape Town, South Africa. *Accident Analysis & Prevention*, *99*, pp.202-209.
4. Lieu, D.K. and Sorby, S.A., 2015. *Visualization, modeling, and graphics for engineering design*. Cengage Learning.
5. Park, G.J., Ro, Y.S., Do Shin, S., Song, K.J., Hong, K.J. and Jeong, J., 2018. Preventive effects of car safety seat use on clinical outcomes in infants and young children with road traffic injuries: A 7-year observational study. *Injury*, *49*(6), pp.1097-1103.
6. Pešić, D., Trifunović, A. and Petrović, M., 2019a. Road safety education for children: results of children's behavior on traffic playground and simulated traffic situations. *Facta Universitatis, Series: Teaching, Learning and Teacher Education*, pp.001-010.
7. Pešić, D., Trifunović, A., Ivković, I., Čičević, S. and Žunjić, A., 2019b. Evaluation of the effects of daytime running lights for passenger cars. *Transportation research part F: traffic psychology and behaviour*, *66*, pp.252-261.
8. Poudel-Tandukar, K., Nakahara, S., Ichikawa, M., Poudel, K.C. and Jimba, M., 2007. Risk perception, road behavior, and pedestrian injury among adolescent students in Kathmandu, Nepal. *Injury prevention*, *13*(4), pp.258-263.
9. Tabibi, Z., & Pfeffer, K. (2007). Finding a safe place to cross the road: the effect of distractors and the role of attention in children's identification of safe and dangerous road-crossing sites. *Infant and Child Development: An International Journal of Research and Practice*, *16*(2), 193-206.
10. Traffic Safety Agency, 2020. *Statistical report on the state of traffic safety in the Republic of Serbia in 2019*.
11. Trifunović, A., Čičević, S., Lazarević, D., Mitrović, S. and Dragović, M., 2018. Comparing tablets (touchscreen devices) and PCs in preschool children'education: testing spatial relationship using geometric symbols on traffic signs. *IETI Transactions on Ergonomics and Safety*, *2*(1), pp.35-41.
12. Trifunović, A., Pešić, D., Čičević, S. and Antić, B., 2017. The importance of spatial orientation and knowledge of traffic signs for children's traffic safety. *Accident Analysis & Prevention*, *102*, pp.81-92.
13. Trifunović, A.V., 2020. *Primena geometrijskog modeliranja za određivanje spremnosti dece za samostalno bezbedno učestvovanje u saobraćaju* (Doctoral dissertation, Univerzitet u Beogradu-Saobraćajni fakultet).
14. Twisk, D.A.M., Vlakveld, W.P. and Commandeur, J.J.F., 2007. *When Is Education Effective? Systematic Evaluation of Education Projects* (Vol. 2006, No. 28).
15. Wang, H., Morgan, C., Li, D., Huang, R. and Schwebel, D.C., 2021. Children’s fear in traffic and its association with pedestrian decisions. *Journal of safety research*, *76*, pp.56-63

# AESTHETICS OF VISUAL COMMUNICATIONS COURSE AT THE COMPUTER GRAPHICS - ENGINEERING ANIMATION STUDIES

Jelena Letić[1*], Milan Miščević[1], Marija Varga[1], Ivana Vasiljević[1], Branislav Popkonstantinović[1], Ratko Obradović[1]

[1]University of Novi Sad, Faculty of Technical Sciences, Computer Graphics Chair, 21000 Novi Sad, Serbia

jelena.letic@uns.ac.rs

***ABSTRACT***

*This paper presents the content of the course Aesthetics of Visual Communications (AVC). The course AVC is studied during the sixth semester of the undergraduate study program of Computer Graphics – Engineering Animation, at the Faculty of Technical Sciences, University of Novi Sad and covers different definitions, concepts and principles of aesthetics of visual communications (Faculty of Technical Sciences, 2021). Before taking AVC course, students have mastered 3D character modeling, mapping, lighting and rendering. Also, they are familiar with rigid body animation, as well as with simple animal and humanoid character animation requiring rigging. In order to develop the skills for forming the judgment of aesthetic evaluation of visual impression in all forms of visual communications, within the practical part of the AVC course, student are required to do three projects on different topics. This paper presents the topics of these tasks, details about them and their sequence as well as the evaluation of students' work. The first students' task is to rig and animate the car or vehicle of their choice. The second project task is deal with digital portrait study within ZBrush, digital sculpting program. This students' project requires modeling a 3D portrait of themselves and the final project is to rig this 3D portrait and to animate different facial expressions. After completing these course, students acquire enough skills and knowledge for further studying basics of animation techniques as well as software programs needed for digital production of animated films and visual effects*

**Keywords:** Computer graphics; 3D animation; rigging; 3D portrait modeling; character animation

## 1. INTRODUCTION

Computer Graphics—Engineering Animation (CG-EA) study program were accredited for the first time in the 7th accreditation cycle in the Republic of Serbia, on December 24th, 2010, at the Faculty of Technical Sciences (University of Novi Sad, Serbia) and the first generation of students enrolled in October 2011. Engineering Animation is an interdisciplinary program which connects the courses of electrical engineering and computer science with mathematics (Obradović et al., 2012). The program is designed to enable high quality education in interdisciplinary visualizations and in applying Computer Graphics in interdisciplinary researches in different fields, particularly in medicine, in visualization in technical and engineering disciplines, industrial engineering, civil ant traffic engineering, architecture, etc. In addition, today Computer Graphics is widely used for educational interdisciplinary presentations, in the film and gaming industry. Considering this, the CG-EA program is created to provide two basic educational modules for our students: the first one is creating 3D computer animations and the second one deals with all programming techniques which refer to image, i.e. for image creating or analyzing (Obradović et al., 2010).

New accreditation for undergraduate Academic Studies comprises 49 subjects - 38 compulsory subjects and 11 elective positions (with a choice of several subjects). The course Aesthetics of Visual Communications (AVC), the content of which is presented in this paper, is studied in the sixth semester of the study program CG-EA, and encompasses three hours (four classes per 45 min) of lectures and three hours of practical exercises a week. Hence, during the 14 weeks of a semester, the students have 56 classes of practical exercises in the computer laboratory (Obradović et al., May 2019).

## 2. AESTHETICS OF VISUAL COMMUNICATIONS COURSE

Subjects covered in this course are the continuation of the previous four courses: Spatial Shape Design, 3D Modeling, Character Animation and Fundamentals of Engineering Animation. By the time they come to the AVC course the students have studied various techniques for modeling 3D shapes, texturing and mapping, rendering techniques, animations with rigid bodies and the use of constraints, rigging and controllers creating for some animals/objects which have a relatively simple skeleton, (e.g. fish, duck or table lamp) as well as manlike characters rigging and animation (Obradović et al., 2019).

The main topics covered in the AVC course are advanced techniques of rigging and animation of the complex rigid bodies (e.g. car or vehicle) and humanoid character face, including digital portrait study of that character. These topics are studied through the practical part of the course consists of two project tasks and one Final Project. The distribution of tasks and points is shown in Table 1.

| *Obligations* | *Points* | *Available time (weeks)* |
|---|---|---|
| *First Project Task* | *15* | *4* |
| *Second Project Task* | *20* | *6* |
| *Final Project* | *30* | *4* |
| *Activity at exercises* | *5* | *-* |

**Table 1**: Distribution of tasks and points

All obligations from Table 1 in the summary are worth 70 points and represent the pre-exam assignments on the course that carry most of the points. The pre-exam obligations take 14 weeks to complete and must be fulfilled during the semester. A student must obtain a minimum of 40 points out of a maximum of 70 and at least 1/3 of the points for each task. If a student does not meet these requirements and does not collect 40 points, he/she must attend the course again next year (Obradović et al., 2019).

### 2.1 Student Projects Tasks

The main features of each task and its representative examples will be represented in detail in the following sections.

#### 2.2.1 First Project Task

The aim of the First Project Task is practicing advanced techniques of rigging and animation of complex rigid bodies. The task is to rig and animate the car or vehicle of their choice and should be carried out by using own 3D models or the one downloaded from the internet. In the rigid body animation, movement is a complex event and it needs to be presented with an evident influence of weight, force and speed of the vehicle, that is, animation should correspond to realistic model of vehicle behaviour. The vehicle should have a minimum of 4 wheels, with wheel steering. Animation should include driving along a given path, over rough terrain, with bends on the road. It is necessary to animate basic vehicle movements such as: wheel rotation, front-wheel steering, shock absorbers function, vehicle body roll and drifting (Computer Graphics - Engineering Animation, 2021).

Before starting the rigging process it is very important to explore vehicle movement, find a good references, notice the different movement and how to represent them best into the rig. Each individual vehicle movement (wheel rotation, wheel steering, body roll, etc.) should be controlled by one control which manipulates the part of the vehicle geometry. Locator objects i.e. helpers should be used as intermediaries between the controls and geometry of 3D model. Some controls affect the position and rotation of other controls. This is because the controls and helpers in a rig are connected to form a hierarchical structure. The hierarchical structure can be seen metaphorically as ‘a parent-child’ relationship. ‘A parent’ is an object at the top of the hierarchy, while ‘a child’ is an object at the bottom of the hierarchy. (Letić et al., 2020). Within the vehicle rig, wheel steering control represents 'the parent' in the hierarchical structure, and the wheel rotation control are 'the child'. It is very important to link all the elements into a whole to form a hierarchical structure.

The requirements that students must complete in the present project:

- main control and shock absorbers need to be able to adapt to rough terrain,
- turning the vehicle should be preceded by turning the front wheels,
- rotation of the wheels should correspond to the movement of the vehicle,
- during the animation, the vehicle has to do two laps along a given path, so that it has a different trajectory and movement,
- vehicle body roll and drifting needs to be demonstrated on the roadway horizontal curves,
- position the camera in order that all elements and movements are visible during the animation, and
- all controls and helpers must be colour coded, organized into layers with clear naming.

Project is scored according to the quality and functionality of the rig and the level of realism and persuasiveness of the vehicle movement in animation.

### 2.2.2 **Second Project Task**

The objective of the second task is to practice digital sculpting through the creation of 3D portrait within ZBrush, a digital sculpting software. Considering the fact that students meet a digital sculpting on this study program for the first time, it is planned to dedicate two weeks to studying the software and then four weeks to practise on the present project. Their task is to make a self-portrait and it has to be as realistic as possible to the person being portrayed. The portrait should be displayed as a turntable video. Textures are not required (Computer Graphics - Engineering Animation, 2021).

Before sculpting, students should take reference pictures, i.e. to photograph themselves. They need to create a set of photos, although for reference images within the software they will use only two photos - a front view photo (full face picture) and a side view photo of the model (profile picture). In order to obtain as realistic portraits as possible, perspective distortions should be avoided when taking photos. The next step is to study anatomy of the head, especially facial anatomy. The recommendation for students is to start working on the portrait from the basic low resolution model of 3D head which has already set the ears, the construction of the nose, mouth and eyes. Further, hair of the model can be styled in masses, similar to classic clay sculpture techniques.

Project is scored according to the quality of the portrait through persuasiveness and realism of the portrait, properly conveyed proportions and masses, the impression of skeletal construction, musculature and skin, as well as the quality of the final video, which should be clear, well framed and well lit.

### 2.2.3 **Final Project**

The aim of the Final Project is to develop a training process of rigging and skinning for humanoid character's face as well as practicing the principles of character animation. For this task, the students use the character, 3D portrait of themselves that was created during the previous task. The task is to make a short video with animation of five different facial poses: wide open mouth, happiness, sadness, anger and astonishment. Each facial pose should last about three seconds and each transition should last about one second (Computer Graphics - Engineering Animation, 2020).

Before starting the rigging process students need to do retopology of the 3D model. The recommendation for students is to use 3ds Max tools for manual retopology instead an automatic retopology tools within ZBrush. Retopology is the act of recreating an existing surface with more optimal geometry including clean, quad-based mesh (CGCookie, 2021). Clean topology is important in order to make the skinning process easier and to create more realistic muscle movement of the character (Letić et al., 2020). Topology should supports the correct creasing in required areas, thus an edge loops must be created around mouth, nose and eyes.

The rigging process starts with the creation of the bone structure for 3D model. Bones should be placed on key parts of the character, specifically, moving parts of the head: neck, lower jawbone, eyes, eyelids, eyebrows and nostrils. The bones in a rig are connected to form a hierarchical structure. This is followed by setting skeleton controls outside of the geometry of the 3D model in order to allow the animator to move the character to the desired position. Skinning is the next stage and represent the process of attaching the geometry of a 3D model to the digital skeleton. This is one of the most delicate and time-consuming tasks in creating a 3D animation. The weight of each bone needs to be assigned to the 3D model vertices so that every vertex follows the required bone. Ultimately, animation of the required facial expressions should be done. Considering that the keyframe animation is too demanding for this specific task, the students are advised to use morphing technique by adding the Morpher modifier within the 3ds Max. The advantage of using the Morpher is that you can set individual expressions and swap between them freely, or combine them with varying strengths for each one.

Project is scored according to the quality of the rig (including intuitiveness of the rig), skin, facial expressions and video representation. The face rig should contain the following controls:

- global control for the whole head (scaling this control should properly scale the whole rig and other controls)
- head control (with the pivot in the point of connection of the skull and neck, which will enable rotation of the head around this point)
- jaw control (for mouth opening)
- eye guidance control
- control for individual eyelids and eyes closing control (with possibility of manual animation of individual eyelids)
- eyebrow controls (with possibility of manual animation of eyebrows)
- controls for mouth movements (with possibility of manual animation of lips)

Intuitive rig refers to the ease of use of that rig. Skinning should be done correctly, in order to properly and harmoniously deform the geometry of the character face. Facial expressions should be clearly expressed and recognizable. Avoiding the symmetry of the left and right halves of the face will make the poses look more natural and interesting. The representation refers to the quality of the final video itself, which should be clear, well framed and well lit.

### 2.2 Results

In this section we will present the most successful and most attractive student projects that have been done in the last two academic years.

Last year (2019/2020 School year) the course was attended by 66 students and the pre-exam requirements were successfully completed by 63 students, i.e. 95%. This year (2020/2021 School year) the course was attended by 62 students and the pre-exam requirements were successfully completed by 57 students, i.e. 92%.

Figures 1 to 5 show renders of moving car in several characteristics keyframes. Figures 6 to 9 present the digital 3D portraits of the students. On figures 10 to 13 are shown the heads of the characters with different facial expressions.

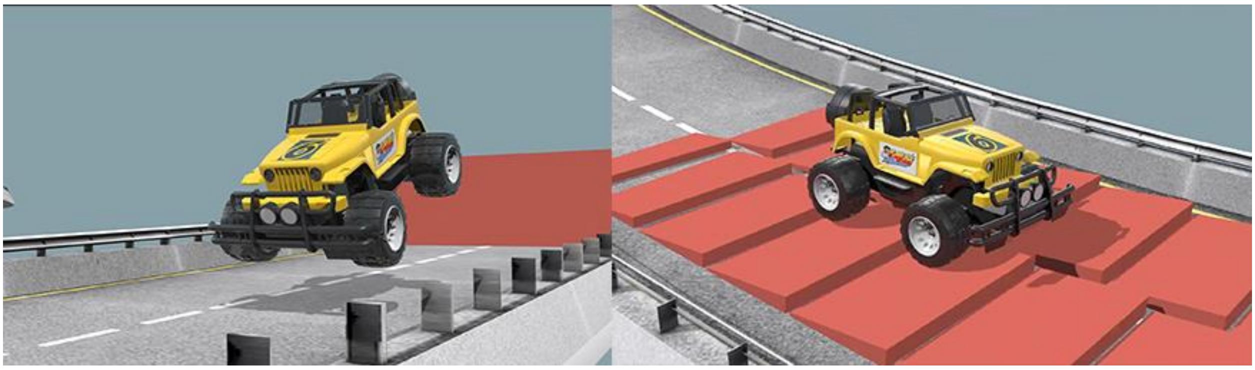

**Figure 1**: Car in motion, by student Anja Barnjak

**Figure 2**: Car in motion, by student Silvija Orsić

**Figure 3**: Car in motion, by student Teodora Micić

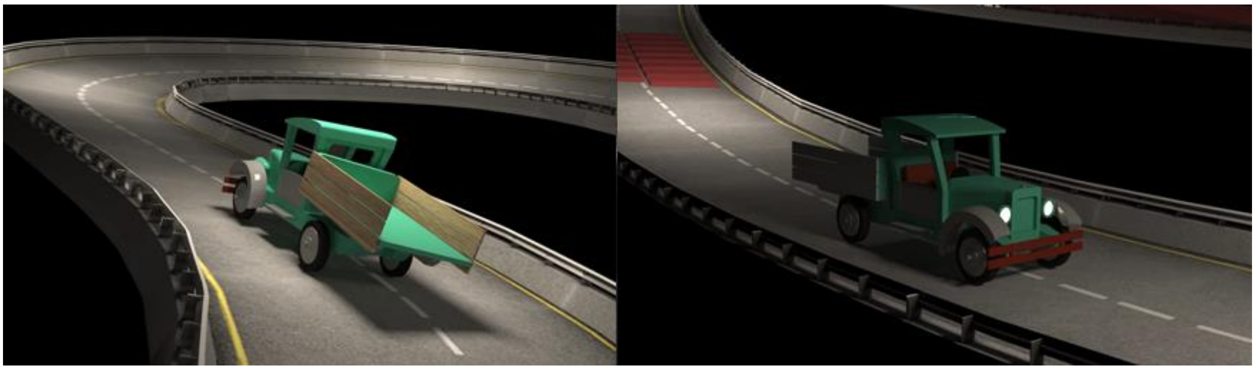

**Figure 4**: Car in motion, by student Tara Đurđević

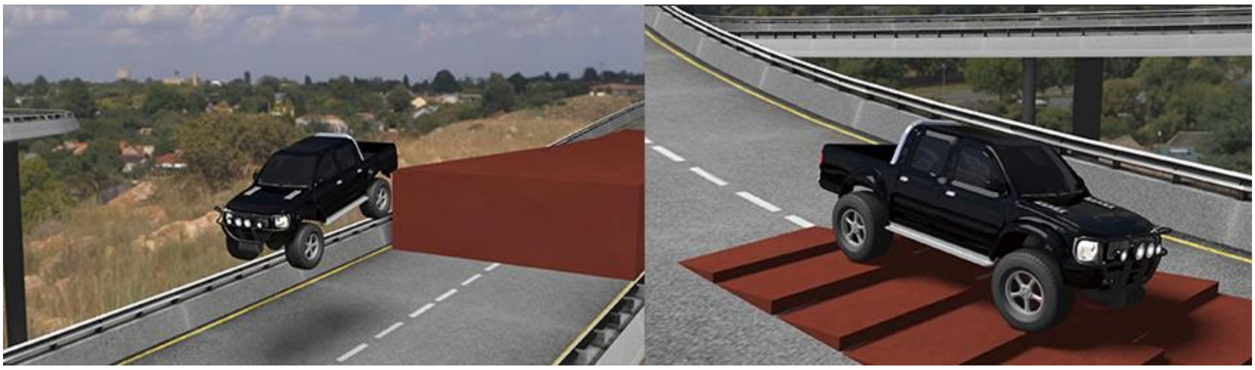

**Figure 5**: Car in motion, by student Nataša Sremac

**Figure 6**: 3D portrait, by student Miloš Nestorović

**Figure 7**: 3D portrait, by student Anja Barnjak

**Figure 8**: 3D portrait, by student Uroš Marković

**Figure 9**: 3D portrait, by student Nataša Erdeljan

**Figure 10**: Selected facial expressions, by student Tamara Jovanović

**Figure 11**: Selected facial expressions, by student Tamara Miljković

**Figure 12**: Selected facial expressions, by student Nataša Sremac

**Figure 13**: Selected facial expressions, by student Ognjen Petković

## 3. CONCLUSION

This paper presents the course Aesthetics of Visual Communications from the sixth semester at the study program Computer Graphics—Engineering Animation at the University of Novi Sad, Serbia. Within the practical part of the AVC course, student are required to do three projects on different topics. The first students' task is to rig and animate the car or vehicle of their choice. The second project task is deal with digital portrait study and the final project is to rig this 3D portrait and to animate different facial expressions. This paper presents a way of evaluating students work on these three tasks and their successful completion of the course, with the pass rate between 92 and 95%.

In addition to very high exam pass rate, the methodology of the AVC course is well accepted by the students, and they are motivated in the work which is interesting for them. This course presents a continuation of the four subjects (in the first, second and third year of the study) and is followed by the courses Special Visual Effects and Advanced Engineering Animation (in the third and fourth year of the study). These subjects are interestingly incorporated and it is expected, as the outcome, that students will be able to apply acquired knowledge in the further process of education as well as in the future of their professional work (Obradović et al., 2019).

## REFERENCES


1. CGCookie, Introduction to Retopology, https://cgcookie.com/course/introduction-to-retopology [Accessed: June, 2021]

2. Computer Graphics - Engineering Animation, http://www.racunarska-grafika.com [Accessed: June, 2021]

3. Faculty of Technical Sciences, Undergraduate Academic Studies Engineering Animation, http://www.ftn.uns.ac.rs/2028806618/engineering-animation [Accessed: June, 2021]

4. Letić, J., Mirčeski, F., Đurić, I., Vasiljević, I., Kekeljević, I., Obradović, R., 2020. Teaching Rigging for Animation at the Computer Graphics - Engineering Animation Studies, In: Jeli, Z. (ed.) 7th International Scientific Conference on Geometry and Graphics moNGeometrija 2020. University of Belgrade, Belgrade, Serbia.

5. Obradović, R., Popkonstantinović, B., Šidjanin, P., Vujanović, M., Milojević, Z., 2010. Computer graphics and computer animation studies at Serbian faculties. In: Popkonstantinović, B. (ed.) 2nd International Scientific Conference on Geometry and Graphics moNGeometrija 2010. University of Belgrade, Belgrade, Serbia.

6. Obradović, R., Vujanović, M., 2012. New Curriculum at the Faculty of Technical Sciences: Computer Graphics—Engineering Animation. In: Obradović, R. (ed.) 3rd International Scientific Conference moNGeometrija 2012, University of Novi Sad, Faculty of Technical Sciences, Novi Sad, Serbia. pp. 481–486.

7. Obradović, R., Vujanović, M., Kekeljević, I., 2019. Teaching 3D Character Animation Through Four Related Tasks, Advances in Intelligent Systems and Computing 809, ICGG 2018—Proceedings of the 18th International Conference on Geometry and Graphics, pp. 1671–1681.

8. Obradović, R., Vujanović, M., Popkonstantinović, B., Ivetić, D., Šiđanin, P., May 2019. Computer Graphics - Engineering Animation study program at the Faculty of Technical Sciences in Novi Sad, JIGED, Volume 14, Issue 1, pp. 319-326.

# SPECIAL VISUAL EFFECTS COURSE AT THE COMPUTER GRAPHICS - ENGINEERING ANIMATION STUDIES

Filip Mirčeski[1], Aleksa Paunović[2], Nikola Milinković[3], Igor Kekeljević[4], Ratko Obradović[5]

[1-5]University of Novi Sad, Faculty of Technical Sciences, Department of Fundamental Sciences, 21101 Novi Sad, Serbia

[1]filip.mirceski@uns.ac.rs, [2]aleksa.paunovic@uns.ac.rs, [3]nikolam@uns.ac.rs, [4]igor.kekeljevic@uns.ac.rs, [5]obrad_r@uns.ac.rs

***ABSTRACT***

*This paper shows the content of the course on Special visual effects, which students attend during the third year of their undergraduate studies of Computer Graphics - Engineering Animation. Through this paper, we present techniques of developing VFX, through the use of tools like particles, physical and cloth simulations. The course focuses on correctly applying the methods mentioned above, by describing three assignments and a course project which students complete during the semester. The subject Special visual effects is a continuation of the subjects 3D modeling and Character animation, which students attend during their second year of studies where the acquire the knowledge of advanced 3D modeling and animation techniques. After completing this third-year course, the students have obtained all the necessary skills for making basic animated movies which contained elementary VFX.*

**Keywords:** Computer Graphics, VFX, Particles, Physical Simulations, Cloth Simulations.

## 1. INTRODUCTION

The academic study programme in Engineering Animation was established at the Faculty of Technical Sciences, University of Novi Sad in 2011 as an interdisciplinary program which combines the courses of electrical engineering and computer science with mathematics. This study program is designed to enable high quality education in interdisciplinary visualizations and in applying Computer Graphics in interdisciplinary researches in different fields (Obradović et al., 2010).

Undergraduate Academic Studies last for four years and comprise 40 subjects, of which 31 are compulsory subjects and nine elective positions with a choice of several subjects (Obradović et al., 2012). During the studies, especially in professional courses, independent work is highly rated, the students are encouraged to participate in professional and development projects, and the focus is on the development of the skills for solving real problems.

## 2. COURSE CONTENT

This course improves the knowledge previously acquired during the fourth and fifth semesters. It focuses primarily on visual effects which are commonly used today in movie and gaming industries. The topics covered in this course include Particles, Physical Simulations, Cloth Simulations which are crucial part of VFX. This subject is divided into four different assignments. First two tasks cover the previously mentioned terms, starting with Particle Systems and finishing with *MassFX Plugin*, while the third assignment focuses on Cloth Simulations.

The implementation of the projects mentioned above will be explained in detail in the next section.

This course puts focus on teaching the students about VFX, Particles, Physical Simulations, Cloth Simulations. Through four assessments the students acquire all the necessary knowledge about the principles of VFX. In previous courses students acquired knowledge of modeling, texturing and lighting, while in this course that knowledge will be supplemented with advanced utilization of Special Visual Effects.

By describing four assignments which students completed within three different courses during the fourth, the fifth and the sixth semester, we will present the process of developing the skills of rigging and skinning different types of characters. These subjects are studied through the following three courses: Character Animation - in the second year of study, Fundamentals of Engineering Animation and Aesthetics of Visual Communications, both in the third year of studies. During the 15 weeks of the semester, the students have 60 classes of practical exercises in the computer laboratory for each of these courses (Obradović et al., 2019). Independent student work is accentuated, still it is supervised by teachers and teaching assistants.

## 3. PRACTICAL PART OF THE COURSE - COURSE PROJECTS

### 3.1 First Course Assignment (Particle System)

The term particle system is vaguely defined in Computer Graphics. In Computer Graphics, particles are used to simulate the appearance of physical phenomena that can be simulated as a set of variable models. For example, some typical particle systems include: fire, smoke, dust, explosions, snow, rainfalls and glass shatters. It has been used to describe different modeling techniques, rendering techniques, and even types of animation. In fact, the definition of a particle system seems to depend on the application that it is being used for. The criteria that holds true for all particle systems are the following:

- Collection of particles - A particle system can be made of an arbitrary number of same or different particles. Each of these particles has attributes that influence the behavior of the particle. Often, particles are graphical primitives such as points, lines or simple three-dimensional geometry, but they are not limited to this.
- Nonlinearly defined attributes - The other common characteristic of all particle systems is the introduction of some type of random element. This random element can be used to control the particles basic attributes such as position, velocity and color. Usually the random element is controlled by some type of predefined variable, such as an integer, bound, variance, or a type of distribution.

The first assignment students have to complete is to create a complex Particle System which simulates a natural occurrence which abides by all laws of physics. Some of the more common themes students generally approach are events, such as rainfall, fire, smoke, etc.

Workflow generally includes creating either basic or procedurally generated geometry that will spawn as particles, creating a spawn point (or using existing geometry as source) for the particles, setting boundaries, triggers, as well as forces (such as motion, gravity, etc.) that will affect the particle system.

The main task of the first assignment is to, in detail, create a *Particle Flow* System, within *3DStudio Max* software, which gives user a great deal of options and variables that can be used to create a visually pleasing and physically correct render. The students are required to implement particle systems in their renders based on lifelike models, using reference from real life, while respecting natural laws such as speed, gravity, wind, drag and interaction with environment. The behavior of the particles should correspond to the natural model.

The students work is also graded depending on the complexity of the system. Complexity refers to the quantity of the *Particle Flow* systems and the actual number of particles included in the systems. It is measured according to the number of significant and effective changes in the behavior of particles, or the number of used *Particle Flow* systems. An example of a high complexity achieved through one *Particle Flow*'s system is the imitation of rain: a drop falls, hits an object, one part of the drop bursts, the other slides down the geometry, accelerates again and falls to the ground, becomes a geometric shape of the crown of scattered water, etc.

Besides the complexity and the implementation of this system, visual appeal is also graded. The display refers to the quality of the final video file. The material (reflection, refraction, roughness, metalness, etc.) and geometry of the particles should correspond to the realistic appearance of the simulated phenomenon. Clarity scenes are achieved by adequate framing and exposure, which should clearly show the phenomenon that we imitate with the help of the *Particle Flow* System.

### 3.2 Results of the First Course Assignment

This section will showcase the most visually pleasing and the most complex Particle Systems that students have created in the last three academic years.

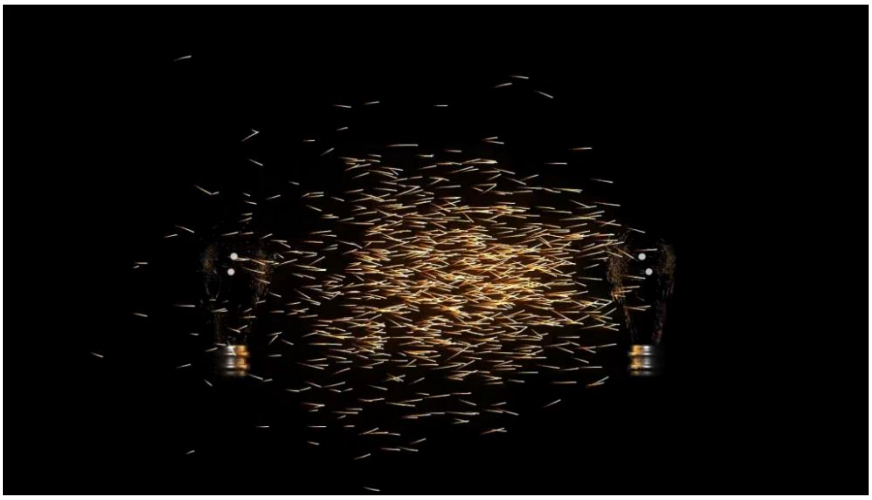

**Figure 1**: Energy transfer from one bulb to another (presented through photon simulation), by Aleksa Paunović

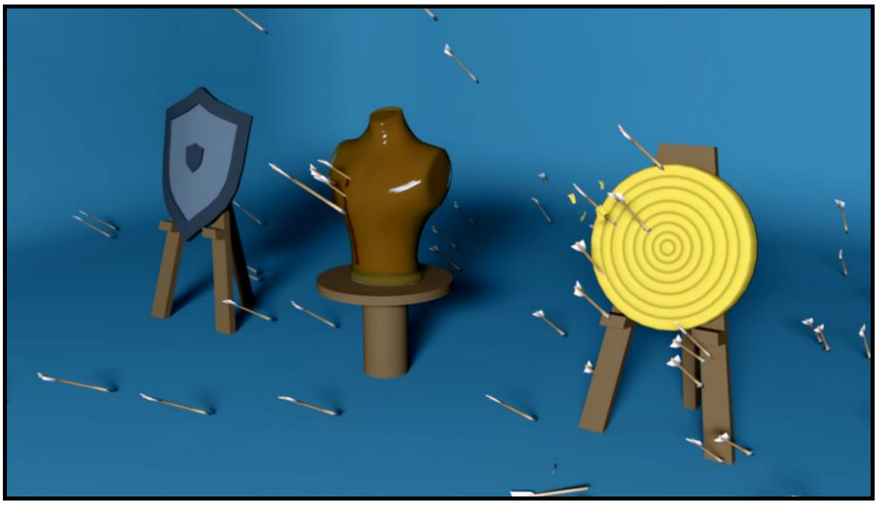

**Figure 2**: Simulation of arrows penetrating different targets, by Andrej Krstić

**Figure 3**: Popcorn popping simulation, by Ilija Rajić; Multiple base geometries of popcorn are being spawned in a limited base geometry

**Figure 4**: Rainfall simulation by Stojan Dobrički

**Figure 5**: Moths gathering around a light source, by Svetlana Bobić

### 3.3 Second Course Assignment (*MassFX Plugin*)

The second assignment includes creating a Rude Goldberg's machine using *MassFX Plugin* included in the base version of *3DStudio Max* software.

A Rube Goldberg machine, named after American cartoonist Rube Goldberg, is a chain reaction-type machine or contraption intentionally designed to perform a simple task in an indirect and overly complicated way. Usually, these machines consist of a series of simple unrelated devices; the action of each triggers the initiation of the next, eventually resulting in achieving a stated goal [1].

*MassFX* is a commonly used toolset in Computer Graphics which main application is adding realistic physics simulations to a project. *MassFX* simulations use rigid bodies, objects that do not change shape during the simulation, while, depending on their interaction with other objects, they can be dynamic, kinematic or static, the terms regularly used in physics simulation. Dynamic objects are entirely controlled by the simulation, as they are object of gravity, interactions, cloth simulations, etc. Kinematic objects can be animated using standard methods, but they can also be stationary, meaning they can affect dynamic objects, but can't be affected by them. Lastly, static objects cannot be animated, they can only be used as an obstacle.

With this knowledge, *MassFX* has its use in animating complex systems of simple interactions between objects, such as domino effect, bowling pin collisions, cloth animations, destructible meshes, and so on.

As previously mentioned, the assignment includes implementing Rube Goldberg's machine, while the three crucial grading parameters are complexity, physics realism and overall appeal. The reason for choosing Rude Goldberg's machine as an  assignment is because it emphasizes the use of creative thinking, while urging students to utilize tools that are available inside *MassFX Plugin*'s toolset, such as kinematic, dynamic and static types of objects, constraints, *mCloth* and ragdolls, and generating complex system through its application.

The most important part of this grading system, or the one that generates the highest part of the grade, is the physics, or the interaction between objects in the scene, since it requires that students create logical chain of events that can be seen in real world, without the feeling of it being simulated. Finally, similar to the first assignment, visual appeal comprises using correct lighting, material and camera animation setup, that was previously taught through the *3D Animation* subjects syllabus in the 3rd semester.

### 3.4 Results of the Second Course Assignment

This section will showcase the most visually pleasing and the most complex Rube Goldberg's machines that students have created in the last three academic years.

**Figure 6**: Rube Goldberg's machine, where the left image shows the effect before, and the right image shows the effect after the simulation's complete, by Ana Šaler

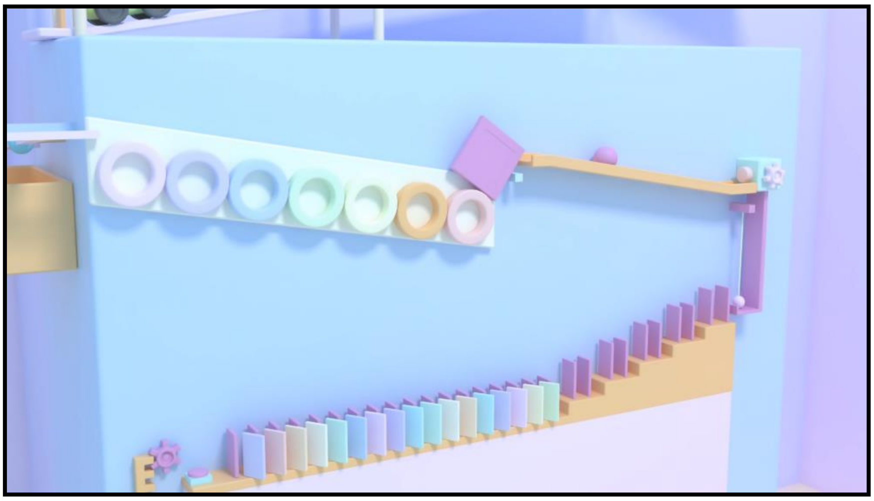

**Figure 7**: Rude Goldberg's machine, by Anja Barnak

**Figure 8**: Rude Goldberg's machine, by Lorena Ignjatović Ivanović

**Figure 9**: Rude Goldberg’s machine, by Nina Škrijelj


**Figure 10**: Paper animation, simulated using a wind force, by Strahinja Milošev

### 3.5 Third Course Assignment (Cloth Simulation)

Third course assignment (or the course project), unlike previous two assignments, focuses on Cloth Simulation. In the software used for this assignment, practical workflow includes using two separate geometries, one as a medium for Cloth Simulation and another, previously prepared geometry, as a static object with whom cloth object interacts and shapes itself. The main theme of this task involves creating garment for a fictional character, as clothing is probably the most intuitive piece of cloth, and, on the other hand, it encourages creative thinking and problem solving.

Unlike the standard way of creating geometry, objects used for Cloth Simulation are made from two or more separate 2D panels, connected together using custom seams. 2D panels are prepared using basic curves, filled out with triangle polygons, which, depending on the complexity of the model, allows the geometry to transform up to a certain degree, during the simulation process. Before the actual simulation, the panels are supposed to be positioned in a way that is intuitive, or in a way that best fits the body of the static object which garment envelops. The process of transforming 2D panels, and merging into 3D geometry is shown in Figure 11.

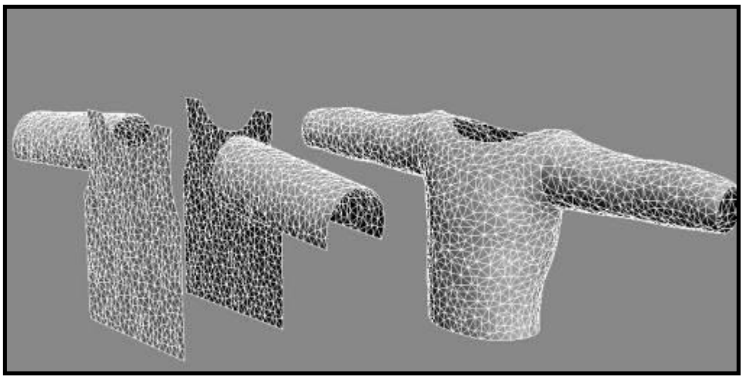

**Figure 11**: On the left side, cloth simulation is not yet applied, while on the right side the model is simulated, the static model, or the body of the model, is set to invisible [2]

Specifications for this task are as follows:

1. The character for which the clothing is made must be independently created by the student or, alternatively, the character modeled in the subject *Basics of Animation Engineering,* during the 5th semester can be used. The character movement does not have to be created by the student.
2. The clothing simulation should last for at least 5 seconds.
3. The character must contain at least 3 pieces of clothing. The clothes must be made independent from one another.
4. At least 2 pieces of clothing should have different physical characteristics, such as cotton T-shirt, twill pants, synthetic coat, jeans, tuxedo, etc.
5. At least 2 pieces of clothing must significantly overlap with one another (vest over a T-shirt, T-shirt over pants, etc.)
6. Each piece of clothing must have a minimum of 2 panels.
7. Only one piece of clothing can be tight around the characters body, since these type of clothes have very scarce simulation capabilities.
8. There must be at least one sleeve on at least one piece of clothing.

Grading system for this final assignment, similarly to the previous tasks, includes complexity of the simulation created, realism of the physics simulated, and finally, visual appeal. Complexity is measured according to the complexity of the clothes, geometry subdivision, depending on how many pieces of clothes were used, how many panels the clothes consist of and the way the clothes are joined.

Physics and interaction are scored according to the credibility of the behavior of the clothes during the simulation. The goal is to make the clothes behave as realistically as possible, to clearly see the differences in the physical specifics of the material used for the garment objects, while not allowing any geometry intersections between pieces of clothing to appear. This is the most important part of the task, as it carries the highest number of points.

Lastly, visual appeal consists of using correct lighting technique (using singular ambient light, using direct light, bounce, back and edge light, etc.), generating intuitive materials that show the pieces of garment (making a certain difference between a material of jeans and cotton, etc.) and finally creating stimulating character animations and garment simulations.

### 3.6 Results of the Third Course Assignment

This section will showcase the most visually pleasing and the most complex Cloth Simulation results that students have created in the last two academic years.

**Figure 12**: Cloth animation, by Nataša Sremac

**Figure 13**: Cloth animation, by Anja Barnak

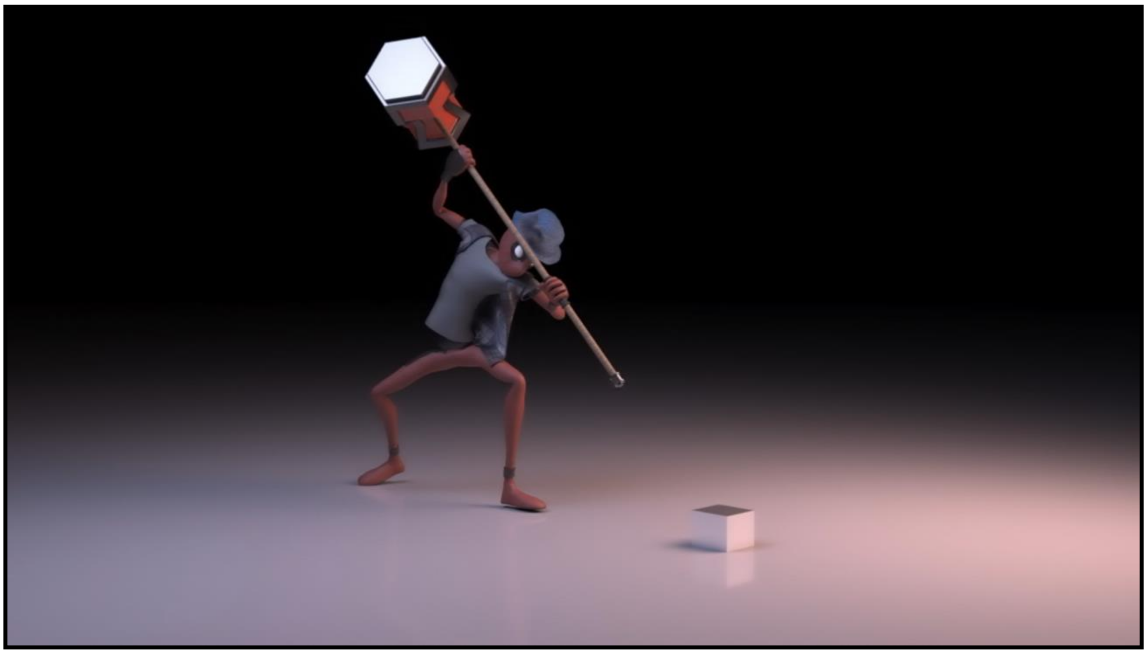

**Figure 14**: Cloth animation, by Aleksa Paunović

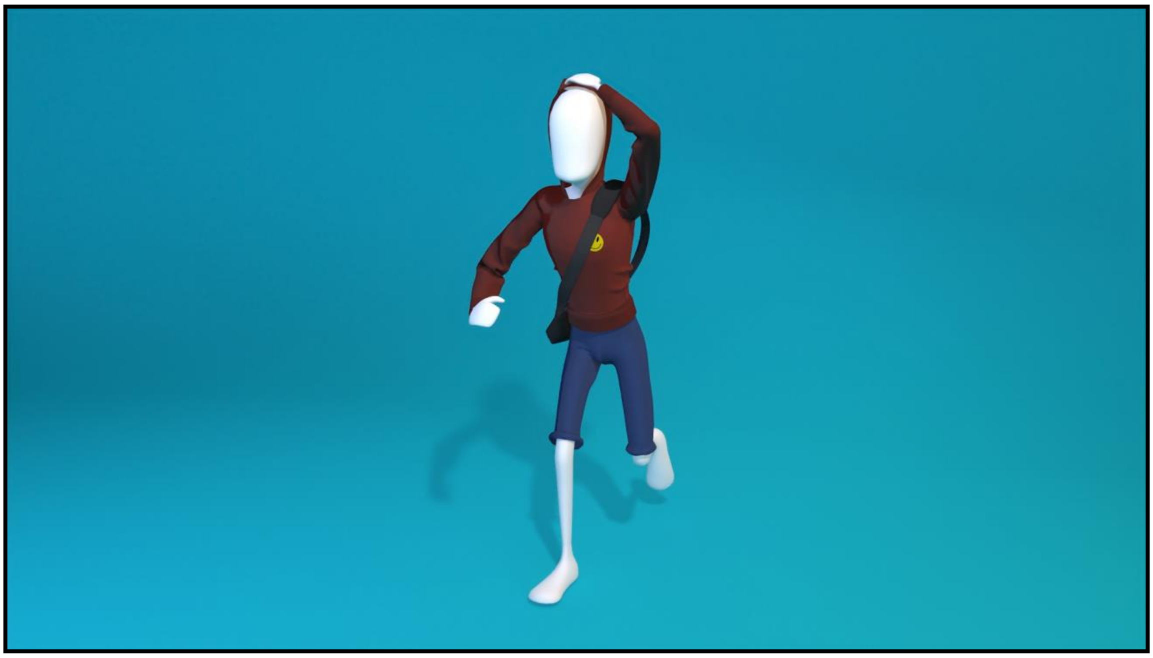

**Figure 15**: Cloth animation, by Strahinja Milošev

## 4. CONCLUSION

This paper present a teaching process of implementing complex particle, physics and cloth simulations through the content of the course Special Visual Effects, un undergraduate course of the Computer Graphics study program at the Faculty of Technical Sciences, University of Novi Sad. Through the implementation of this course, a gradual learning of the addressed topics was achieved. Different simulation workflows are covered through three mandatory projects during the third year of study, and they are all presented in detail in this paper. The students attend the course mentioned above during their 6th semester, while, during their 8th semester, their knowledge of different simulating techniques is further broadened, through the mandatory subject, *Advanced Engineering Animation.*

The most significant outcomes of this method of teaching are:

1. The majority of students successfully complete the courses
2. Interesting and properly completed students' projects, and
3. Distinct progress in learning process of the specified topic.

In addition, this methodology of the courses is well accepted by the students, and they are motivated to work on the assignments which they find interesting.

**REFERENCES**


1. Jon Gress: Visual Effects & Compositing, 1st Edition, New Riders Pub (October 22, 2014)
2. Lee Lanier: Compositing Visual Effects in After Effects: Essential Techniques, 1st Edition, Routledge (November 6, 2015)
3. Chad Perkins: The After Effects Illusionist: All the Effects in One Complete Guide, 2nd Edition, Routledge (October 4, 2012)
4. Rube Goldberg's machine, Wikipedia: https://en.wikipedia.org/wiki/Rube_Goldberg_machine
5. 3DStudio Max, Cloth Modifier, Autodesk: https://knowledge.autodesk.com/support/3ds-max/learn-explore/caas/CloudHelp/cloudhelp/2020/ENU/3DSMax-Simulation-Effects/files/GUID-1663898B-7C53-4123-9D54-7B7EE843FB92-htm.html#GUID-1663898B-7C53-4123-9D54-7B7EE843FB92
6. Computer Graphics - Engineering Animation. Available online: http://www.racunarska-grafika.com (accessed on 20 June 2021).
7. Obradovic, R., Vujanovic, M., Popkonstantinovic, B., Ivetic, D., & Sidanin, P. (2019). COMPUTER GRAPHICS-ENGINEERING ANIMATION STUDY PROGRAM AT THE FACULTY OF TECHNICAL SCIENCES IN NOVI SAD. Journal of Industrial Design and Engineering Graphics, Volume 14(1), pp. 319-326,
8. Obradović, R., Vujanović, M., 2012. New curriculum at the faculty of technical sciences: computer graphics—engineering animation. In: Obradović, R. (ed.) 3rd International Scientific Conference moNGeometrija 2012, pp. 481–486. University of Novi Sad, Faculty of Technical Sciences, Novi Sad, Serbia

www.mongeometrija.org